

PALACKÝ UNIVERSITY IN OLOMOUC
FACULTY OF SCIENCE

Laboratory of Growth Regulators & Department of Botany

Jan Šimura

NEW APPROACHES TO PHYTOHORMONE
ANALYSIS IN PLANTS

IN PROGRAMME BIOLOGY – BOTANY

Ph.D. THESIS

Olomouc

2017

Acknowledgements

It is my great pleasure to thank my supervisor Dr. Ondřej Novák for introducing me and professionally guiding me through the often tricky field of applied mass spectrometry. I express appreciation foremost for his kindness, encouragement and his patience. I would also like to express my gratitude to Dr. Danuše Tarkowská for her valuable advices, remarks and support during my struggles with mass-spec. instrumentation. My special thanks go to Prof. Dr. Karin Ljung, who supported my work in Sweden. I would like to express my thanks to Dr. Ioanna Antoniadis and Dr. Jitka Šíroková for encouragement and help during the final stages of my experiments, Dr. Aleš Pěňčík, Dr. Kristýna Floková and Dr. Lenka Plačková for consultations, advices and remarks during the preparation of this thesis and Dr. Alexander Oulton for the final English correction. I consider myself lucky that I have had the opportunity to work and study in such a friendly and supportive environment as the Laboratory of Growth Regulators certainly is, and therefore, I am expressing my sincere gratitude to Prof. Miroslav Strnad for the opportunity to be a member of his group. I would like to extend my thanks to my lab colleagues, especially Eva Hirnerová, for the inspirational and joyful atmosphere and of course for their friendship.

This work was funded by the Internal Grant Agency of Palacký University (project no. IGA_PrF_2017_010).

Bibliographical identification

Author's first name and surname: Jan Šimura

Title: New approaches to phytohormone analysis in plants

Type of thesis: Ph.D. Thesis

Department: Department of Botany

Laboratory of Growth Regulators & Department of Chemical Biology and Genetics,
Centre of the Region Haná for Biotechnological and Agricultural Research, Institute of
Experimental Botany AS CR & Faculty of Science of Palacký University

Supervisor: Mgr. Ondřej Novák, Ph.D.

Adviser I.: Mgr. Danuše Tarkowská, Ph.D.

Adviser II.: Prof. Dr. Karin Ljung

The year of presentation: 2017

Keywords: Plant hormones, Solid-phase extraction (SPE), Ultra-high performance
liquid chromatography (UHPLC), Tandem mass spectrometry (MS/MS)

Number of pages: 86

Number of supplements: 6

Language: English

Bibliografická identifikace

Jméno a příjmení autora: Jan Šimura

Název práce: Nové přístupy k analýze fytohormonů v rostlinách

Typ práce: disertační práce

Pracoviště: Laboratoř růstových regulátorů & Oddělení chemické biologie a genetiky, Centrum regionu Haná pro biotechnologický a zemědělský výzkum, Ústav experimentální botaniky AV ČR, v.v.i. & Přírodovědecká fakulta, Palackého Universita.

Školitel: Mgr. Ondřej Novák, Ph.D.

Konzultant I.: Mgr. Danuše Tarkowská, Ph.D.

Konzultant II.: Prof. Dr. Karin Ljung

Rok obhajoby: 2017

Klíčová slova: Rostlinné hormony, Extrakce na pevné fázi (SPE), Ultra-vysokoúčinná kapalinová chromatografie (UHPLC), tandemová hmotnostní spektrometrie (MS/MS)

Počet stran: 86

Počet příloh: 6

Jazyk: Anglický

Abstract

Plant hormones are highly bioactive signalling molecules with broad functions as chemical messengers that stimulate growth and development including flowering, seed germination, senescence and various stress responses. Plant hormones are an extremely large family of diverse compounds divided into several structurally different groups such as purine and indole derivatives, plant steroids, lipid-based substances and terpenoid carboxylic acids. The characteristic of all hormones is that they are typically found in tissues in minute concentrations. Thus, direct quantification in complex plant extracts poses a difficult analytical task.

The primary objectives of this thesis are as follows: the development of a rapid UHPLC-MS/MS based method for complex phytohormone analysis, a method for miniaturizing tRNA bound cytokinin extraction, their determination in algal and cyanobacteria species, and the application of these newly developed methods (and well-established ones) to plant hormone determination with a focus on signalling and crosstalk.

Keywords: Plant hormones, Solid-phase extraction (SPE), Ultra-high performance liquid chromatography (UHPLC), Tandem mass spectrometry (MS/MS), crosstalk

Number of pages: 86

Number of supplements: 6

Language: English

Declaration I

I hereby, declare that the presented Ph.D. thesis is my original work. The literature used is listed in the References section.

Olomouc,

Mgr. Jan Šimura

Declaration II

I declare that my role in preparation of the papers listed above was as follows:

Supplement I: First author - Plant hormonomics: multiple phytohormone profiling by targeted metabolomics

Supplement II: Co-author - Control of cytokinin and auxin homeostasis in cyanobacteria and algae

Supplement III: Co-author - Light influences cytokinin biosynthesis and sensing in *Nostoc* (Cyanobacteria)

Supplement IV: First author - Cytokinin, auxin and physiological polarity in the aquatic carnivorous plants *Aldrovanda vesiculosa* and *Utricularia australis*

Supplement V: Co-author - Endogenous abscisic acid promotes hypocotyl growth and affects endoreduplication during dark-induced growth in tomato (*Solanum lycopersicum* L.)

Supplement VI: Co-author - CHASE domain-containing receptors play an essential role in the cytokinin response of the moss *Physcomitrella patens*

Table of contents

List of papers.....	9
List of abbreviations.....	10
1 Introduction.....	14
2 The main aims and objectives.....	15
3 Literature review	16
3.1 Plant hormones.....	16
3.1.1 Cytokinins.....	16
3.1.2 Auxins	21
3.1.3 Abscisates	25
3.1.4 Jasmonates	27
3.1.5 Salicylic acid.....	30
3.1.6 Gibberellins.....	32
3.1.7 Brassinosteroids	36
3.1.8 Other plant growth regulators and phytohormones.....	39
3.2 Phytohormone crosstalk	41
3.2.1 Physiological polarity.....	42
3.2.2 Skotomorphogenesis to photomorphogenesis transition (de-etiolation).....	43
3.2.3 Salinity stress	44
3.3 Plant hormone analysis.....	46
3.3.1 Extraction.....	46
3.3.2 Purification	47
3.3.3 LC-MS Analysis	48
4 Experimental	50
4.1 Materials and methods.....	50
4.1.1 Chemicals	50
4.1.2 Plant Materials	51
4.1.3 Methods of phytohormone isolations.....	53
4.1.4 Instrumentation and phytohormone detection	56
4.2 Survey of results	58
4.2.1 Plant hormonomics.....	58
4.2.2 <i>t</i> RNA-bound cytokinins	66
4.4.3 Phytohormone signalling and crosstalk.....	69
5 Conclusion and future prospects	72
6 References.....	74
7 Supplements I-VI	86

List of papers

This thesis is based on the following publications, referred to in the text by corresponding supplement No. I-VI attached in the Supplement section.

- I. **Šimura, J.**, Antoniadis, I., Šírková, J., Tarkowská, D., Strnad, M., Ljung, K., Novák, O. (2017) Plant hormonomics: A multiple phytohormone profiling by targeted metabolomics approach. (manuscript submitted, *Plant Physiology*)
- II. Žižková, E., Kubeš, M., Dobrev, P., I., Příbyl, P., **Šimura, J.**, Zahajská, L., Závěská Drábková, L., Novák, O., & Motyka, V. (2017). Control of cytokinin and auxin homeostasis in cyanobacteria and algae. *Annals of Botany*, 119(1), 151–166.
- III. Frébortová, J. Plíhal, O., Florová, V., Kokáš, F., Kubiasová, K., Greplová, M., **Šimura, J.**, Novák, O., Frébort, I. (2017) Light influences cytokinin biosynthesis and sensing in *Nostoc* (Cyanobacteria). *Journal of Phycology*, 53, 703–714.
- IV. **Šimura, J.**, Spíchal, L., Adamec, L., Pěňčík, A., Rolčík, J., Novák, O., & Strnad, M. (2016). Cytokinin, auxin and physiological polarity in the aquatic carnivorous plants *Aldrovanda vesiculosa* and *Utricularia australis*. *Annals of Botany*, 117(6), 1037-1044.
- V. Humplík, J. F., Bergougnoux, V., Jandová, M., **Šimura, J.**, Pěňčík, A., Tomanec, O., Rolčík, J., Novák, O., & Fellner, M. (2015). Endogenous abscisic acid promotes hypocotyl growth and affects endoreduplication during dark-induced growth in tomato (*Solanum lycopersicum* L.). *PLoS ONE*, 10(2).
- VI. Von Schwartzenberg, K., Lindner, A. C., Gruhn, N., **Šimura, J.**, Novák, O., Strnad, M., Gonneau, M., Nogué, F., & Heyl, A. (2015). CHASE domain-containing receptors play an essential role in the cytokinin response of the moss *Physcomitrella patens*. *Journal of Experimental Botany*, 67(3), 667-679.

List of abbreviations

Chemicals & Analytes

Chl _a	chlorophyll a
Chl _b	chlorophyll b
DEPC	diethyl pyrocarbonate
AcA	acetic acid
FA	formic acid
2,4-D	2,4-dichlorophenoxyacetic acid
2-MeS CKs	2-methylthio cytokinins
4-Cl-IAA	4-chloroindol-3-acetic acid
7'-OH-ABA	7'-hydroxy- abscisic acid
8'-OH-ABA	8'-hydroxy- abscisic acid
9'-OH-ABA	9'-hydroxy- abscisic acid
ABA	abscisic acid
ACN	acetonitrile
AP	alkaline phosphatase
BAP	<i>N</i> 6-benzylaminopurine
BL	brassinolide
BRs	brassinosteroids
<i>cis</i> -(+)-OPDA	<i>cis</i> -(+)- <i>I</i> 2-oxo-phytodienoic acid
dnOPDA	dinor- <i>I</i> 2-oxo-phytodienoic acid
CKs	cytokinins
CS	castasterone
<i>cZ</i>	<i>cis</i> -zeatin
<i>cZR</i>	<i>cis</i> -zeatin riboside
<i>cZRMP</i>	<i>cis</i> -zeatin riboside-5'-monophosphate
DPA	dihydrophaseic acid
DZ	dihydrozeatin
DZR	dihydrozeatin riboside
EtOH	ethanol
GAs	gibberellins
IAA	indole-3-acetic acid
IAA-Ala	IAA- <i>L</i> -alanin
IAA-Asp	IAA- <i>L</i> -aspartate
IAA-Glu	IAA- <i>L</i> -glutamate
IAA-Gly	IAA- <i>L</i> -glycine
IAA-Leu	IAA- <i>L</i> -leucine
IAM	indole-3-acetamide
IAN	indole-3-acetonitrile
IGP	indol-3-glycerol phosphate
iP	<i>N</i> ⁶ -(Δ^2 -isopentenyl)adenine
IPA	propan-2-ol (isopropanol)
iPR	<i>N</i> ⁶ -isopentenyladenine riboside
iPRMP	<i>N</i> ⁶ -isopentenyladenine riboside-5'-monophosphate
JA	jasmonic acid
JA-Ile	jasmonoyl- <i>L</i> -isoleucin
JAs	jasmonates
JA-Trp	jasmonoyl- <i>L</i> -tryptophan
K	kinetin
KAR1	karrikinolide
L-Trp	L-tryptophan
MeJA	methyl jasmonate
MeOH	methanol
MEP	2-C-methyl- <i>D</i> -erythritol-4-phosphate
MeSA	methyl salicylate
<i>mT</i>	<i>meta</i> -topolin

NeoPA	neophaseic acid
<i>o</i> T	<i>ortho</i> -topolin
PA	phaseic acid
PAA	phenylacetic acid
<i>p</i> T	<i>para</i> -topolin
SA	salicylic acid
SLs	strigolactones
<i>t</i> RNA	transfer ribonucleic acid
<i>t</i> Z	<i>trans</i> -zeatin
<i>t</i> ZR	<i>trans</i> -zeatin riboside
<i>t</i> ZRMP	<i>trans</i> -zeatin riboside-5'-monophosphate
α -NAA	α -naphthaleneacetic acid
2-MeSiPR	2-methylthio- N^6 -(Δ^2 -isopentenyl)adenine riboside
2-MeScZR	2-methylthio- <i>cis</i> -zeatin riboside

Genes & Proteins

ABCB/MDR/PGP	ATP-binding cassette subfamily B/ multidrug resistance phosphoglycoprotein
ABP1	AUXIN BINDING PROTEIN 1
ADP	adenosine diphosphate
AHK2/3/4	AUTHENTIC HIS- KINASE (Arabidopsis histidine kinase 2/3/4)
AHPs	<i>Arabidopsis thaliana</i> histidine phosphotransfer proteins
AOC1/2	allene oxide cyclase 1/2
AOS	allene oxide synthase
ARFs	AUXIN RESPONSE FACTORs
ATP	adenosine triphosphate
Aux/IAA	AUXIN/INDOLE-3-ACETIC ACID
AUX/LAX	AUXIN RESISTANT 1/LIKE AUX
BAK1	ASSOCIATED RECEPTOR KINASE 1
BES1	BRI1-EMS-SUPPRESSOR 1
BIN2	BRASSINOSTEROID-INSENSITIVE 2
BKI	BRI1 KINASE INHIBITOR 1
BRI1	BRASSINOSTEROID-INSENSITIVE 1
BSKs	BR SIGNALING KINASEs
BSU1	BRI1 SUPPRESSOR 1
BZR1	BRASSINAZOLE RESISTANT 1
CDG1	CONSTITUTIVE DIFFERENTIAL GROWTH 1
CHASE	CYCLASE HISTIDINE-KINASE ASSOCIATED SENSORY
CHKs	the CHASE domain-containing histidine kinases
PpCHK	<i>Physcomitrella patens</i> CHASE domain-containing histidine kinases
CKX	cytokinin oxidase/dehydrogenase
COI1	CORONATINE-INSENSITIVE PROTEIN 1
COP/DET/FUS	photomorphogenic/deetiolated/fusca
COP1	CONSTITUTIVE PHOTOMORPHOGENIC 1
CRE1	CK RESPONSE 1
CYP	cytochrome P450 mono-oxygenase
DET1	DE-ETIOLATED 1
ETR1	ETHYLENE RECEPTOR 1
GA2ox	gibberellin 2-oxidase
GA3ox	gibberellin 3-oxidase
GH3	GRETCHEN HAGEN 3
GID1	GIBBERELLIN INSENSITIVE DWARF 1

GID2	GIBBERELLIN INSENSITIVE DWARF 2
HY5	ELONGATED HYPOCOTYL 5
IBR5	INDOLE-3-BUTYRIC ACID RESPONSE5
ICS	isochorismate synthase
IPT	isopentenyl transferase
KAI2	KARRIKIN INSENSITIVE 2
LOG	“lonely guy” gene, phosphoribohydrolase
LOX3	lipoxygenase 3
NCED3	9-cis-epoxycarotenoid dioxygenase 3
NPR	NONEXPRESSER OF PR GENES
OPR3	OPDA reductase 3
Phy	phytochrome
PIF	phytochrome interacting factor
PILS	PIN-LIKES
PIN1-8	PINFORMED 1-8
PP2A	protein phosphatase 2
PP2C	clade A protein phosphatase
PYL	PYR-LIKE
PYR	PYRABACTIN RESISTANT
RCAR	REGULATORY COMPONENT OF ABA RECEPTOR
SAURs	SMALL AUXIN UP RNAs
SCF	SKP, CULLIN, F-box containing complex
SKP1	S-PHASE KINASE-ASSOCIATED PROTEIN 1
SKP2A	S-PHASE KINASE-ASSOCIATED PROTEIN 2A
SLY1	SLEEPY 1
SNF1	SUCROSE NON-FERMENTING 1
SnRKs	Snf1-related protein kinases
SPA	SUPPRESSOR OF PHYA-105
TIR1/AFB	TRANSPORT INHIBITOR RESPONSE 1/AUXIN SIGNALING F-BOX
tRNA-IPT9	tRNA isopentenyl transferase 9
TRP3	MULTIFUNCTIONAL TRYPTOPHAN BIOSYNTHESIS PROTEIN
Type-B ARR	type-B AUTHENTIC RESPONSE REGULATOR
UGT	UDP-glucosyltransferase
WOL	WOODEN LEG
YUCCA	YUC family of flavin monooxygenases

Instrumentation

BEH	ethylene bridged hybrid
CAPV	capillary voltage
CE	collision energy
CSH	charged surface hybrid
CV	cone voltage
ESI	electrospray ionisation
GC	gas chromatography
HESI	heated electrospray ionization
HPLC	high performance liquid chromatography
HRMS	high-resolution mass spectrometry
LC	liquid chromatography
MS	mass spectrometry
MS/MS	tandem mass spectrometry

RPM	rounds per minute
UHPLC	ultra-high performance liquid chromatography

Methodology

ANOVA	analysis of variance
DSPE	dispersive solid-phase extraction
DW	dry weight
FW	fresh weight
HLB	hydrophilic lipophilic balance
IAC	immunoaffinity chromatography
LOD	limit of detection
LOQ	limit of quantification
MCX	mixed-mode cation exchange
MRM	multi reaction monitoring
OPLSDA	orthogonal projections to latent structures discriminant analysis
PCA	principal component analysis
SPE	solid phase extraction

Other

SAR	systemic acquired resistance
ER	endoplasmic reticulum
AM	arbuscular mycorrhiza
RNA	ribonucleic acid
tRNA	transfer ribonucleic acid
UN	unit
PR	pathogenesis-related

1 Introduction

A general definition of a plant hormone is a natural compound in plants with the ability to affect physiological processes at concentrations far below those of nutrients or vitamins (Davies, 2010). Plant hormones, otherwise known as phytohormones, are highly bioactive compounds which are directly responsible for organized plant growth and development including flowering, seed germination, senescence and various stress responses. It is a group of diverse compounds, which can be divided into several structurally different families. Over the last two decades, evidence has emerged suggesting four new classes of substances (brassinosteroids, jasmonates, salicylic acid and most recently strigolactones) acting as signalling molecules with growth-regulating activities.

There are a number of methods and approaches to plant hormone determination, analysis of compounds from one plant hormone family or analysis of a wider range of bioactive compounds from different plant hormone families during specific physiological processes, e.g. stress. There is now increasing interest in obtaining complex information from given biological materials, such as lipidomic analysis, proteomic analysis and metabolomics, in most cases using modern instrumentation based on liquid or gas chromatography combined with mass spectrometry. In a similar way, a comprehensive view on plant hormones including related compounds could provide valuable insight into plant hormone signalling and crosstalk.

The present thesis combines the results of targeted analysis of cytokinins and auxins in various plant materials, some suggesting potential for the application of more versatile and universal analytical methods for simultaneous analysis of biologically active compounds from other phytohormone classes. We have established a generalized liquid chromatography-mass spectrometry based method for such screening including more than one hundred analytes, members of all the main classes of plant hormones: cytokinins, auxins, brassinosteroids, gibberellins, jasmonates, abscisates, strigolactones and salicylates.

2 The main aims and objectives

Plant hormones are highly bioactive compounds usually found in very low concentrations ranging from 10^{-10} – 10^{-15} mol/g fresh weight (FW), depending on the plant tissue, physiological state and environmental conditions. The plant cell wall however complicates the extraction and the matrix contains other compounds (e.g. pigments, oils, lipids, phenolic compounds, saccharides) which interfere with the analysis. Thus precise analysis of phytohormones combines effective sample preparation (extraction and purification) favouring the targeted compounds and more importantly requires highly sensitive and selective instrumentation.

The main objectives elaborated and discussed in this doctoral thesis are as follows:

1. To establish a novel method for simultaneous determination of selected biosynthetic precursors, catabolites and metabolites of six phytohormone classes, including
 - a) optimizing extraction and purification of targeted compounds to a total number more than one hundred,
 - b) the development of a sensitive, accurate and high-throughput method utilizing ultra-high performance liquid chromatography combined with triple quadrupole tandem mass spectrometry (UHPLC-ESI-MS/MS) for simultaneous analysis of these compounds,
 - c) the analytical and biological validations of the newly developed methodology.
2. To miniaturize a method for isolation of *t*RNA-bound CKs and to monitor cytokinin homeostasis in non-vascular plants (algae and cyanobacteria).
3. To apply developed and well-established LC-MS/MS methods for studying phytohormone signalling and crosstalk, such as
 - a) the distribution of auxins and cytokinins in rootless carnivorous aquatic plants,
 - b) the role of abscisic acid and cytokinins during the de-etiolation process,
 - c) the characterization of cytokinin receptors in moss.

3 Literature review

In the following chapters, the main classes of plant hormones involved in this work, structure, biosynthesis/metabolism, signalling, biological functions and crosstalk are briefly introduced. Progress in the field of phytohormone determination in plant material utilizing LC-MS based methods is also reviewed.

3.1 Plant hormones

A general definition of a plant hormone (phytohormone) could be as follows: “An organic substance, other than a nutrient, that in minute amounts modifies a plant physiological process through a specialized signal perception and transduction system (Davies, 2010).

3.1.1 Cytokinins

History

The idea of diffusible factor that positively regulates cell division and cytokinesis was introduced in 1913 by Gottlieb Haberlandt who discovered that phloem exudates from various plants have a stimulating effect on cell division (Haberlandt, 1913). Intensive research of cytokinins began later in the 1940s in the search for proper additives for culture media essential for explant cultivation. Philip White prepared cultivation media with coconut milk, where during cultivation, induction of cell division leading to creation of callus was observed (Caplin and Steward, 1948). This suggested the presence of a highly biologically active compound. The first identified and isolated cytokinin was 6-furfurylamonipurin, known as kinetin, isolated from autoclaved herring sperm (Miller et al., 1955). The presence of kinetin in coconut milk (*Cocos nucifera*) was confirmed relatively recently (Ge et al., 2005). In the following decades, the discovery of kinetin initiated search for similar naturally occurring compounds regulating cell division.

Structure, biosynthesis and metabolism

Natural cytokinins are chemically N^6 -substituted adenine derivatives. According to the structural character of the side chain located on N^6 , this substitution can be either isoprenoid or aromatic (Figure 1). To the isoprenoid CK group belong N^6 -(Δ^2 -isopentenyl)adenine (iP), *cis*- and *trans*-zeatin (*cZ*, *tZ*) with an unsaturated aliphatic side chain and dihydrozeatin (DZ) with saturated aliphatic side chain. The aromatic cytokinins, carry an aromatic ring of either furfuryl origin, e.g. kinetin (K) or benzyl origin, e.g. N^6 -benzylaminopurine (BAP), that can be further substituted (hydroxylated) in *para*, *meta* or *ortho* positions giving rise to compounds known as topolins (*oT*, *mT*, *pT*). Aromatic cytokinins probably share the same biosynthetic pathway with isoprenoid moiety, however, the enzymes responsible for the final transformation and synthesis of *pT*, *mT*, *oT* and BAP remain unknown (Davies, 2010). Furthermore, hydrophobic 2-methylthio cytokinin derivatives (2-MeS CKs) have been found in *tRNA*, adjacent to the anticodon that recognize codons beginning with uracil and they probably affect the proper translation (Persson et al., 1994).

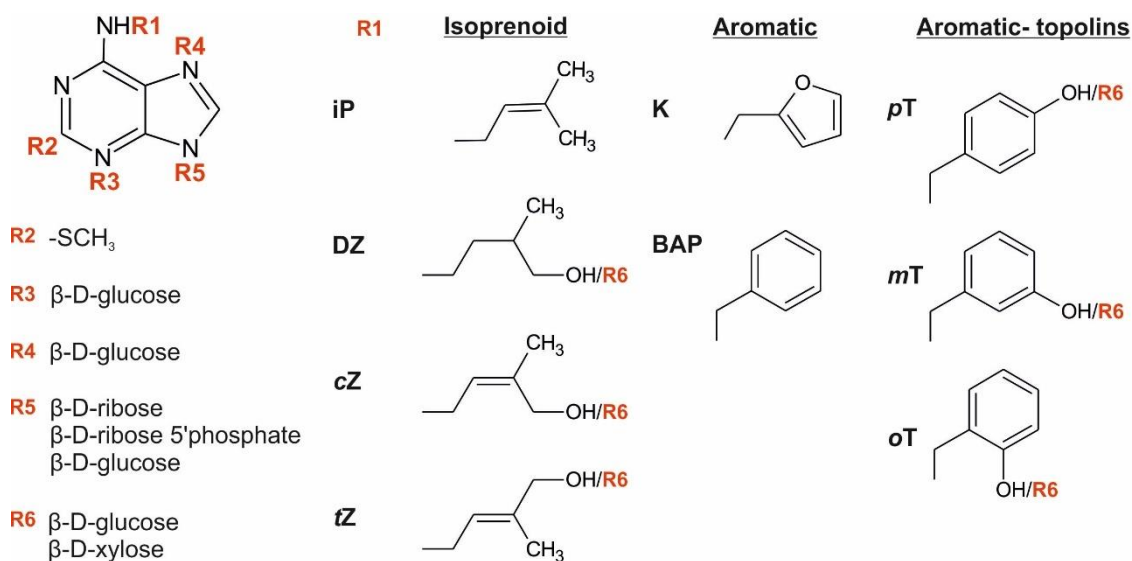


Figure 1. Structure of adenine-type CKs. The R1 characterizes the determinant side chain, R2 to R6 indicate the type of CK conjugation resulting from the metabolic interconversions summarised in Fig. 2. iP, N^6 -(Δ^2 -isopentenyl)adenine; DZ, dihydrozeatin; *tZ*, *trans*-zeatin; *cZ*, *cis*-zeatin; K, kinetin; BAP, N^6 -benzylaminopurine; *mT*, *meta*-topolin; *oT*, *ortho*-topolin; *pT*, *para*-topolin.

The CK metabolic pathway is shown in Figure 2. Shortly, cytokinins are present in active forms – free bases and ribosides (e.g. *tZ*, *tZR*), in the form of their biosynthetic precursors – the corresponding nucleotides (e.g. *tZRMP*), and in conjugated forms (with

sugars or amino acids). In *Arabidopsis*, CK biosynthesis starts with the synthesis of cytokinin mono/di or triphosphates. This process is controlled by nine adenosine phosphate-isopentenyl transferases (IPTs), which are divided into two classes of IPTs: the ATP/ADP-IPT class responsible for biosynthesis of iP and tZ-type CKs, and the tRNA-IPT class, which is responsible for biosynthesis of cZ CKs (Nishiyama et al., 2012). Inactive CK ribotides are further converted to appropriate ribosides and then to bioactive bases. These reactions are carried out by 5'-ribonucleotide phosphohydrolase and adenosine nucleosidase, respectively (Figure 2). More recently, an alternative pathway controlled by CK phosphoribohydrolase 'Lonely guy (LOG)' has been described (review by Spíchal, 2012).

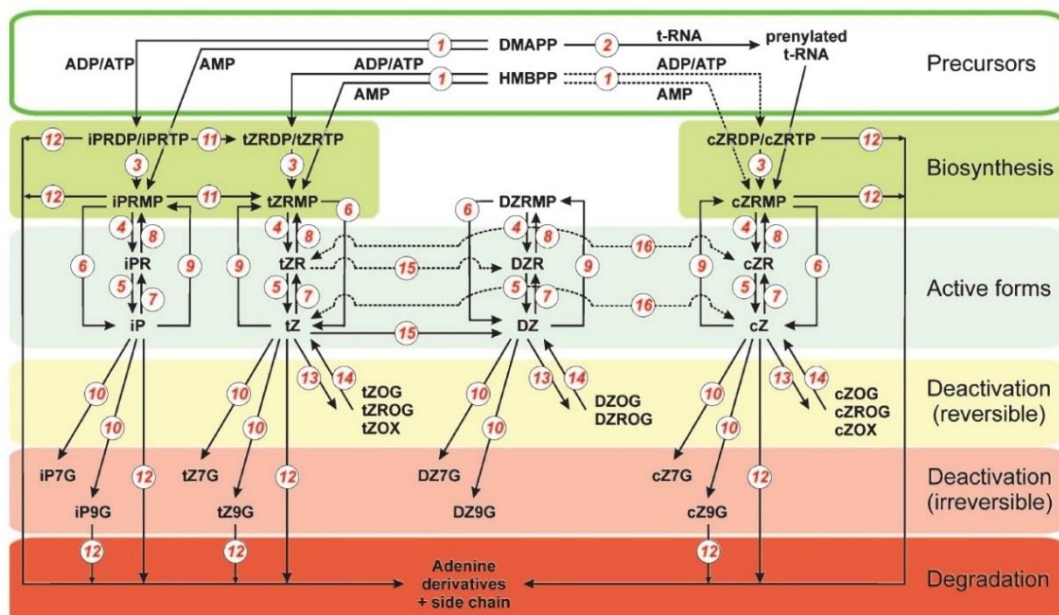


Figure 2. Scheme of cytokinin biosynthesis, interconversions and degradation in plants (from Spíchal, 2012). Enzymes involved in these interconversions are indicated by red numbers. Dashed lines show pathways that have not yet been sufficiently proven. (1) adenylate isopentenyltransferase (EC 2.5.1.27); (2) tRNA-specific isopentenyltransferase (EC2.5.1.8); (3) phosphatase (EC 3.1.3.1); (4) 5'-ribonucleotide phosphohydrolase (EC 3.1.3.5); (5) adenosine nucleosidase (EC 3.2.2.7); (6) CK phosphoribohydrolase „Lonely guy“; (7) purine nucleoside phosphorylase (EC 2.4.2.1); (8) adenosine kinase (EC 2.7.1.20); (9) adenine phosphoribosyltransferase (EC 2.4.2.7); (10) N-glucosyl transferase (EC 2.4.1.118); (11) cytochrome P450 mono-oxygenase; (12) cytokinin oxidase/dehydrogenase (EC 1.5.99.12); (13) zeatin-O-glucosyltransferase, either *trans*-zeatin specific (EC 2.4.1.203) or *cis*-zeatin specific (EC 2.4.1.215), utilising xylose instead of glucose (EC 2.4.2.40); (14) β -glucosidase (EC 3.2.1.21); (15) zeatin reductase (EC 1.3.1.69); (16) zeatin isomerase. *Abbreviations*: DMAPP, dimethylallylpyrophosphate; HMBPP, 4-hydroxy-3- methyl-2-(*E*)-butenyl diphosphate; iPRDP, *N*⁶-isopentenyladenosine-5'-diphosphate; iPRTP, *N*⁶-isopentenyladenosine-5'-triphosphate; iPRMP, *N*⁶-isopentenyladenosine-5'-monophosphate; iPR, *N*⁶-isopentenyladenosine; iP7G, *N*⁶-isopentenyladenine-*N*7-glucoside; iP9G, *N*⁶-isopentenyladenine-*N*9-glucoside, and the equivalents for tZ, DZ and cZ; tZOG, *trans*-zeatin-O-glucoside; tZROG, *trans*-zeatin-O-glucoside riboside and the equivalents for DZ and cZ; tZOX, *trans*-zeatin-O-xyloside; cZOX, *cis*-zeatin-O-xyloside.

The CK conjugates serve either as reversibly inactivated storage forms (*O*-glucosides) or probably as part of a degradation system (*N*7- or *N*9-glucosides) with the exception of *N*3-glucosides, which can be hydrolysed back to corresponding bases by β -glucosidase (EC 3.2.1.21). The precise function of the *N*-glucosyl-derivatives, however, is still unknown (Brzobohatý et al., 1993; Werner et al., 2001; Sakakibara, 2005; Bajguz and Piotrowska, 2009; Spíchal, 2012). Despite the wide range of conjugates, the main player in cytokinin homeostasis is enzyme cytokinin oxidase/dehydrogenase (CKX, EC 1.5.99.12; Frébortová et al., 2004), which catalyzes the degradation of the side chain of cytokinins from *iP*, *cZ* and *tZ* moiety (ribosides, ribotides, *N*-glucosides; Galuszka et al., 2007; Kowalska et al., 2010) to oxidation products (adenine and corresponding aldehydes). *O*-glucosides and DZ-type CKs are resistant to CKX (McGaw and Hobgan, 1985). Aromatic CKs are also known as substrates of this degradation but with much slower rate (Frébortová et al., 2004; Galuszka et al., 2007).

Perception and signalling

As signalling molecules, CKs are active in nanomolar concentrations and their interaction with a specific receptor represents a crucial step leading to conversion of the chemical signal to specific physiological response. A two-component system employed to transduce the cytokinin signal to the target genes consists of a sensory histidine kinase and response regulator (Osugi and Sakakibara, 2015). In *Arabidopsis thaliana*, the cytokinin signal is perceived by three sensor histidine kinases (AHK2, AHK3 and CRE1/AHK4/WOL), five histidine-containing phosphotransfer proteins (AHPs; AHP1–AHP5) and eleven type-B response regulators (type-B ARR; ARR1, ARR2, ARR10–ARR14 and ARR18–ARR21). Recent studies suggest that the AHK receptors are localized in the plasma membrane and the endoplasmic reticulum (ER) (Wulfetange et al., 2011). Moreover, CRE1 (CK RESPONSE 1; Inoue et al., 2001) and WOL (WOODEN LEG; Mähönen et al., 2000) were found to be identical to AHK4 (Yamada et al., 2001; Suzuki et al., 2001). CKs are perceived by a ligand binding region of the receptor called the CHASE domain (CYCLASE HISTIDINE-KINASE ASSOCIATED SENSORY EXTRACELLULAR) that is common among prokaryotes and lower eukaryotes, where it serves as a ligand-binding domain for low molecular weight ligands and small peptides (Mougel and Zhulin, 2001; Von Schwartzberg et al., 2016). The CK signalling pathway is depicted in Figure 3.

CK receptors differ in ligand affinity, and experiments using single, double, and triple mutants, also showed differences in how modulation of signalling through specific receptors affects the plant physiological and morphological responses (Riefler et al., 2006; Werner and Schmülling, 2009 and Wulfetange et al., 2011).

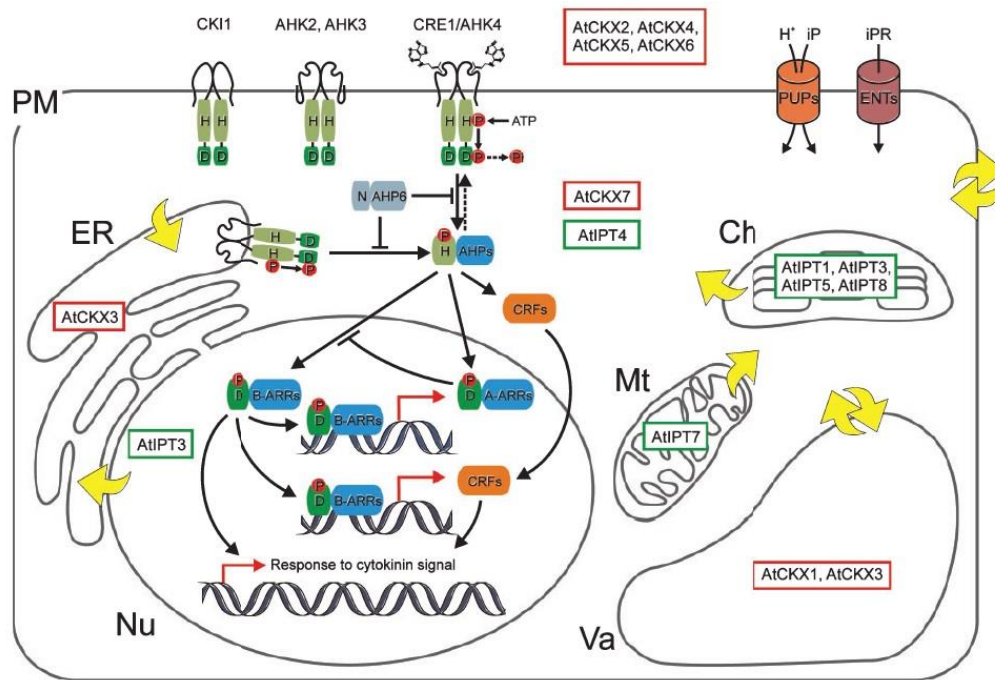


Figure 3. Model of CK signalling and cellular distribution of biosynthetic CKs in *Arabidopsis* (from Spíchal, 2012). CK signalling involves AHK receptors (AHK2, AHK3 and CRE1/AHK4) localized in the plasma membrane and endomembrane of ER. After CK binding, the signal is transduced via phosphorelay through conserved His (H) and Asp (D) residues from AHKs (ARABIDOPSIS HISTIDINE KINASES) to AHPs (ARABIDOPSIS HISTIDINE PHOSPHOTRANSFER PROTEINS) and then to the nuclei localized Type B RESPONSE REGULATORS (RRs) that induce expression of effector genes directly or through CRFs (CYTOKININ RESPONSE FACTORS), or Type A ARR (ARABIDOPSIS RESPONSE REGULATORS) acting as negative feedback regulators. PUPs, PURINE TRANSPORTERS; ENTs, EQUILBRATIVE NUCLEOSIDE TRANSPORTERS; PM, plasmatic membrane; Nu, nucleus; Va, vacuole; Mt, mitochondria; Ch, chloroplast. Biosynthetic AtIPTs (ARABIDOPSIS ISOPENTENYL TRANSFERASES) showed in green rectangles and degradation CKs via AtCKXs (ARABIDOPSIS CYTOKININ OXIDASE/DEHYDROGENASE), in red rectangles.

Biological function

Cytokinins, besides inducing cell division (Skoog and Miller, 1957), have a very wide spectrum of physiological effects. Various experiments, including exogenous application of cytokinins to plants and plant tissues, modulation of endogenous cytokinin content utilizing CK overproducers and mutants with enhanced CKs catabolism, have provided evidence of the physiological roles of cytokinins (Akiyoshi et al., 1984; Barry et al., 1984). These include root growth and root branching

inhibition, delay in senescence, chloroplast maturation and nutrient accumulation, regulation of apical dominance, increased resistance to environmental stresses and initiation of seed development (Richmond and Lang, 1957; Mok, 1994; Riefler et al., 2006; Sakakibara, 2006; Werner and Schmülling, 2009; Spíchal, 2012).

3.1.2 Auxins

History

Auxin was the first discovered plant hormone, observed only as an unspecified chemical signal transported through the plant resulting in plant growth response (Darwin, 1880). This “signal” was later identified as indole-3-acetic acid (IAA), called auxin (Koeogl and Kostermans, 1934; Went and Thimann, 1937).

Structure, biosynthesis and metabolism

After the discovery of IAA, other natural auxins, such as 4-Cl-IAA (4-chloroindole-3-acetic acid) and PAA (phenylacetic acid), were identified in plants. Several synthetic compounds such as α -naphthalene acetic acid (α -NAA) and 2,4-dichlorophenoxyacetic acid (2,4-D) have IAA-like activity and are widely used in horticulture, agriculture, and research (Ljung, 2013). Auxin activity is regulated by a combination of active transport, local biosynthesis, degradation and conjugation (Woodward and Bartel, 2005; Normanly, 2010).

IAA can be synthesized by the L-tryptophan (L-Trp)-dependent pathway which is believed to be the main source of IAA in plants (Mano and Nemoto, 2012), and also through an Trp-independent pathway. In *Arabidopsis*, IAA is synthesized directly from indole-3-glycerol phosphate (IGP) (Ouyang et al., 1999; Wang et al., 2015) though this pathway remains a matter of debate since the cytosolic “indole to auxin” conversion is not elucidated (Nonhebel, 2015). The content of free IAA may be regulated via catabolic oxidation (decarboxylative or non-decarboxylative), or by conjugation with amino acids or sugars (Normanly, 2010; Ljung, 2013) producing either hydrolysable conjugates (e.g. with alanine and leucine – IAA-Ala and IAA-Leu) or non-hydrolysable conjugates (with aspartic and glutamic acids – IAA-Asp and IAA-Glu). These two groups of conjugates are believed to have storage and/or inactive functions (Bajguz and

Piotrowska, 2009). Trp-dependent biosynthesis, together with auxin catabolism and conjugation are shown in Figure 4.

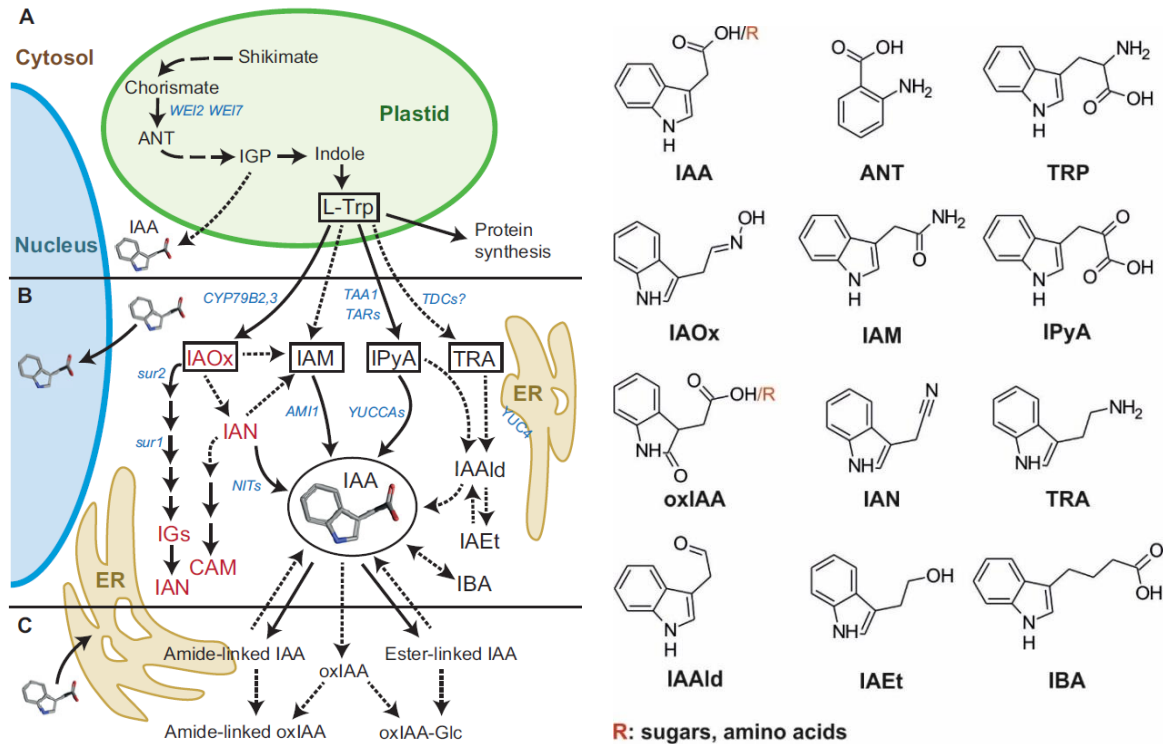


Figure 4. Auxin metabolism in higher plants and chemical structures of involved compounds (adapted from Ljung, 2013). (A) The biosynthesis of IAA precursors, such as IGP and L-Trp, takes place in plastids. L-Trp, the major IAA precursor, is generated via the shikimate pathway. (B) The subsequent L-Trp-dependent IAA biosynthesis pathways are believed to be located in the cytosol. Four putative pathways for L-Trp-dependent IAA biosynthesis in higher plants are shown: the IAOx, IAM, IPyA and TRA pathways. The enzymes known to operate in each pathway are shown in blue. Intermediates that also act as precursors and degradation products of defence compounds (such as IGs and CAM) are in red. (C) Pathways for IAA degradation and conjugation. IAA can be conjugated to amino acids and sugars, or catabolized to form oxIAA. Some IAA conjugates can be regarded as storage forms that can be hydrolysed to form free IAA. Solid arrows indicate pathways in which the enzymes, genes or intermediates are known, and dashed arrows indicate pathways that are not well defined. *Abbreviations:* ANT, anthranilate; CAM, camalexin; Glc, glucose; IAA, indole-3-acetic acid; IAAld, indole-3-acetaldehyde; IAEt, indole-3-ethanol; IAM, indole-3-acetamide; IAN, indole-3-acetonitrile; IAOx, indole-3-acetaldoxime; IBA, indole-3-butyric acid; IGP, indole-3-glycerol phosphate; IGs, indole glucosinolates; IPyA, indole-3-pyruvic acid; L-Trp, L-tryptophan; oxIAA, 2-oxoindole-3-acetic acid; TDCs, tryptophan decarboxylases; TRA, tryptamine; AMI, amidase; CYP79B, cytochrome P450 monooxygenase; NITs, nitrilases; SURs, SUPERROOTS; TAA, tryptophan aminotransferase Arabidopsis; TARs, tryptophan aminotransferases related; TDCs, tryptophan decarboxylases; WEIs, WEAK ETHYLENE INSENSITIVES; YUCCAs, flavin monooxygenases.

Perception and signalling

Intracellular auxin binds to its nuclear receptor from the TRANSPORT INHIBITOR RESPONSE 1/AUXIN SIGNALING F-BOX (TIR1/AFB) family of F-box proteins, which together form the SCF E3-ligase protein complex (Kepinski and Leyser, 2005). Activation of this complex leads to ubiquitination followed by the proteasome-mediated specific degradation of auxin Aux/IAA (AUXIN/INDOLE 3-ACETIC ACID) transcriptional repressors. The auxin response factors (ARFs) then activate auxin-inducible gene expression (Paciorek and Friml, 2006; Ljung, 2013). Roles for TIR1/AFB pathway components in the auxin response are well understood (Figure 5), but additional factors implicated in auxin responses require more study. The function of these factors, including S-Phase Kinase-Associated Protein 2A (SKP2A), SMALL AUXIN UP RNAs (SAURs), INDOLE 3-BUTYRIC ACID RESPONSE5 (IBR5), and AUXIN BINDING PROTEIN1 (ABP1), remain largely obscure (reviewed in Powers and Strader, 2016).

Active transport

Typical for auxin is that many of its actions depend on its differential distribution within plant tissues, where it forms local maxima or gradients between cells. This is possible because of basipetal polar transportation regulated through several influx and efflux mechanisms that include both passive and active processes (Van Berkel et al., 2013; Petrášek and Friml, 2009). The auxin influx is carried out by the AUX1/LAX (AUXIN RESISTANT 1/LIKE AUX) family of transmembrane proton-gradient-driven transporters (Bennett et al., 1996; Swarup et al., 2008). Moreover, the low pH in cell walls causes auxin to become protonated, allowing it to pass through cell membranes relatively easily. Efflux of auxin is managed through a family of PIN (PINFORMED) proteins, hitherto, eight members of the PIN protein family have been isolated in *Arabidopsis* (PIN1-8; Vieten et al., 2007; Zažímalová et al., 2007). They typically have a polar cellular distribution. Thus auxin transport is directed only across those membranes where PINs are localized (Van Berkel et al., 2013). Dynamic changes in subcellular localization of PINs are strongly regulated by auxin itself (Paciorek et al., 2005).

Other proteins playing a role in auxin efflux are plant orthologues of the mammalian ATP-binding cassette subfamily B (ABCB)-type transporters of the

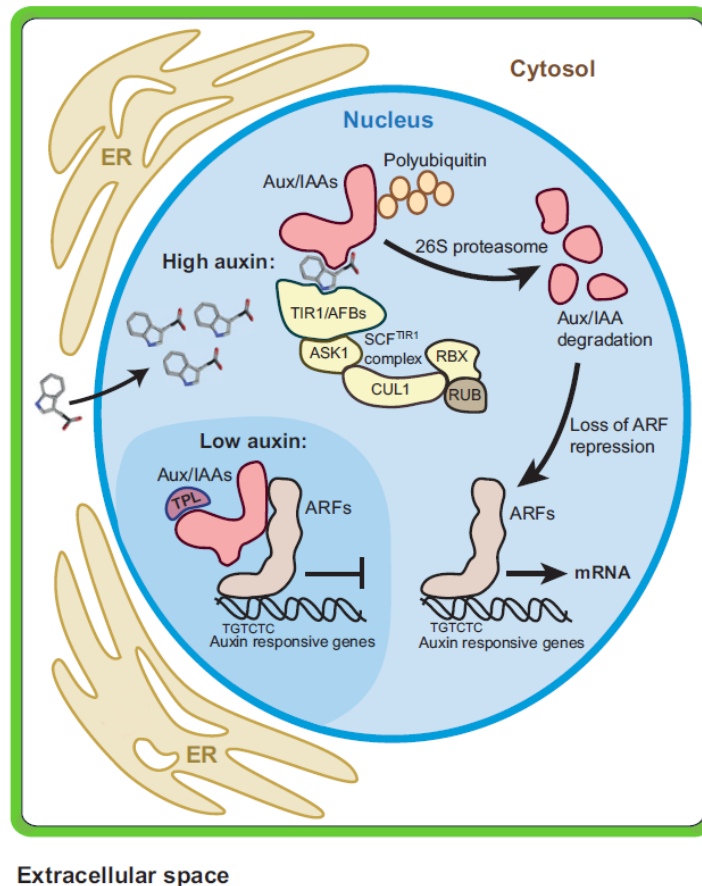


Figure 5. Scheme of auxin perception and signalling (adapted from Ljung, 2013). In the nucleus, IAA binds to its receptors, the TIR1/AFBs, and to the Aux/IAA proteins. TIR1/AFBs are F-box proteins that form part of the SCF^{TIR1} complex, which consists of four subunits – TIR1/AFB, ARABIDOPSIS SKP1 HOMOLOGUE (ASK1), CULLIN 1 (CUL1) and RING-BOX 1 (RBX). An additional protein, RUB, binds to the SCF^{TIR1} complex to regulate its function. The TIR1/AFB and Aux/IAA proteins function as co-receptors for IAA, binding IAA with high affinity. When IAA levels are low (darker blue background), the Aux/IAA proteins form heterodimers with auxin response factors (ARFs) to repress gene transcription. The TOPLESS (TPL) protein functions as a transcriptional co-repressor for Aux/IAAs. However, when IAA levels are high, the binding of IAA to its co-receptors targets the Aux/IAA proteins for degradation by the 26S proteasome, which leads to de-repression of ARF transcriptional regulation and the expression of auxin responsive genes.

multidrug resistance phosphoglycoprotein (ABC/MDR/PGP) family. However, in contrast to PIN proteins, only a subset of ABCBs has been reported to transport auxin (Cho and Cho, 2013; Petrášek and Friml, 2009). More recently, a new group of transport PIN-LIKES proteins (PILS) have been identified, and these are postulated to have a function in IAA transport between the cytosol and the ER (Barbez et al., 2012).

Biological function

Auxin is a hormone vital to a broad range of physiological activities including cell division and differentiation, stem elongation and root development (Perrot-

Rechenmann, 2010), various tropisms, abscission, apical dominance, senescence and flowering (Woodward and Bartel, 2005; Tanaka et al., 2006; Nakamura et al., 2012).

3.1.3 Abscisates

History

Abscisic acid (ABA), also known as abscisin II or dormin, was discovered in the early 1960s when it was found to be involved in the control of seed dormancy and organ abscission (Liu and Carnsdagger, 1961; Ohkuma et al., 1963; Cornforth et al., 1965).

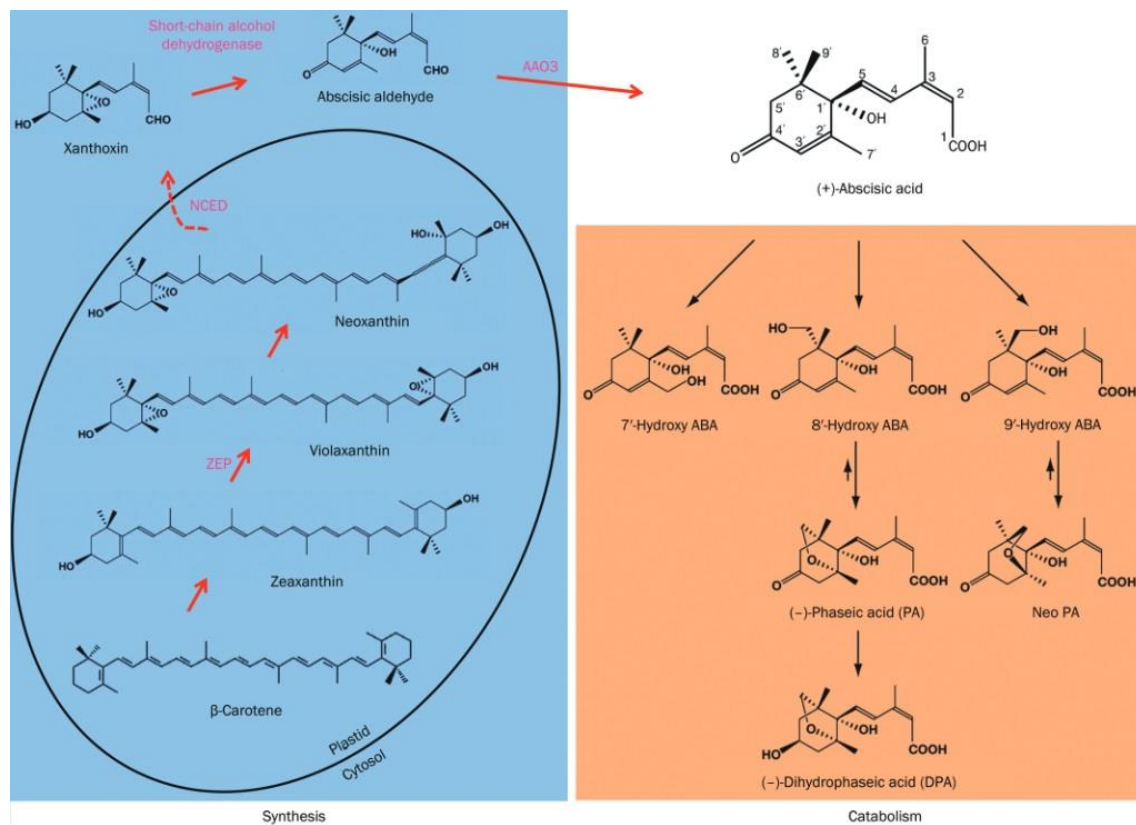


Figure 6. Scheme of ABA biosynthesis and catabolism (from Ng et al., 2014). ABA is derived from C_{40} epoxy-carotenoid precursors through oxidative cleavage reactions that occur in the plastid. The C_{15} intermediate xanthoxin is exported into the cytosol, where it is converted to ABA through a two-step reaction involving an abscisic aldehyde intermediate. The ABA biosynthetic enzymes zeaxanthin epoxidase (ZEP), 9-cis-epoxycarotenoid dioxygenase (NCED), short-chain alcohol dehydrogenase and abscisic aldehyde oxidase (AAO3) are shown in pink. In the right panel, three catabolic pathways involving C-7', C-8', and C-9' hydroxylation are shown. ABA is fully inactivated after the formation of the biologically inactive compound DPA.

Structure, biosynthesis and metabolism

ABA is a C₁₅ isoprenoid plant hormone (sesquiterpene). Its naturally occurring form is S-(+)-ABA with a side chain in the 2-*cis*, 4-*trans* configuration (Addicott et al., 1968). The C₁₅ backbone of ABA is formed after cleavage of C₄₀ carotenoids (zeaxanthin) in the plastidal 2-C-methyl-*D*-erythritol-4-phosphate (MEP) pathway. Endogenous ABA levels are largely controlled by the balance between biosynthesis and catabolism (Figure 6, p. 25). The content of bioactive ABA is regulated by oxidation producing 8'-hydroxy-ABA (8'-OH-ABA), which spontaneously isomerizes to phaseic acid (PA) with following reduction to inactive dihydrophaseic acid (DPA), by the C-9' hydroxylation pathway with the 9'-OH-ABA subsequently cyclised into neophaseic acid (NeoPA), or by a minor oxidation pathway with formation of 7'-hydroxy-ABA (7'-OH-ABA; Zhou et al., 2004). In addition, ABA and its metabolites may be conjugated with glucose, forming corresponding glucose esters (reviewed in Nambara and Marion-Poll, 2005).

Perception and signalling

The best-characterized ABA receptors are a family of soluble proteins known as PYR (PYRABACTIN RESISTANT), PYL (PYR-LIKE) or RCAR (REGULATORY COMPONENT OF ABA RECEPTOR) discovered in 2009 using pyrabactin, a synthetic sulfonamide with physiological effects similar to those of ABA (Park et al., 2009). Sequence comparisons identified 13 related genes, designated PYR-like and PYL1-PYL12. These, show overlapping expression patterns and the ability to form and enhance the stability of a complex with one of the clade A protein phosphatase 2Cs (PP2Cs). This conjunction inactivates the PP2C and releases the inhibition of SNF1-related kinases (SnRKs) required to activate transcription factors, ion channels and numerous other mediators of the ABA response (reviewed in Guo et al., 2011; Finkelstein, 2013). As an example, the scheme of the ABA mediated stress response is shown in Figure 7.

Biological function

ABA's primary function is regulation of seed dormancy, maturation, germination and stomata opening (Patterson, 2001). However, ABA plays an important role in many other physiological processes such as inducing adaptive responses to various abiotic

stresses (Nambara and Marion-Poll, 2005), shoot elongation, root growth maintenance (Sharp and LeNoble, 2002), morphogenesis of submerged plants (Hoffmann-Benning and Kende, 1992; Kuwabara et al., 2003) and skotomorphogenesis (Humplík et al., 2015).

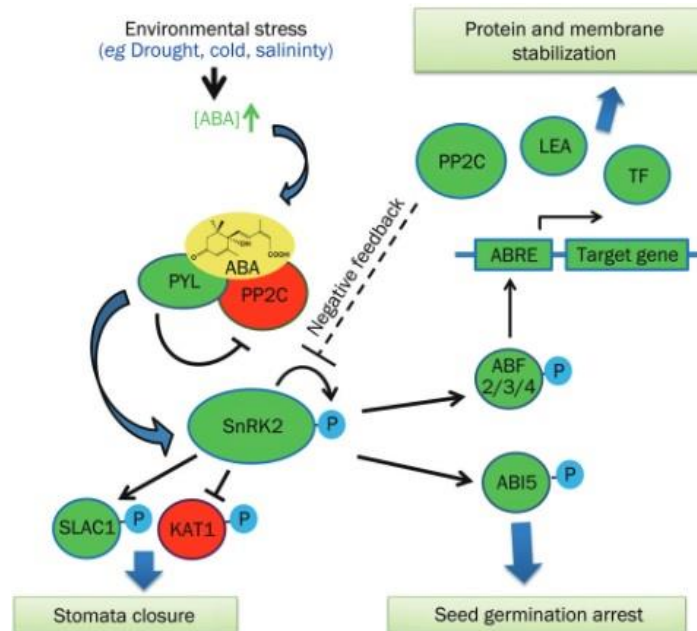


Figure 7. Overview of the ABA-mediated abiotic stress response (from Ng et al., 2014). ABA accumulation, induced by stress signals, activates PYL ABA receptors to inhibit group A PP2Cs. PP2C inhibition in turn allows Snf1-related protein kinases 2 (SnRK2) activation through autophosphorylation. Active SnRK2s mediate the ABA response through the phosphorylation of downstream targets. In guard cells, SnRK2s phosphorylate the slow-type anion channel (SLAC1) and inward-rectifying potassium channel (KAT1), resulting in stomatal closure to prevent transpirational water loss. In seeds, ABI5 (ABA-insensitive) phosphorylation by SnRK2s leads to the inhibition of seedling growth. The phosphorylation of the AREB/ABF (AREB1/ABF2, AREB2/ABF4, and ABF3) transcription factors activates the transcription of target genes such as Late Embryogenesis Abundant (LEA)-class genes as well as transcription factors (TF) involved in stress tolerance. Transcriptional increases in the expression of group A PP2C genes may function as a negative feedback loop in the ABA response pathway by inhibiting SnRK2 activity. Positive regulators of the ABA signalling pathway are shown in green. Negative regulators are shown in red.

3.1.4 Jasmonates

History

Jasmonates (JAs, a group of jasmonic acid, JA, and its related compounds) are metabolites derived from oxolipins. Methyl jasmonate (MeJA) as a floral scent compound was isolated in 1962 from the aromatic oil of *Jasminum grandiflorum* (Demole et al., 1962). However, physiological effects of MeJA and JA were unknown

until the 80's when their senescence promoting and growth inhibition activity in *Vicia faba* was observed (Dathe et al., 1981).

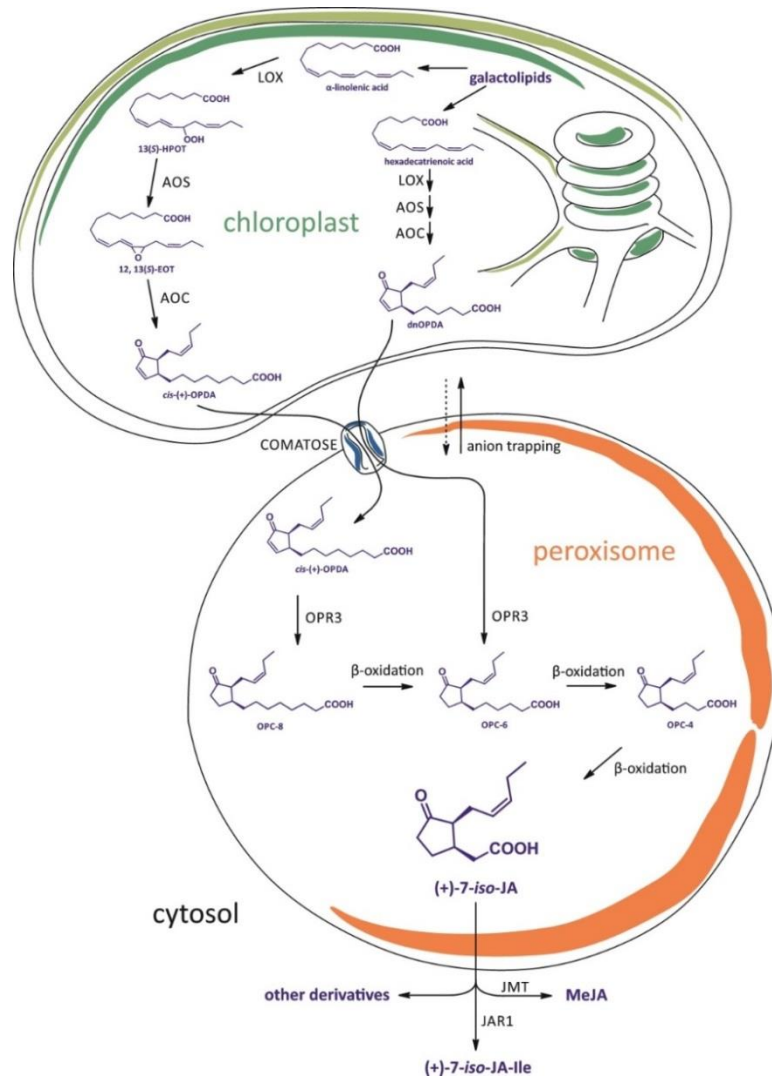


Figure 8. The octadecanoid and hexadecanoid pathway of JAs biosynthesis (the scheme was generously provided by Kristýna Floková, from her PhD thesis, 2014, and modified based on Wasternack and Kombrink, 2010). Upon release of the polyunsaturated fatty acids α -linolenic (18:3) and hexadecatrienoic acid (16:3) – from plastid galactolipids, 13-lipoxygenase (LOX) introduces molecular oxygen to 16 form a corresponding hydroperoxides. 13(*S*)-hydroperoxy-octadecatrienoic acid (13-HPOT) is a substrate of allene oxide synthase (AOS) generating the unstable allene oxide 12,13(*S*)-EOT which is further converted to *cis*-(+)-12-oxo-phytodienoic acid (*cis*-(+)-OPDA) by allene oxide cyclase (AOC). Analogously, dinor-12-oxo-phytodienoic acid (dnOPDA) is generated by the hexadecanoid pathway using the same set of enzymes. Compounds are exported by an unknown mechanism from chloroplasts. Import into peroxisomes is mediated by the ABC transporter COMATOSE (PXA1) and presumable ion trapping. Both OPDAs are reduced by OPDA reductase 3 (OPR3) to OPC-8 and OPC-6, respectively. The carboxylic side chain is shortened by the fatty acid β -oxidation enzymes to the final product (+)-7-*iso*-JA. Subsequent conjugation of (+)-7-*iso*-JA with isoleucine (JAR1) leads to the most bioactive compound (+)-7-*iso*-JA-Ile. Methylation generating the volatile MeJA, and also formation of the other JA derivatives takes place in the cytosol.

Structure, biosynthesis and metabolism

As compounds originating from polyunsaturated fatty acids, JAs are biosynthesized by the allene oxide synthase (AOS), one branch of lipoxygenase (LOX), using α -linolenic acid (18:3) as a substrate and by several subsequent β -oxidation steps producing (+)-7-*iso*-JA which spontaneously epimerizes into more stable *trans* configuration, (-)-JA. Jasmonic acid further undergoes modifications to produce diverse JA derivatives (Yan et al., 2013) The JA precursor, *cis*-(+)-12-oxo-phytodienoic acid (*cis*-(+)-OPDA), the free JA and MeJA, conjugates jasmonyl- *L*-isoleucin (JA-Ile) and jasmonyl-*L*-tryptophan (JA-Trp) are assumed the most active JA forms in plants (Fonseca et al., 2009), see Figure 8 (p. 28).

Perception and signalling

In the case of JAs, the bioactive compound is *L*-isoleucine acid amid of jasmonic acid, (+)-7-*iso*-JA-Ile. As a bioactive compound, it operates through the jasmonate receptor COI1, which is an F-box protein part of the complex Skp1/Cullin/F-box (SCF^{COI1}; Xie et al., 1998; Fonseca et al., 2009). Analogously to auxin, the multisubunit SCF complex serves as E3 ubiquitin ligase and has responsibility for the ubiquitination of target protein and its degradation in 26S proteasome. The F-box protein is a variable subunit bearing substrate specificity (Santner and Estelle, 2010). The mechanism of JA-Ile perception and regulation of gene expression are shown in Figure 9.

Biological function

Jasmonates alone or in combination with other phytohormones, such as SA and ABA, play a crucial role in defensive responses against a wide spectrum of pathogens (Adie et al., 2007; Browse, 2009) as well as to different abiotic stresses (Conconi et al., 1996; Browse, 2005). It has been observed that mechanical wounding or damage caused by herbivore insects result in accumulation of JAs at the site of wounding (Glauser et al., 2008; Floková et al., 2014). Moreover, increase in JA content was observed throughout the whole plant resulting in systemic resistance (Reymond et al., 2004). Due to the volatile character of MeJA, like methyl salicylate (MeSA), it allows this signal to spread to surrounding plants. JAs also play essential roles in development of the male organ of bisexual flowers (Browse, 2009). Today, JAs are regarded as one of the major hormones regulating both plant defence and development. JA, MeJA and JA-Ile are

essential cellular regulators (Staswick & Tiryaki, 2004) involved in various developmental processes, such as seed germination, root growth, fertility, fruit ripening, and senescence (Wasternack and Hause, 2002).

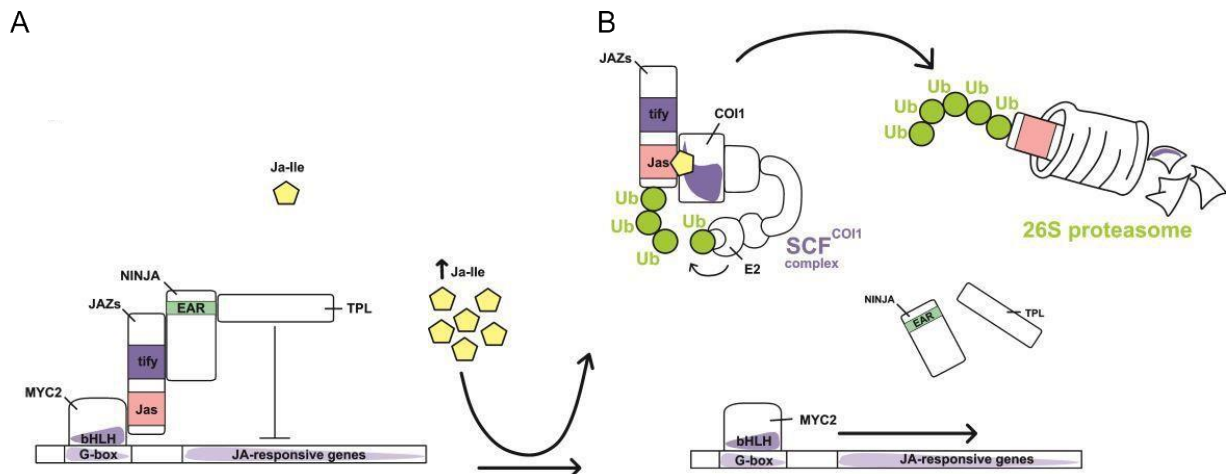


Figure 9. Mechanism of JA-Ile perception and regulation of gene expression (the scheme was provided by Kristýna Floková, from her PhD thesis, 2014, and modified based on Wasternack and Hause, 2013). (A) At the low level of JA-Ile, bHLH (a basic helix-loop-helix) transcriptional factor MYC2 is arrested by interaction with the Jas domain of JAZ (JASMONATE ZIM-DOMAIN) proteins. Repression is stabilized by co-repressor TOPLESS (TPL) bound to the EAR motif of the adaptor protein novel interactor of JAZ (NINJA) that interacts with the tify (ZIM) domain of JAZs. (B) Upon external stimuli (e.g. wounding) or developmental cues, JA biosynthesis is promoted and (+)-7-*iso*-JA-Ile is accumulated. This compound is bound to the active site of the E3 22 ubiquitin ligase of the SCF^{COI1} –JAZ-co-receptor complex. Recognition of (+)-7-*iso*-JA-Ile by the complex enables the interaction of COI1 (CORONATINE INSENSITIVE 1) with JAZ proteins via their Jas domain. The repressor JAZ is polyubiquitinated and subsequently degraded by the 26S proteasome. Release of the transcription factor MYC2 from JAZ-mediated repression leads to activation of JA-responsive gene expression.

3.1.5 Salicylic acid

History

Salicylic acid (2-hydroxybenzoic acid, SA) is a simple phenolic compound. Long before salicylates (group of SA and related compounds) were isolated, identified, and their role in plant hormone signalling recognized, plants containing these compounds were used medicinally in large quantities. In modern medicine its derivative, acetylsalicylic acid, is a commonly used an anti-inflammatory drug, a pain reliever and antiplatelet agent (Pawar et al., 1998). The idea of SA being an endogenous plant signal was first raised in 1974, by analysing different fractions of honeydew collected from aphids feeding on vegetative or flowering *Xanthium strumarium*. Later SA was identified as a phloem

mobile compound capable of inducing flowering in *Lemna gibba* (Cleland and Ajami, 1974; Cleland, 1974).

Structure, biosynthesis and metabolism

In *Arabidopsis*, SA can be synthesized through two metabolic pathways (Figure 10). The synthesis of the major portion of endogenous SA (80%) is regulated by the enzyme isochorismate synthase 1 (ICS; Wildermuth et al., 2001; Garcion et al., 2008), the other pathway is regulated by the enzyme phenylalanine ammonia-lyase (PAL; Chen et al., 2009).

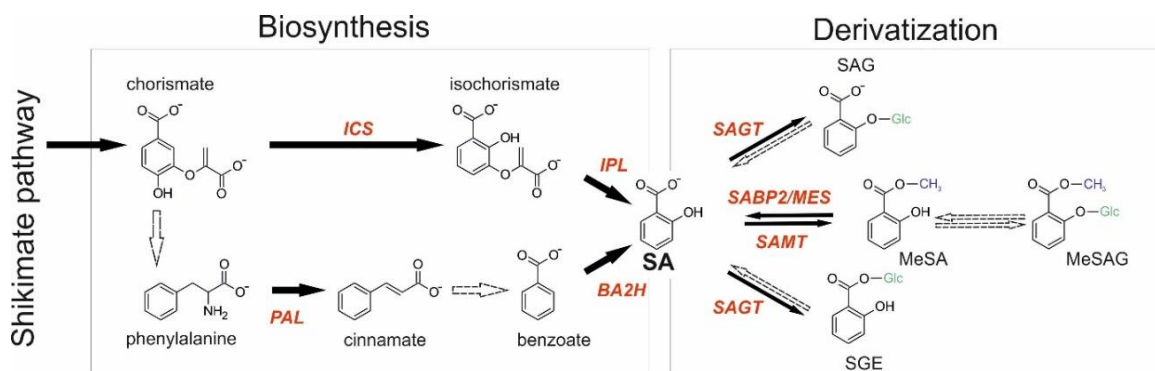


Figure 10. Schematic of SA biosynthetic and derivatization pathways (glycosylation-green and methylation-blue), adapted from Vlot et al., 2009. *Abbreviations:* PAL, phenylalanine ammonia lyase; ICS, isochorismate synthase; IPL, isochorismate pyruvate lyase; BA2H, benzoic acid-2-hydroxylase; SA, salicylic acid; SAGT, SA glucosyltransferase; SAMT, SA methyltransferase; SABP2, SA-binding protein 2; MES, methyl esterase; MeSA, methyl salicylate; MeSAG, methyl salicylate *O*- β -glucoside; SAG, SA-*O*- β -glucoside; SGE, salicyloyl glucose ester.

Perception and signalling

Salicylic acid functions through binding with NPR3 and NPR4 (NONEXPRESSER OF PR GENES, transcription co-activators, homologs to NPR1) which interact with NPR1 and E3-ubiquitin ligase leading to NPR1 degradation. The level of NPR1 determines cell death or survival during pathogen infection (Fu et al., 2012; Kuai et al., 2015). NPR3 and NPR4 have different affinity towards NPR1 and their interaction with it depends on SA level as shown in Figure 11. Although NPR1 plays a major role in SA-mediated transcriptional reprogramming, there are indications of other SA-dependent but NPR1-independent pathways that regulate defence gene expression (An and Mou, 2011).

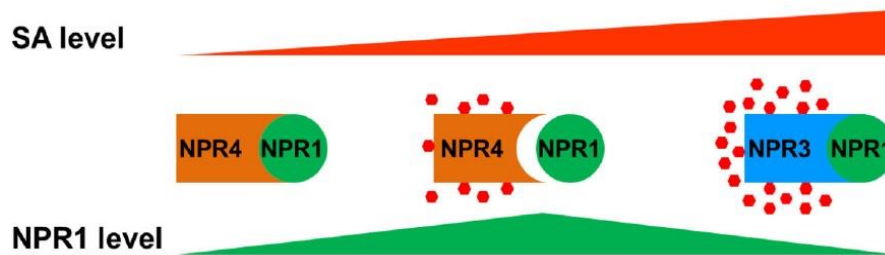


Figure 11. Scheme of SA perception by NPR-dependent manner (from Yan and Dong, 2014). NPR4 is a high affinity SA receptor in unaffected cells - allowing for the continuous ubiquitination and turnover of NPR1 by the proteasome. The NPR3 is a low affinity SA receptor in SAR (Systemic Acquired Resistance) induced cell state. Pathogen infection creates an SA gradient around the infection site and NPR1 suppresses programmed cell death during ETI (Effector Triggered Immunity). In infected tissues, the SA level is high enough to facilitate NPR3 and NPR1 interaction to degrade NPR1, allowing cell death and ETI to occur. In the surrounding tissues, the lower SA level is sufficient to disrupt NPR4-NPR1 interaction but not high enough to mediate NPR3-NPR1 interaction, allowing the accumulation of NPR1 protein, which promotes cell survival and SA-mediated resistance.

Biological function

SA is predominantly active in mediating the plant defence against pathogens by inducing the production of pathogenesis-related proteins (Pieterse and Van Loon, 2004) and by reducing the systemic replication of viruses. Subsequently, SA transportation via phloem also leads to systemic acquired resistance (SAR) in which a pathogenic attack on one part of the plant induces resistance in other non-infected parts (Van Huijsdijnen et al., 1986; Raskin, 1992; Singh et al., 2014). Moreover, by SA conversion to the volatile MeSA, the stress signal can also spread to nearby plants. Besides plant resistance to pathogens, SA also plays a role in other physiological aspects of plant development such as seed germination, seedling establishment, cell growth, respiration, stomatal closure, senescence-associated gene expression, responses to abiotic stresses, basal thermotolerance, nodulation in legumes, and fruit yield (Vlot et al., 2009).

3.1.6 Gibberellins

History

The discovery of the gibberellins originated from an investigation of a soil-borne disease in rice caused by the fungus *Gibberella fujikuroi*. At an early stage of the disease, the leaves and stems of some seedlings elongate more rapidly than those of healthy plants. In 1926, the Japanese scientist Eiichi Kurosawa showed that application of cell-free filtrates from cultures of the fungus *Giberella fujikuroi* on healthy seedlings

led to elongation symptoms characteristic for the disease. In 1938 and 1939, Yabuta and co-workers (Sumiki, Hayashi) succeeded in isolating a crystalline bioactive material from such culture fluids which they named gibberellin A (reviewed in Grove, 1961). Currently there are 136 gibberellin structures identified in various organisms (bacteria, fungi, lower and higher plants) with assigned trivial names gibberellin A₁–A₁₃₆, abbreviated as GA₁, GA₃ *etc.* They are numbered in order of their discovery (MacMillan & Takahashi, 1968, Yamaguchi, 2008).

Structure, biosynthesis and metabolism

Gibberellins (GAs) are a large group of diterpenoid carboxylic acids with an either tetracyclic *ent*-gibberellane skeleton (consisting of 20 carbon atoms, *i.e.* C₂₀-GAs) or 20-nor-*ent*-gibberellane skeleton (consisting of only 19 carbon atoms, *i.e.* C₁₉-GAs) – Figure 12. C₂₀-GAs with a carbon atom attached to C10 are considered precursors of C₁₉-GAs (Oh et al., 2007). The C₁₉-GAs include the biologically active forms, which must contain a hydroxyl group on C-3 β , a γ -lactone between C-4 and C-10 and a free carboxyl group on C-6 for optimal binding to the GA receptor GID1 (Shimada et al., 2008) – see below. Interestingly, only a small number of GAs members are biologically active including C₁₉-GAs GA₁, GA₃, GA₄, GA₅, GA₆ and GA₇ while the others are their biosynthetic precursors (*e.g.* GA₁₂, GA₅₃) or deactivation products (*e.g.* GA₈, GA₃₄, GA₅₁). Thus, the concentrations of bioactive GAs are determined by the rates of their synthesis and deactivation (reviewed in Yamaguchi, 2008; Hedden and Thomas, 2012; Figure 12).

In higher plants, GAs are synthesized by the action of terpene cyclases operating in plastids (CPS, KS), cytochrome P450 mono-oxygenases operating in endoplasmic reticulum (KO) and 2-oxoglutarate-dependent dioxygenases localized in the cytosol, respectively (GA20ox, GA13ox, GA3ox and GA2ox; reviewed in Yamaguchi, 2008; Hedden and Thomas, 2012).

Deactivation of GAs is carried out through several mechanisms, the most prevalent being oxidation on C₂ (2 β -hydroxylation), catalysed by GA 2-oxidases (GA2ox). A second mechanism of GAs deactivation would be epoxidation, catalysed by cytochrome P450 mono-oxygenase (CYP714A1/A2; in *Arabidopsis*) converting GAs into their 16 α ,17-epoxides (Zhang et al., 2011). Moreover, GAs could be converted into

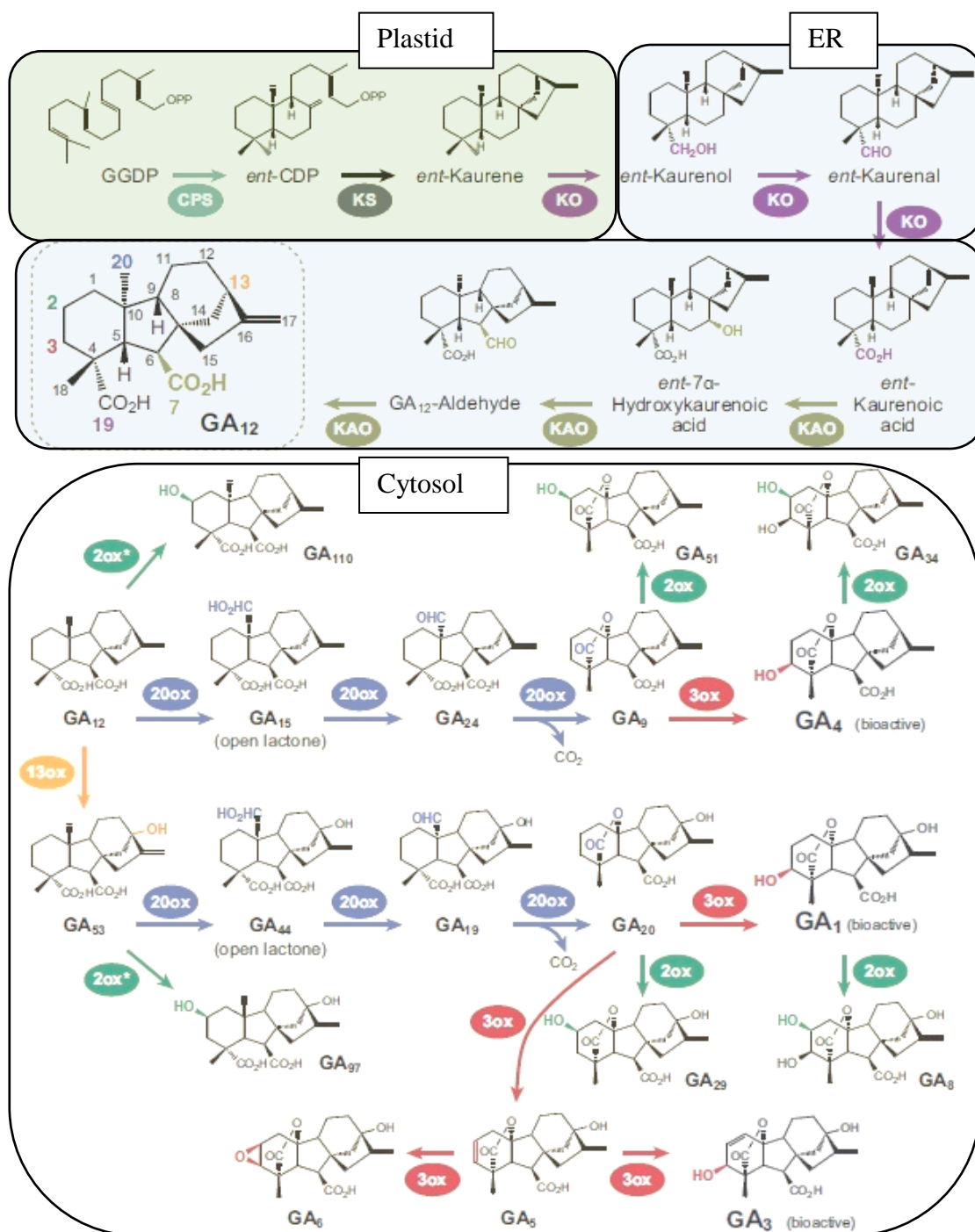


Figure 12. Scheme of gibberellin biosynthesis and structures (adapted from Yamaguchi, 2008). Modifications highlighted in color. GA₇ (13-nonhydroxy GA₃) is biosynthesized from GA₉ in a similar pathway to the synthesis of GA₃ from GA₂₀, but is not shown in this figure. Abbreviations: ER, endoplasmic reticulum; CPS, *ent*-copalyl diphosphate synthase; GGDP, geranylgeranyl diphosphate; KS, *ent*-kaurene synthase; KO, *ent*-kaurene oxidase; KAO, *ent*-kaurenoic acid oxidase; 2ox, GA 2-oxidase (Class I and II); 2ox* GA 2-oxidase (Class III); 3ox, GA 3-oxidase; 13ox, GA 13-oxidase; 20ox, GA 20-oxidase. Epoxidation and conjugation are not shown.

conjugates predominantly with glucose, either through a hydroxyl group to give respective GA-*O*-glucosyl ether or via the 6-carboxyl group to give a GA-glucosyl ester

(Schneider et al., 1992). Although the formation of these GA conjugates may also serve to deactivate GAs, it remains unclear whether GA conjugations play any regulatory role in the control of bioactive GA levels (reviewed by Hedden and Thomas, 2012).

Perception and signalling

Gibberellins are perceived by soluble receptors **GID1** (**GIBBERELLIN INSENSITIVE DWARF 1**), see Figure 13. Bioactive GA binding to **GID1** leads to conformational change enabling **DELLA** (nuclear-localized repressors and transcription factor, Willige et al., 2007) to join in creating the **GA-GID1-DELLA** complex, which promotes **DELLA** interaction with E3 ubiquitin **SCF^{SLY1/GID2}** ligase; **SLY1** (**SLEEPY 1**) and **GID2** (**GIBBERELLIN INSENSITIVE DWARF 2**) are F-box proteins in *Arabidopsis* and *Oryza sativa*, respectively. This **DELLA - E3 ubiquitin SCF^{SLY1/GID2}** ligase interaction leads to **DELLA** degradation via the 26S proteasome pathway. **DELLA** degradation activates the transcription factors or regulators, previously inactivated by **DELLA**, which promotes or represses the expression of targeted genes. Moreover, without the presence of **SCF^{SLY1/GID2}**, the formation of **GA-GID1-DELLA** complex by itself inhibits the transactivation activity of **DELLA**. In short, the GA signal promotes plant growth by overcoming **DELLA**-mediated growth restraint (Davière and Achard, 2013).

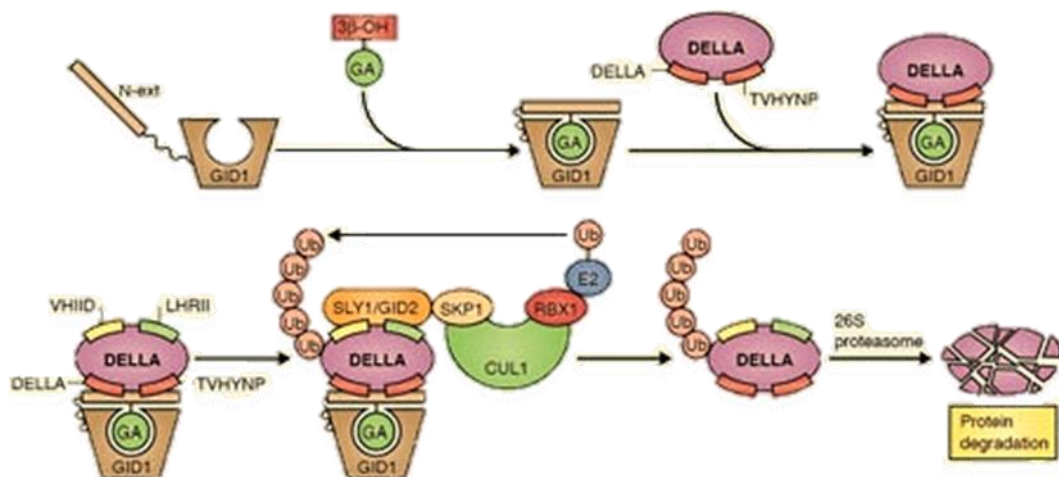


Figure 13. Scheme of GA signalling (from Davière and Achard, 2013). Formation of **GA-GID1-DELLA** complex with subsequent **DELLA** interaction with E3 ubiquitin ligase **SCF^{SLY1/GID2}**, followed by **DELLA** polyubiquitination, and ultimately **DELLA** degradation.

Biological function

Biologically active GAs control diverse aspects of plant growth and development such as seed germination and development, stem elongation, leaf expansion, transition from juvenile to adult phases, flowering, sex determination, pollen development, fruit set and parthenocarpy (Taiz and Zeiger, 2010; Yamaguchi, 2008).

3.1.7 Brassinosteroids

History

Brassinosteroids are a relatively young group of compounds with determined hormonal function in plants (Caño-Delgado et al., 2004). The first brassinosteroid was discovered in 1979 (Grove et al., 1979). It was isolated after extraction and purification of 227 kg of bee-collected *Brassica napus* pollen, while only 4 mg of pure material was obtained and further identified using X-ray analysis as a compound with a steroidal lactone. The results showed that the new compound was a steroidal lactone and the name was given after its source brassinolide (BL; figure 14). To date, there are over 70 isolated and characterised compounds structurally related to brassinolide forming members of the plant hormone group called brassinosteroids (BRs; Choe, 2010).

Structure, biosynthesis and metabolism

BRs are triterpenoid polyhydroxylated substances, while their common structural feature is a C₂₇-membered 5 α -cholestane skeleton (Figure 14). Other compounds of the BR group differ from BL by variations at C-2 and C-3 in the A ring; the presence of a lactone, ketone, or de-oxo function at C-6 in the B ring; the stereochemistry of the hydroxyl groups in the side chain, and the presence or absence of a methyl (methylene) or ethyl (ethylene) group at C-24 forming C₂₈ and C₂₉ BRs, respectively (Clouse, 2011; Tarkowská et al., 2016).

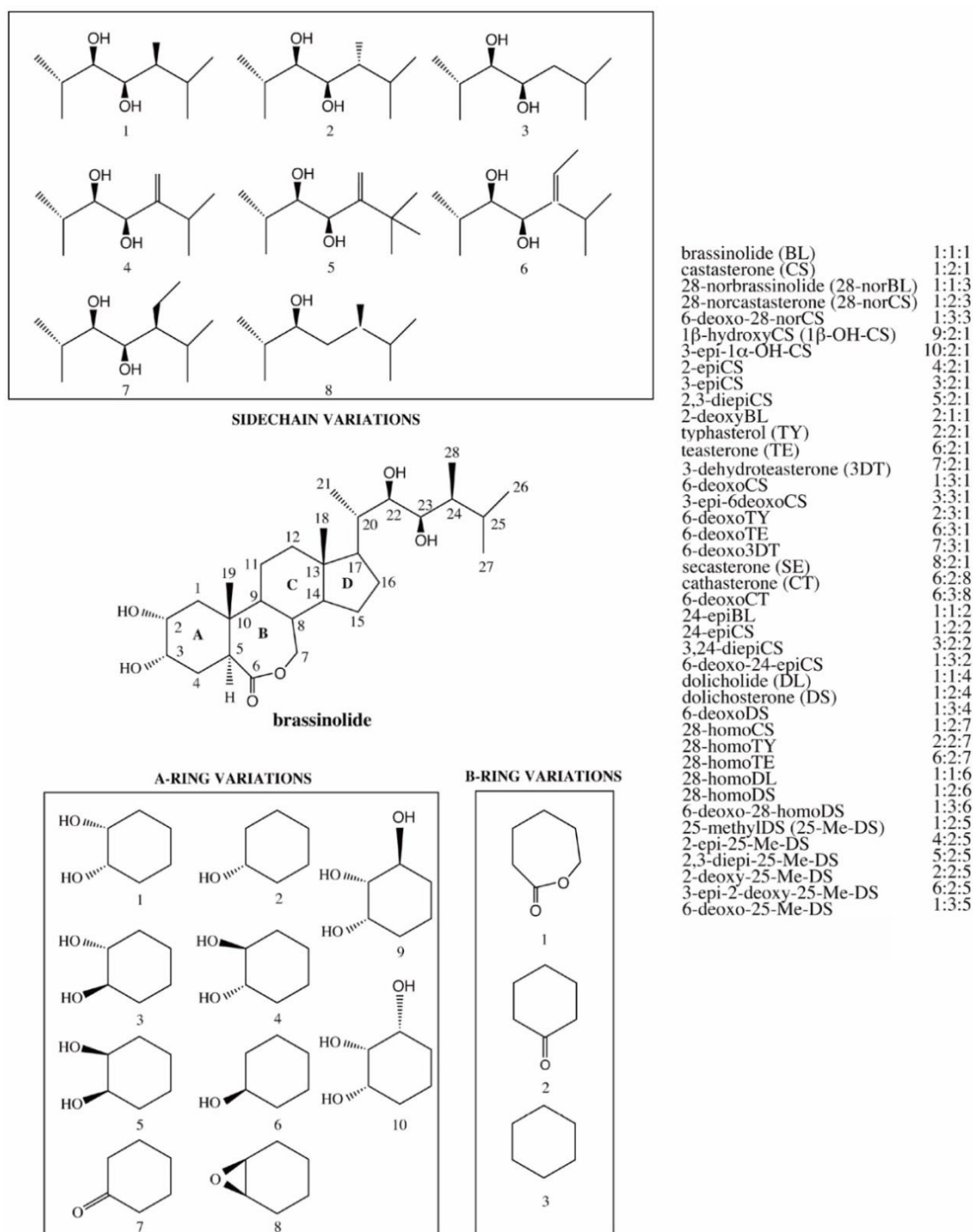


Figure 14. Structure of naturally occurring brassinosteroids (from Clouse, 2011). The structure of brassinolide is presented with possible variations in the A and B rings and the side chain shown in boxes. Compounds to the right have been identified in plants and the numbers represent structures of A-Ring: B-Ring: Side Chain. The C and D rings remain the same for all compounds.

BRs are synthesized from campesterol (C_{28}), sitosterol (C_{29}) and cholesterol (C_{27}). The main biosynthetic precursor of BRs is campesterol, which is first converted to campestanol and then via a series of oxidation reactions finally to bioactive castasteron

(CS) using either the so called *early* or *late C-6 oxidation pathway*. The final step in BRs biosynthesis is the formation of BL from CS. The levels of bioactive BRs are regulated by negative feedback loop, activating BRs response genes via BRs signal perception and transduction in cells leads to repression of BRs biosynthetic genes (see Figure 15). There are several mechanisms by which BL is inactivated, including epimerization, oxidation, hydroxylation, sulphonation and conjugation to glucose (Chung and Choe, 2013; Taiz and Zeiger, 2010). Moreover, BRs can conjugate with a variety of fatty acids such as lauric acid and myristic acid (Bajguz, 2011). Teasterone 3-laurate and teasterone 3-myristate were identified in lily pollen. Studies of endogenous BRs levels during pollen development suggested that conjugated teasterone may serve as a storage form which releases teasterone during pollen maturation with subsequent biosynthesis of BL (reviewed in Clouse, 2011).

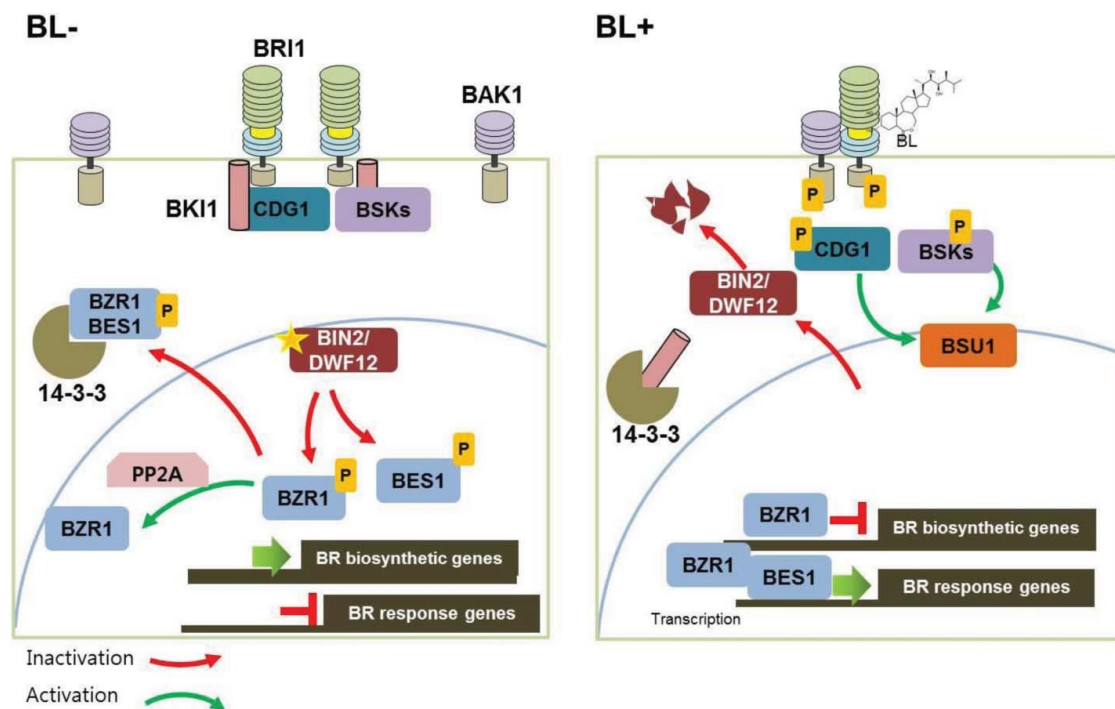


Figure 15. The scheme of brassinosteroid signalling pathway (from Chung and Choe, 2013). In the absence and presence of BL (BL-, BL+). The activation of BRs signalling pathway results in inhibition of BR biosynthetic gene transcription, thus, providing negative regulatory feedback loop.

Perception and signalling

BR signalling starts with the binding of bioactive BRs, *e.g.*, brassinolide, to an *island domain* of a plasma membrane-localized receptor kinase, BRI1 (BRASSINOSTEROID-INSENSITIVE 1; Wang et al., 2001b). Followed by auto- and transphosphorylation

events between BRI1 and its co-receptor BRI1-Associated-Kinase1 (BAK1), the plasma membrane-localized inhibitor (BKI) disassociates from BRI1, which results in subsequent release of BR-Signalling Kinases (BSKs) and Constitutive Differential Growth 1 (CDG1) originally anchored in the plasma membrane. They further transmit the BR signal by activating a protein phosphatase, BRI1 suppressor 1 (BSU1). BSU1 dephosphorylates BIN2 (BRASSINOSTEROID INSENSITIVE 2), the dephosphorylated BIN2 is inactive and is degraded by the 26S proteasome. BIN2 is a component with kinase activity that negatively regulates BR signalling by phosphorylating BR-specific transcription factors BZR1 and BES1, leaving them inactive, and forcing them out of the nucleus into the cytoplasm where they are retained by 14-3-3 proteins. However, in the presence of BRs, BIN2 is degraded and BZR1 and BES1 transcriptionally regulate their target genes. The reactivation of phosphorylated BZR1 is mediated by dephosphorylation through PP2A-type protein phosphatases (Cheon et al., 2013; Chung and Choe, 2013).

Biological function

The endogenous levels of BRs are extremely low even compared to those of other plant hormones (fg-pg/g FW). BRs are most abundant in reproductive tissues, such as pollen, flowers and immature seeds, but their levels are extremely low in vegetative tissues (Tarkowská et al., 2014). BRs regulate the expression of numerous genes, affect the activity of complex metabolic pathways and participate with other plant hormones in a broad spectrum of physiological actions; such as increase in tolerance towards stress caused by temperature, water, or salinity. They also contribute to the regulation of cell division, differentiation and flowering (Fujioka and Sakurai, 1997; Sakurai, 1999; Khripach et al., 2000; Sasse, 2003).

3.1.8 Other plant growth regulators and phytohormones

To provide a more comprehensive overview, other plant hormones and plant growth regulators are briefly reviewed in this sub-chapter below.

Ethylene

The gaseous hormone ethylene regulates many aspects of plant growth and development. It is perceived by a family of high-affinity receptors typified by the ETR1 protein of *Arabidopsis* (Bleecker et al., 1998). It is formed essentially in all cells but often most abundantly in fruits and wounded tissues. Ethylene regulates many aspects of the plant life cycle, including seed germination, root initiation, flower development, fruit ripening, senescence, and responses to biotic and abiotic stresses. It thus plays a key role in responses to the environment that have a direct bearing on a plant's fitness for adaptation and reproduction (Lin et al., 2009).

Strigolactones

Strigolactones (SLs) are the most recently described class of plant hormones. They are terpenoid lactones derived from carotenoids, plant secondary metabolites, originally identified as an allelochemical involved in plant host-parasite interactions (Xie et al., 2010). As environmental signals, SLs induce hyphal branching of AM (arbuscular mycorrhizal) fungi and germination of parasitic plants in *Striga* and *Orobancha* species. SLs are also used by host plants as endogenous hormones for inhibiting shoot branching and mediating light transduction, where light is perceived in aerial part of the host plants and then, through mobile factor (X), stimulates strigolactone production in roots (Tsuchiya and McCourt, 2012). To date, more than 20 compounds in this group of sesquiterpene lactones have been identified from root exudates of various plant species. The most well-known SLs are strigol and orobanchol (Xie et al., 2010).

Karrikins

Karrikins are a family of compounds produced by wildfires that can stimulate the germination of dormant seeds of plants from numerous families. Seed plants could have 'discovered' karrikins during fire-prone times in the Cretaceous period when flowering plants were evolving rapidly. Recent research suggests that karrikins mimic an unidentified endogenous compound that has roles in seed germination and early plant development. The endogenous signalling compound is presumably not only similar to karrikins, but also to the related, above mentioned, strigolactones. The first karrikin discovered was KAR1, also known as karrikinolide. Since karrikins can be produced by burning sugars such as xylose, the pyran ring of karrikins is probably derived from such

pyranose sugars. Both karrikins and strigolactone hormones such as strigol have a butenolide ring (Flematti et al., 2015). Moreover, karrikins are perceived by paralog to strigolactone receptor (DWARF14, Yao et al., 2016), the KAI2 (KARRIKIN INSENSITIVE 2; Bythell-Douglas et al., 2013; Waters et al., 2014).

Polyamines

Polyamines are plant growth regulators, amines with aliphatic linear structure, which are biosynthesized from amino acids. They act as antioxidant agents, delaying senescence, neutralizing acidic compounds and have a role in membrane stabilization. Typical members are spermidine, spermine, putrescine and cadaverine (Galston and Sawhney, 1990).

3.2 Phytohormone crosstalk

The activity of every plant hormone is determined by its availability which is controlled at the level of its biosynthesis and metabolism, transportation, distribution and efficiency in signal perception and transduction. From foregoing chapters that provide a brief overview of phytohormones, it is self-evident that multiple hormones are often involved in particular physiological processes; this is referred to as *hormone crosstalk*. Simply put, it is a process in which different hormone signalling pathway interact. The outcome of the activated response is therefore influenced by the composition and kinetics of the hormonal blend at the site of action.

Crosstalk mechanisms can be classified into three categories based on the level of their interaction. In primary (direct) crosstalk, phytohormonal pathways converge on the same target and regulate or control the expression of a common gene or modulate the activity of the same protein. Secondary (indirect) crosstalk is where one hormone modulates the perception, sensitivity or component availability of another hormone. A third category of hormone interaction is co-regulation, when two or more hormones contribute to regulation of the same physiological process but their action is mediated through independent pathways (Vanstraelen and Benková, 2012; Tvorogova et al., 2013).

This complex signalling network provides powerful regulatory potential to flexibly control the plant's adaptive response to a vast variety of physiological and/or environmental cues. Therefore, how different hormones cooperatively regulate these growth and developmental aspects of plant life is an important question. Several developmental aspects of plant growth, such as physiological polarity, skotomorphogenesis and salt stress, are discussed in this thesis.

3.2.1 Physiological polarity

Physiological polarity is an observable asymmetry in plant morphology (the shape and direction of plant growth). The major impact of this phenomenon is on apical dominance, organ maturation, senescence and abscission, all regulated through complex plant hormone signalling pathways.

An example of such polarity on a cellular level is auxin transport, where the AUX/LAX influx carriers pump auxin into cells and the PIN family of efflux carriers pump auxin out of cells. The coordinated PIN protein polarisation within the tissue, together with other transport components form the auxin transport network, mediate local auxin distribution and trigger different cellular responses during developmental processes such as embryogenesis, organogenesis, leaf venation and axial bud outgrowth inhibition (Paciorek and Friml, 2006; Petrášek and Friml, 2009; Nakamura et al., 2012). Auxin biosynthesis occurs in both aerial portions of the plant and in roots; thus, the auxin required for root development could come from either source, or both (Ljung et al., 2005).

Cytokinins also have a major role in apical dominance and the overall polar development of a plant. As mentioned above, their accumulation in tissue delays senescence, induces chloroplast maturation and has a key function in nutrient accumulation. Cytokinins are mainly produced in root tissues and transported from the root to the shoot via the xylem. However, during active growth periods, cytokinins are synthesized in both root and shoot meristems. Long-distance transport can be envisaged in the case of roots only, whereas cytokinins produced in shoot meristem is distributed to the tissue lying close to the site of production (Davies, 2010).

In many cases, auxin's effect on cytokinins is antagonistic, as is nicely illustrated in the crosstalk of these two hormones during tissue regeneration, root stem-cell specification, and lateral root formation. On the other hand, auxin and cytokinin

have also been found to act synergistically, for example, in the shoot apical meristem (reviewed in Schaller et al., 2015; Zürcher and Müller, 2016).

3.2.2 Skotomorphogenesis to photomorphogenesis transition (de-etiolation)

Light is one of the most important factors influencing plant growth and development. One light-regulated process is de-etiolation; the switch from dark-induced growth, skotomorphogenesis, to photomorphogenesis. Skotomorphogenesis is a developmental process characterized by rapid elongation of the hypocotyl, closed cotyledons and a hook at the upper part of the hypocotyl, protecting the apical shoot meristem from any damage during growth through the soil. It should be noted that this process fully relies on limited seed reserves. As soon as the seedling emerges from the soil and perceives light, it switches to photomorphogenesis. This process is marked by a number of dramatic phenotypic changes, such as a significant reduction in the rate of shoot elongation, opening of the apical hook, expansion of true leaves and the development of mature chloroplasts, ensuring the autotrophy of the developing young plant (Josse and Halliday, 2008; Arsovski et al., 2012; Humplík et al., 2015).

On a molecular level, skotomorphogenesis is achieved by the active repression of the genes that would lead to de-etiolation and photomorphogenic development. The process is regulated by the constitutive photomorphogenic/deetiolated/fusca (COP/DET/FUS) genes and seven basic helix-loop-helix loci encoding phytochrome interacting factors (PIF1, PIF3-8; Leivar et al., 2008). PIF1 directly interacts with the COP1 (CONSTITUTIVE PHOTOMORPHOGENIC 1) and SPA (SUPPRESSOR OF PHYA-105) complex and acts as a cofactor of COP1-SPA E3 ubiquitin ligase complex to synergistically degrade the positively acting factor HY5 (ELONGATED HYPOCOTYL 5) to repress photomorphogenesis in the dark (Ang et al., 1998; Zhu et al., 2015). Moreover, DET1 (DE-ETIOLATED 1) positively regulates PIF protein levels primarily by their stabilization and synergistically represses photomorphogenesis in the dark. The nuclear localized PIF1 homodimers bind to the promoter region of light-regulated target genes and repress their expression to prevent photomorphogenesis (Dong et al., 2014; Zhu et al., 2015).

The light signals triggering the transition from skoto- to photomorphogenesis are perceived by sensory photoreceptors. Members of the phytochrome (phy) family (phyA through phyE in *Arabidopsis*) which mediate the responses to red and far-red

wavelengths (Rockwell et al., 2006). Light perception results in a proportional decrease in the nuclear abundance of COP1, thus allowing the accumulation of HY5 leading to photomorphogenesis (Osterlund et al., 2000). The light-activated forms of phytochromes directly interact with PIFs and induce their rapid phosphorylation, binding to the $CUL4^{COP1-SPA}$ complex and subsequent PIF1 ubiquitylation. The destruction of the negative regulator, PIF1, depresses the light-regulated gene expression and thereby promotes photomorphogenesis.

De-etiolation is very complex developmental process, while its main initiator is light, the following developmental processes (e.g. cell elongation, chloroplast maturation) are regulated by plant hormones which act as transducers of the light signal. A number of plant hormones have been implicated in the regulation of morphological changes during de-etiolation, including GAs, IAA, ABA, CKs, BRs and ethylene (reviewed by Symons and Reid, 2003).

3.2.3 Salinity stress

Salinity is a major abiotic stress factor that limits crop production. High salinity affects plants in two main ways: high concentrations of salt in the soil disturb the capacity of roots to extract water, and high concentrations of salt within the plant itself can be toxic, resulting in an inhibition of many physiological and biochemical processes such as nutrient uptake and assimilation (Munns et al., 1995; Hasegawa et al., 2000; Munns, 2002; Munns and Tester, 2008). Together, these effects reduce plant growth, development and survival. Comprehensive study on what is salinity stress and how the exposure to high salinity affects the plant development can be found in Carillo et al., (2011).

Phytohormones are thought to be the most important endogenous substances that are critical in modulating physiological responses that eventually lead to adaptation to salinity. In recent years, there have been several reviews published describing the vital role of hormones in mediating diverse physiological and biochemical processes by which the plant survives salt stress conditions (Javid et al., 2011; Fahad et al., 2015; Ryu and Cho, 2015). Abscisic acid is often regarded as the main stress hormone. ABA and its rapid and significant accumulation under salinity stress is pivotal to plant protective mechanisms (Shakirova et al., 2010). It acts as an endogenous messenger regulating plant's water status, through guard cells; it can limit transpiration and

resulting water loss by regulating stomatal closure (Wilkinson and Davies, 2010). Plant hormone auxin plays an essential role in plant growth and development. It contributes to vascular tissue development, cell elongation, organogenesis and apical dominance by formation of auxin maxima (Lau et al., 2008). It was observed that high salt stress greatly remodelled root architecture by altering auxin accumulation. This suggests that changes in redistribution of auxin maxima are correlated with reduced growth observed under salinity stress (Petersson et al., 2009; Wang et al., 2009). Reductions of cytokinin and gibberellin levels contribute to limited growth under salt stress conditions. Indeed exogenously applied cytokinins and gibberellins have been reported to alleviate the adverse effect of salinity stress on plant water relations and water use efficiency. By the exogenous application of CKs or GAs, they reverse leaf and fruit abscission that are induced by ABA or water stress. This treatment results in enhanced source potential and redistribution of photosynthates thus increasing sink strength in treated tissues which support further growth (Khan et al., 2007; Yamaguchi, 2008; Iqbal et al., 2014). CKs and GAs are generally considered to be ABA antagonists in several developmental processes including stomatal opening (Blackman and Davies, 1984) and seed germination (Gonai et al., 2004; Thomas, 1992).

It is apparent that although an individual hormone may play a predominant role in a particular physiological process, the final response is the result of complex coordination of multiple overlapping signalling pathways that include stress recognizing sensor proteins, signal transducers, transcription factors and stress responsive genes and metabolites (Zhu, 2002). The phytohormone metabolome thus reflects the environmental conditions.

3.3 Plant hormone analysis

3.3.1 Extraction

The first step in sample preparation for hormone analysis is extraction; dissolution and transfer of the analytes from the solid material into a liquid form of sample. This is also the first step where choice of proper extraction solvent can significantly reduce sample complexity while maintaining high extraction efficiency of desired compounds. The crude plant extract composition is mainly dependent on the chemical properties of extraction solvent; it may contain large quantities of substances that will interfere with subsequent LC-MS analyses (e.g., pigments, proteins, carbohydrates or lipids). Organic solvents, such as methanol (MeOH), ethanol (EtOH), acetonitrile (ACN), isopropanol (IPA), chloroform (CHCl₃) and their combination, are primarily used due to the greater solubility of the organic analytes in such solvents. However, increasing the organic portion in the solvent mixture also readily increases the extraction of above-mentioned interfering compounds. On the other hand, in an aqueous environment, the chemical degradation and/or enzyme activation leading to metabolic changes, such as conjugate hydrolysis, may occur. Therefore, extraction must be performed at low temperatures. Reduction of extraction time to a minimum and the use of antioxidants are also recommended (Ernsten et al., 1986; Novák et al., 2014).

Herein, the overview of recently used extraction solvents for the respective plant hormone analysis is listed below:

- **Cytokinins:** modified Bielecki buffer MeOH/H₂O/formic acid (FA) (15:4:1, v/v/v) in Dobrev and Kamínek (2002) ice-cold EtOH/H₂O (7:3, v/v) in Novák et al. (2008); Bielecki buffer MeOH/CHCl₃/FA/H₂O (12:5:2:1, v/v/v/v) in Svačinová et al. (2012); ice-cold MeOH/H₂O (1:9, v/v) in Plačková et al. (2017).
- **Auxins:** 65% isopropanol and 35% 0.2 M imidazole (pH 7.0) in Liu X. et al. (2012); cold phosphate buffer (50mM; pH 7.0) containing 0.02% sodium diethyldithiocarbamate (antioxidant) in (Pěňčík et al., 2009; Novák et al., 2012).
- **Abscisates:** MeOH/H₂O (4:1, v/v) in Gómez-Cadenas et al. (2002); modified Bielecki buffer MeOH/H₂O/FA (15:4:1, v/v/v) in Dobrev and Kamínek (2002);

MeOH/H₂O/AcA (10:89:1, v/v/v) in Turečková et al. (2009); ice-cold MeOH/H₂O (1:9, v/v) in Floková et al. (2014).

- **Gibberellins:** ACN/H₂O/FA (16:3:1, v/v/v) in Urbanová et al. (2013); MeOH/H₂O/FA (75:20:5, v/v/v) in Li et al., (2016).
- **Brassinosteroids:** ACN/H₂O (6:4, v/v) in Tarkowská et al. (2016); cold 100% ACN in Deng et al. (2016).
- **Jasmonates (stress-induced hormones):** cold 100% MeOH in Balcke et al. (2012); ice-cold MeOH/H₂O (1:9, v/v) in Floková et al. (2014).
- **Hormonomics (a multi-phytohormone profiling):** IPA/acetic acid (AcA) (99:1, v/v) in Chiwocha et al. (2003); IPA/H₂O/HCl (2:1:0.002, v/v/v) in Pan et al. (2008); modified Bielecki buffer MeOH/H₂O/FA (15:4:1, v/v/v) in Kojima et al. (2009), Van Meulebroek et al. (2012) and Schäfer et al. (2016); ice cold MeOH/H₂O/FA (15:10:5, v/v/v) in Drábková et al. (2015); MeOH/H₂O (4:1, v/v) in Cao et al. (2016); ACN/H₂O (4:1, v/v) in Cai et al. (2016).

3.3.2 Purification

All phytohormones are small organic molecules with diverse chemical properties and abundance levels. Their analysis in various materials is further complicated by different matrix composition of tissues. Optimized sample purification is important for the highest sensitivity possible in mass spectrometric analysis. By removing undesired compounds such as salts, pigments, polysaccharides, lipids and proteins from the sample we reduce the background noise during the analysis and also remove possible co-eluting agents. Moreover, less complex and analyte-enriched samples are friendlier towards the high sensitive instrumentation (MS source spotting, LC system clogging).

Consequently, many new sample preparation techniques have been published over the past decade, such as batch immunoaffinity chromatography (Hauserová et al., 2005; Hradecká et al., 2007; Novák et al., 2008), in-tip solid-phase extraction (SPE) (Deng et al., 2016; Liu et al., 2012a; Svačinová et al., 2012), magnetic solid-phase extraction (Cai et al., 2014, 2015; Ding et al., 2014; Liu et al., 2012b; Zhang et al., 2010; Zhang et al., 2016), molecularly imprinted monolithic solid-phase extraction (Du et al., 2012), boronate affinity polymer monolith micro extraction (Ding et al., 2013) hydrophilic solid-phase extraction (Cai et al., 2013), or mixed-mode SPE combining

reverse phase with sorbent of ion-exchange properties (Dobrev and Kamínek, 2002; Urbanová et al., 2013).

3.3.3 LC-MS Analysis

The most used analytical methods for phytohormone determination utilize liquid chromatography (LC) or gas chromatography (GC) separation combined with mass spectrometer, with the main advantages being sensitivity and versatility. Most plant hormones are non-volatile and thus require derivatization steps prior to GC. This leaves the LC approach as more suitable for this application. Moreover, with no need for high temperature, the LC is friendlier towards less stable compounds. A number of analytical methods for determination of a single compound or specific class have been described (López-Carbonell and Jáuregui, 2005; Novák et al., 2008, 2012; Pěňčík et al., 2009; Turečková et al., 2009; Tarkowski et al., 2010; Urbanová et al., 2013, Tarkovská et al., 2016). However, the increasing interest in multiple hormone screenings and the availability of the advancing technology calls for method development for simultaneous analysis of phytohormones and related compounds involved in metabolism and signalling from multiple classes. Ideally, a method capable of providing general qualitative overview as well as precise information about concentration levels of targeted compounds. Considering the complexity of plant cell matrix where minor phytohormones are present in the background of more abundant primary and secondary metabolites, the chemical stability and structural diversity of phytohormones, the method requires a combination of proper sample preparation and high instrument performance (robustness and sensitivity).

Multi-phytohormone profiling was first successfully applied in a study on lettuce seed dormancy (Chiwocha et al., 2003) where in 50-100 mg dry weight (DW) material, using Sep-Pak C18 column for sample purification, four CKs and 10 acidic plant hormones (IAA, five abscisates and four GAs) were determined utilizing high-performance liquid chromatography (HPLC) combined with electrospray ionization tandem mass spectrometry (ESI-MS/MS) in total, sample to sample, 40 minutes long run. Pan et al. (2008) presented a study utilizing a similar approach (HPLC-ESI-MS/MS), without purification or derivatization. Using 50-100 mg FW *Arabidopsis* material, in crude extract they focused on 17 plant hormones and related compounds in 20 minutes long

analytical run. A complex study on plant hormone profiling across *Bryophytes*, in 100 mg FW material, utilizing mixed-mode cation exchange SPE and two separate LC separation methods have been published (Drábková et al., 2015). In this study, more than 40 compounds were determined using HPLC-ESI-MS/MS. In 2009, Kojima and co-authors developed an UHPLC-ESI-MS/MS based method using derivatization of negatively charged compounds, enabling screening in more sensitive ESI positive mode. They employed automated solid phase extraction for simultaneous analysis of 43 plant hormones in *Oryza sativa*, including cytokinins, auxins, ABA and GAs in 100 mg FW material. Similarly, an HPLC-MS/MS based experiment was carried out by Cao et al. (2016), in 200 mg FW (*Oryza sativa*) material, 43 phytohormones and related compounds were determined utilizing ion exchange SPE for sample purification. Cai et al. (2016) utilized a one-step dispersive solid-phase extraction (DSPE) combined with UHPLC-MS/MS for determination of 54 phytohormones (auxins, ABA, SA, JA, GAs and CKs) from a single rice sample extract in a 52-min long analysis. The heated electrospray ionization (HESI) included in an UHPLC-MS/MS system was also recently used for targeted analysis of more than 100 primary and secondary metabolites (Schäfer et al., 2016). A complex multistep extraction approach combined with ion exchange sample purification and three independent LC-MS runs for determination of targeted compounds were used, including plant hormones and their derivatives. Another UHPLC-ESI-MS/MS method using SPE for sample purification focusing specifically on stress-induced hormones (e.g. JAs, IAA, ABA and SA) in *Arabidopsis* was described (Balcke et al., 2012; Floková et al., 2014). The high-resolution mass spectrometry (HRMS) utilizing the combination of UHPLC-Fourier Transform Orbitrap MS has also been recently applied in the field of plant hormone screening for identification and quantification of a large number of compounds related to plant hormones, in 100 mg FW samples of tomato fruits and leaf tissues. The HRMS-based method was validated for eight compounds (GA₃, ABA, SA, IAA, *tZ*, BAP and 24-*epiBL*) as representatives of major classes of phytohormones (Van Meulebroek et al., 2012). Overall, hyphenated techniques have become the most versatile, rapid, selective and sensitive technique available for identifying and quantifying small molecules. Thus, the combination of LC-MS is replacing all other quantitative approaches in plant hormone analysis.

4 Experimental

All the obtained results are summarized and discussed in this section separately, according to the three main objectives of this doctoral thesis:

1. Development of a novel method for simultaneous determination of all the main classes of plant hormones (Chapter 4.2.1).
2. Miniaturization and application of a *t*RNA-bound CKs isolation method (Chapter 4.2.2).
3. Study of phytohormone signalling and crosstalk (Chapter 4.2.3).

The majority of methods and results are described in detail in publications attached as Supplement I-VI.

4.1 Materials and methods

This section briefly summarizes chemicals used, experimental equipment and methods required to carry out the analyses in the attached publications (**Supplements I–VI**).

4.1.1 Chemicals

- Authentic standards of cytokinins (isoprenoid, aromatic and 2-MeS CKs), auxins, gibberellins, jasmonates, salicylic acid, abscisic acid, phaseic acid, brassinosteroids and their corresponding isotopically labelled analogues were purchased from Olchemim Ltd. (Olomouc, Czech Republic) and Chemiclones (Waterloo, Canada). Dihydrophaseic acid, neophaseic acid, 7-hydroxy-abscisic acid and their corresponding isotopically labelled analogues were provided from the compound library of Laboratory of Growth Regulators (Olomouc, Czech Republic; Turečková, 2009).
- Chromatographic solvents (acetonitrile and methanol) of hyper grade quality, eluent additives (FA and NH₄OH) were obtained from Sigma-Aldrich (St. Louis, MO, USA) and Merck (Darmstadt, Germany). Potassium hydroxide (KOH), sodium and potassium acetate (CH₃COONa, CH₃COOK), sodium bicarbonate (NaHCO₃) and 99.8% EtOH were purchased from Lach-Ner, s.r.o. (Neratovice, Czech Republic).

Deionised (Milli-Q) water prepared by a Simplicity 185 water system (Millipore, Bedford, MA, USA) was used for all aqueous solutions except *t*RNA extraction. For that purpose, we used the DEPC treated nuclease free water (Carl Roth, Germany). Alkaline phosphatase (AP) from *E. coli* was purchased from Sigma-Aldrich (St. Louis, MO, USA).

4.1.2 Plant Materials

- *Arabidopsis thaliana* (ecotype Col-0) was used for the method validation and for the salt stress experiment. Seedlings were grown in petri dishes in standard Murashige and Skoog media, vertically, in a growth chamber under long day conditions at a light intensity of $100 \mu\text{Em}^{-2} \text{ s}^{-1}$ (16 h light, 24°C/8 h dark, 18°C) for 12 days. The plants were then transferred in new media supplemented with 150mM NaCl (8,77g/l) prior autoclaving and seedlings were grown vertically for an additional 48 hours (total 14 days old plants). A control group of seedling was grown the same way and 12-day-old seedlings were transferred as well in standard Murashige and Skoog media. The seedlings were harvested, shoots and roots separated, weighted into micro tubes and immediately frozen in liquid nitrogen. Samples were stored at -80°C until extraction and analysis (Šimura et al., manuscript submitted; **Supplement I**).
- Pre-cultures of microalgae *Scenedesmus obliquus* were cultured in bubble columns of 3.8 cm inner diameter (Kavalierglass, Prague, Czech Republic) at a continuous incident light intensity of $500 \text{ mmol m}^{-2} \text{ s}^{-1}$ PAR at $30 \pm 0.5^\circ\text{C}$ and bubbled with 2 % CO₂ (v/v) in air. The cell density was quantified using a Bürker counting chamber (Hecht-Assistent, Sondheim, Germany); at least 600 cells were counted for each sample. Material for CK analysis was collected during cellular growth phase (0–14 d) by separation from the growth medium using centrifugation (10 000 g, 8 min) and the biomass was freeze-dried (Scanvac CoolSafe 110-4, Fisher Scientific, USA) in a vacuum for 7 h. (Žižková et al., 2017; **Supplement II**).
- *Nostoc* sp. PCC 7120 was obtained from the Pasteur Culture collection of Cyanobacteria (Paris, France). *Nostoc* sp. PCC 7120 was cultivated in 50 mL of nitrogen-free medium BG-110 (Rippka et al., 1971) in a chamber (Sanyo MLR

350H, Osaka, Japan) with 16h light / 8 h dark cycles, at 24°C and a photon flux density of 35 $\mu\text{mol}\cdot\text{m}^{-2}\cdot\text{s}^{-1}$. Humidity was kept at 60%. Fresh BG-110 medium in each flask was inoculated with the stock culture to reach chlorophyll-a concentration of 0.1 $\text{mg}\cdot\text{L}^{-1}$. The cells were harvested after 28 days by centrifugation at 10 000 g for 10 min at 4°C, washed by deionized water and stored at -80°C. Samples were collected every second hour starting 1 h after the beginning of the light period (Frébortová et al., 2017; **Supplement III**).

- Plants of *Aldrovanda vesiculosa* (originating from Poland) were collected from the dystrophic (humic) fen lake Karlštejn in the Třeboň Basin Biosphere Reserve in South Bohemia, Czech Republic, on 26th July 2008. *Utricularia australis* were collected from the dystrophic inlet of the Ruda fishpond in the same region as above on 28th July 2008. Plants were thoroughly washed, deprived of all attached macro organisms, and their branches were removed. The main shoots were separated into four segments (apices, young, medium, old) for phytohormone analyses. Thirty mature turions of *A. vesiculosa*, 6–7 mm long, and 12 mature turions of *U. australis*, 8–11 mm long, were collected from the sites on 15 October 2008. They were washed in tap water and all dead leaves were removed from their surfaces. All separated plant material was stored at -80°C prior lyophilisation (Šimura et al., 2016; **Supplement IV**).
- The etiolated seedlings of *Solanum lycopersicum* L., tomato mutants (*sitiens*) and wild type (cv. *Rheinlands Ruhm*) were used for CK analysis; harvested 4 days after germination. The seeds were soaked in 3% sodium hypochlorite (Bochemie, Czech Republic) for 20 minutes and rinsed extensively with sterile distilled water prior to sowing. The seeds were then sown on the basal Murashige and Skoog medium supplemented with 0.7% (w/v) agar in square Petri dishes (120 x 120 mm). The pH was adjusted to 6.1 with 1.0 MKOH before autoclaving. The Petri dishes were placed vertically in the dark for 3 days at 23°C to induce germination. The collected samples were stored at -80°C and prior to analysis homogenized with a mortar and pestle in liquid nitrogen (Humplík et al., 2015; **Supplement V**).
- The sequenced wild-type *Physcomitrella patens* was grown under the following conditions, 25°C, in white light ($100 \mu\text{E m}^{-2} \text{s}^{-1}$) for a light:dark cycle of 16:8 h. For transformation and cytokinin profiling, liquid cultures were regularly disintegrated

and grown in A'BCD(N)TV medium [0.356 mM Ca(NO₃)₂, 1.01 mM MgSO₄, 1.84 mM KH₂PO₄, 10 mM KNO₃, 0.044 mM FeSO₄ supplemented with Hoagland trace element solution (1 ml l⁻¹) and the vitamins nicotinic acid (8 μM), *p*-aminobenzoic acid (1.8 μM), and thiamine HCl (1.5 μM)]. Liquid cultures of the wild type and the three double mutants (*Δchk1,2*; *Δchk1,3*; *Δchk2,3*) as well as the triple mutant (*Δchk1,2,3*) were grown for 21 d and harvested as described in (Von Schwartzenberg et al., 2007). Three biological replicates were grown separately for the wild type and each mutant line. For CK profiling, samples from each line were lyophilized and subsequently homogenized under liquid nitrogen (Von Schwartzenberg et al., 2016; **Supplement VI**).

4.1.3 Methods of phytohormone isolations

- Sample purification was mainly performed using solid phase extraction sorbents:
 - Oasis[®] HLB (30mg/1 ml) and Oasis[®] MCX (30mg/1 ml) purchased from Waters Co. (Milford, MA, USA),
 - C8 and C18 (Bond Elut, 500 mg/3 ml) obtained from Agilent Technologies, Inc. (Santa Clara, CA, USA).
- The SPE protocol for a simultaneous quantification of different plant hormones and their metabolites is fully described in **Supplement I** and the method development is summarized in Chapter 4.2.1.

Briefly, the *Arabidopsis* material, roots and shoots separately, 20 mg FW/sample was ground into fine powder using liquid nitrogen. After addition of cold extraction solvent (1 ml of ice-cold 50% ACN), a mixture of isotopically labelled internal standards, and 3-mm ceria stabilised zirconium oxide beads (Next Advance Inc., Averill Park, NY, USA), the samples were extracted. Extraction began with homogenization using an MM 301 vibration mill (Retsch GmbH & Co. KG, Haan, Germany) with pre-chilled components at a frequency of 27 Hz for 5 min, followed by sonification for 5 min at 4°C. Samples were extracted during stirring using a benchtop laboratory rotator Stuart SB3 (Bibby Scientific Ltd., Staffordshire, UK) at 4°C, 60 min. The homogenates were subsequently centrifuged and corresponding supernatants were purified on Oasis[®] HLB columns (30mg/1 ml) using the Visiprep[™] Solid Phase Extraction Vacuum Manifold (Supelco[™], Bellefonte, PA,

USA). The SPE sorbent was washed by 1 ml of 100% MeOH and 1 ml of H₂O, and afterwards equilibrated with 1 ml of 50% ACN (v/v). After loading the sample (supernatant), the flow-through fraction was collected into a glass tube (Fisherbrand™) and the SPE column was then rinsed with 1 ml of 30% ACN (v/v). This fraction was collected into the same glass tube as the flow-through fraction. The samples were evaporated to dryness under a gentle stream of nitrogen using a TurboVap® LV evaporation system (Caliper Life Sciences, Hopkinton, MA, USA) and stored in a freezer at -20°C until analysis. Each sample residue was then dissolved in 40 µl of 30% aqueous acetonitrile (v/v), transferred into conical insert equipped vials and analysed by UHPLC-MS/MS method (**Supplement I**).

- In **Supplement II** and **III**, the miniaturized method for tRNA extraction, hydrolysis and dephosphorylation were applied.

The tRNA extraction was carried out in 2 ml microcentrifuge tubes. Lyophilized material 20–40 mg was extracted using 800 µl of 100mM NaCl/10mM tris/HCl buffer (pH=7.5), 800 µl phenol with 100 µl *m*-cresol, and three 3-mm ceria stabilised zirconium oxide beads added to each sample prior to homogenization in a vibration mill (27 Hz, 3 min, 4°C). The samples were sonicated (benchtop ultrasound 5 min at 4°C), incubated using a laboratory rotator for 30 min at 4°C, afterwards left on ice for 10 min, and then centrifuged (15 min, 23 000 g at 0°C). Each supernatant (600 µl of water phase) was transferred into a new microcentrifuge tube, 60 µl of 20% potassium acetate (m/m) and 1.2 ml EtOH were added and samples were left for precipitation overnight at -20°C. After the RNA precipitation, the samples were centrifuged (23 000 g, 30 min, 0°C), pellets were dried, the tRNA portion dissolved over time in 0.5 ml of 3M sodium acetate using a laboratory rotator for 60 min at 4°C and afterwards centrifuged (45 min, 23 000 g at 4°C). The supernatants were transferred into new microcentrifuge tubes and 1 ml of EtOH were added for overnight tRNA precipitation (-20°C). Finally, after centrifugation (45 min, 23 000 g at 4°C), tRNA pellets were dried and dissolved in DEPC treated water. The quantity and purity of extracted tRNA was determined using spectrophotometry by measuring the absorbance at 260/280nm and electrophoresis (Teare et al., 1997; Philipps, 1971, respectively).

The extracted tRNA was then hydrolysed using 2M KOH, each sample was neutralized using 10% HClO₄ (v/v) and the precipitated KClO₄ was removed by

centrifugation. The supernatant was transferred into a new microcentrifuge tube; the pH of the samples was adjusted to approx. 8.0 using a NaHCO₃ buffer (0.42g/10ml) and 0.1M HCl. The nucleotides were dephosphorylated by alkaline phosphatase (AP) from *Escherichia coli* (1 UN, 1h at 37°C and 1h at 40°C). Enzyme was subsequently removed by centrifugation after overnight precipitation in EtOH at -20°C. The supernatants were evaporated to dryness using a SpeedVac concentrator, dissolved in 2 ml of 1M FA and immediately passed through an Oasis[®] MCX column (see below).

- The extraction and purification of cytokinins in algae (**Supplement II**), cyanobacteria (**Supplement III**), tomato (**Supplement V**) and moss (**Supplement VI**), were carried out as follows: each sample was homogenized under liquid nitrogen, extracted in modified Bielecki buffer (MeOH/H₂O/FA, 15/4/1, v/v/v; (Hoyerová et al., 2006) with the stable isotope-labelled internal standards added. After centrifugation (15 min, 23 000 g at 4°C), the supernatant was purified using two solid phase extraction columns, a C18-based column (500 mg of sorbent,) and a mixed-mode Oasis[®] MCX column (30 mg) as described by Dobrev and Kamínek, 2002, with slight modifications.

Briefly, in the first step, all samples were purified by SPE using C18 columns activated with 2 ml of MeOH and modified Bielecki buffer. After loading the supernatants, the flow-through fractions were collected, evaporated to water phase and dissolved in 2 ml of 1M FA. The second step utilized the Oasis[®] MCX cartridges conditioned with 1 ml each of 100% MeOH and H₂O, equilibrated sequentially with 1ml of 50% (v/v) nitric acid, 1 ml of H₂O, and 1 ml of 1M FA. After sample application onto an MCX column, unretained compounds were removed by a wash step using 1 ml of 1M FA and 1 ml 100% MeOH, preconcentrated analytes were eluted by two-step elution using 1 ml of 0.35M NH₄OH aqueous solution and 2 ml of 0.35M NH₄OH in 60% (v/v) MeOH solution. The eluates were then evaporated to dryness *in vacuo* and stored at -20°C until LC-MS/MS analysis.

- For cytokinin analysis in **Supplement IV**, the samples of *A. vesiculosa* and *U. australis* were purified using a combination of a cation (SCX cartridge) exchanger, an anion (DEAE-Sephadex-C18 cartridge) exchanger and immunoaffinity chromatography (IAC) based on monoclonal antibodies specific for a wide range of

cytokinins (Novák et al., 2003). Moreover, IAA and its amide conjugates were analysed by a method described by Pěňčík et al. (2009). The auxins were extracted with phosphate buffer, pre-purified by C8-based solid-phase extraction and further purified by an auxin-specific immunoaffinity extraction. The eluates from the IAC columns were evaporated to dryness, dissolved in the mobile phase and used for quantitative analysis.

4.1.4 Instrumentation and phytohormone detection

- All samples in **Supplements I-VI** were prepared using the following laboratory equipment: MM 301 vibration mill (Retsch GmbH & Co. KG, Haan, Germany), benchtop laboratory rotator Stuart SB3 (Bibby Scientific Ltd., Staffordshire, UK), benchtop ultrasound Transonic 310 (Elma, Germany) Visiprep™ Solid Phase Extraction Vacuum Manifold (Supelco™, Bellefonte, PA, USA), TurboVap® LV evaporation system (Caliper Life Sciences, Hopkinton, MA, USA).
- The hormonomics method development (**Supplement I**) and all quantification experiments (**Supplements II-IV & VI**) were performed using an Acquity UPLC® System (Waters, Milford, MA, USA) coupled to a triple quadrupole mass spectrometer Xevo™ TQ-S MS with electrospray interface (Waters MS Technologies, Manchester, UK). The multi-phytohormone profiling method was also co-developed using Agilent 6490 UHPLC-QqQMSMS (Agilent Technologies, Santa Clara, CA, USA) during stay in UPSC, Umea, Sweden.
- The CKs and auxin determination in aquatic carnivorous plants (**Supplement V**) was performed on an Acquity UPLC™ System coupled with a Quattro Micro API triple quadrupole mass spectrometer (Waters MS Technologies, Manchester, UK).
- Analytes were separated using a reversed phase columns as follows:
 - Acquity UPLC CSH® C18 (150 × 2.1 mm; 1.7 µm; Waters; **Supplement I**),
 - Acquity UPLC BEH® C18 (150 × 2.1 mm, 1.7 µm; Waters; **Supplements II-VI**),
 - Jupiter® C4 (250 × 2.0 mm, 5 µm; Phenomenex, Torrance, CA, USA; **Supplements III-IV**),
 - Symmetry® C18 (150 × 2.1 mm, 5 µm; Waters; **Supplement V**).

- All analytes were determined using an ultra-high performance liquid chromatography-electrospray tandem mass spectrometry (UHPLC-MS/MS) with stable isotope-labelled internal standards as a reference (Pratt, 1986). The analysed compounds and appropriate internal standards were determined in multiple ion monitoring mode (MRM) using these optimized MS conditions. Full details of the hormonomics method are described in **Supplement I**. Cytosolic (so called free) and tRNA-bound isoprenoid cytokinin levels were analysed based on the LC-MS/MS methods published by Novák et al. (2008) and Svačinová et al. (2012). The 2-MeS CKs derivatives were determined according to Tarkowski et al. (2010) and auxin metabolites by method published previously by Pěňčík et al. (2009).
- The instrument control, acquisition and MS data processing was carried out by the MassLynx™ software package (versions 4.0 and 4.1, Waters, Milford, MA, USA; **Supplements I-VI**) and Mass Hunter Qualitative Analysis B.05.00 (Agilent Technologies, Santa Clara, USA).

4.2 Survey of results

4.2.1 Plant hormonomics

The first aim of this doctoral thesis was to provide a fast and sensitive targeted MS-based approach for simultaneous phytohormone profiling comprising all the main classes: cytokinins, auxins, gibberellins, brassinosteroids, abscisates, jasmonates and salicylates. Including bioactive forms, their precursors, catabolites and metabolites, the developed and optimized protocol combines the rapid non-selective extraction and purification with extremely sensitive MS/MS quantification from a milligram amount of plant material. The method is fully described and discussed in **Supplement I** (Šimura *et al.*, submitted June 2017).

Sample extraction and purification

Cold acetonitrile (ACN) was often used in previous phytohormone profiling studies (Urbanová *et al.*, 2013; Tarkowská *et al.*, 2016). To effectively extract hydrophobic phytohormones such as gibberellins or brassinosteroids, we performed experiments with rising organic content in ACN solutions focusing on the solubility of brassinosteroids (the most hydrophobic compounds in this study) and the extractability of plant pigment chlorophylls a (Chl_a) and b (Chl_b). Based on a compromise from these experiments, we selected the optimal extraction solvent as an ice-cold aqueous solution 50% ACN (v/v) providing the highest signal for selected phytohormones and lower chlorophyll yield compared with solvents of higher organic content.

Second, the chemical stability of targeted analytes during the extraction and purification steps was also tested by an experiment using aqueous solutions of 1M FA (pH < 3) and 0.35M NH₄OH (pH > 14) and 50% ACN as controls. After incubation and gentle evaporation under a stream of nitrogen, the samples were analysed by LC-MS/MS and the recovery of each compound was compared to the initial concentration. Several GAs and also amino acid conjugates with JA and IAA showed much lower yields in acidic pH, therefore, the ice-cold 50% ACN with no additives was chosen as an optimal extraction solvent. All subsequent phytohormone analyses were performed using 1 ml of ice cold 50% ACN as the extraction solvent. The scheme and full description of the final sample preparation protocol is shown in **Supplement I**, chapter **Online methods** and **figure I**.

Development of UHPLC-ESI-MS/MS method

The other aim of this project was to develop a rapid, derivatization free MS-based method for quantification of more than 100 phytohormones with often similar core structure, e.g. *cis-/trans-* isomers with the same fragment ions. To obtain an optimal baseline separation of all critical pairs, we tested two reversed-phase UHPLC chromatographic columns Acquity UPLC[®] CSH[™] (Charged Surface Hybrid) and Acquity UPLC[®] BEH shield (Ethylene Bridged Hybrid) with diameters 2.1 × 150 mm and particle size 1.7 μm. The Acquity UPLC[®] CSH[™] column provided a better peak shape and peak-to-peak resolution compared to the Acquity UPLC[®] BEH column (Figure 18B). Using isocratic elution and 0.01% formic acid in both A (water) and B (ACN) mobile phase utilizing the Acquity UPLC[®] CSH[™] column, the baseline separation of all isomers was achieved (**Supplement I, figure 2**).

Retention times for each of 101 plant hormone metabolites were determined and multiple reaction monitoring (MRM) combined with isotope dilution analysis were used for precise quantification. Appropriate precursor to product transitions for each compound were selected, afterwards the optimization of the collision energy (CE), cone voltage (CV) and capillary voltage (CAPV) was carried out in order to achieve the highest signal intensity possible. All values are listed in **Supplement I, supplementary table 3**. Isoprenoid CKs, 2-MeS CKs, auxins, BRs and some JAs (e.g. *cis-(+)-OPDA* and *JA-Ile*) were scanned in positive ESI(+) mode, however, abscisates, GAs, SA and JAs were determined in negative ESI(-) mode. Importantly, all overlapping compounds had the specific precursor to product transitions.

Use of polarity switching for the simultaneous analysis of 101 phytohormones was the main goal of this method development (Figure 16). Unfortunately, to monitor positive and negative ions in one chromatographic run resulted in lowering the sensitivity of negatively charged compounds approximately 3 to 10 times. Therefore, the method was divided according to the ESI mode (positive and negative) and all samples were analysed in two separate injections during 17 and 15 minutes, respectively. For detailed information see **Supplement I, figure 2**.

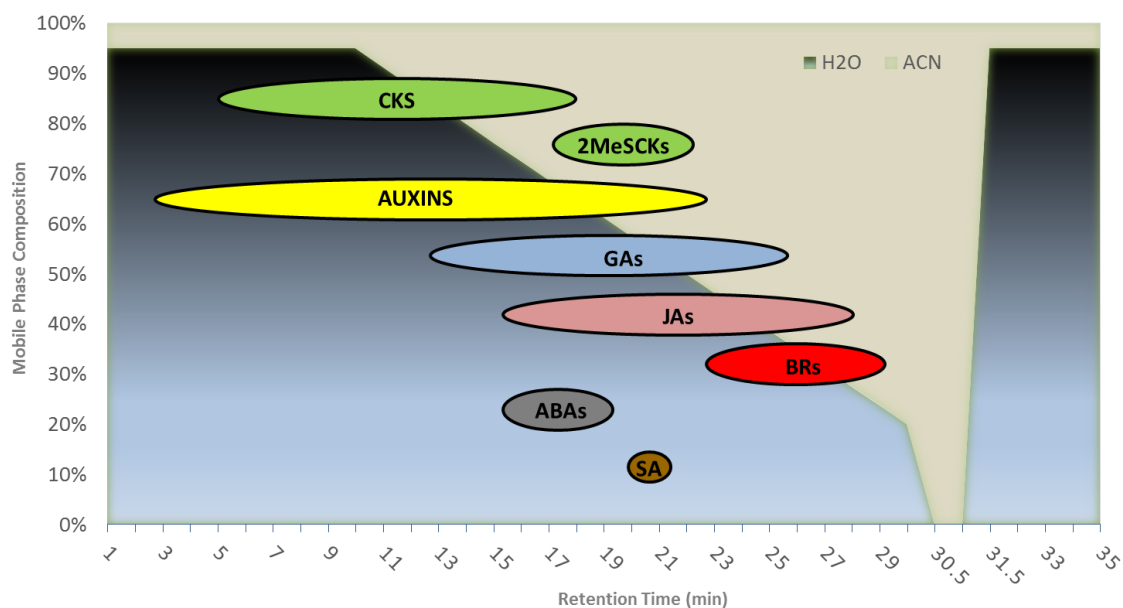


Figure 16. Scheme of LC separation, using the proposed LC-MS/MS method for simultaneous analysis of $[M+H]^+$ and $[M-H]^-$ ions utilizing both MRM and ion polarity switching in one analytical run.

Finally, limits of detection (LOD) and quantification (LOQ) were calculated for each analyte as 3 or 10 times the noise level, respectively. LOD ranged on average from 0.01 fmol for CKs ribosides to 100.5 fmol for *norCS*, full data are included in **Supplement I, supplementary table 2**.

More detailed description of this UHPLC-ESI-MS/MS method is included in **Supplement I**.

Analytical method validation

It is important to emphasize that regardless which analytical technology is applied for final analyte determination, the proper use of isotopically labelled internal standards, their addition to extraction mixture at beginning of the sample preparation, is essential to ensure accurate quantitative results, allowing compensations for losses from the whole sample preparation process and during the MS analysis itself (Ljung et al., 2010).

To evaluate the purification process and validate the developed method, sets of spiked samples were prepared and the recovery of each standard added was then calculated (see **Supplement I**, chapter **Online methods**). For assessment of the method accuracy and precision, the concentration of each analyte was calculated using the standard isotope dilution method (Rittenberg and Foster, 1940). The concentration of each non-labelled standard added into samples was calculated after subtraction of

determined endogenous levels and compared with the known theoretical amounts spiked. The mean precision, expressed as relative standard deviation, was 4.2% and the mean accuracy (expressed as percentage bias) was 1.0%. The mean total extraction yields per phytohormone class ranged from 52 to 97% (**Supplement I, supplementary table 2**).

Biological cross-validation of the hormonomics method

To illustrate the applicability of the newly developed targeted metabolomics approach, the hormonomics analysis was performed on 20 mg FW root and shoot *Arabidopsis thaliana* material grown under salinity stress conditions as described in chapter 4.1 (Materials and methods). The salt stress conditions were determined using GENEVESTIGATOR[®] tool based on predicted alterations in phytohormone levels under salt stress condition.

In total, utilizing the newly developed hormonomics method, 43 members of the main classes of plant hormones were determined and quantified in both root and shoot samples. Using a t-test on root samples, 23 out of 43 the mentioned compounds showed significant changes compared to control groups. In shoot samples, applying the same statistical approach identified 15 compounds with significantly altered concentrations. When multivariate statistics were used for data interpretation, the results showed clear separation between root and shoot samples as well as between control and treated groups where samples were closely grouped together accordingly. OPLSDA based S-plots as well as results from t-test revealed compounds whose levels were strongly affected during salinity stress.

The hormonomics results were further cross-validated with the transcriptomics data (GENEVESTIGATOR[®]) to investigate if the transcript profiles matched the metabolite profiles of plant hormones under salt stress. The following results highlight the importance and value of the hormonomics method as a unique way of examining not only the hormonal transcript levels but their respective deriving metabolites from a single sample.

Experimental design, statistical and Genenvestigatior analysis are described in **Supplement I**.

1) Abscisates

ABA, often referred to as plant stress hormone, is an essential signalling mediator during various developmental processes as well as adaptive responses during abiotic stresses (Zhu, 2002). In vegetative tissues, the concentration of ABA increases up to 40-fold under drought and salt stress (Zeevaart and Creelman, 1988). Indeed, ABA and its oxidation products phaseic acid (PA) and dihydrophaseic acid (DPA) were significantly increased in response to salt stress in whole seedlings.

This observation is in accordance with the elevated transcript levels of both ABA biosynthesis and oxidation genes. Moreover, gene coding 9-cis-epoxycarotenoid dioxygenase (NCED3), the enzyme catalysing the synthesis of the xanthoxin- precursor of abscisic aldehyde, which is a direct precursor to ABA, was up-regulated almost twice as much in roots compared to the shoots. This finding corresponds with the increased ABA levels in treated roots rather than in treated shoots. The overall higher expression of cytochromes (CYP707A1/A3/A4) involved in ABA oxidation under salt stress in roots is also reflected in DPA levels, which were almost 10 times higher in treated root samples than in treated shoot samples.

2) Jasmonates

JA, MeJA and JA-Ile are essential cellular regulators (Staswick and Tiryaki, 2004) involved in various developmental processes, such as seed germination, root growth, fertility, fruit ripening, and senescence (Wasternack and Hause, 2002). Jasmonates also play a role in defence against herbivory and in responses to abiotic stress, such as drought, low temperature and salinity (Wang et al., 2001a; Cheong and Choi, 2003). Large-scale transcriptomic studies have shown that some JA-biosynthesis genes coding AOC1, AOC2, AOS, LOX3 and OPR3 proteins are up regulated in roots under salt stress (Jiang and Deyholos, 2006; Ma et al., 2006; Kilian et al., 2007; Geng et al., 2013) which implies that higher amounts of JA should be expected. This hypothesis was supported in Wang et al., (2001a). Exposure to salinity stress caused significant increase in levels of JA in *Iris hexagona*. However, another study performed on rice cultivars showed that JA concentration does not increase with the higher magnitude of salt stress, but rather the opposite. The salt stress initially led to a sharp increase in the concentrations of JA in 20mM NaCl treatment, but then the concentrations of JA progressively decreased with increasing NaCl levels (Kang et al., 2005). Another report describes no increase in jasmonates after exposure of

barley leaf segments to NaCl (Lehmann et al., 1995). In our study, levels of JA, 9,10-dihydro-JA and *cis*-(+)-OPDA (the JA biosynthetic precursor) were significantly elevated in treated roots, while the concentration of another precursor - dnOPDA (dinor-12-oxo-phytodienoic acid) was significantly lower compared to root control. We suggest that the increased OPR3 expression in roots led to more pronounced exhaustion of the dnOPDA as a substrate for JA biosynthesis, since the OPR3 expression in shoot was not significantly altered and the dnOPDA levels in this tissue showed no substantial change. Interestingly, the concentration of bioactive JA-Ile in treated roots remained unchanged. In treated shoot samples compared to shoot control we observed significantly lower concentration of 9,10-dihydro-JA and JA-Ile, the observed decrease of JA content was not significant. Both determined biosynthetic precursors dnOPDA, *cis*OPDA showed only slightly increased concentrations compared to shoot control samples.

3) Auxins

IAA in plants is synthesized by Trp-dependent and Trp-independent biosynthesis pathways (Figure 4). L-Trp is an amino acid synthesized in chloroplast from chorismate, the final product of the shikimate pathway (Radwanski and Last, 1995). The significant increase in Trp level observed in roots, but not in shoots, is consistent with the transcriptomics data where the gene coding TRP3 (MULTIFUNCTIONAL TRYPTOPHAN BIOSYNTHESIS PROTEIN) was up regulated in roots. In shoots, the *trp3* expression was not altered and Trp levels remained similar in both treated and control shoot samples. The Trp-dependent pathway via flavin monooxygenases family (YUCCAs) is the main auxin biosynthesis pathway in *Arabidopsis thaliana* (Zhao, 2012). Genes involved in the YUCCA-pathway (Figure 23) were downregulated consistently with reduced IAA levels in the stressed seedlings in both shoots and roots. Interestingly, the genes involved in auxin biosynthesis pathway through indole-3-acetamide (IAM) and indole-3-acetonitrile (IAN) were induced predominantly in the root. The corresponding metabolites (IAM and IAN) were significantly increased compared to root control samples, however, the IAA levels in treated roots were still reduced as a response to salt stress. The induction of genes and metabolites of this parallel pathway indicate possible homeostatic mechanism for the reduced IAA levels in roots. The auxin conjugation pathway was also induced in the stressed roots in accordance with respective genes coding GH3 (GRETCHEN

HAGEN 3) and UGT (UDP-glucosyltransferase) upregulation, as a response to salt stress. The main conjugates determined were IAA-Asp, IAA-Glu and IAA-Glycine, where the last two mentioned compounds showed significantly increased levels in roots. In the shoot this upregulation concerned fewer genes and with weaker inductions and thus in accordance there was no significant change in shoot IAA conjugated forms.

4) Cytokinins

In 2011, Nishiyama et al., presented research describing decrease in cytokinin content and down regulation of CKs biosynthetic genes in *Arabidopsis* exposed to salt stress. In 2012, the same authors provided results showing how the altered gene expression profile of the salt-treated *ipt1,3,5,7* mutant significantly overlapped with that of the salt-treated WT, pointing out that the reduction of IPT (isopentenyl transferase) expression promotes salt stress tolerance (Nishiyama et al., 2012). In our experiment, according to transcriptomics data, the *ipt* genes were overall down-regulated under salt stress (besides *ipt9* in roots) implying reduced levels of CK phosphates and further bioactive cytokinins in affected tissues as well. However, in our study we observed significantly higher levels of *cZR* and *iPR* in treated samples (both root and shoot), while changes in *tZR* and *DZR* levels were not significant. This increase in *cZR* and *iPR* levels is in accordance with up-regulated expression of *tRNA-IPT9* (*tRNA*- isopentenyl transferase 9) in roots, while in shoots the *tRNA-IPT9* is downregulated and the increased levels in treated shoot samples is probably due to xylem transport (reviewed by Ryu and Cho, 2015).

In 2010, Atanasova observed an increase in *tRNA*-bound CKs (*iPR* and *cZR*) under salinity stress in *Zea Mays L.* This observation together with the decreased stability of RNA machinery, described among salinity stress effects by other authors (Rauser and Hanson, 1966; Aspinall, 1986; Munns and Termaat, 1986), suggest *tRNA* is a source of these compounds. To support this suggestion, our results also show significantly higher levels of 2-methylthio CK derivatives, 2-MeSiPR and 2-MeScZR, in roots. These compounds are *tRNA* specific components (Björk et al., 1987), thus the *tRNA* degradation with consequent release of *tRNA* bound CKs contributed to increased levels of *cZR* and *iPR* observed in root samples.

In accordance with the literature (Javid et al., 2011; Fahad et al., 2015; Ryu and Cho, 2015), the bioactive *tZ* and *cZ* were indeed found in lower concentrations in

treated root samples compared to root control. However, these changes were not significant. Moreover, the iP was significantly more abundant in root tissue than in the root control group. The iP change in shoot samples was not significant. Overall, the bioactive *tZ* and *cZ* levels in shoot samples were significantly lower to those in root samples. These findings are in accord with the fact that all *LOG* genes were upregulated in the root and not in the shoot.

5) *Gibberellins*

Four gibberellins were determined namely GA₃, GA₄, GA₅ and GA₂₄. The GA₄ and GA₃ are biologically active compounds while GA₂₄ and GA₅ serve as their biosynthetic intermediates, respectively (Yamaguchi, 2008). GA₄ displayed differential response to salt stress between shoots and roots, while GA₄ production was induced in the stressed shoots; it was reduced in the stressed roots. On the transcriptomic level, the GA inactivation (*GA2ox* genes) and precursor biosynthesis (gene for *ent*-kaurene oxidase, KO) were induced in both tissues. The *GA3ox* gene which controls the last biosynthetic step of bioactive GAs, such as GA₄ (Figure 12), was induced in the shoots but down-regulated in the roots, which agrees with the observed metabolite trend. Moreover, significantly decreased levels of GA₂₄ in salt stressed shoot samples point to rapid metabolic change to bioactive GA₄ with increased levels in this tissue compared to the shoot control group.

Taken together, the validation experiments and the calculated accuracy and precision of the newly developed method demonstrate its reliability and usefulness for routine phytohormone analysis using minute amounts of plant tissue. Moreover, cross-validation of the method via analysis of salt stress-induced hormones and genes, in combination with multivariate data analysis, showed that our technique has the potential to provide a deeper level of understanding of how signalling molecules achieve plant stress adaptation mainly through modulations in gene expression.

Graphical interpretations of these results are included in **Supplement I, figure 3 and 4.**

4.2.2 *t*RNA-bound cytokinins

Miniaturized method for tRNA extraction, hydrolysis and dephosphorylation

We developed a miniaturized extraction and purification method for determination of *t*RNA bound cytokinin ribosides and their 2-methylthio derivatives, originally performed according to a protocol described by Maaß and Klämbt (1981) with modifications by Stirk et al. (2012).

Although *t*RNA isolation is well-known and widely used, we have optimized the published method with the aim of designing a cheaper, faster, miniaturized and more high-throughput approach. The optimized protocol is step-by-step described in Chapter 4.1.3. Our method was designed on the micro-scale with the main goal of decreasing both sample and solvent volumes. Compared to Stirk et al. (2012), the application of modified protocol decreased tenfold the amount of plant tissues required per extraction. Moreover, due to the lower amounts of contaminants, it was possible to determine directly *t*RNA levels using spectrophotometry.

The extraction method was further successfully utilized for cytokinin profiling in green algae *Scenedesmus obliquus* and cyanobacteria *Nostoc sp.* (**Supplements II and III**, respectively), following the purification scheme summarized in Figure 17.

Regulation of cytokinin homeostasis in non-vascular organisms (Supplement II)

The main goal of this study was to characterize auxin and CK metabolism in 20 representatives of taxonomically major lineages of cyanobacteria and algae as the ancestors of vascular plants. The phytohormone profile screening showed that endogenous free IAA and its oxidation catabolite were predominantly indole auxin forms. Interestingly, the abundance of free *cZ*-type CKs and the occurrence of 2-MeS CK derivatives pointed to the *t*RNA pathway as a substantial source of CKs.

With the aim of deciphering the regulation of CK homeostasis in non-vascular organisms, *Scenedesmus obliquus* was used as representative green algae of the chlorophyte clade. The endogenous CK (free and *t*RNA-bound) pools were determined during the cellular growth cycle. The total free CK concentration was at least 3-fold higher during exponential and linear growth phases (0-4 d) than in the stationary growth phase (7-14 d); the *cZ* nucleotides, bases and ribosides were the most abundant forms, followed by *iP* type. The importance of the *t*RNA biosynthetic pathway was

subsequently proved by the detection of *t*RNA-bound CKs using a novel miniaturized *t*RNA extraction method. The most abundant metabolites were *c*ZR and *i*PR as well as its 2-methylthio derivatives, 2-MeScZR and 2-MeSiPR. Thus, it can be assumed that *t*RNA degradation is an essential source of CKs, representing a predominant biosynthetic pathway of CKs in evolutionarily older non-vascular organisms, such as cyanobacteria and algae.

For insight into the complexity of phytohormone regulation during 14 d of *Scenedesmus obliquus* cell growth, the auxin metabolite profile was also determined. The correlation between *Scenedesmus obliquus* growth and levels of both CKs and auxins suggest an indispensable role of the two phytohormones in algal cell division, with a complex network of metabolic pathways that apparently differ from those in vascular plants. More information is given in Žižková et al., (2017).

Light influences cytokinin biosynthesis and sensing in Nostoc (Supplement III)

In this work, we have characterized the second IPT present in *Nostoc* sp. PCC 7120 (NoIPT2) as *t*RNA-IPT. In agreement with the observed enzymatic activity, analysis of *t*RNA-bound CKs showed that *t*RNA predominantly contains *i*PRMP, together with *c*ZRMP and their 2-MeS derivatives. In addition, the screening of the gene expression involved in CK biosynthesis in *Nostoc* sp. PCC 7120 showed that cytokinin biosynthesis is activated during the dark period of growth leading to enhanced cytokinin content after the start of light period. Furthermore, cytokinins in conjunction with light affect expression of a number of genes related to signal transduction, including two-component sensor histidine kinases and two-component hybrid sensors and regulators. Domain organization of these *Nostoc* signalling components is very complex and several domains typical for bacterial two-component systems have been identified. From the evolutionary perspective, *Nostoc* and other cyanobacteria may represent an interesting model for studies on the development of cytokinin signalling. The experimental results are presented and discussed in Frébortová et al. (2017).

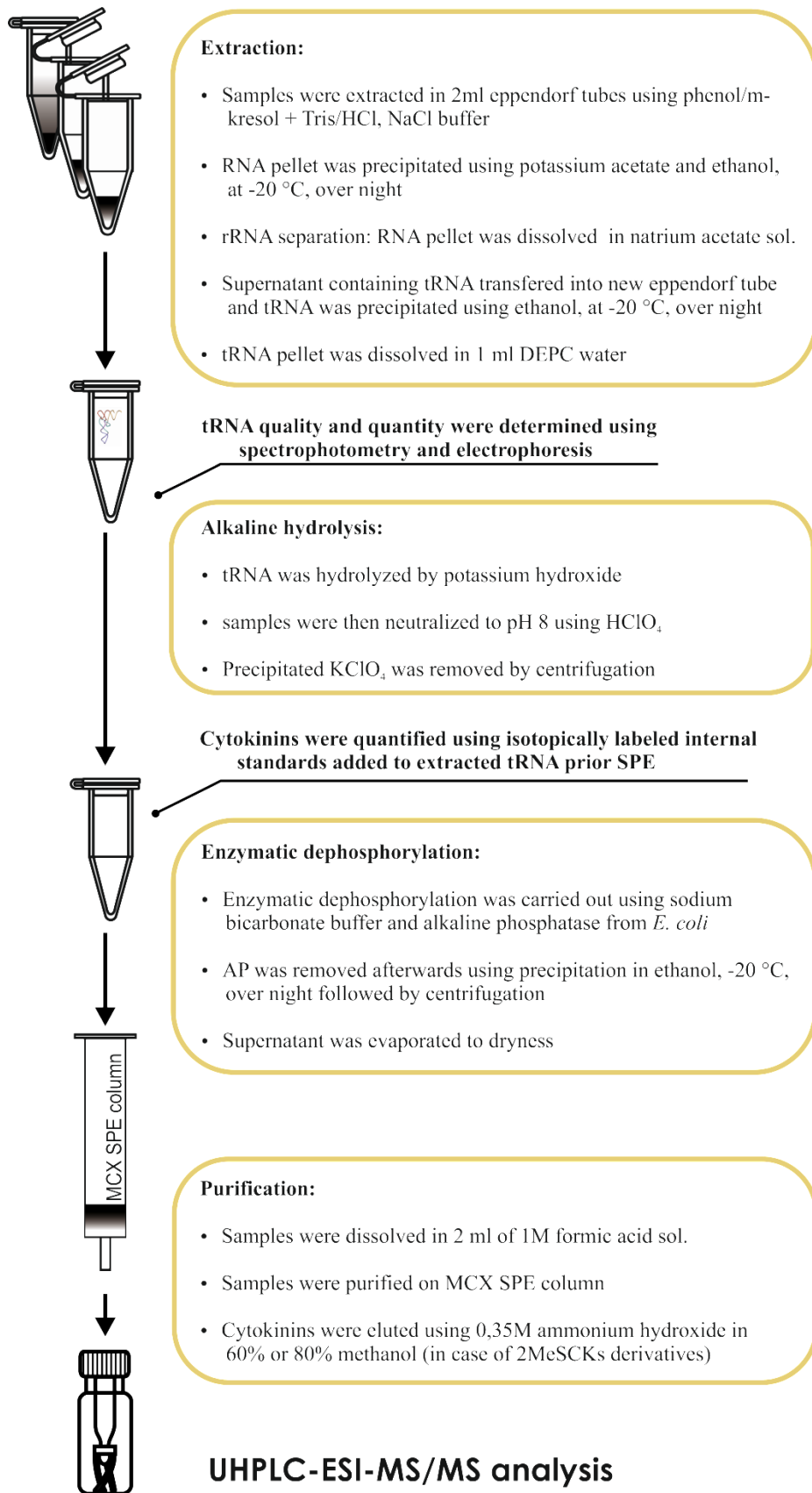


Figure 17. Miniaturized extraction and purification method for determination of tRNA bound cytokinins.

4.4.3 Phytohormone signalling and crosstalk

Besides the method development, new applications of developed and well-established LC-MS/MS methods for phytohormone profiling were employed to study a complex signalling network of plant hormones. In this chapter, an overview of results from both projects is summarized.

Auxin and cytokinin distribution and physiological polarity (Supplement IV)

In Šimura et al., (2016), we focused on the distribution of auxin and cytokinins in segmented shoots and turions of rootless carnivorous aquatic plants *Aldrovanda vesiculosa* and *Utricularia australis*. Most species of aquatic carnivorous plants have linear, poorly branched shoots and are rootless. They usually exhibit very rapid apical shoot growth (1–4 leaf nodes per day) and high relative growth rates, while their basal shoot segments decay at the same rate as new shoots are produced. Our analyses showed that cytokinin and auxin activity, which were originally studied and described in model rooting terrestrial plant species (*Arabidopsis thaliana*, *Nicotiana tabacum*), strongly correlate with physiological aspects of the rapid and polar growth and the development of these rootless aquatic species. Analysis of the apical parts of these plants has shown that the rapidly growing shoot apices have high cytokinin and auxin biosynthetic activity. The apex acts as a very strong physiological sink, attracting the allocation of both essential minerals and organic nutrients and thus promoting the growth and development of new tissues in this segment, while maintaining active meristems.

A basipetal decrease in the content of biologically active cytokinins leads to a change in the cytokinin/auxin balance throughout the whole plant in favour of auxin in tissues further from the apex. Such a change in the cytokinin/auxin ratio may be reflected in a change in chlorophyll content, and thus in a progressive decrease in photosynthetic rate, in tissues (leaves and traps). A low content of active cytokinins is also associated with ageing processes in plants, such as maturation of leaves and traps, changes in leaf and trap function and senescence. All of the above occur along the observed gradient of decrease in active cytokinin content, and contribute to the growth and physiological polarity of these plants.

The auxin and cytokinin profiling along the plant shoot point to the importance of the dynamic balance of phytohormones, suggesting that physiological processes such

as senescence are not controlled only by the presence of one particular hormone but rather through a combination of several compounds and their optimal ratio. Direct and detailed analysis of complex plant hormone metabolism provides valuable information about the regulatory mechanisms and the roles played by phytohormone crosstalk.

The role of cytokinins in de-etiolation (Supplements V)

As an example of hormone cross talk during the de-etiolation process, the role of ABA and CKs has been studied (Humplík et al., 2015). Data presented in this publication support and contribute to the idea of ABA role in stimulating and maintenance of the shoot growth during etiolation of *Solanum lycopersicum*. It has been observed that ABA deficiency caused a reduction in hypocotyl growth at the level of cell elongation and that the growth in ABA-deficient plants could be improved by treatment with exogenous ABA in a concentration dependent matter showing that ABA is essential for hypocotyl elongation during skotomorphogenesis. ABA promotes DNA endoreduplication during skotomorphogenesis by enhancing the expression of the genes encoding inhibitors of cyclin-dependent kinases and by reducing CKs levels. In contrast, during de-etiolation (exposure to blue light) accumulation of CKs was observed, corresponding to accumulation of *SILOG2* transcripts (encoding enzyme responsible for free CK bases biosynthesis) correlated with the inhibition of endoreduplication. Additionally, treatment with exogenous ABA significantly inhibited the *SILOG2* transcript accumulation emphasizing the antagonistic roles of CKs and ABA during de-etiolation.

Cytokinin signal transduction in *Physcomitrella patens* (Supplement VI)

Currently studies are underway to investigate the impact of the CHASE domain-containing histidine kinase (CHK) receptors on multiple physiological and developmental aspects, and we anticipate that this research will contribute to understanding how hormonal regulation was established at the level of bryophytes. This study showed that at the evolutionary stage of bryophytes, cytokinin signalling is fully established and uses classical receptors of the *CHK* gene family (CHK1, CHK2, and CHK3). Previously, it has been shown in *Arabidopsis* that deficiencies in cytokinin receptors can result in changes in cytokinin homeostasis (Riefler et al., 2006). Surprisingly, no significant changes in CK profiles were measured in the cytokinin

receptor double ($\Delta chk1,2$, $\Delta chk1,3$, and $\Delta chk2,3$) and triple ($\Delta chk1,2,3$) mutants compared with the wild type. In summary, in the moss *P. patens* – in contrast to flowering plants – there is only a minor contribution of the CHK1, CHK2, and CHK3 receptors to CK homeostasis.

However, our experiments highlight the common and different properties of the receptors and their roles in developmental processes such as bud formation and gametophore development. The importance of cytokinin receptors for sexual reproduction was also emphasized by the inability of the triple mutant to form sporophytes. The results of this study demonstrate the functionality of the classical PpCHK receptors, which are crucial for key steps in the life cycle of *P. patens*. This plant is apparently dependent on functionality in the level of cytokinin homeostasis as well as of cytokinin perception. All experiments are fully described in Von Schwartzberg et al. (2016).

5 Conclusion and future prospects

The present work whose main aim was to develop an efficient, robust and sensitive UHPLC-ESI-MS/MS based method for phytohormone screening, was inspired by determination of cytokinins in various plant materials (*A. vesiculosa*, *U. australis* and *S. lycopersicum sp.*) with the main focus on cytokinin crosstalk with other classes of plant hormones such as auxins and abscisic acid during plant growth and development. A newly established method for phytohormone profiling provide a simple, sensitive and powerful tool for such studies on phytohormonal inter- and intra-cellular communications and evolution in plants, as suggested above.

The UHPLC-ESI-MS/MS based method capable of a wide range plant-hormone profiling throughout several classes of plant hormones was later established. This method allows determination of more than 100 plant hormones related compounds and metabolites in one sample. This was achieved using sub-2 μm particle reversed-phase column, combined with the optimized mobile phase composition and chromatographic conditions. The baseline separation of the crucial isomers was achieved in a 15 minutes long chromatographic run. Targeted compounds in the same crude extract were purified by single step non-selective reverse phase solid phase extraction, while avoiding the use of acidified solvents during sample preparation, which minimized the degradation of sensitive analytes, thus preventing the undesired changes in analyte composition. Targeted compounds were determined using the specific MRM transitions in both ESI(+) and ESI(-) modes with optimized CE, CV and CAPV conditions. The proposed method was successfully applied to the phytohormone profiling of real samples (roots and shoots) of *Arabidopsis thaliana* grown under salinity stress and normal conditions.

Another part of this thesis focused on *tRNA* bound cytokinins which are important agents in cytokinin biosynthesis and signalling. A well-established UHPLC-ESI-MS/MS method for cytokinin determination (Svačinová et al., 2012) was used for studies of evolution of cytokinin signalling pathway in *Physcomitrella patens* and during studies of cytokinin roles in *Nostoc sp.* and *Scenedesmus obliquus* growth. These studies also required an efficient method for determination of *tRNA* bound cytokinins. This objective was fulfilled by miniaturization and optimization of the *tRNA* extraction protocol previously described by Maaß and Klämbt (1981) and modified by Stirk et al. (2012). The tailor-made protocol requires 10 times lower amounts of analysed material

and can be carried out in standard 2ml laboratory tubes with also significantly reduced amounts of necessary chemicals.

In future, the ongoing development of increasingly sensitive and selective mass spectrometers and methods will likely allow the analysis of most plant hormones at cellular and even organelle levels. Nevertheless, higher sensitivity comes with its own problems, such as contamination and high background noise. Ultraclean laboratories and dedicated instruments will be needed to avoid problems with sample contamination; further higher resolution will be needed to reduce the background noise (Nováková, 2013). Work in the MS area is already responding to these challenges with a shift from low-resolution to ultra-high-resolution tandem mass analysers, a shift from conventional LC-MS to ultra-fast LC-MS techniques, the adoption of two-dimensional LC-MS for complex samples, and/or use of other dimensions in MS, such as ion mobility spectrometry (Holčapek et al., 2012). Moreover, highly efficient extraction and purification methods remain essential if we are to obtain a high enough sensitivity in the MS-based analyses for all compounds. New types of adsorbents, miniaturization, and online purification have the potential to increase the sensitivity even further.

6 References

- Addicott, F. T., Lyon, J. L., Okhuma, K., Thiessen, W. E., Carns, H. R., Smith, O. E., Cornforth, J. W., Milborrow, B. V., Ryback, G., & Wareing, P. F. (1968). Abscisic acid: a new name for abscisin II (dormin). *Science*, *159*(3822), 1493–1493.
- Adie, B. A. T., Pérez-Pérez, J., Pérez-Pérez, M. M., Godoy, M., Sánchez-Serrano, J.-J., Schmelz, E. A., & Solano, R. (2007). ABA is an essential signal for plant resistance to pathogens affecting JA biosynthesis and the activation of defenses in *Arabidopsis*. *Plant Cell*, *19*(5), 1665–81.
- Akiyoshi, D. E., Klee, H., Amasino, R. M., Nester, E. W., & Gordon, M. P. (1984). T-DNA of *Agrobacterium tumefaciens* encodes an enzyme of cytokinin biosynthesis. *Proceedings of the National Academy of Sciences of the United States of America*, *81*(19), 5994–8.
- An, C., & Mou, Z. (2011). Salicylic acid and its function in plant immunity. *Journal of Integrative Plant Biology*, *53*(6), 412–428.
- Ang, L. H., Chattopadhyay, S., Wei, N., Oyama, T., Okada, K., Batschauer, A., & Deng, X. W. (1998). Molecular interaction between COP1 and HY5 defines a regulatory switch for light control of *Arabidopsis* development. *Molecular Cell*, *1*(2), 213–222.
- Arsovski, A. A., Galstyan, A., Guseman, J. M., & Nemhauser, J. L. (2012). Photomorphogenesis. In *The Arabidopsis book* (Vol. 10). American Society of Plant Biologist.
- Aspinall, D. (1986). Metabolic effects of water and salinity stress in relation to expansion of the leaf surface. *Australian Journal of Plant Physiology*, *13*(1), 59.
- Atanasova, L. (2010). Long-term salinity affects tRNA and rRNA cytokinins in maize (*Zea Mays* L.). *Comptes Rendus de l'Académie Bulgare Des Sciences: Sciences Mathématiques et Naturelles*, *63*(12), 1741–1748.
- Bajguz, A. (2011). Brassinosteroids - occurrence and chemical structures in plants. In S. Hayat & A. Ahmad (Eds.), *Brassinosteroids: A Class of Plant Hormone* (1–27). Dordrecht: Springer Netherlands.
- Bajguz, A., & Piotrowska, A. (2009). Conjugates of auxin and cytokinin. *Phytochemistry*, *70*(8), 957–969.
- Balcke, G. U., Handrick, V., Bergau, N., Fichtner, M., Henning, A., Stellmach, H., Tissier, A., Hause, B., & Frolov, A. (2012). An UPLC-MS/MS method for highly sensitive high-throughput analysis of phytohormones in plant tissues. *Plant Methods*, *8*(1), 47.
- Barbez, E., Kubeš, M., Rolčík, J., Béziat, C., Pěňčík, A., Wang, B., Rosquete, M. R., Zhu, J., Dobrev P. I., Lee, Y., Zažímalová, E., Petrášek, J., Geisler, M., Friml, J., & Kleine-Vehn, J. (2012). A novel putative auxin carrier family regulates intracellular auxin homeostasis in plants. *Nature*, *485*(7396), 119–122.
- Barry, G. F., Rogers, S. G., Fraley, R. T., & Brand, L. (1984). Identification of a cloned cytokinin biosynthetic gene. *Proceedings of the National Academy of Sciences of the United States of America*, *81*(15), 4776–80.
- Bennett, M. J., Marchant, A., Green, H. G., May, S. T., Ward, S. P., Millner, P. A., Walker, A., R., Schulz, B., & Feldmann, K. A. (1996). *Arabidopsis* AUX1 gene: a permease-like regulator of root gravitropism. *Science*, *273*(5277), 948–950.
- Björk, G. R., Ericson, J. U., Gustafsson, C. E., Hagervall, T. G., Jönsson, Y. H., & Wikström, P. M. (1987). Transfer RNA modification. *Annual Review of Biochemistry*, *56*, 263–287.
- Blackman, P. G., & Davies, W. J. (1984). Modification of the CO₂ responses of maize stomata by abscisic acid and by naturally-occurring and synthetic cytokinins. *Journal of Experimental Botany*, *35*(2), 174–179.
- Bleecker, A. B., Esch, J. J., Hall, A. E., Rodríguez, F. I., & Binder, B. M. (1998). The ethylene-receptor family from *Arabidopsis*: structure and function. *Philosophical Transactions of the Royal Society of London. Series B, Biological Sciences*, *353*(1374), 1405–1412.
- Browse, J. (2005). Jasmonate: An oxylipin signal with many roles in plants. *Vitamins and Hormones*, *72*, 431–456.

- Browse, J.** (2009). The power of mutants for investigating jasmonate biosynthesis and signaling. *Phytochemistry*, *70*(13–14), 1539–1546.
- Brzobohatý, B., Moore, I., Kristoffersen, P., Bako, L., Campos, N., Schell, J., & Palme, K.** (1993). Release of active cytokinin by a beta-glucosidase localized to the maize root meristem. *Science*, *262*(5136), 1051–4.
- Bythell-Douglas, R., Waters, M. T., Scaffidi, A., Flematti, G. R., Smith, S. M., & Bond, C. S.** (2013). The structure of the karrikin-insensitive protein (KAI2) in *Arabidopsis thaliana*. *PLoS ONE*, *8*(1).
- Cai, B. D., Yin, J., Hao, Y. H., Li, Y. N., Yuan, B. F., & Feng, Y. Q.** (2015). Profiling of phytohormones in rice under elevated cadmium concentration levels by magnetic solid-phase extraction coupled with liquid chromatography tandem mass spectrometry. *Journal of Chromatography A*, *1406*.
- Cai, B. D., Zhu, J. X., Gao, Q., Luo, D., Yuan, B. F., & Feng, Y. Q.** (2014). Rapid and high-throughput determination of endogenous cytokinins in *Oryza sativa* by bare Fe₃O₄ nanoparticles-based magnetic solid-phase extraction. *Journal of Chromatography A*, *1340*, 146–150.
- Cai, B. D., Zhu, J. X., Shi, Z. G., Yuan, B. F., & Feng, Y. Q.** (2013). A simple sample preparation approach based on hydrophilic solid-phase extraction coupled with liquid chromatography–tandem mass spectrometry for determination of endogenous cytokinins. *Journal of Chromatography B*, *942–943*, 31–36.
- Cai, W. J., Ye, T. T., Wang, Q., Cai, B. D., & Feng, Y. Q.** (2016). A rapid approach to investigate spatiotemporal distribution of phytohormones in rice. *Plant Methods*, *12*(1), 47.
- Caño-Delgado, A., Yin, Y., Yu, C., Vafeados, D., Mora-García, S., Cheng, J.-C., Nam, K. H., Li, J., & Chory, J.** (2004). BRL1 and BRL3 are novel brassinosteroid receptors that function in vascular differentiation in *Arabidopsis*. *Development*, *131*(21), 5341–5351.
- Cao, Z. Y., Sun, L. H., Mou, R. X., Zhang, L. P., Lin, X. Y., Zhu, Z. W., & Chen, M. X.** (2016). Profiling of phytohormones and their major metabolites in rice using binary solid-phase extraction and liquid chromatography-triple quadrupole mass spectrometry. *Journal of Chromatography A*, *1451*, 67–74.
- Caplin, S. M., & Steward, F. C.** (1948). Effect of coconut milk on the growth of explants from carrot root. *Science*, *108*(2815), 655–657.
- Carillo, P., Annunziata, M. G., Pontecorvo, G., Fuggi, A., & Woodrow, P.** (2011). Salinity stress and salt tolerance. In A. Shanker & B. Venkateswarlu (Eds.), *Abiotic Stress in Plants - Mechanisms and Adaptations*. Rijeka: InTech.
- Cleland, C. F.** (1974). Isolation of flower-inducing and flower-inhibitory factors from aphid honeydew. *Plant Physiology*, *54*(6), 899–903.
- Cleland, C. F., & Ajami, A.** (1974). Identification of the flower-inducing factor isolated from aphid honeydew as being salicylic acid. *Plant Physiology*, *54*(6), 904–906.
- Clouse, S. D.** (2011). Brassinosteroids. In *The Arabidopsis book* (Vol. 9). *American Society of Plant Biologists*.
- Conconi, A., Smerdon, M. J., Howe, G. A., & Ryan, C. A.** (1996). The octadecanoid signalling pathway in plants mediates a response to ultraviolet radiation. *Nature*, *383*(6603), 826–829.
- Cornforth, J. W., Milborrow, B. V., Ryback, G., & Wareing, P. F.** (1965). Chemistry and physiology of “dormins” in sycamore: identity of sycamore “dormin” with abscisic acid. *Nature*, *205*(4978), 1269–1270.
- Dathe, W., Rönsch, H., Preiss, A., Scgade, W., Sembdner, G., & Schreiber, K.** (1981). Endogenous plant hormones of the broad bean, *Vicia faba* L. (—)-jasmonic acid, a plant growth inhibitor in pericarp. *Planta*, *153*(6), 530–535.
- Darwin, C. R.** (1880). *The power of movement in plants*. London: John Murray.
- Davière, J.-M., & Achard, P.** (2013). Gibberellin signaling in plants. *Development*, *140*(6), 1147–51.
- Davies, P. J.** (2010). The plant hormones: Their nature, occurrence, and functions. In P. J. Davies (Ed.), *Plant Hormones: Biosynthesis, Signal Transduction, Action!* (1–15). Dordrecht: Springer Netherlands.
- Demole, E., Lederer, E., & Mercier, D.** (1962). Isolement et détermination de la structure du jasmonate de méthyle, constituant odorant caractéristique de l'essence de jasmin. *Helvetica Chimica Acta*, *45*(2), 675–685.

- Deng, T., Wu, D., Duan, C., & Guan, Y.** (2016). Ultrasensitive quantification of endogenous brassinosteroids in milligram fresh plant with a quaternary ammonium derivatization reagent by pipette-tip solid-phase extraction coupled with ultra-high-performance liquid chromatography tandem mass spectrometry. *Journal of Chromatography A*, 1456, 105–112.
- Ding, J., Mao, L. J., Yuan, B. F., & Feng, Y. Q.** (2013). A selective pretreatment method for determination of endogenous active brassinosteroids in plant tissues: double layered solid phase extraction combined with boronate affinity polymer monolith microextraction. *Plant Methods*, 9(1), 13.
- Ding, J., Wu, J. H., Liu, J. F., Yuan, B. F., & Feng, Y. Q.** (2014). Improved methodology for assaying brassinosteroids in plant tissues using magnetic hydrophilic material for both extraction and derivatization. *Plant Methods*, 10(1), 39/1-39/11, 11 .
- Dobrev, P. I., & Kamínek, M.** (2002). Fast and efficient separation of cytokinins from auxin and abscisic acid and their purification using mixed-mode solid-phase extraction. *Journal of Chromatography A*, 950(1–2), 21–29.
- Dong, J., Tang, D., Gao, Z., Yu, R., Li, K., He, H., Terzaghi, W., Deng, X. W., & Chen, H.** (2014). *Arabidopsis* DE-ETIOLATED1 represses photomorphogenesis by positively regulating phytochrome-interacting factors in the dark. *Plant Cell*, 26(9), 3630–45.
- Drábková, L. Z., Dobrev, P. I., & Motyka, V.** (2015). Phytohormone profiling across the bryophytes. *PLoS ONE*, 10(5).
- Du, F., Ruan, G., Liang, S., Xie, F., & Liu, H.** (2012). Monolithic molecularly imprinted solid-phase extraction for the selective determination of trace cytokinins in plant samples with liquid chromatography-electrospray tandem mass spectrometry. *Analytical and Bioanalytical Chemistry*, 404(2), 489–501.
- Ernsten, A., Sandberg, G., & Crozier, A.** (1986). Effects of sodium diethyldithiocarbamate, solvent, temperature and plant extracts on the stability of indoles. *Physiologia Plantarum*, 68(3), 519–522.
- Fahad, S., Hussain, S., Matloob, A., Khan, F. A., Khaliq, A., Saud, S., Hassan, S., Shan, D., Khan, F., Ullah, N., Faiq, M., Khan, M. R., Tareen A. K., Khan, A., Ullah, A., Ullah, N., & Huang, J.** (2015). Phytohormones and plant responses to salinity stress: a review. *Plant Growth Regulation*, 75(2), 391–404.
- Finkelstein, R.** (2013). Abscisic acid synthesis and response. In *The Arabidopsis book* (Vol. 11). *American Society of Plant Biologists*.
- Flematti, G. R., Dixon, K. W., & Smith, S. M.** (2015). What are karrikins and how were they “discovered” by plants? *BMC Biology*, 13(1), 108.
- Floková, K., Tarkowská, D., Miersch, O., Strnad, M., Wasternack, C., & Novák, O.** (2014). UHPLC-MS/MS based target profiling of stress-induced phytohormones. *Phytochemistry*, 105(July), 147–157.
- Fonseca, S., Chini, A., Hamberg, M., Adie, B., Porzel, A., Kramell, R., Miersch, O., Wasternack, C., & Solano, R.** (2009). (+)-7-iso-Jasmonoyl-L-isoleucine is the endogenous bioactive jasmonate. *Nature Chemical Biology*, 5(5), 344–350.
- Frébortová, J., Fraaije, M. W., Galuszka, P., Šebela, M., Peč, P., Hrbáč, J., Novák, O., Bilyeu, K., D., English, T., & Frébort, I.** (2004). Catalytic reaction of cytokinin dehydrogenase: preference for quinones as electron acceptors. *Biochemical Journal*, 380(1), 121–130.
- Frébortová, J., Plíhal, O., Florová, V., Kokáš, F., Kubiasová, K., Greplová, M., Šimura, J., Novák, O., Frébort, I.** (2017) Light influences cytokinin biosynthesis and sensing in *Nostoc* (Cyanobacteria). *Journal of Phycology*, 53, 703–714.
- Fu, Z. Q., Yan, S., Saleh, A., Wang, W., Ruble, J., Oka, N., Mohan, R., Spoel, S. H., Tada, Y., Zheng, N., & Dong, X.** (2012). NPR3 and NPR4 are receptors for the immune signal salicylic acid in plants. *Nature*, 486(7402), 228–32.
- Fujioka, S., & Sakurai, A.** (1997). Brassinosteroids. *Natural Product Reports*, 14(1), 1–10.
- Galston, W., & Sawhney, R. K.** (1990). Polyamines in plant physiology. *Plant Physiology*, 94(2), 406–410.
- Galuszka, P., Popelková, H., Werner, T., Frébortová, J., Pospíšilová, H., Mik, V., Köllmer, I., Schmölling, T., & Frébort, I.** (2007). Biochemical characterization of cytokinin oxidases/dehydrogenases from *Arabidopsis thaliana* expressed in *Nicotiana tabacum* L. *Journal of Plant Growth Regulation*, 26(3), 255–267.

- Garcion, C., Lohmann, A., Lamodière, E., Catinot, J., Buchala, A., Doermann, P., & Métraux, J.-P.** (2008). Characterization and biological function of the *ISOCHORISMATE SYNTHASE2* gene of *Arabidopsis*. *Plant Physiology*, *147*(3), 1279–87.
- Ge, L., Yong, J. W. H., Goh, N. K., Chia, L. S., Tan, S. N., & Ong, E. S.** (2005). Identification of kinetin and kinetin riboside in coconut (*Cocos nucifera* L.) water using a combined approach of liquid chromatography-tandem mass spectrometry, high performance liquid chromatography and capillary electrophoresis. *Journal of Chromatography B*, *829*(1–2), 26–34.
- Geng, Y., Wu, R., Wee, C. W., Xie, F., Wei, X., Chan, P. M. Y., Tham, C., Duan, L., & Dinnen, J. R.** (2013). A spatio-temporal understanding of growth regulation during the salt stress response in *Arabidopsis*. *Plant Cell*, *25*(6), 2132–54.
- Glauser, G., Grata, E., Dubugnon, L., Rudaz, S., Farmer, E. E., & Wolfender, J. L.** (2008). Spatial and temporal dynamics of jasmonate synthesis and accumulation in *Arabidopsis* in response to wounding. *Journal of Biological Chemistry*, *283*(24), 16400–16407.
- Gómez-Cadenas, A., Pozo, O. J., García-Augustín, P., & Sancho, J. V.** (2002). Direct analysis of abscisic acid in crude plant extracts by liquid chromatography—electrospray/tandem mass spectrometry. *Phytochemical Analysis*, *13*(4), 228–234.
- Gonai, T., Kawahara, S., Tougou, M., Satoh, S., Hashiba, T., Hirai, N., Kawaide, H., Kamiya, Y., & Yoshioka, T.** (2004). Abscisic acid in the thermoinhibition of lettuce seed germination and enhancement of its catabolism by gibberellin. *Journal of Experimental Botany*, *55*(394), 111–118.
- Grove, J. F.** (1961). The gibberellins. *Quarterly Reviews Chemical Society*, *15*(1), 56–70.
- Grove, M. D., Spencer, G. F., Rohwedder, W. K., Mandava, N., Worley, J. F., Jr., Warthen, J. D. Jr., Steffens, G. L., Flippen-Anderson, J. L., & Cook, C. J. Jr.** (1979). Brassinolide, a plant growth-promoting steroid isolated from *Brassica napus* pollen. *Nature*, *281*, 216–217.
- Guo, J., Yang, X., Weston, D. J., & Chen, J.-G.** (2011). Abscisic acid receptors: past, present and future. *Journal of Integrative Plant Biology*, *53*(6), 469–79.
- Haberlandt, G.** (1913). Zur Physiologie der Zellteilung. *Sitzber. K. Preuss. Akad. Wiss.*, 318–345.
- Hasegawa, P. M., Bressan, R. A., Zhu, J. K., & Bohnert, H. J.** (2000). Plant cellular and molecular responses to high salinity. *Annual Review of Plant Physiology and Plant Molecular Biology*, *51*, 463–499.
- Hauserová, E., Swaczynová, J., Doležal, K., Lenobel, R., Popa, I., Hajdúch, M., Vydra, D., Fuksová, K., & Strnad, M.** (2005). Batch immunoextraction method for efficient purification of aromatic cytokinins. *Journal of Chromatography A*, *1100*(1), 116–125.
- Hedden, P., & Thomas, S. G.** (2012). Gibberellin biosynthesis and its regulation. *Biochemical Journal*, *444*(1), 11–25.
- Hoffmann-Benning, S., & Kende, H.** (1992). On the role of abscisic acid and gibberellin in the regulation of growth in rice. *Plant Physiology*, *99*(3), 1156–61.
- Holčápek, M., Jirásko, R., & Lísa, M.** (2012). Recent developments in liquid chromatography-mass spectrometry and related techniques. *Journal of Chromatography A*, *1259*(2012), 3–15.
- Hoyerová, K., Gaudinová, A., Malbeck, J., Dobrev, P. I., Kocábek, T., Šolcová, B., Trávníčková, A., & Kamínek, M.** (2006). Efficiency of different methods of extraction and purification of cytokinins. *Phytochemistry*, *67*(11), 1151–1159.
- Hradecká, V., Novák, O., Havlíček, L., & Strnad, M.** (2007). Immunoaffinity chromatography of abscisic acid combined with electrospray liquid chromatography-mass spectrometry. *Journal of Chromatography B*, *847*(2), 162–173.
- Humplik, J. F., Bergougnoux, V., Jandová, M., Šimura, J., Pěňčík, A., Tomanec, O., Rolčík, J., Novák, O., & Fellner, M.** (2015). Endogenous abscisic acid promotes hypocotyl growth and affects endoreduplication during dark-induced growth in tomato (*Solanum lycopersicum* L.). *PLoS ONE*, *10*(2), 1–23.
- Chen, Z., Zheng, Z., Huang, J., Lai, Z., & Fan, B.** (2009). Biosynthesis of salicylic acid in plants. *Plant Signaling & Behavior*, *4*(6), 493–496.
- Cheon, J., Fujioka, S., Dilkes, B. P., & Choe, S.** (2013). Brassinosteroids regulate plant growth through distinct signaling pathways in *Selaginella* and *Arabidopsis*. *PLoS ONE*, *8*(12), 1–9.
- Cheong, J. J., & Choi, Y. Do.** (2003). Methyl jasmonate as a vital substance in plants. *Trends in Genetics*, *19*(7), 409–413.

- Chiwocha, S. D. S., Abrams, S. R., Ambrose, S. J., Cutler, A. J., Loewen, M., Ross, A. R. S., & Kermodé, A. R.** (2003). A method for profiling classes of plant hormones and their metabolites using liquid chromatography-electrospray ionization tandem mass spectrometry: An analysis of hormone regulation of thermodormancy of lettuce (*Lactuca sativa* L.) seeds. *Plant Journal*, 35(3), 405–417.
- Cho, M., & Cho, H. T.** (2013). The function of ABCB transporters in auxin transport. *Plant Signaling & Behavior*, 8(2), e22990.
- Choe, S.** (2010). Brassinosteroid biosynthesis and metabolism. In P. J. Davies (Ed.), *Plant Hormones: Biosynthesis, Signal Transduction, Action!* (156–178). Dordrecht: Springer Netherlands.
- Chung, Y., & Choe, S.** (2013). The regulation of brassinosteroid biosynthesis in *Arabidopsis*. *Critical Reviews in Plant Sciences*, 32(6), 396–410.
- Inoue, T., Higuchi, M., Hashimoto, Y., Seki, M., Kobayashi, M., Kato, T., Tabata, S., Shinozaki, K., & Kakimoto, T.** (2001). Identification of CRE1 as a cytokinin receptor from *Arabidopsis*. *Nature*, 409(6823), 1060–1063.
- Iqbal, N., Umar, S., Khan, N. A., & Khan, M. I. R.** (2014). A new perspective of phytohormones in salinity tolerance: regulation of proline metabolism. *Environmental and Experimental Botany*, 100(2014), 34–42.
- Javid, M. G., Sorooshzadeh, A., Moradi, F., Sanavy, S. A. M. M., & Allahdadi, I.** (2011). The role of phytohormones in alleviating salt stress in crop plants. *Australian Journal of Crop Science*, 5(6), 726–734.
- Jiang, Y., & Deyholos, M. K.** (2006). Comprehensive transcriptional profiling of NaCl-stressed *Arabidopsis* roots reveals novel classes of responsive genes. *BMC Plant Biology*, 6(1), 25.
- Josse, E. M., & Halliday, K. J.** (2008). Skotomorphogenesis: the dark side of light signalling. *Current Biology*, 18(24), 1144–1146.
- Kang, D. J., Seo, Y. J., Lee, J. D., Ishii, R., Kim, K. U., Shin, D. H., Park, S. K., Jang, S. W., & Lee, I. J.** (2005). Jasmonic acid differentially affects growth, ion uptake and abscisic acid concentration in salt-tolerant and salt-sensitive rice cultivars. *Journal of Agronomy and Crop Science*, 191(4), 273–282.
- Kepinski, S., & Leyser, O.** (2005). The *Arabidopsis* F-box protein TIR1 is an auxin receptor. *Nature*, 435(7041), 446–451.
- Khan, N. A., Singh, S., Nazar, R., & Lone, P. M.** (2007). The source-sink relationship in mustard. *Asian and Australasian Journal of Plant Science and Biotechnology*, 1(1), 10–18.
- Khripach, V., Zhabinskii, V., & de Groot, A.** (2000). Twenty years of brassinosteroids: steroidal plant hormones warrant better crops for the XXI century. *Annals of Botany*, 86(3), 441–447.
- Kilian, J., Whitehead, D., Horak, J., Wanke, D., Weinl, S., Batistic, O., D'Angelo, C., Bornberg-Bauer, E., Kudla, J., & Harter, K.** (2007). The AtGenExpress global stress expression data set: Protocols, evaluation and model data analysis of UV-B light, drought and cold stress responses. *Plant Journal*, 50(2), 347–363.
- Koegl, F., & Kostermans, D. G. F. R.** (1934). Hetero- auxin als Stoffwechselprodukt niederer pflanzlicher Organismen. Isolierung aus Hefe. *Hoppe-Seyler's Zeitschrift Für Physiologische Chemie*, 228, 113–121.
- Kojima, M., Kamada-Nobusada, T., Komatsu, H., Takei, K., Kuroha, T., Mizutani, M., Ashikari, M., Ueguchi-Tanaka, M., Matsuoka, M., Suzuki, K., & Sakakibara, H.** (2009). Highly sensitive and high-throughput analysis of plant hormones using ms-probe modification and liquid chromatography-tandem mass spectrometry: An application for hormone profiling in *Oryza sativa*. *Plant and Cell Physiology*, 50(7), 1201–1214.
- Kowalska, M., Galuszka, P., Frébortová, J., Šebela, M., Béres, T., Hluska, T., Šmehilová, M., Bilyeu, K., D., & Frébort, I.** (2010). Vacuolar and cytosolic cytokinin dehydrogenases of *Arabidopsis thaliana*: Heterologous expression, purification and properties. *Phytochemistry*, 71(17–18), 1970–1978.
- Kuai, X., MacLeod, B. J., & Després, C.** (2015). Integrating data on the *Arabidopsis* NPR1/NPR3/NPR4 salicylic acid receptors; a differentiating argument. *Frontiers in Plant Science*, 6, 235.
- Kuwabara, A., Ikegami, K., Koshihara, T., & Nagata, T.** (2003). Effects of ethylene and abscisic acid upon heterophylly in *Ludwigia arcuata* (Onagraceae). *Planta*, 217(6), 880–887.

- Lau, S., Jürgens, G., & De Smet, I. (2008). The evolving complexity of the auxin pathway. *Plant Cell*, 20(7), 1738–1746.
- Lehmann, J., Atzorn, R., Brückner, C., Reinbothe, S., Leopold, J., Wasternack, C., & Parthier, B. (1995). Accumulation of jasmonate, abscisic acid, specific transcripts and proteins in osmotically stressed barley leaf segments. *Planta*, 197(1), 156–162.
- Leivar, P., Monte, E., Oka, Y., Liu, T., Carle, C., Castillon, A., Huq, E., & Quail, P. H. (2008). Multiple phytochrome-interacting bHLH transcription factors repress premature seedling photomorphogenesis in darkness. *Current Biology*, 18(23), 1815–1823.
- Li, D., Guo, Z., & Chen, Y. (2016). Direct derivatization and quantitation of ultra-trace gibberellins in sub-milligram fresh plant organs. *Molecular Plant*, 9(1), 175–177.
- Lin, Z., Zhong, S., & Grierson, D. (2009). Recent advances in ethylene research. *Journal of Experimental Botany*, 60(12), 3311–3336.
- Liu, W. C., & Carnsdagger, H. R. (1961). Isolation of abscisic acid, an abscission accelerating substance. *Science*, 134(3476), 384–5.
- Liu, X., Hegeman, A. D., Gardner, G., & Cohen, J. D. (2012a). Protocol: high-throughput and quantitative assays of auxin and auxin precursors from minute tissue samples. *Plant Methods*, 8(1), 31.
- Liu, Z., Cai, B. D., & Feng, Y. Q. (2012b). Rapid determination of endogenous cytokinins in plant samples by combination of magnetic solid phase extraction with hydrophilic interaction chromatography-tandem mass spectrometry. *Journal of Chromatography B*, 891–892, 27–35.
- Ljung, K. (2013). Auxin metabolism and homeostasis during plant development. *Development*, 140(5), 943–950.
- Ljung, K., Hull, A. K., Celenza, J., Yamada, M., Estelle, M., Normanly, J., & Sandberg, G. (2005). Sites and regulation of auxin biosynthesis in *Arabidopsis* roots. *Plant Cell*, 17(4), 1090–1104.
- Ljung, K., Sandberg, G., & Moritz, T. (2010). Methods of plant hormone analysis. In P. J. Davies (Ed.), *Plant Hormones: Biosynthesis, Signal Transduction, Action!* (717–740). Dordrecht: Springer Netherlands.
- López-Carbonell, M., & Jáuregui, O. (2005). A rapid method for analysis of abscisic acid (ABA) in crude extracts of water stressed *Arabidopsis thaliana* plants by liquid chromatography—mass spectrometry in tandem mode. *Plant Physiology and Biochemistry*, 43(4), 407–411.
- Ma, S., Gong, Q., & Bohnert, H. J. (2006). Dissecting salt stress pathways. *Journal of Experimental Botany*, 57(5), 1097–1107.
- Maaß, H., & Klämbt, D. (1981). Cytokinin biosynthesis in higher plants. In J. Guern & C. Péaud-Lenoël (Eds.), *Metabolism and Molecular Activities of Cytokinins: Proceedings of the International Colloquium of the Centre National de la Recherche Scientifique held at Gif-sur-Yvette (France) 2-6 September 1980* (27–33). Berlin, Heidelberg: Springer.
- MacMillan, J., & Takahashi, N. (1968). Proposed procedure for the allocation of trivial names to the gibberellins. *Nature*, 217(5124), 170–171.
- Mähönen, A. P., Bonke, M., Kauppinen, L., Riikonen, M., Benfey, P. N., & Helariutta, Y. (2000). A novel two-component hybrid molecule regulates vascular morphogenesis of the *Arabidopsis* root. *Genes and Development*, 14(23), 2938–2943.
- Mano, Y., & Nemoto, K. (2012). The pathway of auxin biosynthesis in plants. *Journal of Experimental Botany*, 63(8), 2853–2872.
- McGaw, B. A., & Hobgan, R. (1985). Cytokinin metabolism and the control of cytokinin activity. *Biologia Plantarum*, 27(2–3), 180–187.
- Miller, C. O., Skoog, F., Von Saltza, M. H., & Strong, F. M. (1955). Kinetin, a cell division factor from deoxyribonucleic acid. *Journal of the American Chemical Society*, 77(5), 1392–1392.
- Mok, D. W. S. (1994). Cytokinin metabolic enzymes. In D. W. S. Mok & M. C. Mok (Eds.), *Cytokinins: Chemistry, Activity and Function* (29–137). CRC Press, Boca Raton, FL.
- Mougel, C., & Zhulin, I. B. (2001). CHASE: An extracellular sensing domain common to transmembrane receptors from prokaryotes, lower eukaryotes and plants. *Trends in Biochemical Sciences*, 26(10), 582–584.
- Munns, R. (2002). Comparative physiology of salt and water stress. *Plant, Cell & Environment*, 25(2), 239–250.

- Munns, R., Schachtman, D., & Condon, A.** (1995). The significance of a two-phase growth response to salinity in wheat and barley. *Australian Journal of Plant Physiology*, 22(4), 561–569.
- Munns, R., & Termaat, A.** (1986). Whole-plant responses to salinity. *Australian Journal of Plant Physiology*, 13(1), 143–160.
- Munns, R., & Tester, M.** (2008). Mechanisms of salinity tolerance. *Annual Review of Plant Biology*, 59, 651–81.
- Nakamura, M., Kiefer, C. S., & Grebe, M.** (2012). Planar polarity, tissue polarity and planar morphogenesis in plants. *Current Opinion in Plant Biology*, 15(6), 593–600.
- Nambara, E., & Marion-Poll, A.** (2005). Abscisic acid biosynthesis and catabolism. *Annual Review of Plant Biology*, 56(1), 165–185.
- Ng, L. M., Melcher, K., Teh, B. T., & Xu, H. E.** (2014). Abscisic acid perception and signaling: structural mechanisms and applications. *Acta Pharmacologica Sinica*, 35(5), 567–584.
- Nishiyama, R., Le, D. T., Watanabe, Y., Matsui, A., Tanaka, M., Seki, M., Yamaguchi-Shinozaki, K., Shinozaki, K., & Tran, L. S. P.** (2012). Transcriptome analyses of a salt-tolerant cytokinin-deficient mutant reveal differential regulation of salt stress response by cytokinin deficiency. *PLoS ONE*, 7(2), 1–12.
- Nishiyama, R., Watanabe, Y., Fujita, Y., Le, D. T., Kojima, M., Werner, T., Vaňková, R., Yamaguchi-Shinozaki, K., Shinozaki, K., Kakimoto, T., Sakakibara, H., Schmülling, T., & Tran, L.-S. P.** (2011). Analysis of cytokinin mutants and regulation of cytokinin metabolic genes reveals important regulatory roles of cytokinins in drought, salt and abscisic acid responses, and abscisic acid biosynthesis. *Plant Cell*, 23(6), 2169–2183.
- Nonhebel, H. M.** (2015). Tryptophan-independent IAA synthesis: critical evaluation of the evidence. *Plant Physiology*, 169(2), 1001–1005.
- Normanly, J.** (2010). Approaching cellular and molecular resolution of auxin biosynthesis and metabolism. *Cold Spring Harbor Perspectives in Biology*, 2(1), 1–17.
- Novák, O., Hauserová, E., Amakorová, P., Doležal, K., & Strnad, M.** (2008). Cytokinin profiling in plant tissues using ultra-performance liquid chromatography-electrospray tandem mass spectrometry. *Phytochemistry*, 69(11), 2214–2224.
- Novák, O., Hényková, E., Sairanen, I., Kowalczyk, M., Pospíšil, T., & Ljung, K.** (2012). Tissue-specific profiling of the *Arabidopsis thaliana* auxin metabolome. *Plant Journal*, 72(3), 523–536.
- Novák, O., Pěňčík, A., & Ljung, K.** (2014). Identification and profiling of auxin and auxin metabolites. In E. Zažímalová, J. Petrášek, & E. Benková (Eds.), *Auxin and Its Role in Plant Development* (39–60). Vienna: Springer.
- Novák, O., Tarkowski, P., Tarkowská, D., Doležal, K., Lenobel, R., & Strnad, M.** (2003). Quantitative analysis of cytokinins in plants by liquid chromatography-single-quadrupole mass spectrometry. *Analytica Chimica Acta*, 480(2), 207–218.
- Nováková, L.** (2013). Challenges in the development of bioanalytical liquid chromatography-mass spectrometry method with emphasis on fast analysis. *Journal of Chromatography A*.
- Oh, E., Yamaguchi, S., Hu, J., Yusuke, J., Jung, B., Paik, I., Lee, H.-S., Sun, T.-P., Kamiya, Y., & Choi, G.** (2007). PIL5, a phytochrome-interacting bHLH protein, regulates gibberellin responsiveness by binding directly to the *GAI* and *RGA* promoters in *Arabidopsis* seeds. *Plant Cell*, 19(4), 1192–1208.
- Ohkuma, K., Lyon, J. L., Addicott, F. T., & Smith, O. E.** (1963). Abscisin II, an abscission-accelerating substance from young cotton fruit. *Science*, 142(3599), 1592–3.
- Osterlund, M. T., Hardtke, C. S., Wei, N., & Deng, X. W.** (2000). Targeted destabilization of HY5 during light-regulated development of *Arabidopsis*. *Nature*, 405(6785), 462–466.
- Osugi, A., & Sakakibara, H.** (2015). Q&A: How do plants respond to cytokinins and what is their importance? *BMC Biology*, 13(1), 102.
- Ouyang, J., Chen, M., & Li, J.** (1999). Measurement of soluble tryptophan and total indole-3-acetic acid in *Arabidopsis* by capillary electrophoresis. *Analytical Biochemistry*, 271(1), 100–102.
- Paciorek, T., & Friml, J.** (2006). Auxin signaling. *Journal of Cell Science*, 9(7), 448–453.
- Paciorek, T., Zažímalová, E., Ruthardt, N., Petrášek, J., Stierhof, Y. D., Kleine-Vehn, J., Morris, D. A., Emans, N., Jürgens, G., Geldner, N., & Friml, J.** (2005). Auxin inhibits endocytosis and promotes its own efflux from cells. *Nature*, 435(7046), 1251–1256.

- Pan, X., Welti, R., & Wang, X.** (2008). Simultaneous quantification of major phytohormones and related compounds in crude plant extracts by liquid chromatography-electrospray tandem mass spectrometry. *Phytochemistry*, *69*(8), 1773–1781.
- Park, S., Fung, P., Nishimura, N., Jensen, D. R., Zhao, Y., Lumba, S., Santiago, J., Rodrigues, A., Chow, T-F. F., Alfred, S. E., Bonetta, D., Finkelstein, R., Provart, N.J., Desveaux, D., Rodriguez, P. L., McCourt, P., Zhu, J-K., Schroeder, J. I., Volkman, B. F., & Cutler, S. R.** (2009). Abscisic acid inhibits PP2Cs via the PYR/PYL family of ABA-binding START proteins. *Science*, *324*(5930), 1068–1071.
- Patterson, S. E.** (2001). Cutting loose. Abscission and dehiscence in *Arabidopsis*. *Plant Physiology*, *126*(2), 494–500.
- Pawar, D., Shahani, S., & Maroli, S.** (1998). Aspirin - the novel antiplatelet drug. *Hong Kong Medical Journal*, *4*(4), 415–418.
- Pěňčík, A., Rolčík, J., Novák, O., Magnus, V., Barták, P., Buchčík, R., Salopek-Sondi, B., & Strnad, M.** (2009). Isolation of novel indole-3-acetic acid conjugates by immunoaffinity extraction. *Talanta*, *80*(2), 651–655.
- Perrot-Rechenmann, C.** (2010). Cellular responses to auxin: division versus expansion. *Cold Spring Harbor Perspectives in Biology*, *2*(5).
- Persson, B. C., Esberg, B., Ólafsson, Ó., & Björk, G. R.** (1994). Synthesis and function of isopentenyl adenosine derivatives in tRNA. *Biochimie*, *76*(12), 1152–1160.
- Peterson, S. V., Johansson, A. I., Kowalczyk, M., Makoveychuk, A., Wang, J. Y., Moritz, T., Grebe, M., Benfey, P. N., Sandberg, G., & Ljung, K.** (2009). An auxin gradient and maximum in the *Arabidopsis* root apex shown by high-resolution cell-specific analysis of IAA distribution and synthesis. *Plant Cell*, *21*(6), 1659–1668.
- Petrásek, J., & Friml, J.** (2009). Auxin transport routes in plant development. *Development*, *136*(16), 2675–2688.
- Philipps, G. R.** (1971). Analysis of purified tRNA species by polyacrylamide gel electrophoresis. *Analytical Biochemistry*, *44*(2), 345–357.
- Pieterse, C. M. J., & Van Loon, L. C.** (2004). NPR1: The spider in the web of induced resistance signaling pathways. *Current Opinion in Plant Biology*, *7*(4), 456–464.
- Plačková, L., Oklestkova, J., Pospíšková, K., Poláková, K., Buček, J., Stýskala, J., Zatloukal, M., Šafařík, I., Zbořil, R., Strnad, M., Doležal, K., & Novák, O.** (2017). Microscale magnetic microparticle-based immunopurification of cytokinins from *Arabidopsis* root apex. *Plant Journal*, *89*(5), 1065–1075.
- Powers, S. K., & Strader, L. C.** (2016). Up in the air: untethered factors of auxin response. *F1000Research*, *5*.
- Pratt, J. J.** (1986). Isotope dilution analysis using chromatographic separation of isotopic forms of the compound to be measured. *Annals of Clinical Biochemistry*, *23*(3), 251–276.
- Radwanski, E. R., & Last, R. L.** (1995). Tryptophan biosynthesis and metabolism: biochemical and molecular genetics. *Plant Cell*, *7*(7), 921–34.
- Raskin, I.** (1992). Salicylate, a new plant hormone. *Plant Physiology*, *99*, 799–803.
- Rauser, W. E., & Hanson, J. B.** (1966). The metabolic status of ribonucleic acid in soybean roots exposed to saline media. *Canadian Journal of Botany*, *44*(6), 759–776.
- Reymond, P., Bodenhausen, N., Van Poecke, R. M. P., Krishnamurthy, V., Dicke, M., & Farmer, E. E.** (2004). A conserved transcript pattern in response to a specialist and a generalist herbivore. *Plant Cell*, *16*(11), 3132–3147.
- Riefler, M., Novák, O., Strnad, M., & Schmülling, T.** (2006). *Arabidopsis* cytokinin receptor mutants reveal functions in shoot growth, leaf senescence, seed size, germination, root development, and cytokinin metabolism. *Plant Cell*, *18*(1), 40–54.
- Richmond, A. E., & Lang, A.** (1957). Effect of kinetin on protein content and survival of detached *Xanthium* leaves. *Science*, *125*(3249), 650–651.
- Rippka, R., Neilson, A., Kunisawa, R., & Cohen-Bazire, G.** (1971). Nitrogen fixation by 16 unicellular blue-green algae. *Archives of Microbiology*, *76*, 341–348.
- Rittenberg, D., & Foster, G. L.** (1940). A new procedure for quantitative analysis by isotope dilution, with application to the determination of amino acids and fatty acids. *The Journal of Biological Chemistry*, *133*, 737–744.

- Rockwell, N. C., Su, Y.-S., & Lagarias, J. C.** (2006). Phytochrome structure and signaling mechanisms. *Annual Review of Plant Biology*, *57*, 837–858.
- Ryu, H., & Cho, Y.-G.** (2015). Plant hormones in salt stress tolerance. *Journal of Plant Biology*, *58*(3), 147–155.
- Sakakibara, H.** (2005). Cytokinin Biosynthesis and Regulation. *Vitamins and Hormones*, *72*(5), 271–287.
- Sakakibara, H.** (2006). Cytokinins: activity, biosynthesis, and translocation. *Annual Review of Plant Biology*, *57*, 431–449.
- Sakurai, A.** (1999). Brassinosteroid biosynthesis. *Plant Physiology and Biochemistry*, *37*(5), 351–361.
- Santner, A., & Estelle, M.** (2010). The ubiquitin proteasome system regulates plant hormone signalling. *Plant Journal*, *61*(6), 1029–1040.
- Sasse, J. M.** (2003). Physiological actions of brassinosteroids: an update. *Journal of Plant Growth Regulation*, *22*(4), 276–288.
- Shakirova, F. M., Avalbaev, A. M., Bezrukova, M. V., & Kudoyarova, G. R.** (2010). Role of endogenous hormonal system in the realization of the antistress action of plant growth regulators on plants. *Plant Stress*, *4*(1), 32–38.
- Sharp, R. E., & LeNoble, M. E.** (2002). ABA, ethylene and the control of shoot and root growth under water stress. *Journal of Experimental Botany*, *53*(366), 33–37.
- Shimada, A., Ueguchi-Tanaka, M., Nakatsu, T., Nakajima, M., Naoe, Y., Ohmiya, H., Kato, H., & Matsuoka, M.** (2008). Structural basis for gibberellin recognition by its receptor *GID1*. *Nature*, *456*(7221), 520–523.
- Schäfer, M., Brütting, C., Baldwin, I. T., & Kallenbach, M.** (2016). High-throughput quantification of more than 100 primary- and secondary-metabolites, and phytohormones by a single solid-phase extraction based sample preparation with analysis by UHPLC-HESI-MS/MS. *Plant Methods*, *12*(1), 30.
- Schaller, G. E., Bishopp, A., & Kieber, J. J.** (2015). The yin-yang of hormones: cytokinin and auxin interactions in plant development. *Plant Cell*, *27*(1), 44–63.
- Schneider, G., Jensen, E., Spray, C. R., & Phinney, B. O.** (1992). Hydrolysis and reconjugation of gibberellin *A*₂₀ glucosyl ester by seedlings of *Zea mays* L. *Proceedings of the National Academy of Sciences*, *89*(17), 8045–8048.
- Singh, V., Roy, S., Singh, D., & Nandi, A. K.** (2014). *Arabidopsis* *FLOWERING LOCUS D* influences systemic-acquired-resistance- induced expression and histone modifications of *WRKY* genes. *Journal of Biosciences*, *39*(1), 119–126.
- Skoog, F., & Miller, C. O.** (1957). Chemical regulation of growth and organ formation in plant tissues cultured in vitro. *Symposia of the Society for Experimental Biology*, *11*, 118–131.
- Spíchal, L.** (2012). Cytokinins - Recent news and views of evolutionally old molecules. *Functional Plant Biology*, *39*(4), 267–284.
- Staswick, P. E., & Tiryaki, I.** (2004). The oxylipin signal jasmonic acid is activated by an enzyme that conjugates it to isoleucine in *Arabidopsis*. *Plant Cell*, *16*(8), 2117–2127.
- Stirk, W. A., Václavíková, K., Novák, O., Gajdošová, S., Kotland, O., Motyka, V., Strnad, M., & van Staden, J.** (2012). Involvement of *cis*-zeatin, dihydrozeatin, and aromatic cytokinins in germination and seedling establishment of maize, oats, and lucerne. *Journal of Plant Growth Regulation*, *31*(3), 392–405.
- Suzuki, T., Miwa, K., Ishikawa, K., Yamada, H., Aiba, H., & Mizuno, T.** (2001). The *Arabidopsis* sensor His-kinase, *AHK4*, can respond to cytokinins. *Plant and Cell Physiology*, *42*(2), 107–113.
- Svačinová, J., Novák, O., Plačková, L., Lenobel, R., Holík, J., Strnad, M., & Doležal, K.** (2012). A new approach for cytokinin isolation from *Arabidopsis* tissues using miniaturized purification: pipette tip solid-phase extraction. *Plant Methods*, *8*, 17.
- Swarup, K., Benková, E., Swarup, R., Casimiro, I., Peret, B., Yang, Y., Parry, G., Nielsen, E., De Smet, I., Vanneste, S., Levesque, M. P., Carrier, D., James, N., Calvo, V., Ljung, K., Kramer, E., Roberts, R., Graham, N., Marillonnet, S., Patel, K., Jones, J. D. G., Taylor, C. G., Schachtman, D. P., May, S., Sandberg, G., Benfey, P., Friml, J., Kerr, I., Beeckman, T., Laplaze, L., & Bennett, M. J.** (2008). The auxin influx carrier *LAX3* promotes lateral root emergence. *Nature Cell Biology*, *10*(8), 946–954.

- Symons, G. M., & Reid, J. B.** (2003). Interactions between light and plant hormones during de-etiolation. *Journal of Plant Growth Regulation*, 22(1), 3–14.
- Šimura, J., Spíchal, L., Adamec, L., Pěňčík, A., Rolčík, J., Novák, O., & Strnad, M.** (2016). Cytokinin, auxin and physiological polarity in the aquatic carnivorous plants *Aldrovanda vesiculosa* and *Utricularia australis*. *Annals of Botany*, 117(6), 1037–1044.
- Taiz, L., & Zeiger, E.** (2010). *Plant physiology*. (5th ed.). Sunderland: Sinauer Associated.
- Tanaka, M., Takei, K., Kojima, M., Sakakibara, H., & Mori, H.** (2006). Auxin controls local cytokinin biosynthesis in the nodal stem in apical dominance. *Plant Journal*, 45(6), 1028–1036.
- Tarkowská, D., Novák, O., Floková, K., Tarkowski, P., Turečková, V., Grúz, J., Rolčík, J., & Strnad, M.** (2014). Quo vadis plant hormone analysis? *Planta*, 240(1), 55–76.
- Tarkowská, D., Novák, O., Oklestkova, J., & Strnad, M.** (2016). The determination of 22 natural brassinosteroids in a minute sample of plant tissue by UHPLC--ESI--MS/MS. *Analytical and Bioanalytical Chemistry*, 408(24), 6799–6812.
- Tarkowski, P., Václavíková, K., Novák, O., Pertry, I., Hanuš, J., Whenham, R., Verecke, D., Šebela, M., & Strnad, M.** (2010). Analysis of 2-methylthio-derivatives of isoprenoid cytokinins by liquid chromatography-tandem mass spectrometry. *Analytica Chimica Acta*, 680(1–2), 86–91.
- Teare, J. M., Islam, R., Flanagan, R., Gallagher, S., Davies, M. G., & Grabau, C.** (1997). Measurement of nucleic acid concentrations using the DyNA QuantTM and the GeneQuantTM. *BioTechniques*, 22(6), 1170–1174.
- Thomas, T. H.** (1992). Some reflections on the relationship between endogenous hormones and light-mediated seed dormancy. *Plant Growth Regulation*, 11(3), 239–248.
- Tsuchiya, Y., & McCourt, P.** (2012). Strigolactones as small molecule communicators. *Molecular BioSystems*, 8(2), 464–469.
- Turečková, V., Novák, O., & Strnad, M.** (2009). Profiling ABA metabolites in *Nicotiana tabacum* L. leaves by ultra-performance liquid chromatography-electrospray tandem mass spectrometry. *Talanta*, 80(1), 390–399.
- Tvorogova, V. Y., Osipova, M. A., Doduyeva, I. Y., & Lutova, L. A.** (2013). Interactions between transcription factors and phytohormones in the regulation of plant meristem activity. *Russian Journal of Genetics: Applied Research*, 3(5), 325–337.
- Urbanová, T., Tarkowská, D., Novák, O., Hedden, P., & Strnad, M.** (2013). Analysis of gibberellins as free acids by ultra performance liquid chromatography-tandem mass spectrometry. *Talanta*, 112, 85–94.
- Van Berkel, K., de Boer, R. J., Scheres, B., & ten Tusscher, K.** (2013). Polar auxin transport: models and mechanisms. *Development*, 140(11), 2253–68.
- Van Huijsduijnen, R., Alblas, S., De Rijk, D., & Bol, J.** (1986). Induction by salicylic acid of pathogenesis-related proteins and resistance to alfalfa mosaic virus infection in various plant species. *Journal of General Virology*, 67(1986), 2135–2143.
- Van Meulebroek, L., Bussche, J. Vanden, Steppe, K., & Vanhaecke, L.** (2012). Ultra-high performance liquid chromatography coupled to high resolution Orbitrap mass spectrometry for metabolomic profiling of the endogenous phytohormonal status of the tomato plant. *Journal of Chromatography A*, 1260, 67–80.
- Vanstraelen, M., & Benková, E.** (2012). Hormonal interactions in the regulation of plant development. *Annual Review of Cell and Developmental Biology*, 28, 463–87.
- Vieten, A., Sauer, M., Brewer, P. B., & Friml, J.** (2007). Molecular and cellular aspects of auxin-transport-mediated development. *Trends in Plant Science*, 12(4), 160–168.
- Vlot, A. C., Dempsey, D. A., & Klessig, D. F.** (2009). Salicylic acid, a multifaceted hormone to combat disease. *Annual Review of Phytopathology*, 47(1), 177–206.
- Von Schwartzenberg, K., Lindner, A. C., Gruhn, N., Šimura, J., Novák, O., Strnad, M., Gonneau, M., Nogué, F., & Heyl, A.** (2016). CHASE domain-containing receptors play an essential role in the cytokinin response of the moss *Physcomitrella patens*. *Journal of Experimental Botany*, 67(3), 667–679.
- Von Schwartzenberg, K., Núñez, M. F., Blaschke, H., Dobrev, P. I., Novák, O., Motyka, V., & Strnad, M.** (2007). Cytokinins in the bryophyte *Physcomitrella patens*: analyses of activity, distribution, and cytokinin oxidase/dehydrogenase overexpression reveal the role of extracellular cytokinins. *Plant Physiology*, 145(3), 786–800.

- Wang, B., Chu, J., Yu, T., Xu, Q., Sun, X., Yuan, J., Xiong, G., Wang, G., Wang, Y., & Li, J.** (2015). Tryptophan-independent auxin biosynthesis contributes to early embryogenesis in *Arabidopsis*. *Proceedings of the National Academy of Sciences*, *112*(15), 4821–4826.
- Wang, Y., Li, K., & Li, X.** (2009). Auxin redistribution modulates plastic development of root system architecture under salt stress in *Arabidopsis thaliana*. *Journal of Plant Physiology*, *166*(15), 1637–1645.
- Wang, Y., Mopper, S., & Hasenstein, K. H.** (2001a). Effects of salinity on endogenous ABA, IAA, JA, and SA in *Iris hexagona*. *Journal of Chemical Ecology*, *27*(2), 327–342.
- Wang, Z. Y., Seto, H., Fujioka, S., Yoshida, S., & Chory, J.** (2001b). BRI1 is a critical component of a plasma-membrane receptor for plant steroids. *Nature*, *410*(6826), 380–383.
- Wasternack, C., & Hause, B.** (2002). Jasmonates and octadecanoids: signals in plant stress responses and development. *Progress in Nucleic Acid Research and Molecular Biology*, *72*, 165–221.
- Wasternack, C., & Hause, B.** (2013). Jasmonates: biosynthesis, perception, signal transduction and action in plant stress response, growth and development. An update to the 2007 review in *Annals of Botany*. *Annals of Botany*, *111*(6), 1021–1058.
- Wasternack, C., & Kombrink, E.** (2010). Jasmonates: structural requirements for lipid-derived signals active in plant stress responses and development. *ACS Chemical Biology*.
- Waters, M. T., Scaffidi, A., Sun, Y. K., Flematti, G. R., & Smith, S. M.** (2014). The karrikin response system of *Arabidopsis*. *Plant Journal*, *79*(4), 623–631.
- Went, F. W., & Thimann, K. V.** (1937). *Phytohormones*. New York The Macmillan Company.
- Werner, T., Motyka, V., Strnad, M., & Schmülling, T.** (2001). Regulation of plant growth by cytokinin. *Proceedings of the National Academy of Sciences of the United States of America*, *98*(18), 10487–92.
- Werner, T., & Schmülling, T.** (2009). Cytokinin action in plant development. *Current Opinion in Plant Biology*, *12*(5), 527–538.
- Wildermuth, M. C., Dewdney, J., Wu, G., & Ausubel, F. M.** (2001). Isochorismate synthase is required to synthesize salicylic acid for plant defence. *Nature*, *414*(6863), 562–565.
- Wilkinson, S., & Davies, W. J.** (2010). Drought, ozone, ABA and ethylene: new insights from cell to plant to community. *Plant, Cell and Environment*, *33*(4), 510–525.
- Willige, B. C., Ghosh, S., Nill, C., Zourelidou, M., Dohmann, E. M. N., Maier, A., & Schwechheimer, C.** (2007). The DELLA domain of GA INSENSITIVE mediates the interaction with the GA INSENSITIVE DWARF1A gibberellin receptor of *Arabidopsis*. *Plant Cell*, *19*(4), 1209–20.
- Woodward, A. W., & Bartel, B.** (2005). Auxin: regulation, action, and interaction. *Annals of Botany*, *95*(5), 707–735.
- Wulfetange, K., Lomin, S. N., Romanov, G. a, Stolz, A., Heyl, A., & Schmülling, T.** (2011). The cytokinin receptors of *Arabidopsis* are located mainly to the endoplasmic reticulum. *Plant Physiology*, *156*(8), 1808–1818.
- Xie, D.-X., Feys, B. F., James, S., Nieto-Rostro, M., & Turner, J. G.** (1998). *COI1*: An *Arabidopsis* Gene Required for Jasmonate-Regulated Defense and Fertility. *Science*, *280*(5366), 1091–1094.
- Xie, X., Yoneyama, K., & Yoneyama, K.** (2010). The Strigolactone Story. *Annual Review of Phytopathology*, *48*(1), 93–117.
- Yamada, H., Suzuki, T., Terada, K., Takei, K., Ishikawa, K., Miwa, K., Yamashino, T., & Mizuno, T.** (2001). The *Arabidopsis* AHK4 histidine kinase is a cytokinin-binding receptor that transduces cytokinin signals across the membrane. *Plant and Cell Physiology*, *42*(9), 1017–23.
- Yamaguchi, S.** (2008). Gibberellin Metabolism and its Regulation. *Annual Review of Plant Biology*, *59*(1), 225–251.
- Yan, S., & Dong, X.** (2014). Perception of the plant immune signal salicylic acid. *Current Opinion in Plant Biology*, *0*, 64–68.
- Yan, Y., Borrego, E., & Kolomiets, M. V.** (2013). Jasmonate Biosynthesis, Perception and Function in Plant Development and Stress Responses. In R. V. Baez (Ed.), *Lipid Metabolism* (Chapter 16). *InTech*.

- Yao, R., Ming, Z., Yan, L., Li, S., Wang, F., Ma, S., Yu, C., Yang, M., Chen, L., Chen, L., Li, Y., Yan, C., Miao, D., Sun, Z., Yan, J., Sun, Y., Wang, L., Chu, J., Fan, S., He, W., Deng, H., Nan, F., Li, J., Rao, Z., Lou, Z., & Xie, D.** (2016). DWARF14 is a non-canonical hormone receptor for strigolactone. *Nature*, 536(7617), 469–473.
- Zažimalová, E., Křeček, P., Skůpa, P., Hoyerová, K., & Petrášek, J.** (2007). Polar transport of the plant hormone auxin - The role of PIN-FORMED (PIN) proteins. *Cellular and Molecular Life Sciences*, 64(13), 1621–1637.
- Zeevaart, J. A. D., & Creelman, R. A.** (1988). Metabolism and physiology of abscisic acid. *Annual Review of Plant Physiology and Plant Molecular Biology*, 39, 439–473.
- Zhang, Q., Li, G., Xiao, X., Zhan, S., & Cao, Y.** (2016). Efficient and selective enrichment of ultratrace cytokinins in plant samples by magnetic perhydroxy-cucurbit[8]uril microspheres. *Analytical Chemistry*, 88(7), 4055–4062.
- Zhang, Y., Li, Y., Hu, Y., Li, G., & Chen, Y.** (2010). Preparation of magnetic indole-3-acetic acid imprinted polymer beads with 4-vinylpyridine and β -cyclodextrin as binary monomer via microwave heating initiated polymerization and their application to trace analysis of auxins in plant tissues. *Journal of Chromatography A*, 1217(47), 7337–7344.
- Zhang, Y., Zhang, B., Yan, D., Dong, W., Yang, W., Li, Q., Zeng, L., Wang, J., Wang, L., Hicks, L. M., & He, Z.** (2011). Two *Arabidopsis* cytochrome P450 monooxygenases, CYP714A1 and CYP714A2, function redundantly in plant development through gibberellin deactivation. *Plant Journal*, 67(2), 342–353.
- Zhao, Y.** (2012). Auxin biosynthesis: a simple two-step pathway converts tryptophan to indole-3-Acetic acid in plants. *Molecular Plant*, 5(2), 334–338.
- Zhou, R., Cutler, A. J., Ambrose, S. J., Galka, M. M., Nelson, K. M., Squires, T. M., Loewen, M. K., Jadhav, A. S., Ross, A. R. S., Taylor, D. C., & Abrams, S. R.** (2004). A new abscisic acid catabolic pathway. *Plant Physiology*, 134(1), 361–369.
- Zhu, J. K.** (2002). Salt and drought stress signal transduction in plants. *Annual Review of Plant Biology*, 53(1), 247–273.
- Zhu, L., Bu, Q., Xu, X., Paik, I., Huang, X., Hoecker, U., Deng, X. V., & Huq, E.** (2015). CUL4 forms an E3 ligase with COP1 and SPA to promote light-induced degradation of PIF1. *Nature Communications*, 6, 7245.
- Zürcher, E., & Müller, B.** (2016). Cytokinin synthesis, signaling, and function—advances and new insights. In *International Review of Cell and Molecular Biology* (Vol. 324).
- Žižková, E., Kubeš, M., Dobrev, P. I., Příbyl, P., Šimura, J., Zahajská, L., Záveská Drábková, L., Novák, O., & Motyka, V.** (2017). Control of cytokinin and auxin homeostasis in cyanobacteria and algae. *Annals of Botany*, 119(1), 151–166.

7 Supplements I-VI

The work undertaken by the author of this thesis is fully described in the multi-author papers attached as Supplements I-VI.

- I. **Šimura, J.**, Antoniadis, I., Šíroká, J., Tarkowská, D., Strnad, M., Ljung, K., Novák, O. (2017) Plant hormonomics: multiple phytohormone profiling by targeted metabolomics. (manuscript submitted, *Plant Physiology*)
- II. Žižková, E., Kubeš, M., Dobrev, P., I., Příbyl, P., **Šimura, J.**, Zahajská, L., Záveská Drábková, L., Novák, O., & Motyka, V. (2017). Control of cytokinin and auxin homeostasis in cyanobacteria and algae. *Annals of Botany*, 119(1), 151–166.
- III. Frébortová, J. Plíhal, O., Florová, V., Kokáš, F., Kubiasová, K., Greplová, M., **Šimura, J.**, Novák, O., Frébort, I. (2017) Light influences cytokinin biosynthesis and sensing in *Nostoc* (Cyanobacteria). *Journal of Phycology*, 53, 703–714.
- IV. **Šimura, J.**, Spíchal, L., Adamec, L., Pěňčík, A., Rolčík, J., Novák, O., & Strnad, M. (2016). Cytokinin, auxin and physiological polarity in the aquatic carnivorous plants *Aldrovanda vesiculosa* and *Utricularia australis*. *Annals of Botany*, 117(6), 1037-1044.
- V. Humplík, J. F., Bergougnoux, V., Jandová, M., **Šimura, J.**, Pěňčík, A., Tomanec, O., Rolčík, J., Novák, O., & Fellner, M. (2015). Endogenous abscisic acid promotes hypocotyl growth and affects endoreduplication during dark-induced growth in tomato (*Solanum lycopersicum L.*). *PLoS ONE*, 10(2).
- VI. Von Schwartzenberg, K., Lindner, A. C., Gruhn, N., **Šimura, J.**, Novák, O., Strnad, M., Gonneau, M., Nogué, F., & Heyl, A. (2015). CHASE domain-containing receptors play an essential role in the cytokinin response of the moss *Physcomitrella patens*. *Journal of Experimental Botany*, 67(3), 667-679.

Supplement I

Šimura, J., Antoniadou, I., Široká, J., Tarkowská, D., Strnad, M., Ljung, K., Novák, O. (2017)
Plant hormonomics: multiple phytohormone profiling by targeted metabolomics. (manuscript
submitted, *Plant Physiology*)

RUNNING TITLE

Multiple phytohormone screening method

CORRESPONDING AUTHORS

Ondřej Novák

Laboratory of Growth Regulators, Centre of the Region Haná for Biotechnological and Agricultural Research, Institute of Experimental Botany AS CR & Faculty of Science of Palacký University, Šlechtitelů 27, CZ-78371 Olomouc, Czech Republic

E-mail: novako@ueb.cas.cz

tel: +420585634853, fax: +420585634870.

RESEARCH AREAS

Breakthrough Technologies

Plant hormonomics: multiple phytohormone profiling by targeted metabolomics

Jan Šimura, Ioanna Antoniadis, Jitka Šíroková, Danuše Tarkowská, Miroslav Strnad, Karin Ljung, Ondřej Novák*

Laboratory of Growth Regulators, Centre of the Region Haná for Biotechnological and Agricultural Research, Institute of Experimental Botany, Czech Academy of Sciences, and Faculty of Science, Palacký University, Šlechtitelů 27, CZ-783 71, Olomouc, Czech Republic (J.Š., Ji.Š., D.T., M.S., O.N.); Department of Chemical Biology and Genetics, Centre of the Region Haná for Biotechnological and Agricultural Research, Faculty of Science, Palacký University, Šlechtitelů 27, CZ-783 71, Olomouc, Czech Republic (J.Š.); Umeå Plant Science Centre, Department of Forest Genetics and Plant Physiology, Swedish University of Agricultural Sciences, SE-90183 Umeå, Sweden (I.A., K.L.)

ONE SENTENCE SUMMARY

A method for concurrent quantification of 101 metabolites representing the metabolic flux of seven major classes of plant hormones provides a simple and sensitive tool for phytohormonal studies.

FOOTNOTES

List of author contributions

J.Š., I.A., K.L. and O.N. designed the study; J.Š., D.T. and O.N. participated in development of the experimental protocol; J.Š. performed most of the experiments; J.Š., I.A. and Ji.Š. analyzed data; J.Š. and O.N. wrote the article with contributions of all the authors; D.T., M.S., K.L. and O.N. supervised the research.

Funding information

This work was funded by the Internal Grant Agency of Palacký University (project no. IGA_PrF_2017_010), the Ministry of Education, Youth and Sports of the Czech Republic (National Program for Sustainability I, grant no. LO1204) and the Czech Science Foundation (grant no. GA14-34792S). Support was also provided by the Swedish Governmental Agency for Innovation Systems (Vinnova) and the Swedish Research Council (VR) to K.L. and I.A.

* Address correspondence to novako@ueb.cas.cz

ABSTRACT

Plant hormones are highly physiologically important signaling molecules divided into several structurally different groups, such as purine and indole derivatives, plant steroids, lipid-based substances and terpenoid carboxylic acids. We present a method for simultaneous targeted profiling of 101 phytohormone-related analytes from minute amounts of fresh plant material (<20 mg). Rapid and non-selective extraction, fast one-step sample purification and extremely sensitive ultra-high liquid chromatography-tandem mass spectrometry (UHPLC-MS/MS) enables concurrent quantification of the main phytohormonal classes: cytokinins, auxins, brassinosteroids, gibberellins, jasmonates, salicylates and abscisates. Our targeted analysis allows quantification of a large spectrum of these hormonal compounds, which play essential roles in intricate signaling networks that regulate diverse processes in plants. This ‘hormonomic’ approach was validated by application to salt-stressed and control *Arabidopsis thaliana* seedlings. Subsequent multivariate statistics data processing and cross-validation with transcriptomic data clearly highlighted the main hormone metabolites involved in plant adaptation to salt stress.

INTRODUCTION

During the last decade, techniques used in metabolomic analyses have advanced tremendously. In plant science, the mostly widely used methods are based on separation by liquid chromatography (LC) or gas chromatography (GC) combined with tandem mass spectrometric detection (MS/MS). The main advantages of these combinations are high sensitivity and versatility. To enhance signals of trace compounds, such as the plant hormones (phytohormones) considered here, it is essential to reduce the influence of abundant interfering compounds present in plant matrices by rigorous purification of extracts before the instrumental analysis (Du et al., 2012). The sample preparation steps usually include solid phase extraction (SPE) with general purpose sorbents or more selective immunosorbents that specifically target selected compounds (Pěňčík et al., 2009; Turečková et al., 2009; Plačková et al., 2017; Oklestkova et al., 2017). Many analytical methods (particularly the immunological methods) have been described for determination of a single compound or specific class of phytohormones (Du et al., 2012; Tarkowská et al., 2014). However, there is growing interest in methods capable of simultaneously analyzing phytohormones of several classes together with their precursors and metabolites, for the following reasons.

Phytohormones are naturally occurring signaling molecules, which play key roles in the complex cell-cell communication required for regulation of plant physiology, development, and adaptation to environmental stimuli. Generally, their concentrations in plant tissues are extremely low (fmol-pmol/g fresh weight, FW). They are also extremely diverse compounds with wide ranges of physicochemical properties, divided into several structural classes: cytokinins (CKs) and 2-methylthio cytokinins (2MeSCKs), auxins (AXs), ethylene, gibberellins (GAs), abscisic acid and its metabolic products (hereafter abscisates, ABAs), brassinosteroids (BRs), jasmonates (JAs), salicylic acid (SA) and strigolactones (Davies, 2010; Zwanenburg et al., 2016). Their biological activities depend on their availability, which is controlled by their biosynthetic and metabolic rates, cellular and subcellular localization, transport, and responses of the signal perception and transduction pathways (Davies, 2010). Modulations at all these levels can directly affect myriads of physiological processes. Moreover, although certain phytohormones are usually related to specific biological functions or responses, there is increasing evidence that plant hormone signaling involves complex interactions ('crosstalk') among all the pathways involved (Vanstraelen and Benková, 2012). Indeed, this is hardly surprising as plants in natural environments may have to cope simultaneously with (for example) salt, water and temperature stresses, pathogen attack, competition and a need to complete certain physiological processes within environmentally-dictated timeframes. Thus, plants' physiological regulation involves complex coordination of the biosynthesis, transport and metabolism of multiple hormones, their highly interacting signal transduction pathways, transcription factors and responsive genes.

Clearly, a convenient method to simultaneously quantify as wide ranges as possible of plant signaling molecules of all known classes would greatly facilitate the investigation of hormone functions and networks. Thus, several plant hormone profiling techniques have been published, and the number of covered compounds is increasing (Chiwoka et al., 2003; Pan et al., 2008; Kojima et al., 2009; Farrow and Emery, 2012; Cao et al. 2016; Wang et al., 2017). The most extensive analysis of primary and secondary metabolites published to date included 53 plant hormone-related compounds (Schäfer et al., 2016), and a more focused analysis of plant growth substances covered 54 compounds (Cai et al., 2016). However, there is scope for further extension. An ideal method should provide both a qualitative overview and precise quantitative information for all covered compounds. It also requires appropriate sample preparation and high instrumental performance (in terms of both robustness and sensitivity), due to phytohormones' low concentrations (relative to those of primary and secondary metabolites) and wide ranges of chemical structure and stability.

Here we present methodology with these features, designed to afford rapid, sensitive and simultaneous LC-MS/MS-based profiling of 101 CKs, AXs, GAs, BRs, ABAs, JAs and SA. The analytes include bioactive forms of the hormones, their precursors and metabolites to acquire quantitative snapshots of sampled tissues' physiological status (Supplemental Table S1). The protocol for isolating all 101 compounds combines rapid one-step non-selective extraction from milligram amounts of plant tissues (< 20 mg FW) followed by their LC separation and extremely sensitive MS-based quantification. To assess the practical utility of this 'hormonomic' approach it was applied to characterize phytohormone profiles in root and shoot tissues of control and salt-stressed *Arabidopsis* seedlings. Our results highlight the value of such analysis, which (together with multivariate data analysis and cross-validation with transcriptomic data), revealed the seedlings' hormonal responses to salinity stress—one of the major factors limiting crop production (Munns and Tester, 2008) and differences in responses of their roots and shoots.

RESULTS

One-step extraction of distinct phytohormone classes

In an attempt to effectively extract targeted compounds while avoiding their decomposition by elevated temperatures and enzymatic degradation (Ulijn et al., 2002), we used ice-cold acetonitrile (ACN) as an organic solvent. This has also been used in several previous analyses of hydrophobic phytohormones, such as diterpenoid GAs (Urbanová et al., 2013) and triterpenoid BRs (Tarkowská et al., 2016). We tested aqueous water:ACN mixtures with ACN contents ranging from 0 to 100% (vol/vol), focusing on the solubility of the most hydrophobic compounds included in our study (BRs). Further, to quantify impairment of the final LC-MS/MS analysis by signal suppression, contents of the

most abundant interfering plant pigments, chlorophyll a (Chl_a) and b (Chl_b), were determined. The solubility of all investigated BRs (measured as a percentage of maximal signal intensity) reached on average 95 % in solvents with $\geq 50\%$ ACN (vol/vol) (Fig. 1A), however, the concentration of interfering plant pigments also rapidly increased with increases in ACN (Fig. 1B). Thus, cold 50% ACN was selected as the optimal extraction solvent, providing the best balance between signal intensity for selected phytohormones and chlorophyll co-extraction (Fig. 1).

It was also essential to consider the chemical stability of the wide spectrum of targeted analytes during sample preparation. For instance, GAs are pH-sensitive and should only be exposed to solvents with pH 2.5 – 8.5 (Urbanová et al., 2013). To test the pH sensitivity of our analytes, we dissolved selected metabolites (Fig. 1C) in aqueous solutions of 1 M formic acid (pH < 3), 0.35 M NH₄OH in 60% MeOH (vol/vol, pH > 12) and 50% ACN solution (as a control); solutions that are often used during sample preparation of CKs and other phytohormones using ion-exchange SPE (Dobrev and Kamínek, 2002; Kojima et al., 2009; Závěská Drábková et al., 2015; Schäfer et al., 2016). A mixture with known amounts of each compound (0.4 pmol of CKs and JAs, with 4 pmol of AXs and GAs) was incubated in each solution for 15 min at 4 °C. After evaporation under a gentle stream of gaseous nitrogen, samples were dissolved in 30% ACN and analyzed by LC-MS/MS. Peak areas of each compound relative to corresponding peaks area in control samples were then calculated (Fig. 1C). In alkaline solvents, levels of most of the tested compounds remained close to those found in control samples, but in tested acidic extraction solvents recoveries of GAs, JAs and indole-3-acetic acid (IAA) amino acid conjugates were significantly lower compared to control samples. To preserve levels of all targeted compounds, and limit their possible structural changes and hydrolysis during sample preparation, the extraction solvent with no additives was used in all subsequent phytohormone experiments (see scheme in Fig. 1D).

Reduction of a complex plant matrix by a highly efficient purification step

In the simultaneous analysis of phytohormones several multistep SPE methods combining use of either silica-based reversed-phase (RP) sorbents with long 18-carbon alkyl chains (C₁₈) or polymer-based RP materials with ion-exchange properties (mixed-mode sorbents) have proven efficacy for purifying samples and enrichment of the targeted analyte fraction (Kojima et al, 2009; Balcke et al., 2012; Floková et al., 2014; Závěská Drábková et al., 2015; Schäfer et al., 2016; Cao et al., 2016). These approaches often work with solvents of various pH values, but (as mentioned above) the pH sensitivity of some of our analytes limited the use of acidic conditions during sample preparation. Moreover, sample preparation utilizing multiple step SPEs is very time consuming and often includes several evaporation steps, which significantly reduce the effectiveness of sample preparation protocols, especially for highly volatile compounds such as jasmonates (Floková et al., 2014). To avoid these problems, we used the initially applied organic solvent without any additives as both

sample extraction and SPE loading solution (Fig. 1D), thus eliminating one evaporation step, reducing effects of the plant matrix and minimizing losses caused by enzymatic degradation and pH-dependent hydrolysis. To remove co-extracted plant pigments with maximum efficiency while maintaining high analyte recovery, we utilized RP polymer-based SPE Oasis[®] HLB columns packed with a hydrophilic-lipophilic-balanced water-wettable sorbent. Recoveries following this purification step were studied using extracts from 20 mg FW of *Arabidopsis* plant material supplemented with authentic phytohormone standards before and after SPE purification steps (Caban et al., 2012; see Materials and Methods). The HLB sorbent was used to retain possible interfering compounds while targeted compounds passed through the SPE column sorbent in the loading step (the flow-through fraction) or were subsequently eluted with 30% ACN (vol/vol). These fractions were pooled, and average total extraction yields per class ranged from 87 to 97 % except for brassinosteroids 52 % (Table 1; Supplemental Table S2). Samples were further evaporated under a gentle stream of gaseous nitrogen then dissolved in 40 µl of 30% ACN prior to MS/MS-based analysis (Fig. 2).

Profiling of 101 phytohormones by ultrafast LC-MS/MS

One of the main inherent difficulties in profiling more than 100 plant hormones (Supplemental Table S1) is that many of the compounds have similar core structures, including isomers with the same MS fragmentation patterns (*e.g.* *cis*- and *trans*-zeatin, topolin isomers, brassinolide and 24-*epi*brassinolide, castasterone and 24-*epi*castasterone). To optimize baseline separation, we tested two RP ultra-high performance liquid chromatography (UHPLC) columns packed with charged surface hybrid (CSH) and ethylene bridged hybrid (BEH) polymer-based sub-2 µm sorbents. In good agreement with previously reported results (Urbanová et al., 2013; Floková et al., 2014), the CSH column provided better peak shapes and peak-to-peak resolution of the above-mentioned isomeric compounds than the BEH column (Fig. 2A). Moreover, the composition of the mobile phase and use of different mobile phase additives strongly influenced the separation, peak shapes and analyte ionization. Cao et al. (2016) found that increasing the concentration of formic acid in the range from 0.05 to 0.2 % impaired CK separation, we achieved baseline separation of CK isomers on the CSH column using isocratic elution with 0.01% formic acid in both mobile phase solutions (water and ACN) (Fig. 2B). Moreover, volatile buffers and additives are commonly used in LC-MS/MS analyses due to their ability to enhance analyte ion yields during ionization in the electrospray ion source (ESI) of the MS instrument. Under our chromatographic conditions, limits of detection (LODs) for the 101 targeted plant hormones and their metabolites ranged on average from 0.01 fmol for CKs ribosides to 100.5 fmol for *nor*CS. The LODs and limits of quantification (LOQs) were defined as 3 and 10 times the noise level, respectively (for details, see Table 1 and Supplemental Table S2).

Retention times of the 101 targeted compounds were further determined by separate injections and compared with those of 71 stable-isotope-labelled standards. Each non-labelled and stable-

isotope-labelled couple co-eluted with the same or almost identical retention time, although deuterated analogues usually eluted slightly earlier than corresponding authentic standards due to the chromatographic isotope effect (Pratt, 1986). Not all compounds were separated to baseline (Fig. 2), but their determination in multiple reaction monitoring (MRM) mode allowed precise detection due to specific precursor to product ion transitions in the fragmentation of co-eluting compounds (see Supplemental Table S3). Appropriate precursor ions ($[M+H]^+$ or $[M-H]^-$) and the most abundant product ions for each compound were carefully selected, partly for this purpose. The metabolites of CKs, 2-methylthio CKs (2MeSCKs), AXs, BRs, some JA precursors and its amino acid conjugates were determined in positive ESI(+) mode, which provided good agreement with previously published data (Tarkowski et al., 2010; Novák et al., 2012; Svačinová et al., 2012; Floková et al., 2014; Tarkovská et al., 2016). All other phytohormones (including ABAs, GAs, SA and JAs) were determined in negative ESI(-) mode (Turečková et al., 2009; Urbanová et al., 2013; Floková et al., 2014). Finally, the collision energy and cone voltage were optimized to maximize signal intensities. The optimized conditions are listed in Supplemental Table S3.

The proposed method was initially designed for simultaneous analysis of positively and negatively charged ions, utilizing both MRM modes (polarity switching) in single analytical run. However, the ESI(-) mode is known to be generally less sensitive than the positive mode, and polarity switching for simultaneous analysis of 101 phytohormones caused further 5- to 10-fold reductions in signal intensity of negatively charged compounds (*see* Supplemental Fig. 1). Therefore, to improve the sensitivity of MS-based detection, samples were analyzed in two separate runs under the same chromatographic conditions, with the flow rate set to 0.5 ml min^{-1} and the column temperature to 50°C . Under these conditions, UHPLC-ESI-MS/MS analysis of the targeted compounds in one sample takes 32 min in total (Fig. 2, C and D). To further increase signal intensity, the 17 and 15 min chromatographic separations of the targeted analytes in ESI(+) and ESI(-) modes, respectively, were both divided into nine MRM scan segments.

Calibration curves constructed after repeatedly injecting standard solutions revealed a broad linear concentration range for most compounds, spanning at least three orders of magnitude with R^2 values ≥ 0.993 (Supplemental Table S3). The method sensitivity and linearity were found to be comparable to those reported by authors using tandem mass spectrometry for simultaneous phytohormone analysis (Kojima et al., 2009; Balcke et al., 2012; Floková et al., 2014; Závěská Drábková et al., 2015; Cai et al., 2016; Schäfer et al., 2016; Delatorre et al., 2017).

Method validation and quantification of hormones in plants under salinity stress

Using the standard isotope dilution method, concentrations of all the analytes were calculated as ratios of non-labelled compounds to labelled internal standards or closely eluting stable isotope-labelled tracers (Supplemental Table S3). To validate the UHPLC-MS/MS method, spiked

Arabidopsis seedling extracts were analyzed and the endogenous levels were subtracted from the amounts of non-labelled standards added (see Materials and Methods). Finally, the calculated concentrations of each analyte were compared with the known amounts added to samples and are presented as method accuracy, ranging in average from 5.2% bias (CKs) to 8.68% bias (SA). Method precision was calculated as the relative standard deviation of analyte concentrations determined in three replicates. The mean precision ranged in average from 1.06% RSD (ABAs) to 7.8% RSD (BRs) (Table 1, Supplemental Table S2). The overall validation parameters of the developed method demonstrate its reliability and utility for simultaneous quantification of multiple classes of phytohormones in minute amounts of plant material.

To assess the applicability of the newly developed targeted metabolomics approach, we used it in a comparison of hormone-related transcript and metabolite levels in samples of root and shoot tissues (<20 mg FW) of stressed *Arabidopsis* plants and controls. Published microarray data sets were screened to identify a stimulus that affects genes involved in most phytohormone metabolic pathways (Fig. 4, Supplemental Table S4). This bioinformatics analysis was performed in an unsupervised manner (without checking for up- or down-regulation). Salinity stress was identified as an appropriate condition, which is likely to cause major alterations in metabolite levels of most hormones and corresponding changes in transcript profiles.

Therefore, we gently transferred 12-day-old *Arabidopsis* seedlings to new media with and without Supplemental 150 mM NaCl for an additional 48 hours. Shoots and roots were harvested separately, and their hormonomic profiles were examined (Supplemental Table S7). In total, 45 endogenous compounds out of the 101 phytohormone-related analytes were detected in both root and shoot samples. Two brassinosteroids (24-*epi*BL and 28-*nor*CS) were identified, but their levels were sub-LOQ. Thus, they were omitted in subsequent statistical data analysis. According to Student's t-test, levels of 23 of 43 determined compounds significantly differed between samples of roots of salt-stressed and control seedlings (Fig. 3E), and levels of 15 differed between their shoots (Fig. 3F). In addition, multivariate statistical analysis revealed clear separation between root and shoot samples' hormone profiles, and between control and salt-stressed seedlings' profiles (Fig. 3B). OPLSDA based S-plots revealed compounds that were strongly affected by salinity stress, and thus were primarily responsible for the latter separation (Fig. 3, C and D).

The hormonomic results (Fig. 3, E and F) were further cross-validated by comparing the transcriptomic data (Fig. 4, C and D, and Supplemental Tables 5 and 6) and hormonal profiles (Fig. 3, E and F). ABAs and JAs, often referred to as plant stress hormones, have been previously shown to promote salt tolerance (Ryu and Cho, 2015). Accordingly, salt stress was associated with increases in levels of ABA, its oxidation products phaseic acid (PA) and dihydrophaseic acid (DPA) and JA in roots, together with up-regulation of JA biosynthesis and ABA biosynthesis and oxidation genes. Similar correspondence was found between GA metabolite and transcript profiles, and differential

responses of the active GA₄ to salt stress in shoots and roots. GA biosynthesis and inactivation genes (*KO* and *GA2ox*, encoding *ent*-kaurene oxidase and gibberellin 2-oxidase, respectively) were induced in both tissues under salt stress. However, *GA3ox*, catalyzing the last biosynthetic step of bioactive GAs, was only induced in shoots, in accordance with an observed increase in GA₄ concentration in this tissue. In contrast, auxin and cytokinin metabolite outputs showed a more dynamic balance that could not be readily linked to changes in expression profiles of genes involved in their biosynthesis and metabolism under salinity stress. These findings suggest that physiological responses to stimuli such as salinity are not controlled solely by a single active form of a hormone (or even single active forms of several hormones), but by combined activities and ratios of multiple hormones, metabolites and (hence) genes. Our hormonomic analysis and the cross-validation with transcriptomic data highlight the value of such profiling methods, which provide potent tools to assess not only transcript levels but also levels of corresponding metabolites in samples, thereby obtaining global views of hormonal responses and interactions.

DISCUSSION

We present here a ‘plant hormonomics’ technique, involving a non-selective extraction and SPE purification followed by high-throughput UHPLC-ESI-MS/MS separation and analysis, for profiling 101 phytohormones and their metabolites in a single plant sample. Several challenges were addressed during its development, and should be considered in any attempts to establish such techniques. First, use of an appropriate extraction solvent is crucial to reduce levels of interfering substances, but efficiently extract the analytes from plant tissues. This poses a dilemma, because increasing concentrations of organic solvents, such as methanol, ethanol, acetonitrile, isopropanol and chloroform (singly or in various combinations) generally increases the extraction efficiency of both the analytes and interfering substances (*e.g.* pigments, proteins, phenolics or lipids). Such ballast compounds increase background noise, detection limits, risks of analytes co-eluting with other substances and fouling of the instruments (Tarkowská et al., 2014). Thus, at least one effective purification step before final MS-based analysis is desirable (Nováková and Vlčková, 2009), or even essential for high-throughput analyses. Therefore, our protocol includes extraction of samples with an optimized solvent (50 % aqueous ACN) and purification of the extracts by one-step non-selective reversed phase SPE. Moreover, to prevent pH-dependent hydrolysis and/or other structural changes that may occur during extraction (Novák et al., 2012), we have avoided use of acidified solvents during sample extraction and purification.

LC was selected partly because most known phytohormones are non-volatile compounds that require chemical derivatization for GC- (but not LC-) MS-based multi-targeted profiling (Müller et al.,

2002; Birkemeyer et al., 2003). The increasing availability of chromatographic columns with diverse physicochemical properties has also significantly improved the versatility of LC techniques. Furthermore, the rapid development of ultra-high performance liquid chromatography (UHPLC), using columns with sub-2 μm particles, has greatly improved separation, resolution, sensitivity and overall speed of LC-based analytical methods (Nováková, 2013). Thus, LC is now the most robust, convenient and widely utilized technique for simultaneous phytohormone analysis (Kojima et al., 2009; Müller & Munné-Bosch, 2011; Balcke et al., 2012; Floková et al., 2014; Závěská Drábková et al., 2015; Cai et al., 2016; Cao et al., 2016; Schäfer et al., 2016; Delatorre et al., 2017; Wang et al., 2017).

Combining one-step non-selective SPE with optimized UHPLC-MS/MS, including use of a 1.7 μm particle size reversed-phase C_{18} column, enabled sensitive and selective quantification of 101 underivatized phytohormones and related compounds in two independent 17-min ($[\text{M}+\text{H}]^+$) and 15-min ($[\text{M}+\text{H}]^-$) chromatographic runs. The optimized method was applied to the phytohormone profiling of *Arabidopsis* plants grown under salt stress and control conditions. More than 40 phytohormones and their metabolites in single plant samples were quantified simultaneously. Uni- and multi-variate analysis of the acquired data revealed significant differences in profiles of these compounds between roots and shoots, and between controls and salt-stressed plants. The analysis also revealed compounds primarily responsible for the significant differences in profiles, which mostly corresponded well with transcriptomic data. The cross-validation of the hormonal results with salt stress- induced changes in gene expression thus highlights the potential of this technique in unravelling the network of plant hormone signaling cascades.

In summary, our method for phytohormone profiling provides a simple, sensitive and powerful tool for phytohormonal studies. The validation experiments, in conjunction with the demonstration of the hormonal method's accuracy and precision, confirm its reliability and utility for routine quantifications of phytohormones in minute amounts of plant tissue.

MATERIALS AND METHODS

Chemicals and material

Authentic standards and their isotopically labelled counterparts are listed in Supplementary Table 1). Cytokinins, auxins, gibberellins, jasmonates, salicylic acid, abscisic acid, phaseic acid, brassinosteroids and their corresponding isotopically labelled analogues were purchased from Olchemim Ltd. (Olomouc, Czech Republic) and Chemiclones (Waterloo, Canada), dihydrophaseic acid, neophaseic acid, 7-hydroxy-abscisic acid and their corresponding isotopically labelled analogues were obtained from the compound library of the Laboratory of Growth Regulators (Olomouc, Czech Republic; Turečková et al., 2009). Formic acid (FA), acetonitrile (ACN, UHPLC hypergrade) and methanol (MeOH, UHPLC hypergrade) were purchased from Merck (Darmstadt, Germany). Deionized (Milli-Q) water was obtained using a Simplicity 185 water system (Millipore, Bedford, MA, USA) and used to prepare all aqueous solutions.

Plant material and salinity stress experiment

Arabidopsis thaliana (ecotype Col-0) was used for method validation and the salt stress experiments. Seedlings were grown in petri dishes in standard Murashige and Skoog media, vertically, in a growth chamber under long day conditions at a light intensity of $100 \mu\text{Em}^{-2} \text{s}^{-1}$ (16 h light, 24 °C/8 h dark cycles, 18 °C) for 12 days. On the 12th day, plants assigned to the salt stress treatment were transferred to new medium supplemented with 150 mM NaCl (8.77 g/l) prior to autoclaving, and seedlings were grown vertically for an additional 48 hours. Control seedlings were grown in the same way, and transferred during the 12th day to standard Murashige and Skoog medium. On the 14th day seedlings of both sets were harvested, then shoots and roots were separated, weighed into micro tubes, immediately frozen in liquid nitrogen and stored at - 80 °C until extraction and analysis.

Chlorophyll extraction

Chlorophyll a (Chl_a) and b (Chl_b) were extracted from 100 mg FW samples of *Arabidopsis* seedlings using 1 ml of aqueous ACN at concentrations ranging from 10 to 100% (vol/vol) (n=4, extraction solvent). After extraction and removal of solid particles by centrifugation (20 000 RPM, 4°C, 10 min.), the supernatants were transferred to new Eppendorf tubes and evaporated to dryness under a gentle stream of gaseous nitrogen using a TurboVap[®] LV evaporation system (Caliper Life Sciences, Hopkinton, MA, USA). Before chlorophyll determination the pellets were dissolved in acetone p.a. (Lach-ner, Czech Republic). The light absorbance of the resulting suspensions was measured at 663.2, 646.8 and 750 nm wavelengths using an Infinite[®] 200 PRO spectrophotometer (Tecan, Switzerland) and the sample's chlorophyll contents were calculated according to Lichtenthaler (1987).

Solubility experiment

The solubility of selected brassinosteroids (Supplementary Table 10) was tested by adding 40 μl portions of aqueous ACN, with concentrations ranging from 10 to 70 % (vol/vol), to mixtures containing 50 pmol of each of the compounds in solid state. The samples were thoroughly mixed by sonication for 5 min at 4 °C in a Transsonic T310a laboratory ultrasonicator with an ice block-filled bathtub (Elma GmbH & Co KG, Singen, Germany), then filtered using modified nylon 0.2 μm Centrifugal Filters (VWR International, Czech Republic). Portions (20 μl) of the filtrates were transferred to new insert-equipped vials and analyzed by UHPLC-ESI-MS/MS (2 μl /injection). Finally, average peak areas of each compound extracted in each solvent and relative yields (percentages of average peak areas in each solvent relative to those obtained using the most effective tested solvent) were calculated.

Stability experiment

Portions of solutions containing known amounts of selected analytes (0.4 pmol of CKs and JAs, with 4 pmol of AXs and GAs per sample, n=3; Supplementary Table 9) were transferred to new vials and evaporated to dryness under a gentle stream of gaseous nitrogen using a TurboVap[®] LV evaporation system (Caliper Life Sciences, Hopkinton, MA, USA). The compounds were then dissolved in 1 ml of aqueous solutions of 1 M formic acid (pH < 3), 0.35 M NH₄OH (60% MeOH, vol/vol; pH > 12), or 50% ACN, using ultrasound (5 min, 4 °C; Transsonic T310a laboratory ultrasonicator, Elma GmbH & Co KG, Singen, Germany). After incubation for 15 min at 4 °C, samples were filtered using modified nylon 0.2 μm Centrifugal Filters (VWR International, Czech Republic). Filtered samples were evaporated to dryness as described above, dissolved in 40 μl of 30% ACN and UHPLC-MS/MS analysis (10 μl /injection). Relative peak areas (%) of the compounds were calculated as ratios to respective peak areas obtained from analyses of reference samples in 50% ACN (Fig. 1c).

Sample extraction

For the quantification of targeted plant hormones and related compounds, plant material of 20 mg FW portions of separately harvested roots and shoots were weighed into 2 ml plastic micro tubes (Eppendorf, Germany) and frozen in liquid nitrogen. Before extraction, three 3 mm ceria stabilized zirconium oxide beads (Next Advance Inc., Averill Park, NY, USA) were added to each sample. A mixture of stable isotopically labelled internal standards (IS) was added to validate the method and enable precise quantification of endogenous levels of targeted compounds. The amounts of IS ranged from 0.4 – 50 pmol per sample (precise amounts are listed in Supplementary Table 3). Frozen plant material was extracted in 1 ml of ice-cold 50% aqueous ACN (vol/vol) using a MM 301 vibration mill (Retsch GmbH & Co. KG, Haan, Germany) operating at a frequency of 27 Hz for 5 min. Samples

were then sonicated for 3 min at 4 °C using a Transsonic T310 ultrasonicator with an ice block-filled bathtub (Elma GmbH & Co KG, Singen, Germany) and subsequently extracted using a Stuart SB3 benchtop laboratory rotator (Bibby Scientific Ltd., Staffordshire, UK) for 30 min, 15 rpm at 4 °C. After centrifugation (10 min, 20 000 rpm, 4 °C; Beckman Avanti™ 30) the supernatant was transferred to clean plastic microtubes. Samples were further purified according to the scheme shown in Fig. 3D.

Sample purification

All samples were purified using Oasis® HLB reversed-phase polymer-based solid phase extraction (RP-SPE) cartridges (1 cc/30 mg), obtained from Waters Co. (Milford, MA, USA) that had been washed with 1 ml of 100% MeOH and 1 ml of deionized water, then equilibrated with 50% aqueous ACN (vol/vol). After loading a sample (supernatant obtained following the procedure described above), the flow-through fraction was collected in a glass tube (Fisherbrand™). The cartridge was then rinsed with 1 ml of 30% ACN (vol/vol) and this fraction was collected in the same glass tube as the flow-through fraction. After this single-step SPE, the samples were evaporated to dryness under a gentle stream of nitrogen using a TurboVap® LV evaporation system (Caliper Life Sciences, Hopkinton, MA, USA) and stored at -20 °C until analysis. For UHPLC–ESI–MS/MS analysis, the samples were dissolved in 40 µl of 30% ACN (vol/vol) and transferred to insert-equipped vials, then 20 µl portions of each sample were injected (in two 10 µl injections) into the UHPLC-ESI-MS/MS system.

UHPLC-ESI-MS/MS conditions

Targeted compounds were analyzed using an Acquity UPLC® System equipped with an Acquity UPLC® CSH™ C18 RP column (150 x 2.1 mm, particle size of 1.7 µm) coupled to a triple quadrupole mass spectrometer Xevo® TQ-S MS, all from Waters (Manchester, UK). The mobile UPLC phase consisted of binary gradients of ACN with 0.01% (vol/vol) FA (A) and 0.01% (vol/vol) aqueous FA (B), flowing at 0.5 ml min⁻¹, which depended on the ESI mode, as described below. MassLynx™ software (version 4.1, Waters, Milford, MA, USA) was used to control the instrument and to acquire and then process the MS data.

Separation of compounds detected in ESI positive mode. Analytes were initially eluted isocratically with 5% A (vol/vol) for 5 min, then the proportion of A was increased linearly to 80% over following 10 min. After this the column was washed with 100% A and then re-equilibrated under the initial conditions for 2 min. The column temperature was held at 50 °C.

Separation of compounds detected in ESI negative mode. The mobile phase was the same until the A:B ratio reached 65:35 (vol/vol), in the 13th minute. Then the column was washed with 100% A and re-equilibrated under the initial conditions for 2 min.

During analytical runs in both ESI modes the UHPLC eluate was switched to waste until acquisition of the first targeted compound, and back to waste after elution of the last compound, to minimize impairment of the MS system's sensitivity by ballast compounds. During acquisition of analytes, the eluate was introduced into the electrospray ion source of the tandem MS analyzer operating under the following conditions: source/desolvation temperature, 125/600 °C; cone/desolvation gas flow, 150/1000 L h⁻¹; capillary voltage, 2.1 kV ESI(+), 1.5 kV ESI(-); cone voltage, 10–40 V; collision energy, 12–30 eV; collision gas flow (argon), 0.21 mL min⁻¹. The analyzed compounds and appropriate internal standards were quantified in multiple ion monitoring mode (MRM) using optimized MS conditions (Supplementary Table 3). The dwell times ranged from 8 to 100 ms to provide at least 15 data points across each chromatographic peak using automatic mode. The MRM transitions were recorded over each chromatographic run in 9 targeted scan windows to maximize the MS signal intensity for each compound. For ESI(+) runs these windows were: 1.00–5.30, 5.31–7.65, 7.30–8.40, 8.35–8.85, 8.86–10.00, 10.10–10.95, 11.30–11.85, 11.50–12.70 and 12.60–15.00 min. For ESI(-) runs they were: 6.30–7.30, 7.30–8.25, 8.20–8.70, 8.70–9.30, 9.00–9.90, 9.80–10.85, 10.90–11.30, 11.30–12.00 and 12.00–13.00 min.

Method validation

UHPLC–ESI–MS/MS calibration curves were constructed using serially diluted phytohormone standards, listed in Supplementary Table 3, and the internal labelled standards (added in known concentrations). Limits of detection and quantification were defined as signal-to-noise ratios of 3:1 and 10:1, respectively.

To evaluate losses of analytes during the purification process and validate the method, three sets of samples were each prepared in triplicate and analyzed by the UHPLC–ESI–MS/MS system. In the first set, 20 mg FW of *Arabidopsis* seedlings were extracted in 50% ACN spiked with known amounts of stable isotope-labelled internal standards (at levels listed in Supplementary Table 2), and subsequently purified by SPE protocol (Fig. 1d). The second set consisted of identical plant tissue extracts spiked with a mixture of authentic and stable isotope-labelled internal standards (at levels listed in Supplementary Table 2) before SPE. The third set consisted of 20 mg FW portions of *Arabidopsis* plant tissue extracted and spiked by adding non-labelled standards, in varied concentrations, directly to purified eluates after the SPE step.

Analyte recovery (RE, %; Caban et al., 2012) following the purification process was calculated as the ratio of the mean peak area of a non-labelled analyte spiked before SPE (set 2) to the mean peak area of the same analyte spiked after SPE purification (set 3) multiplied by 100.

Concentrations of plant hormones were quantified using the standard isotope dilution method (Rittenberg and Foster, 1940). Concentrations of non-labelled targeted compounds added to samples from sample set 2 were calculated after subtracting their determined endogenous levels (average

values for each compound obtained from analyses of sample set 1). Finally, determined analyte concentrations were compared with known theoretical amounts of appropriate standards added to samples and presented as method accuracy (expressed as percentage bias). Method precision, for each analyte, was calculated as the relative standard deviation of its determined concentration in three replicates of samples of set 2.

Genevestigator analysis

The meta-analytical approach of Genevestigator (Hruz et al., 2008) has proven value for designing new experiments and validating existing results (Saito et al., 2008). Therefore, the software was initially used (in an unsupervised manner) to identify a single stress condition that alters the expression of genes involved in most hormones' biosynthesis and metabolism pathways (Supplementary Table 4). Salt stress was identified as the most appropriate condition by screening using the *Differential expression* tool (Genevestigator Experiment ID: AT-00656), and its suitability was confirmed by screening shifts in expression of hormone-related genes in one more salt stress experiment (Genevestigator Experiment ID: AT-00120).

To compare the data on hormonal and transcriptomic shifts under salt stress, the *Perturbations* tool was used. The genes listed in Supplementary Table 4 that were significantly up- or down-regulated (fold change ≥ 1.5 , $p < 0.01$) in response to salinity stress were identified. Log values of changes in their expression were then extracted and their activities in hormone pathways were noted to check the consistency between their responses and changes we detected in the corresponding hormones and metabolites (Supplementary Tables 5 and 6).

The Genevestigator interface is a JAVA applet running in the user's browser. Information about the individual tools and respective statistical analysis on the data is provided on the Genevestigator website (www.genevestigator.ethz.ch).

Statistical analysis (Uni- and multi-variate statistics)

Before multivariate statistical analysis, measured concentrations of compounds in roots or shoots up to 50% below the limit of detection were replaced with two thirds of their respective LODs, and compounds for which more than 50% of values were missing were removed from the dataset. Multivariate analysis was performed using SIMCA software (version 14, Umetrics). Unsupervised principal component analysis (PCA) and supervised orthogonal partial least squares discriminant analysis (OPLS-DA) were applied to log-transformed and Pareto-scaled data. PCA was used to obtain a general overview of the data structure, and OPLS-DA derived S-plots to identify compounds responsible for separation of roots and shoots, and samples from control and salinity-stressed plants. Differences in levels of each determined metabolite between these groups were also evaluated using Student's t-test at $P < 0.05$, $P < 0.01$, and $P < 0.001$ levels.

SUPPLEMENTAL DATA

The following supplemental materials are available.

Supplemental Figure S1. Comparison of signal intensities of indicated analytes of various phytohormone classes

Supplemental Table S1. List of targeted compounds.

Supplemental Table S2. Method validation data.

Supplemental Table S3. Optimized UHPLC–MS/MS parameters.

Supplemental Table S4. Phytohormone-related genes used in the experimental design process.

Supplemental Table S5. Genes showing shifts in expression levels under salt stress in roots.

Supplemental Table S6. Genes showing shifts in expression levels under salt stress in shoots.

Supplemental Table S7. Determined levels of plant hormones in root and shoot samples of salt-stressed and control *Arabidopsis* plants.

Supplemental Table S8. Determination of chlorophyll (Chl_{a,b}).

Supplemental Table S9. Tests of pH stability.

Supplemental Table S10. Solubility of brassinosteroids.

ACKNOWLEDGMENTS

We thank the Swedish Metabolomics Centre for the use of instrumentation and Sees-editing Ltd. for careful revision of the manuscript. We would also like to thank Eva Hirnerová for technical support and sample preparation during the plant hormone analyses.

TABLES

Table 1. Overview of average recovery, limit of detection (LOD), method precision and analytical accuracy (absolute value) for each phytohormone class. See Supplemental Table 2 for detailed information.

Phytohormone class	Number of compounds	Average recovery (%)	Spiked contents (pmol)	Average LOD (fmol)	Analytical precision (% RSD)	Analytical accuracy (% bias)
CYTOKININS	41	87.0	0.5 - 5	0.23	3.30	7.49
AUXINS	15	91.5	1 - 50	3.98	4.31	6.93
JASMONATES	11	95.3	10	18.64	5.70	5.20
ABSCISATES	5	95.9	10	7.19	1.06	5.91
GIBBERELLINS	14	89.2	5	28.88	3.00	5.54
SALICYLIC ACID	1	97.3	100	51.16	4.05	8.68
BRASSINOSTEROIDS	14	52.5	10	24.44	7.80	5.26

FIGURES

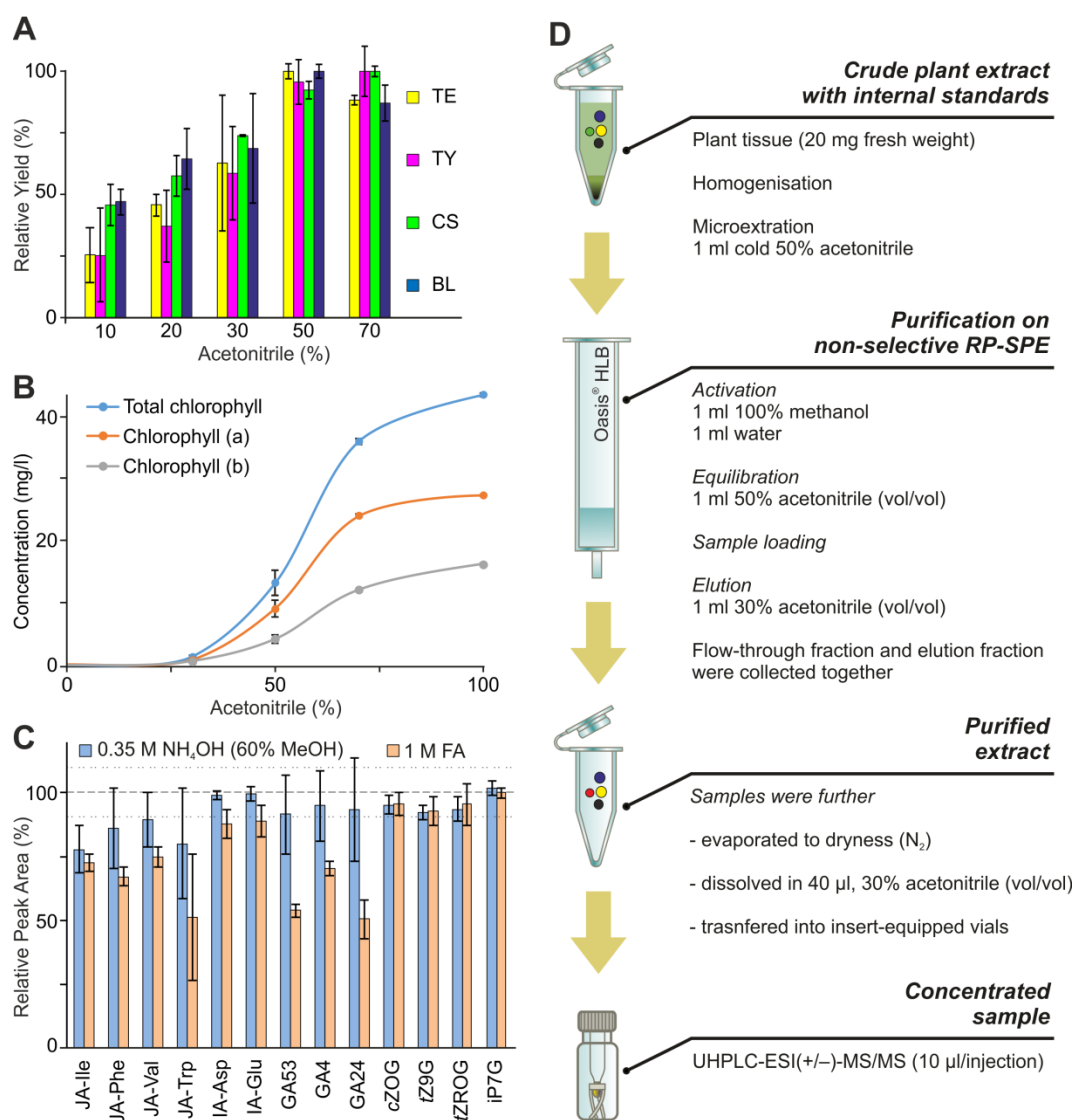


Figure 1. Optimization of sample preparation. A, Solubility of selected compounds (TE, teasterone; TY, typhasterol; CS, castasterone; BL, brassinolide) from the most hydrophobic phytohormone class included in our study (brassinosteroids) in extraction solvents with varied acetonitrile (ACN) content. Relative yield (ratio, in percent, of average peak area to maximal average peak area per extraction solvent; Supplemental Table S10). B, Amounts of chlorophyll extracted (mg/l) using extraction solvents with indicated ACN concentrations (Supplemental Table S8). C, pH-dependent stability (relative peak area, %) of selected compounds dissolved in 0.35 M ammonium hydroxide in 60% methanol (0.35 M NH₄OH in 60% MeOH) and 1 M formic acid (1 M FA), based on peak areas relative to peak areas of compounds dissolved in control solvent (50% ACN). The dashed line represents the average peak area and dotted line the average of standard deviations for compounds dissolved in control solvent; asterisks indicate significant changes compared to control (Student's t-test, P<0.05 (*); Supplemental Table S9). D, Scheme of sample micro-extraction and purification prior to UHPLC-ESI-MS/MS analysis.

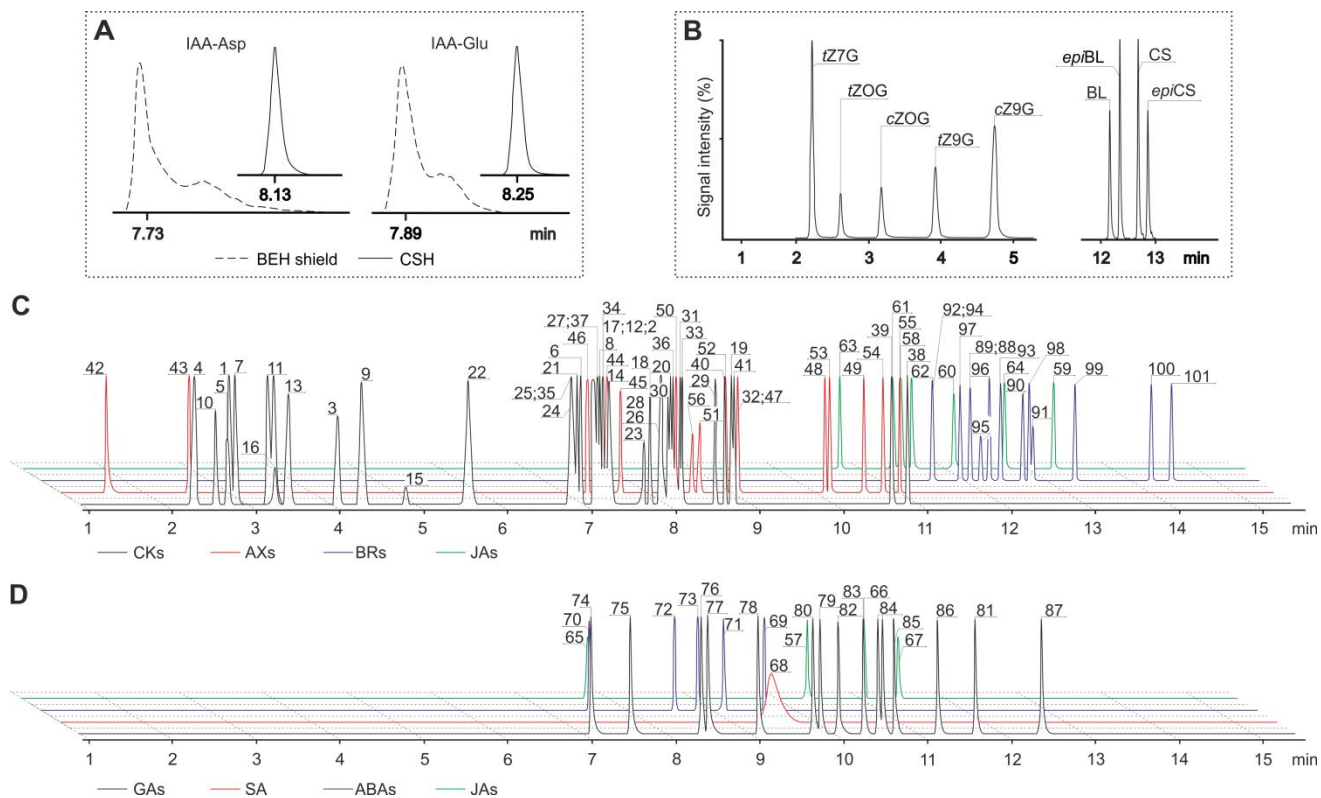


Figure 2. Optimization of baseline chromatographic separation. A, Peak shape of IAA-aspartate (IAA-Asp) and IAA-glutamate (IAA-Glu) separated on Acquity UPLC® CSH™ (full line) and Acquity UPLC® BEH shield (dashed line) columns. B, Isomer separation of *N/O*-glucoside forms of *cis/trans*-zeatins (left) and brassinolide (BL/*epi*BL) and castasterone (CS/*epi*CS) isobars (right) using an Acquity UPLC® CSH™ column. C and D, Scheme of UHPLC-ESI-MS/MS separation of targeted compounds in ESI(+) mode (C) and ESI(-) mode (D). Phytohormones are numbered according to Supplemental Table S1.

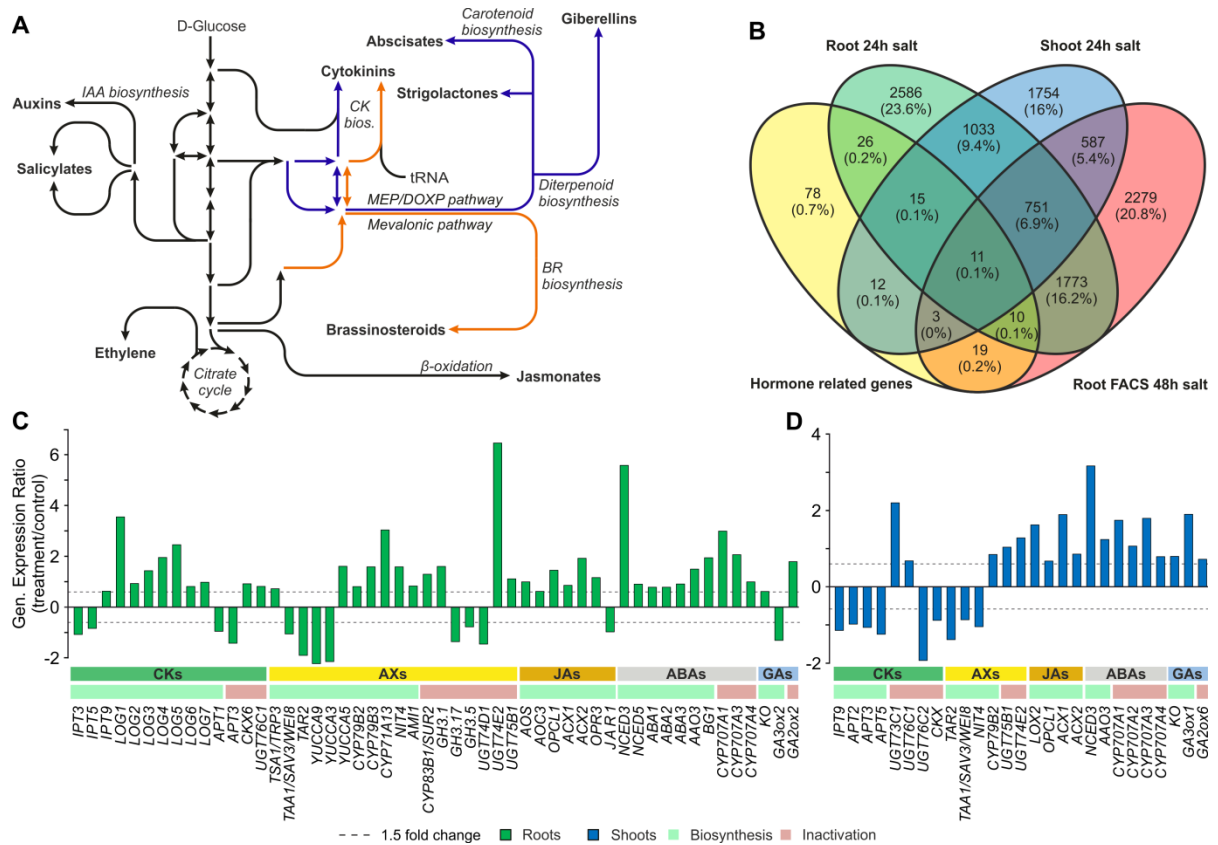


Figure 4. Alterations in expression level of plant hormone-related genes induced by salinity stress in *Arabidopsis*. **A**, Simplified scheme of plant hormone biosynthesis pathways. **B**, Venn diagram showing numbers, percentages and overlaps of hormone-related genes (Supplemental Table S4) and transcripts with affected levels (≥ 1.5 -fold change, $p < 0.01$) during different salt stress experiments as indicated (dashed line). **C** and **D**, Changes in hormone-related gene expression levels in shoot (**C**) and root (**D**) tissues under salinity stress (log ratio treated/control, fold change ≥ 1.5 , $p < 0.01$; Supplemental Tables 5 and 6).

LITERATURE CITED

- Balcke GU, Handrick V, Bergau N, Fichtner M, Henning A, Stellmach H, Tissier A, Hause B, Frolov A** (2012) An UPLC-MS/MS method for highly sensitive high-throughput analysis of phytohormones in plant tissues. *Plant Methods* **8**: 47
- Birkemeyer C, Kolasa, A, Kopka J** (2003) Comprehensive chemical derivatization for gas chromatography–mass spectrometry-based multi-targeted profiling of the major phytohormones. *J Chromatogr A* **993**: 89–102
- Caban M, Migowska N, Stepnowski P, Kwiatkowski M, Kumirska J** (2012) Matrix effects and recovery calculations in analyses of pharmaceuticals based on the determination of β -blockers and β -agonists in environmental samples. *J Chromatogr A* **1258**: 117–127
- Cai W J, Ye TT, Wang Q, Cai BD, Feng YQ** (2016) A rapid approach to investigate spatiotemporal distribution of phytohormones in rice. *Plant Methods* **12**: 47
- Cao ZY, Sun LH, Mou RX, Zhang LP, Lin XY, Zhu ZW, Chen MX** (2016) Profiling of phytohormones and their major metabolites in rice using binary solid-phase extraction and liquid chromatography-triple quadrupole mass spectrometry. *J Chromatogr A* **1451**: 67–74
- Chiwocha SD, Abrams SR, Ambrose SJ, Cutler AJ, Loewen M, Ross AR, Kermode AR** (2003) A method for profiling classes of plant hormones and their metabolites using liquid chromatography-electrospray ionization tandem mass spectrometry: An analysis of hormone regulation of thermodormancy of lettuce (*Lactuca sativa* L.) seeds. *Plant J* **35**: 405–417
- Davies P.J.** (2010) *Plant Hormones: Biosynthesis, Signal Transduction, Action!* 3rd Edition. Kluwer Academic Publishers, Dordrecht, Netherlands
- Delatorre C, Rodríguez A, Rodríguez L, Majada JP, Ordás RJ, Feito I** (2017) Hormonal profiling: Development of a simple method to extract and quantify phytohormones in complex matrices by UHPLC–MS/MS. *J Chromatogr B* **1040**: 239–249
- Dobrev PI, Kamínek M** (2002) Fast and efficient separation of cytokinins from auxin and abscisic acid and their purification using mixed-mode solid-phase extraction. *J Chromatogr A* **950**: 21–29
- Du F, Ruan G, Liu H** (2012) Analytical methods for tracing plant hormones. *Anal Bioanal Chem* **403**: 55–74
- Farrow SC, Emery RN** (2012) Concurrent profiling of indole-3-acetic acid, abscisic acid, and cytokinins and structurally related purines by high-performance-liquid-chromatography tandem electrospray mass spectrometry. *Plant Methods* **8**: 42
- Floková K, Tarkowská D, Miersch O, Strnad M, Wasternack C, Novák O** (2014) UHPLC–MS/MS based target profiling of stress-induced phytohormones. *Phytochemistry* **105**: 147–157

- Hruz T, Laule O, Szabo G, Wessendorp F, Bleuler S, Oertle L, Widmayer P, Gruissem W, Zimmermann P** (2008) GENEVESTIGATOR V3: a reference expression database for the meta-analysis of transcriptomes. *Adv Bioinformatics* **2008**: 420747
- Kojima M, Kamada-Nobusada T, Komatsu H, Takei K, Kuroha T, Mizutani M, Ashikari M, Ueguchi-Tanaka M, Matsuoka M, Suzuki K, Sakakibara H** (2009) Highly sensitive and high-throughput analysis of plant hormones using MS-probe modification and liquid chromatography-tandem mass spectrometry: An application for hormone profiling in *Oryza sativa*. *Plant Cell Physiol* **50**: 1201–1214
- Lichtenthaler HK** (1987) Chlorophylls and carotenoids: Pigments of photosynthetic biomembranes. *Methods Enzymol* **148**: 350–382
- Müller A, Düchting P, Weiler E** (2002) A multiplex GC-MS/MS technique for the sensitive and quantitative single-run analysis of acidic phytohormones and related compounds, and its application to *Arabidopsis thaliana*. *Planta* **216**: 44–56
- Müller M, Munné-Bosch S** (2011) Rapid and sensitive hormonal profiling of complex plant samples by liquid chromatography coupled to electrospray ionization tandem mass spectrometry. *Plant Methods* **7**: 37
- Munns R, Tester M** (2008) Mechanisms of salinity tolerance. *Annu Rev Plant Biol* **59**: 651–681
- Novák O, Hényková E, Sairanen I, Kowalczyk M, Pospíšil T, Ljung K** (2012) Tissue-specific profiling of the *Arabidopsis thaliana* auxin metabolome. *Plant J*. **72**: 523–536
- Nováková L, Vlčková H** (2009) A review of current trends and advances in modern bio-analytical methods: Chromatography and sample preparation. *Anal Chim Acta* **656**: 8–35
- Nováková L** (2013) Challenges in the development of bioanalytical liquid chromatography-mass spectrometry method with emphasis on fast analysis. *J Chromatogr A* **1292**: 25–37
- Oklestkova J, Tarkowská D, Eyer L, Elbert T, Marek A, Smržová Z, Novák O, Fránek M, Zhabinskii VN, Strnad M** (2017) Immunoaffinity chromatography combined with tandem mass spectrometry: a new tool for the selective capture and analysis of brassinosteroid plant hormones. *Talanta* **170**: 432–440
- Pan X, Welti R, Wang X** (2008) Simultaneous quantification of major phytohormones and related compounds in crude plant extracts by liquid chromatography–electrospray tandem mass spectrometry. *Phytochemistry* **69**: 1773–1781
- Pěňčík A, Rolčík J, Novák O, Magnus V, Barták P, Buchtík R, Salopek-Sondi B, Strnad M** (2009) Isolation of novel indole-3-acetic acid conjugates by immunoaffinity extraction. *Talanta* **80**: 651–655
- Plačková L, Oklestkova J, Pospíšková K, Poláková K, Buček J, Stýskala J, Zatloukal M, Šafařík I, Zbořil R, Strnad M, Doležal K, Novák O** (2017) Microscale magnetic microparticle-based immunopurification of cytokinins from *Arabidopsis* root apex. *Plant J* **89**: 1065–1075

- Pratt JJ** (1986) Isotope dilution analysis using chromatographic separation of isotopic forms of the compound to be measured. *Ann Clin Biochem* **23**: 251–276
- Rittenberg D, Foster GL** (1940) A new procedure for quantitative analysis by isotope dilution, with application to the determination of amino acids and fatty acids. *J Biol Chem* **133**: 737–744
- Ryu H, Cho Y** (2015) Plant hormones in salt stress tolerance. *J Plant Biol* **58**: 147–155
- Saito K, Hirai MY, Yonekura-Sakakibara K** (2008) Decoding genes with coexpression networks and metabolomics: ‘majority report by precogs’. *Trends Plant Sci* **13**: 36–43
- Schäfer M, Brütting C, Baldwin IT, Kallenbach M** (2016) High-throughput quantification of more than 100 primary- and secondary-metabolites, and phytohormones by a single solid-phase extraction based sample preparation with analysis by UHPLC-HESI-MS/MS. *Plant Methods* **12**: 30
- Svačinová J, Novák O, Plačková L, Lenobel R, Holík J, Strnad M, Doležal K** (2012) A new approach for cytokinin isolation from *Arabidopsis* tissues using miniaturized purification: Pipette tip solid-phase extraction. *Plant Methods* **8**: 17
- Tarkowská D, Novák O, Floková K, Tarkowski P, Turečková V, Grúz J, Rolčík J, Strnad M** (2014). Quo vadis plant hormone analysis? *Planta* **240**: 55–76
- Tarkowská D, Novák O, Oklestkova J, Strnad M** (2016). The determination of 22 natural brassinosteroids in a minute sample of plant tissue by UHPLC–ESI–MS/MS. *Anal Bioanal Chem* **408**: 6799–6812
- Tarkowski P, Václavíková K, Novák O, Pertry I, Hanuš J, Whenham R, Vereecke D, Šebela M, Strnad M** (2010) Analysis of 2-methylthio-derivatives of isoprenoid cytokinins by liquid chromatography–tandem mass spectrometry. *Anal Chim Acta* **680**, 86–91
- Turečková V, Novák O, Strnad M.** (2009) Profiling ABA metabolites in *Nicotiana tabacum* L. leaves by ultra-performance liquid chromatography–electrospray tandem mass spectrometry. *Talanta* **80**: 390–399
- Ulijn RV, Janssen AE, Moore BD, Halling PJ, Kelly SM, Price NC** (2002). Reversible acetonitrile-induced inactivation/activation of thermolysin. *Chembiochem* **3**: 1112–1116
- Urbanová T, Tarkowská D, Novák O, Hedden P, Strnad M** (2013) Analysis of gibberellins as free acids by ultra performance liquid chromatography–tandem mass spectrometry. *Talanta* **112**: 85–94
- Vanstraelen M, Benková E** (2012) Hormonal interactions in the regulation of plant development. *Annu Rev Cell Dev Biol* **28**: 463–487
- Wang Q, Cai WJ, Yu L, Ding J, Feng YQ** (2017). Comprehensive profiling of phytohormones in honey by sequential liquid–liquid extraction coupled with liquid chromatography–mass spectrometry. *J Agric Food Chem* **65**: 575–585

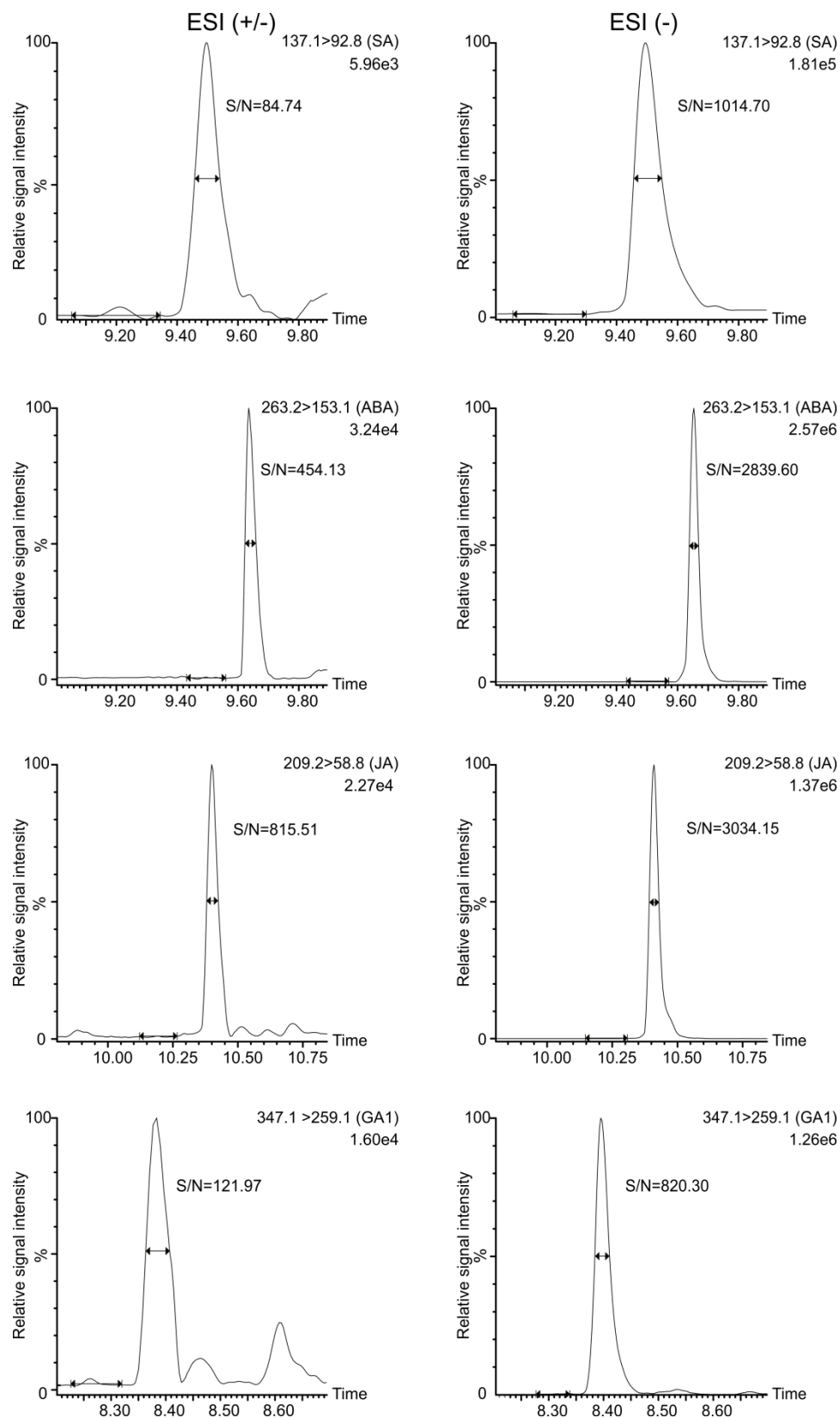
Záveská Drábková L, Dobrev PI, Motyka V (2015) Phytohormone profiling across the Bryophytes.

PLoS One **10**: e0125411

Zwanenburg B, Pospíšil T, Čavar Zeljković S (2016) Strigolactones: new plant hormones in action.

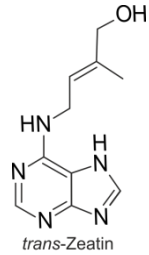
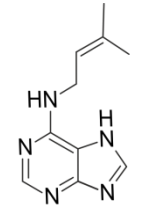
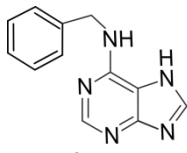
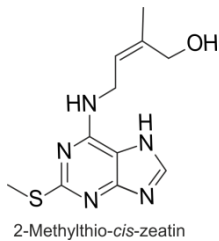
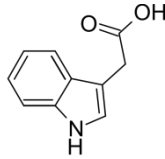
Planta **243**: 1311–1326

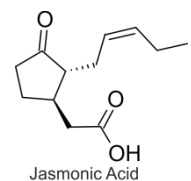
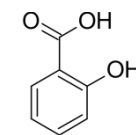
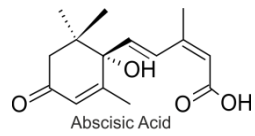

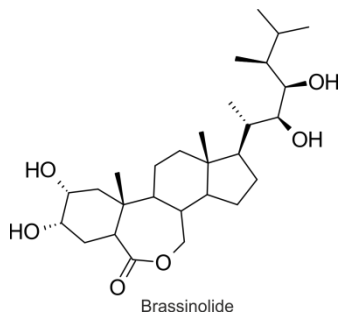
Supplemental Data



Supplemental Figure 1 | Comparison of signal intensities of indicated analytes of various phytohormone classes (SA, salicylic acid; ABA, abscisic acid; JA, jasmonic acid; GA₁, gibberellin A1) in polarity switching [ESI (+/-)] mode and ESI (-) mode.

Supplemental Table 1. List of targeted compounds with abbreviations and representative structures.

Tab. 1/2	Compound name	Abbreviation	Representative Structure
1	<i>trans</i> -zeatin	<i>tZ</i>	 <p><i>trans</i>-Zeatin</p>
2	<i>trans</i> -zeatin riboside	<i>tZR</i>	
3	<i>trans</i> -zeatin-9-glucoside	<i>tZ9G</i>	
4	<i>trans</i> -zeatin-7-glucoside	<i>tZ7G</i>	
5	<i>trans</i> -zeatin-O-glucoside	<i>tZOG</i>	
6	<i>trans</i> -zeatin riboside-O-glucoside	<i>tZROG</i>	
7	Dihydrozeatin	DHZ	
8	Dihydrozeatin riboside	DHZR	
9	Dihydrozeatin-9-glucoside	DHZ9G	
10	Dihydrozeatin-7-glucoside	DHZ7G	
11	Dihydrozeatin-O-glucoside	DHZOG	
12	Dihydrozeatin riboside-O-glucoside	DHZROG	
13	<i>cis</i> -zeatin	<i>cZ</i>	 <p><i>N</i>⁶-Isopentenyladenine</p>
14	<i>cis</i> -zeatin riboside	<i>cZR</i>	
15	<i>cis</i> -zeatin-9-glucoside	<i>cZ9G</i>	
16	<i>cis</i> -zeatin-O-glucoside	<i>cZOG</i>	
17	<i>cis</i> -zeatin riboside-O-glucoside	<i>cZROG</i>	
18	<i>N</i> ⁶ -isopentenyladenine	<i>iP</i>	
19	<i>N</i> ⁶ -isopentenyladenenosine	<i>iPR</i>	 <p><i>N</i>⁶-Benzyladenine</p>
20	<i>N</i> ⁶ -isopentenyladenine-9-glucoside	<i>iP9G</i>	
21	<i>N</i> ⁶ -isopentenyladenine-7-glucoside	<i>iP7G</i>	
22	<i>para</i> -topolin	<i>pT</i>	
23	<i>para</i> -topolin riboside	<i>pTR</i>	
24	<i>para</i> -topolin-9-glucoside	<i>pT9G</i>	
25	<i>meta</i> -topolin	<i>mT</i>	
26	<i>meta</i> topolin riboside	<i>mTR</i>	
27	<i>meta</i> topolin-9-glucoside	<i>mT9G</i>	
28	<i>ortho</i> -topolin	<i>oT</i>	
29	<i>ortho</i> -topolin riboside	<i>oTR</i>	 <p>2-Methylthio-<i>cis</i>-zeatin</p>
30	<i>ortho</i> -topolin-9-glucoside	<i>oT9G</i>	
31	<i>N</i> ⁶ -benzyladenine	<i>BAP</i>	
32	<i>N</i> ⁶ -benzyladenosine	<i>BAPR</i>	
33	<i>N</i> ⁶ -benzyladenine-9-glucoside	<i>BAP9G</i>	
34	benzyladenine-7-glucoside	<i>BAP7G</i>	
35	Kinetin	<i>K</i>	
36	Kinetin riboside	<i>KR</i>	
37	Kinetin-9-glucoside	<i>K9G</i>	
38	2-methylthio-isopentenyladenine	<i>2MeSiP</i>	
39	2-methylthio-isopentenyladenosine	<i>2MeSiPR</i>	
40	2-methylthio- <i>cis</i> -zeatin	<i>2MeScZ</i>	
41	2-methylthio- <i>cis</i> -zeatin riboside	<i>2MeScZR</i>	
42	Tryptamine	<i>TRA</i>	 <p>Indol-3-acetic Acid</p>
43	Tryptophan	<i>TRP</i>	
44	Indol-3-acetamide	<i>IAM</i>	
45	2-oxoindole-3-acetic acid	<i>oxIAA</i>	
46	Anthranilic acid	<i>ANT</i>	
47	Indol-3-acetic acid	<i>IAA</i>	
48	Indole-3-acetonitrile	<i>IAN</i>	
49	Indol-3-butyric acid	<i>IBA</i>	
50	IAA-glycine	<i>IAA-Gly</i>	
51	IAA-glutamate	<i>IAA-Glu</i>	
52	IAA-alanine	<i>IAA-Ala</i>	
53	IAA-valine	<i>IAA-Val</i>	
54	IAA-leucine	<i>IAA-Leu</i>	
55	IAA-phenylalanine	<i>IAA-Phe</i>	
56	IAA-aspartate	<i>IAA-Asp</i>	

Tab. 2/2	Compound name	Abbreviation	Representative Structure
57	Jasmonic acid	JA	 <p>Jasmonic Acid</p>
58	JA-isoleucine	JA-Ile	
59	<i>cis</i> -12-oxo-phytodienoic acid	<i>cis</i> OPDA	
60	dinor-12-oxo-phytodienoic acid	dnOPDA	
61	JA-tryptophan	JA-Trp	
62	JA-phenylalanine	JA-Phe	
63	JA-valine	JA-Val	
64	3-oxo-2-(2-(<i>Z</i>)-pentenyl)cyclopentane-1-hexanoic acid	OPC-6	 <p>Salicylic Acid</p>  <p>Abscisic Acid</p>
65	12-hydroxy-jasmonic acid	12-OH-JA	
66	9,10-dihydrojasmonic acid	9,10-dh-JA	
67	3-oxo-2-(2-(<i>Z</i>)-pentenyl) cyclopentane-1-butyric acid	OPC-4	
68	Salicylic acid	SA	
69	Abscisic acid	ABA	
70	Dihydrophaseic acid	DPA	
71	<i>neo</i> -phaseic acid	NeoPA	 <p>Gibberellin 1</p>
72	Phaseic acid	PA	
73	7-hydroxy-ABA	7-OH-ABA	
74	Gibberellin A ₈	GA ₈	
75	Gibberellin A ₂₉	GA ₂₉	
76	Gibberellin A ₃	GA ₃	
77	Gibberellin A ₁	GA ₁	
78	Gibberellin A ₆	GA ₆	
79	Gibberellin A ₅	GA ₅	
80	Gibberellin A ₁₉	GA ₁₉	
81	Gibberellin A ₂₄	GA ₂₄	
82	Gibberellin A ₄₄	GA ₄₄	
83	Gibberellin A ₃₄	GA ₃₄	
84	Gibberellin A ₅₁	GA ₅₁	
85	Gibberellin A ₅₃	GA ₅₃	
86	Gibberellin A ₄	GA ₄	
87	Gibberellin A ₁₅	GA ₁₅	
88	28-norcastasterone	<i>nor</i> CS	 <p>Brassinolide</p>
89	Dolichosterone	DS	
90	Castasterone	CS	
91	24-epicastasterone	<i>epi</i> CS	
92	28-norbrassinolide	<i>nor</i> BL	
93	Homodolichosterone	homoDS	
94	Dolicholide	DL	
95	Brassinolide	BL	
96	24- <i>epi</i> brassinolide	<i>epi</i> BL	
97	Homodolicholide	homoDL	
98	Homobrassinolide	homoBL	
99	Homocastasterone	homoCS	
100	Teasterone	TE	
101	Typhasterol	TY	

Supplemental Table 2. Method validation data. R², coefficient of determination; LOD, limit of detection; LOQ, limit of quantification; IS, internal standard; and RE, recovery for indicated compounds. LOD and LOQ defined as signal-to-noise ratios of 3:1 and 10:1, respectively.

Tab. 1/3	Compound	Dynamic range (pmol)	R ²	LOD (fmol)	LOQ (fmol)	Spiked content (pmol)	IS/sample (pmol)	RE (%)	Method precision (%RSD)	Method accuracy (%bias)
1	<i>t</i> Z	1*10 ⁻¹⁵ - 1*10 ⁻¹²	0.999	0.32	1.08	5.00	0.40	86.82	3.06	-1.11
2	<i>t</i> ZR	1*10 ⁻¹⁵ - 5*10 ⁻¹³	0.999	0.01	0.05	5.00	0.40	86.65	1.51	-17.99
3	<i>t</i> Z9G	1*10 ⁻¹⁵ - 1*10 ⁻¹²	0.999	0.12	0.40	5.00	0.40	88.09	13.02	-11.58
4	<i>t</i> Z7G	1*10 ⁻¹⁵ - 1*10 ⁻¹²	0.999	0.05	0.15	5.00	0.40	82.64	2.08	11.57
5	<i>t</i> ZOG	1*10 ⁻¹⁵ - 1*10 ⁻¹²	0.999	0.25	0.82	5.00	0.40	95.54	5.30	-8.16
6	<i>t</i> ZROG	1*10 ⁻¹⁵ - 5*10 ⁻¹³	0.998	0.06	0.20	5.00	0.40	74.94	4.73	-19.74
7	DHZ	1*10 ⁻¹⁵ - 1*10 ⁻¹²	0.999	0.04	0.14	5.00	0.40	91.58	5.54	14.44
8	DHZR	1*10 ⁻¹⁵ - 5*10 ⁻¹³	0.999	0.09	0.30	5.00	0.40	80.66	1.64	4.62
9	DHZ9G	1*10 ⁻¹⁵ - 1*10 ⁻¹²	0.999	0.21	0.69	5.00	0.40	98.52	3.39	1.63
10	DHZ7G	1*10 ⁻¹⁵ - 1*10 ⁻¹²	0.999	0.20	0.65	5.00	0.40	81.25	10.00	6.28
11	DHZOG	1*10 ⁻¹⁵ - 1*10 ⁻¹²	0.998	0.10	0.35	0.50	0.40	96.75	8.77	6.70
12	DHZROG	1*10 ⁻¹⁵ - 1*10 ⁻¹²	0.999	0.16	0.53	0.50	0.40	73.16	3.10	7.80
13	<i>c</i> Z	1*10 ⁻¹⁵ - 1*10 ⁻¹²	0.999	0.09	0.29	5.00	0.40	86.12	2.43	1.41
14	<i>c</i> ZR	1*10 ⁻¹⁵ - 5*10 ⁻¹³	0.999	0.09	0.30	5.00	0.40	80.66	1.64	4.62
15	<i>c</i> Z9G	1*10 ⁻¹⁵ - 1*10 ⁻¹²	0.999	0.01	0.05	5.00	0.40	83.32	6.12	-17.57
16	<i>c</i> ZOG	1*10 ⁻¹⁵ - 1*10 ⁻¹²	0.999	0.04	0.14	5.00	0.40	93.63	10.79	-2.88
17	<i>c</i> ZROG	1*10 ⁻¹⁵ - 1*10 ⁻¹²	0.999	0.34	1.13	5.00	0.40	75.91	1.08	4.26
18	iP	1*10 ⁻¹⁵ - 1*10 ⁻¹²	0.999	0.04	0.15	5.00	0.40	86.26	2.59	13.75
19	iPR	1*10 ⁻¹⁵ - 5*10 ⁻¹³	0.999	0.04	0.15	5.00	0.40	88.45	2.18	-1.40
20	iP9G	1*10 ⁻¹⁵ - 5*10 ⁻¹³	0.999	0.16	0.54	5.00	0.40	88.37	1.51	-0.05
21	iP7G	1*10 ⁻¹⁵ - 5*10 ⁻¹³	0.999	0.03	0.10	5.00	0.40	96.14	1.50	2.27
22	pT	1*10 ⁻¹⁵ - 1*10 ⁻¹²	0.999	0.47	1.56	1.00	0.40	82.53	0.03	0.06
23	pTR	1*10 ⁻¹⁵ - 1*10 ⁻¹²	0.999	0.92	3.05	1.00	0.40	96.55	0.01	-4.56
24	pT9G	1*10 ⁻¹⁵ - 5*10 ⁻¹³	0.999	0.03	0.10	1.00	0.40	99.28	0.02	-17.12
25	mT	1*10 ⁻¹⁵ - 1*10 ⁻¹²	0.999	0.03	0.10	5.00	0.40	81.40	0.19	2.90
26	mTR	1*10 ⁻¹⁵ - 1*10 ⁻¹²	0.999	0.67	2.24	5.00	0.40	93.83	0.10	7.56
27	mT9G	1*10 ⁻¹⁵ - 5*10 ⁻¹³	0.999	0.21	0.71	5.00	0.40	84.53	5.26	15.66
28	oT	1*10 ⁻¹⁵ - 1*10 ⁻¹²	0.999	0.04	0.15	5.00	0.40	84.30	1.60	5.29
29	oTR	1*10 ⁻¹⁵ - 1*10 ⁻¹²	0.999	0.34	1.13	5.00	0.40	85.00	0.02	-1.40
30	oT9G	1*10 ⁻¹⁵ - 5*10 ⁻¹³	0.999	1.13	3.76	5.00	0.40	96.18	0.04	-3.27
31	BAP	1*10 ⁻¹⁵ - 5*10 ⁻¹³	0.999	0.28	0.93	0.50	0.40	80.87	2.75	7.97
32	BAPR	1*10 ⁻¹⁵ - 1*10 ⁻¹²	0.998	0.01	0.05	0.50	0.40	92.66	1.69	-1.28

Tab. 2/3	Compound	Dynamic range (pmol)	R ²	LOD (fmol)	LOQ (fmol)	Spiked content (pmol)	IS/sample (pmol)	RE (%)	Method precision (%RSD)	Method accuracy (%bias)
33	BAP9G	1*10 ⁻¹⁵ - 1*10 ⁻¹²	0.999	0.15	0.50	5.00	0.40	98.92	2.49	-7.26
34	BAP7G	1*10 ⁻¹⁵ - 1*10 ⁻¹²	0.999	0.13	0.45	5.00	0.40	85.98	0.43	-7.62
35	K	1*10 ⁻¹⁵ - 1*10 ⁻¹²	0.999	0.12	0.41	5.00	0.40	82.61	4.23	7.52
36	KR	1*10 ⁻¹⁵ - 1*10 ⁻¹²	0.998	0.44	1.47	5.00	0.40	97.44	2.85	3.81
37	K9G	1*10 ⁻¹⁵ - 1*10 ⁻¹²	0.995	1.15	3.82	5.00	0.40	97.45	2.30	-14.14
38	2MeSiP	1*10 ⁻¹⁵ - 1*10 ⁻¹²	0.996	0.36	1.19	5.00	0.40	54.19	5.18	12.30
39	2MeSiPR	1*10 ⁻¹⁵ - 1*10 ⁻¹²	0.996	0.06	0.21	0.50	0.40	78.58	8.63	7.32
40	2MeScZ	1*10 ⁻¹⁵ - 1*10 ⁻¹²	0.997	0.16	0.52	5.00	0.40	84.70	4.56	-14.71
41	2MeScZR	1*10 ⁻¹⁵ - 1*10 ⁻¹³	0.999	0.06	0.21	5.00	0.40	92.48	0.77	-5.54
42	TRA	5*10 ⁻¹⁴ - 1*10 ⁻¹¹	0.999	9.12	30.41	1.00	1.00	99.90	0.59	1.18
43	TRP	2.5*10 ⁻¹³ - 1*10 ⁻¹¹	0.999	5.45	18.18	50.00	50.00	97.62	4.11	5.31
44	IAM	5*10 ⁻¹⁵ - 5*10 ⁻¹³	0.999	2.84	9.46	1.00	1.00	89.00	0.03	-9.27
45	oxIAA	5*10 ⁻¹⁵ - 5*10 ⁻¹¹	0.999	1.77	5.89	10.00	1.00	89.52	2.66	5.00
46	ANT	5*10 ⁻¹⁴ - 2*10 ⁻¹²	0.999	5.03	16.77	10.00	1.00	83.19	7.08	-3.52
47	IAA	5*10 ⁻¹⁴ - 1*10 ⁻¹¹	0.999	6.90	23.02	10.00	1.00	92.43	10.91	12.73
48	IAN	5*10 ⁻¹⁵ - 5*10 ⁻¹¹	0.999	0.31	1.02	10.00	50.00	74.23	2.61	-4.01
49	IBA	5*10 ⁻¹⁵ - 2*10 ⁻¹²	0.999	1.24	4.13	1.00	50.00	89.26	7.66	3.89
50	IAA-Gly	5*10 ⁻¹⁵ - 2*10 ⁻¹²	0.999	1.01	3.36	10.00	1.00	99.99	1.26	-17.97
51	IAA-Glu	5*10 ⁻¹⁵ - 2*10 ⁻¹²	0.999	2.77	9.23	1.00	1.00	92.87	2.08	-9.00
52	IAA-Ala	5*10 ⁻¹⁵ - 2*10 ⁻¹²	0.998	1.64	5.46	1.00	1.00	95.22	14.91	6.04
53	IAA-Val	5*10 ⁻¹⁵ - 2*10 ⁻¹²	0.999	0.63	2.09	1.00	1.00	97.92	5.81	9.15
54	IAA-Leu	5*10 ⁻¹⁵ - 2*10 ⁻¹²	0.999	9.03	30.10	1.00	1.00	85.23	2.90	9.44
55	IAA-Phe	5*10 ⁻¹⁵ - 2*10 ⁻¹²	0.999	1.22	4.06	1.00	1.00	94.98	0.74	-2.83
56	IAA-Asp	5*10 ⁻¹⁴ - 2*10 ⁻¹²	0.999	10.78	35.93	1.00	1.00	91.00	1.33	4.56
57	JA	5*10 ⁻¹⁴ - 1*10 ⁻¹¹	0.999	15.32	51.06	10.00	20.00	93.51	0.26	3.41
58	JA-Ile	1*10 ⁻¹⁴ - 1*10 ⁻¹²	0.999	3.53	11.75	10.00	0.80	99.30	2.98	5.33
59	cisOPDA	1*10 ⁻¹⁴ - 2*10 ⁻¹¹	0.996	1.21	4.02	10.00	8.00	94.08	13.22	12.89
60	dnOPDA	1*10 ⁻¹³ - 1*10 ⁻¹¹	0.999	25.46	84.88	10.00	8.00	91.38	5.67	1.12
61	JA-Trp	1*10 ⁻¹⁴ - 2*10 ⁻¹²	0.999	2.43	8.11	10.00	0.80	99.00	10.37	-0.61
62	JA-Phe	1*10 ⁻¹⁴ - 2*10 ⁻¹²	0.999	1.59	5.31	10.00	0.80	99.00	5.41	11.54
63	JA-Val	1*10 ⁻¹⁴ - 2*10 ⁻¹²	0.999	0.97	3.22	10.00	20.00	99.66	4.25	9.91
64	OPC-6	1*10 ⁻¹³ - 1*10 ⁻¹⁰	0.997	35.89	119.63	10.00	0.80	91.50	6.08	0.96
65	12-OH-JA	1*10 ⁻¹³ - 1*10 ⁻¹⁰	0.999	31.01	103.38	10.00	20.00	95.87	0.88	3.85
66	9,10-dh-JA	1*10 ⁻¹³ - 1*10 ⁻¹⁰	0.994	28.08	93.61	10.00	20.00	94.81	12.76	-0.46
67	OPC-4	1*10 ⁻¹³ - 1*10 ⁻¹⁰	0.998	59.56	198.54	10.00	20.00	89.69	0.80	-7.13
68	SA	1*10 ⁻¹² - 1*10 ⁻¹⁰	0.999	51.16	170.55	100.00	20.00	97.28	4.05	-8.68
69	ABA	5*10 ⁻¹⁴ - 1*10 ⁻¹⁰	0.998	16.71	55.72	10.00	20.00	99.74	0.62	9.71
70	DPA	5*10 ⁻¹⁴ - 1*10 ⁻¹⁰	0.999	6.08	20.27	10.00	20.00	91.82	1.89	5.45

Tab. 3/3	Compound	Dynamic range (pmol)	R ²	LOD (fmol)	LOQ (fmol)	Spiked content (pmol)	IS/sample (pmol)	RE (%)	Method precision (%RSD)	Method accuracy (%bias)
71	NeoPA	5*10 ⁻¹⁴ - 1*10 ⁻¹⁰	0.999	7.16	23.85	10.00	20.00	96.21	0.23	-0.55
72	PA	5*10 ⁻¹⁴ - 1*10 ⁻¹⁰	0.999	4.32	14.39	10.00	20.00	93.89	2.13	2.31
73	7-OH-ABA	5*10 ⁻¹⁴ - 1*10 ⁻¹⁰	0.999	1.67	5.57	10.00	20.00	97.70	0.45	11.53
74	GA ₈	2.5*10 ⁻¹³ - 5*10 ⁻¹¹	0.999	12.72	42.39	5.00	8.00	99.36	0.12	-2.13
75	GA ₂₉	2.5*10 ⁻¹³ - 5*10 ⁻¹¹	0.999	3.81	12.69	5.00	8.00	99.97	0.18	7.66
76	GA ₃	2.5*10 ⁻¹³ - 5*10 ⁻¹¹	0.998	17.08	56.92	5.00	8.00	99.55	0.07	-0.03
77	GA ₁	2.5*10 ⁻¹³ - 5*10 ⁻¹¹	0.999	7.18	23.95	5.00	8.00	97.64	0.17	10.80
78	GA ₆	2.5*10 ⁻¹³ - 5*10 ⁻¹¹	0.996	18.16	60.53	5.00	8.00	76.11	5.87	7.28
79	GA ₅	2.5*10 ⁻¹³ - 5*10 ⁻¹¹	0.999	47.66	158.86	5.00	8.00	68.58	5.80	2.98
80	GA ₁₉	2.5*10 ⁻¹³ - 5*10 ⁻¹¹	0.997	4.98	16.59	5.00	8.00	99.26	0.02	6.49
81	GA ₂₄	2.5*10 ⁻¹³ - 5*10 ⁻¹¹	0.999	15.17	50.58	5.00	8.00	98.64	0.14	2.40
82	GA ₄₄	2.5*10 ⁻¹³ - 5*10 ⁻¹¹	0.993	28.07	93.56	5.00	8.00	67.82	14.84	-16.66
83	GA ₃₄	2.5*10 ⁻¹³ - 5*10 ⁻¹¹	0.997	20.20	67.33	5.00	8.00	71.95	10.99	-9.57
84	GA ₅₁	2.5*10 ⁻¹³ - 5*10 ⁻¹¹	0.998	39.65	132.18	5.00	8.00	98.97	0.23	3.21
85	GA ₅₃	2.5*10 ⁻¹³ - 5*10 ⁻¹¹	0.999	72.72	242.39	5.00	8.00	92.30	0.25	3.85
86	GA ₄	2.5*10 ⁻¹³ - 5*10 ⁻¹¹	0.996	73.52	245.07	5.00	8.00	81.33	2.97	1.44
87	GA ₁₅	2.5*10 ⁻¹³ - 5*10 ⁻¹¹	0.998	43.45	144.82	5.00	8.00	96.89	0.39	3.09
88	norCS	1*10 ⁻¹³ - 1*10 ⁻¹¹	0.995	100.50	334.98	10.00	4.00	53.91	15.93	0.86
89	DS	1*10 ⁻¹³ - 5*10 ⁻¹²	0.997	23.95	79.84	10.00	4.00	65.81	2.55	3.22
90	CS	1*10 ⁻¹³ - 1*10 ⁻¹¹	0.999	42.51	141.71	10.00	4.00	41.81	3.31	0.70
91	epiCS	1*10 ⁻¹³ - 1*10 ⁻¹¹	0.995	22.07	73.56	10.00	4.00	52.02	14.68	4.15
92	norBL	1*10 ⁻¹³ - 1*10 ⁻¹¹	0.993	21.64	72.12	10.00	4.00	72.24	7.02	-7.55
93	homoDS	1*10 ⁻¹³ - 1*10 ⁻¹¹	0.997	13.31	44.37	10.00	4.00	52.36	9.53	-7.27
94	DL	1*10 ⁻¹³ - 1*10 ⁻¹¹	0.999	29.03	96.76	10.00	4.00	64.85	5.18	6.11
95	BL	1*10 ⁻¹³ - 1*10 ⁻¹¹	0.998	7.59	25.30	10.00	4.00	60.81	5.95	-0.14
96	epiBL	1*10 ⁻¹³ - 1*10 ⁻¹¹	0.999	15.62	52.06	10.00	4.00	60.29	5.81	-1.28
97	homoDL	1*10 ⁻¹³ - 1*10 ⁻¹¹	0.997	15.33	51.10	10.00	4.00	70.47	4.98	4.26
98	homoBL	1*10 ⁻¹³ - 1*10 ⁻¹¹	0.998	1.39	4.62	10.00	4.00	53.84	10.84	-11.67
99	TE	1*10 ⁻¹³ - 1*10 ⁻¹¹	0.999	9.68	32.25	10.00	4.00	23.81	1.63	10.92
100	TY	1*10 ⁻¹³ - 1*10 ⁻¹¹	0.993	12.09	40.31	10.00	4.00	10.34	18.71	4.91
101	homoCS	1*10 ⁻¹³ - 1*10 ⁻¹¹	0.997	27.49	91.62	10.00	4.00	52.36	3.11	10.66

Supplemental Table 3. Optimized UHPLC–MS/MS parameters for the quantification of targeted compounds. ESI, electrospray ionization; MRM, multiple reaction monitoring; RT, retention time; CV, cone voltage; CE, collision energy; IS, internal standard.

Tab. 1/3	Compound	Scan mode (ESI)	MRM transition	RT (min)	CV (V)	CE (eV)	IS	IS RT (min)	MRM transition
1	<i>t</i> Z	+	220.1 > 136.1	2.61	30	16	[¹³ C ₃]- <i>t</i> Z	2.61	225.1 > 141.0
2	<i>t</i> ZR	+	352.2 > 220.1	7.02	30	18	[² H ₅]- <i>t</i> ZR	6.97	357.2 > 220.1
3	<i>t</i> Z9G	+	382.2 > 220.1	3.87	30	20	[² H ₅]- <i>t</i> Z9G	3.82	387.2 > 225.1
4	<i>t</i> Z7G	+	382.2 > 220.2	2.20	30	20	[² H ₅]- <i>t</i> Z7G	2.15	387.2 > 225.1
5	<i>t</i> ZOG	+	382.2 > 220.3	2.58	30	20	[² H ₅]- <i>t</i> ZOG	2.53	387.2 > 225.1
6	<i>t</i> ZROG	+	514.2 > 382.2	6.85	32	20	[² H ₅]- <i>t</i> ZROG	6.80	519.2 > 387.1
7	DHZ	+	222.1 > 136.1	2.75	32	20	[² H ₃]-DHZ	2.70	222.1 > 136.0
8	DHZR	+	354.2 > 222.1	7.10	30	20	[² H ₃]-DHZR	7.05	357.2 > 220.1
9	DHZ9G	+	384.2 > 222.1	4.20	27	22	[² H ₃]-DHZ9G	4.15	387.2 > 225.1
10	DHZ7G	+	384.2 > 222.3	2.50	27	22	[² H ₃]-DHZ9G	4.15	387.2 > 225.1
11	DHZOG	+	384.2 > 222.2	3.15	27	22	[² H ₅]- <i>t</i> ZOG	2.53	387.2 > 225.1
12	DHZROG	+	516.2 > 384.2	7.01	35	21	[² H ₅]- <i>t</i> ZROG	6.80	519.2 > 387.1
13	<i>c</i> Z	+	220.1 > 136.2	3.30	30	16	[¹³ C ₃]- <i>c</i> Z	3.30	225.1 > 141.1
14	<i>c</i> ZR	+	352.2 > 220.1	7.19	30	18	[² H ₅]- <i>t</i> ZR	6.97	357.2 > 220.1
15	<i>c</i> Z9G	+	382.2 > 220.4	4.64	30	20	[² H ₅]- <i>t</i> Z9G	3.89	387.2 > 225.1
16	<i>c</i> ZOG	+	382.2 > 220.5	3.15	30	20	[² H ₅]- <i>t</i> ZOG	2.53	387.2 > 225.1
17	<i>c</i> ZROG	+	514.2 > 382.2	6.99	32	20	[² H ₅]- <i>t</i> ZROG	6.80	519.2 > 387.1
18	iP	+	204.3 > 136.1	7.72	35	14	[² H ₆]-iP	7.67	210.3 > 137.1
19	iPR	+	336.4 > 204.2	8.68	25	17	[² H ₆]-iPR	8.63	342.4 > 210.2
20	iP9G	+	366.2 > 204.1	7.95	35	18	[² H ₆]-iP9G	7.90	372.2 > 210.1
21	iP7G	+	366.2 > 204.1	6.83	30	20	[² H ₆]-iP7G	6.78	372.2 > 210.1
22	pT	+	242.1 > 136.1	5.46	20	16	[¹⁵ N ₄]-pT	5.46	246.1 > 140.1
23	pTR	+	374.2 > 242.1	7.63	20	30	[¹⁵ N ₄]-pTR	7.63	378.2 > 246.1
24	pT9G	+	404.2 > 242.1	6.77	40	22	[¹⁵ N ₄]-pT9G	6.77	408.2 > 246.1
25	mT	+	242.1 > 107.1	6.75	20	22	[¹⁵ N ₄]-mT	6.75	246.1 > 107.0
26	mTR	+	374.2 > 242.1	7.84	20	30	[¹⁵ N ₄]-mTR	7.84	378.2 > 246.2
27	mT9G	+	404.2 > 242.1	7.09	40	22	[¹⁵ N ₄]-mT9G	7.09	408.2 > 246.1
28	oT	+	242.1 > 136.0	7.85	35	16	[¹³ C ₃]-oT	7.85	247.1 > 141.0
29	oTR	+	374.4 > 242.2	8.49	15	16	[¹⁵ N ₄]-oTR	8.49	378.4 > 246.2
30	oT9G	+	404.2 > 242.1	7.82	35	20	[¹⁵ N ₄]-oT9G	7.82	408.2 > 246.1
31	BAP	+	226.3 > 91.0	8.09	29	22	[² H ₇]-BAP	8.04	233.3 > 98.0
32	BAPR	+	358.4 > 226.2	8.79	30	18	[² H ₇]-BAPR	8.74	365.4 > 233.2
33	BAP9G	+	388.2 > 226.1	8.09	25	22	[² H ₇]-BAP9G	8.04	395.2 > 233.1

Tab. 2/3	Compound	Scan mode (ESI)	MRM transition	RT (min)	CV (V)	CE (eV)	IS	IS RT (min)	MRM transition
34	BAP7G	+	388.2 > 226.1	7.15	35	24	[² H ₆]-iP7G	6.78	372.2 > 210.1
35	K	+	216.1 > 81.1	6.77	20	15	[¹⁵ N ₄]-pT	5.46	246.1 > 140.1
36	KR	+	348.2 > 216.1	7.97	40	18	[¹⁵ N ₄]-pTR	7.92	348.2 > 216.1
37	K9G	+	378.2 > 216.1	7.06	40	20	[¹⁵ N ₄]-pT9G	6.72	408.2 > 246.1
38	2MeSiP	+	250.1 > 182.1	10.81	30	22	[² H ₆]-2MeSiP	10.76	256.1 > 183.1
39	2MeSiPR	+	382.1 > 250.1	10.61	30	22	[² H ₆]-2MeSiPR	10.56	388.1 > 256.1
40	2MeScZ	+	266.1 > 182.1	8.63	30	22	[² H ₅]-2MeScZ	8.58	271.1 > 182.1
41	2MeScZR	+	398.1 > 266.1	8.72	30	22	[² H ₅]-2MeScZR	8.67	403.1 > 271.1
42	TRA	+	161.1 > 144.1	1.28	15	10	[² H ₄]-TRA	1.23	165.1 > 148.1
43	TRP	+	205.2 > 146.1	2.17	20	16	[² H ₅]-TRP	2.12	210.2 > 150.1
44	IAM	+	175.2 > 130.1	7.15	30	14	[² H ₅]-IAM	7.11	180.2 > 134.1
45	oxIAA	+	192.2 > 146.1	7.34	15	14	[¹³ C ₆]-OxIAA	7.34	198.2 > 152.1
46	ANT	+	138.1 > 120.1	7.05	20	10	[² H ₄]-ANT	7.00	142.1 > 124.1
47	IAA	+	176.1 > 130.1	8.77	30	16	[¹³ C ₆]-IAA	8.77	182.1 > 136.1
48	IAN	+	157.2 > 130.1	9.82	15	10	[² H ₄]-IAN	9.77	161.2 > 134.1
49	IBA	+	204.2 > 186.2	10.29	30	12	[² H ₄]-IBA	9.77	161.2 > 134.1
50	IAA-Gly	+	233.2 > 130.1	7.98	10	16	[¹⁵ N, ² H ₅]-IAA-Leu	10.48	295.2 134.1
51	IAA-Glu	+	305.2 > 130.1	8.25	15	24	[¹³ C ₆]-IAA-Glu	8.25	311.2 > 136.1
52	IAA-Ala	+	247.2 > 130.1	8.58	10	18	[¹⁵ N, ² H ₅]-IAA-Leu	10.46	295.2 134.1
53	IAA-Val	+	275.2 > 130.1	9.86	30	26	[¹⁵ N, ² H ₅]-IAA-Val	9.84	281.2 > 134.1
54	IAA-Leu	+	289.2 > 130.1	10.50	15	25	[¹⁵ N, ² H ₅]-IAA-Leu	10.48	295.2 134.1
55	IAA-Phe	+	323.2 > 130.1	10.69	15	26	[¹⁵ N, ² H ₅]-IAA-Phe	10.67	329.2 > 134.1
56	IAA-Asp	+	291.2 > 130.1	8.13	15	16	[¹³ C ₆]-IAA-Asp	8.13	297.2 > 136.1
57	JA	-	209.2 > 58.8	10.42	20	14	[² H ₆]-JA	10.38	215.2 > 58.8
58	JA-Ile	+	324.3 > 151.2	11.51	30	23	[² H ₂]-JA-Ile	11.49	326.3 > 151.2
59	cisOPDA	+	293.3 > 275.3	13.31	35	12	[² H ₅]-cisOPDA	13.29	298.3 > 279.3
60	dnOPDA	+	265.3 > 247.3	12.16	30	20	[² H ₅]-cisOPDA	13.29	298.3 > 279.3
61	JA-Trp	+	397.3 > 351.3	11.41	30	17	[² H ₂]-JA-Ile	11.49	326.3 > 151.2
62	JA-Phe	+	358.8 > 151.2	11.62	30	23	[² H ₂]-JA-Ile	11.49	326.3 > 151.2
63	JA-Val	+	310.3 > 151.3	10.79	30	23	[² H ₆]-JA	10.38	215.2 > 58.8
64	OPC-6	+	267.3 > 135.2	12.76	15	16	[² H ₂]-JA-Ile	11.49	326.3 > 151.2
65	12-OH-JA	-	225.2 > 58.2	7.76	35	22	[² H ₃]-DPA	7.55	284.1 > 240.1
66	9,10-dh-JA	-	211.2 > 58.8	11.08	10	12	[² H ₆]-JA	10.38	215.2 > 58.8
67	OPC-4	-	237.2 > 58.8	11.44	30	23	[² H ₆]-JA	10.38	215.2 > 58.8
68	SA	-	137.1 > 92.8	9.55	25	13	[² H ₄]-SA	9.50	141.1 > 96.8
69	ABA	-	263.2 > 153.1	9.66	25	10	[² H ₆]-ABA	9.63	269.2 > 159.1
70	DPA	-	281.1 > 237.1	7.56	20	14	[² H ₃]-DPA	7.55	284.1 > 240.1
71	NeoPA	-	279.1 > 205.1	9.16	25	14	[² H ₃]-NeoPA	9.14	282.1 > 208.1

Tab. 3/3	Compound	Scan mode (ESI)	MRM transition	RT (min)	CV (V)	CE (eV)	IS	IS RT (min)	MRM transition
72	PA	-	279.1 > 205.1	8.56	25	14	[² H ₃]-PA	8.53	282.1 > 208.1
73	7-OH-ABA	-	279.1 > 151.1	8.85	10	16	[² H ₄]-7-OH-ABA	8.83	283.1 > 155.1
74	GA ₈	-	363.1 > 275.1	6.95	35	18	[² H ₂]-GA ₈	6.94	365.1 > 277.1
75	GA ₂₉	-	347.1 > 303.1	7.45	30	15	[² H ₂]-GA ₂₉	7.44	349.1 > 261.1
76	GA ₃	-	345.1 > 239.1	8.32	25	14	[² H ₂]-GA ₃	8.31	347.1 > 241.1
77	GA ₁	-	347.1 > 259.1	8.39	32	18	[² H ₂]-GA ₁	8.39	347.1 > 259.1
78	GA ₆	-	345.1 > 119.1	8.99	30	26	[² H ₂]-GA ₆	8.98	347.1 > 119.1
79	GA ₅	-	329.1 > 145.1	9.74	28	14	[² H ₂]-GA ₅	9.73	331.1 > 287.1
80	GA ₁₉	-	361.1 > 273.1	9.66	32	27	[² H ₂]-GA ₁₉	9.65	363.1 > 275.1
81	GA ₂₄	-	345.1 > 257.1	11.62	35	25	[² H ₂]-GA ₂₄	11.61	347.1 > 259.1
82	GA ₄₄	-	345.1 > 301.1	9.95	32	23	[² H ₂]-GA ₄₄	9.94	347.1 > 303.1
83	GA ₃₄	-	347.1 > 259.1	10.27	30	17	[² H ₂]-GA ₃₄	10.27	349.1 > 261.1
84	GA ₅₁	-	331.1 > 287.1	10.52	33	18	[² H ₂]-GA ₅₁	10.51	333.1 > 289.1
85	GA ₅₃	-	347.1 > 329.1	10.64	35	26	[² H ₂]-GA ₅₃	10.63	349.1 > 331.1
86	GA ₄	-	331.1 > 257.1	11.12	33	24	[² H ₂]-GA ₄	11.11	333.1 > 259.1
87	GA ₁₅	-	329.1 > 257.1	12.39	37	22	[² H ₂]-GA ₁₅	13.38	331.1 > 259.1
88	<i>nor</i> CS	+	451.1 > 433.1	12.08	25	12	[² H ₃]-CS	12.75	468.1 > 432.1
89	DS	+	463.1 > 427.1	12.11	35	16	[² H ₃]-CS	12.75	468.1 > 432.1
90	CS	+	465.1 > 429.1	12.76	27	17	[² H ₃]-CS	12.75	468.1 > 432.1
91	<i>epi</i> CS	+	465.1 > 429.1	12.87	27	17	[² H ₃]- <i>epi</i> CS	12.82	468.1 > 432.1
92	<i>nor</i> BL	+	467.1 > 431.1	11.68	25	12	[² H ₃]- <i>nor</i> BL	11.67	470.1 > 434.1
93	homoDS	+	477.1 > 459.1	12.47	35	10	[² H ₃]-BL	12.21	484.1 > 445.1
94	DL	+	479.1 > 349.1	11.63	15	14	[² H ₃]-BL	12.21	484.1 > 445.1
95	BL	+	481.1 > 445.1	12.23	25	12	[² H ₃]-BL	12.21	484.1 > 445.1
96	<i>epi</i> BL	+	481.1 > 445.1	12.35	25	12	[² H ₃]- <i>epi</i> BL	12.34	484.1 > 445.1
97	homoDL	+	493.1 > 349.2	11.99	25	14	[² H ₃]-BL	12.21	484.1 > 445.1
98	homoBL	+	495.1 > 459.1	12.82	25	14	[² H ₃]-BL	12.21	484.1 > 445.1
99	homoCS	+	479.1 > 443.1	13.36	35	10	[² H ₃]-CS	12.75	468.1 > 432.1
100	TE	+	449.1 > 283.1	14.26	10	20	[² H ₃]-TY	14.43	451.7 > 434.2
101	TY	+	449.1 > 431.1	14.47	15	14	[² H ₃]-TY	14.43	451.7 > 434.2

Supplemental Table 4. Hormone-related genes used in the experimental design process.

Tab. 1/3				Auxins				Brassinosteroids	
Gene Name	Accession Number	Gene Name	Accession Number	Gene Name	Accession Number	Gene Name	Accession Number	Gene Name	Accession Number
<i>YUCCA1</i>	AT4G32540	<i>TAR2</i>	AT4G24670	<i>NIT2</i>	AT3G44300	<i>GH3.3</i>	AT2G23170	<i>BASI/CYP734A1</i>	AT2G26710
<i>YUCCA2</i>	AT4G13260	<i>TAR3</i>	AT1G34040	<i>NIT3</i>	AT3G44320	<i>GH3.4</i>	AT1G59500	<i>SOB7/CH12/CYP72C1</i>	AT1G17060
<i>YUCCA3</i>	AT1G04610	<i>TAR4</i>	AT1G34060	<i>NIT4</i>	AT5G22300	<i>GH3.6</i>	AT5G54510	<i>BR6ox1/CYP85A1</i>	AT5G38970
<i>YUCCA4</i>	AT5G11320	<i>TSA1/TRP3</i>	AT3G54640	<i>AMI1</i>	AT1G08980	<i>GH3.9</i>	AT2G47750	<i>BR6ox2/CYP85A2</i>	AT3G30180
<i>YUCCA5</i>	AT5G43890	<i>TSA1 homolog</i>	AT4G02610	<i>CYP71A13</i>	AT2G30770	<i>GH3.17</i>	AT1G28130	<i>CPD/CYP90A1</i>	AT5G05690
<i>YUCCA6</i>	AT5G25620	<i>TSB2/TRP2</i>	AT4G27070	<i>CYP83B1/SUR2</i>	AT4G31500	<i>UGT84B1</i>	AT2G23260	<i>DWF4/CYP90B1</i>	AT3G50660
<i>YUCCA7</i>	AT2G33230	<i>TSB2 homolog</i>	AT5G38530	<i>SUR1</i>	AT2G20610	<i>UGT84B2</i>	AT2G23250	<i>ROT3/CYP90C1</i>	AT4G36380
<i>YUCCA8</i>	AT4G28720	<i>TSB2 homolog</i>	AT5G28237	<i>IAR3</i>	AT1G51760	<i>UGT74E2</i>	AT1G05680	<i>CYP90D1</i>	AT3G13730
<i>YUCCA9</i>	AT1G04180	<i>VAS1/ISS1</i>	AT1G80360	<i>ILL1</i>	AT5G56650	<i>UGT74D1</i>	AT2G31750	<i>DET2</i>	AT2G38050
<i>YUCCA10</i>	AT1G48910	<i>CYP79B2</i>	AT4G39950	<i>ILL2</i>	AT5G56660	<i>UGT75B1</i>	AT1G05560	<i>DWF1/DIM</i>	AT3G19820
<i>YUCCA11</i>	AT1G21430	<i>CYP79B3</i>	AT2G22330	<i>ILR1</i>	AT3G02875	<i>UGT75B2</i>	AT1G05530	<i>STE1/DWF7</i>	AT3G02580
<i>TAA1/SAV3/WEI8</i>	AT1G70560	<i>AAO1</i>	AT5G20960	<i>GH3.1</i>	AT2G14960	<i>IAMT1</i>	AT5G55250	<i>DWF5</i>	AT1G50430
<i>TAR1</i>	AT1G23320	<i>NIT1</i>	AT3G44310	<i>GH3.2</i>	AT4G37390	<i>DAO2</i>	AT1G14120	<i>UGT73C5</i>	AT2G36800

Tab. 2/3						Gibberellins			
		Cytokinins							
Gene Name	Accession Number	Gene Name	Accession Number	Gene Name	Accession Number	Gene Name	Accession Number	Gene Name	Accession Number
<i>IPT1</i>	AT1G68460	<i>LOG3</i>	AT2G37210	<i>CKX7</i>	AT5G21482	<i>ATCPS/GA1</i>	AT4G02780	<i>ATGA3OX3</i>	AT4G21690
<i>IPT2</i>	AT2G27760	<i>LOG4</i>	AT3G53450	<i>UGT76C1</i>	AT5G05870	<i>ATKS/GA2</i>	AT1G79460	<i>ATGA3OX4</i>	AT1G80330
<i>IPT3</i>	AT3G63110	<i>LOG5</i>	AT4G35190	<i>UGT76C2</i>	AT5G05860	<i>ATKO/GA3</i>	AT5G25900	<i>ATGA2OX1</i>	AT1G78440
<i>IPT4</i>	AT4G24650	<i>LOG6</i>	AT5G03270	<i>UGT73C1</i>	AT2G36750	<i>ATKAO1</i>	AT1G05160	<i>ATGA2OX2</i>	AT1G30040
<i>IPT5</i>	AT5G19040	<i>LOG7</i>	AT5G06300	<i>UGT73C5</i>	AT2G36800	<i>ATKAO2</i>	AT2G32440	<i>ATGA2OX3</i>	AT2G34555
<i>IPT6</i>	AT1G25410	<i>LOG8</i>	AT5G11950	<i>UGT85A1</i>	AT1G22400	<i>ATGA20OX1/GA5</i>	AT4G25420	<i>ATGA2OX4</i>	AT1G47990
<i>IPT7</i>	AT3G23630	<i>LOG9</i>	AT5G26140	<i>AK1</i>	AT3G09820	<i>ATGA20OX2</i>	AT5G51810	<i>ATGA2OX5</i>	AT3G17203
<i>IPT8</i>	AT3G19160	<i>CKX1</i>	AT2G41510	<i>AK2</i>	AT5G03300	<i>ATGA20OX3</i>	AT5G07200	<i>ATGA2OX6</i>	AT1G02400
<i>IPT9</i>	AT5G20040	<i>CKX2</i>	AT2G19500	<i>APT1</i>	AT1G27450	<i>ATGA20OX4</i>	AT1G60980	<i>ATGA2OX7</i>	AT1G50960
<i>CYP735A1</i>	AT5G38450	<i>CKX3</i>	AT5G56970	<i>APT2</i>	AT1G80050	<i>ATGA20OX5</i>	AT1G44090	<i>ATGA2OX8</i>	AT4G21200
<i>CYP735A2</i>	AT1G67110	<i>CKX4</i>	AT4G29740	<i>APT3</i>	AT4G22570	<i>ATGA3OX1/GA4</i>	AT1G15550	<i>GAMT1</i>	AT4G26420
<i>LOG1</i>	AT2G28305	<i>CKX5</i>	AT1G75450	<i>APT4</i>	AT4G12440	<i>ATGA3OX2</i>	AT1G80340	<i>GAMT2</i>	AT5G56300
<i>LOG2</i>	AT2G35990	<i>CKX6</i>	AT3G63440	<i>APT5</i>	AT5G11160				

Tab. 3/3		Jasmonates				Salicylates			
Abscisates		Gene Name		Accession Number		Gene Name		Accession Number	
Gene Name	Accession Number	Gene Name	Accession Number	Gene Name	Accession Number	Gene Name	Accession Number	Gene Name	Accession Number
<i>ABA1/ZEP</i>	AT5G67030	<i>DAD1</i>	AT2G44810	<i>JMT</i>	AT1G19640	<i>ICS1/SID2</i>	AT1G74710		
<i>ABA4</i>	AT1G67080	<i>DGL</i>	AT1G05800	<i>ATST2A</i>	AT5G07010	<i>ICS2</i>	AT1G18870		
<i>NCED2</i>	AT4G18350	<i>LOX2</i>	AT3G45140	<i>IAR3</i>	AT1G51760	<i>BSMT1</i>	AT3G11480		
<i>NCED3</i>	AT3G14440	<i>AOS</i>	AT5G42650	<i>ILL6</i>	AT1G44350	<i>UGT74F1</i>	AT2G43840		
<i>NCED5</i>	AT1G30100	<i>AOC1</i>	AT3G25760			<i>UGT74F2</i>	AT2G43820		
<i>NCED6</i>	AT3G24220	<i>AOC2</i>	AT3G25770			<i>ATMES1</i>	AT2G23620		
<i>NCED9</i>	AT1G78390	<i>AOC3</i>	AT3G25780			<i>ATMES2</i>	AT2G23600		
<i>ABA2</i>	AT1G52340	<i>OPR3</i>	AT2G06050			<i>ATMES7</i>	AT2G23560		
<i>AAO3</i>	AT2G27150	<i>OPCL1</i>	AT1G20510			<i>ATMES9</i>	AT4G37150		
<i>ABA3</i>	AT1G16540	<i>ACX1</i>	AT4G16760			<i>ATMES10</i>	AT2G23580		
<i>CYP707A1</i>	AT4G19230	<i>ACX2</i>	AT5G65110			<i>S3H</i>	AT4G10500		
<i>CYP707A2</i>	AT2G29090	<i>ACX3</i>	AT1G06290						
<i>CYP707A3</i>	AT5G45340	<i>ACX4</i>	AT3G51840						
<i>CYP707A4</i>	AT3G19270	<i>ACX5</i>	AT2G35690						
<i>BG1</i>	AT1G52400	<i>JAR1</i>	AT2G46370						

Supplemental Table 5. Genes showing shifts in expression levels under salt stress in roots (Figure 3c), abbreviated and full names of the encoded enzymes, the classes of phytohormones affected, log ratios of shifts in expression levels, and functions of the enzymes.

Tab. 1/2		ROOTS				
Gene ID	Enzyme abb.	Name	Class	Log Ratio	Function	
AT3G63110	IPT3	Adenylate isopentenyltransferase	CKs	-1.0709		
AT5G19040	IPT5	Adenylate isopentenyltransferase	CKs	-0.8306		
AT5G20040	IPT9	rRNA dimethylallyltransferase	CKs	0.6334		
AT2G28305	LOG1	Cytokinin riboside 5'-monophosphate phosphoribohydrolase	CKs	3.5571		
AT2G35990	LOG2	Cytokinin riboside 5'-monophosphate phosphoribohydrolase	CKs	0.9355	Biosynthesis	
AT2G37210	LOG3	Cytokinin riboside 5'-monophosphate phosphoribohydrolase	CKs	1.4418		
AT3G53450	LOG4	Cytokinin riboside 5'-monophosphate phosphoribohydrolase	CKs	1.9621		
AT4G35190	LOG5	Cytokinin riboside 5'-monophosphate phosphoribohydrolase	CKs	2.4630		
AT5G03270	LOG6	Cytokinin riboside 5'-monophosphate phosphoribohydrolase	CKs	0.8193		
AT5G06300	LOG7	Cytokinin riboside 5'-monophosphate phosphoribohydrolase	CKs	0.9856		
AT1G27450	APT1	Adenine phosphoribosyltransferase	CKs	-0.9455		
AT4G22570	APT3	Adenine phosphoribosyltransferase	CKs	-1.4150	Inactivation	
AT3G63440	CKX6	Cytokinin dehydrogenase	CKs	0.9246		
AT5G05870	UGT76C1	UDP-glycosyltransferase	CKs	0.8225		
AT4G02610	TSA1/TRP3	Tryptophan synthase alpha chain	AXs	0.7317	Biosynthesis	
AT1G70560	TAA1/SAV3/WEI8	L-tryptophan-pyruvate aminotransferase	AXs	-1.0493		
AT4G24670	TAR2	Tryptophan aminotransferase-related protein	AXs	-1.8919		
AT5G43890	YUCCA5	Indole-3-pyruvate monooxygenase	AXs	1.6154	Biosynthesis	
AT1G04610	YUCCA3	Indole-3-pyruvate monooxygenase	AXs	-1.9446		
AT1G04180	YUCCA9	Indole-3-pyruvate monooxygenase	AXs	-2.6278		
AT4G39950	CYP79B2	Tryptophan N-monooxygenase	AXs	0.8139		
AT2G22330	CYP79B3	Tryptophan N-monooxygenase	AXs	1.5571		
AT2G30770	CYP71A13	Indoleacetaldoxime dehydratase	AXs	3.0427	Biosynthesis	
AT5G22300	NIT4	Nitrilase/nitrile hydratase	AXs	1.5918		
AT1G08980	AMI1	Amidase	AXs	0.8391		
AT4G31500	CYP83B1/SUR2	Cytochrome P450	AXs	1.3032		
AT2G14960	GH3.1	Indole-3-acetic acid-amido synthetase	AXs	1.6081		
AT1G28130	GH3.17	Indole-3-acetic acid-amido synthetase	AXs	-1.3290		
AT4G27260	GH3.5	Indole-3-acetic acid-amido synthetase	AXs	-0.7478		
AT2G31750	UGT74D1	UDP-glycosyltransferase	AXs	-1.4148	Inactivation	
AT1G05680	UGT74E2	UDP-glycosyltransferase	AXs	6.4651		
AT1G05560	UGT75B1	UDP-glycosyltransferase	AXs	1.1194		

Tab.2/2		ROOTS			
Gene ID	Enzyme abb.	Name	Class	Log Ratio	Function
AT5G42650	AOS	Allene oxide synthase	JAs	1.0007	
AT3G25780	AOC3	Allene oxide cyclase	JAs	0.6270	
AT1G20510	OPCL1	4-coumarate-CoA ligase	JAs	1.4586	
AT4G16760	ACX1	Acyl-coenzyme A oxidase	JAs	0.8648	Biosynthesis
AT5G65110	ACX2	Acyl-coenzyme A oxidase	JAs	1.9296	
AT2G06050	OPR3	12-oxophytodienoate reductase	JAs	1.1686	
AT2G46370	JAR1	Jasmonic acid-amido synthetase	JAs	-0.967	
AT3G14440	NCED3	9-cis-epoxycarotenoid dioxygenase	ABAs	5.5859	
AT1G30100	NCED5	9-cis-epoxycarotenoid dioxygenase	ABAs	0.9134	
AT5G67030	ABA1	Zeaxanthin epoxidase	ABAs	0.7910	Biosynthesis
AT1G52340	ABA2	Xanthoxin dehydrogenase	ABAs	0.7901	
AT1G16540	ABA3	Molybdenum cofactor sulfurase	ABAs	0.9172	
AT2G27150	AAO3	Abscisic-aldehyde oxidase	ABAs	1.5040	
AT1G52400	BG1	Beta-D-glucopyranosyl abscisate beta-glucosidase	ABAs	1.9507	Reactivation
AT4G19230	CYP707A1	Abscisic acid 8'-hydroxylase	ABAs	2.9988	
AT5G45340	CYP707A3	Abscisic acid 8'-hydroxylase	ABAs	2.0716	Inactivation
AT3G19270	CYP707A4	Abscisic acid 8'-hydroxylase	ABAs	1.0005	
AT5G25900	KO	Ent-kaurene oxidase	GAs	0.6231	Biosynthesis
AT1G80340	GA3ox2	Gibberellin 3-beta-dioxygenase	GAs	-1.3109	
AT1G30040	GA2ox2	Gibberellin 2-beta-dioxygenase	GAs	1.7884	Inactivation

Supplemental Table 6. Genes showing shifts in expression levels under salt stress in shoots (Figure 3d), abbreviated and full names of the encoded enzymes, the classes of phytohormones affected, log ratios of shifts in expression levels, and functions of the enzymes.

SHOOTS					
Gene ID	Enzyme	Name	Class	Log Ratio	Function
AT5G20040	IPT9	<i>t</i> RNA isopentenyltransferase	CK	-1.1413	
AT1G80050	APT2	Adenine phosphoribosyltransferase	CK	-0.9771	Biosynthesis
AT4G22570	APT3	Adenine phosphoribosyltransferase	CK	-1.0633	
AT5G11160	APT5	Adenine phosphoribosyltransferase	CK	-1.2414	
AT2G36750	UGT73C1	UDP-glycosyltransferase	CK	2.1987	
AT5G05870	UGT76C1	UDP-glycosyltransferase	CK	0.6807	Inactivation
AT5G05860	UGT76C2	UDP-glycosyltransferase	CK	-1.9277	
AT3G63440	CKX6	Cytokinin dehydrogenase	CK	-0.8776	
AT4G24670	TAR2	Tryptophan aminotransferase-related protein	AXs	-1.3820	
AT1G70560	TAA1/SAV3/WEI8	L-tryptophan--pyruvate aminotransferase	AXs	-0.8621	Biosynthesis
AT5G22300	NIT4	Nitrilase/nitrile hydratase	AXs	-1.0426	
AT4G39950	CYP79B2	Tryptophan N-monooxygenase	AXs	0.8458	
AT1G05560	UGT75B1	UDP-glycosyltransferase	AXs	1.0386	Inactivation
AT1G05680	UGT74E2	UDP-glycosyltransferase	AXs	1.2817	
AT3G45140	LOX2	Lipoxygenase	JAs	1.6230	
AT1G20510	OPCL1	4-coumarate-CoA ligase	JAs	0.6749	Biosynthesis
AT4G16760	ACX1	Acyl-coenzyme A oxidase	JAs	1.8911	
AT5G65110	ACX2	Acyl-coenzyme A oxidase	JAs	0.8560	
AT3G14440	NCED3	9- <i>cis</i> -epoxycarotenoid dioxygenase	ABAs	3.1663	Biosynthesis
AT2G27150	AAO3	Abscisic-aldehyde oxidase	ABAs	1.2404	
AT4G19230	CYP707A1	Abscisic acid 8'-hydroxylase	ABAs	1.7435	
AT2G29090	CYP707A2	Abscisic acid 8'-hydroxylase	ABAs	1.0673	Inactivation
AT5G45340	CYP707A3	Abscisic acid 8'-hydroxylase	ABAs	1.7931	
AT3G19270	CYP707A4	Abscisic acid 8'-hydroxylase	ABA	0.7905	
AT5G25900	KO	<i>ent</i> -kaurene oxidase	GAs	0.7977	Biosynthesis
AT1G15550	GA3ox1	Gibberellin 3-oxidase	GAs	1.8984	
AT1G02400	GA2ox6	Gibberellin 2-oxidase	GAs	0.7219	Inactivation

Supplemental Table 7. Determined levels of plant hormones in root and shoot samples of salt-stressed and control *A. thaliana* plants (pmol/g FW; n=3), p-values (Student's t-test) and asterisks indicating significance (p>0.05, "-", p>0.01; "*"; p>0.001; "***"; p<0.001, "****").

		ROOTS			
	Compound	Control	Salt-stressed	p-value	Significance
CKs	iP	0.03 ± 0.01	0.11 ± 0.01	0.00157	**
	iPR	2.07 ± 0.38	6.37 ± 1.53	0.01798	*
	iP7G	21.7 ± 4.98	18.9 ± 2.20	0.49705	-
	iP9G	1.30 ± 0.27	1.15 ± 0.18	0.54473	-
	tZ	0.74 ± 0.15	0.57 ± 0.08	0.23242	-
	tZR	3.28 ± 0.96	4.49 ± 0.14	0.15224	-
	tZ7G	5.87 ± 1.20	3.54 ± 0.36	0.05799	-
	tZ9G	7.77 ± 1.70	5.03 ± 0.55	0.09621	-
	tZOG	26.9 ± 7.2	25.6 ± 3.55	0.82071	-
	tZROG	0.08 ± 0.01	0.07 ± 0.01	0.46222	-
	DHZR	0.12 ± 0.04	0.11 ± 0.01	0.73354	-
	DHZ7G	3.07 ± 0.38	2.17 ± 0.07	0.02928	*
	DHZ9G	0.09 ± 0.03	0.07 ± 0.01	0.28480	-
	cZ	0.34 ± 0.08	0.26 ± 0.01	0.27173	-
	cZR	3.24 ± 0.33	5.93 ± 0.52	0.00351	**
	cZ9G	6.27 ± 0.67	10.1 ± 0.65	0.00447	**
	cZOG	5.73 ± 0.36	6.59 ± 0.83	0.24659	-
cZROG	0.97 ± 0.27	1.04 ± 0.05	0.24659	-	
2MeSiPR	0.72 ± 0.16	1.26 ± 0.20	0.04150	*	
2MeScZR	3.46 ± 0.40	4.62 ± 0.05	0.01526	*	
AXs	TRP	5439 ± 1281	20513 ± 1603	0.00049	****
	IAM	0.06 ± 0.03	0.18 ± 0.03	0.01437	*
	IAN	8058 ± 2273	20938 ± 4482	0.02228	*
	IAA	297 ± 2.56	213 ± 30.0	0.03391	*
	OxIAA	579 ± 0.30	306 ± 61.2	0.00322	**
	IAA-Asp	17.4 ± 6.94	16.3 ± 0.12	0.87138	-
	IAA-Glu	31.8 ± 1.78	121 ± 25.6	0.03161	*
	IAA-Gly	2.60 ± 0.16	8.63 ± 1.43	0.00409	**
JAs	cisOPDA	42.8 ± 3.16	93.9 ± 12.8	0.00531	**
	dnOPDA	1564 ± 142	474 ± 102	0.00094	****
	9.10-dh-JA	6.33 ± 0.84	9.76 ± 1.51	0.04873	*
	JA	12.3 ± 0.84	21.2 ± 3.49	0.02474	*
	JA-Ile	3.89 ± 0.12	3.44 ± 1.27	0.64126	-
	JA-Trp	0.84 ± 0.09	2.60 ± 0.06	0.00002	****
	JA-Phe	0.97 ± 0.19	0.76 ± 0.14	0.28207	-
ABAs	ABA	1.66 ± 0.06	31.2 ± 8.13	0.00680	**
	PA	0.13 ± 0.0002	15.6 ± 3.10	0.00214	**
	DPA	30.7 ± 3.90	882 ± 189	0.00312	**
SA	SA	498 ± 170	523 ± 81.2	0.86237	-
GAs	GA ₂₄	<LOD	<LOD	n/a	-
	GA ₃	0.58 ± 0.16	1.19 ± 0.46	0.15149	-
	GA ₄	10.1 ± 1.52	3.88 ± 2.35	0.03440	*
	GA ₅	6.23 ± 1.40	6.19 ± 1.28	0.97888	-
BRs	epiBL	<LOQ	<LOQ	n/a	-
	norCS	<LOQ	<LOQ	n/a	-

SHOOTS					
	Compound	Control	Salt-stressed	p-value	Significance
CKs	iP	0.09 ± 0.02	0.14 ± 0.03	0.12963	-
	iPR	2.53 ± 0.85	7.52 ± 2.40	0.02502	*
	iP7G	65.8 ± 1.56	70.5 ± 4.34	0.22195	-
	iP9G	5.08 ± 0.78	4.95 ± 0.38	0.83714	-
	iZ	0.22 ± 0.04	0.25 ± 0.02	0.32486	-
	iZR	0.99 ± 0.16	1.01 ± 0.02	0.88306	-
	iZ7G	6.03 ± 1.11	5.06 ± 1.00	0.41221	-
	iZ9G	4.05 ± 0.26	3.66 ± 0.42	0.33160	-
	iZOG	37.0 ± 3.01	32.8 ± 2.52	0.20485	-
	iZROG	0.38 ± 0.02	0.31 ± 0.04	0.08893	-
	DHZR	0.02 ± 0.01	0.003 ± 0.0001	0.01334	*
	DHZ7G	3.81 ± 0.49	2.89 ± 0.33	0.18777	-
	DHZ9G	0.07 ± 0.01	0.05 ± 0.01	0.04413	*
	cZ	0.08 ± 0.01	0.08 ± 0.01	0.53465	-
	cZR	0.57 ± 0.05	1.06 ± 0.21	0.03249	*
	cZ9G	4.88 ± 0.05	4.71 ± 0.40	0.60139	-
	cZOG	3.74 ± 0.48	3.12 ± 0.27	0.18818	-
	cZROG	8.20 ± 0.55	5.92 ± 0.70	0.02258	*
	2MeSiPR	0.67 ± 0.21	0.98 ± 0.55	0.51127	-
	2MeScZR	20.5 ± 0.58	15.1 ± 1.84	0.01719	*
AXs	TRP	9184 ± 1283	8743 ± 117	0.65359	-
	IAM	0.72 ± 0.15	0.80 ± 0.15	0.62552	-
	IAN	22168 ± 2225	23021 ± 2132	0.71529	-
	IAA	211 ± 7.03	158 ± 25.6	0.04531	*
	OxIAA	553 ± 31.85	435 ± 39.5	0.02980	*
	IAA-Asp	239 ± 34.72	235 ± 17.8	0.91214	-
	IAA-Glu	719 ± 85.2	648 ± 148	0.69439	-
	IAA-Gly	14.8 ± 5.19	7.83 ± 3.52	0.19059	-
JAs	cisOPDA	12224 ± 1511	14127 ± 3875	0.55294	-
	dnOPDA	24683 ± 3923	32747 ± 2566	0.07182	-
	9.10-dh-JA	33.4 ± 2.64	13.4 ± 1.75	0.00087	***
	JA	51.0 ± 12.9	36.3 ± 13.0	0.31887	-
	JA-Ile	12.6 ± 1.40	3.03 ± 0.48	0.00079	***
	JA-Trp	<LOD	<LOD	n/a	-
	JA-Phe	<LOD	<LOD	n/a	-
ABAs	ABA	6.11 ± 1.87	20.7 ± 4.16	0.01070	*
	PA	0.14 ± 0.003	85.7 ± 42.4	0.04627	*
	DPA	45.3 ± 0.25	89.3 ± 14.7	0.01319	*
SA	SA	318 ± 21.2	324 ± 35.18	0.82340	-
GAs	GA ₂₄	17.4 ± 3.20	3.21 ± 0.60	0.00350	**
	GA ₃	0.15 ± 0.03	0.77 ± 0.46	0.12672	-
	GA ₄	2.36 ± 0.05	3.90 ± 0.30	0.00431	**
	GA ₅	<LOD	<LOD	n/a	-
BRs	epiBL	<LOQ	<LOQ	n/a	-
	norCS	<LOQ	<LOQ	n/a	-

Supplemental Table 8. Determination of chlorophyll (Chl_{a,b}) extracted using water:acetonitrile (ACN) mixtures with indicated ACN contents. Chlorophyll concentration expressed in mg/l (n=4); SD, standard deviation. N.D., not detected.

Extraction solvent	Replicate	Chlorophyll Conc (Mean ± SD; mg/l)									
		750 nm	663.2 nm	646.8 nm	Chl _(a)		Chl _(b)		Chl _(a) +Chl _(b)		
H₂O	1.	0.0478	0.0433	0.0454							
	2.	0.0571	0.0526	0.0545	N.D.		N.D.		N.D.		
	3.	0.0483	0.0442	0.0462							
	4.	0.0553	0.0515	0.0537							
10% ACN	1.	0.0436	0.0380	0.0390							
	2.	0.0491	0.0458	0.0469	N.D.		N.D.		N.D.		
	3.	0.0630	0.0630	0.0638							
	4.	0.0492	0.0459	0.0468							
30% ACN	1.	0.0795	0.1576	0.1303	0.81	0.72 ± 0.09	0.69	0.62 ± 0.08	1.51	1.34 ± 0.17	
	2.	0.0530	0.1155	0.0946	0.65		0.58		1.23		
	3.	0.0778	0.1524	0.1273	0.78		0.68		1.46		
	4.	0.0547	0.1149	0.0942	0.63		0.54		1.17		
50% ACN	1.	0.0504	1.0236	0.5090	10.64	9.21 ± 1.61	4.90	4.23 ± 0.75	15.54	13.44 ± 2.36	
	2.	0.0536	0.7728	0.3912	7.87		3.59		11.46		
	3.	0.0494	1.0153	0.5046	10.56		4.86		15.42		
	4.	0.0532	0.7639	0.3877	7.77		3.57		11.34		
70% ACN	1.	0.0762	2.2325	1.1318	23.47	23.80 ± 0.39	11.70	11.94 ± 0.18	35.17	35.74 ± 0.56	
	2.	0.0541	2.2760	1.1445	24.18		12.11		36.29		
	3.	0.0726	2.2307	1.1377	23.47		11.89		35.36		
	4.	0.0504	2.2653	1.1358	24.10		12.04		36.14		
100% ACN	1.	0.0430	2.5768	1.3875	27.29	27.33 ± 0.05	15.98	16.17 ± 0.24	43.27	43.49 ± 0.29	
	2.	0.0467	2.5912	1.4134	27.36		16.41		43.76		
	3.	0.0430	2.5753	1.3849	27.28		15.94		43.21		
	4.	0.0463	2.5919	1.4098	27.38		16.33		43.71		

Supplemental Table 9. Results of tests of pH stability of selected compounds in 50% acetonitrile (control), an alkaline solvent and an acidic solvent. Standard deviation (SD%; n=3). Significance (*) is based on Student's t-test, P<0.05. FA, formic acid; MeOH, methanol.

Class	Compound	Treatment	Average Area	Relative to control (%) ± SD%	Significance
JAs	JA-Ile	control	1082554	100 ± 9.92	
		0.35 M NH ₄ OH in 60% MeOH	843317	78 ± 9.15	-
		1 M FA in H ₂ O	788192	73 ± 3.20	*
	JA-Phe	control	693114	100 ± 9.99	
		0.35 M NH ₄ OH in 60% MeOH	598110	86 ± 15.88	-
		1 M FA in H ₂ O	466689	67 ± 3.49	*
	JA-Val	control	438487	100 ± 17.57	
		0.35 M NH ₄ OH in 60% MeOH	393394	90 ± 10.72	-
		1 M FA in H ₂ O	329475	75 ± 3.96	-
JA-Trp	control	626693	100 ± 13.99		
	0.35 M NH ₄ OH in 60% MeOH	503238	80 ± 21.41	-	
	1 M FA in H ₂ O	320746	51 ± 24.65	*	
AXs	IAA-Asp	control	421687	100 ± 2.04	
		0.35 M NH ₄ OH in 60% MeOH	417608	99 ± 1.75	-
		1 M FA in H ₂ O	370910	88 ± 5.77	*
	IAA-Glu	control	1030594	100 ± 1.26	
		0.35 M NH ₄ OH in 60% MeOH	1028582	100 ± 2.88	-
		1 M FA in H ₂ O	915294	89 ± 6.12	*
GAs	GA ₅₃	control	20453	100 ± 11.25	
		0.35 M NH ₄ OH in 60% MeOH	18730	92 ± 15.28	-
		1 M FA in H ₂ O	11056	54 ± 2.49	*
	GA ₄	control	10560	100 ± 11.48	
		0.35 M NH ₄ OH in 60% MeOH	10024	95 ± 13.57	-
		1 M FA in H ₂ O	7431	70 ± 2.73	*
	GA ₂₄	control	19351	100 ± 12.19	
		0.35 M NH ₄ OH in 60% MeOH	18139	94 ± 20.25	-
		1 M FA in H ₂ O	9790	51 ± 7.77	*
CKs	cZOG	control	868298	100 ± 8.38	
		0.35 M NH ₄ OH in 60% MeOH	828850	95 ± 3.62	-
		1 M FA in H ₂ O	830865	96 ± 4.42	-
	tZ9G	control	2472940	100 ± 9.71	
		0.35 M NH ₄ OH in 60% MeOH	2289342	93 ± 2.85	-
		1 M FA in H ₂ O	2298027	93 ± 5.79	-
	tZROG	control	1688755	100 ± 6.10	
		0.35 M NH ₄ OH in 60% MeOH	1582395	94 ± 4.86	-
		1 M FA in H ₂ O	1612154	95 ± 7.90	-
	iP7G	control	2247776	100 ± 3.43	
		0.35 M NH ₄ OH in 60% MeOH	2288729	102 ± 2.75	-
		1 M FA in H ₂ O	2248139	100 ± 1.97	-

Supplemental Table 10. Solubility of selected representatives of the most hydrophobic phytohormone class (brassinosteroids) using extraction solvents with indicated acetonitrile (ACN) concentration (n=3). APA, average peak area; SD, standard deviation; RY, relative yield (ratio of average peak area to maximal average peak area per extraction solvent). TY, typhasterol; TE, teasterone; BL, brassinolide; CS, castasterone.

Tab.	10% ACN		20% ACN		30% ACN		50% ACN		70% ACN		
	1/2	APA (%)	SD	APA (%)	SD	APA (%)	SD	APA (%)	SD	APA (%)	SD
TY		46325 ± 8818		68166 ± 10095		107478 ± 20603		175455 ± 16273		183292 ± 19087	
TE		12162 ± 1358		21839 ± 953		29888 ± 8301		47581 ± 1563		42030 ± 896	
BL		79393 ± 4136		108491 ± 13659		115675 ± 25981		168312 ± 5119		146625 ± 11008	
CS		62518 ± 5372		78696 ± 6699		100966 ± 577		126220 ± 4804		136623 ± 3250	

Tab.	10% ACN		20% ACN		30% ACN		50% ACN		70% ACN		
	2/2	RY (%)	SD	RY (%)	SD	RY (%)	SD	RY (%)	SD	RY (%)	SD
TY		25.27 ± 19.04		37.19 ± 14.81		58.64 ± 19.17		95.72 ± 9.27		100.00 ± 10.41	
TE		25.56 ± 11.17		45.90 ± 4.37		62.81 ± 27.77		100.00 ± 3.28		88.33 ± 2.13	
BL		47.17 ± 5.21		64.46 ± 12.59		68.73 ± 22.46		100.00 ± 3.04		87.11 ± 7.51	
CS		45.76 ± 8.59		57.60 ± 8.51		73.90 ± 0.57		92.39 ± 3.81		100.00 ± 2.38	

Supplement II

Žižková, E., Kubeš, M., Dobrev, P., I., Příbyl, P., **Šimura, J.**, Zahajská, L., Závěská Drábková, L., Novák, O., & Motyka, V. (2017). Control of cytokinin and auxin homeostasis in cyanobacteria and algae. *Annals of Botany*, 119(1), 151–166.

Control of cytokinin and auxin homeostasis in cyanobacteria and algae

Eva Žižková¹, Martin Kubeš^{1,2}, Petre I. Dobrev¹, Pavel Příbyl³, Jan Šimura², Lenka Zahajská⁴,
Lenka Závěská Drábková⁵, Ondřej Novák⁶ and Václav Motyka^{1,*}

¹Laboratory of Hormonal Regulations in Plants, Institute of Experimental Botany CAS, Rozvojová 263, CZ-165 02 Prague 6, Czech Republic, ²Department of Chemical Biology and Genetics, Centre of the Region Haná for Biotechnological and Agricultural Research, Faculty of Science, Palacký University, Šlechtitelů 27, CZ-783 71 Olomouc, Czech Republic, ³Centre for Phycology and Biorefinery Research Centre of Competence, Institute of Botany CAS, Dukelská 135, CZ-379 82 Třeboň, Czech Republic, ⁴Isotope Laboratory, Institute of Experimental Botany CAS, Vídeňská 1083, CZ-142 20 Prague 4, Czech Republic, ⁵Department of Taxonomy and Biosystematics, Institute of Botany CAS, Zámek 1, CZ-252 43 Průhonice, Czech Republic and ⁶Laboratory of Growth Regulators, Centre of the Region Haná for Biotechnological and Agricultural Research, Faculty of Science of Palacký University and Institute of Experimental Botany CAS, Šlechtitelů 27, CZ-783 71 Olomouc, Czech Republic

*For correspondence. E-mail vmotyka@ueb.cas.cz

Received: 15 June 2016 Returned for revision: 18 July 2016 Accepted: 11 August 2016

- **Background and Aims** The metabolism of cytokinins (CKs) and auxins in vascular plants is relatively well understood, but data concerning their metabolic pathways in non-vascular plants are still rather rare. With the aim of filling this gap, 20 representatives of taxonomically major lineages of cyanobacteria and algae from Cyanophyceae, Xanthophyceae, Eustigmatophyceae, Porphyridiophyceae, Chlorophyceae, Ulvophyceae, Trebouxiophyceae, Zygnematophyceae and Klebsormidiophyceae were analysed for endogenous profiles of CKs and auxins and some of them were used for studies of the metabolic fate of exogenously applied radiolabelled CK, [³H]trans-zeatin (*transZ*) and auxin ([³H]indole-3-acetic acid (IAA)), and the dynamics of endogenous CK and auxin pools during algal growth and cell division.
- **Methods** Quantification of phytohormone levels was performed by high-performance or ultrahigh-performance liquid chromatography–electrospray tandem mass spectrometry (HPLC-MS/MS, UHPLC-MS/MS). The dynamics of exogenously applied [³H]transZ and [³H]IAA in cell cultures were monitored by HPLC with on-line radioactivity detection.
- **Key Results** The comprehensive screen of selected cyanobacteria and algae for endogenous CKs revealed a predominance of bioactive and phosphate CK forms while *O*- and *N*-glucosides evidently did not contribute greatly to the total CK pool. The abundance of *cis*-zeatin-type CKs and occurrence of CK 2-methylthio derivatives pointed to the tRNA pathway as a substantial source of CKs. The importance of the tRNA biosynthetic pathway was proved by the detection of tRNA-bound CKs during the course of *Scenedesmus obliquus* growth. Among auxins, free IAA and its oxidation catabolite 2-oxindole-3-acetic acid represented the prevailing endogenous forms. After treatment with [³H]IAA, IAA-aspartate and indole-3-acetyl-1-glucosyl ester were detected as major auxin metabolites. Moreover, different dynamics of endogenous CKs and auxin profiles during *S. obliquus* culture clearly demonstrated diverse roles of both phytohormones in algal growth and cell division.
- **Conclusions** Our data suggest the existence and functioning of a complex network of metabolic pathways and activity control of CKs and auxins in cyanobacteria and algae that apparently differ from those in vascular plants.

Key words: Cytokinin, auxin, cyanobacteria, algae, metabolism, cytokinin oxidase/dehydrogenase, cytokinin 2-methylthioderivatives, *trans*-zeatin, indole-3-acetic acid, tRNA.

INTRODUCTION

Many aspects of plant growth and development are coordinated by plant hormones. Among them, cytokinins (CKs) represent one of the most important groups, playing a key role in cytokinesis and regulation of the cell cycle. In addition, CKs affect a number of other physiological processes, such as morphogenesis, apical dominance, leaf senescence, chloroplast development and seed dormancy (Miller *et al.*, 1956; Hwang *et al.*, 2012). Naturally occurring CKs are *N*⁶-substituted adenine derivatives with isoprenoid or aromatic side-chain functioning specifically at minute concentrations (10⁻⁶ to 10⁻⁹ M) in plant

tissues (Santner *et al.*, 2009; Kieber and Schaller, 2014). [In this article, CKs are abbreviated as proposed and modified by Kamínek *et al.* (2000).] While *N*⁶-(Δ^2 -isopentenyl)adenine (iP), *trans*-zeatin (*transZ*), *cis*-zeatin (*cisZ*), dihydrozeatin (DHZ) and their derivatives are typical representatives of isoprenoid CKs, *N*⁶-benzyladenine (BA) and its hydroxylated forms *ortho*-topolin and *meta*-topolin represent common aromatic CKs. According to their structure and physiological activity, CKs are categorized into (1) bioactive forms, including free bases and corresponding nucleosides and their precursors (nucleotides), and (2) non-active or weakly active forms, CK-*O*- and CK-*N*-glucosides (Sakakibara, 2006). In the plant kingdom, a wide

spectrum of CK derivatives has been found to occur ubiquitously in vascular plants (Gajdošová et al., 2011; Spíchal, 2012) as well as in bryophytes (Záveská Drábková et al., 2015) and fungi (Morrison et al., 2015). In contrast to vascular plants, none or only trace amounts of CK *N*-glucosylated forms and mostly rather low levels of CK *O*-glucosides have been reported in cyanobacteria or algae (Stirk et al., 2003, 2013; Ördög et al., 2004; Tarakhovskaya et al., 2007; Hussain et al., 2010).

Cyanobacteria as photosynthetic microorganisms exhibit beneficial effects on plant growth through their CK-like activity in processes of atmospheric nitrogen fixation, and thus are successfully utilized in agriculture (Stirk et al., 1999, 2002; Abdel-Raouf et al., 2012). A relatively simple CK metabolism in cyanobacteria was predicted based on a search of CK-related homologous genes involved in CK biosynthesis and degradation pathways. Frébort et al. (2011) and Kakimoto (2003) confirmed that isopentenyltransferases (IPTs) catalysing the first step in CK biosynthesis in cyanobacteria have a high level of similarity with bacterial tRNA isopentenyltransferases (tRNA-IPTs) and adenylate isopentenyltransferases (AMP/ADP/ATP-IPTs). Recently, the function of gene encoded adenylate-IPT in the cyanobacterium *Nostoc* sp. PCC 7120 has been reported, although it clusters to plant tRNA-IPT (Frébortová et al., 2015). Interestingly, a putative CK oxidase/dehydrogenase (CKX) homologous gene sequence involved in CK degradation was discovered in *Nostoc* sp. PCC 7120 (*NsCKX1*), but the predicted *NsCKX1* similarity to plant CKX proteins was very low (Schmülling et al., 2003). Moreover, functional analysis of the recombinant CKX protein named in the study as NoCKX1 revealed no detectable activity for CK downregulation (Frébortová et al., 2015). In addition, no matching CKX sequences were detected in *Synechocystis* sp. PCC 6803 and *Prochlorococcus marinus*, in contrast to some other cyanobacterial species (Schmülling et al., 2003; Frébort et al., 2011). On the other hand, the regulatory effect of CKs on cyanobacteria metabolism has been reported for *Synechocystis* sp. PCC 6803 strain, where BA and *transZ* enhanced RNA synthesis *in vitro*. Strongly activated RNA transcription in the presence of *transZ* and CK-binding protein suggested the existence of a potential system of CK signal recognition, which might be transferred to the plant cell in cyanobacteria (Selivankina et al., 2006). Although a gene sequence with high similarity to CK membrane receptor CRE1 in *Synechocystis* sp. PCC 6803 was found, there are still no details concerning gene expression and function (Anantharaman and Aravind, 2001; Selivankina et al., 2006).

Algae are a highly diverse, non-monophyletic group of photosynthetic eukaryotes occurring in marine, freshwater and land habitats, where sufficient photosynthetic light is available (Lewis and McCourt, 2004). Variable profiles of both isoprenoid and aromatic CKs have been assigned to various algal taxa with some general trends, including *cisZ*-type prevalence and low or undetectable contents of DHZ forms and CK conjugates (Stirk et al., 2003, 2013; Tarakhovskaya et al., 2007). In addition, variation of endogenous CK levels was demonstrated during the cell division cycle of *Chlorella minutissima* in response to light/dark treatment, suggesting a potential requirement of CKs for algal growth (Stirk et al., 2011, 2014). Even though genes coding for CK metabolic pathways have been identified in several algal species, most of them occur sporadically in

comparison with vascular plants (Pils and Heyl, 2009; Kiseleva et al., 2012; Lu et al., 2014). Like cyanobacterial IPTs, algal IPTs are related to tRNA-IPTs rather than to adenylate ones, supporting the origin of CKs from tRNA (Lu and Xu, 2015). Taking these data together, the full set of proteins participating in CK metabolism has apparently evolved in particular in green plants (Pils and Heyl, 2009; Lu et al., 2014), although as yet unknown mechanisms controlling CK homeostasis probably exist in evolutionarily older organisms, such as cyanobacteria and algae.

The phytohormone auxin is well known for its key role in the regulation of plant growth and development, especially for its impact on cell polarity and cell patterning during embryogenesis and postembryonic development, plant tropic responses, phyllotaxis, floral organs, leaf and vascular tissue formation, root development and *de novo* organogenesis (Friml et al., 2003; Blilou et al., 2005; Woodward and Bartel, 2005; Cheng et al., 2006, 2007; Benková et al., 2009; Pernisová et al., 2011). In recent years our knowledge about auxin biosynthetic pathways has increased dramatically. Tryptophan-dependent biosynthesis is believed to be the main route of IAA synthesis, and currently four individual pathways are proposed, each named after the intermediate immediately downstream of tryptophan: the indole-3-acetaldoxime (IAOx), indole-3-acetamide (IAM), tryptamine and indole-3-pyruvic acid (IPyA) pathways (reviewed by Ljung, 2013; Tivendale et al., 2014). A tryptophan-independent indole-3-glycerol phosphate (IGP) pathway has been described in *Arabidopsis* (Normanly et al., 1993; Ouyang et al., 2000; Tivendale et al., 2014; Wang et al., 2015).

Based on physiological activity and chemical structure, naturally occurring auxins and its derivatives can be classified to: (1) biologically active forms such as indole-3-acetic acid (IAA), 4-chloroindole-3-acetic acid (4-Cl-IAA) and indole-3-butyric acid (IBA); (2) proposed precursors of IAA biosynthetic pathways such as IAOx, IAM, tryptamine, IPyA, indole-3-acetonitrile (IAN) and indole-3-acetaldehyde (IAAld); and (3) auxin metabolites such as methyl-IAA (MeIAA) with a proposed storage role, amino acid conjugates as proposed metabolites of a degradation pathway [indole-3-acetic acid-aspartate (IAA-Asp); indole-3-acetic acid-glutamate (IAA-Glu) or inhibitors of auxin action (indole-3-acetic acid-tryptophan, IAA-tryptophan)]. Moreover, some auxin conjugates can also be hydrolysed back to free IAA via activity of amino acid conjugate hydrolases [indole-3-acetic acid-alanine, (IAA-Ala); indole-3-acetic acid-leucine (IAA-Leu); indole-3-acetic acid-phenylalanine (IAA-Phe)], auxin catabolite 2-oxindole-3-acetic acid (OxIAA) ensuring rapid inactivation of IAA via oxidation, and conjugates with sugars such as indole-3-acetyl-1-glucosyl ester (IAA-GE) and oxindole-3-acetic acid-glucosyl ester (oxIAA-GE) (Ludwig-Müller, 2011; Korasick et al., 2013).

Endogenous IAA has been detected in cyanobacteria (Sergeeva et al., 2002; Hussain et al., 2010; Mazhar et al., 2013) as well as in brown algae (Le Bail et al., 2010), red algae (Ashen et al., 1999; Yokoya et al., 2010) and green algae (Mazur et al., 2001; Cooke et al., 2002; Stirk et al., 2013). Likewise, other auxin precursors and metabolites represented by tryptophan, anthranilate, IAM, indole-3-ethanol and IAOx were reported in substantial amounts in algae (Yokoya et al., 2010; Stirk et al., 2013, 2014), while in some cyanobacteria the

species IBA was found as a predominant metabolite (Hashtroudi *et al.*, 2013). Similarly, the presence of endogenous phenylacetic acid (PAA) has been detected in red and green algae (Abe *et al.*, 1974; Rocha *et al.*, 2011) and the effect of PAA application in comparison with IAA on the levels of metabolically active compounds and growth of the green alga *Chlorella vulgaris* has been described by Piotrowska-Niczyporuk and Bajguz (2014). Moreover, Sugawara *et al.* (2015) have recently shown the basic characteristics of PAA transport and metabolism and its role in auxin signalling in vascular as well as non-vascular plants.

Positive effects of IAA exogenous application have been reported, e.g. for improvement of algal growth rate (Park *et al.*, 2013), oil content increase (Maor, 2010; Jusoh *et al.*, 2015) and induction of tolerance of higher salinities and temperatures (Nowak *et al.*, 1988; Piotrowska-Niczyporuk and Bajguz, 2014). Additionally, the enhancement of growth parameters and biomass production after inoculation with some cyanobacterial strains due to their auxin-like activity were observed in wheat (Mazhar *et al.*, 2013) and sunflower (Varalakshmi and Malliga, 2012), for instance.

The goal of this study was to characterize CK and auxin metabolism in cyanobacteria and algae as the ancestors of vascular plants. In order to get insight into potential metabolic pathways involved in the control of the homeostasis of the two phytohormones, we quantified the endogenous profiles of CKs and auxins and determined their levels following exogenous application of radiolabelled *transZ* and IAA in distinct taxa of cyanobacteria and algae. Last but not least, endogenous CK and auxin pools were determined during the culture of *Scenedesmus obliquus* with the aim of demonstrating the roles of both phytohormones in algal growth and cell division.

MATERIALS AND METHODS

Chemicals

All CKs were supplied by Olchemim, Ltd (Olomouc, Czech Republic); other chemicals were purchased from Sigma-Aldrich. (St Louis, MO, USA). [^3H]*trans*-zeatin ([^3H]*transZ*; specific radioactivity 29.7 Ci mmol $^{-1}$), [^3H]*cis*-zeatin ([^3H]*cisZ*; specific radioactivity 29.7 Ci mmol $^{-1}$) and [^3H] N^6 -(Δ^2 -isopentenyl)adenine ([^3H]iP; specific

radioactivity 35.1 Ci mmol $^{-1}$) were supplied by the Isotope Laboratory, Institute of Experimental Botany CAS (Prague, Czech Republic). [^3H]indole-3-acetic acid ([^3H]IAA), [^3H]2,4-dichlorophenoxy acetic acid ([^3H]2,4-D) and [^3H]naphthalene-1-acetic acid ([^3H]NAA) (specific radioactivity 20.0 Ci mmol $^{-1}$ each) were supplied by American Radiolabeled Chemicals (St Louis, MO, USA).

Experimental material

Twenty representatives of taxonomically major lineages of cyanobacteria and algae belonging to nine classes (Cyanophyceae, Xanthophyceae, Eustigmatophyceae, Porphyridiophyceae, Chlorophyceae, Ulvophyceae, Trebouxiophyceae, Zygnematophyceae and Klebsormidiophyceae) were provided by the Culture Collection of Autotrophic Organisms (CCALA, <http://ccala.butbn.cas.cz/index.php>). An overview of the selected species used in the study as well as their taxonomic classification is given in Supplementary Data Table S1, and their position within a simplified phylogenetic tree is shown in Fig. 1.

Culture conditions for cyanobacteria and algae

In CCALA, cyanobacterial and algal strains have been maintained on agar slants under controlled light and temperature conditions, i.e. light intensity 23 $\mu\text{mol photons m}^{-2} \text{s}^{-1}$ of photosynthetically active radiation (PAR), a 12-h light/12-h dark photoperiod and temperature 12–15 °C. In order to adapt them for culture experiments, the cells were transferred to flasks containing 100 mL of 1/2 S&S; medium (Přibyl *et al.*, 2015) and pre-cultured at 80 $\mu\text{mol m}^{-2} \text{s}^{-1}$ PAR at room temperature for a few days until appropriate amounts of biomass were reached. Cultures were shaken manually several times a day. Strains for experiments with exogenously applied phytohormones were then transferred into bubble columns of 3.8 cm inner diameter (Kavalierglass, Prague, Czech Republic) at a continuous incident light intensity of 230 $\mu\text{mol m}^{-2} \text{s}^{-1}$ PAR at room temperature and bubbled with 2 % CO $_2$ (v/v) in air. Cultures were collected in the early stationary growth phase (after 10–14 d) and subsequently used for further experiments. Strains for phytohormone profiling were cultured in the same flasks and under the same culture conditions as given above for

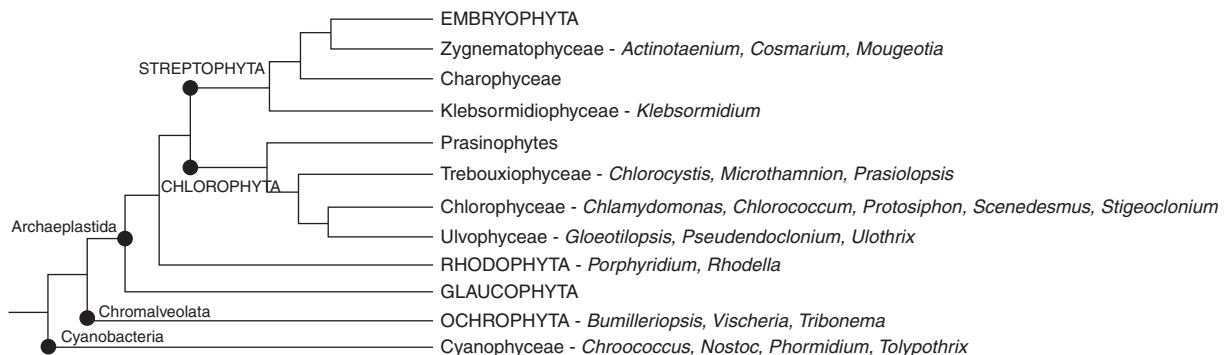


Fig. 1. The position of selected cyanobacterial and algal taxa within a simplified phylogenetic tree. The phylogenetic tree is based on different data sources from the whole chloroplast genome and nuclear rDNA (Riisberg *et al.*, 2009; Ruhfel *et al.*, 2014). For a complete list of analysed species see Table S1.

another 3–4 weeks to reach the early stationary growth phase. Before identification and quantification of CKs and auxins, cyanobacterial and algal suspension cultures were centrifuged for 20 min at 20 000 *g* and 4 °C (Beckman Coulter, Palo Alto, CA, USA). Subsequently, supernatants were removed by pipetting and pellets were immediately frozen in liquid nitrogen.

Endogenous cytokinin and auxin profiles in cyanobacterial and algal species

Endogenous CKs and auxins were extracted from homogenized samples of cyanobacteria and algae (0.108–0.251 g fresh weight) according to a previously described method (Dobrev and Kamínek, 2002). Determination and quantification of CKs and auxins were performed with a high-performance liquid chromatography (HPLC) system (Ultimate 3000, Dionex) coupled to a hybrid triple quadrupole/linear ion trap mass spectrometer (3200 Q TRAP, Applied Biosystems) using a multi-level calibration graph with [³H]-labelled internal standards, as described previously (Dobrev et al., 2005; Djilianov et al., 2013; Žižková et al., 2015). Detection of 2-methylthio derivatives of iP, *transZ* and their ribosides was set up in a selected reaction-monitoring mode.

*Metabolism of exogenously applied [³H]*transZ*, [³H]IAA, [³H]NAA and [³H]2,4-D in cyanobacterial and algal cells*

Metabolic profiles of exogenously applied radiolabelled *transZ* ([³H]*transZ*, 1.5 × 10⁶ d.p.m. μL⁻¹) added to the culture medium at final concentration 1 μM or 20 nM were determined in one cyanobacterial strain (*Chroococcus minutus*, CCALA 55) and three strains of algae (*Chlorococcum elbense*, CCALA 282; *Klebsormidium flaccidum*, CCALA 786; *Scenedesmus obliquus*, CCALA 454) cultured in liquid media as described previously and regenerated overnight in a culture room (16 h light/8 h dark, 20 °C) under continuous shaking (120 rpm, orbital diameter 20 mm). Cells and media (200 mg fresh weight and 10 mL per sample) were collected separately by filtering through Whatman GF/C glass fibre filters (5 cm diameter) at time points 0, 0.5, 1, 2, 4 and 24 h.

Similarly, radiolabelled [³H]IAA, [³H]NAA or [³H]2,4-D was added to the culture medium of four algal strains (*Chlorococcum ellipsoideum*, CCALA 283; *Stigeoclonium helveticum*, CCALA 868; *Scenedesmus obliquus*, CCALA 454; and *Microthamnion kuetzingianum*, CCALA 368) at a final concentration of 20 nM. Cells and media were collected separately by filtering through Whatman GF/C glass fibre filters (5 cm diameter) at time points 0, 1, 2 and 6 h.

Radiolabelled metabolites of *transZ* and auxins were separately analysed by HPLC coupled to an on-line radioactivity detector under the same analytical conditions, with the exception of the different gradients. A Luna HPLC column C18(2) (150 × 4.6 mm, 3 μm; Phenomenex, Torrance, CA, USA), was used; mobile phase A was 40 mM CH₃COONH₄ (pH 4) and mobile phase B was CH₃CN/CH₃OH, 1/1 (v/v), and flow rate was 0.6 mL min⁻¹. The linear gradient programme for *transZ* metabolites was 10–40 % B for 12 min, 40–100 % B for 1 min, 100 % B for 2 min and 100–10 % B for 1 min. The linear gradient programme for auxin metabolites was 30–50 % B for

10 min, 50–100 % B for 1 min, 100 % B for 2 min and 100–30 % B for 1 min. The column eluate was monitored with a Ramona 2000 on-line radioactivity detector (Raytest, Straubenhardt, Germany) after on-line mixing with three volumes (1.8 mL min⁻¹) of liquid scintillation cocktail (Flo-Scint III, Perkin Elmer Life and Analytical Sciences, Shelton, CT, USA). The radioactive metabolites were identified on the basis of comparison of their retention times with authentic standards. Results of auxin metabolic profiles are presented as total integrated area of chromatogram plots normalized to the equalization of total accumulated radiolabel.

Cytokinin oxidase/dehydrogenase in vitro assay

The enzyme preparations were extracted and partially purified using the method described by Motyka et al. (2003). The CKX activity was determined by *in vitro* assays based on the conversion of [2-³H]-labelled CKs ([³H]*transZ*, [³H]*cisZ* and [³H]iP) to [³H]adenine. Separation of the substrate from the product of the enzyme reaction was achieved by HPLC as described by Gaudinová et al. (2005). The CKX activity was determined in duplicate in two independent experiments.

Growth of Scenedesmus obliquus

Pre-cultures of microalgae *Scenedesmus obliquus* were diluted with 1/2 SŠ fresh medium (Příbyl et al., 2015) to obtain the cell density of 1.0–1.5 × 10⁶ cells mL⁻¹ (around 0.15–0.20 g L⁻¹ dry weight). The cell density was determined using a Bürker counting chamber (Hecht-Assistent, Sondheim, Germany); at least 400 cells were counted. The culture was cultured in bubble columns of 3.8 cm inner diameter (Kavalierglass, Prague, Czech Republic) at a continuous incident light intensity of 500 μmol m⁻² s⁻¹ PAR at 30 ± 0.5 °C and bubbled with 2 % CO₂ (v/v) in air. The dilution procedure was repeated twice each 24 h and the resulting inoculum was used for batch-culture experiments in an initial volume of 150 mL under the same conditions as described above for 14 d. During culture, samples were taken regularly for analysis following the replenishment of water evaporated from the bubble columns. Growth was determined gravimetrically based on increased cell dry weight as follows: culture samples (1.5 mL) were centrifuged (10 000 *g*, 8 min) in pre-weighed microtubes and the sediment was dried at 105 °C. The cell density was quantified using a Bürker counting chamber (Hecht-Assistent, Sondheim, Germany); at least 600 cells were counted for each sample. Samples for CK analyses were collected at the same intervals; biomass was separated from the growth medium by centrifugation (10 000 *g*, 8 min) and both biomass and medium were immediately frozen in liquid nitrogen.

Endogenous cytokinin profiles during Scenedesmus obliquus growth

The frozen pellets (as described above) used for determination of CKs were freeze-dried (Scanvac CoolSafe 110-4, Fisher Scientific) in a vacuum (SavantTM SPD 121P SpeedVacTM Concentrator, Thermo ScientificTM) for 7 h. For

analysis of free CKs, *Scenedesmus obliquus* samples (5 mg dry weight of each) were homogenized under liquid nitrogen, extracted in modified Bielecki buffer (methanol/water/formic acid, 15/4/1, v/v/v) containing 0.2 pmol of [²H]- or [¹³C]-labelled CK free bases/ribosides/*N*-glucosides and 0.5 pmol of [²H]-labelled CK-*O*-glucosides/nucleotides (Novák et al., 2003, 2008), and then purified using two solid-phase extraction columns, the C18 octadecylsilica-based column and the MCX column (Dobrev and Kamínek, 2002). Analytes were eluted by two-step elution using a 0.35 M NH₄OH aqueous solution and 0.35 M NH₄OH in 60 % (v/v) MeOH. Levels of CKs were determined by ultrahigh-performance liquid chromatography-electrospray tandem mass spectrometry (UHPLC-MS/MS) with stable isotope-labelled internal standards as a reference (Svačinová et al., 2012).

Extraction and purification of tRNA were performed according to a protocol described by Maass and Klämbt (1981) including modifications described by Stirk et al. (2011). Aliquots of extracted total tRNA were hydrolysed with 2 M KOH overnight and dephosphorylated using alkaline phosphatase. Addition of internal standards (0.2 pmol of each [²H]-labelled CK riboside), sample purification on a mixed-mode cation exchange (MCX) column and tRNA-bound CK quantification was performed by UHPLC-MS/MS as described above. 2-Methylthio derivatives of tRNA-bound isoprenoid CKs were analysed with an HPLC-MS/MS system as described previously (Tarkowski et al., 2010). The extraction and purification of *Scenedesmus obliquus* samples were carried out in two technical replicates for each biological replicate.

Presentation of results

Each evaluation was carried out in duplicate in two or three independent experiments. The results are expressed as mean values and standard deviations of the means in the figures and/or tables.

RESULTS

Selection of cyanobacterial and algal species

In order to extend our current knowledge concerning CK and auxin metabolism in non-vascular organisms, a search for suitable cyanobacterial and algal candidates was performed with respect to their distinct evolutionary history, taxonomic position and habitat requirements. The complete list and abbreviations of all representatives analysed for CK and auxin profiles, including cyanobacteria and the major lineages brown algae (Ochrophyta), red algae (Rhodophyta) and green algae (Chlorophyta and Streptophyta), is shown in Table S1.

The position of selected taxa within a simplified phylogenetic tree based on different data sources from the whole chloroplast genome and nuclear rDNA (Riisberg et al., 2009; Ruhfel et al., 2014) is demonstrated in Fig. 1. In addition to Prokaryota, represented by three cyanobacterial species (*Chroococcus minutus*, *Phormidium animale* and *Nostoc microscopicum*), three ochrophytes (*Tribonema aequale*, *Bumilleriopsis filiformis* and *Vischeria helvetica*), two red algae (*Porphyridium purpureum* and *Rhodella violacea*) and two

major lineages of green algae referred to the chlorophyte and charophyte/streptophyte clades (see Table S1) were included in the analysed set of eukaryotic organisms. Nine Chlorophyta species belonging to three major groups (Chlorophyceae, Ulvophyceae and Trebouxiophyceae) and two Streptophyta species (*Actinotaenium curtum* and *Klebsormidium flaccidum*) as representatives of evolutionarily more advanced organisms closely related to vascular plants were selected within the green algae for analyses of CK and auxin spectra (Fig. 1, Table S1). Another Chlorophyta species, *Chlorococcum elbense*, was chosen for metabolic studies only. To summarize, the set of analysed samples was representative enough to enable a very comprehensive survey of the regulation of CK and auxin metabolism in photoautotrophic microorganisms of different phylogenetic origin.

Cytokinin profiles in cyanobacteria and algae differ substantially from those in vascular plants

In analogy to vascular plants, a wide spectrum of isoprenoid CKs was detected in both cyanobacteria and algae. Total CK levels in different species varied from picomoles per gram fresh weight (FW) (e.g. *Porphyridium purpureum*, 2.53 pmol g⁻¹ FW) to hundreds of picomoles (e.g. *Phormidium animale*, 178.55 pmol g⁻¹ FW) (Fig. 2, Supplementary Data Table S2). Bioactive CKs (free bases and ribosides) and CK phosphates were the prevalent CK forms, being present in concentrations from 1.01 pmol g⁻¹ FW (*Porphyridium purpureum*) to 100.19 pmol g⁻¹ FW (*Chlamydomonas segnis*) and from 0.56 pmol g⁻¹ FW (*Chlamydomonas segnis*) to 65.36 pmol g⁻¹ FW (*Phormidium animale*), respectively. On the other hand, CK-*N*-glucosides were not detected or detected in only trace amounts throughout the set of analysed species. Similarly, CK-*O*-glucosides occurred only in minute concentrations or were absent in the tested samples (Fig. 2A, Table S2). In general, the iP-, cisZ- and transZ-type CKs predominated in all analysed cyanobacteria and algae, while DHZ types contributed only insignificantly (with concentrations ranging from 0.35 to 3.95 pmol g⁻¹ FW) to the total CK pool. Interestingly, whereas monophosphate forms of iP, transZ and DHZ were relatively abundant in most of the species, cisZ was found only in biologically active free-base and riboside forms in all of the analysed taxa. In 13 (out of 19) analysed taxa, the levels of cisZ and its riboside exceeded those of corresponding transZ counterparts, in most of them being more than at least 3-fold higher (Fig. 2B, Table S2). Interestingly, 2-methylthio-*N*⁶-(Δ^2 -isopentenyl)adenosine (2MeSiPR) was detected in moderate or high concentrations in almost all of the analysed samples, representing a predominant metabolite in some Cyanobacteria (*Chroococcus minutus*, *Phormidium animale*) and Chlorophyta (*Chlorococcum ellipsoideum*, *Pseudendoclonium basilense*, *Scenedesmus obliquus*, *Microthamnion kuetzingianum*) species (Fig. 2B, Table S2). In summary, the profiles of endogenous CKs in selected cyanobacteria and algae revealed a predominance of biologically active and phosphate CK forms and relatively small amounts of CK-*O*- and *N*-glucosides. Moreover, it is demonstrated that cisZ-type CKs and 2MeSiPR substantially contribute to the overall CK pool, indicating the existence of

diverse metabolic pathways in cyanobacteria and algae compared with vascular plants.

Spectra of auxin metabolites in cyanobacteria and algae are rather narrow

In all of the selected cyanobacteria and algae, the screen of endogenous CKs was supplemented by analysis of endogenous indole auxin levels. In the whole spectrum of analysed species and biological samples, the auxins IAA, its primary catabolite OxIAA and an amino acid conjugate, IAA-Asp, were detected. The total auxin concentrations ranged from 10.93 to 290.69 pmol g⁻¹ FW, with the lowest as well as the highest endogenous levels in Chlorophyta species *Pseudendoclonium basilense* and *Stigeoclonium helveticum*, respectively (Fig. 2C, Supplementary Data Table S3). The main auxins were represented by free IAA (occurring in concentrations from 3.26 to 287.57 pmol g⁻¹ FW; *Porphyridium purpureum* and *Stigeoclonium helveticum*, respectively) and OxIAA (ranging from 1.78 to 43.54 pmol g⁻¹ FW; *Bumilleriopsis filiformis* and *Protosiphon botryoides*, respectively) whereas concentrations of

IAA-Asp were close to the detection limit in all of the tested species (Fig. 2C, Table S3). Taking these results together, endogenous free IAA and OxIAA evidently represent predominant indole auxin forms in the selected cyanobacterial and algal samples.

Cyanobacteria and algae metabolize exogenously applied [³H]transZ

In order to study the regulation of CK levels in non-vascular plants and to compare it with regulation in vascular plants, radiolabelled *transZ* was exogenously applied to cultures of cyanobacteria (*Chroococcus minutus*) and selected algae (*Chlorococcum elbense*, *Klebsormidium flaccidum* and *Scenedesmus obliquus*). Following [³H]*transZ* treatment, some relatively rapid metabolic changes in cultured cells were observed as early as after 1 h of incubation (Fig. 3A–D). After 4 h of incubation, the degradation products adenine [retention time (RT)=4.15 min] and adenosine (RT=7.12 min) together with other substances, such as AMP/ADP/ATP (RT=4.0 min), DHZ (RT=16.5 min) and its riboside (RT=18.5 min), were found, based on their retention times on

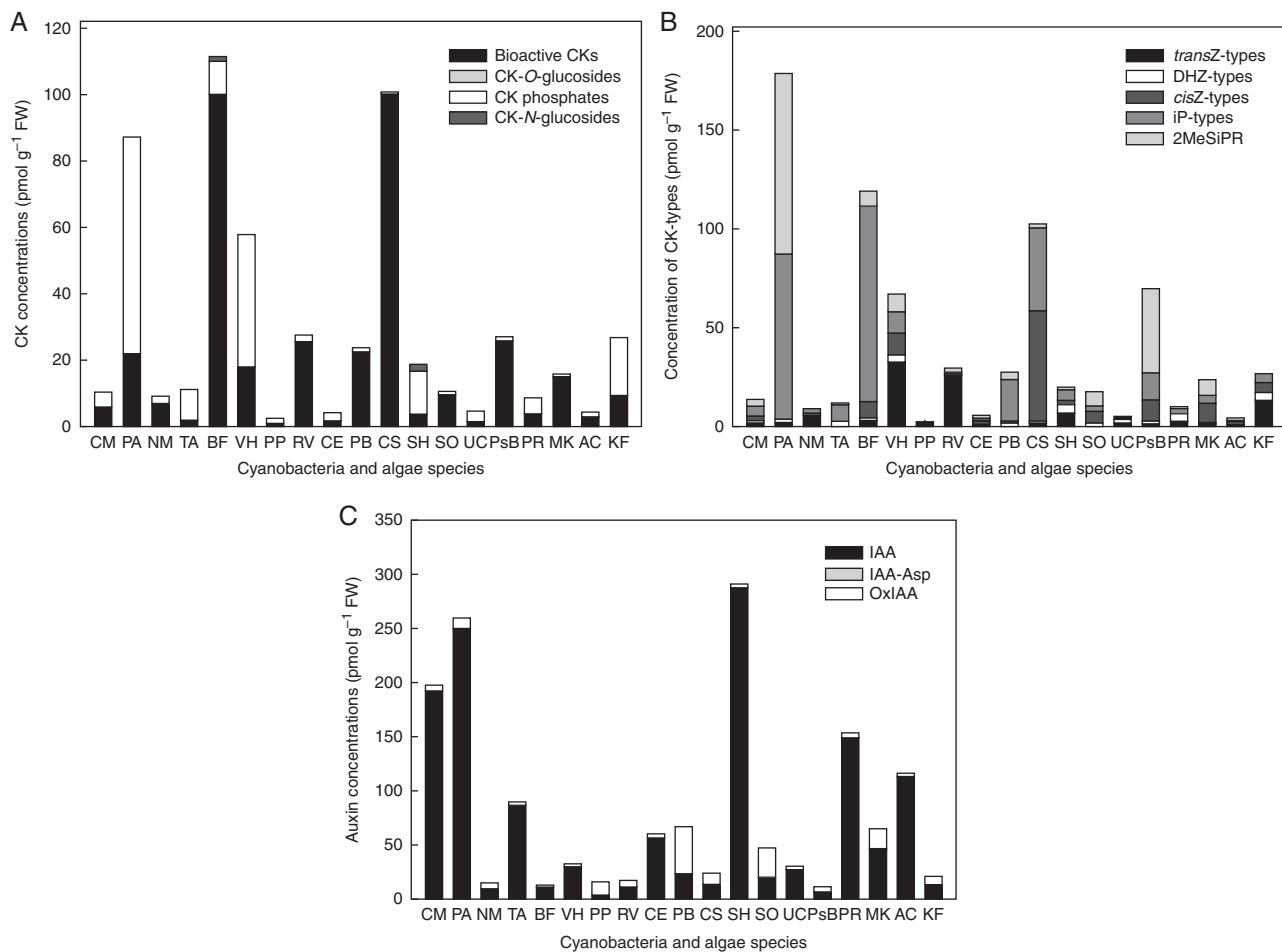


Fig. 2. Endogenous cytokinin and auxin profiles in selected cyanobacterial and algal species. Cytokinin profiles were determined in the early stationary growth phase and are based on conjugation status/physiological function (A) and the chemical structure of the purine ring (B). Endogenous levels of both cytokinins and auxins (C) are expressed in pmol g⁻¹ FW. Abbreviations of selected cyanobacterial and algal representatives are given in Table S1.

HPLC. After 24 h, almost complete conversion of [^3H]transZ was apparent in *Chroococcus minutus*, *Scenedesmus obliquus* and *Chlorococcum elbense* (Fig. 3A–C), which was in contrast to *Klebsormidium flaccidum*, where a relatively high amount of [^3H]transZ persisted (about one-fourth of the initial amount; Fig. 3D). Interestingly, relatively high concentrations of rapidly formed, unknown metabolites were detected after [^3H]transZ treatment in all four analysed species (Fig. 3A–D).

Metabolism of [^3H]transZ was also followed in the culture medium of *Chroococcus minutus* and *Klebsormidium flaccidum*. After incubation (4 and 24 h), [^3H]transZ was largely converted in the *Klebsormidium flaccidum* medium with subsequent accumulation of DHZ and several unidentified metabolites (Supplementary Data Fig. S1). Similarly, a decline in [^3H]transZ 24 h after its supply was recorded and some unidentified metabolites were detected in the medium of *Chlorococcum minutus* (data not shown). Altogether, our data strongly suggest a potential intra- as well as extracellular regulation of CK status in both cyanobacterial and algal cells.

The intense *in vivo* formation of adenine and adenosine as products of [^3H]transZ metabolism in selected cultures raises the question of the potential involvement of CKX activity in the degradation of CKs in cyanobacteria and algae. To investigate this subject, degradation of [^3H]transZ, [^3H]cisZ and [^3H]iP by the CKX activity isolated from crude protein preparations of eight species, including Cyanobacteria, Rhodophyta, Ochrophyta and Chlorophyta, was determined. *In vitro* enzymatic assays performed at two pH values, pH 7.0 and pH 8.5 (Supplementary Data Figs S2 and S3 for [^3H]iP; data not shown for [^3H]transZ and [^3H]cisZ) revealed no CKX activity for any of the tested samples. Interestingly, an unknown metabolite (RT = 2.5 min) was formed *in vitro* as a product of radiolabelled CK substrates in all analysed samples (Figs S2 and S3; data not shown). To summarize our finding, in spite of the intense *in vivo* conversion of [^3H]transZ to adenine and/or adenosine, the assumed CKX activity was not detected.

Exogenously applied [^3H]IAA is gradually metabolized in algal cell cultures

In order to characterize more precisely the auxin metabolism in non-vascular plants, radiolabelled [^3H]IAA was exogenously applied to cultures of the four Chlorophyta species *Stigeoclonium helveticum*, *Chlorella vulgaris*, *Microthamnion kuetzingianum* and *Scenedesmus obliquus*. In all of the analysed green algae, exogenously applied [^3H]IAA was gradually metabolized in both cells (Fig. 4) and media (Fig. 5). During 6 h of [^3H]IAA treatment, formation of IAA-Asp (RT = 6.6 min), IAA-GE (RT = 8.12 min) and eight other unidentified metabolites with a major product with RT 14.23 min was detected. To compare auxin metabolic profiles in algal cells after addition of synthetic radiolabelled auxin compounds, [^3H]NAA and [^3H]2,4-D were applied. Surprisingly, in comparison with numerous conversions of exogenously applied IAA, no significant effect on substrate metabolism in selected algal cells and media was observed (data not shown), probably due to missing metabolic pathway(s) for such unnaturally occurring substrates or an inability to transport them inside the cells.

Cytokinin and auxin metabolite profiles are differently affected during Scenedesmus obliquus growth

With the aim of deciphering the regulation of CK and auxin homeostasis in non-vascular organisms, *Scenedesmus obliquus* was used as a representative green alga of the chlorophyte clade because of its relatively easy culture. The cellular growth and concentrations of CKs (both free and tRNA-bound) and auxins were recorded during the course of *Scenedesmus obliquus* culture (Fig. 6).

After a short lag phase, a rapid increase in cell number was detected, reaching the stationary growth phase after 2–3 d of culture. Biomass dry weight showed a similar pattern, but with a substantial delay in entering the stationary growth phase (Fig. 6A). Within the exponential and linear phases of cellular growth (0–4 d), the total free CK concentration was at least 3-fold higher than in the stationary phase (7–14 d). Among CK groups, CK phosphates represented the predominant CK forms (67–81 % of the total), whereas the rest of the CK pool comprised mainly bioactive free bases and ribosides. CK-*O*-glucosides were found at very low concentrations, close to the detection limit (ranging from 0.09 to 0.58 pmol g⁻¹ FW) and CK-*N*-glucosides were not detected at all (Fig. 6B). Remarkably, the highest levels of CK phosphates and bioactive CKs were reached at day 2 (168.48 ± 12.56 and 50.50 ± 3.06 pmol g⁻¹ FW, respectively) while at least 9-fold decreased contents of both CK groups (12.38 ± 1.90 and 5.29 ± 0.26 pmol g⁻¹ FW, respectively) were observed in the stationary phase of *Scenedesmus obliquus* growth (Fig. 6B). The CK profiling also revealed that endogenous levels of cisZ and its metabolites considerably exceeded concentrations of other CK types during *Scenedesmus obliquus* growth and that iP types represented the second most abundant CK forms (Fig. 6C).

To characterize the contribution of the tRNA biosynthetic pathway to the CK pool in the course of *Scenedesmus obliquus* growth, tRNA-bound CKs were further assessed. The profile of individual CK ribosides derived from tRNA revealed a dominant proportion of cisZ-9-riboside (cisZR) and N⁶-(Δ²-isopentenyl)adenosine (iPR) during the first 7 d of *Scenedesmus obliquus* culture (Fig. 6D). The highest concentration of cisZR (52.45 ± 2.42 pmol g⁻¹ dry weight) was reached at day 1 of the exponential phase of growth, whereas its lowest level was found at the beginning of the stationary phase (day 9; 2.11 ± 0.56 pmol g⁻¹ dry weight). Interestingly, very low concentrations of transZ-9-riboside (transZR) and DHZ-9-riboside (DHZR), varying from 0.07 ± 0.03 to 0.75 ± 0.10 pmol g⁻¹ dry weight, were detected during the whole *Scenedesmus obliquus* growth cycle (Fig. 6D). Consistently, a prevalence of cisZR and iPR was found also when concentrations of tRNA-bound CKs were recalculated in relation to milligrams of isolated tRNA instead of dry weight (Supplementary Data Table S4). In addition, determination of tRNA-bound 2-methylthio derivatives revealed the presence of 2-methylthio-cisZ-9-riboside (2MeScisZR) and 2MeSiPR during the whole *Scenedesmus obliquus* growth cycle (Fig. 6E). Both 2MeScisZR and 2MeSiPR were detected at the highest concentrations after day 1 of the algal cell growth cycle (reaching 26.10 ± 1.84 and 16.02 ± 0.55 pmol g⁻¹ dry weight, respectively), followed by a continuous decline until day 9 and subsequently by an obvious

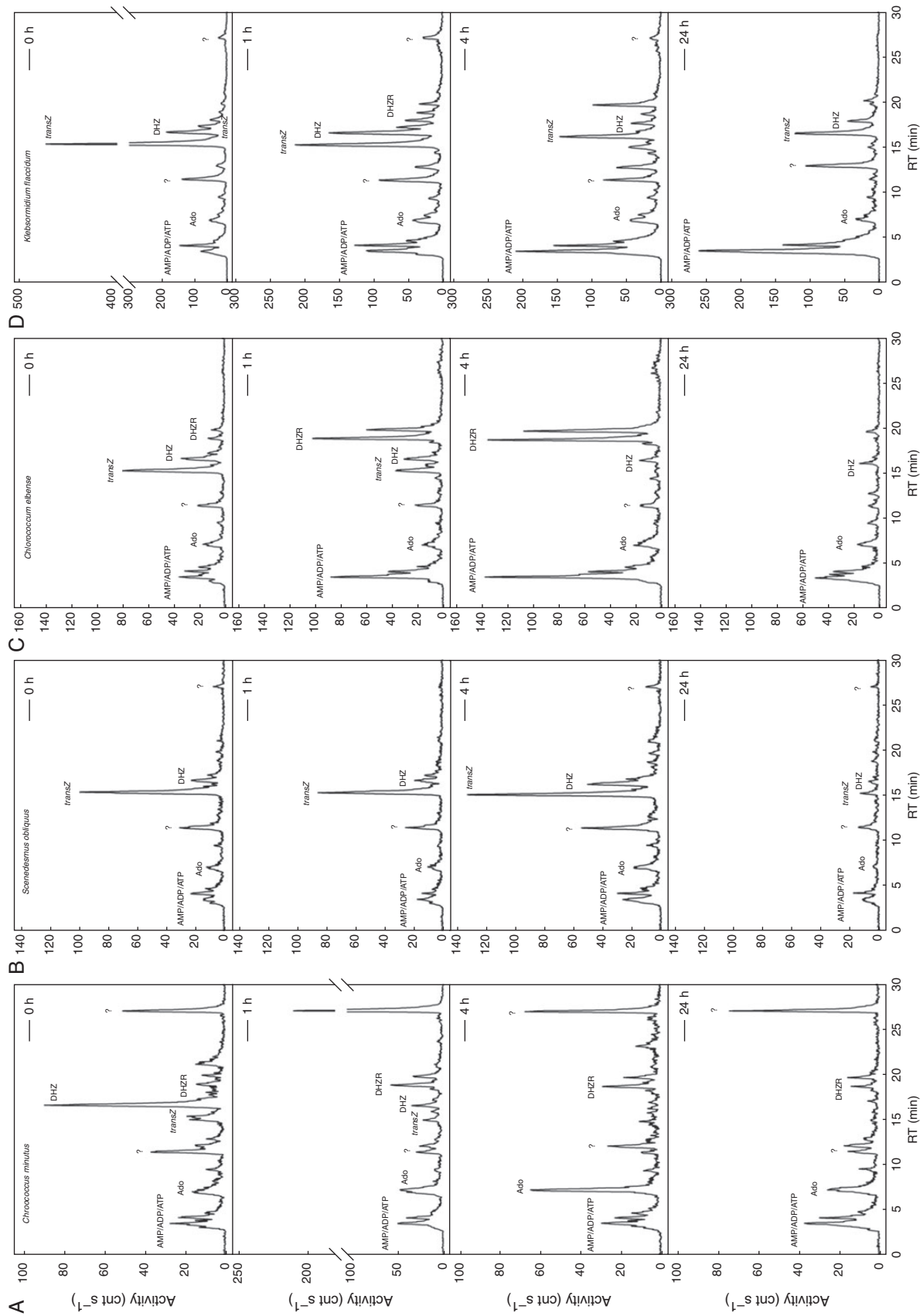


Fig. 3. Metabolism of exogenously applied [³H]transZ in cells of selected cyanobacterial and algal species. Radiolabelled [³H]transZ was applied to cultures of cyanobacteria *Chroococcus minutus* (A) and algal *Scenedesmus obliquus* (B), *Chlorococcum elbense* (C) and *Klebsormidium flaccidum* (D) in the early stationary growth phase. The peaks represent distributions of radioactivity associated with individual metabolites in the cells 0, 1, 4 and 24 h after [³H]transZ application. The products of [³H]transZ metabolism were analysed by an HPLC system coupled to an online radioactivity detector. cnt, counts; RT, retention time; Ado, adenosine.

increase at the end of the stationary phase (Fig. 6E). When related to pmol mg^{-1} tRNA, the contents of 2MeScisZR and 2MeSiPR showed variations, especially during the exponential phase of growth (Table S4).

To get insight into the complexity of phytohormone regulation during 14 d of *Scenedesmus obliquus* cell growth, the auxin metabolite profile was also determined (Supplementary Data Table S5). The content of IAA gradually increased from the start of the experiment, reaching its maximum after 13 d of culture ($84.9 \pm 0.96 \text{ pmol g}^{-1}$ FW) and then decreasing rapidly and noticeably to approximately one-half of this value (14 d;

$41.4 \pm 11.65 \text{ pmol g}^{-1}$ FW) (Fig. 6F). Concentrations of auxin precursors IAM and IAN were considerably lower than those of free IAA, exhibiting moderate variation in their levels during *Scenedesmus obliquus* growth. The auxin catabolite OxIAA reached its maximum at a stage similar to IAA (at 13 d), whereas the endogenous conjugated forms IAA-Asp and OxIAA-GE were detected at very low concentrations within the exponential and linear growth phases (Table S5). Surprisingly, the main auxin metabolite was PAA, with an amount about one order of magnitude higher than IAA, but without showing any significant dynamic changes during the culture period (Fig. 6F).

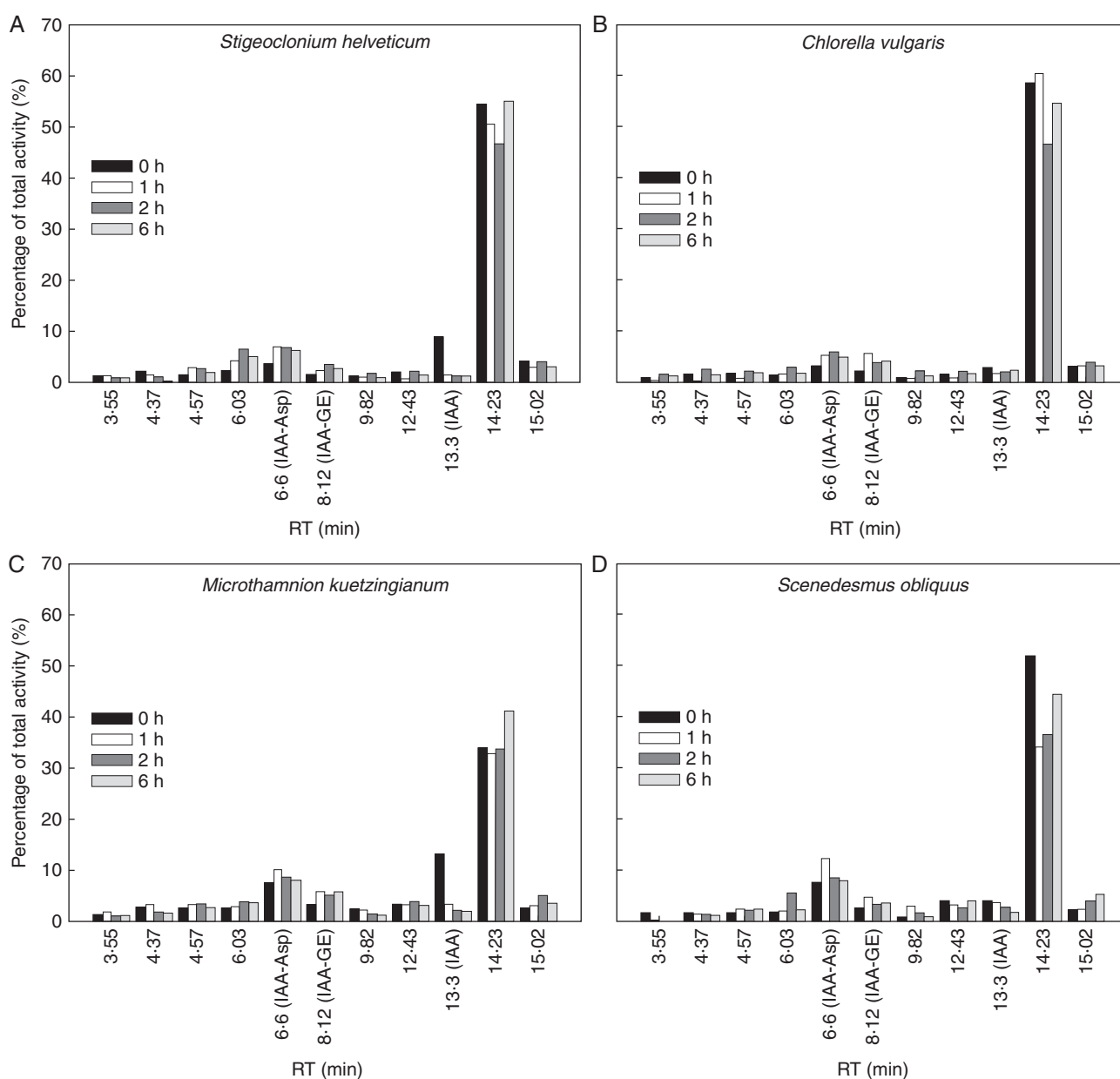


FIG. 4. Metabolism of exogenously applied $[^3\text{H}]$ IAA in the cells of selected algal species. Radiolabelled $[^3\text{H}]$ IAA was applied to cultures of Chlorophyta species *Stigeoclonium helveticum* (A), *Chlorella vulgaris* (B), *Microthamnion kuetzingianum* (C) and *Scenedesmus obliquus* (D) in the early stationary growth phase. Bars represent distribution of radioactivity associated with individual metabolites in cells 0, 1, 2 and 6 h after $[^3\text{H}]$ IAA application. Products of $[^3\text{H}]$ IAA metabolism were analysed by HPLC coupled to an on-line radioactivity detector. Values are percentages of total extracted radioactivity in cells. RT, retention time.

Taken together, our data demonstrate a dynamic regulation of CK and auxin homeostasis during the *Scenedesmus obliquus* cell growth cycle. The enhanced concentration of CKs in cells during the phase of their intensive growth is mainly due to an enormous amount of CK phosphates, especially those of *cisZR* (*cisZRMP*) and *iPR* (*iPRMP*). Substantial amounts of *cisZR*, *iPR* and their 2-methylthioderivatives seem to be delivered mainly through the tRNA biosynthetic pathway (Fig. 6). In contrast, concentrations of auxins (mainly of biologically active IAA) gradually increase from the exponential to the linear growth phase. In summary, the

distinct proportions of CK and auxin profiles during *Scenedesmus obliquus* growth may indicate their different functioning and physiological consequences in algal cells.

DISCUSSION

It has been postulated that physiological and structural changes in the metabolism of vascular plants developed progressively with the transition from an aqueous to a gaseous environment (Kenrick and Crane, 1997). Thus, the components of the CK

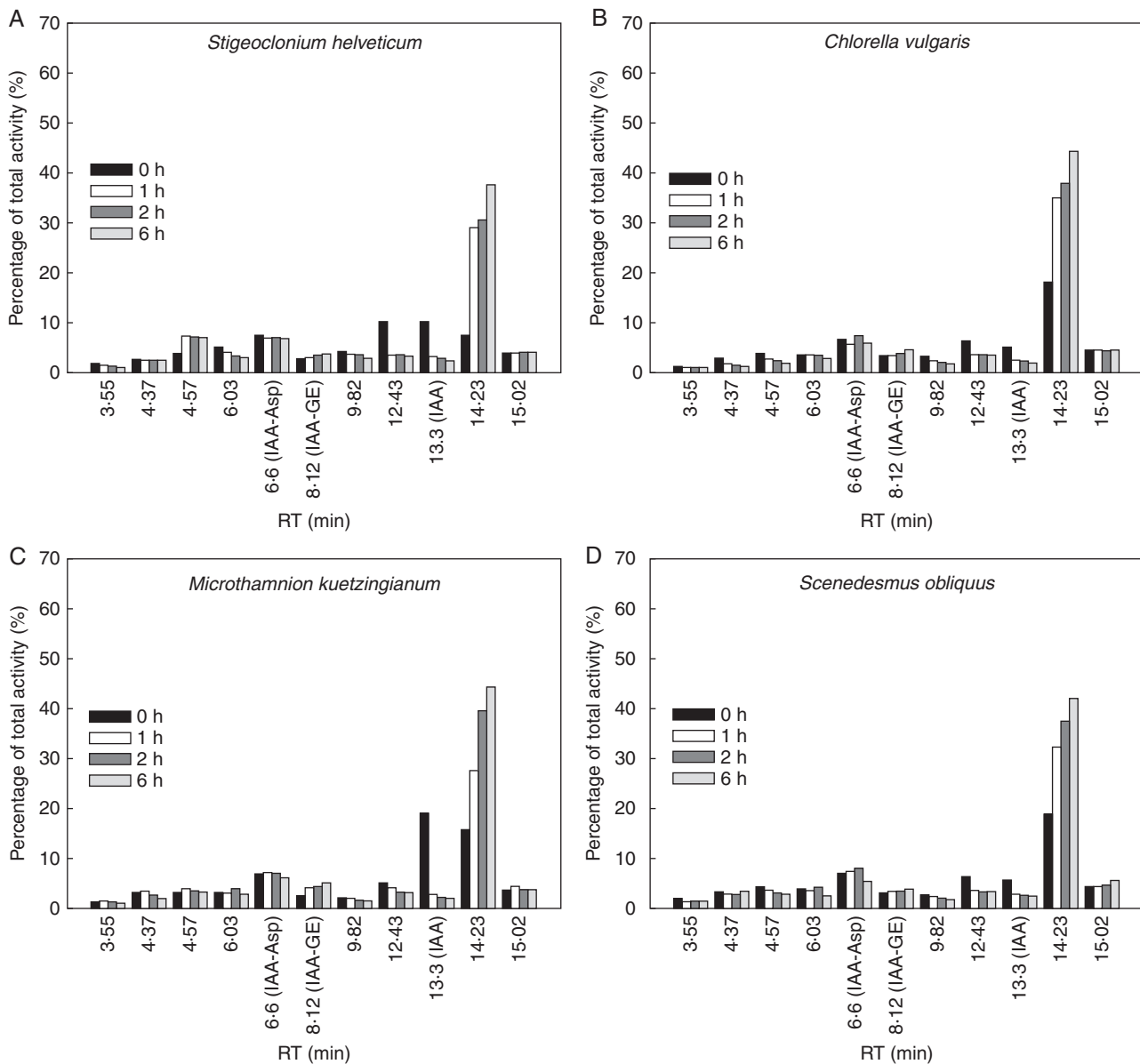


Fig. 5. Metabolism of exogenously applied $[^3\text{H}]\text{IAA}$ in culture media of selected algal species. Radiolabelled $[^3\text{H}]\text{IAA}$ was exogenously applied to cultures of Chlorophyta species *Stigeoclonium helveticum* (A), *Chlorella vulgaris* (B), *Microthamnion kuetzingianum* (C) and *Scenedesmus obliquus* (D) in the early stationary growth phase. Bars represent distribution of radioactivity associated with individual metabolites in media 0, 1, 2 and 6 h after $[^3\text{H}]\text{IAA}$ application. Products of $[^3\text{H}]\text{IAA}$ metabolism were analysed by HPLC coupled to on-line radioactivity detector. Values are percentages of total extracted radioactivity in the media. RT, retention time.

and auxin metabolic pathways identified in vascular plants probably arose from pre-existing elements of bacterial primary metabolism via endosymbiosis and horizontal gene transfer (Spíchal, 2012; Yue *et al.*, 2014). However, in contrast to the relatively well-characterized regulation of CK and auxin homeostasis via different metabolic pathways in vascular plants (e.g. Normanly, 2010; Korasick *et al.*, 2013; Kieber and Schaller, 2014), data concerning the regulatory mechanisms of

both phytohormone levels in evolutionarily older non-vascular organisms are rather limited. To attempt to fill this gap, selected cyanobacterial and algal species belonging to divergent evolutionary lineages (Fig. 1, Table S1) were screened and analysed for CK and auxin profiles and metabolic pathways involved in their homeostasis control.

For all cyanobacterial and algal species used in this study, some common traits regarding the profiles of isoprenoid CK

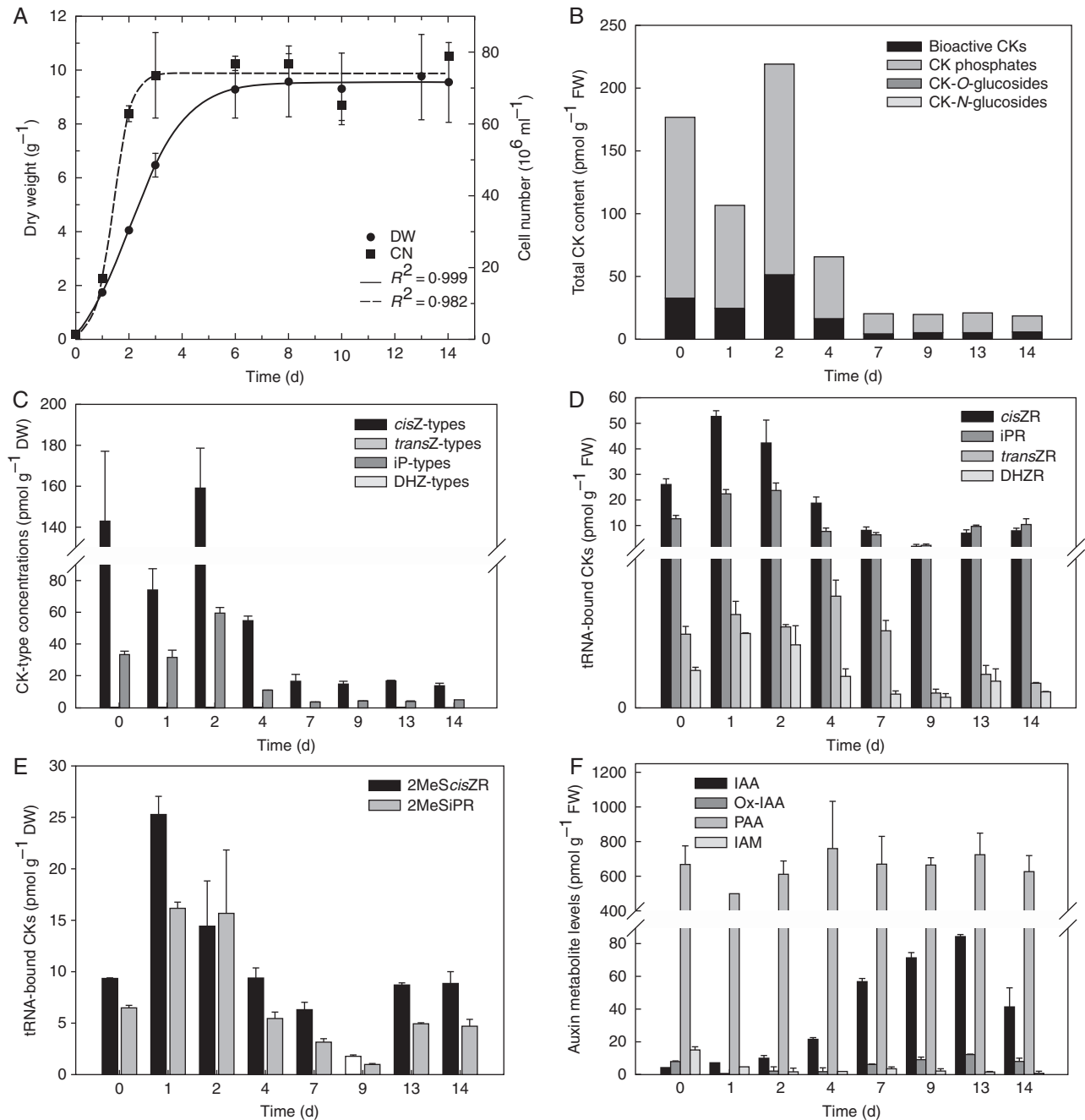


FIG. 6. Growth characteristics and endogenous cytokinin and auxin profiles during the *Scenedesmus obliquus* growth cycle. The cycle was characterized by dry weight and cell number increase (A), variations in profiles of endogenous free cytokinins based on conjugation status/physiological function (B) and the chemical structure of the purine ring (C), as well as tRNA-bound cytokinins (D), including methylthio derivatives (E) and changes in the spectra and concentrations of endogenous auxins (F). Levels of free and tRNA-bound cytokinins and auxins are expressed in pmol g⁻¹ dry weight.

derivatives were found. In general, bioactive CKs and CK phosphates represented the prevailing CK forms, in contrast to CK-*O*- and *N*-glucosides, which occurred only in moderate or hardly detectable concentrations (Fig. 2A, Table S2). Cytokinin spectra similar to those found here have been reported previously by Stirk *et al.* (2013) and Yokoya *et al.* (2010), but there are also a few exceptions demonstrating higher proportions of CK-*O*-glucosides in some microalgal and macroalgal strains than shown in our study (Stirk *et al.*, 2003; Ördög *et al.*, 2004; Lu *et al.*, 2014). Among the CK derivatives detected, 2MeSiPR was present in most tested species (Table S2), suggesting its tRNA origin, as reported by e.g. Prinsen *et al.* (1997). Additionally, the enzyme catalysing the methylation of CK derivatives was discovered in chloroplasts of the light-grown photosynthetic protozoan *Euglena gracilis* (Swaminathan and Bock, 1977). Thus, it can be assumed that tRNA degradation is an essential source of CKs, representing a predominant biosynthetic pathway of CKs in evolutionarily older non-vascular organisms, such as cyanobacteria and algae.

Among the bioactive CKs, free bases of iP, *cisZ* and in some species also *transZ* were found as major CK forms. Their ribosides were detected mostly in lower amounts, and *transZR* was completely missing in cyanobacteria and just sporadically detected in algae (Table S2). Regarding zeatins, *cis* forms were more common than *trans* forms; the contents of *cisZ* and its riboside exceeded those of *transZ* counterparts in 13 (out of 19) cyanobacterial and algal samples. This prevalence of *cisZ* over *transZ* types corresponds well with findings reported by other authors (Ördög *et al.*, 2004; Stirk *et al.*, 2002, 2003, 2013). Based on these data, we suggest that the function of CK-*N*-glucosides (i.e. deactivation or reduction of biological activity) in cyanobacteria and algae may be, at least partially, substituted by *cisZ* types, which represent prevailing and generally less active forms compared with *transZ* types (Gajdošová *et al.*, 2011).

As expected, CK status in cyanobacteria and algae was not steady and could be dramatically affected by internal as well as external factors. In our study, substantially lower concentrations of isoprenoid CKs than those published by Stirk *et al.* (2013) were found in the green algae *Chlorococcum ellipsoideum*, *Protosiphon botryoides* and *Klebsormidium flaccidum*. The differences could be mainly due to the distinct growth phases of the analysed species; whereas the measurements of our samples were performed in the early stationary growth phase, the analyses by Stirk's group were done in the exponential phase of growth. Additionally, environmental factors might affect the CK profiles of cyanobacteria and algae. For instance, the CK spectra were found to be dependent on water temperature in the Chlorophyta seaweed *Ulva* sp. (Stirk *et al.*, 2003), and the effects of light during the cell cycle of *Chlorella minutissima* (Stirk *et al.*, 2011) and nitrogen depletion in *Nannochloropsis oceanica* (Lu *et al.*, 2014) on CK profiles have been reported.

The present study also showed a wide concentration range of auxins (free IAA, OxIAA and IAA-Asp) in selected cyanobacterial and algal species (Table S3). This is consistent with previously published results demonstrating wide variation in concentrations of IAA and other auxin metabolites, such as IAA-Glu, IAA-Leu and IAM, in cyanobacteria and algae (Tarakhovskaya *et al.*, 2007; Hussain *et al.*, 2010; Yokoya *et al.*, 2010; Yokoya and Yoneshigue-Valentin, 2011). The

auxin derivatives OxIAA and IAA-Asp detected in our study represent metabolic products of two major catabolic pathways of IAA in plants. The first is IAA oxidation to the primary catabolite OxIAA (Kai *et al.*, 2007a) and the second is an amino acid conjugation of IAA with aspartate, leading to the formation of IAA-Asp (Ljung *et al.*, 2002; Ludwig-Müller, 2011). Our data revealed that free IAA and OxIAA were the main auxins, while IAA-Asp occurred only at concentrations close to the detection limit, if present at all (Table S3), indicating a higher relevance of the oxidative than the conjugative pathway in IAA catabolism in cyanobacteria and algae.

Fast regulation of bioactive CK and auxin pools after [³H]*transZ* and [³H]IAA treatments strongly suggests that cyanobacteria and algae possess effective mechanism(s) controlling CK and auxin homeostasis in cells. Using exogenously applied [³H]*transZ*, a swift conversion within 1 h of incubation, especially in *Chroococcus minutus* and *Chlorococcum elbense*, was observed (Fig. 3A, C). In spite of the extensive formation of radiolabelled adenine and/or adenosine following [³H]*transZ* treatment, no CKX activity was detected *in vitro* for any of the species analysed (Figs S2 and S3). This is in accordance with recently published data demonstrating only a very sporadic detection of homologous CKX sequences in algae (Lu *et al.*, 2014) and no detectable enzymatic activity of NoCKX1 in cyanobacterium *Nostoc* sp. PCC 7120 (Frébortová *et al.*, 2015). Notably, the occurrence of [³H]*transZ* metabolite peaks with retention times corresponding to DHZ and DHZR (Fig. 3) suggests a potential involvement of zeatin reductase activity, detected so far only rather rarely in some vascular plant species (Martin *et al.*, 1989; Gaudinová *et al.*, 2005).

It was previously found that feeding *Arabidopsis* seedlings with IAA led to increased accumulation of IAA-Asp, IAA-Glu, IAA-GE, OxIAA and OxIAA-GE (Kai *et al.*, 2007b), most likely due to the activation of multiple metabolic pathways in response to the exogenous IAA supply. Consistently with these results, our findings in selected algal species (*Scenedesmus obliquus*, *Chlorococcum elbense*, *Stigeoclonium helveticum* and *Microthamnion kuetzingianum*) revealed a gradual metabolization of exogenously applied [³H]IAA to IAA-Asp and IAA-GE as two major products. Detection of eight more unidentified metabolites in both cells and medium may indicate the existence of other, probably unknown IAA metabolic pathway(s) in green algae (Figs 4 and 5). Surprisingly, exogenous application of [³H]NAA or [³H]2,4-D did not have any significant effect on substrate metabolization (data not shown), although both of these synthetic auxins were shown to stimulate cell growth and to increase cell fresh and dry weight in *Chlorella pyrenoidosa* cultures (Czerpak *et al.*, 1994). It may be speculated that the absence of metabolization of [³H]NAA or [³H]2,4-D is due to non-functional transport mechanisms or absent metabolic pathways for rapid inactivation of these unnatural auxins.

The apparent correlation between *Scenedesmus obliquus* growth and levels of both CKs and auxins, as demonstrated in Fig. 6, suggests an indispensable role of the two phytohormones in algal cell division. Corresponding to the data of Stirk *et al.* (2014), *cisZ* and iP types mainly contributed to the total CK pool. Enhanced content of CK phosphates, particularly *cisZRMP* and *iPRMP*, during the exponential and linear growth phases (0–3 d) indicated higher CK biosynthetic rates in algal cells in comparison with the stationary phase (Fig. 6B). Our

data are fully compatible with the assumed roles of *cisZ* and iP nucleotides as immediate products in CK biosynthesis, in contrast to *transZ* and DHZ nucleotides, formed particularly by side-chain modification (Takei *et al.*, 2004; Hwang and Sakakibara, 2006; Kieber and Schaller, 2014). Screening of tRNA-bound CKs during *Scenedesmus obliquus* growth also revealed a prevalence of *cisZR* and iPR, contrary to *transZR* and DHZR (Fig. 6E). iPR and *cisZR* have also been reported previously as predominantly tRNA-bound as well as free CK forms in several cyanobacterial and microalgal species by Šimura *et al.* (2014). The significance of *cisZ*-type CKs in the *Scenedesmus obliquus* growth cycle demonstrated in our observations and their potential origin from the tRNA pathway suggested by recent phylogenetic studies, in which higher similarity of IPTs from cyanobacteria and microalgae related to tRNA-IPTs was reported (Frébortová *et al.*, 2015; Lu and Xu, 2015), is thus likely. The prevalence of tRNA-bound *cisZR* and iPR, indicating an important involvement of a tRNA-dependent CK biosynthetic pathway, was also described in the moss *Physcomitrella patens* (Yevdakova *et al.*, 2008). However, a comparison between total concentrations of free CK forms and tRNA-bound CKs during *Scenedesmus obliquus* growth indicated a more pronounced production of CKs through *de novo* biosynthesis (Fig. 6C, D). Likewise, free *cisZ*- and iP-type CK forms were found in considerably higher concentrations than tRNA-bound CKs in vascular plants, such as oat, lucerne and maize, during their germination and early seedling establishment (Stirk *et al.*, 2012).

A subsequent metabolization of CK nucleotides in *Scenedesmus obliquus* culture is not clear because there was no increase in production of CK metabolites in the cells and the medium after stopping cell divisions (Fig. 6B and data not shown). Moreover, the genes involved in CK conjugation (*UGT*) and degradation (*CKX*) have not been functionally characterized in algae yet (Lu *et al.*, 2014; Frébortová *et al.*, 2015). Thus, it can be hypothesized that CK homeostasis during algal growth is controlled basically by modulation of the pool of CK ribotides functioning at least partially as storage metabolites. However, a more detailed characterization of this type of regulation needs further investigation.

In contrast to the CK profile, a gradual enhancement of IAA levels during the subculture period of *Scenedesmus obliquus* correlated with an increase in cell division during the exponential growth phase (2–8 d). Subsequently, IAA concentrations reached their maxima at the stationary phase (13 d) and then declined (Fig. 6F). These findings are consistent with those of Mähönen *et al.* (2014), who showed that higher auxin levels inhibit cell division and expansion but not cell differentiation in *Arabidopsis*. The presence of IAM, a precursor of auxin biosynthesis (reviewed by Woodward and Bartel, 2005; Korasick *et al.*, 2013), indicated an involvement of tryptophan-dependent pathway(s) in *Scenedesmus obliquus*. Detection of OxIAA in *Scenedesmus obliquus* in our experiment pointed to the importance of this auxin metabolic product (Östin *et al.*, 1998) in regulating bioactive IAA levels in non-vascular organisms in addition to vascular plants. Although the biological activity of PAA is generally lower compared with IAA (Sugawara *et al.*, 2015), the endogenous levels of PAA considerably exceeded those of IAA in *Scenedesmus obliquus* cells, which corresponds to data reported for numerous vascular plants [e.g. *Avena sativa*

coleoptiles (Wightman and Lighty, 1982) and *Pisum sativum* roots (Schneider *et al.*, 1985)]. Moreover, PAA and IAA seem to function similarly by regulating auxin-responsive genes through the TIR1/AFB pathway, as demonstrated for *Arabidopsis* (Löbner and Klämbt, 1985), although direct interaction of PAA with TIR1/AFB and Aux/IAA proteins has yet to be investigated both in vascular plants (Shimizu-Mitao and Kakimoto, 2014) and in non-vascular plants. A relatively steady PAA content without any significant dynamic changes during the *Scenedesmus obliquus* growth cycle, however, raises the question of its spatiotemporal regulation in algae. To conclude, our results clearly demonstrate a diverse involvement of CKs and auxins during algal cell growth (Fig. 6), indicating specificities of their functioning in analogy to processes known for vascular plants (Coenen and Lomax, 1997).

CONCLUSIONS

In summary, we present here an insight into the control of CK and auxin homeostasis in evolutionarily older non-vascular organisms, such as cyanobacteria and algae. The comprehensive screen of selected representatives for endogenous CK and auxin profiles reveals the prevalence of CK phosphates and *cisZ*-type CKs in the total CK pool, while in the auxinome free IAA and its primary catabolite OxIAA predominate. For both CKs and auxins, the conjugated forms were not found or were detected only in very low concentrations in cyanobacteria and algae. In contrast to vascular plants, CK downregulation by CKX activity was not observed in any of the tested species. Our data also demonstrate the occurrence and significance of CK methylthio derivatives, which indicates the importance of the tRNA pathway as a substantial source of CKs in cyanobacteria and algae. In addition, we show here the metabolic fate of exogenously applied [³H]*transZ* and [³H]IAA in the selected taxa as well as changes in endogenous CK and auxin pools during the course of *Scenedesmus obliquus* culture, when high concentrations of non-indole PAA, exceeding those of indole auxins, were detected. Our results suggest the existence and operation of a complex network of metabolic pathways and regulation of activities of CKs and auxins in cyanobacteria and algae, apparently differing from those in vascular plants, and reveal a whole range of not yet answered questions regarding the control of phytohormone homeostasis in non-vascular plants.

SUPPLEMENTARY DATA

Supplementary data are available online at www.aob.oxfordjournals.org and consist of the following. Table S1: list and abbreviations of cyanobacterial and algal species analysed for endogenous cytokinin and auxin profiles in this study. Table S2: endogenous cytokinin spectra and concentrations (in pmol g⁻¹ FW) in selected cyanobacterial and algal species in the early stationary growth phase. Table S3: endogenous auxin spectra and concentrations (in pmol g⁻¹ FW) in selected cyanobacterial and algal species in the early stationary growth phase. Table S4: endogenous spectra and concentrations of tRNA-bound cytokinins (pmol mg⁻¹ tRNA) during the *Scenedesmus obliquus* growth cycle. Table S5: endogenous spectra and concentrations of auxins (pmol g⁻¹ FW) during the *Scenedesmus*

obliquus growth cycle. Figure S1: metabolism of exogenously applied [^3H]transZ in the culture medium of *Klebsormidium flaccidum* in the early stationary growth phase. Figure S2: metabolic conversion of [^3H]N 6 -(Δ^2 -isopentenyl)adenine incubated *in vitro* with cytokinin oxidase/dehydrogenase preparations extracted and partially purified from selected cyanobacterial and algal species in the early stationary growth phase. Figure S3: metabolic conversion of [^3H]N 6 -(Δ^2 -isopentenyl)adenine incubated *in vitro* with cytokinin oxidase/dehydrogenase preparations extracted and partially purified from selected cyanobacterial and algal species in the early stationary growth phase.

ACKNOWLEDGEMENTS

The authors wish to thank Dr Miroslav Kamínek for critical reading of the manuscript, Andrew Leppard for language editing and Marie Korecká for her excellent and invaluable technical support. This work was supported by the Czech Science Foundation (16-14649S and GA15-22322S), the Program of Postdoctoral Fellowship from the Czech Academy of Sciences (E.Ž., M.K.) and a long-term research development project (RVO 67985939). Part of this work was also funded by the Ministry of Education, Youth and Sports of the Czech Republic through the National Program of Sustainability (grant no. LO1204) and by the internal Grant Agency of Palacký University (IGA PrF 2016 011).

LITERATURE CITED

- Abdel-Raouf N, Al-Homaidan AA, Ibraheem IBM. 2012. Agricultural importance of algae. *African Journal of Biotechnology* **11**: 11648–11658.
- Abe H, Uchiyama M, Sato R. 1974. Isolation of phenylacetic acid and its p-hydroxy derivative as auxin-like substances from *Undaria pinnatifida*. *Agricultural and Biological Chemistry* **38**: 897–898.
- Anantharaman V, Aravind L. 2001. The CHASE domain: a predicted ligand-binding module in plant cytokinin receptors and other eukaryotic and bacterial receptors. *Trends in Biochemical Sciences* **26**: 579–582.
- Ashen JB, Cohen JD, Goff LJ. 1999. GC-SIM-MS detection and quantification of free indole-3-acetic acid in bacterial galls on the marine alga *Prionitis lanceolata* (Rhodophyta). *Journal of Phycology* **35**: 493–500.
- Le Bail A, Billoud B, Kowalczyk N, et al. 2010. Auxin metabolism and function in the multicellular brown alga *Ectocarpus siliculosus*. *American Society of Plant Biologists* **153**: 128–144.
- Benková E, Ivanchenko MG, Friml J, Shishkova S, Dubrovsky JG. 2009. A morphogenetic trigger: is there an emerging concept in plant developmental biology? *Trends in Plant Science* **14**: 189–193.
- Blilou I, Xu J, Wildwater M, Willemssen V, et al. 2005. The PIN auxin efflux facilitator network controls growth and patterning in *Arabidopsis* roots. *Nature* **433**: 39–44.
- Coenen C, Lomax TL. 1997. Auxin-cytokinin interactions in higher plants: old problems and new tools. *Trends in Plant Science* **2**: 351–356.
- Cooke TJ, Poli DB, Szeiten AE, Cohen JD. 2002. Evolutionary patterns in auxin action. *Plant Molecular Biology* **49**: 319–338.
- Cheng Y, Dai X, Zhao Y. 2006. Auxin biosynthesis by the YUCCA flavin monooxygenases controls the formation of floral organs and vascular tissues in *Arabidopsis*. *Genes & Development* **20**: 1790–1799.
- Cheng Y, Dai X, Zhao Y. 2007. Auxin synthesized by the YUCCA flavin monooxygenases is essential for embryogenesis and leaf formation in *Arabidopsis*. *The Plant Cell* **19**: 2430–2439.
- Czepak R, Bajguz A, Bialecka B, Wierzychowska LE, Wolanska MM. 1994. Effect of auxin precursors and chemical analogs on the growth and chemical composition in *Chlorella pyrenoidosa* Chick. *Acta Societatis Botanicorum Poloniae* **6**: 279–286.
- Djilianov DL, Dobrev PI, Moyankova DP, et al. 2013. Dynamics of endogenous phytohormones during desiccation and recovery of the resurrection plant species *Haberlea rhodopensis*. *Journal of Plant Growth Regulation* **32**: 564–574.
- Dobrev PI, Kamínek M. 2002. Fast and efficient separation of cytokinins from auxin and abscisic acid and their purification using mixed-mode solid-phase extraction. *Journal of Chromatography A* **950**: 21–29.
- Dobrev PI, Havlíček L, Vágner M, Malbeck J, Kamínek M. 2005. Purification and determination of plant hormones auxin and abscisic acid using solid phase extraction and two-dimensional high performance liquid chromatography. *Journal of Chromatography A* **1075**: 159–166.
- Frébort I, Kowalska M, Hluska T, Frébortová J, Galuszka P. 2011. Evolution of cytokinin biosynthesis and degradation. *Journal of Experimental Botany* **62**: 2431–2452.
- Frébortová J, Greplová M, Seidl MF, Heyl A, Frébort I. 2015. Biochemical characterization of putative adenylate dimethylallyltransferase and cytokinin dehydrogenase from *Nostoc* sp. PCC 7120. *PLoS One* **10**: e0138468.
- Friml J, Vieten A, Sauer M, et al. 2003. Efflux-dependent auxin gradients establish the apical-basal axis of *Arabidopsis*. *Nature* **426**: 147–153.
- Gajdošová S, Spichal L, Kamínek M, et al. 2011. Distribution, biological activities, metabolism, and the conceivable function of *cis*-zeatin-type cytokinins in plants. *Journal of Experimental Botany* **62**: 2827–2840.
- Gaudinová A, Dobrev PI, Šolcová B, et al. 2005. The involvement of cytokinin oxidase/dehydrogenase and zeatin reductase in regulation of cytokinin levels in pea (*Pisum sativum* L.) leaves. *Journal of Plant Growth Regulation* **24**: 188–200.
- Hashtroudi MS, Ghassempour A, Riahi H, Shariatmadari Z, Khanjir M. 2013. Indogenous auxins in plant growth-promoting Cyanobacteria – *Anabaena vaginicola* and *Nostoc calcicola*. *Journal of Applied Phycology* **25**: 379–386.
- Hussain A, Kruschke M, Roitsch T, Hasnain S. 2010. Rapid determination of cytokinins and auxin in cyanobacteria. *Current Microbiology* **61**: 361–369.
- Hwang I, Sakakibara H. 2006. Cytokinin biosynthesis and perception. *Physiologia Plantarum* **126**: 528–538.
- Hwang I, Sheen J, Müller B. 2012. Cytokinin signaling networks. *Annual Review of Plant Biology* **63**: 353–380.
- Jusoh M, Loh SH, Chuah TS, Aziz A, Cha TS. 2015. Indole-3-acetic acid (IAA) induced changes in IOL content, fatty acid profiles and expression of four fatty acid biosynthetic genes in *Chlorella vulgaris* at early stationary growth phase. *Phytochemistry* **111**: 65–71.
- Kai K, Horita J, Wakasa K, Miyagawa H. 2007a. Three oxidative metabolites of indole-3-acetic acid from *Arabidopsis thaliana*. *Phytochemistry* **68**: 1651–1663.
- Kai K, Nakamura S, Wakasa K, Miyagawa H. 2007b. Facile preparation of deuterium-labeled standards of indole-3-acetic acid (IAA) and its metabolites to quantitatively analyze the disposition of exogenous IAA in *Arabidopsis thaliana*. *Bioscience Biotechnology and Biochemistry* **71**: 1946–1954.
- Kakimoto T. 2003. Biosynthesis of cytokinins. *Journal of Plant Research* **116**: 233–239.
- Kamínek M, Březinová A, Gaudinová A, Motyka V, Vaňková R, Zažímalová E. 2000. Purine cytokinins: a proposal of abbreviations. *Plant Growth Regulation* **32**: 253–256.
- Kenrick P, Crane PR. 1997. The origin and early evolution of plants on land. *Nature* **389**: 33–39.
- Kieber JJ, Schaller GE. 2014. Cytokinins. *The Arabidopsis Book* **11**: e0168. doi:10.1199/tab.0168.
- Kiseleva AA, Tarachvskaya ER, Shishova MF. 2012. Biosynthesis of phytohormones in algae. *Russian Journal of Plant Physiology* **59**: 595–610.
- Korasick DA, Enders TA, Strader LC. 2013. Auxin biosynthesis and storage forms. *Journal of Experimental Botany* **64**: 2541–2555.
- Lewis LA, McCourt RM. 2004. Green algae and the origin of land plants. *American Journal of Botany* **91**: 1535–1556.
- Ljung K. 2013. Auxin metabolism and homeostasis during plant development. *Development* **140**: 943–950.
- Ljung K, Hull AK, Kowalczyk M, et al. 2002. Biosynthesis, conjugation, catabolism and homeostasis of indole-3-acetic acid in *Arabidopsis thaliana*. *Plant Molecular Biology* **49**: 249–272.
- Löbler M, Klämbt D. 1985. Auxin-binding protein from coleoptile membranes of corn (*Zea mays* L.). I. Purification by immunological methods and characterization. *Journal of Biological Chemistry* **260**: 9848–9853.
- Lu Y, Xu J. 2015. Phytohormones in microalgae: a new opportunity for microalgal biotechnology? *Trends in Plant Science* **20**: 273–282.
- Lu Y, Tarkowská D, Turečková V, et al. 2014. Antagonistic roles of abscisic acid and cytokinin during response to nitrogen depletion in oleaginous

- microalga *Nannochloropsis oceanica* expand the evolutionary breadth of phytohormone function. *The Plant Journal* **80**: 52–68.
- Ludwig-Müller J. 2011.** Auxin conjugates: their role for plant development and in the evolution of land plants. *Journal of Experimental Botany* **62**: 1757–1773.
- Maass H, Klämbt D. 1981.** On the biogenesis of cytokinins in roots of *Phaseolus vulgaris*. *Planta* **151**: 353–358.
- Mähönen AP, Tusscher K, Siligato R, et al. 2014.** PLETHORA gradient formation mechanism separates auxin responses. *Nature* **515**: 125–129.
- Maor R. 2010.** Compositions and methods for increasing oil content in algae. European Patent Application WO2010IL00247 20100324.
- Martin RC, Mok MC, Shaw G, Mok DWS. 1989.** An enzyme mediating the conversion of zeatin to dihydrozeatin in *Phaseolus* embryos. *Plant Physiology* **90**: 1630–1635.
- Mazhar S, Cohen JD, Hasnain S. 2013.** Auxin producing non-heterocystous cyanobacteria and their impact on the growth and endogenous auxin homeostasis of wheat. *Journal of Basic Microbiology* **53**: 996–1003.
- Mazur H, Konop A, Synak R. 2001.** Indole-3-acetic acid in the culture medium of two axenic green microalgae. *Journal of Applied Phycology* **13**: 35–42.
- Miller CO, Skoog F, von Saltza MH, Strong FM. 1956.** Isolation, structure and synthesis of kinetin, a substance promoting cell division. *Journal of American Chemical Society* **78**: 1375–1380.
- Morrison EN, Knowles S, Hayward A, Thorn RG, Saville BJ, Emery RJN. 2015.** Detection of phytohormones in temperate forest fungi predicts consistent abscisic acid production and a common pathway for cytokinin biosynthesis. *Mycologia* **107**: 245–257.
- Motyka V, Vaňková R, Čapková V, Petrášek J, Kamínek M, Schmölling T. 2003.** Cytokinin-induced upregulation of cytokinin oxidase activity in tobacco includes changes in enzyme glycosylation and secretion. *Physiologia Plantarum* **117**: 11–21.
- Normanly J. 2010.** Approaching cellular and molecular resolution of auxin biosynthesis and metabolism. *Cold Spring Harbor Perspectives in Biology* **2**: a001594.
- Normanly J, Cohen JD, Fink GR. 1993.** *Arabidopsis thaliana* auxotrophs reveal a tryptophan-independent biosynthetic pathway for indole-3-acetic acid. *Proceedings of the National Academy of Sciences of the USA* **21**: 10355–10359.
- Novák O, Tarkowski P, Tarkowská D, Doležal K, Lenobel R, Strnad M. 2003.** Quantitative analysis of cytokinins in plants by liquid chromatography–single-quadrupole mass spectrometry. *Analytica Chimica Acta* **480**: 207–218.
- Novák O, Hauserová E, Amakorová P, Doležal K, Strnad M. 2008.** Cytokinin profiling in plant tissues using ultra-performance liquid chromatography-electrospray tandem mass spectrometry. *Phytochemistry* **69**: 2214–2224.
- Nowak J, Sonaike B, Lawson GW. 1988.** Auxin induced stress tolerance in algae. *Environmental Pollution* **51**: 213–218.
- Ouyang J, Shao X, Li J. 2000.** Indole-3-glycerol phosphate, a branchpoint of indole-3-acetic acid biosynthesis from the tryptophan biosynthetic pathway in *Arabidopsis thaliana*. *The Plant Journal* **24**: 327–334.
- Ördög V, Stirk WA, van Staden J, Novák O, Strnad M. 2004.** Endogenous cytokinins in three genera of microalgae from the Chlorophyta. *Journal of Phycology* **40**: 88–95.
- Östín A, Kowalyczk M, Bhalerao RP, Sandberg G. 1998.** Metabolism of indole-3-acetic acid in *Arabidopsis*. *Plant Physiology* **118**: 285–296.
- Park W, Yoo G, Moon M, Kim C, Choi YE, Yang JW. 2013.** Phytohormone supplementation significantly increases growth of *Chlamydomonas reinhardtii* cultivated for biodiesel production. *Applied Biochemistry and Biotechnology* **171**: 1128–1142.
- Pernisová M, Kuderová A, Hejátko J. 2011.** Cytokinin and auxin interactions in plant development: metabolism, signalling, transport and gene expression. *Current Protein and Peptide Science* **12**: 137–147.
- Pils B, Heyl A. 2009.** Unraveling the evolution of cytokinin signaling. *Plant Physiology* **151**: 782–791.
- Piotrowska-Niczyporuk A, Bajguz A. 2014.** The effect of natural and synthetic auxins on the growth, metabolite content and antioxidant response of green alga *Chlorella vulgaris* (Trebouxiophyceae). *Plant Growth Regulation* **73**: 57–66.
- Příbýl P, Cepák V, Kašťánek P, Zachleder V. 2015.** Elevated production of carotenoids by a new isolate of *Scenedesmus* sp. *Algal Research* **11**: 22–27.
- Prinsen E, Kamínek M, van Onckelen HA. 1997.** Cytokinin biosynthesis: a black box? *Plant Growth Regulation* **23**: 3–15.
- Rocha OP, Felício R, Rodrigues AHB, et al. 2011.** Chemical profile and biological potential of non-polar fractions from *Centroceras clavulatum* (C. Agardh) Montagne (Ceramiales, Rhodophyta). *Molecules* **16**: 7105–7114.
- Riisberg I, Orr RJS, Kluge R, et al. 2009.** Seven gene phylogeny of heterokonts. *Protist* **160**: 191–204.
- Ruhfel BR, Gitzendanner MA, Soltis PS, Soltis DE, Burleigh JG. 2014.** From algae to angiosperms – inferring the phylogeny of green plants (Viridiplantae) from 360 plastid genomes. *BMC Evolutionary Biology* **14**: 23.
- Sakakibara H. 2006.** Cytokinins: activity, biosynthesis, and translocation. *Annual Review of Plant Biology* **57**: 431–449.
- Santner A, Calderon-Villalobos LIA, Estelle M. 2009.** Plant hormones are versatile chemical regulators of plant growth. *Nature Chemical Biology* **5**: 301–307.
- Schmölling T, Werner T, Riefler M, Krupková E, Bartriba y Manns I. 2003.** Structure and function of cytokinin oxidase/dehydrogenase genes of maize, rice, *Arabidopsis* and other species. *Journal of Plant Research* **116**: 241–252.
- Schneider EA, Kazakoff CW, Wightman F. 1985.** Gas chromatography–mass spectrometry evidence for several endogenous auxins in pea seedling organs. *Planta* **165**: 232–241.
- Selivankina SY, Zubkova NK, Kupriyanova EV, et al. 2006.** Cyanobacteria respond to cytokinin. *Russian Journal of Plant Physiology* **53**: 751–755.
- Sergeeva E, Liaimer A, Bergman B. 2002.** Evidence for production of the phytohormone indole-3-acetic acid by cyanobacteria. *Planta* **215**: 229–238.
- Shimizu-Mitao Y, Kakimoto T. 2014.** Auxin sensitivities of all *Arabidopsis* Aux/IAAs for degradation in the presence of every TIR1/AFB. *Plant Cell Physiology* **55**: 1450–1459.
- Spíchal L. 2012.** Cytokinins – recent news and views of evolutionarily old molecules. *Functional Plant Biology* **39**: 267–284.
- Stirk WA, Ördög V, van Staden J. 1999.** Identification of the cytokinin isopenentenyladenine in a strain of *Arthonema africanum* (Cyanobacteria). *Journal of Phycology* **35**: 89–92.
- Stirk WA, Ördög V, van Staden J, Jäger K. 2002.** Cytokinin- and auxin-like activity in Cyanophyta and microalgae. *Journal of Applied Phycology* **14**: 215–221.
- Stirk WA, Novák O, Strnad M, van Staden J. 2003.** Cytokinins in macroalgae. *Plant Growth Regulation* **41**: 13–24.
- Stirk WA, van Staden J, Novák O, et al. 2011.** Changes in endogenous cytokinin concentrations in *Chlorella* (Chlorophyceae) in relation to light and the cell cycle. *Journal of Phycology* **47**: 291–301.
- Stirk WA, Václavíková K, Novák O, et al. 2012.** Involvement of *cis*-zeatin, dihydrozeatin, and aromatic cytokinins in germination and seedling establishment of maize, oats and lucerne. *Journal of Plant Growth Regulation* **31**: 392–405.
- Stirk WA, Ördög V, Novák O, Rolčík J, Strnad M, Van Staden J. 2013.** Auxin and cytokinin relationships in 24 microalgal strains. *Journal of Phycology* **49**: 459–467.
- Stirk WA, Tarkowska D, Turecova V, Strnad M, van Staden J. 2014.** Abscisic acid, gibberellins and brassinosteroids in Kelpak (R), a commercial seaweed extract made from *Ecklonia maxima*. *Journal of Applied Phycology* **26**: 561–567.
- Sugawara S, Mashiguchi K, Tanaka K, et al. 2015.** Distinct characteristics of indole-3-acetic acid and phenylacetic acid, two common auxins in plants. *Plant Cell Physiology* **56**: 16411654.
- Svačinová J, Novák O, Plačková L, et al. 2012.** A new approach for cytokinin isolation from *Arabidopsis* tissues using miniaturized purification: pipette tip solid-phase extraction. *Plant Methods* **8**: 17.
- Swaminathan S, Bock RM. 1977.** Isolation and identification of cytokinins from *Euglena gracilis* transfer ribonucleic acid. *Biochemistry* **16**: 1355–1360.
- Šimura J, Novák O, Strnad M, Nedbal L. 2014.** Cytokinin profiling in Cyanobacteria and microalgae species using UHPLC-MS/MS. In: *Abstracts of the International Symposium 2014: Auxins and Cytokinins in Plant Development ... and Interactions with Other Phytohormones*, Prague, Czech Republic. Abstract P1–15.
- Takei K, Yamaya T, Sakakibara H. 2004.** *Arabidopsis* CYP735A1 and CYP735A2 encode cytokinin hydroxylases that catalyze the biosynthesis of trans-zeatin. *Journal of Biological Chemistry* **279**: 41866–41872.
- Tarakhovskaya ER, Maslov YI, Shishova MF. 2007.** Phytohormones in algae. *Russian Journal of Plant Physiology* **54**: 186–194.

- Tarkowski P, Václavíková K, Novák O, et al. 2010.** Analysis of 2-methylthio-derivatives of isoprenoid cytokinins by liquid chromatography-tandem mass spectrometry. *Analytica Chimica Acta* **680**: 86–91.
- Tivendale ND, Ross JJ, Cohen JD. 2014.** The shifting paradigms of auxin biosynthesis. *Trends in Plant Science* **19**: 44–51.
- Yevdakova NA, Motyka V, Malbeck J, et al. 2008.** Evidence for importance of tRNA-dependent cytokinin biosynthetic pathway in the moss *Physcomitrella patens*. *Journal of Plant Growth Regulation* **27**: 271–281.
- Yokoya NS, Stirk WA, van Staden J, et al. 2010.** Endogenous cytokinins, auxins and abscisic acid in red algae from Brazil. *Journal of Phycology* **46**: 1198–1205.
- Yokoya NS, Yoneshigue-Valentin Y. 2011.** Micropropagation as a tool for sustainable utilization and conservation of populations of Rhodophyta. *Revista Brasileira De Farmacognosia – Brazilian Journal of Pharmacognosy* **21**: 334–339.
- Yue J, Xiangyang H, Huang J. 2014.** Origin of plant auxin biosynthesis. *Trends in Plant Science* **19**: 764–770.
- Varalakshmi P, Malliga P. 2012.** Evidence for production of indole-3-acetic acid from a fresh water cyanobacteria (*Oscillatoria annae*) on the growth of *H. annuus*. *International Journal of Scientific and Research Publications* **3**: 1–15.
- Wang B, Chu J, Yu T, et al. 2015.** Tryptophan-independent auxin biosynthesis contributes to early embryogenesis in *Arabidopsis*. *Proceedings of the National Academy of Sciences of the USA* **112**: 4821–4826.
- Wightman F, Lighty DL. 1982.** Identification of phenylacetic acid as natural auxin in the shoots of higher plants. *Physiologia Plantarum* **55**: 17–24.
- Woodward AW, Bartel B. 2005.** Auxin: regulation, action, and interaction. *Annals of Botany* **95**: 707–735.
- Záveská Drábková L, Dobrev PI, Motyka V. 2015.** Phytohormone profiling across the bryophytes. *PLoS One* **10**: e0125411.
- Žižková E, Dobrev PI, Muhovski Y, et al. 2015.** Tomato (*Solanum lycopersicum* L.) SIIPT3 and SIIPT4 isopentenyltransferases mediate salt stress response in tomato. *BMC Plant Biology* **15**: 85.

SUPPLEMENTARY DATA

Supplementary data are available in the online version of this article at www.aob.oxfordjournals.org.

Table S1:

The list and abbreviations of cyanobacteria and algae species analysed for endogenous cytokinin and auxin profiles in this study.

Table S2:

Endogenous cytokinin spectra and concentrations (in pmol g⁻¹ FW) in selected cyanobacteria and algae species in the early stationary growth phase. Abbreviations of selected representatives as given in Table S1; abbreviations of cytokinins adopted and modified according to Kamínek *et al.* (2000).

Table S3:

Endogenous auxin spectra and concentrations (in pmol g⁻¹ FW) in selected cyanobacteria and algae species in the early stationary growth phase. Abbreviations of selected representatives as given in Table S1.

Table S4:

Endogenous spectra and concentrations of tRNA-bound cytokinins (related to pmol mg⁻¹ tRNA) during *Scenedesmus obliquus* growth cycle. Abbreviations of cytokinins adopted and modified according to Kamínek *et al.* (2000).

Table S5:

Endogenous spectra and concentrations of auxins (in pmol g⁻¹ FW) during *Scenedesmus obliquus* growth cycle.

Figure S1:

Metabolism of exogenously applied [^3H]*transZ* in the culture medium of *Klebsormidium flaccidum* in the early stationary growth phase. The peaks represent distribution of radioactivity associated with individual metabolites in the medium 4 and 24 h after [^3H]*transZ* application. The products of [^3H]*transZ* metabolism were analysed by HPLC coupled to on-line radioactivity detector.

transZ = *trans*-zeatin; DHZ = dihydrozeatin.

Figure S2:

Metabolic conversion of [^3H] N^6 -(Δ^2 -isopentenyl)adenine incubated *in vitro* with enzyme cytokinin oxidase/dehydrogenase preparations extracted and partially purified from selected cyanobacteria and algae species in the early stationary growth phase. The *in vitro* assays were performed in 100 mM MOPS-NaOH buffer containing 75 μM 2,6-dichloroindophenol at pH 7.0.

Figure S3: Metabolic conversion of [^3H] N^6 -(Δ^2 -isopentenyl)adenine incubated *in vitro* with enzyme cytokinin oxidase/dehydrogenase preparations extracted and partially purified from selected cyanobacteria and algae species in the early stationary growth phase. The *in vitro* assays were performed in 100 mM TAPS-NaOH buffer containing 75 μM 2,6-dichloroindophenol at pH 8.5.

TABLE S1

Phylum	Order	Class	CCALA #	Species, authority	Abb.
Cyanobacteria	Chroococcales	Cyanophyceae	55	<i>Chroococcus minutus</i> (Kuetzing) Naegeli	CM
	Nostocales	Cyanophyceae	139	<i>Phormidium animale</i> (C. Agardh ex Gomont) Anagnostidis et Komárek	PA
	Nostocales	Cyanophyceae	124	<i>Nostoc microscopicum</i> Carmichael	NM
Ochrophyta	Tribonematales	Xanthophyceae	512	<i>Tribonema aequale</i> Pascher	TA
	Mischococcales	Xanthophyceae	223	<i>Bumilleriopsis filiformis</i> Vischer	BF
	Eustigmatales	Eustigmatophyceae	514	<i>Vischeria helvetica</i> (Vischer et Pascher) Hibberd	VH
Rhodophyta	Porphyridiales	Porphyridiophyceae	416	<i>Porphyridium purpureum</i> (Bory de Saint-Vincent) K. M. Drew & R. Ross	PP
	Rhodellales	Porphyridiophyceae	925	<i>Rhodella violacea</i> (Kornmann) Wehrmeyer	RV
Chlorophyta	Chlamydomonadales	Chlorophyceae	283	<i>Chlorococcum ellipsoideum</i> Deason et Bold	CE
	Chlamydomonadales	Chlorophyceae	282	<i>Chlorococcum elbense</i> Archibald	ChE
	Chlamydomonadales	Chlorophyceae	421	<i>Protosiphon botryoides</i> (Kuetzing) Klebs	PB
	Chlamydomonadales	Chlorophyceae	248	<i>Chlamydomonas segnis</i> Ettl	CS
	Chaetophorales	Chlorophyceae	868	<i>Stigeoclonium helveticum</i> Vischer	SH
	Sphaeropleales	Chlorophyceae	454	<i>Scenedesmus obliquus</i> (Turpin) Kuetzing	SO
	Ulotrichales	Ulvophyceae	926	<i>Ulothrix crenulata</i> Kuetzing	UC
	Ulvales	Ulvophyceae	423	<i>Pseudendoclonium basiliense</i> Vischer	PsB
	Prasiolales	Trebouxiophyceae	420	<i>Prasiolopsis ramosa</i> Vischer	PR
	Microthamniales	Trebouxiophyceae	368	<i>Microthamnion kuetzingianum</i> Naegeli	MK
Streptophyta	Desmidiales	Zygnematophyceae	836	<i>Actinotaenium curtum</i> (Ralfs) Teiling ex Ruzicka et Pouzar	AC
	Klebsormidiales	Klebsormidiophyceae	786	<i>Klebsormidium flaccidum</i> (Kützing) P.C. Silva, K.R. Mattox et W.H. Blackwell	KF

TABLE S2

Phyllum	Species	<i>transZ</i>	<i>transZR</i>	<i>transZ7G</i>	<i>transZ9G</i>	<i>transZOG</i>	<i>transZROG</i>	<i>transZRMP</i>	Σ<i>transZ</i>-types
Cyanobacteria	<i>Chroococcus minutus</i> (CM)	0.51 ± 0.18	-	-	-	-	-	1.36 ± 0.28	1.87
	<i>Phormidium animale</i> (PA)	0.43 ± 0.10	-	-	-	-	-	1.69 ± 0.68	2.12
	<i>Nostoc microscopicum</i> (NM)	4.95 ± 3.06	-	-	-	-	-	-	4.95
Ochrophyta	<i>Tribonema aequale</i> (TA)	0.18 ± 0.05	-	-	-	0.02 ± 0.01	-	0.49 ± 0.36	2.81
	<i>Bumilleriopsis filiformis</i> (BF)	0.79 ± 0.27	0.37 ± 0.30	-	0.38 ± 0.29	-	0.09 ± 0.02	1.33 ± 0.43	2.96
	<i>Vischeria helvetica</i> (VH)	2.28 ± 0.73	-	-	-	-	-	30.34 ± 1.30	32.62
Rhodophyta	<i>Porphyridium purpureum</i> (PP)	0.55 ± 0.40	0.02 ± 0.00	-	-	-	-	0.98 ± 0.11	1.55
	<i>Rhodella violacea</i> (RV)	23.93 ± 9.57	-	-	-	-	-	1.44 ± 0.78	25.37
Chlorophyta	<i>Chlorococcum ellipsoideum</i> (CE)	0.27 ± 0.07	-	-	-	0.06 ± 0.03	0.03 ± 0.00	1.17 ± 0.00	1.53
	<i>Protosiphon botryoides</i> (PB)	0.30 ± 0.03	-	-	-	-	-	-	0.30
	<i>Chlamydomonas segnis</i> (CS)	1.38 ± 0.23	-	-	-	-	-	0.46 ± 0.10	1.84
	<i>Stigeoclonium helveticum</i> (SH)	-	-	-	-	-	-	6.89 ± 0.24	6.89
	<i>Scenedesmus obliquus</i> (SO)	0.29 ± 0.08	-	0.02 ± 0.01	0.18 ± 0.03	-	-	-	0.49
	<i>Ulothrix crenulata</i> (UC)	0.13 ± 0.02	-	-	-	-	-	1.65 ± 0.22	1.78
	<i>Pseudendoclonium basiliense</i> (PsB)	1.02 ± 0.34	-	-	-	-	-	0.49 ± 0.08	1.51
	<i>Prasiolopsis ramosa</i> (PR)	0.63 ± 0.41	-	-	0.25 ± 0.13	-	0.44 ± 0.38	1.33 ± 0.61	2.65
	<i>Microthamnion kuetzingianum</i> (MK)	1.35 ± 0.03	-	-	-	0.02 ± 0.01	-	-	1.37
Streptophyta	<i>Actinotaenium curtum</i> (AC)	-	-	-	-	-	-	1.29 ± 0.01	1.29
	<i>Klebsormidium flaccidum</i> (KF)	0.22 ± 0.06	-	-	-	-	-	13.08 ± 0.45	13.30

Species	DHZ	DHZR	DHZ9G	DHZOG	DHZRMP	Σ DHZ-types	<i>cisZ</i>	<i>cisZR</i>	Σ <i>cisZ</i> -types
CM	0.36 ± 0.15	0.54 ± 0.15	-	-	0.24 ± 0.11	1.14	2.42 ± 0.37	-	2.42
PA	0.55 ± 0.26	0.63 ± 0.50	-	-	-	1.18	0.39 ± 0.06	-	0.39
NM	0.50 ± 0.36	-	-	-	-	0.50	0.98 ± 0.16	0.49 ± 0.35	1.47
TA	0.32 ± 0.07	0.52 ± 0.01	0.07 ± 0.02	-	1.07 ± 0.45	1.98	-	-	-
BF	0.41 ± 0.16	-	-	-	1.00 ± 0.05	1.41	7.77 ± 0.54	0.66 ± 0.11	8.43
VH	0.35 ± 0.03	0.31 ± 0.10	-	-	2.78 ± 0.10	3.44	3.69 ± 0.38	7.77 ± 1.06	11.46
PP	0.34 ± 0.10	-	0.04 ± 0.03	-	0.15 ± 0.05	0.53	-	-	-
RV	0.35 ± 0.09	-	-	-	-	0.35	0.32 ± 0.12	0.77 ± 0.17	1.09
VCE	0.19 ± 0.06	-	-	-	0.61 ± 0.16	0.80	0.46 ± 0.05	0.32 ± 0.02	0.78
PB	0.24 ± 0.11	0.14 ± 0.07	-	-	1.13 ± 0.19	1.51	0.74 ± 0.18	0.19 ± 0.06	0.93
CS	0.37 ± 0.01	0.16 ± 0.04	0.20 ± 0.03	0.06 ± 0.01	-	0.79	55.91 ± 5.61	-	55.91
SH	0.24 ± 0.02	0.26 ± 0.19	-	-	3.45 ± 0.75	3.95	0.99 ± 0.05	1.74 ± 0.31	2.73
SO	0.31 ± 0.00	0.34 ± 0.01	-	-	0.71 ± 0.21	1.36	3.65 ± 0.87	2.30 ± 1.00	5.95
UC	0.37 ± 0.11	0.37 ± 0.10	0.10 ± 0.06	-	1.20 ± 0.06	2.04	-	0.37 ± 0.03	0.37
PsB	0.24 ± 0.03	0.45 ± 0.06	-	-	0.41 ± 0.02	1.10	10.93 ± 1.24	-	10.93
PR	0.31 ± 0.04	0.21 ± 0.15	-	-	3.00 ± 0.10	3.52	0.54 ± 0.08	-	0.54
MK	0.46 ± 0.12	0.20 ± 0.04	-	-	-	0.66	9.69 ± 1.22	-	9.69
AC	-	0.83 ± 0.19	-	-	-	0.83	0.68 ± 0.22	0.22 ± 0.00	0.90
KF	0.53 ± 0.17	0.51 ± 0.13	0.07 ± 0.05	-	2.74 ± 1.12	3.85	1.13 ± 0.12	4.13 ± 0.95	5.26

Species	iP	iPR	iP7G	iP9G	iPRMP	ΣiP-types	2MeSiPR	Total CKs
CM	1.37 ± 0.14	0.67 ± 0.16	-	-	2.89 ± 0.15	4.93	3.43 ± 0.16	13.79
PA	12.21 ± 0.48	7.77 ± 0.19	-	-	63.67 ± 7.50	83.65	91.21 ± 1.94	178.55
NM	-	-	-	-	2.19 ± 1.70	2.19	-	9.11
TA	0.76 ± 0.03	0.17 ± 0.03	-	0.14 ± 0.10	7.37 ± 0.74	8.44	0.80 ± 0.10	14.03
BF	78.35 ± 2.31	11.71 ± 0.94	-	0.99 ± 0.05	7.73 ± 0.30	98.78	7.44 ± 0.18	119.02
VH	0.61 ± 0.05	2.99 ± 0.46	-	-	6.77 ± 0.61	10.37	9.14 ± 0.14	67.03
PP	0.10 ± 0.03	-	-	-	0.35 ± 0.02	0.45	-	2.53
RV	0.11 ± 0.09	-	-	-	0.54 ± 0.15	0.65	2.11 ± 0.98	29.57
VCE	0.28 ± 0.01	-	-	-	0.84 ± 0.21	1.12	1.41 ± 0.05	5.64
PB	20.50 ± 1.19	0.40 ± 0.19	-	-	0.25 ± 0.05	21.15	3.34 ± 1.54	27.23
CS	42.37 ± 1.18	-	0.01 ± 0.00	-	0.10 ± 0.02	42.48	0.98 ± 0.28	102
SH	0.36 ± 0.00	-	1.96 ± 0.24	-	2.79 ± 0.04	5.11	1.41 ± 0.01	20.09
SO	1.31 ± 0.29	1.44 ± 0.08	-	0.08 ± 0.02	-	2.83	7.04 ± 0.80	17.67
UC	0.04 ± 0.01	0.20 ± 0.05	-	-	0.27 ± 0.10	0.51	0.28 ± 0.21	4.98
PsB	12.26 ± 1.41	0.95 ± 0.17	-	-	0.32 ± 0.15	13.53	42.76 ± 8.47	69.83
PR	1.17 ± 0.17	0.86 ± 0.02	-	-	0.42 ± 0.05	2.45	0.70 ± 0.26	9.86
MK	3.25 ± 0.11	-	-	-	0.82 ± 0.04	4.07	8.10 ± 1.80	23.89
AC	1.08 ± 0.03	-	-	-	0.24 ± 0.07	1.32	-	4.34
KF	2.25 ± 0.24	0.28 ± 0.21	-	0.09 ± 0.05	1.70 ± 0.03	4.32	0.29 ± 0.00	27.02

TABLE S3

Phyllum	Species	IAA	IAA-Asp	OxIAA	Σauxins
Cyanobacteria	<i>Chroococcus minutus</i> (CM)	192.95 ± 5.90	0.03 ± 0.02	5.47 ± 0.12	198.45
	<i>Phormidium animale</i> (PA)	250.17 ± 12.32	0.09 ± 0.05	9.51 ± 0.09	259.77
	<i>Nostoc microscopicum</i> (NM)	9.40 ± 2.82	0.05 ± 0.03	5.24 ± 2.00	14.69
Ochrophyta	<i>Tribonema aequale</i> (TA)	86.36 ± 7.68	-	3.37 ± 0.72	89.73
	<i>Bumilleriopsis filiformis</i> (BF)	11.00 ± 0.51	-	1.78 ± 0.09	12.78
	<i>Vischeria helvetica</i> (VH)	29.82 ± 1.32	0.04 ± 0.01	3.16 ± 0.21	33.02
Rhodophyta	<i>Porphyridium purpureum</i> (PP)	3.26 ± 1.22	0.05 ± 0.03	13.19 ± 0.77	16.5
	<i>Rhodella violacea</i> (RV)	11.18 ± 1.96	-	5.90 ± 0.59	17.8
Chlorophyta	<i>Chlorococcum ellipsoideum</i> (CE)	56.19 ± 3.91	0.22 ± 0.09	3.78 ± 0.26	60.19
	<i>Protosiphon botryoides</i> (PB)	23.47 ± 2.30	0.10 ± 0.02	43.54 ± 4.77	67.11
	<i>Chlamydomonas segnis</i> (CS)	13.39 ± 1.52	-	10.83 ± 1.65	91.34
	<i>Stigeoclonium helveticum</i> (SH)	287.57 ± 19.89	0.03 ± 0.01	3.09 ± 0.45	290.69
	<i>Scenedesmus obliquus</i> (SO)	19.59 ± 1.73	0.70 ± 0.17	27.32 ± 9.75	47.61
	<i>Ulothrix crenulata</i> (UC)	27.17 ± 0.51	-	3.18 ± 0.30	30.35
	<i>Pseudendoclonium basiliense</i> (PsB)	6.43 ± 0.52	-	4.50 ± 1.12	10.93
	<i>Prasiolopsis ramosa</i> (PR)	148.72 ± 9.48	0.15 ± 0.04	4.53 ± 0.06	153.4
	<i>Microthamnion kuetzingianum</i> (MK)	45.70 ± 1.29	0.21 ± 0.02	19.16 ± 3.74	65.07
Streptophyta	<i>Actinotaenium curtum</i> (AC)	113.34 ± 4.56	0.06 ± 0.03	2.76 ± 0.15	116.16
	<i>Klebsormidium flaccidum</i> (KF)	13.61 ± 0.35	-	7.61 ± 0.66	21.22

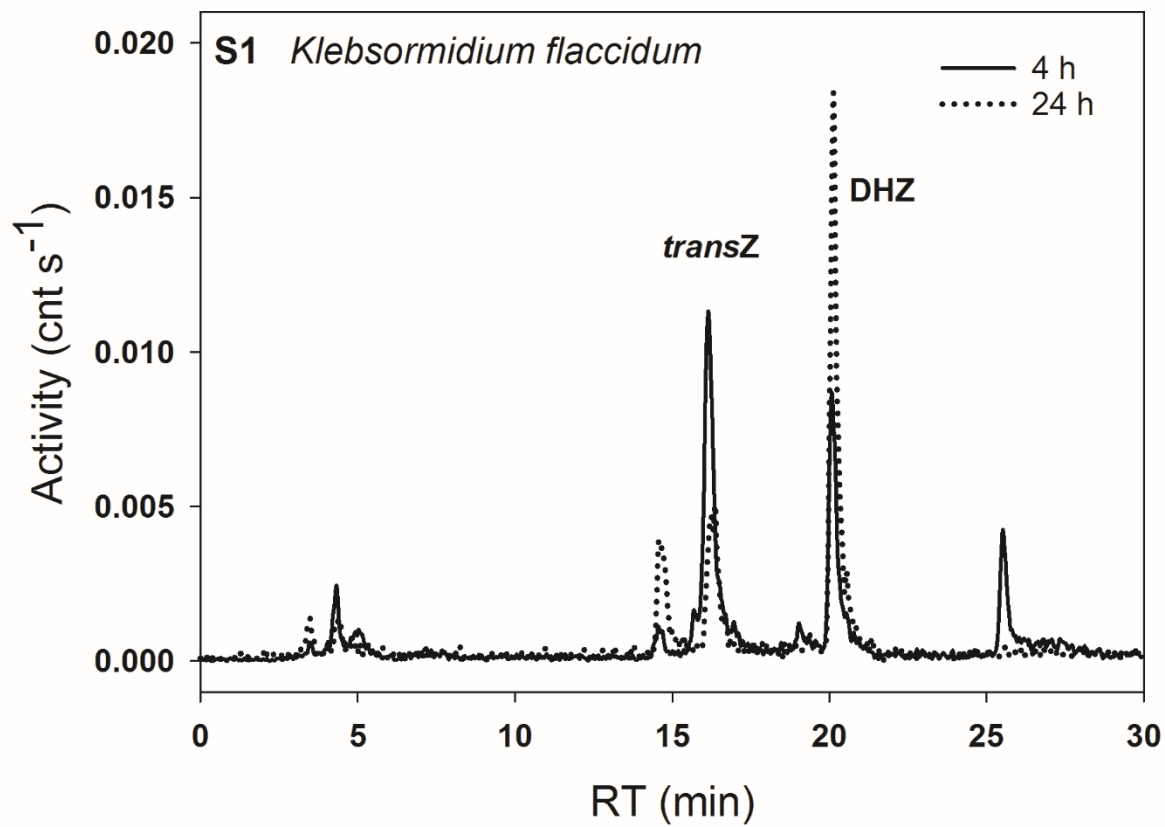
TABLE S4

Time (d)	ng tRNA/g DW	tRNA (ng/ul)	pmol mg ⁻¹ tRNA				pmol mg ⁻¹ tRNA	
			<i>trans</i> ZR	<i>cis</i> ZR	DHZR	iPR	2MeScisZR	2MeSiPR
0	0.50 ± 0.04	9.10 ± 1.38	0.97 ± 0.03	51.45 ± 0.44	0.49 ± 0.00	24.92 ± 0.63	19.26 ± 1.45	12.77 ± 0.55
1	0.91 ± 0.10	12.94 ± 0.82	0.69 ± 0.02	58.32 ± 4.00	0.56 ± 0.07	24.87 ± 1.03	28.94 ± 1.28	17.84 ± 1.44
2	0.70 ± 0.17	13.78 ± 3.70	0.81 ± 0.17	61.05 ± 1.85	0.59 ± 0.04	34.92 ± 4.07	21.12 ± 1.35	21.45 ± 3.52
4	0.25 ± 0.04	5.12 ± 1.13	3.00 ± 0.36	74.36 ± 5.83	0.85 ± 0.10	31.20 ± 2.98	38.85 ± 3.94	21.58 ± 3.02
7	0.24 ± 0.04	8.58 ± 1.93	2.12 ± 0.26	33.96 ± 2.66	0.38 ± 0.04	26.18 ± 2.50	27.13 ± 2.75	12.74 ± 1.78
9	0.15 ± 0.06	3.89 ± 0.78	0.70 ± 0.12	15.06 ± 2.24	0.45 ± 0.01	15.70 ± 2.36	13.98 ± 4.60	8.40 ± 3.80
13	0.21 ± 0.00	7.24 ± 4.50	1.07 ± 0.30	35.12 ± 5.31	0.85 ± 0.41	46.29 ± 3.21	42.89 ± 0.71	23.38 ± 0.06
14	0.23 ± 0.01	7.56 ± 0.24	0.71 ± 0.01	34.40 ± 2.14	0.46 ± 0.01	44.51 ± 7.54	39.30 ± 3.15	19.89 ± 1.92

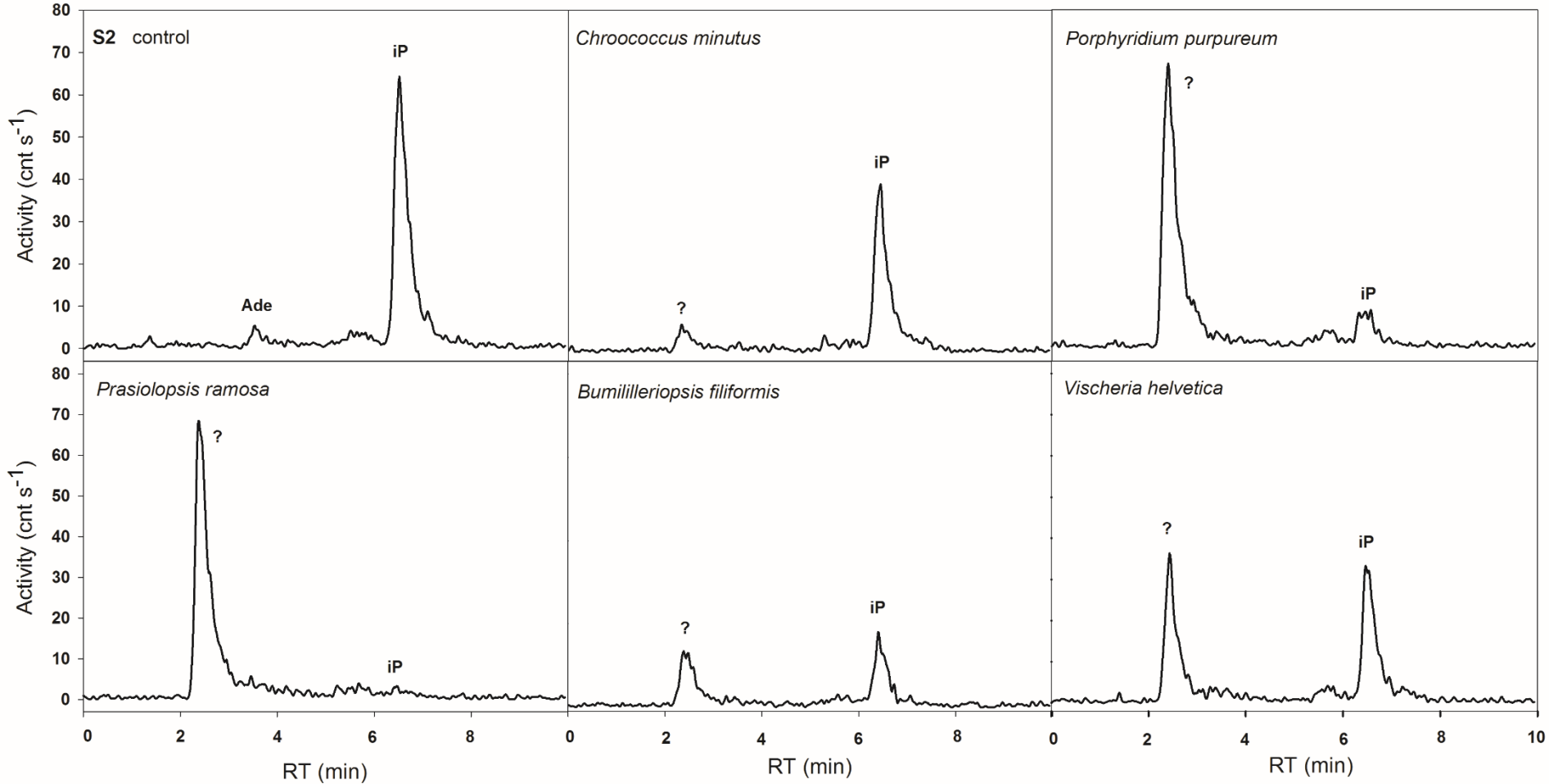
TABLE S5

Time (d)	IAA	OxIAA	IAM	PAA	IAA-Asp	OxIAA-GE	IAN
0	4.33 ± 0.03	8.07 ± 0.48	15.27 ± 1.68	668.91 ± 106.69	0.26 ± 0.10	0.04 ± 0.05	0.17 ± 0.04
1	7.37 ± 0.15	0.63 ± 0.13	4.74 ± 0.95	495.28 ± 99.06	0.30 ± 0.06	-	0.11 ± 0.02
2	10.13 ± 1.34	2.17 ± 2.54	1.72 ± 2.25	608.36 ± 77.72	0.28 ± 0.33	0.11 ± 0.15	1.73 ± 0.01
4	21.58 ± 0.98	1.77 ± 2.39	1.97 ± 0.19	757.79 ± 274.09	0.08 ± 0.12	0.31 ± 0.22	0.36 ± 0.30
7	57.13 ± 1.78	6.23 ± 0.56	3.51 ± 1.10	669.93 ± 159.02	0.32 ± 0.07	0.31 ± 0.01	1.37 ± 0.89
9	71.62 ± 3.23	9.18 ± 1.31	2.31 ± 1.17	662.70 ± 41.37	0.22 ± 0.08	0.10 ± 0.14	2.10 ± 1.73
13	84.90 ± 0.96	12.18 ± 0.47	1.50 ± 0.47	724.37 ± 123.24	0.05 ± 0.08	0.11 ± 0.15	0.79 ± 0.16
14	41.42 ± 11.65	7.93 ± 2.22	0.87 ± 0.97	625.74 ± 92.14	0.21 ± 0.10	0.35 ± 0.24	0.41 ± 0.08

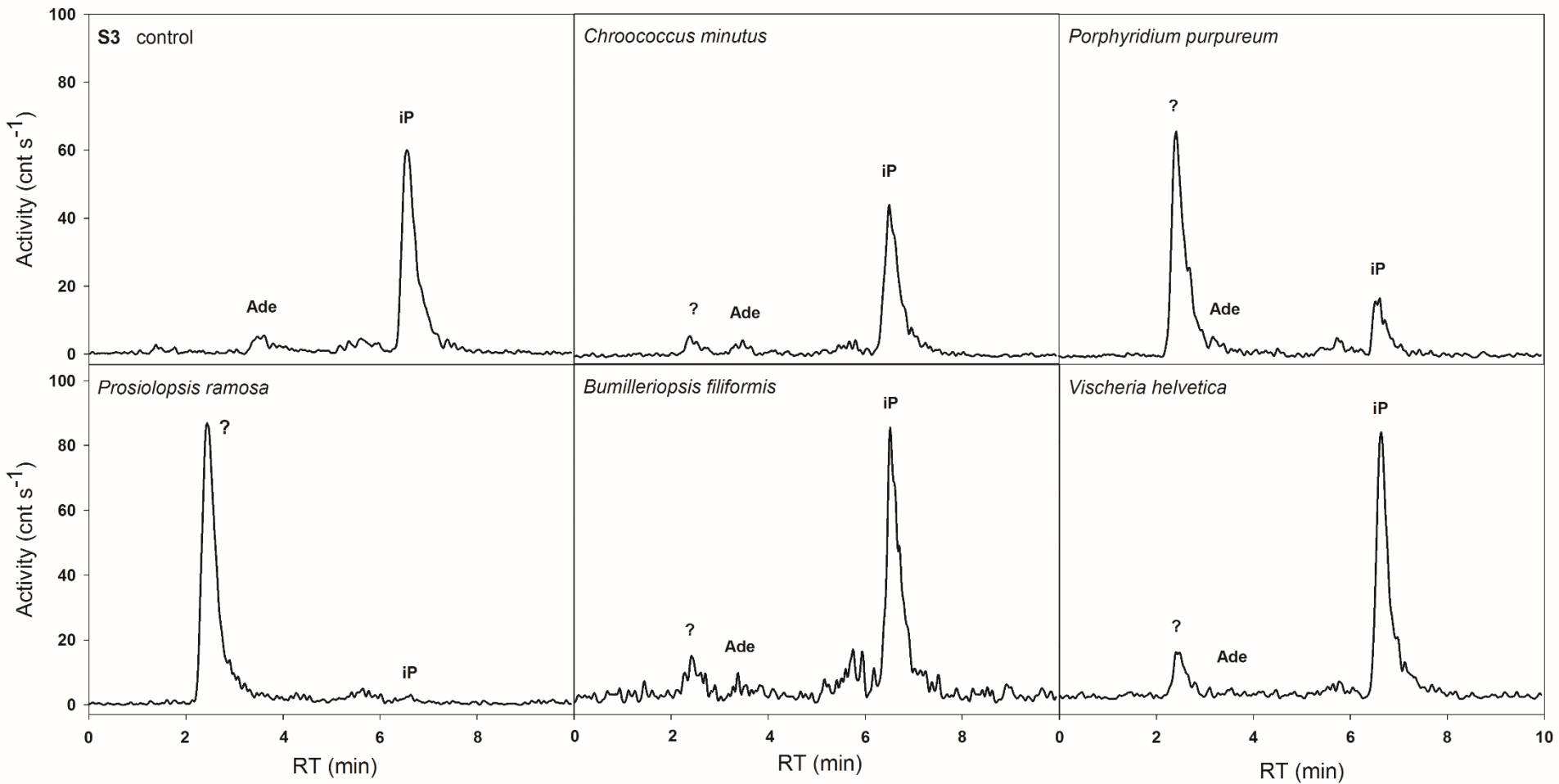
Supplementary Data Fig. S1



Supplementary Data Fig. S2



Supplementary Data Fig. S3



Supplement III

Frébortová, J. Plíhal, O., Florová, V., Kokáš, F., Kubiasová, K., Greplová, M., **Šimura, J.**, Novák, O., Frébort, I. (2017) Light influences cytokinin biosynthesis and sensing in *Nostoc* (Cyanobacteria). *Journal of Phycology*, 53, 703–714.

LIGHT INFLUENCES CYTOKININ BIOSYNTHESIS AND SENSING IN *NOSTOC* (CYANOBACTERIA)¹

Jitka Frébortová²

Department of Chemical Biology and Genetics, Centre of the Region Haná for Biotechnological and Agricultural Research,
Faculty of Science, Palacký University, Šlechtitelů 27, 783 71 Olomouc, Czech Republic

Ondřej Plíhal, Vendula Florová, Filip Kokáš, Karolína Kubiasová, Marta Greplová

Department of Molecular Biology, Centre of the Region Haná for Biotechnological and Agricultural Research, Faculty of Science,
Palacký University, Šlechtitelů 27, 783 71 Olomouc, Czech Republic

Jan Šimura

Department of Chemical Biology and Genetics, Centre of the Region Haná for Biotechnological and Agricultural Research,
Faculty of Science, Palacký University, Šlechtitelů 27, 783 71 Olomouc, Czech Republic

Ondřej Novák

Laboratory of Growth Regulators, Centre of the Region Haná for Biotechnological and Agricultural Research, Faculty of Science,
Palacký University and Institute of Experimental Botany, The Czech Academy of Sciences, Šlechtitelů 27, 783 71 Olomouc,
Czech Republic

and Ivo Frébort

Department of Molecular Biology, Centre of the Region Haná for Biotechnological and Agricultural Research, Faculty of Science,
Palacký University, Šlechtitelů 27, 783 71 Olomouc, Czech Republic

Cytokinins are an important group of plant hormones that are also found in other organisms, including cyanobacteria. While various aspects of cytokinin function and metabolism are well understood in plants, the information is limited for cyanobacteria. In this study, we first experimentally confirmed a prenylation of tRNA by recombinant isopentenyl transferase *NoIPT2* from *Nostoc* sp. PCC 7120, whose encoding gene we previously identified in *Nostoc* genome along with the gene for adenylate isopentenyl transferase *NoIPT1*. In contrast to *NoIPT2*, the transcription of *NoIPT1* was strongly activated during the dark period and was followed by an increase in the cytokinin content several hours later in the light period. Dominant cytokinin metabolites detected at all time points were free bases and monophosphates of isopentenyladenine and *cis*-zeatin, while *N*-glucosides were not detected at all. Whole transcriptome differential expression analysis of cultures of the above *Nostoc* strain treated by cytokinin compared to untreated controls indicated that cytokinin together with light trigger expression of several genes related to signal transduction, including two-component sensor histidine kinases and two-component hybrid sensors and regulators. One of the affected histidine kinases

with a cyclase/histidine kinase-associated sensory extracellular domain similar to the cytokinin-binding domain in plant cytokinin receptors was able to modestly bind isopentenyladenine. The data show that the genetic disposition allows *Nostoc* not only to produce free cytokinins and prenylate tRNA but also modulate the cytokinin biosynthesis in response to light, triggering complex changes in sensing and regulation.

Key index words: cytokinin; expression profiling; *miaA*; *Nostoc*; RNA-seq; sensor kinase; tRNA IPT

Abbreviations: CHASE, cyclase/histidine kinase-associated sensory extracellular; CKX, cytokinin dehydrogenase; *cZ*, *cis*-zeatin; *cZR*, *cis*-zeatin 9-riboside; *cZRMP*, *cis*-zeatin 9-riboside-5'-monophosphate; *DHZ*, dihydrozeatin; *DMAPP*, dimethylallyl pyrophosphate; *DW*, dry weight; *GO*, gene ontology; *HMBPP*, 4-hydroxy-3-methyl-but-2-enyl pyrophosphate; *iP*, N^6 - (Δ^2 -isopentenyl) adenine; *iPRMP*, N^6 - (Δ^2 -isopentenyl) adenosine-5'-monophosphate; *iPR*, N^6 - (Δ^2 -isopentenyl) adenosine; *IPT*, isopentenyl transferase; *MBP*, maltose-binding protein; *tZR*, trans-zeatin 9-riboside; *tZ*, trans-zeatin

¹Received 21 December 2016. Accepted 29 March 2017.

²Author for correspondence: e-mail jitka.frebortova@upol.cz.
Editorial Responsibility: J. Raven (Associate Editor)

Cytokinins are a group of phytohormones, chemicals functioning as signal molecules in regulation of plant growth (Mok and Mok 2001). Since the discovery of a first cytokinin in 1950s (Miller et al.

1955), numerous studies describing cytokinin occurrence, metabolism, and physiological function in plants were published. Cytokinins were also found in other photosynthetic organisms, cyanobacteria, and algae, as well as nonphotosynthetic bacteria, amoeba, and fungi (Tsavkelova et al. 2006). Information on metabolism and physiological function of cytokinins in these phylogenetically diverse organisms, including both prokaryotes and eukaryotes with different life strategies, is, however, only emerging (Pertry et al. 2010, Hussain et al. 2013, Lu and Xu 2015, Radhika et al. 2015, Samanovic et al. 2015, Chanclud and Morel 2016, Miri et al. 2016).

Cytokinins are derivatives of adenine and can be classified based on the nature of their side chain as isoprenoid or aromatic (Mok and Mok 2001). While the biosynthetic pathway of aromatic cytokinins is yet unknown, biosynthesis of isoprenoid cytokinins is catalyzed by two different classes of isopentenyl transferases (IPT), one of which transfers isopentenyl chain from dimethylallyl pyrophosphate (DMAPP) or 4-hydroxy-3-methyl-but-2-enyl pyrophosphate (HMBPP) to N⁶-amino group of AMP, ADP, or ATP (adenylate IPT; EC 2.5.1.27; Sakakibara 2006) and the other to tRNA-bound adenosine phosphate in tRNAs recognizing the UNN codon (tRNA IPT; EC 2.5.1.75; Persson et al. 1994). Adenylate IPT is present in some bacteria, amoeba *Dicystelium discoideum*, and in plants (Kakimoto 2003, Sakakibara 2006, Anjard and Loomis 2008) and was recently also found in fungus *Claviceps purpurea* (Hinsch et al. 2015). In plants, they are responsible for biosynthesis of most of the cytokinins (Barnes et al. 1980), except for their *cis*-zeatin type, which is a degradation product of prenylated tRNA (Miyawaki et al. 2006). Degradation of tRNA is a major source of cytokinins in many other organisms (Persson et al. 1994, Koenig et al. 2002, Morrison et al. 2015) due to ubiquitous distribution of tRNA IPTs, encoded by *miaA* genes, in almost all living organisms, excluding Archaea (Persson et al. 1994). Recent phylogenetic analysis indicated that most cyanobacteria contain only tRNA IPTs, which all form separate clade distinct from plant IPTs (Frébortová et al. 2015). Adenylate IPT was found in only three cyanobacterial species, *Nostoc* sp. PCC 7120, closely related *Anabaena variabilis* ATCC 29413 and *Microcystis aeruginosa* NIES-843. Interestingly, these adenylate IPTs were more related to plant tRNA IPTs than existing adenylate IPTs of plant origin. In addition, there is so far no evidence for the presence of an adenylate IPT in algae (Frébortová et al. 2015, Lu and Xu 2015).

Cytokinin biosynthesis by adenylate IPT and degradation of prenylated tRNA both give cytokinin nucleotides as the final product. Analysis of cytokinin content in several cyanobacteria as well as algae revealed the presence of various cytokinin metabolites, including free bases, ribosides and nucleotides of isopentenyladenine (iP), *cis*-zeatin

(cZ), *trans*-zeatin (tZ) and dihydrozeatin (DHZ), and zeatin *O*-glucosides (Stirk et al. 2003, 2011, Ördög et al. 2004, Hussain et al. 2010, Lu et al. 2014, Frébortová et al. 2015, Žižková et al. 2017), indicating existence of metabolic pathways controlling levels of individual cytokinins. Observed prevalence of free bases and nucleotides of iP and cZ points to different regulation of cytokinin homeostasis in cyanobacteria and algae compared to plants (Žižková et al. 2017). In addition, pathways leading to an inactivation of cytokinins through the formation of biologically inactive N⁹-glucosides by N-glucosyltransferase or side chain cleavage by cytokinin dehydrogenase (CKX) are absent in all analyzed cyanobacterial species and most algal species (Ördög et al. 2004, Stirk et al. 2011, Lu et al. 2014, Frébortová et al. 2015, Žižková et al. 2017). These findings led to a suggestion that formation of cZ type of cytokinins, in most plants biologically less active form of cytokinins (Gajdošová et al. 2011), may modulate pool of biologically active cytokinins in cyanobacteria and algae (Žižková et al. 2017).

In contrast to the wealth of information on many aspects of cytokinin action in plants, to date only little is known about their metabolic conversions and function in other photosynthetic organisms. It was recently reported that endogenous cytokinins were involved in the responses to light and cell division in unicellular eukaryotic algae *Chlorella minutissima* and *Chlorella* sp. (Stirk et al. 2011) and that cytokinin biosynthesis was suppressed in unicellular oleaginous alga *Nannochloropsis oceanica* under nitrogen deprivation (Lu et al. 2014). In cyanobacteria, a group of photosynthetic prokaryotes, most information on cytokinin action comes from exogenous application of cytokinins. Growth promotion by kinetin was observed with *Anabaena doliolum* (Kapoor and Sharma 1981) and *Synechococcus leopoliensis* (Suzuki et al. 2004); kinetin also enhanced nitrogen fixation in *Anabaena* (Kapoor and Sharma 1981). Stimulation of *in vitro* transcription by cytokinins benzyladenine and tZ was reported in *Synechosystis* sp. (Selivankina et al. 2006). Involvement of cytokinins in rice and wheat root colonization by *Nostoc* sp. was suggested (Hussain et al. 2013).

Our recent study of homologs of key enzymes in plant cytokinin biosynthesis and degradation in *Nostoc* sp. PCC 7120 showed that adenylate IPT homolog (*NoIPT1*) is a functional enzyme, catalyzing formation of isopentenyladenosine-5'-monophosphate (iPRMP), while gene homologous to plant CKXs does not encode an active protein (Frébortová et al. 2015). In addition to *NoIPT1*, *Nostoc* sp. PCC 7120 contains another IPT annotated as tRNA IPT, whose enzymatic activity, however, was not experimentally confirmed. In the work reported herein, we thus cloned the gene, expressed it in *Escherichia coli* and characterized the protein product, confirming its function in tRNA prenylation.

A further aim of this study was to evaluate if there are variations in expression of the two *IPT* genes during the light and dark period of *Nostoc* growth under nitrogen-fixing conditions and if they are reflected in changes of cytokinin content. In addition, whole transcriptome differential expression analysis of *Nostoc* cultures treated by cytokinin compared to untreated controls was performed to evaluate the response of cyanobacteria to exogenous cytokinin exposure and light conditions on the gene expression level.

MATERIALS AND METHODS

Culture conditions. *Nostoc* sp. PCC 7120 was obtained from the Pasteur Culture collection of Cyanobacteria (Paris, France). *Nostoc* sp. PCC 7120 was cultivated in 50 mL of nitrogen-free medium BG-11₀, pH 7.1 (Rippka et al. 1971) in a chamber (Sanyo MLR 350H, Osaka, Japan) with 16:8 light-dark cycles, at 24°C and a photon flux density of 35 $\mu\text{mol} \cdot \text{m}^{-2} \cdot \text{s}^{-1}$. Humidity was kept at 60%. Fresh BG-11₀ medium in each flask was inoculated with the stock culture to reach chlorophyll-*a* concentration of 0.1 $\text{mg} \cdot \text{L}^{-1}$. The cells were harvested after 28 d (corresponding to early stationary phase) by centrifugation at 10,000*g* for 10 min at 4°C, washed by deionized water, and stored at -80°C. Samples were collected every second hour during the 24 h period starting 1 h after beginning of light period on day 28. For analysis of free cytokinins, cyanobacteria from four different flasks per sampling time were combined. For expression analysis, three replicate samples per time point, each combined from two different flasks, were used. The experiment was carried out with two sets of independently cultivated *Nostoc* cells. For whole transcriptome shotgun sequencing, *Nostoc* cultures cultivated for 28 d under conditions described above were treated with 5 μM isopentenyladenosine (iPR) 10 h after the start of light period on day 28 or 3 h after the start of subsequent dark period on day 28 and the cells were collected 3 h later. Control cultures were treated with DMSO at the volume identical to the volume of added iPR solution in DMSO. Three replicate samples per each condition, each combined from three different flasks, were used.

Cloning, expression, and purification of tRNA IPT (NoIPT2). - Genomic DNA was isolated from *Nostoc* sp. PCC 7120 using method based on a published protocol (Fiore et al. 2000). Gene encoding *NoIPT2* (*abr5266*) was amplified from genomic DNA of *Nostoc* sp. PCC 7120 by PCR with each of the two specific primers, *NoIPT2*_Ndelfw (5'-GGAATTCATATGAC TAAATTAATCGTAATTTG-3') and *NoIPT2*_Sallrev (5'-ACGC GTCGACCTACGGTTGT-3'), using Phusion DNA Polymerase (Finnzymes, Espoo, Finland). The amplified DNA was first cloned into an expression plasmid pTYB12 (New England Biolabs, Ipswich, MA, USA). *NoIPT2* gene was subsequently cleaved from pTYB12 plasmid with HindIII and PstI and cloned to pMAL-c4X plasmid (New England Biolabs). Plasmid constructs were transformed into *Escherichia coli* TOP10 by heat shock and the transformants were selected on LB medium containing ampicillin. The DNA sequence of the plasmid was confirmed by sequencing and the recombinant plasmid was transformed into expression cells *E. coli* BL21 Star (DE3; Thermo Fisher Scientific, Waltham, MA, USA).

Escherichia coli was cultivated in 50 mL liquid LB media containing ampicillin (100 $\mu\text{g} \cdot \text{mL}^{-1}$) and 1% glucose in a 250 mL Erlenmeyer flask at 37°C and 160 rpm until reaching OD₆₀₀ of 0.5. Expression of *NoIPT2* protein was induced by adding isopropyl- β -D-thiogalactopyranoside to a final concentration of 0.3 mM. Cultures were then incubated at 18°C on

an orbital shaker (160 rpm) overnight. Cells were harvested by centrifugation at 5,000*g* for 15 min and stored at -80°C until used. The pellet from 1 L of expression culture was suspended in 25 mL lysis buffer (20 mM Tris/HCl, pH 7.5, 10 mM MgCl₂, 200 mM NaCl, 1 mM PMSF) and the cells were then disrupted by sonication (4 \times 5 min, pulse 6 s, pause 9 s). The cell lysates were clarified by centrifugation at 14,000*g* for 30 min at 4°C.

NoIPT2 fused with maltose-binding protein (MBP) at *NoIPT2* N-terminus was purified on an amylose resin (New England Biolabs). The protein sample was loaded onto the column (10 \times 1 cm) equilibrated by 20 mM Tris/HCl, pH 7.5, containing 10 mM MgCl₂ and 200 mM NaCl, and washed with 100 mL of the same buffer. *NoIPT2*-MBP fusion protein was subsequently eluted with 60 mL of the equilibration buffer supplemented with 10 mM maltose. The buffer in eluted fraction was then exchanged with 50 mM Tris/HCl, pH 7.5, containing 10 mM MgCl₂ (buffer A) using an Amicon Ultra-15 centrifugal filter unit with 10 kDa cut-off (Millipore, Darmstadt, Germany), and *NoIPT2* was further purified on High Q column (BioRad, Hercules, CA, USA; 20 cm \times 1.5 cm) equilibrated with buffer A. After sample loading, the column was washed by 100 mL of the same buffer and retained proteins were then eluted by a linear gradient of KCl (0–1 M) in buffer A (total volume 180 mL), followed by an isocratic elution with 1 M KCl in buffer A (50 mL). Fractions (5 mL each) containing *NoIPT2* without apparent contaminating proteins (as judged from SDS-PAGE) were collected and concentrated by centrifugal filter unit with 10 kDa cut-off.

Determination of tRNA-IPT activity. The tRNA IPT activity assay was based on the reaction of a synthetic 17-base consensus oligoribonucleotide with a sequence 5'-GCCGACU CAAAUCCGC-3', an analog of the unmodified stem-loop region of tRNA^{Phe} (Soederberg and Poulter 2000), as an acceptor substrate and dimethylallyl pyrophosphate or 4-hydroxy-3-methyl-but-2-enyl pyrophosphate as donor substrates. Cytokinin ribonucleotide was then released from the prenylated oligonucleotide by enzymatic hydrolysis with nuclease P1 from *Penicillium citrinum* and dephosphorylated by alkaline phosphatase (Gehrke et al. 1982). The RNA oligonucleotide (Sigma-Aldrich, St. Louis, MO, USA) was diluted to 100 μM concentration in RNase-free 10 mM Tris/1 mM EDTA (TE) buffer, pH 8, containing 7 mM MgCl₂, incubated in a water bath at 100°C for 5 min and then rapidly cooled on ice for 30 min to form stem-loop structure (Soederberg and Poulter 2000). The reaction mixture (total volume of 30 μL) consisting of 35 mM Tris/HCl pH 8.5, 2 mM mercaptoethanol, 3.5 mM MgCl₂, 50 μM annealed oligoribonucleotide, 50 μM DMAPP, or *trans*-HMBPP (Echelon BioSciences, Salt Lake City, UT, USA) and an appropriate amount of the enzyme solution was incubated at 37°C for 1–6 h. The enzymatic reaction was stopped by heating for 10 min at 95°C, then the sample mixture diluted by 30 μL of 500 mM Tris/HCl, pH 7, and resulting oligonucleotide cleaved overnight by 0.2 U of nuclease P1 (Sigma-Aldrich) at 37°C. The nuclease was deactivated by heating for 10 min at 95°C and liberated cytokinin monophosphate converted to riboside by 0.2 U of FastAP thermosensitive alkaline phosphatase (Thermo Fisher Scientific) at 37°C for 2 h. The alkaline phosphatase was then deactivated at 75°C for 5 min and the mixture centrifuged at 17,000*g* for 5 min. Control reactions in the absence of the donor substrate or enzyme were also performed. Obtained supernatant was analyzed for the formation of cytokinin riboside by HPLC with UV detection at 268 nm. Reaction products, iPR or *trans*-zeatin riboside (tZR), were determined on a Symmetry C18 column (2.1 \times 150 mm, 5 μm ; Waters, Milford, MA, USA) connected to an Alliance e2695 high-performance liquid chromatograph

(Waters) and Waters 2998 photodiode array detector. The analyzed products were eluted by a linear gradient of 15 mM ammonium formate, pH 4.0 (A) and acetonitrile (B) using the following solvent mixture: 0–30 min, 5%–24% B, 30–31 min, 24%–100% B. The flow rate was $0.25 \text{ mL} \cdot \text{min}^{-1}$ and the column temperature 30°C . The concentration of each product was determined by a calibration curve method using authentic standard compound (OlChemIm, Olomouc, Czech Republic). The identity of the product was confirmed by Q-TOF mass spectrometer (Waters) connected to HPLC at the method development stage.

The soluble protein content in enzyme samples was determined by the Bradford method (Bradford 1976) with BSA as a standard.

Analysis of free and tRNA-bound cytokinins. *Nostoc* samples (5 mg of freeze-dried cells) were homogenized and extracted in 1 mL of modified Bielecki buffer (60% MeOH, 10% HCOOH, and 30% H₂O) together with a cocktail of stable isotope-labeled internal standards (0.25 pmol of cytokinin bases, ribosides, *N*-glucosides, 0.5 pmol of cytokinin *O*-glucosides, and nucleotides per sample added). The extracts were purified using mixed-mode cation exchange columns (Oasis MCX cartridges, $30 \text{ mg} \cdot \text{mL}^{-1}$; Waters) as described by Dobrev and Kamínek (2002), with modifications (Antoniadi et al. 2015). Analytes were eluted by two-step elution using 0.35 M NH₄OH aqueous solution and 0.35 M NH₄OH in 60% (v/v) MeOH solution. Extractions and purifications were carried out in three technical replicates.

Extraction and purification of tRNA-bound cytokinins, including 2-methylthio derivatives, were performed according to a protocol described by Maass and Klämbt (1981) with modifications by Stirk et al. (2012). tRNA was isolated from 50 mg of freeze-dried cells that were collected after 28 d of cultivation and 5 h after the start of light period. Extracted tRNA was subsequently hydrolyzed with 2 M KOH and dephosphorylated using alkaline phosphatase. After enzyme removal (overnight precipitation using ethanol in -20°C), the samples were further purified using MCX columns as mentioned above. Stable isotope-labeled internal standards were used as a reference (0.2 pmol of each [²H]-labeled cytokinin riboside). Extractions and purifications were carried out in four technical replicates.

Cytokinin concentrations were determined by the isotope dilution method (Rittenberg and Foster 1940) using ultra-high-performance liquid chromatography-electrospray tandem mass spectrometry (UHPLC-MS/MS). Quantification of free and tRNA-bound cytokinin metabolites was performed according to the method described by Svačinová et al. (2012). 2-methylthio derivatives of tRNA-bound isoprenoid cytokinins were analyzed with an HPLC-MS/MS system as described previously (Tarkowski et al. 2010).

qPCR expression profiling. Pelleted *Nostoc* cells were homogenized in the presence of TRI Reagent Solution (Applied Biosystems, Waltham, MA, USA) and glass beads (0.2 mm; Sigma-Aldrich) using oscillatory mill (Retsch MM400; Retsch GmbH, Haan, Germany). Cell homogenate was clarified by centrifugation, and RNA was separated from DNA and proteins by chloroform extraction. RNA was precipitated from the aqueous phase with isopropanol in the presence of a high salt precipitation solution according to the manufacturer's manual, washed with ethanol, and suspended in nuclease-free water. Isolated RNA was treated twice with the TURBO DNase-free kit (Thermo Fisher Scientific) and purified using Agencourt RNAClean XP (Beckman Coulter, Pasadena, CA, USA) magnetic beads. RNA was then used in a first strand cDNA synthesis with the RevertAid™ H Minus M-MuLV reverse transcriptase and oligo-dT mixture (Thermo Fisher Scientific). Diluted cDNA samples were used as templates in

real-time PCR reactions containing the gb SG PCR Master Mix (Generi Biotech, Hradec Králové, Czech Republic), passive reference dye (Generi Biotech) and 300 nM primers, which were designed using Primer Express 3.0 software (Applied Biosystems). Each cDNA sample was analyzed in two technical replicates on a StepOnePlus Real-Time PCR System using the default program (Life Technologies, Carlsbad, CA, USA). *C_t* values were normalized with respect to *petB* (cytochrome *b₆*) and *secA* (protein translocase subunit SecA) genes (Pinto et al. 2012). Expression values were determined and statistically evaluated using the DataAssist v3.0 Software package (Thermo Fisher Scientific).

RNA-seq and data analysis. Total RNA (4 µg) from each sample was processed using Ribo-Zero rRNA Removal Kit for Bacteria (Illumina, San Diego, CA, USA) to remove contaminating rRNA. Subsequently, 40 ng isolated mRNA per sample was used for cDNA synthesis using Illumina® TruSeq® Stranded mRNA Sample Preparation Kit. cDNA library was prepared using the manufacturer's protocol with one modification: isolated mRNA (0.5–1 µL) was directly added to 18.5 µL of Fragment, Prime, and Finish mix and incubated for 10 min at 94°C for RNA fragmentation and priming. Three replicate samples per each condition were used to generate cDNA libraries. Prepared libraries were validated using DNA 1000 chip with 2100 Bioanalyzer Instrument (Agilent Technologies, Santa Clara, CA, USA), and all concentrations were assessed using a Kapa Library Quantification Kit (Kapa Biosystems, Wilmington, MA, USA). Prepared libraries were pooled to a final concentration of $12 \text{ pmol} \cdot \text{L}^{-1}$ for cluster generation and sequencing. The final libraries were sequenced on a MiSeq Sequencing System (Illumina) using MiSeq Reagent Kits v3 (150 cycle).

The reads generated by sequencing were mapped to the reference genome of *Nostoc* sp. PCC 7120 v.31 using Ensembl genome annotation system release 87 (Yates et al. 2016) using a TopHat v.2.0.12 splice-read mapper (Kim et al. 2013) with default parameters. The reads mapped to the transcripts annotated in the reference genome were quantified with HTSeq v.0.6.0 software (Anders et al. 2014) with respect to the stranded library. The tests for differential gene expression were performed using the DESeq2 package (Love et al. 2014) implemented in R (R Development Core Team, 2008). Gene ontology (GO) annotation (Ashburner et al. 2000) of the reference genome was improved using the Blas2GO v.3.0 program (Conesa et al. 2005) and nt database (b2g_Sep2016).

Cloning of all2875 and cytokinin-binding assay. Coding sequence of *all2875* was obtained by gene synthesis (Life Technologies) and subcloned in pDEST14 vector by LR recombination reaction (Gateway® technology; Thermo Fisher Scientific). The DNA sequence of the plasmid was confirmed by sequencing and the recombinant plasmid was transformed into expression cells *E. coli* BL21 Star (DE3; Thermo Fisher Scientific). The binding assay was performed according to a method described by Romanov et al. (2005) with slight modifications. *Escherichia coli* was grown in liquid M9 medium supplemented with $100 \text{ µg} \cdot \text{mL}^{-1}$ ampicillin and 0.1% (w/v) casamino acids at 25°C , with shaking (180 rpm), to OD₆₀₀ 0.6–0.7. Cell suspension (1 mL) was transferred to microcentrifuge tubes, followed by addition of 3 pmol of [³H] tZ (Isotope Laboratory, Institute of Experimental Botany, AS CR, Prague, Czech Republic) and varying concentrations of unlabeled tZ or iP. After 30 min incubation at 4°C , the sample was centrifuged (6,000g, 6 min, 4°C), the supernatant was carefully removed, and pelleted *E. coli* cells were suspended in 1 mL of scintillation cocktail (Beckman, Ramsey, MN, USA). Radioactivity was measured by a Hidex 300 SL scintillation counter (Hidex, Turku, Finland).

RESULTS AND DISCUSSION

NoIPT2 catalyzes prenylation of tRNA *in vitro*. In addition to recently characterized adenylate IPT (*NoIPT1*), *Nostoc* sp. PCC 7120 contains another IPT (*NoIPT2*) annotated as tRNA IPT (Frébortová et al. 2015). To confirm the predicted function, encoding gene was cloned into several plasmid expression vectors, such as pET-28b (+), pTYB12, and pMAL-c4X, and tested for expression in *E. coli*. While the former two systems produced only minute amounts of recombinant tRNA IPT, successful expression was achieved from pMAL-c4X plasmid, which led to the production of tRNA IPT as a fusion protein with MBP. Protein was initially purified from clarified cell lysates by amylose affinity chromatography, and remaining impurities were removed by High Q ion-exchange chromatography. Analysis of purified protein by SDS-PAGE revealed the presence of tRNA IPT-MBP fusion protein (75.5 kDa) and a band of ~60 kDa, reminiscent of chaperonin GroEL co-expressing with NoCKX (Frébortová et al. 2015). Chaperonin could be removed from tRNA IPT by purification on High Q column after cleavage of tRNA IPT-MBP fusion protein by factor Xa; the removal, however, resulted in rapid degradation of tRNA IPT protein. Fusion protein exhibited an enzyme activity in tRNA IPT assay employing synthetic RNA oligonucleotide mimicking stem-loop region of tRNA^{Phe} (Soederberg and Poulter 2000). Both DMAPP and *trans*-HMBPP were used by the enzyme to prenylate RNA oligonucleotide, showing specific activities of 253.4 ± 13.6 pkat \cdot mg⁻¹ and 6.6 ± 0.7 pkat \cdot mg⁻¹ (mean value \pm SD, $n = 3$), respectively. AMP was not used by the enzyme as side chain accepting substrate.

In agreement with the observed enzymatic activity of *NoIPT2*, analysis of tRNA-bound cytokinins showed that tRNA predominantly contains iPRMP, together with *cis*-zeatin 9-riboside-5'-monophosphate (cZRMP) and their 2-methylthio derivatives (Fig. 1). Total concentrations of cZ types and iP types were similar, reaching ~100 fmol \cdot μ g⁻¹ of tRNA. In contrast to iP, cZ was present mainly in the form of its 2-methylthio derivative, which is the final product of hypermodification of tRNA-bound iPR by methylthiotransferase MiaB (Pierrel et al. 2004) and hydroxylase MiaE (Persson and Björk 1993). Very low concentrations of tZ and DHZ (less than 0.1 fmol \cdot μ g⁻¹ of tRNA; data not shown) were also detected.

Expression profiling of cytokinin biosynthesis genes and cytokinin content in Nostoc cells in response to light conditions. Expressions of the two genes involved in cytokinin biosynthesis, *NoIPT1* and *NoIPT2*, were determined in *Nostoc* cells grown in a nitrogen-free medium to early stationary phase at 16:8 light:dark regimen, after collecting samples every second hour during the 24 h period. Expression of *NoIPT1* started to decrease after the start of light period,

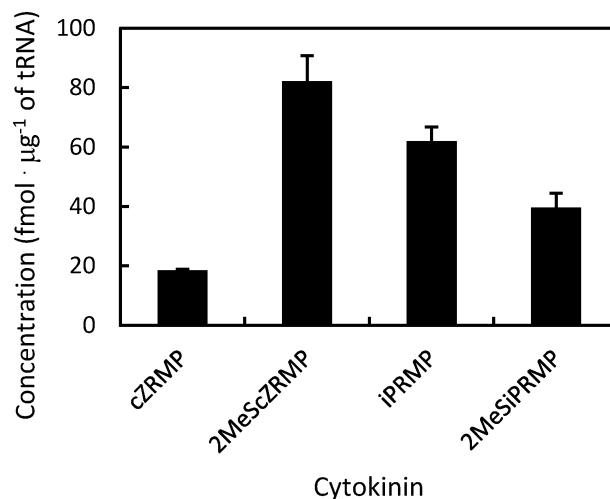


Fig. 1. Cytokinins detected in tRNA of *Nostoc*. The bars indicate concentration of individual cytokinins (mean \pm SD, $n = 4$). cZRMP, *cis*-zeatin 9-riboside-5'-monophosphate, iPRMP, N⁶-(Δ^2 -isopentenyl) adenosine-5'-monophosphate; 2MeScZRMP, 2-methylthio-*cis*-zeatin 9-riboside-5'-monophosphate, 2MeSiPRMP, 2-methylthio-N⁶-(Δ^2 -isopentenyl) adenosine-5'-monophosphate.

become steady between seventh and fifteenth hour of the light period, and increased gradually after the start of dark period, reaching the peak at 23 h, with the expression 30 times higher compared to the lowest expression at 13 h (Fig. 2A). However, although the expression of *NoIPT2* appeared to decrease after the start of the light period and then gradually return to steady state, the changes were not statistically significant (Fig. 2B).

To determine whether changes in expression of *NoIPT1* gene are also reflected in changes in the cytokinin content, concentrations of free cytokinins were measured in *Nostoc* cells collected at the same time points as those used for expression analysis. At all the followed time points, iP and cZ metabolites represented the dominant cytokinins (more than 97% of total cytokinin pool; Fig. 3A), while tZ and particularly DHZ metabolites were present at low concentrations. Cytokinin monophosphates and free bases together represented more than 95% of all cytokinin metabolites present. Remaining 5% were represented by cytokinin ribosides and zeatin-*O*-glucosides (Fig. 3B); cytokinin-*N*-glucosides were not detected. Most free bases were derived from iP (Fig. 3, B and C). cZRMP was always present in higher concentrations than cZ (Fig. 3D).

As shown in Figure 3C, concentrations of iP gradually increased at the beginning of light period, reaching maximum at 7 h. Concentration of iP then decreased and stabilized after 11 h. The same profile was also observed for cZ. Although iPRMP is a first product of the *de novo* cytokinin biosynthesis, its concentration was at most of the time points invariable (Fig. 3C) and did not immediately follow the increase in *NoIPT1* expression. The peak of iP production at 7 h of light period (in contrast to

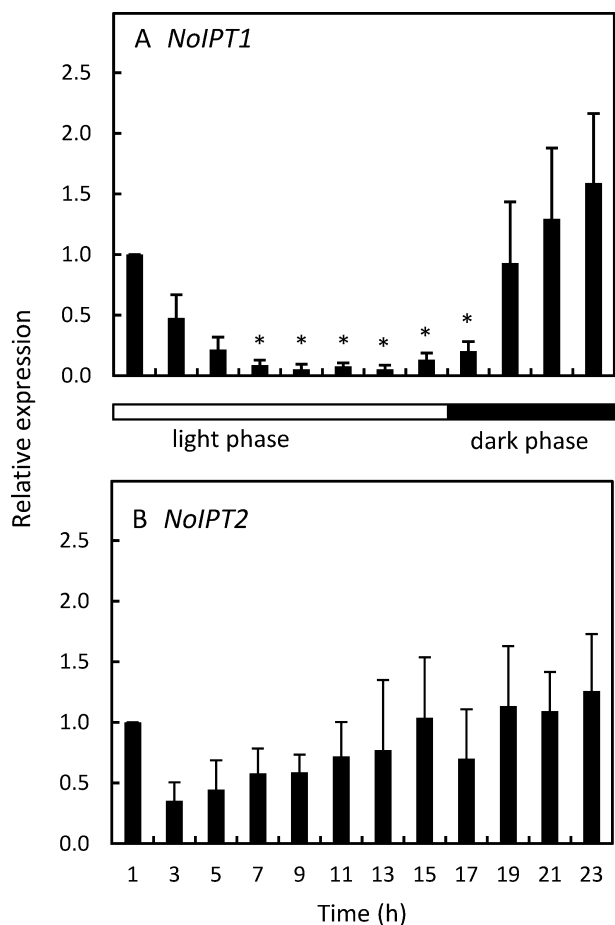


Fig. 2. Expression profiles of IPTs in *Nostoc* during 24 h period (16:8 h light:dark). The bars indicate relative gene expression and the error bars indicate SD values ($n = 4$). Expression values were determined and statistically evaluated using the DataAssist v3.0. Gene expression was normalized to 1 h. Asterisks denote significant difference compared to 1 h, $P \leq 0.05$.

peak of *NoIPT1* expression at the end of dark period) together with limited changes in iPRMP concentration suggests that the enzymatic reaction catalyzed by *NoIPT1* is a rate limiting step of the active cytokinin production and that excessive iPRMP is rapidly converted to iP, probably by a process analogous to plants, which involves a phosphoribohydrolase known as a “Lonely guy” (Kurakawa et al. 2007). Changes in concentrations of cZ followed those of iP (Fig. 3D), but origin of cZ at the moment uncertain. Although it may appear that cZ metabolites are present due to a conversion of free iPRMP or iP, the only recognized source of cZ so far is degradation of tRNA (Miyawaki et al. 2006). In contrast to cytochrome P450 monooxygenases that catalyze hydroxylation of iP-nucleotides to tZ-nucleotides (Takei et al. 2004), a similar enzyme converting iP type of cytokinins to cZ type was not discovered to date. Likewise, direct production of cZ type of cytokinins by transferring isoprenoid precursor HMBPP with a hydroxyl group in the

cis-position to adenine ring was not described. While the increase of cytokinin content can be attributed either to enhanced cytokinin biosynthesis by *NoIPT1* or to enhanced tRNA degradation or both, a mechanism of subsequent reduction of cytokinin concentrations is unclear, since putative cytokinin dehydrogenase NoCKX1 was not active nor was its activity observed in cell extracts or culture medium (Frébortová et al. 2015). Interestingly, conversion of iP to an unknown polar product by a crude protein extract from cyanobacterium *Chroococcus minutus* was observed recently (Žižková et al. 2017) and may represent a novel cytokinin deactivation pathway.

Whole transcriptome analysis of Nostoc in response to light conditions and cytokinin treatment. Similar to the findings in green unicellular algae *Chlorella* (Stirk et al. 2011), cytokinin content and expression of a gene involved in cytokinin biosynthesis in *Nostoc* sp. PCC 7120 differ during light and dark periods of cultivation. However, to date no information is available on the response of cyanobacteria to exogenous cytokinin exposure on the gene expression level. Thus, we next performed a whole transcriptome differential expression analysis of cultures treated by iPR relative to those without cytokinin treatment. The cells were treated and collected either during light period or dark period of the cultivation. Direct comparison between the cytokinin-treated cultures and respective control cultures collected under the same conditions, however, failed to show significantly affected differently regulated genes (DEGs), and therefore, the combined effect of light and the cytokinin treatment was evaluated. The comparison of expression profiles of untreated cultures collected during the light period with those collected in the dark revealed 605 significantly affected genes from the total number of 3,005 annotated genes (adjusted $P < 0.05$). Similar results were obtained by comparing cultures treated by iPR; in this case, significant alterations of 658 genes were observed. All genes affected by light in either control group (C group) or cytokinin-treated group (CK group) were assigned corresponding GO number, and the distribution of GO terms in both data sets was performed at level 5 and higher. The results showing 15 most affected GO terms among up-regulated and down-regulated DEGs are summarized in Table 1. As expected, the most affected DEGs were linked to light-dependent photosynthetic reactions. A large number of alterations in GO:0009772 “photosynthetic electron transport in photosystem II” was observed in the group of up-regulated genes. Accordingly, electron transport chain-related protein products of genes belonging to GO:0015992 “proton transport” or GO:0008137 “NADH dehydrogenase (ubiquinone) activity” and GO:0016655 “oxidoreductase activity acting on NAD(P)H, quinone or similar compound as acceptor” were also found among the most affected GO terms. The

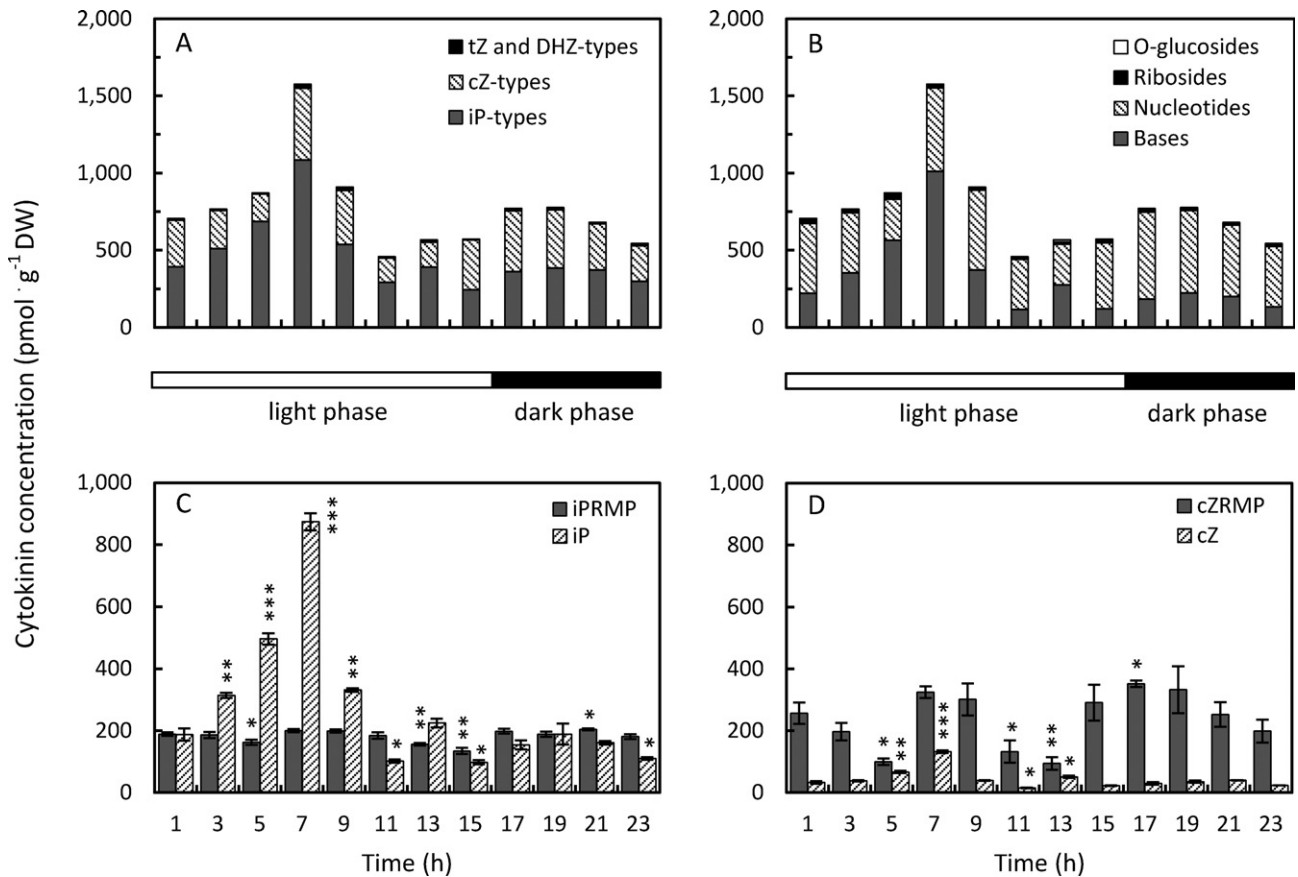


FIG. 3. Endogenous cytokinins detected in *Nostoc* cells during 24 h period (16:8 h light:dark). (A) Total cytokinins grouped according to the structure of a side chain. (B) Total cytokinins grouped according to conjugating molecules. (C) Content of major iP metabolites. (D) Content of major cZ metabolites. The bars indicate concentration of individual cytokinins (mean \pm SD, $n = 3$). Asterisks denote significant differences compared to 1 h for each cytokinin (* $P \leq 0.05$, ** $P \leq 0.01$, *** $P \leq 0.001$).

comparison between C group and CK group of DEGs confirmed that changes between these two data sets were small for highly enriched GO terms, indicating that photosynthesis and related processes are not significantly iPR dependent. In contrast to up-regulated DEGs, GO analysis in the group of down-regulated DEGs did not show any major enrichment in a specific pathway in response to light conditions and cytokinin treatment (Table 1). Changes were observed in diverse processes including oligosaccharide and lipopolysaccharide synthesis (GO:0009311 and GO:0009103, respectively), chemical homeostasis (GO:0048878), or sigma factor activity (GO:0016987).

Next, GO enrichment data from both data sets (i.e., C group and CK group) were scanned for changes in the pattern of enriched GO terms (Table 2). While differences in the number of DEGs for GO terms related to photosynthesis were insignificant, differential enrichment and up-regulation of DEGs in the CK group of genes were observed in GO:0044260 “cellular macromolecule metabolic process,” GO:0044271 “cellular nitrogen compound biosynthetic process,” and several signal

transduction-related categories. Notably, the latter included two interlinked terms GO:0000160 “phosphorelay signal transduction system” and GO:0000155 “phosphorelay sensor kinase activity.” Conversely, some GO terms contained down-regulated DEGs, which were mostly linked to aromatic amino acid metabolic processes. This down-regulation may lead to decreased tryptophan levels since GO:0000162 “tryptophan biosynthetic process” was one of the affected terms. In this context, it is interesting to note that tryptophan pathway is in plants utilized for production of volatile indolics, important plant defense compounds, as well as glucosinolates, phytoalexins, and, notably, phytohormone auxin (Radwanski and Last 1995), whose function is complementary to cytokinin (Faiss et al. 1997, Nordström et al. 2004, Tanaka et al. 2006) and which was shown to be produced by cyanobacteria (Hussain et al. 2010, Lu and Xu 2015).

Differential analysis of GO terms in the C group and CK group pointed to the fact that cytokinin treatment in *Nostoc* leads to reprogramming of gene transcription in response to cytokinin treatment on condition that the effect of the hormone is

TABLE 1. Most affected gene ontology (GO) terms assigned to up-regulated or down-regulated differentially expressed genes (adjusted $P < 0.05$) in *Nostoc* sp. PCC 7120 cultures collected during light period relative to samples collected in dark.

GO number	Domain	Description	Total no.	Regulated genes (%)	
				CK	C
<i>GO categories for up-regulated DEGs</i>					
GO:0009772	BP	Photosynthetic electron transport in photosystem II	9	88.9	88.9
GO:0009145	BP	Purine nucleoside triphosphate biosynthetic process	9	88.9	88.9
GO:0015992	BP	Proton transport	8	87.5	87.5
GO:0098662	BP	Inorganic cation transmembrane transport	9	77.8	77.8
GO:0008137	MF	NADH dehydrogenase (ubiquinone) activity	14	71.4	78.6
GO:0042451	BP	Purine nucleoside biosynthetic process	13	69.2	69.2
GO:0016655	MF	Oxidoreductase activity acting on NAD(P)H, quinone or similar compound as acceptor	18	66.7	72.2
GO:0030076	CC	Light-harvesting complex	27	51.9	51.9
GO:0042168	BP	Heme metabolic process	6	50.0	50.0
GO:0022904	BP	Respiratory electron transport chain	18	50.0	44.4
GO:0015980	BP	Energy derivation by oxidation of organic compounds	33	45.5	36.4
GO:0009163	BP	Nucleoside biosynthetic process	20	45.0	45.0
GO:1901659	BP	Glycosyl compound biosynthetic process	20	45.0	45.0
GO:0009156	BP	Ribonucleoside monophosphate biosynthetic process	18	44.4	50.0
GO:0003899	MF	DNA-directed RNA polymerase activity	9	44.4	44.4
<i>GO categories for down-regulated DEGs</i>					
GO:0009583	BP	Detection of light stimulus	8	50.0	50.0
GO:0009311	BP	Oligosaccharide metabolic process	8	50.0	50.0
GO:0016868	MF	Intramolecular transferase activity, phosphotransferases	6	50.0	50.0
GO:0048878	BP	Chemical homeostasis	6	50.0	50.0
GO:0009103	BP	Lipopolysaccharide biosynthetic process	7	42.9	42.9
GO:0016987	MF	Sigma factor activity	15	40.0	40.0
GO:0015112	MF	Nitrate transmembrane transporter activity	8	37.5	25.0
GO:0045226	BP	Extracellular polysaccharide biosynthetic process	6	33.3	33.3
GO:0009522	CC	Photosystem I	15	33.3	33.3
GO:0004553	MF	Hydrolase activity, hydrolyzing O-glycosyl compounds	23	30.4	26.1
GO:0000270	BP	Peptidoglycan metabolic process	17	29.4	23.5
GO:0030076	CC	Light-harvesting complex	27	25.9	25.9
GO:0018904	BP	Ether metabolic process	8	25.0	25.0
GO:0044272	BP	Sulfur compound biosynthetic process	12	25.0	25.0
GO:1903509	BP	Lipopolysaccharide metabolic process	12	25.0	25.0

BP, biological process; CC, cellular component; MF, molecular function.

The early stationary phase cultures were treated by 5 μ M iPR or equal volume of DMSO (mock). DEGs were grouped into two data sets: light-regulated in the presence of cytokinin (CK) and light-regulated control (C). The most affected GO terms at level 5 or higher are shown for both groups. Percentages of DEGs are calculated from the total number of genes in *Nostoc* sp. PCC 7120 genome with the same GO number (total no.).

evaluated between the light and dark phase of cultivation, or in other words, the effect of cytokinin is light-dependent. To evaluate the effects of cytokinin treatment in more detail, individual DEGs in CK group and in C group of genes were further analyzed. Comparison of these two groups revealed that there was a substantial overlap; 406 up-regulated and 554 down-regulated DEGs common to both C group and CK group were detected (Fig. 4). Nevertheless, 179 up-regulated DEGs and 126 down-regulated DEGs were unique only for the CK group of genes. Closer inspection of these genes showed that number of affected processes was again related to signal transduction. Specifically, the examination of the individual genes in GO:0000155 “phosphorelay sensor kinase activity” revealed that 11 DEGs were specific only for CK group, 14 DEGs were present both in C group and CK group, and only two DEGs were present specifically in C group (Table 3).

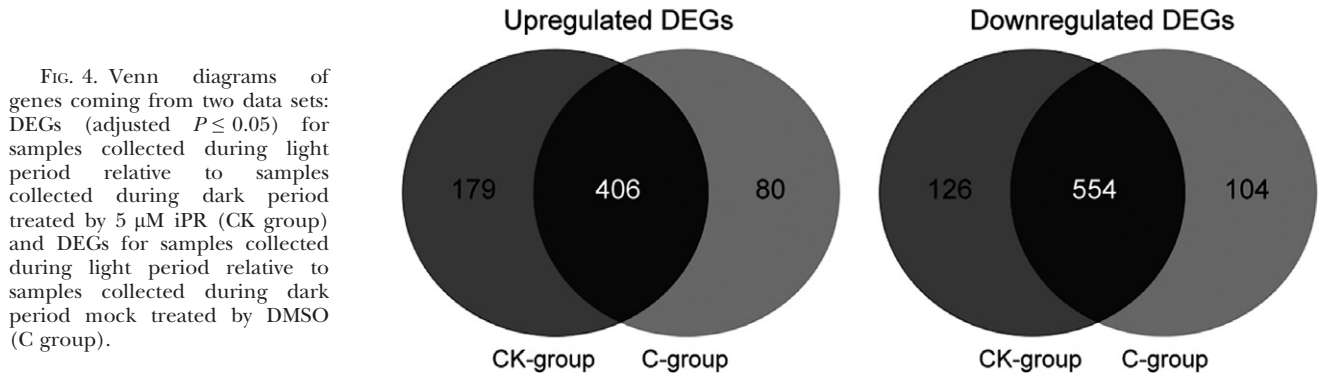
Analysis of signaling components with GO:0000155 responding to the combined effect of light and cytokinin in Nostoc. The genes with GO:0000155 encode protein products annotated mostly as two-component (hybrid) sensor histidine kinase or serine/threonine kinase with two-component sensor domain. The protein lengths were rather variable, reaching from ~400 to 1,800 amino acids. The domain architecture of affected proteins, however, showed some common features. Importantly, all two-component histidine kinases in the list contain a histidine kinase A domain (HisKA; pfam 00512) followed by a histidine kinase-, DNA gyrase B-, and HSP90-like ATPase domain (HATPase; pfam02518). Hybrid sensor histidine kinases/response regulators such as *abr1231* and *abr3121* (specific only for the CK group) contain in addition to aforementioned domains also a response regulator receiver domain (REC; cd00156), which is atypically located at the protein

TABLE 2. Differential distribution of gene ontology (GO) terms for *Nostoc* sp. PCC 7120 cultures collected during light period relative to samples collected in dark.

GO number	Domain	Description	Total no.	Number of regulated genes		
				CK	C	Δ_{CK-C}
GO:0044260	BP	Cellular macromolecule metabolic process	597	89	60	29
GO:0044271	BP	Cellular nitrogen compound biosynthetic process	429	87	71	16
GO:0007165	BP	Signal transduction	230	22	9	13
GO:0000160	BP	Phosphorelay signal transduction system	154	19	8	11
GO:0000155	MF	Phosphorelay sensor kinase activity	130	12	4	8
GO:0038023	MF	Signaling receptor activity	132	12	4	8
GO:0009072	BP	Aromatic amino acid family metabolic process	24	<i>8</i>	<i>2</i>	<i>6</i>
GO:0042430	BP	Indole-containing compound metabolic process	13	<i>6</i>	<i>2</i>	<i>4</i>
GO:0000162	BP	Tryptophan biosynthetic process	7	<i>3</i>	<i>1</i>	<i>2</i>
GO:0006520	BP	Cellular amino acid metabolic process	95	<i>5</i>	<i>7</i>	<i>-2</i>
GO:0009126	BP	Purine nucleoside monophosphate metabolic process	35	16	18	-2
GO:0034220	BP	Ion transmembrane transport	20	11	13	-2
GO:0022804	MF	Active transmembrane transporter activity	102	10	14	-4
GO:0006139	BP	Nucleobase-containing compound metabolic process	507	<i>34</i>	<i>39</i>	<i>-5</i>
GO:0010556	BP	Regulation of macromolecule biosynthetic process	169	<i>20</i>	<i>25</i>	<i>-5</i>
GO:0034645	BP	Cellular macromolecule biosynthetic process	313	<i>25</i>	<i>33</i>	<i>-8</i>

BP, biological process; MF, molecular function.

The early stationary phase cultures were treated by 5 μ M iPR or equal volume of DMSO (mock). DEGs were grouped into two data sets: light-regulated in the presence of cytokinin (CK) and light-regulated control (C). Selected GO terms at level 5 or higher were sorted according to the differential distribution of either up-regulated DEGs (shown in bold, adjusted $P < 0.05$) or down-regulated DEGs (shown in italics, adjusted $P < 0.05$) in both groups; total number of genes in *Nostoc* sp. PCC 7120 genome in each selected GO category is shown (total no.); Δ_{CK-C} shows the number of DEGs that were differently regulated between CK group and control group of genes.



N-terminus. Interestingly, these domains are present in histidine kinase cytokinin receptors in higher plants (Heyl and Schmölling 2003), with the REC domain located at the C-terminus. Similarly, REC domain can also be found near the C-terminus of cytokinin response regulators.

Other two-component histidine kinases in the list show more elaborate domain architecture. Two genes, *abr3170* and *cyaC*, both specific only for the CK group, encode proteins with GGDEF diguanylate cyclase domain (pfam00990) and AcyC adenylate cyclase domain (COG2114), respectively. *Nostoc cyaC* again shows unusual domain architecture starting with a REC domain followed by two GAF domains (pfam 01590), HisKA domain, HATPase domain, and another REC domain to finish with the adenylate cyclase domain. Importantly, adenylate cyclase AcrA, a cyclase with the same domain architecture

as *cyaC*, was previously described in *Dictyostelium discoideum* as a cytokinin-responsive element necessary for initiation of sporulation (Anjard and Loomis 2008).

Several other two-component histidine kinases with GO:0000155 contain repeated PAS domains (pfam 00989) located at the N-terminal portion of the protein that were found to act as sensors for light and oxygen in signal transduction. This is the case of *abr3170* mentioned above or *all0824*, *abr2137*, and *all2875*. The latter gene encodes a large protein with a complex protein architecture: it contains a N-terminal CHASE (cyclases/histidine kinases-associated sensing extracellular) domain (pfam 03924), which may represent a cytokinin sensing domain in parallel with plant histidine kinase receptors, followed by four PAS domains, GAF domain, HisKA domain, HATPase domain, and two REC domains.

TABLE 3. Distribution of differentially expressed genes in GO:0000155 (phosphorelay sensor kinase activity) between cytokinin-treated group (CK) and control group (C).

Protein ID	Gene	Description	Log2 fold change	
			CK	C
BAB76888	alr5189	Two-component sensor histidine kinase	2.4	1.7
BAB74574	all2875	Histidine kinase	2.0	1.9
BAB74736	alr3037	Two-component sensor histidine kinase	1.7	NA
BAB73188	alr1231	Two-component hybrid sensor and regulator	1.4	NA
BAB73613	all1914	Histidine kinase	1.3	1.4
BAB74820	alr3121	Two-component hybrid sensor and regulator	1.3	NA
BAB74869	alr3170	Alr3170 protein	1.3	NA
BAB74974	all3275	Two-component hybrid sensor and regulator	1.0	NA
BAB73665	alr1966	Two-component sensor histidine kinase	0.8	0.8
BAB76195	hepK	Two-component system sensory histidine kinase	0.8	NA
BAB73836	alr3137	Two-component sensor histidine kinase	0.7	NA
BAB73503	all1804	Two-component hybrid sensor and regulator	0.7	NA
BAB74271	alr2572	Two-component sensor histidine kinase	NA	0.3
BAB75684	all3985	Histidine kinase	NA	-1.1
BAB73265	alr1308	Two-component sensor histidine kinase	-0.6	-1.0
BAB76662	cyuC	Adenylate cyclase carrying two-component hybrid sensor and regulator domains	-0.6	NA
BAB72386	alr0428	Two-component sensor histidine kinase	-0.9	-1.1
BAB75466	all3767	Two-component sensor histidine kinase	-1.0	-1.3
BAB74858	alr3159	Two-component hybrid sensor and regulator	-1.8	-1.9
BAB72781	all0824	Two-component hybrid sensor and regulator	-2.2	NA
BAB77991	all1625	Serine/threonine kinase with two-component sensor domain	-2.3	NA
BAB75464	all3765	Two-component hybrid sensor and regulator	-2.5	-2.7
BAB74856	aphA	Cyanobacterial phytochrome A	-2.8	-2.8
BAB75796	all4097	Two-component hybrid sensor and regulator	-3.0	-2.2
BAB72782	all0825	Two-component sensor histidine kinase	-3.3	-3.5
BAB72281	all0323	Serine/threonine kinase with two-component sensor domain	-4.0	-3.2
BAB72857	alr0900	Serine/threonine kinase with two-component sensor domain	-4.0	-3.3

NA, not significantly affected.

Gene expression values were calculated as log2-ratios of the signals for samples collected during light period relative to samples collected during dark period, with addition of cytokinin (CK) or mock treated by DMSO (C).

The combination of light-sensitive PAS domain with ligand-binding CHASE domain is rather unusual and evidently differs from the domain organization present in cytokinin HK receptors of land plants.

Sequence homology of *Nostoc* CHASE domain was low compared to *Arabidopsis* and other known CHASE domains, but recent findings indicated that some of the highly conserved residues within the CHASE domain of land plants were not essential for ligand-binding (Gruhn et al. 2014). Since *all2875* is the only histidine kinase with CHASE domain among the affected DEGs, we expressed protein encoded by *all2875* in *E. coli* and tested it for its ligand binding ability in a cytokinin-binding assay with radiolabeled tZ. As shown in Figure S1 in the Supporting Information, iP and to lesser extent tZ, used as ligand competitors, bound to the CHASE domain in a dose-dependent manner. However, activation of signal transduction by any of the cytokinin ligands tested (tZ, iP, cZ, DHZ, and discadenine) was not observed in a receptor activation assay (Suzuki et al. 2001), which suggests that *all2875* was not compatible with the phosphorelay pathway in the *E. coli* strain KMI001 previously used for AHK receptor screenings (Spíchal et al. 2004) and other in vivo assays will be

necessary to confirm its cytokinin downstream signaling properties.

CONCLUSIONS

The screening of endogenous cytokinins and expression of genes involved in cytokinin biosynthesis in *Nostoc* sp. PCC 7120 showed that cytokinin biosynthesis is activated during the dark period of growth leading to enhanced cytokinin content after the start of light period. Although the proteins involved in cytokinin metabolism in *Nostoc* and cyanobacteria in general are for the most part unknown, the spectrum of detected cytokinin metabolites and their variations over the time suggest that *Nostoc* metabolizes cytokinins in a manner similar to and yet different from plants. In addition, cytokinin in conjunction with light affects expression of a number of genes related to signal transduction, including two-component sensor histidine kinases and two-component hybrid sensors and regulators. Some of the signaling components share on the protein level many similarities with cytokinin signaling components found in higher plants. Domain organization of these *Nostoc* signaling components is, however, very complex, and several domains

typical for bacterial two-component systems were identified. From the evolutionary perspective, *Nostoc* and other cyanobacteria may represent an interesting model for studies on development of the cytokinin signaling.

The authors acknowledge Petr Galuszka for inspiring discussions, Jaromír Kábrt for technical assistance with protein purification, and Hana Martínková for help with cytokinin analyses. This study was supported by research grant P501/12/0161 from the Czech Science Foundation and by grant LO1204 from the National Program of Sustainability I from the Ministry of Education, Youth and Sports, Czech Republic.

- Anders, S., Pyl, P. T. & Huber, W. 2014. HTSeq – A Python framework to work with high-throughput sequencing data. *Bioinformatics* 31:166–9.
- Anjard, C. & Loomis, W. F. 2008. Cytokinins induce sporulation in *Dictyostelium*. *Development* 135:819–27.
- Antoniadi, I., Plačková, L., Simonovik, B., Doležal, K., Turnbull, C., Ljung, K. & Novák, O. 2015. Cell-type specific cytokinin distribution within the *Arabidopsis* primary root apex. *Plant Cell* 27:1955–67.
- Ashburner, M., Ball, C. A., Blake, J. A., Botstein, D., Butler, H., Cherry, J. M., Davis, A. P. et al. 2000. Gene ontology: tool for the unification of biology. *Nat. Genet.* 25:25–9.
- Barnes, F. M., Cheng, L. T. & Gray, J. S. 1980. Biosynthesis of cytokinins by potato cell cultures. *Phytochemistry* 19:409–12.
- Bradford, M. M. 1976. A rapid and sensitive method for the quantitation of microgram quantities of protein utilizing the principle of protein-dye binding. *Anal. Biochem.* 72:248–54.
- Chanclud, E. & Morel, J. B. 2016. Plant hormones: a fungal point of view. *Mol. Plant Pathol.* 17:1289–97.
- Conesa, A., Götz, S., García-Gómez, J. M., Terol, J., Talón, M. & Robles, M. 2005. Blast2GO: a universal tool for annotation, visualization and analysis in functional genomics research. *Bioinformatics* 21:3674–6.
- Dobrev, P. I. & Kamínek, M. 2002. Fast and efficient separation of cytokinins from auxin and abscisic acid and their purification using mixed-mode solid-phase extraction. *J. Chromatogr. A* 950:21–9.
- Faiss, M., Zalubilová, J., Strnad, M. & Schmülling, T. 1997. Conditional transgenic expression of the *ipt* gene indicates a function for cytokinins in paracrine signaling in whole tobacco plants. *Plant J.* 12:401–15.
- Fiore, M. F., Moon, D. H., Tsai, S. M., Lee, H. & Trevors, J. T. 2000. Miniprep DNA isolation from unicellular and filamentous cyanobacteria. *J. Microbiol. Methods* 39:159–69.
- Frébortová, J., Greplová, M., Seidl, M. F., Heyl, A. & Frébort, I. 2015. Biochemical characterization of putative adenylate dimethylallyltransferase and cytokinin dehydrogenase from *Nostoc* sp. PCC 7120. *PLoS ONE* 10:e0138468.
- Gajdošová, S., Spíchal, L., Kamínek, M., Hoyerová, K., Novák, O., Dobrev, P. I., Galuszka, P. et al. 2011. Distribution, biological activities, metabolism, and the conceivable function of *cis*-zeatin-type cytokinins in plants. *J. Exp. Bot.* 62:2827–40.
- Gehrke, C. W., Kuo, K. C., McCune, R. A. & Gerhard, K. O. 1982. Quantitative enzymatic hydrolysis of tRNAs. Reversed-phase high-performance liquid chromatography of tRNA nucleosides. *J. Chromatogr.* 230:297–308.
- Gruhn, N., Halawa, M., Snel, B., Seidl, M. F. & Heyl, A. 2014. A subfamily of putative cytokinin receptors is revealed by an analysis of the evolution of the two-component signaling system of plants. *Plant Physiol.* 165:227–37.
- Heyl, A. & Schmülling, T. 2003. Cytokinin signal perception and transduction. *Curr. Opin. Plant Biol.* 6:480–8.
- Hinsch, J., Vrabka, J., Oeser, B., Novák, O., Galuszka, P. & Tudzynski, P. 2015. De novo biosynthesis of cytokinins in the biotrophic fungus *Claviceps purpurea*. *Environ. Microbiol.* 17:2935–51.
- Hussain, A., Hamayun, M. & Shah, S. T. 2013. Root colonization and phyto-stimulation by phytohormones producing entophytic *Nostoc* sp. AH-12. *Curr. Microbiol.* 67:624–30.
- Hussain, A., Krischke, M., Roitsch, T. & Hasnain, S. 2010. Rapid determination of cytokinins and auxin in cyanobacteria. *Curr. Microbiol.* 61:361–9.
- Kakimoto, T. 2003. Biosynthesis of cytokinins. *J. Plant. Res.* 116:233–9.
- Kapoor, K. & Sharma, V. K. 1981. Effect of growth-promoting chemicals on growth, nitrogen fixation and heterocyst frequency in blue-green alga. *Z. Allg. Mikrobiol.* 21:305–11.
- Kim, D., Perte, G., Trapnell, C., Pimentel, H., Kelley, R. & Salzberg, S. L. 2013. TopHat2: accurate alignment of transcriptomes in the presence of insertions, deletions and gene fusions. *Genome Biol.* 14:R36.
- Koenig, R. L., Morris, R. O. & Polacco, J. C. 2002. tRNA is the source of low-level trans-zeatin production in *Methylobacterium* spp. *J. Bacteriol.* 184:1832–42.
- Kurakawa, T., Ueda, N., Maekawa, M., Kobayashi, K., Kojima, M., Nagato, Y., Sakakibara, H. & Kyoizuka, J. 2007. Direct control of shoot meristem activity by a cytokinin-activating enzyme. *Nature* 445:652–5.
- Love, M. I., Huber, W. & Anders, S. 2014. Moderated estimation of fold change and dispersion for RNA-Seq data with DESeq2. *Genome Biol.* 15:550.
- Lu, Y., Tarkowská, D., Turečková, V., Luo, T., Xin, Y., Li, J., Wang, Q., Jiao, N., Strnad, M. & Xu, J. 2014. Antagonistic roles of abscisic acid and cytokinin during response to nitrogen depletion in oleaginous microalga *Nannochloropsis oceanica* expand the evolutionary breadth of phytohormone function. *Plant J.* 80:52–68.
- Lu, Y. & Xu, J. 2015. Phytohormones in microalgae: a new opportunity for microalgal biotechnology? *Trends Plant Sci.* 20:273–82.
- Maass, H. & Klämbt, D. 1981. On the biogenesis of cytokinins in roots of *Phaseolus vulgaris*. *Planta* 151:353–8.
- Miller, C. O., Skoog, F., Okumura, F. S., von Saltza, M. H. & Strong, F. M. 1955. Structure and synthesis of kinetin. *J. Am. Chem. Soc.* 78:2662–3.
- Miri, M., Janakirama, P., Held, M., Ross, L. & Szczygłowski, K. 2016. Into the root: how cytokinin controls rhizobial infection. *Trends Plant Sci.* 21:178–86.
- Miyawaki, K., Tarkowski, P., Matsumoto-Kitano, M., Kato, T., Sato, S., Tarkowska, D., Tabata, S., Sandberg, G. & Kakimoto, T. 2006. Roles of *Arabidopsis* ATP/ADP isopentenyltransferases and tRNA isopentenyltransferases in cytokinin biosynthesis. *Proc. Natl. Acad. Sci. USA* 103:16598–603.
- Mok, D. W. & Mok, M. C. 2001. Cytokinin metabolism and action. *Annu. Rev. Plant Phys. Plant Mol. Biol.* 52:89–118.
- Morrison, E. N., Knowles, S., Hayward, A., Thorn, R. G., Saville, B. J. & Emery, R. J. N. 2015. Detection of phytohormones in temperate forest fungi predicts consistent abscisic acid production and a common pathway for cytokinin biosynthesis. *Mycologia* 107:245–57.
- Nordström, A., Tarkowski, P., Tarkowská, D., Norbaek, R., Astot, C., Doležal, K. & Sandberg, G. 2004. Auxin regulation of cytokinin biosynthesis in *Arabidopsis thaliana*: a factor of potential importance for auxin–cytokinin-regulated development. *Proc. Natl. Acad. Sci. USA* 101:8039–44.
- Ördög, V., Stirk, W. A., van Staden, J., Novák, O. & Strnad, M. 2004. Endogenous cytokinins in three genera of microalgae from the chlorophyta. *J. Phycol.* 40:88–95.
- Persson, B. C. & Björk, G. R. 1993. Isolation of the gene (*miaE*) encoding the hydroxylase involved in the synthesis of 2-methylthio-*cis*-ribozeatin in tRNA of *Salmonella typhimurium* and characterization of mutants. *J. Bacteriol.* 175:7776–85.
- Persson, B. C., Esberg, B., Ólafsson, O. & Björk, G. R. 1994. Synthesis and function of isopentenyl adenosine derivatives in tRNA. *Biochimie* 76:1152–60.
- Pertry, I., Václavíková, K., Gemrotová, M., Spíchal, L., Galuszka, P., Depuydt, S., Temmerman, W. et al. 2010. *Rhodococcus fascians* impacts plant development through the dynamic Fas-

- mediated production of a cytokinin mix. *Mol. Plant Microbe Interact.* 23:1164–74.
- Pierrel, F., Douki, T., Fontecave, M. & Atta, M. 2004. MiaB protein is a bifunctional radical-S-adenosylmethionine enzyme involved in thiolation and methylation of tRNA. *J. Biol. Chem.* 279:47555–63.
- Pinto, F., Pacheco, C. C., Ferreira, D., Moradas-Ferreira, P. & Tamagnini, P. 2012. Selection of suitable reference genes for RT-qPCR analyses in cyanobacteria. *PLoS ONE* 7:e34983.
- R Development Core Team 2008. *R: A Language and Environment for Statistical Computing*. R Foundation for Statistical Computing, Vienna.
- Radhika, V., Ueda, N., Tsuboi, Y., Kojima, M., Kikuchi, J., Kudo, T. & Sakakibara, H. 2015. Methylated cytokinins from the phytopathogen *Rhodococcus fascians* mimic plant hormone activity. *Plant Physiol.* 169:1118–26.
- Radwanski, E. R. & Last, R. L. 1995. Tryptophan biosynthesis and metabolism: biochemical and molecular genetics. *Plant Cell* 7:921–34.
- Rippka, R., Neilson, A., Kunisawa, R. & Cohen-Bazire, G. 1971. Nitrogen fixation by unicellular blue-green algae. *Arch. Mikrobiol.* 76:341–8.
- Rittenberg, D. & Foster, L. 1940. A new procedure for quantitative analysis by isotope dilution, with application to the determination of amino acids and fatty acids. *J. Biol. Chem.* 133:727–44.
- Romanov, G. A., Spíchal, L., Lomin, S. N., Strnad, M. & Schmölling, T. 2005. A live cell hormone-binding assay on transgenic bacteria expressing a eukaryotic receptor protein. *Anal. Biochem.* 347:129–34.
- Sakakibara, H. 2006. Cytokinins: activity, biosynthesis, and translocation. *Annu. Rev. Plant Biol.* 57:431–9.
- Samanovic, M. I., Tu, S., Novák, O., Iyer, L. M., McAllister, F. E., Aravind, L., Gygi, S. P., Hubbard, S. R., Strnad, M. & Darwin, K. H. 2015. Proteasomal control of cytokinin synthesis protects *Mycobacterium tuberculosis* against nitric oxide. *Mol. Cell* 19:984–94.
- Selivankina, S. Y., Zubkova, N. K., Kupriyanova, E. V., Lyukevich, T. V., Kusnetsov, V. V., Los, D. A. & Kulaeva, O. N. 2006. Cyanobacteria respond to cytokinin. *Russ. J. Plant Physiol.* 53:751–5.
- Soederberg, T. & Poulter, D. C. 2000. *Escherichia coli* dimethylallyl diphosphate: tRNA dimethylallyltransferase: essential elements for recognition of tRNA substrates within the anticodon stem-loop. *Biochemistry* 39:6546–53.
- Spíchal, L., Rakova, N. Y., Riefler, M., Mizuno, T., Romanov, G. A., Strnad, M. & Schmölling, T. 2004. Two cytokinin receptors of *Arabidopsis thaliana*, CRE1/AHK4 and AHK3, differ in their ligand specificity in a bacterial assay. *Plant Cell Physiol.* 45:1299–305.
- Stirk, W. A., Novák, O., Strnad, M. & van Staden, J. 2003. Cytokinins in macroalgae. *Plant Growth Regul.* 41:13–24.
- Stirk, W. A., Václavíková, K., Novák, O., Gajdošová, S., Kotland, O., Motyka, V., Strnad, M. & van Staden, J. 2012. Involvement of cis-zeatin, dihydrozeatin, and aromatic cytokinins in germination and seedling establishment of maize, oats, and lucerne. *J. Plant Growth Regul.* 31:392–405.
- Stirk, W. A., van Staden, J., Novák, O., Doležal, K., Strnad, M., Dobrev, P. I., Sipos, G., Ördög, V. & Bálint, P. 2011. Changes in endogenous cytokinin concentrations in *Chlorella* (Chlorophyceae) in relation to light and the cell cycle. *J. Phycol.* 47:291–301.
- Suzuki, T., Miwa, K., Ishikawa, K., Yamada, H., Aiba, H. & Mizuno, T. 2001. The Arabidopsis sensor His-kinase, AHK4, can respond to cytokinins. *Plant Cell Physiol.* 42:107–13.
- Suzuki, T., Nakasato, K., Shapiro, S., Pomati, F. & Neilan, B. A. 2004. Effect of local anaesthetics on the growth of the cyanobacterium *Synechococcus leopoliensis*. *J. Appl. Phycol.* 16:145–52.
- Svačinová, J., Novák, O., Plačková, L., Lenobel, R., Holík, J., Strnad, M. & Doležal, K. 2012. A new approach for cytokinin isolation from Arabidopsis tissues using miniaturized purification: pipette tip solid-phase extraction. *Plant Methods* 8:17.
- Takei, K., Yamaya, T. & Sakakibara, H. 2004. Arabidopsis CYP735A1 and CYP735A2 encode cytokinin hydroxylases that catalyze the biosynthesis of trans-zeatin. *J. Biol. Chem.* 279:41866–72.
- Tanaka, M., Takei, K., Kojima, M., Sakakibara, H. & Mori, H. 2006. Auxin controls local cytokinin biosynthesis in the nodal stem in apical dominance. *Plant J.* 45:1028–36.
- Tarkowski, P., Václavíková, K., Novák, O., Pertry, I., Hanuš, J., Whenham, R., Vereecke, D., Šebela, M. & Strnad, M. 2010. Analysis of 2-methylthioderivatives of isoprenoid cytokinins by liquid chromatography-tandem mass spectrometry. *Anal. Chim. Acta* 680:86–91.
- Tsavkelova, E. A., Klimova, S. Y., Cherdyntseva, T. A. & Netrusov, A. I. 2006. Microbial producers of plant growth stimulators and their practical use: a review. *Appl. Biochem. Microbiol.* 42:117–26.
- Yates, A., Akanni, W., Amode, M. R., Barrell, D., Billis, K., Carvalho-Silva, D., Cummins, C. et al. 2016. Ensembl 2016. *Nucleic Acids Res.* 44:D710–6.
- Žizková, E., Kubeš, M., Dobrev, P. I., Příbyl, P., Šimura, J., Zahajská, L., Závěská Drábková, L., Novák, O. & Motyka, V. 2017. Control of cytokinin and auxin homeostasis in cyanobacteria and algae. *Ann. Bot.* 119:151–66. <https://doi.org/10.1093/aob/mcw194>.

Supporting Information

Additional Supporting Information may be found in the online version of this article at the publisher's web site:

Figure S1. [³H] tZ-specific binding to all2875 expressed in *Escherichia coli*. Radioactivity of the retained [³H] tZ was measured after 30 min incubation of transformed bacteria with radiolabeled tZ and varying concentrations of unlabeled tZ or iP.

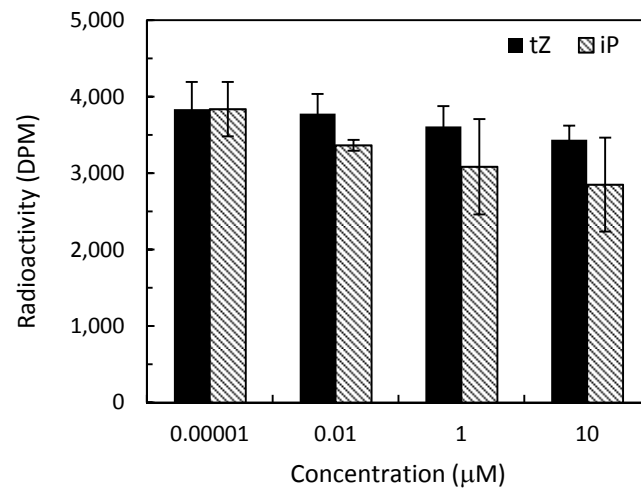


Figure S1. [^3H] tZ specific binding to all2875 expressed in *E. coli*. Radioactivity of the retained [^3H] tZ was measured after 30 min incubation of transformed bacteria with radiolabeled tZ and varying concentrations of unlabeled tZ or iP.

Supplement IV

Šimura, J., Spíchal, L., Adamec, L., Pěňčík, A., Rolčík, J., Novák, O., & Strnad, M. (2016). Cytokinin, auxin and physiological polarity in the aquatic carnivorous plants *Aldrovanda vesiculosa* and *Utricularia australis*. *Annals of Botany*, *117*(6), 1037-1044.

Cytokinin, auxin and physiological polarity in the aquatic carnivorous plants *Aldrovanda vesiculosa* and *Utricularia australis*

Jan Šimura^{1,2}, Lukáš Spíchal^{1,2}, Lubomír Adamec³, Aleš Pěničák², Jakub Rolčík¹, Ondřej Novák¹ and
Miroslav Strnad^{1,*}

¹Laboratory of Growth Regulators, Centre of the Region Haná for Biotechnological and Agricultural Research, Institute of Experimental Botany AS CR and Faculty of Science of Palacký University, Šlechtitelů 27, CZ-78371 Olomouc, Czech Republic,

²Department of Chemical Biology and Genetics, Centre of the Region Haná for Biotechnological and Agricultural Research, Faculty of Science of Palacký University, Šlechtitelů 27, CZ-78371 Olomouc, Czech Republic and ³Institute of Botany of the Czech Academy of Sciences, Section of Plant Ecology, Dukelská 135, CZ-37982 Třeboň, Czech Republic

*For correspondence. E-mail miroslav.strnad@upol.cz

Received: 25 September 2015 Returned for revision: 2 November 2015 Accepted: 18 December 2015

- **Background and Aims** The typical rootless linear shoots of aquatic carnivorous plants exhibit clear, steep polarity associated with very rapid apical shoot growth. The aim of this study was to determine how auxin and cytokinin contents are related to polarity and shoot growth in such plants.
- **Methods** The main auxin and cytokinin metabolites in separated shoot segments and turions of two carnivorous plants, *Aldrovanda vesiculosa* and *Utricularia australis*, were analysed using ultra-high-performance liquid chromatography coupled with triple quad mass spectrometry.
- **Key Results** In both species, only isoprenoid cytokinins were identified. Zeatin cytokinins predominated in the apical parts, with their concentrations decreasing basipetally, and the *trans* isomer predominated in *A. vesiculosa* whereas the *cis* form was more abundant in *U. australis*. Isopentenyladenine-type cytokinins, in contrast, increased basipetally. Conjugated cytokinin metabolites, the *O*-glucosides, were present at high concentrations in *A. vesiculosa* but only in minute amounts in *U. australis*. *N*⁹-glucoside forms were detected only in *U. australis*, with isopentenyladenine-9-glucoside (iP9G) being most abundant. In addition to free indole-3-acetic acid (IAA), indole-3-acetamide (IAM), IAA-aspartate (IAAsp), IAA-glutamate (IAGlu) and IAA-glycine (IAGly) conjugates were identified.
- **Conclusions** Both species show common trends in auxin and cytokinin levels, the apical localization of the cytokinin biosynthesis and basipetal change in the ratio of active cytokinins to auxin, in favour of auxin. However, our detailed study of cytokinin metabolic profiles also revealed that both species developed different regulatory mechanisms of active cytokinin content; on the level of their degradation, in *U. australis*, or in the biosynthesis itself, in the case of *A. vesiculosa*. Results indicate that the rapid turnover of these signalling molecules along the shoots is essential for maintaining the dynamic balance between the rapid polar growth and development of the apical parts and senescence of the older, basal parts of the shoots.

Key words: Auxin, *Aldrovanda vesiculosa*, cytokinin, growth polarity, phytohormones, rootless aquatic plants, *Utricularia australis*.

INTRODUCTION

In plants, developmental and physiological processes are controlled by signalling molecules known as phytohormones. The plant hormones cytokinins and auxins play regulatory roles in many of these processes, and the nature and timing of a plant's responses to environmental and endogenous factors are strongly dependent on the levels of these and/or other phytohormones and the relative amounts of the different hormones (Tarkowski *et al.*, 2014).

Natural cytokinins are *N*⁶-substituted adenine derivatives with either isoprenoid or aromatic side-chains. In higher plants, the predominant cytokinins are the isoprenoid ones – the *N*⁶-isopentenyladenine (iP) type and *cis/trans*-zeatin (*tZ*, *cZ*) types with unsaturated aliphatic side chains, and the dihydrozeatin (DHZ) type with saturated aliphatic side chains. Variations in the structural substituents on the adenine moieties of cytokinins include nucleotide forms, ribosides and free bases, along with a

wide range of other conjugates. It is widely believed that it is the cytokinin free bases that are the bioactive cytokinins (Sakakibara, 2005). However, in cytokinin receptor binding assays, either *in vitro* or in *in vivo* heterologous expression systems, some ribosides also display high affinity for cytokinin receptors (Spíchal, 2012). These phytohormones are involved in the regulation of various processes in plant growth and development, such as shoot differentiation, apical dominance, leaf senescence, nutrient distribution in tissues and plastid differentiation (Sakakibara, 2005; Spíchal, 2012). Indole-3-acetic acid (IAA), also referred to as auxin, is another important phytohormone, which plays crucial roles in virtually every aspect of the regulation of plant growth and development, including cell division and elongation (Perrot-Rechenmann, 2010), gravitropism and phototropism, and phyllotaxis (Kuhlemeier and Reinhardt, 2001; Vernoux *et al.*, 2000), and also in the establishment of apical-basal polarity in individual cells, organs and the whole plant (Tanaka *et al.*, 2006; Nakamura *et al.*, 2012).

Aquatic carnivorous plants comprise the species *Aldrovanda vesiculosa* (Droseraceae), which has snapping traps, and about 50 species of the genus *Utricularia* (Lentibulariaceae) with suction traps (Juniper *et al.*, 1989; Taylor, 1989). They usually grow in shallow, standing, nutrient-poor dystrophic waters (Adamec, 1997a; Guisande *et al.*, 2007). Most species of aquatic carnivorous plants have linear, poorly branched shoots and are rootless. They usually exhibit very rapid apical shoot growth (1–4 leaf nodes d^{-1}) and high relative growth rates, while their basal shoot segments decay at the same rate as new shoots are produced (Friday, 1989; Adamec, 2000, 2008a, 2009; Englund and Harms, 2003; Adamec and Kovářová, 2006). They show adaptations associated with very rapid growth, including mineral nutrient gain from carnivory, efficient N and P reutilization (recycling) from senescent shoots, a very high net photosynthetic rate, a high affinity for mineral nutrient uptake from the ambient water, and, in *Utricularia* spp., possibly also the formation of commensal associations in the traps (Kamiński, 1987; Adamec, 1997b, 2000, 2008b, 2013, 2014; Richards, 2001; Englund and Harms, 2003; Sirová *et al.*, 2009). *Aldrovanda vesiculosa* and *Utricularia australis* are perennial plants with linear shoots that form turions (winter buds), modified shoot apices that serve as vegetative dormant storage organs, enabling the plants to survive under ice over the winter (Adamec, 1999, 2010). Both species have often been used in ecophysiological studies describing the phenomenon of physiological polarity in their shoots, from perspectives including allocation of mineral nutrients and carbohydrate content, net photosynthetic rate, chlorophyll content, allocation of organic carbon derived from carnivory, and studies on trap function (Fabian-Galan and Salageanu, 1968; Kamiński, 1987; Kosiba, 1992a, b; Adamec, 1997a, b, 2000, 2008a, b, 2009, 2011a, 2013; Adamec and Kovářová, 2006). However, no direct phytohormonal screening has hitherto been carried out in aquatic carnivorous plants.

Hence, the aim of the work presented here was to determine levels of cytokinin and auxins and their localization in polar segments of different ages in linear shoots of two aquatic carnivorous plants, *A. vesiculosa* and *U. australis*, which exhibit steep gradients of physiological polarity, and to infer where, in these rootless plants, cytokinins and auxins may be synthesized. For comparison with growing shoots, phytohormone contents were also determined in dormant turions of these species. The levels and distribution of cytokinin and IAA derivatives are interpreted in terms of their possible roles in maintaining physiological and growth polarity.

MATERIALS AND METHODS

Plant material

Around 130 adult plants of *Aldrovanda vesiculosa* (originating from Poland) were collected from the dystrophic (humic) fen lake Karštejn in the Třeboň Basin Biosphere Reserve in South Bohemia, Czech Republic, on 26 July 2008 (Adamec and Kovářová, 2006). The plants were 7–15 cm long with 12–15 mature leaf nodes, and usually branched. They were immediately transferred, without water, to the laboratory for processing. The plants were thoroughly washed in tap water and all larger items

of captured prey were taken out of their traps. All branches were removed. The main shoots were separated into four segments for phytohormone analyses: apices with immature traps; 1st–4th leaf nodes, representing the youngest functional traps; 7th–9th leaf nodes, representing medium-aged traps; and old segments with still-living leaf nodes, which were separated from the medium-aged segments by at least two leaf nodes. Sixty adult plants of *Utricularia australis* were collected from the dystrophic inlet of the Ruda fishpond in the same region as above on 28 July 2008 (Adamec, 2011b). The plants were 45–90 cm long, branched, but non-flowering. After rapid transfer to the laboratory, they were thoroughly washed and deprived of all attached macroorganisms, and their branches were removed. The fact that prey remnants were not removed from the traps should not influence the results. The main shoots were separated, in a similar manner to those of *A. vesiculosa*, into four segments for phytohormone analyses: apices with immature traps (here denoted ‘apices’); 1st–6th leaf nodes, representing the youngest functional traps (‘young’); 21st–26th leaf nodes, representing medium-aged traps (‘medium-aged’); and old segments with still-living leaf nodes but mostly lacking traps (‘old’). Thirty mature turions of *A. vesiculosa*, 6–7 mm long, and 12 mature turions of *U. australis*, 8–11 mm long, were collected from the sites on 15 October 2008. They were washed in tap water and all dead leaves were removed from their surfaces. All separated plant material was stored at $-80\text{ }^{\circ}\text{C}$ for some weeks prior to lyophilization. The freeze-dried biomass of each shoot segment or turion was 0.5–1.0 g. Lyophilized samples were homogenized under liquid nitrogen and split into duplicates for cytokinin analysis and auxin analysis, each replicate containing 100 mg of dry weight (d.w.) material.

Cytokinin analysis

The procedure for cytokinin purification was based on the method described by Novák *et al.* (2003), including modifications described by Novák *et al.* (2008). Isotope-labelled internal standards [$^{13}\text{C}_5$]tZ, [$^2\text{H}_5$]tZR, [$^2\text{H}_5$]tZ9G, [$^2\text{H}_5$]tZOG, [$^2\text{H}_5$]tZROG, [$^2\text{H}_5$]tZRMP, [$^{13}\text{C}_5$]cZ, [$^2\text{H}_3$]DHZ, [$^2\text{H}_3$]DHZR, [$^2\text{H}_3$]DHZ9G, [$^2\text{H}_7$]DHZOG, [$^2\text{H}_3$]DHZRMP, [$^2\text{H}_6$]iP, [$^2\text{H}_6$]iPR, [$^2\text{H}_6$]iP9G, [$^2\text{H}_6$]iPRMP, [$^2\text{H}_7$]BA, [$^2\text{H}_7$]BAR, [$^2\text{H}_7$]BA9G, [$^2\text{H}_7$]BARMP, [$^{15}\text{N}_4$]mT and [$^{15}\text{N}_4$]oT (Olchemim Ltd, Czech Republic) were added, each at 1 pmol per sample, to validate the accuracy of determination (Novák *et al.*, 2008). The samples were purified using a combination of a cation (SCX cartridge) exchanger, an anion (DEAE-Sephadex-C18 cartridge) exchanger and immunoaffinity chromatography (IAC) based on monoclonal antibodies specific for a wide range of cytokinins (Novák *et al.*, 2003). The eluates from the IAC columns were evaporated to dryness and dissolved in 20 μL of the mobile phase used for quantitative analysis. The samples were analysed by ultra-high-performance liquid chromatography (UHPLC; AcquityUPLC[®] System; Waters, Milford, MA, USA) coupled to a triple quadrupole mass spectrometer (MS/MS) equipped with an electrospray interface (Quattro Micro API[™]; Waters, Manchester, UK). The purified samples were injected onto a C18 reversed-phase column (BEH C18; 1.7 μm ; 2.1 \times 50 mm; Waters). The column was eluted with a linear gradient (0 min, 10 % B; 0–8 min, 50 % B; flow rate 0.25 ml min^{-1} ; column temperature 40 $^{\circ}\text{C}$) of 15 mM ammonium formate (pH

4.0, A) and methanol (B). Quantification was achieved by multiple reaction monitoring (MRM) of $[M+H]^+$ and the appropriate product ion. For selective MRM experiments, the optimal conditions, dwell time, cone voltage and collision energy in the collision cell corresponding to the exact diagnostic transition were optimized for each cytokinin compound (Novák *et al.*, 2008). Quantification was performed with MassLynx software using a standard isotope dilution method. The ratio of each endogenous cytokinin to an appropriate labelled standard was determined and used to quantify the level of endogenous compounds in the original extract, according to the known quantity of internal standard added (Novák *et al.*, 2003).

Auxin analysis

Indole-3-acetic acid and its amide conjugates were analysed by a method described by Pěňčík *et al.* (2009). The compounds of interest were extracted with phosphate buffer, pre-purified by C8-based solid-phase extraction and further purified by an auxin-specific immunoaffinity extraction. Final analysis was done using UHPLC–MS/MS detection. The separation was performed on an Acquity UPLC™ System (Waters) equipped with a Symmetry C18 column (5 μ m, 2.1 \times 150 mm; Waters) at 30 °C by gradient elution with a flow rate of 0.25 ml min⁻¹. The mobile phase consisted of 10 mM aqueous formic acid and methanol containing 10 mM formic acid. The content of methanol was held at 25 % during the first minute then increased linearly to 38 % (at 7 min), 40 % (12 min), 58 % (15 min) and 60 % (26 min). The effluent was introduced into the ion source of a Quattro Micro API triple quadrupole mass spectrometer (Waters). The ratio of endogenous IAA and IAA conjugates to appropriate labelled standards (10 pmol per sample of [²H₅]IAA, [¹⁵N,²H₅]IAM, [¹⁵N,²H₅]IAAla, [¹⁵N,²H₅]IAAsp, [¹⁵N,²H₅]IAGlu, [¹⁵N,²H₅]IAGly, [¹⁵N,²H₅]IALeu, [¹⁵N,²H₅]IAPhe, and [¹⁵N,²H₅]IAVal) was determined and used to quantify the levels of endogenous compounds in the original extract (Pěňčík *et al.*, 2009).

RESULTS

Cytokinins

In both species, only isoprenoid cytokinins, the zeatin types (*cZ*, *tZ*, DHZ) and the *iP* type (Fig. 1A, B), were identified (Supplementary Data Tables S1 and S2). The zeatin-type cytokinins were dominant in the apical parts, with concentrations decreasing basipetally, whereas the *iP*-type cytokinins increased in the same direction (Fig. 1A, B). The cytokinin metabolites mainly responsible for these trends were cytokinin biosynthetic precursors, the ribotides, with the highest concentrations of both zeatin ribotides, *cis*-zeatin-9-riboside-5'-monophosphate (*cZR5'MP*) and *trans*-zeatin-9-riboside-5'-monophosphate (*tZR5'MP*), found in the apices, and the highest amount of *N*⁶-isopentenyladenosine-5'-monophosphate (*iPR5'MP*) in the medium-aged and old segments (Fig. 2A, B). Interestingly, whereas in *A. vesiculosa* the dominant zeatin ribotide was the *trans* isomer (*tZR5'MP*; Fig. 2B), in *U. australis* it was the *cis* form (*cZR5'MP*; Fig. 2B). Conjugated cytokinin metabolites, the *O*-glucosides, were present at higher concentrations in

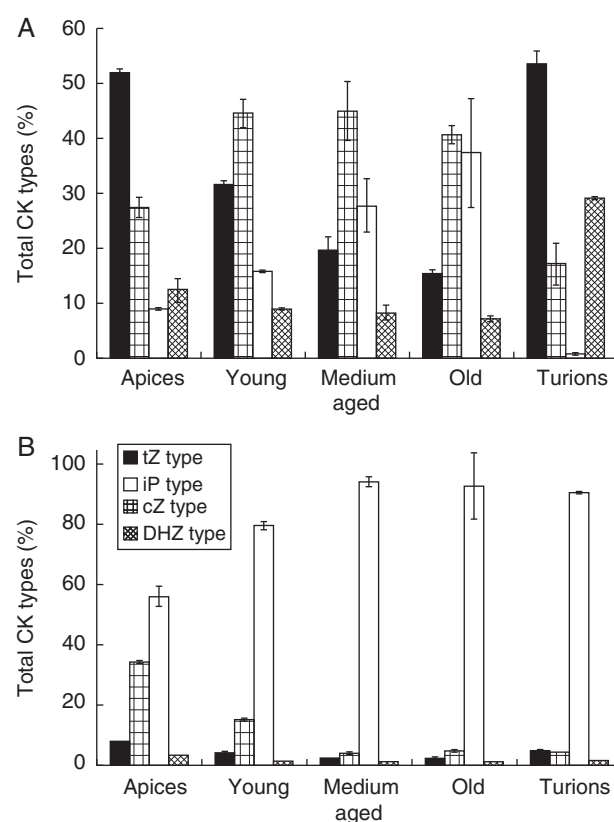


FIG. 1. Percentages of different cytokinin (CK) types in *Aldrovanda vesiculosa* (A) and *Utricularia australis* (B) shoot segments and turions, grouped according to the structure of the *N*⁶-aliphatic side chain: *trans*-zeatin (*tZ*), *cis*-zeatin (*cZ*), dihydrozeatin (DHZ) and isopentenyladenine (*iP*). Error bars represent the standard deviation.

A. vesiculosa, where they stayed at a fairly similar level throughout the whole plant. On the other hand, in *U. australis* the *O*-conjugated cytokinins were found in only minute concentrations. The *N*⁹-glucoside forms were detected only in *U. australis*, in which *N*⁶-isopentenyladenine-9-glucoside (*iP9G*) was found to be the most abundant metabolite (Fig. 3B) (Supplementary Data Table S2).

Turion samples from these species differed greatly in cytokinin content. In *U. australis* the *N*⁹-glucosides, specifically *iP9G*, were the predominant cytokinin metabolites (Fig. 3B, Supplementary Data Table S2). Other forms of cytokinin were present only in minute concentrations. In *A. vesiculosa* turions, the cytokinin spectrum was much broader, including *O*-glucosides and also ribotides. In comparison with *U. australis* turions, in *A. vesiculosa* higher amounts of free bases and ribosides, especially the *tZ* type, were found. Interestingly, no *N*⁹-glucosides were detected in *A. vesiculosa* turions (Fig. 3A), (Supplementary Data Table S1).

Auxins

In *A. vesiculosa* the most abundant metabolite from the auxin family was the amide conjugate with L-aspartic acid (IAAsp), which exceeded the concentration of free IAA, particularly in

the apical part (Supplementary Data Table S3). IAA stayed at the same level of concentration throughout the whole plant (Fig. 4A). In *A. vesiculosa* the highest concentration of indole-3-acetamide (IAM; IAA precursor) was found in the medium-aged and old segments; however, its content showed

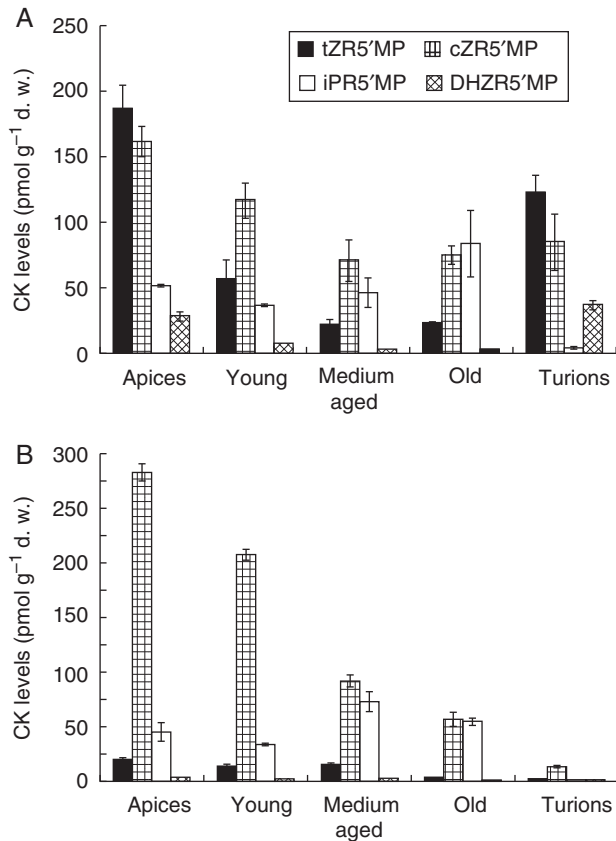


FIG. 2. Content (pmol g⁻¹ d.w.) of cytokinin (CK) biosynthetic precursors, the ribotides (R5'MP), in *Aldrovanda vesiculosa* (A) and *Utricularia australis* (B) shoot segments and turions presented according to the structure of the N⁶-aliphatic side chain: *trans*-zeatin (*tZ*), *cis*-zeatin (*cZ*), dihydrozeatin (DHZ), isopentenyladenine (iP). Error bars represent the standard deviation.

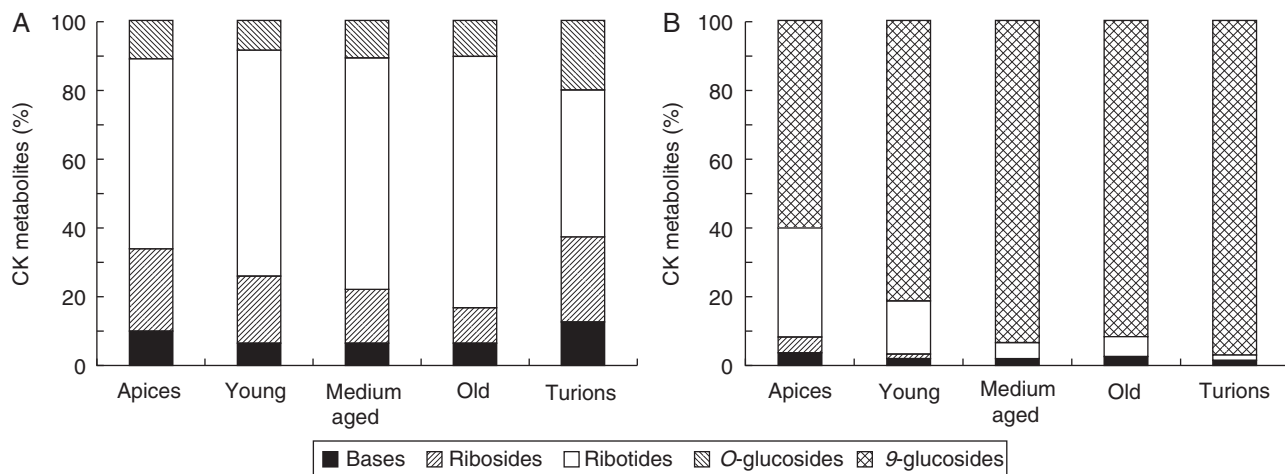


FIG. 3. Composition of cytokinin (CK) metabolites (expressed as percentage) in *Aldrovanda vesiculosa* (A) and *Utricularia australis* (B) shoot segments and turions.

no significant trend with respect to plant growth polarity. The amide conjugate with L-glycine (IAGly) was present only at minor levels. In *U. australis* the free IAA content increased basipetally, reaching a peak in the old segments (Fig. 4B). IAM and IAAsp predominated in the apex (Fig. 4B). The amide conjugate with L-glutamic acid (IAGlu) and IAGly were present only at low concentrations (Supplementary Data Table S4). No other amide conjugates with L-alanine, L-leucine, L-phenylalanine or L-valine (IAAla, IALeu, IAPhe and IAVal, respectively) were detected in *A. vesiculosa* or in *U. australis*.

Turions of both species showed high levels of free IAA, exceeding the levels of conjugated forms of IAA. In *U. australis*, IAM reached a level similar to that of free IAA, whereas in *A. vesiculosa* its content was lower compared with those of free IAA and IAAsp (Fig. 4A). The other two amide conjugates, IAGlu and IAGly, were present in both species only in minute concentrations or were not detected at all (Supplementary Data Tables S3 and S4).

DISCUSSION

In this study, we focused on the analysis of the levels and distribution of cytokinins and auxin in linear shoots of the rootless carnivorous plants *A. vesiculosa* and *U. australis*, which exhibit polar and very rapid linear growth. Plant growth and development are driven by both external environmental conditions and intrinsic growth regulators such as hormones. In this study we focused on two major phytohormone groups, the cytokinins and the auxins. Both groups can be biosynthesized in many, if not all, parts of the plant (Taiz and Zeiger, 2010). They can act as long-distance signalling substances as well as paracrine signals during plant development, and it is known that there is crosstalk between them. It has been reported that auxin regulates cytokinin levels and *vice versa* (Tanaka *et al.*, 2006). For example, it was observed that cytokinin-overproducing tobacco had reduced levels of IAA, whereas overproduction of IAA in the same species led to a reduction in cytokinin content (Palni *et al.*, 1988; Eklöf *et al.*, 1997, 2000). On the other hand, another study showed that an elevation in cytokinin levels leads to a rapid increase in rates of auxin biosynthesis in young, developing *Arabidopsis* tissues, and a reduction in cytokinin

levels leads to lower rates of endogenous auxin biosynthesis (Jones *et al.*, 2010). Despite the difficulty of distinguishing between cause and effect in these experiments, it is obvious that plant developmental processes are driven by changes in hormone levels. Moreover, although an individual hormone may play a predominant role in a particular process, plant responses are likely to be influenced by multiple overlapping factors, including the presence of other hormones; tissue specific responses may depend not only on the absolute concentrations of these hormones but also on the ratios of each to the others (Nordström *et al.*, 2004).

To our knowledge, no detailed study of the distribution of auxins and cytokinins in shoots of submerged aquatic plants has yet been published. Arthur *et al.* (2007) and Stirk and van Staden (2003) reported the contents of IAA and various types of cytokinins in whole shoots of the aquatic ferns *Salvinia molesta* and *Azolla filiculoides*, but the roles of these phytohormones in physiological and growth polarity have not been investigated. Winston and Gorham (1979) published results based on bioassays for gibberellins, cytokinins, auxins and abscisic acid-like activity during the formation and dormancy of turions in *U. vulgaris*. In this study we present cytokinin and auxin metabolite spectra through the rootless shoots of *A. vesiculosa* and *U. australis*.

Cytokinin biosynthesis starts with prenylation at the N^6 position of an adenine nucleotide, catalysed by the enzyme isopentenyltransferase (IPT), to produce either *i*PR5'MP or *t*ZR5'MP.

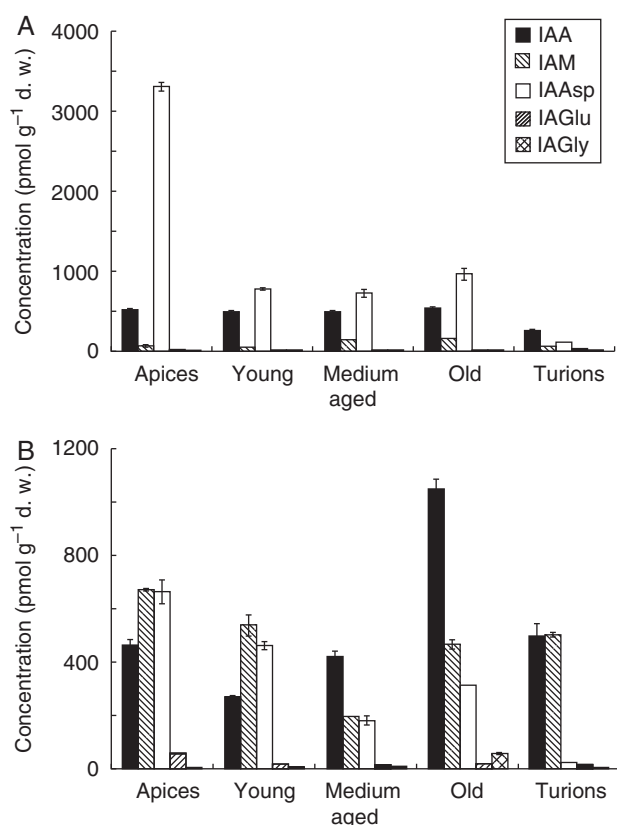


FIG. 4. Content (pmol g⁻¹ d. w.) of auxin metabolites in *Aldrovanda vesiculosa* (A) and *Utricularia australis* (B) shoot segments and turions. IAA, indole-3-acetic acid; IAM, indole-3-acetamide; IAAsp, IAA aspartate; IAGlu, IAA glutamate; IAGly, IAA-glycine.

The *c*Z cytokinin moiety is produced through enzymatic prenylation by tRNA-IPT of adenine residues adjacent to the anticodon in tRNA (Spíchal, 2012). The high levels of *c*ZR5'MP and *t*ZR5'MP in the apices in both species may indicate that these parts are the main sites of biosynthesis of the corresponding cytokinins. Nordström *et al.* (2004) observed that the greatest capacity for cytokinin biosynthesis in *Arabidopsis* is in young developing leaves with active cell division; our findings are consistent with this since in *A. vesiculosa* the apex is the only place where new leaves (whorls) are produced (Fig. 2A, B). Interestingly, the level of *i*PR5'MP showed a basipetal increase, reaching its peak in medium-aged segments in the case of *U. australis* and in old segments in *A. vesiculosa*. However, this increase was not as significant as in the case of zeatin ribotides. Moreover, in *A. vesiculosa* the higher content of *i*PR5'MP was not reflected in an increase in the active compounds, the bases (*i*P) and ribosides (*i*PR) (Supplementary Data Table S1). In *U. australis* we saw very large amounts of the conjugated form, *i*P9G, as well as an increase in active compounds (Supplementary Data Table S2). Cytokinin conjugation can be reversible in the case of the formation of *O*-glucosides, but it is irreversible in the case of *N*⁹-glucoside formation. Products of cytokinin conjugation serve purposes similar to those of auxins, playing roles as storage and transport forms because they are resistant to degradation by cytokinin oxidase/dehydrogenase, and because of their low, or lack of, biological activity. Thus, conjugation contributes to the regulation of cytokinin activity in plants (Bajguz and Piotrowska, 2009). In *U. australis*, conjugation resulted in a substantial increase in the total local cytokinin concentration in the older segments (Fig. 3B), and since very low concentrations of *O*-glucosides were found, the results suggest that *N*⁹-glucosylation plays an important role in the deactivation of cytokinin in *U. australis*. In *A. vesiculosa* the content of biologically active cytokinins is probably regulated differently, because almost no *N*⁹-glucosides were detected anywhere in the plant; only *O*-glucosides were present. Their levels showed no clear connection with possible sites of cytokinin biosynthesis, as they stayed at roughly the same level throughout the whole plant (Fig. 3A). Since the content of ribotides increased in segments further from the apex, we assume that cytokinin regulation may possibly lie at the level of biosynthesis itself. For example, in *Arabidopsis thaliana* the conversion of ribotides to biologically active ribosides and thence to active bases is carried out through enzymatic dephosphorylation via 5'-ribonucleotide phosphohydrolase (EC 3.1.3.5) and adenosine nucleosidase (EC 3.2.2.7), respectively, or directly through cytokinin phosphoribohydrolase, known as 'Lonely Guy', from ribotides to the corresponding cytokinin free bases (Kurakawa *et al.*, 2007). Negative regulation of these enzymes could lead to an increase in the contents of ribotides, as seen here (Fig. 3A). Moreover, active cytokinins in *A. thaliana* can also be degraded directly by cytokinin dehydrogenase (EC 1.5.99.12), as reviewed by Spíchal (2012); if such enzymatic activity also takes place in *A. vesiculosa*, it could explain the missing *N*⁹-glucosides.

The levels of those hormones having auxin activity are regulated by a combination of active transport, local biosynthesis, degradation and conjugation (Woodward and Bartel, 2005; Normanly, 2010). Ljung, 2013). IAA can be synthesized by the so-called L-tryptophan-dependent pathway, which is believed to be the main source of IAA in plants, and also through

an L-tryptophan-independent pathway, by which, in *A. thaliana*, IAA is synthesized directly from indole-3-glycerol phosphate (IGP) (Ouyang *et al.*, 2000). In our analysis we included one IAA precursor, IAM, which is an intermediate in the L-tryptophan-dependent pathway of IAA biosynthesis. Although the IAM content in the shoot of *A. vesiculosa* showed no pronounced trends, we can state that the presence of the compound indicates that the L-tryptophan-dependent pathway is active in this species (Fig. 4A, Supplementary Data Table S3). In *U. australis*, the highest IAM content was found in the apical part, although the highest IAA concentration was observed in the oldest segment. However, taking into account the high level of conjugates in the apex, we suggest that the apical part of this plant is the most active site of IAA biosynthesis (Fig. 4B, Supplementary Data Table S4). The two species exhibited different profiles of free IAA content. In *A. vesiculosa*, IAA was maintained at the same level throughout the whole shoot, while in *U. australis* the levels of free IAA differed greatly among segments, with the peak concentration being in the basal part (Fig. 4A, B); this variation in content in *U. australis* could be associated with the considerably more complex shoot structure and branching in this species compared with *A. vesiculosa*. IAA is conjugated mainly with sugars and amino acids. In general, dicotyledons mostly accumulate amide conjugates, but the formation and also the hydrolysis of conjugates are plant tissue-specific and, moreover, conjugate profiles differ significantly among plant species (Rampey *et al.*, 2004). As with cytokinins, this conjugation can be either reversible or irreversible, and its products are involved in IAA storage and transport or form part of the auxin catabolism pathway. In general, conjugates serve as components in IAA homeostasis, detoxifying excess auxins (Bajguz and Piotrowska, 2009). Their other roles during plant development are still under investigation. In the present study, the most abundant of these compounds in both species was IAA_{sp}. The other two conjugates that we identified, IAGlu and IAGly, were present in minute concentrations (Fig. 4A, B, Supplementary Data Tables S3 and S4).

Analysis of the apical parts of these plants has shown that the rapidly growing shoot apices, which have high cytokinin and auxin biosynthetic activity, act as a very strong physiological sink, attracting the allocation of both essential minerals and organic nutrients into the apex (Adamec 1997a, 2000), and thus promoting the growth and development of new tissues in this segment, while maintaining active meristems.

A basipetal decrease in the content of biologically active cytokinins led to a change in the cytokinin/auxin balance throughout the whole plant in favour of auxin in tissues further from the apex (Fig. 5A, B). Such a change in the cytokinin/auxin ratio may be reflected in a change in chlorophyll content, and thus in a progressive decrease in photosynthetic rate, in tissues (leaves and traps) located further from the apical part, as has been observed in *A. vesiculosa* (described in Adamec, 1997b), *U. vulgaris*, *U. australis* (Adamec, 2013) and *U. macrorhiza* (Knight, 1992).

A low content of active cytokinins is also associated with ageing processes in plants, such as maturation of leaves and traps, changes in leaf and trap function and senescence (Fabian-Galan and Salageanu, 1968; Friday, 1989; Knight, 1992; Adamec, 1997b, 2000, 2008a; Sirová *et al.*, 2009). All of the above occur along the observed gradient of decrease in active cytokinin content, and contribute to the growth and

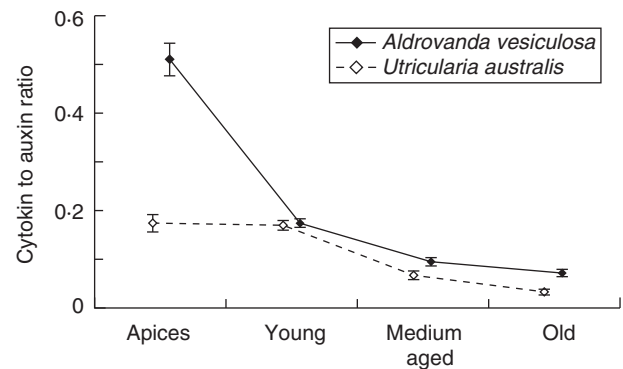


Fig. 5. Ratio (CKs:IAA) of biologically active cytokinins (cytokinin bases and ribosides) to IAA from the apical to the basal part in *Aldrovanda vesiculosa* and *Utricularia australis* shoots.

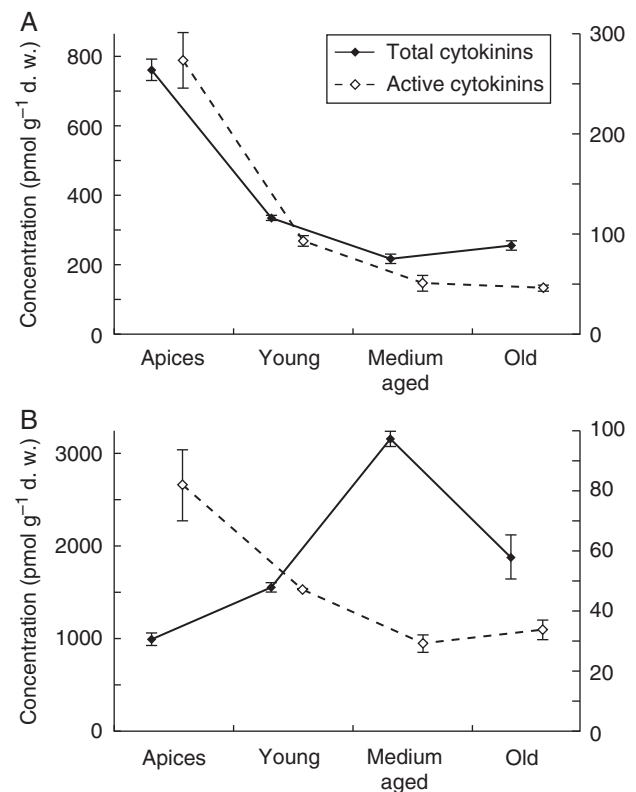


Fig. 6. Total cytokinin content and active cytokinin content (pmol g⁻¹ d.w.) from the apical to the basal part in *Aldrovanda vesiculosa* (A) and *Utricularia australis* (B) shoots.

physiological polarity of these plants (Fig. 6A, B). It should be stressed that both species in this study were collected under optimal growth conditions during a very warm, mid-summer period when the apical shoot growth rate was maximal for both species (Adamec, 2000, 2009). Therefore, the auxin and cytokinin spectra observed along the shoots of both species reflect these optimum growth conditions of maximal apical growth rate. Determination of the auxin and cytokinin spectra along the shoots of both species during the markedly slower apical growth under the sub-optimal conditions (i.e. low temperature,

low light or CO₂ or prey availability; Adamec, 2000, 2008b; Adamec and Kovářová, 2006) were not part of this study. However, Winston and Gorham (1979) observed that, 2 weeks before *U. vulgaris* turion formation and during the whole innate dormancy stage, the abscisic acid and bound gibberellin levels were high, while free gibberellin, cytokinin and auxin levels were low. It is most likely that cytokinin and auxin profiles will reflect changes in the environment and mediate the plant's physiological responses, including turion formation.

Turions are vegetative dormant organs derived from the plant apex, with storage function. Formed in autumn, they accumulate starch, free sugars and also nitrogen in the form of amino acids, and survive winter on the bottom in warmer water, and at the end of winter they rise to the water surface, where they sprout (Adamec, 1999). One of the well-known effects of cytokinins is nutrient allocation, and it is interesting that mature turions from *U. vulgaris* had no detectable levels of cytokinins (Winston and Gorham, 1979), which corresponds also to our findings, where, in turions from *U. australis* >90 % of detected cytokinins were present in biologically inactive form, suggesting metabolomic dormancy of this organ. On the other hand, turions from *A. vesiculosa* in our study showed high contents of active cytokinins, with a similar cytokinin metabolic profile to growing apical parts collected in summer; this suggests still high metabolic activity and ongoing development, which could be explained by the different requirements of environmental conditions needed for mature *A. vesiculosa* turions to enter full dormancy (Adamec, 1999).

In conclusion, our analyses show that cytokinin and auxin activity, which were originally studied and described in model rooting terrestrial plant species (*A. thaliana*, *Nicotiana tabacum*), is strongly correlated with physiological aspects of the rapid and polar growth and the development of the rootless aquatic species *A. vesiculosa* and *U. australis*. Moreover, our results from the analysis of the active CKs and their metabolites combined with the results of auxin levels along the shoots point out the importance of the dynamic balance of these phytohormones, suggesting that physiological processes such as senescence are not controlled only by the presence of one particular hormone but rather through a combination of several compounds and their optimal ratio. The direct and detailed analysis of complex plant hormone metabolism is providing valuable information about the regulatory mechanisms and the roles played by phytohormone crosstalk in developmental processes such as rapid growth, flowering or formation of turions. In future studies, including more phytohormone classes in the analysis could also help us reveal interesting facts about the phylogenetic evolution of signalling pathways and/or species themselves.

SUPPLEMENTARY DATA

Supplementary data are available online at www.aob.oxfordjournals.org and consist of the following. Table S1: cytokinin content in extracted material of *Aldrovanda vesiculosa*. Table S2: cytokinin content in extracted material of *Utricularia australis*. Table S3: auxin content in extracted material of *Aldrovanda vesiculosa*. Table S4: auxin content in extracted material of *Utricularia australis*.

ACKNOWLEDGEMENTS

We thank Sees-editing Ltd. (UK) for the English editing of this manuscript. This study was partly supported by a Czech long-term research development project (project number RVO 67985939) (to L.A.); the Ministry of Education, Youth and Sports of the Czech Republic (National Program for Sustainability I: number LO1204, the 'Návrat' program LK21306) and the Internal Grant Agency of Palacký University (IGA_PrF_2016_011).

LITERATURE CITED

- Adamec L. 1997a. Mineral nutrition of carnivorous plants: a review. *Botanical Review* **63**: 273–299.
- Adamec L. 1997b. Photosynthetic characteristics of the aquatic carnivorous plant *Aldrovanda vesiculosa*. *Aquatic Botany* **59**: 297–306.
- Adamec L. 1999. Turion overwintering of aquatic carnivorous plants. *Carnivorous Plant Newsletter* **28**: 19–24.
- Adamec L. 2000. Rootless aquatic plant *Aldrovanda vesiculosa*: physiological polarity, mineral nutrition, and importance of carnivory. *Biologia Plantarum* **43**: 113–119.
- Adamec L. 2008a. Mineral nutrient relations in the aquatic carnivorous plant *Utricularia australis* and its investment in carnivory. *Fundamental and Applied Limnology* **171**: 175–183.
- Adamec L. 2008b. The influence of prey capture on photosynthetic rate in two aquatic carnivorous plant species. *Aquatic Botany* **89**: 66–70.
- Adamec L. 2009. Photosynthetic CO₂ affinity of the aquatic carnivorous plant *Utricularia australis* (Lentibulariaceae) and its investment in carnivory. *Ecological Research* **24**: 327–333.
- Adamec L. 2010. Tissue mineral nutrient content in turions of aquatic plants: does it represent a storage function? *Fundamental and Applied Limnology* **176**: 145–151.
- Adamec L. 2011a. Functional characteristics of traps of aquatic carnivorous *Utricularia* species. *Aquatic Botany* **95**: 226–233.
- Adamec L. 2011b. Shoot branching of the aquatic carnivorous plant *Utricularia australis* as the key process of plant growth. *Phyton* **51**: 133–148.
- Adamec L. 2013. A comparison of photosynthetic and respiration rates in six aquatic carnivorous *Utricularia* species differing in morphology. *Aquatic Botany* **111**: 89–94.
- Adamec L. 2014. Different reutilization of mineral nutrients in senescent leaves of aquatic and terrestrial carnivorous *Utricularia* species. *Aquatic Botany* **119**: 1–6.
- Adamec L, Kovářová M. 2006. Field growth characteristics of two aquatic carnivorous plants, *Aldrovanda vesiculosa* and *Utricularia australis*. *Folia Geobotanica* **41**: 395–406.
- Arthur GD, Stirk WA, Novak O, Hekera P, van Staden J. 2007. Occurrence of nutrients and plant hormones (cytokinins and IAA) in the water fern *Salvinia molesta* during growth and composting. *Environmental and Experimental Botany* **61**: 137–144.
- Bajguz A, Piotrowska A. 2009. Conjugates of auxin and cytokinin. *Phytochemistry* **70**: 957–969.
- Eklöf S, Åstot C, Blackwell J, Moritz T, Olsson O, Sandberg G. 1997. Auxin-cytokinin interactions in wild-type and transgenic tobacco. *Plant Cell Physiology* **38**: 225–235.
- Eklöf S, Åstot C, Sitbon F, Moritz T, Olsson O, Sandberg G. 2000. Transgenic tobacco plants co-expressing *Agrobacterium* *iaa* and *ipt* genes have wild-type hormone levels but display both auxin- and cytokinin-overproducing phenotypes. *Plant Journal* **23**: 279–284.
- Englund G, Harms S. 2003. Effects of light and microcrustacean prey on growth and investment in carnivory in *Utricularia vulgaris*. *Freshwater Biology* **48**: 786–794.
- Fabian-Galan G, Salageanu N. 1968. Considerations on the nutrition of certain carnivorous plants (*Drosera capensis* and *Aldrovanda vesiculosa*). *Revue Roumaine de Biologie Série Botanique* **13**: 275–280.
- Friday LE. 1989. Rapid turnover of traps in *Utricularia vulgaris* L. *Oecologia* **80**: 272–277.
- Guisande C, Granado-Lorencio C, Andrade-Sossa C, Duque SR. 2007. Bladderworts. *Functional Plant Science and Biotechnology* **1**: 58–68.
- Jones B, Gunneras SA, Petersson SV, Tarkowski P et al. 2010. Cytokinin regulation of auxin synthesis in *Arabidopsis* involves a homeostatic feedback

- loop regulated via auxin and cytokinin signal transduction. *Plant Cell* **22**: 2956–2969.
- Juniper BE, Robins RJ, Joel DM. 1989.** *The carnivorous plants*. London, UK: Academic Press.
- Kamiński R. 1987.** Studies on the ecology of *Aldrovanda vesiculosa* L. I. Ecological differentiation of *A. vesiculosa* population under the influence of chemical factors in the habitat. *Ekologia Polska* **35**: 559–590.
- Kosiba P. 1992a.** Studies on the ecology *Utricularia vulgaris* L. I. Ecological differentiation of *Utricularia vulgaris* L. population affected by chemical factors of the habitat. *Ekologia Polska* **40**: 147–192.
- Kosiba P. 1992b.** Studies on the ecology of *Utricularia vulgaris* L. II. Physical, chemical and biotic factors and the growth of *Utricularia vulgaris* L. in cultures *in vitro*. *Ekologia Polska* **40**: 193–212.
- Knight SE. 1992.** Costs of carnivory in the common bladderwort, *Utricularia macrorhiza*. *Oecologia* **89**: 348–355.
- Kuhlemeier C, Reinhardt D. 2001.** Auxin and phyllotaxis. *Trends in Plant Science* **6**: 187–189.
- Kurakawa T, Ueda N, Maekawa M, et al. 2007.** Direct control of shoot meristem activity by a cytokinin-activating enzyme. *Nature* **445**: 652–655.
- Ljung K. 2013.** Auxin metabolism and homeostasis during plant development. *Development* **140**: 943–950.
- Nakamura M, Kiefer CS, Grebe M. 2012.** Planar polarity, tissue polarity and planar morphogenesis in plants. *Current Opinion in Plant Biology* **15**: 593–600.
- Nordström A, Tarkowski P, Tarkowska D et al. 2004.** Auxin regulation of cytokinin biosynthesis in *Arabidopsis thaliana*: a factor of potential importance for auxin-cytokinin-regulated development. *Proceedings of the National Academy of Sciences of the USA* **101**: 8039–8044.
- Normanly J. 2010.** Approaching cellular and molecular resolution of auxin biosynthesis and metabolism. *Cold Spring Harbor Perspectives in Biology* **2**: a001594.
- Novák O, Tarkowski P, Tarkowska D, Doležal K, Lenobel R, Strnad M. 2003.** Quantitative analysis of cytokinins in plants by liquid chromatography–single-quadrupole mass spectrometry. *Analytica Chimica Acta* **480**: 207–218.
- Novák O, Hauserová E, Amakorová P, Doležal K, Strnad M. 2008.** Cytokinin profiling in plant tissues using ultra-performance liquid chromatography–electrospray tandem mass spectrometry. *Phytochemistry* **69**: 2214–2224.
- Ouyang J, Shao X, Li J. 2000.** Indole-3-glycerol phosphate, a branchpoint of indole-3-acetic acid biosynthesis from the tryptophan biosynthetic pathway in *Arabidopsis thaliana*. *Plant Journal* **24**: 327–334.
- Palni LMS, Burch L, Horgan R. 1988.** The effect of auxin concentration on cytokinin stability and metabolism. *Planta* **174**: 231–234.
- Pěncík A, Rolčik J, Novák O et al. 2009.** Isolation of novel indole-3-acetic acid conjugates by immunoaffinity extraction. *Talanta* **80**: 651–655.
- Perrot-Rechenmann C. 2010.** Cellular responses to auxin: division versus expansion. *Cold Spring Harbor Perspectives in Biology* **2**: a001446.
- Rampey RA, LeClere S, Kowalczyk M, Ljung K, Sandberg G, Bartel B. 2004.** A family of auxin-conjugate hydrolases that contributes to free indole-3-acetic acid levels during *Arabidopsis* germination. *Plant Physiology* **135**: 978–988.
- Richards JH. 2001.** Bladder function in *Utricularia purpurea* (Lentibulariaceae): is carnivory important? *American Journal of Botany* **88**: 170–176.
- Sakakibara H. 2005.** Cytokinin biosynthesis and regulation. *Vitamins and Hormones* **72**: 271–287.
- Sirová D, Borovec J, Černá B, Rejmánková E, Adamec L, Vrba, J. 2009.** Microbial community development in the traps of aquatic *Utricularia* species. *Aquatic Botany* **90**: 129–136.
- Spíchal L. 2012.** Cytokinins - recent news and views of evolutionally old molecules. *Functional Plant Biology* **39**: 267–284.
- Stirk WA, van Staden J. 2003.** Occurrence of cytokinin-like compounds in two aquatic ferns and their exudates. *Environmental and Experimental Botany* **49**: 77–85.
- Taiz L, Zeiger E. 2010.** *Plant physiology*, 5th edn. Sunderland, MA: Sinauer Associates.
- Tanaka M, Takei K, Kojima M, Sakakibara H, Mori H. 2006.** Auxin controls local cytokinin biosynthesis in the nodal stem in apical dominance. *Plant Journal* **45**: 1028–1036.
- Tarkowska D, Novák O, Floková K et al. 2014.** Quo vadis plant hormone analysis? *Planta* **240**: 55–76.
- Taylor P. 1989.** *The genus Utricularia: a taxonomic monograph (Kew Bulletin Additional Series XIV)*. London, UK: HMSO.
- Vernoux T, Kronenberger J, Grandjean O, Laufs P, Traas J. 2000.** PIN-FORMED 1 regulates cell fate at the periphery of the shoot apical meristem. *Development* **127**: 5157–5165.
- Winston RD, Gorham PR. 1979.** Roles of endogenous and exogenous growth regulators in dormancy of *Utricularia vulgaris*. *Canadian Journal of Botany* **57**: 2750–2759.
- Woodward AW, Bartel B. 2005.** Auxin: regulation, action, and interaction. *Annals of Botany* **95**: 707–735.

Table S1: Cytokinin content in extracted material of *Aldrovanda vesiculosa* (pmol/g D.W., Mean \pm Standard Deviation (SD)). *Trans*-zeatin (tZ), *cis*-zeatin (cZ), dihydrozeatin (DHZ), isopentenyladenine (iP) and their derivatives with suffixes: riboside (R), O-glucoside (OG), riboside-O-glucoside (ROG), 9-glucoside (9G), 9-riboside-5'-monophosphate (R5'MP).

<i>Aldrovanda vesiculosa</i> (pmol/g D.W., Mean \pm SD)						
Plant segment	tZ	tZR	tZOG	tZROG	tZ9G	tZR5'MP
<i>Apices</i>	40.39 \pm 6.05	126.24 \pm 14.51	17.24 \pm 2.11	27.17 \pm 2.72	0.0159 \pm 0.0017	185.23 \pm 18.82
<i>Young</i>	5.70 \pm 0.11	28.89 \pm 0.75	4.50 \pm 0.06	8.09 \pm 0.15	<LOD	55.28 \pm 15.29
<i>Medium-aged</i>	2.64 \pm 0.29	9.42 \pm 0.77	2.77 \pm 0.37	4.32 \pm 0.07	<LOD	20.57 \pm 4.66
<i>Old</i>	2.39 \pm 0.31	5.74 \pm 0.63	2.95 \pm 0.08	4.03 \pm 0.37	0.0146 \pm 0.0005	22.77 \pm 0.64
<i>Turion</i>	54.40 \pm 0.98	104.88 \pm 0.37	12.51 \pm 0.29	14.63 \pm 0.83	<LOD	122.38 \pm 12.72
	cZ	cZR	cZOG	cZROG	cZ9G	cZR5'MP
<i>Apices</i>	20.57 \pm 1.51	25.32 \pm 3.80	1.40 \pm 0.22	1.34 \pm 0.01	0.0048 \pm 0.0007	160.90 \pm 11.44
<i>Young</i>	7.62 \pm 0.06	20.57 \pm 4.74	0.69 \pm 0.02	0.82 \pm 0.12	<LOD	116.11 \pm 13.42
<i>Medium-aged</i>	4.81 \pm 0.20	14.88 \pm 4.20	0.76 \pm 0.08	1.57 \pm 0.43	0.0053 \pm 0.0011	70.27 \pm 15.72
<i>Old</i>	6.39 \pm 0.37	15.88 \pm 2.35	1.22 \pm 0.03	2.88 \pm 0.78	0.0047 \pm 0.0004	74.29 \pm 6.86
<i>Turion</i>	3.58 \pm 0.14	7.38 \pm 0.68	1.00 \pm 0.03	1.55 \pm 0.10	<LOD	84.30 \pm 21.22
	DHZ	DHZR	DHZOG	DHZROG	DHZ9G	DHZR5'MP
<i>Apices</i>	3.87 \pm 0.55	25.50 \pm 6.19	16.91 \pm 3.66	19.65 \pm 2.71	<LOD	27.63 \pm 3.49
<i>Young</i>	1.08 \pm 0.00	6.62 \pm 2.07	6.89 \pm 0.79	7.32 \pm 0.04	0.0088	7.17 \pm 0.10
<i>Medium-aged</i>	0.28 \pm 0.01	1.52 \pm 0.03	5.01 \pm 0.63	7.61 \pm 2.07	<LOD	2.45 \pm 0.01
<i>Old</i>	0.32 \pm 0.03	1.04 \pm 0.07	4.43 \pm 1.01	9.87 \pm 2.48	0.0105	1.75 \pm 0.11
<i>Turion</i>	9.72 \pm 0.40	34.33 \pm 2.74	27.55 \pm 0.98	59.73 \pm 0.41	0.0058	35.92 \pm 4.15
	iP	iPR	iP9G	iPR5'MP		
<i>Apices</i>	5.45 \pm 0.26	10.88 \pm 0.93	0.24 \pm 0.01	51.15 \pm 1.50		
<i>Young</i>	4.14 \pm 0.05	10.81 \pm 0.49	<LOD	36.07 \pm 0.75		
<i>Medium-aged</i>	4.76 \pm 0.51	6.49 \pm 0.53	<LOD	45.66 \pm 11.12		
<i>Old</i>	5.06 \pm 0.62	3.91 \pm 0.31	0.26 \pm 0.09	83.18 \pm 25.39		
<i>Turion</i>	0.38 \pm 0.01	0.50 \pm 0.06	<LOD	3.35 \pm 0.83		

Table S2: Cytokinin content in extracted material of *Utricularia australis* (pmol/g D.W., Mean \pm Standard Deviation (SD)). *Trans*-zeatin (tZ), *cis*-zeatin (cZ), dihydrozeatin (DHZ), isopentenyladenine (iP) and their derivatives with suffixes: riboside (R), O-glucoside (OG), riboside-O-glucoside (ROG), 9-glucoside (9G), 9-ribose-5'-monophosphate (R5'MP).

<i>Utricularia australis</i> (pmol/g D.W., Mean \pm SD)						
Segment	tZ	tZR	tZOG	tZROG	tZ9G	tZR5'MP
<i>Apices</i>	3.49 \pm 0.25	7.81 \pm 0.10	1.34 \pm 0.03	1.52 \pm 0.06	45.70 \pm 1.42	18.57 \pm 2.09
<i>Young</i>	2.97 \pm 0.40	4.37 \pm 0.41	1.35 \pm 0.00	1.03 \pm 0.03	38.48 \pm 7.31	12.47 \pm 2.11
<i>Medium-aged</i>	1.48 \pm 0.24	0.97 \pm 0.19	1.52 \pm 0.00	1.24 \pm 0.00	34.11 \pm 1.33	14.14 \pm 1.38
<i>Old</i>	0.84 \pm 0.18	0.22 \pm 0.02	1.18 \pm 0.01	0.92 \pm 0.06	28.48 \pm 8.66	1.98 \pm 0.46
<i>Turion</i>	0.21 \pm 0.01	0.19 \pm 0.04	0.74 \pm 0.16	0.20 \pm 0.04	41.24 \pm 2.91	0.69 \pm 0.22
	cZ	cZR	cZOG	cZROG	cZ9G	cZR5'MP
<i>Apices</i>	19.46 \pm 0.42	41.60 \pm 11.51	1.33 \pm 0.05	1.86 \pm 0.61	12.51 \pm 1.92	282.94 \pm 7.87
<i>Young</i>	8.72 \pm 0.14	17.73 \pm 1.93	0.80 \pm 0.04	0.82 \pm 0.24	14.03 \pm 3.63	207.18 \pm 5.26
<i>Medium-aged</i>	4.56 \pm 0.02	3.92 \pm 0.19	0.72 \pm 0.06	0.97 \pm 0.00	12.67 \pm 2.70	91.35 \pm 5.15
<i>Old</i>	2.06 \pm 0.09	5.12 \pm 0.26	0.61 \pm 0.01	0.68 \pm 0.15	19.80 \pm 3.93	56.29 \pm 6.21
<i>Turion</i>	0.45 \pm 0.03	5.80 \pm 1.87	0.51 \pm 0.06	0.14 \pm 0.04	21.35 \pm 0.27	12.78 \pm 1.25
	DHZ	DHZR	DHZOG	DHZROG	DHZ9G	DHZR5'MP
<i>Apices</i>	0.20 \pm 0.00	1.11 \pm 0.34	0.76 \pm 0.17	0.67 \pm 0.02	26.33 \pm 1.26	2.69 \pm 0.19
<i>Young</i>	0.08 \pm 0.00	0.28 \pm 0.04	0.92 \pm 0.21	0.60 \pm 0.05	13.95 \pm 0.00	0.67 \pm 0.17
<i>Medium-aged</i>	0.04 \pm 0.00	0.04 \pm 0.00	0.24 \pm 0.01	0.98 \pm 0.17	12.24 \pm 0.12	0.59 \pm 0.10
<i>Old</i>	0.03 \pm 0.01	0.08 \pm 0.00	0.26 \pm 0.05	0.60 \pm 0.05	5.17 \pm 0.06	0.09 \pm 0.00
<i>Turion</i>	0.02 \pm 0.01	0.06 \pm 0.02	0.82 \pm 0.08	0.05 \pm 0.01	9.13 \pm 0.26	<LOD
	iP	iPR	iP9G	iPR5'MP		
<i>Apices</i>	4.80 \pm 0.03	3.03 \pm 0.69	542.13 \pm 26.03	44.99 \pm 8.85		
<i>Young</i>	5.76 \pm 0.05	6.19 \pm 0.46	1276.89 \pm 23.46	32.64 \pm 1.09		
<i>Medium-aged</i>	9.55 \pm 0.30	8.35 \pm 1.20	2910.04 \pm 60.83	72.52 \pm 9.35		
<i>Old</i>	18.27 \pm 3.49	7.31 \pm 0.40	1731.86 \pm 208.05	54.23 \pm 3.37		
<i>Turion</i>	0.63 \pm 0.02	0.34 \pm 0.10	914.13 \pm 5.89	0.30 \pm 0.08		

Table S3: Auxin content in extracted material of *Aldrovanda vesiculosa* (pmol/g D.W., Mean \pm Standard Deviation (SD)). Indole-3-acetic acid (IAA), indole-3-acetamide (IAM), IAA-aspartate (IAAsp), IAA-glutamate (IAGlu) and IAA-glycine (IAGly).

<i>Aldrovanda vesiculosa</i> (pmol/g D.W., Mean \pm SD)					
Plant segment	IAA	IAM	IAAsp	IAGlu	IAGly
<i>Apices</i>	503.23 \pm 21.62	52.37 \pm 8.00	3295.71 \pm 53.17	13.11 \pm 0.08	0.81 \pm 0.15
<i>Young</i>	485.49 \pm 12.45	41.03 \pm 8.84	767.83 \pm 19.17	1.84 \pm 0.14	2.78 \pm 1.69
<i>Medium-aged</i>	477.08 \pm 13.72	132.12 \pm 0.34	715.38 \pm 49.60	3.58 \pm 0.37	6.50 \pm 0.60
<i>Old</i>	524.19 \pm 15.71	149.51 \pm 5.01	950.70 \pm 74.64	3.48 \pm 0.31	0.81 \pm 0.01
<i>Turion</i>	241.90 \pm 10.23	45.95 \pm 1.72	100.39 \pm 3.95	1.71 \pm 0.11	<LOD

Table S4: Auxin content in extracted material of *Utricularia australis* (pmol/g D.W., Mean \pm Standard Deviation (SD)). Indole-3-acetic acid (IAA), indole-3-acetamide (IAM), IAA-aspartate (IAAsp), IAA-glutamate (IAGlu) and IAA-glycine (IAGly).

<i>Utricularia australis</i> (pmol/g D.W., Mean \pm SD)					
Plant segment	IAA	IAM	IAAsp	IAGlu	IAGly
<i>Apices</i>	457.83 \pm 21.54	666.56 \pm 3.45	661.32 \pm 44.72	55.11 \pm 1.79	1.38 \pm 0.02
<i>Young</i>	265.59 \pm 1.70	534.36 \pm 39.13	458.50 \pm 14.81	12.66 \pm 0.32	0.97 \pm 0.17
<i>Medium-aged</i>	416.22 \pm 22.17	191.05 \pm 1.95	177.95 \pm 16.88	9.93 \pm 0.41	8.53 \pm 1.06
<i>Old</i>	1044.72 \pm 38.40	463.74 \pm 16.31	308.37 \pm 0.62	14.65 \pm 0.42	53.01 \pm 3.27
<i>Turion</i>	493.49 \pm 47.78	499.78 \pm 8.61	19.02 \pm 0.38	9.02 \pm 0.30	0.74 \pm 0.04

Supplement V

Humplík, J. F., Bergougnoux, V., Jandová, M., **Šimura, J.**, Pěňčík, A., Tomanec, O., Rolčík, J., Novák, O., & Fellner, M. (2015). Endogenous abscisic acid promotes hypocotyl growth and affects endoreduplication during dark-induced growth in tomato (*Solanum lycopersicum* L.). *PLoS ONE*, *10*(2).

RESEARCH ARTICLE

Endogenous Abscisic Acid Promotes Hypocotyl Growth and Affects Endoreduplication during Dark-Induced Growth in Tomato (*Solanum lycopersicum* L.)

Jan F. Humplík^{1*}, Véronique Bergougnoux², Michaela Jandová³, Jan Šimura¹, Aleš Pěňčík¹, Ondřej Tomanec⁴, Jakub Rolčík¹, Ondřej Novák¹, Martin Fellner¹

1 Laboratory of Growth Regulators & Department of Chemical Biology and Genetics, Centre of the Region Haná for Biotechnological and Agricultural Research, Faculty of Science, Palacký University & Institute of Experimental Botany ASCR, Olomouc, Czech Republic, **2** Department of Molecular Biology, Centre of the Region Haná for Biotechnological and Agricultural Research, Faculty of Science, Palacký University, Olomouc, Czech Republic, **3** Department of Botany, Faculty of Science, Palacký University, Olomouc, Czech Republic, **4** Regional Centre of Advanced Technologies and Materials, Department of Physical Chemistry, Palacký University, Olomouc, Czech Republic

* jan.humplik@upol.cz



OPEN ACCESS

Citation: Humplík JF, Bergougnoux V, Jandová M, Šimura J, Pěňčík A, Tomanec O, et al. (2015) Endogenous Abscisic Acid Promotes Hypocotyl Growth and Affects Endoreduplication during Dark-Induced Growth in Tomato (*Solanum lycopersicum* L.). PLoS ONE 10(2): e0117793. doi:10.1371/journal.pone.0117793

Academic Editor: Ricardo Aroca, Estación Experimental del Zaidín (CSIC), SPAIN

Received: July 25, 2014

Accepted: December 31, 2014

Published: February 19, 2015

Copyright: © 2015 Humplík et al. This is an open access article distributed under the terms of the [Creative Commons Attribution License](https://creativecommons.org/licenses/by/4.0/), which permits unrestricted use, distribution, and reproduction in any medium, provided the original author and source are credited.

Data Availability Statement: All relevant data are within the paper and its Supporting Information files.

Funding: This work was supported by the Ministry of Education, Youth and Sports of the Czech Republic grants no. LO1204 and LO1305 (National Program of Sustainability). V. Bergougnoux and M. Fellner were supported by the Operational Programs Education for Competitiveness - European Social Fund, project no. CZ.1.07/2.3.00/20.0165 and project no. CZ.1.07/2.3.00/30.0004, respectively. M. Jandová was supported by internal grants from Palacký University

Abstract

Dark-induced growth (skotomorphogenesis) is primarily characterized by rapid elongation of the hypocotyl. We have studied the role of abscisic acid (ABA) during the development of young tomato (*Solanum lycopersicum* L.) seedlings. We observed that ABA deficiency caused a reduction in hypocotyl growth at the level of cell elongation and that the growth in ABA-deficient plants could be improved by treatment with exogenous ABA, through which the plants show a concentration dependent response. In addition, ABA accumulated in dark-grown tomato seedlings that grew rapidly, whereas seedlings grown under blue light exhibited low growth rates and accumulated less ABA. We demonstrated that ABA promotes DNA endoreduplication by enhancing the expression of the genes encoding inhibitors of cyclin-dependent kinases *SIKRP1* and *SIKRP3* and by reducing cytokinin levels. These data were supported by the expression analysis of the genes which encode enzymes involved in ABA and CK metabolism. Our results show that ABA is essential for the process of hypocotyl elongation and that appropriate control of the endogenous level of ABA is required in order to drive the growth of etiolated seedlings.

Introduction

Abscisic acid (ABA) is very often regarded as an inhibitor of shoot growth e. g. [1], [2], [3]. This is based on the fact that i) ABA accumulates at high concentrations in water stressed plants, correlating with growth inhibition [4], [5], [6] and ii) treatment with exogenous ABA at μM concentrations inhibits shoot growth [7], [5], [8]. However, ABA deficient mutants are

(IGA-PrF-2013-003; IGA-PrF-2014001). The funders had no role in study design, data collection and analysis, decision to publish, or preparation of the manuscript.

Competing Interests: The authors have declared that no competing interests exist.

shorter than the corresponding wild-type (WT) plants, and their growth can be improved by treatment with exogenous ABA. Their reduced growth was attributed to an impaired water balance [9]. The first evidence that ABA could stimulate shoot growth was obtained in a study on etiolated rice seedlings, in which treatment with extremely low concentrations of exogenous ABA stimulated mesocotyl elongation [10]. Later, Saab and co-authors demonstrated that under conditions of high water potential, the ABA-deficient *viviparous* maize mutant exhibited reduced growth compared to WT plants [11]. Similarly, the ABA biosynthesis-impaired *flacca* tomato mutant exhibited reduced shoot growth and elevated ethylene production compared to the WT. The treatment of the *flacca* mutant with exogenous ABA suppressed its excessive ethylene biosynthesis and restored shoot growth to near WT-levels [12]. The inhibition of vegetative growth was also observed in the *Arabidopsis aba1* and *aba2-1* mutants [13], [14], which are defective in different steps of ABA biosynthesis (Fig. 1). It therefore appears that ABA maintains shoot growth rather than inhibiting it, partly by suppressing ethylene synthesis and partly by some ethylene-independent mechanism.

We focused our study on the role of ABA during tomato seedling development, particularly on the growth of hypocotyl. After a seed germinates in the soil, in the absence of light, the seedling undergoes etiolated growth, known as skotomorphogenesis, which is characterized by rapid elongation of the hypocotyl topped by a hook with underdeveloped cotyledons. When the etiolated seedling perceives the light, it begins photomorphogenesis. The transition from skotomorphogenesis to photomorphogenesis, referred to as de-etiolation, involves several developmental changes such as inhibition of the fast hypocotyl growth, activation of the apical meristem, and the development of the cotyledons and plastids [15]. The role of ABA in skotomorphogenesis is poorly documented. Barrero et al. (2008) reported that dark-grown *Arabidopsis aba1* seedlings, deficient in ABA-biosynthesis, had a de-etiolated phenotype [16]. However, since this mutant is also impaired in carotenoid synthesis, the authors concluded that one of ABA's carotenoid biosynthetic precursors was responsible for this effect rather than the ABA itself.

In this work, we investigated the role of ABA during skotomorphogenesis in tomato seedlings (*Solanum lycopersicum* L.). Our study was intended to answer the question: Does ABA contribute to the rapid stem growth observed during skotomorphogenesis or does it play a role in growth inhibition observed during tomato de-etiolation? Using physiological and genetic approaches we demonstrated that finely-tuned regulation of ABA homeostasis is required to promote or inhibit growth. Indeed, ABA was found to promote hypocotyl elongation of etiolated ABA deficient tomato seedlings that exhibited a concentration-dependent response. The results were also supported by the analysis of ABA content, and the expression of ABA metabolic genes in contrasting developmental situations. It seems that ABA stimulates cell expansion by enhancing endoreduplication via the elevated expression of cyclin-dependent kinases (CDK) inhibitors and the inhibition of cytokinin biosynthesis.

Materials and Methods

Plant material and growth conditions

The experiments involving ABA quantification, the analysis of the expression of genes involved in ABA metabolism and pharmacological experiments were performed using wild-type tomato (*Solanum lycopersicum* L.) seedlings of the Rutgers cultivar. In all other experiments that focused on the effects of endogenous ABA deficiency, seedlings of the tomato mutants *sitiens* (*sit*) and *notabilis* (*not*) and the corresponding WTs (cv. Rheinlands Ruhm and cv. Lukullus, respectively) were used. The *sit* mutant is defective in the very last step of ABA biosynthesis [17] (Fig. 1) and consequently produces dramatically less ABA than the corresponding WT

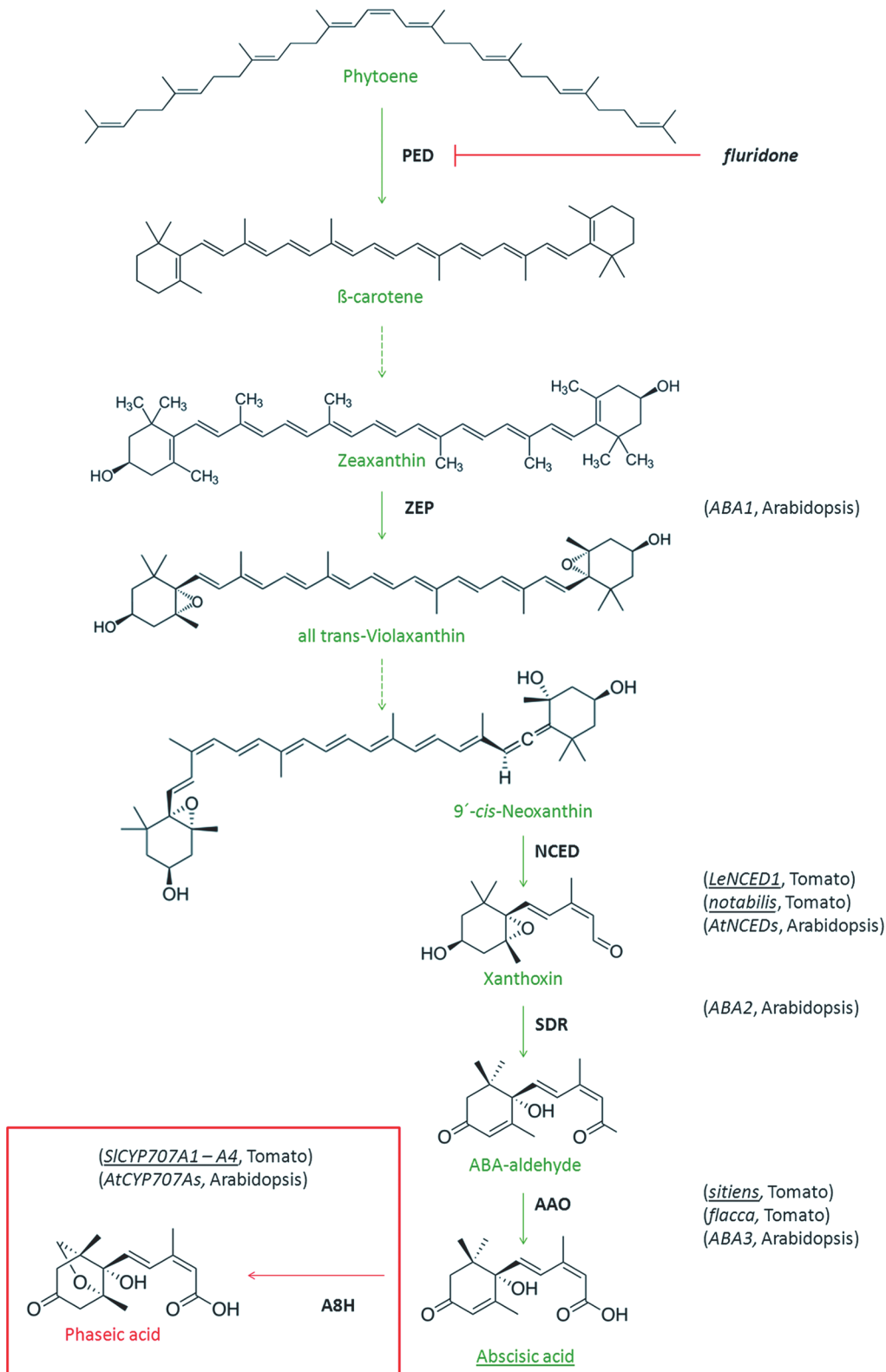


Fig 1. Simplified scheme of ABA biosynthesis and catabolism. Selected enzymatic steps in ABA biosynthesis are shown. The names of the genes encoding the enzymes that catalyze each step in tomato and *Arabidopsis* are indicated; the names of genes examined in this work are underlined. The conversion of phytoene to β -carotene is mediated by phytoene desaturase (PED); this step is blocked by fluridone. Zeaxanthin epoxidase (ZEP) catalyzes the synthesis of violaxanthin, which is then converted to neoxanthin. The subsequent synthesis of xanthoxin is catalyzed by 9'-cis-epoxycarotenoid

dioxygenase (NCED), which is encoded in the gene *LeNCED1* in tomato and disrupted in *notabilis* mutant. Whereas the previous steps occur in plastids, xanthoxin is transported to the cytosol where it is converted to the abscisic aldehyde by short-chain dehydrogenase/reductase (SDR). The final step of ABA biosynthesis is the oxidation of abscisic aldehyde to ABA by an abscisic aldehyde oxidase (AAO), which is encoded in genes that are disrupted in the *sitiens* and *flacca* tomato mutants. ABA degradation (shown in the red frame) is mediated by ABA 8'-hydroxylase (A8H, cytochrome P450 monooxygenase), whose product spontaneously isomerizes to phaseic acid. The genes encoding ABA 8'-hydroxylase in tomato are *SICYP707A1-SICYP707A4*. Dashed arrows represent missing steps in the pathway. These schemes are modified according to Kitahata and co-authors [32] and Nambara and Marion-Poll [70].

doi:10.1371/journal.pone.0117793.g001

[18], [19]. The *not* mutant is impaired in the key regulatory step of ABA biosynthesis, the oxidative cleavage of 9'-*cis*-neoxanthin to xanthoxin [20], and ABA production is also consequently reduced [19], [21].

The seeds were soaked in 3% sodium hypochlorite (Bochemie, Czech Republic) for 20 minutes and rinsed extensively with sterile distilled water prior to sowing. The seeds were then sown on the basal Murashige and Skoog medium [22] supplemented with 0.7% (w/v) agar in square Petri dishes (120 x 120 mm). The pH was adjusted to 6.1 with 1.0 M KOH before autoclaving. The Petri dishes were placed vertically in the dark for 3 days at 23°C to induce germination. For experiments involving blue-light (BL) illumination, the Petri dishes were transferred to a growth chamber (Snijders, The Netherlands) at 23°C with continuous BL illumination provided by fluorescent tubes (TL-D 36W/18-Blue, Philips; total photon fluence rate 10 $\mu\text{mol m}^{-2} \text{s}^{-1}$). The light spectrum was measured using a portable spectroradiometer (model LI-1800; Li-COR, NE, USA). For dark conditions, Petri dishes were wrapped in aluminum foil, and placed in the same growth chamber under the same temperature regime.

Hypocotyl growth measurement

Germinated seeds were transferred to new media that were supplemented as appropriate with abscisic acid or fluridone (both from Sigma-Aldrich, MO, USA) and to new media that were not supplemented with the effectors (control samples). These compounds were added to the medium as 10 mM stock solutions. The stock solution of fluridone was prepared in 10% (v/v) ethanol and the same quantity of solvent was added to the control samples. All samples were placed in a growth chamber for 4 days (96 hours). Hypocotyl length was measured with a ruler and at least 10 seedlings per treatment were measured in each independent experiment. The data of hypocotyl lengths were normalized to the appropriate control samples: the median length of the untreated WT or mutant samples (specified in figure legends) was set as 100% hypocotyl length and all other values were expressed as percentages of this control. The original measured values that were used for data normalization are given in [S1 Table](#). The data are presented as medians and first and third quartiles as they corresponded to the non-parametric statistics. The number of experimental repeats is shown in the figure legends, along with the total number of measured seedlings.

Epidermal cell length measurement

Seedlings of *sit* and WT (*cv.* Rheinlands Ruhm) were grown in dark on the basal Murashige and Skoog medium for 4 days after transfer as described above. Then a 1 cm segment from the hypocotyl base was excised and immediately fixed in a solution of 4% formaldehyde, 0.5% glutaraldehyde in a 1x MTSB buffer (50 mM PIPES, 5 mM MgSO₄, 5 mM EGTA, pH 6.9). Samples were fixed overnight in a vacuum chamber to enhance the penetration of the fixative solution into the hypocotyl tissue. Subsequently samples were washed twice with the 1x MTSB buffer and dehydrated by increasing the concentration of ethanol solution (15%, 30%, 50%, 75%, 90%, 100%). Each dehydration step lasted 20 minutes. Then the 100% ethanol washing was repeated once and samples were incubated overnight. The solution was then replaced by

fresh 100% ethanol solution for storage. Before the analysis hypocotyl segments were mounted on a metal sample holder and ethanol traces evaporated in 3 minutes. Afterwards the sample was immediately transferred to a scanning electron microscope (SEM) and photographed at magnification 100 along the whole length of hypocotyl segment. The epidermal cells were measured in ImageJ software [23] and a non-parametric variant of the t-test (Mann-Whitney test) was applied to prove the significance of the obtained data. The data are presented as medians and first and third quartiles. For each genotype at least 230 cells from three representative hypocotyls were analyzed.

Extraction and quantification of ABA

The seeds and seedlings were cultivated in the dark as described above. For the analysis of ABA, seedlings were harvested at 6, 12, 24, 48, 72, 96 and 120 hours after sowing. To obtain etiolated seedlings for ABA analysis, the Petri dishes were transferred to BL after seed germination, which occurred 72 hours after sowing. Prior to germination at 72 hours, all seeds were collected; after 72 hours, only germinated seeds were used for analysis. For the analysis in the ABA-deficient mutants, the hypocotyls were excised and frozen immediately in liquid nitrogen. The dark-grown samples were harvested under safety green light while BL-grown samples were harvested under BL illumination. The collected samples were homogenized with a mortar and pestle in liquid nitrogen. For determination of the endogenous levels of ABA, 10 mg of homogenized tissue were extracted by using a phosphate buffer. The sample was then purified by solid-phase extraction on a C8 column as described previously for auxins [24], except in this case [$^2\text{H}_6$]ABA was added as an internal standard. After evaporation under reduced pressure, samples were analyzed for free ABA content by UPLC (Acquity UPLCTM; Waters, USA) linked to a triple quadrupole mass detector (Xevo TQ MSTM; Waters, USA). The same trend in relative ABA content was observed in all biological repeats; however, the number of repeats was not sufficient for statistical analysis. All data are presented as the mean of the relative ABA content, with the value observed for dark-grown samples at the last time point (120 hours) set as 100 arbitrary units (a.u.) for each experimental repeat. The absolute values obtained in the independent repeats are reported in tables [S2 Table](#) and [S3 Table](#).

Extraction and quantification of CKs

For the quantification of CKs, the etiolated seedlings of *sit* and WT were harvested 4 days after their germination. The collected samples were homogenized with a mortar and pestle in liquid nitrogen. Fifty mg of the sample were then extracted in a modified Bielecki buffer (methanol/water/formic acid, 15/4/1, v/v/v) [25]. For the purification of free CKs, two SPE columns were used: a C18 octadecylsilica-based column (500 mg of sorbent, Applied Separations) and an MCX column (30 mg of C18/SCX combined sorbent with cation-exchange properties, Waters) [26]. Analytes were eluted by two-step elution using a 0.35 M aqueous solution of NH_4OH and 0.35 M NH_4OH in 60% (v/v) MeOH. Samples were then evaporated to dryness under reduced pressure at 37°C. An Acquity UPLC System (Waters, Milford, MA, USA), linked to a triple quadrupole mass spectrometer XevoTM TQ MS (Waters MS Technologies, Manchester, UK) equipped with an electrospray interface was used to determine cytokinin levels. Stable isotope-labeled CK internal standards (0.5 pmol each for CK bases, ribosides, and *N*-glucosides; 1 pmol each for *O*-glucosides and nucleotides) were added to each sample during the extraction step to enable accurate quantification. The final concentration of each analyte was calculated from its peak area in multiple reaction monitoring mode chromatograms, as described by Svačinová and co-authors [27]. The data are presented as mean relative CK contents, with the measured

values for the WT control samples being set to 100 arbitrary units (a.u.) for each experimental repeat. Absolute values for three independent repeats are given in [S4 Table](#).

Analysis of gene expression by RealTime-qPCR

Seeds and seedlings were cultivated and harvested as described for ABA quantification. Total RNA was extracted using an RNeasy Plant Mini Kit (Qiagen, The Netherlands), with an additional round of DNaseI treatment (Takara, Japan) for 30 minutes at 37°C. The DNase I enzyme was then heat-inactivated at 65°C for 10 minutes, after which the samples were subjected to phenol:chloroform:isoamyl alcohol (25:24:1) purification. The cDNA synthesis was performed using 0.7 µg total RNA with the PrimeScript™ 1st strand cDNA Synthesis Kit (Takara, Japan) according to the manufacturer's instructions. The RNA was then digested with 5 units of RNaseH (Takara, Japan) for 20 minutes at 37°C. The cDNAs were purified on a column and eluted with RNase/DNase-free distilled water. qPCR reactions were performed using the SYBR Premix Ex Taq kit (Takara, Japan) and 200 nM of each primer. Three technical repeats were performed for each sample in a two-step temperature program. The initial denaturation at 95°C for 10 seconds was followed by 45 cycles of 95°C for 5 seconds and 60°C for 20 seconds. The dissociation curve for each sample was monitored during this time. All Ct values were normalized against those for the *PP2Acs* and *Tip41like* genes [28]. The differences in the cycle numbers of the samples during the linear amplification phase, along with the $\Delta\Delta C_T$ method, were used to determine fold changes in gene expression. All results are expressed in term of “fold change”. Relative expression was evaluated using geometrical means calculated from two reference genes in each independent experiment. The quoted values represent the mean relative expressions observed in three independent experiments. While the number of repeats was not sufficient to prove significance in some samples, we observed the same trends in relative gene expression in all experiments (Tables A-D in [S1 File](#)). The primer sequences and gene accession numbers in the SOL genomics network (<http://solgenomics.net/>) are given in [Table 1](#).

Analysis of ploidy—endoreduplication

The seedlings of *sit* mutant and WT were grown in the dark as described above. The hypocotyls were harvested and immediately used to determine the level of DNA endoreduplication using a C6 Flow cytometer (Accuri BD, New Jersey, USA) with a blue laser (488 nm). Ten mm-long segments were excised from the upper part of the hypocotyl and cut with a razor blade in a Petri dish containing 550 µl of ice cold LB01 buffer [29]. The suspension of nuclei was then filtered through a 42 µm nylon mesh and stained with propidium iodide (50 µg.ml⁻¹). For each sample, 5000 particles were measured. A histogram of fluorescence intensity was registered on the FL2 channel using a linear scale. Because the first peak in the histogram corresponded to the G1 (2C) phase of the cell cycle, the ploidy levels of the other peaks were determined by comparison with the position of the G1 peak. The average ratio of the G1 and G2 peak positions was 1.97 (4C) and that of the G1 and G3 positions was 3.69 (8C) with coefficients of variance ranging from 3.7–9.0. For each of the four studied treatments, a total of 10 seedlings were analyzed in three independent experiments.

Statistical analysis

When comparing the results for two samples, the non-parametric variant of the t-test (Mann-Whitney test) was used to assess statistical significance. For multiple-sample experiments, significance was assessed using the non-parametric variant of one-way ANOVA, Kruskal-Wallis test with multiple comparisons post-hoc. The obtained differences were considered as significant when the *p*-value was lower than 0.05 (95% reliability), but in many cases the *p*-values

Table 1. Sequences of primer combinations used in this study.

Gene name	Accession no.	Sequence 5' - 3'	Reference
<i>LeNCED1</i>	SGN-U577478	F: CTTATTTGGCTATCGCTGAACC	[33]
		R: CCTCCAACCTCAAACCTCATTGC	
<i>SICYP707A2</i>	SGN-U583027	F: GCAATGAAAGCGAGGAAAGAG	
		R: TTGTTTCGTCAGTGAGTCCTTC	
<i>SICYP707A3</i>	SGN-U585745	F: GCTCCCAAACCCAATACCTAC	[33]
		R: CAGTTTGGCGAGTTCATTTC	
<i>SICYP707A4</i>	SGN-U583028	F: GCTAGTGTCTTACATGGATCC	[33]
		R: CTCTCATTATCCCCTCTTGCTC	
<i>SIKRP1</i>	AJ441249	F: CAACATTTCAGACCCCTGGTT	
		R: CTCCTTTTCTGCACGGGTAA	
<i>SIKRP3</i>	SGN-U320533	F: TTCGTACAAGAGCTAAAACCCCTAG	
		R: TCTTTTCCCTTCAAACCCAC	
<i>SILOG2</i>		F: TGTTGGAGAAGTAAGAGCAGTG	[35]
		R: ATGAATGCCTAGTTGAGCCC	
<i>PP2Acs</i>	SGN-U567355	F: CGATGTGTGATCTCCTATGGTC	[28]
		R: AAGCTGATGGGCTCTAGAAATC	
<i>Tip41like</i>	SGN-U584254	F: GGTTCCCTATTGCTGCGTT	[28]
		R: CGAAGACAAGGCCTGAAA	

doi:10.1371/journal.pone.0117793.t001

were lower than 0.01 (99% reliability), particular *p*-values are given in figure legends. All statistical analyses were performed using the STATISTICA 12 software (StatSoft, OK, USA). When the number of repeats was not sufficient to prove significance (gene expression and hormone analysis), the original values used for calculation of the means and SE are given in the Supporting information to demonstrate that the data of all replicates in particular experiment showed the same trends.

Results

The effects of ABA deficiency on hypocotyl growth and expansion of hypocotyl cells

The tomato *sit* mutant, which is defective in the last step of ABA biosynthesis, was used as the main tool to investigate the role of ABA in hypocotyl growth. The dark-grown *sit* mutant produced significantly shorter hypocotyls than WT plants grown under identical conditions (Fig. 2A). However, when ABA was added to the growth medium at a concentration of 100 nM, the hypocotyls of the *sit* mutant grew to the same length as those of WT plants. When different concentrations of ABA (50 nM to 5 μM) were applied the hypocotyl length was significantly stimulated by nM but inhibited by concentrations higher than 1 μM in the *sit* mutant (Fig. 2B). On the other hand in the WT inhibition only was observed at the highest ABA concentration treatment (Fig. 2C). A similar response was observed in *not* mutant and corresponding WT (cv. Lukullus). The *not* seedlings were significantly inhibited in the hypocotyl growth compared to the WT, but the treatment with 50 nM ABA led to the improvement of the mutant. WT seedlings did not respond to the exogenous ABA treatment (Fig. 2D). In comparison with *sit* mutant, a lower ABA concentration (50 nM) was chosen as most efficient for *not*, based on the previous test of ABA sensitivity (S1 Fig.). ABA contents in *sit* and *not* mutant and corresponding WT hypocotyls were analyzed to see the effects of mutations in our

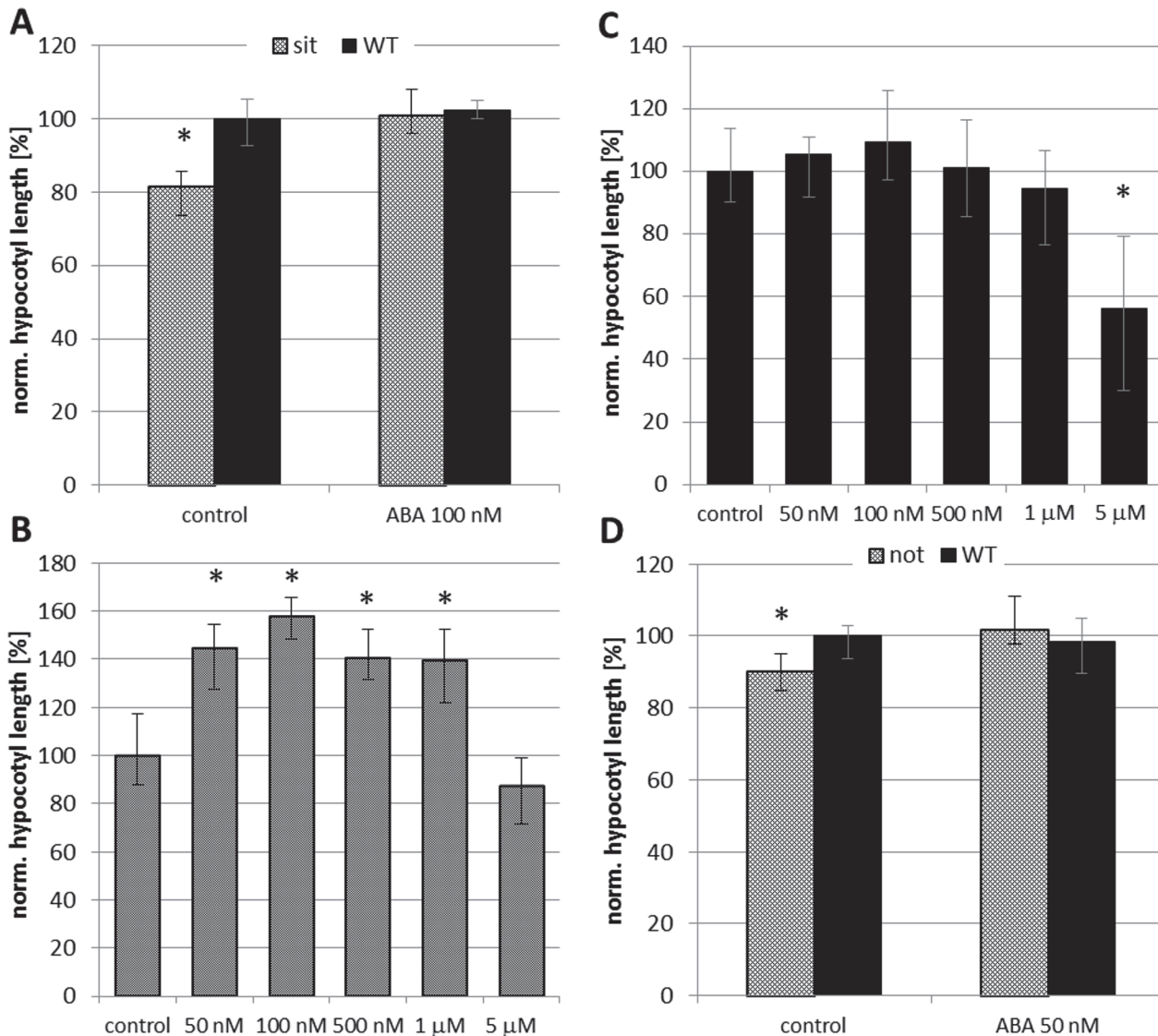


Fig 2. The effects of ABA on the growth of etiolated hypocotyls. A) The effect of ABA-deficiency and exogenous ABA on hypocotyl growth in the *sit* mutant. Germinated seeds of the WT (cv. Rheinlands Ruhm) mutant were transferred to untreated media (control) and media supplemented with 100 nM ABA and grown in the dark for 4 days. The results shown in the figure represent the medians of normalized length of hypocotyls from three independent experiments; the error bars represent the boundaries of the first and third quartiles. The “WT control” was set as 100% hypocotyl length and all other values (medians, quartiles) are expressed as percentages of this value. To prove statistical significance the Mann-Whitney test was performed independently (*sit* versus WT) for control and ABA treated samples. Asterisks denote values that differ significantly (Mann-Whitney test; $p < 0.01$, $n = 136$). B) The hypocotyl elongation of the *sit* mutant treated with various concentrations of ABA. Germinated seeds were transferred to untreated media (control) and media supplemented with ABA and grown in the dark for 4 days. The results shown in the figure represent the medians of normalized length of hypocotyls from two independent experiments; the error bars represent the boundaries of the first and third quartiles. The sample “control” was set as 100% hypocotyl length and all other values (medians, quartiles) are expressed as percentages of this value. To prove statistical significance the Kruskal-Wallis ANOVA with multiple post-hoc comparison was performed. Asterisks denote values that differ significantly from “control” sample ($p < 0.01$; $n = 232$). C) The hypocotyl elongation of the WT (cv. Rheinlands Ruhm) treated with various concentrations of ABA. Germinated seeds were transferred to untreated media (control) and media supplemented with ABA and grown in the dark for 4 days. The results shown in the figure represent the medians of normalized length of hypocotyls from two independent experiments; the error bars represent the boundaries of the first and third quartiles. The sample “control” was set as 100% hypocotyl length and all other values (medians, quartiles) are expressed as percentages of this value. To prove statistical significance the Kruskal-Wallis ANOVA was performed. Asterisks denote values that differ significantly from “control” sample ($p < 0.01$, $n = 200$). D) The effect of ABA-deficiency and exogenous ABA on hypocotyl growth in the *not* mutant. Germinated seeds of the WT (cv. Lukullus) mutant were transferred to untreated media (control) and media supplemented with 50 nM ABA and grown in the dark for 4 days. The results shown in the figure represent the medians of normalized length of hypocotyls from one independent experiment. The “WT control” was set as 100% hypocotyl length and all other values (medians, quartiles) are expressed as percentages of this value. To prove statistical significance the Mann-Whitney test was performed independently (*not* versus WT) for control and ABA treated samples. Asterisks denote values that differ significantly (Mann-Whitney test; $p < 0.03$, $n = 79$).

doi:10.1371/journal.pone.0117793.g002

experimental conditions. Both mutants showed dramatically lowered endogenous ABA compared to the WT samples (Fig. 3, S3 Table). In order to determine the role of ABA during photomorphogenesis, additional experiments were conducted using seedlings grown under BL illumination, which is known to strongly inhibit hypocotyl growth [30], [31]. The *sit* mutation did not have any discernible effect on hypocotyl growth under continuous BL illumination (S2 Fig.).

In parallel to the studies using mutant lines, we conducted a series of experiments using synthetic inhibitor of ABA biosynthesis. Freshly germinated tomato (cv. Rutgers) seedlings were grown in the dark for four days on a medium supplemented with fluridone (10 μM) and then the length of the hypocotyls was measured. Fluridone is an inhibitor of carotenoid pathway, suppressing early steps of ABA synthesis [32] (for details see Fig. 1). The analysis of ABA content in dark-grown WT hypocotyls showed that fluridone lowered endogenous ABA to the less than 50% of the control samples (S3 Fig.). Fluridone caused significant inhibition of hypocotyl growth in the etiolated seedlings (S4 Fig.). To see how ABA deficiency affected hypocotyl cell elongation the microscopic experiments were performed. The measurement of cell length showed significant inhibition (Mann-Whitney test, p value < 0.05) of cell expansion in the dark-grown *sit* mutant compared to the WT (Fig. 4).

Endogenous ABA levels during germination, skotomorphogenesis and photomorphogenesis

The endogenous free ABA contents of whole WT tomato (cv. Rutgers) seedlings were monitored from sowing to early development. The endogenous ABA levels were highest at the first analyzed time point, i.e. 6 hours after sowing, after which they decreased rapidly until germination, 72 hours after sowing. After germination, the ABA content increased gradually in developing seedlings. De-etiolation and photomorphogenesis were initiated by exposure to BL (constant illumination, 10 $\mu\text{mol}\cdot\text{m}^{-2}\cdot\text{s}^{-1}$). Nevertheless, the ABA concentration in dark-grown seedlings was around twice that in seedlings grown under continuous BL and which had undergone de-etiolation and subsequent photomorphogenesis (Fig. 5A).

To determine whether the differences in ABA seen after germination were due to inhibition of ABA biosynthesis or stimulation of ABA degradation, the expression of genes involved in ABA metabolism was investigated. The gene *LeNCED1* encodes 9-cis-epoxycarotenoid dioxygenase, which is the key enzyme involved in ABA synthesis; its expression over time in dark- and BL-grown seedlings is shown in Fig. 5B. The relative abundance of the transcript was below the limit of detection prior to germination but increased progressively in developing seedlings. In addition, the accumulation of *LeNCED1* transcripts in the BL-grown seedlings was almost 60% lower than in those grown in darkness.

We also investigated the expression of four genes which encode the enzymes involved in ABA catabolism (ABA 8'-hydroxylases *SICYP707A1* to *SICYP707A4*) [33]. The *SICYP707A1* transcript was not detected under our conditions, which suggested that the corresponding enzyme was not involved in seedling development. No significant difference was observed between the dark- and BL-grown seedlings with respect to the expression of either *SICYP707A2* or *SICYP707A4* (S4 Fig.). But a BL-induced response was observed in *SICYP707A3* (Fig. 5C). Indeed, this transcript accumulated gradually and at the same rate in the dark- and BL-grown seedlings during the first 48 hours of the experiment (i.e. the seed imbibition period) and then declined between 48 and 72 hours (the point at which germination occurred). In the dark-grown seedlings, the expression of *SICYP707A3* then declined further before reaching a low basal level. Conversely, in the BL-grown seedlings, its expression increased dramatically

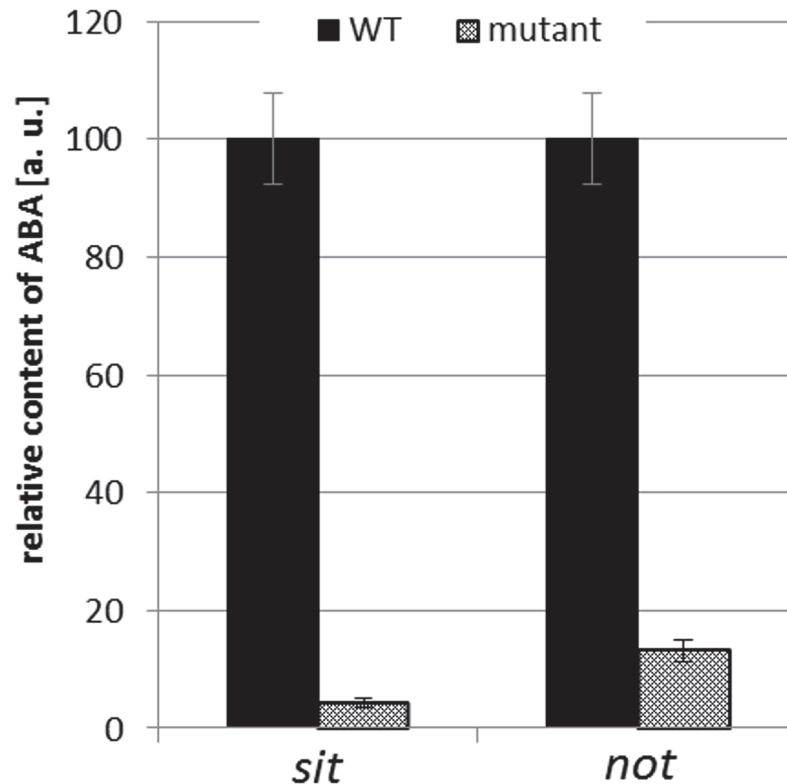


Fig 3. Effect of *sit* and *not* mutations on the endogenous ABA content in etiolated hypocotyls. The dark-grown hypocotyls of *sit* and *not* mutants and corresponding WT were harvested five days after germination and ABA content was measured. Free ABA levels are reported as relative means [a.u.] \pm SE based on two biological repeats. The mutant values are expressed relative to those for corresponding WT, which were assigned a value of 100 a.u.

doi:10.1371/journal.pone.0117793.g003

between 72 and 96 hours before falling again. The developmental stages of tomato germination and post-germination growth considered in this work are shown in [Fig. 5D](#).

The effects of ABA on DNA endoreduplication in etiolated tomato hypocotyls

The results presented above indicated that ABA plays an important role in regulating dark-induced growth. Etiolated hypocotyl growth is primarily due to cell elongation, with cell division only being important in the development of stomata [34]. Moreover, as in *Arabidopsis*, the tomato hypocotyl elongates along a basipetal gradient. Consequently, the upper region of hypocotyl (i.e. the part situated just above the hook and cotyledons) is the active site of elongation [35]. We therefore investigated the effects of ABA on endoreduplication in this part of the seedlings. For this purpose, 10 mm-long segments were excised from the upper parts of the hypocotyls of the etiolated seedlings of both the *sit* mutant and the corresponding WT, and their cell ploidy was measured by flow cytometry. The cell ploidy status was expressed as the ratio of the number of nuclei in the G3 phase to the total number of nuclei [$8C/(2C+4C+8C)$], where G3 represents nuclei in the endoreduplication cycle (8C). Our data clearly showed that the extent of endoreduplication in hypocotyl segments from dark-grown untreated *sit* mutants was significantly lower than in the corresponding WT samples. Treatment with exogenous ABA

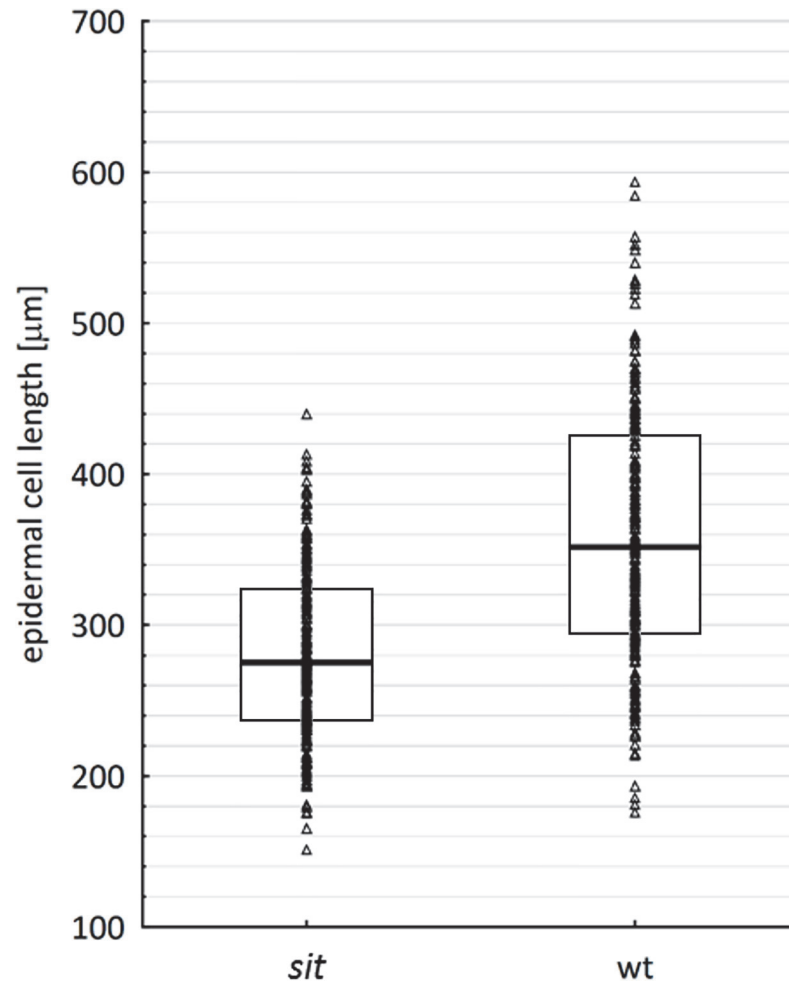


Fig 4. Effect of ABA deficiency on the expansion of hypocotyl cells. The influence of ABA on the elongation of epidermal cells of etiolated hypocotyls in *sit* and WT (cv. Rheinlands Ruhm) was investigated using SEM imaging analysis. Triangles represent all measured values ($n = 471$) for each genotype. The bars within the boxes indicate the median values in each case, while the boxes' upper and lower boundaries indicate the boundaries of the first and third quartiles. The Mann-Whitney test was used to prove statistical significance ($p < 0.01$).

doi:10.1371/journal.pone.0117793.g004

significantly increased the number of G3-phase nuclei in the *sit* hypocotyls but caused only a slight increase in the WT samples (Fig. 6A).

Endoreduplication is controlled by the activity of cyclin-dependent kinase (CDK) proteins, and it has been reported that the expression of the CDK inhibitor *ICK1* is induced by ABA in *Arabidopsis* [36]. Analyses of the expression of two tomato *ICK1* orthologs, *SIKRP1* and *SIKRP3*, [37], [38] indicated that their transcripts were less abundant in the *sit* mutant than in WT plants. Treatment with ABA stimulated the expression of both genes in *sit*, but had no effect on the WT. The overall *SIKRP1* expression was approximately twice that for *SIKRP3* (Fig. 6B).

The effect of ABA on endogenous cytokinin levels

It was recently demonstrated that cytokinins (CKs) accumulate during de-etiolation, probably due to the accumulation of *SILOG2* transcripts, which encode an enzyme responsible for the

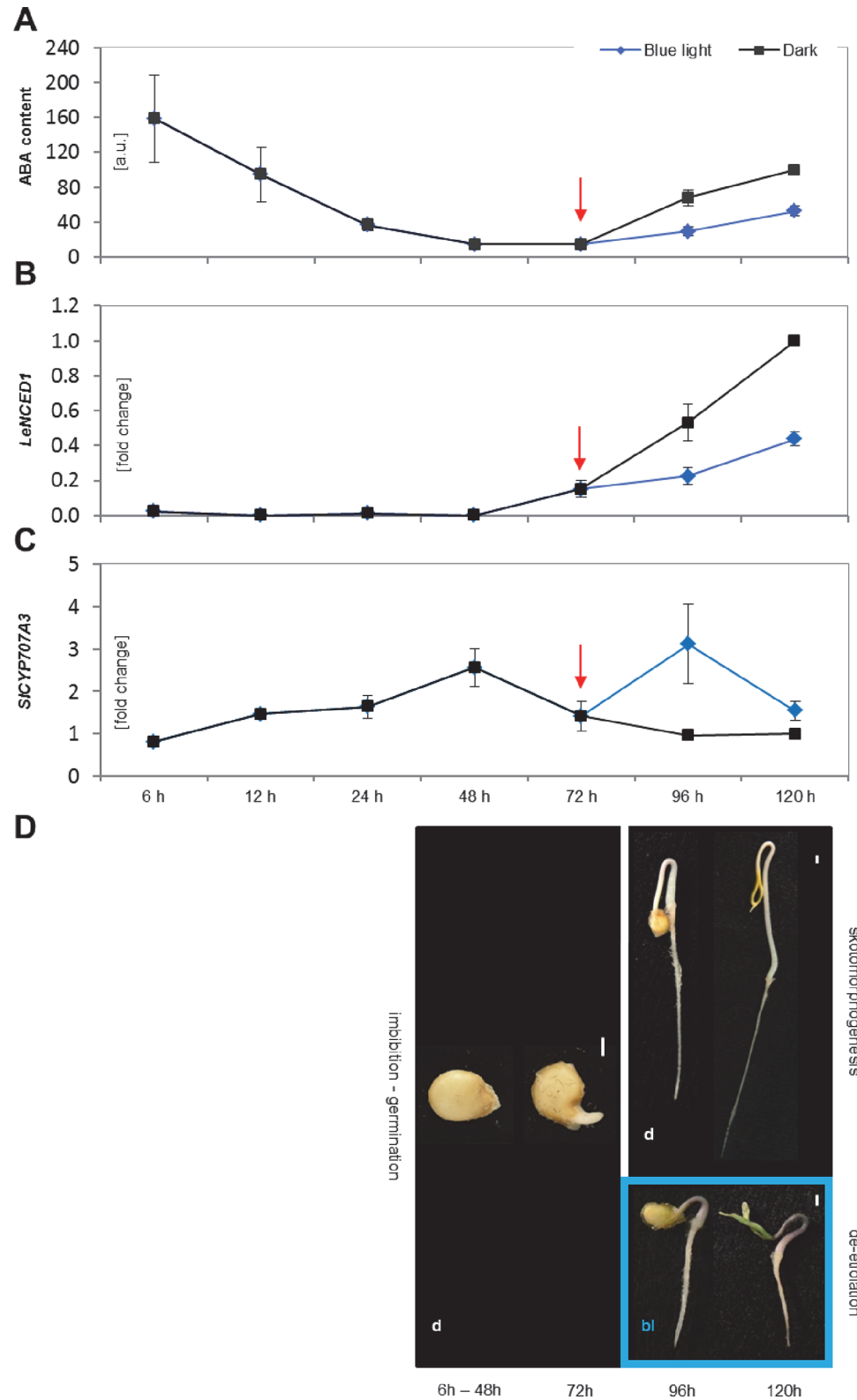


Fig 5. Regulation of ABA metabolism during seed germination and post-germination growth. Free ABA levels are reported as relative means [a.u.] \pm SE based on three independent experiments. All values are expressed relative to those for the dark-grown sample at the 120 hours time point, which was assigned a value of 100 a.u. (A). The fold changes in the expression of the *LeNCED1* (B) and *SICYP707A3* (C) genes are

reported as the means of three independent experiments \pm SE. *Tip41like* and *PP2ACs* were used as housekeeping genes. Relative quantification was performed using the expression levels for the dark-grown sample at 120 hours as a reference. The red arrow marks the point of seed germination. Figure D shows the different stages of tomato seedling development considered in this work. The first is seed imbibition (6h–48h), which is followed by seed germination (72h). Both of these steps occurred in darkness in all experiments. The seedlings were then separated (96h–120h) into two groups: one was kept in darkness (d) to induce skotomorphogenesis while the other was grown under continuous BL (b) to induce de-etiolation. White bars indicate a distance of 1 mm.

doi:10.1371/journal.pone.0117793.g005

synthesis of CK free bases. Moreover, it was evidenced that CK accumulation correlated with the inhibition of endoreduplication [35]. To test the hypothesis that CKs and ABA may act antagonistically during de-etiolation, we measured the endogenous CK contents of dark-grown whole WT and *sit* seedlings grown in the presence and absence of exogenous ABA (Fig. 7A; S4 Table). The *sit* seedlings had much higher levels of CK compounds than the WT plants, and treatment with ABA reduced the abundance of CKs in the mutant but not in the WT. In both cases, the seedlings' CK levels correlated with the expression of the *SLOG2* gene, which was expressed in the hypocotyl segments of the *sit* mutant almost twice as strongly as in the WT. Treatment with exogenous ABA significantly inhibited *SLOG2* transcript accumulation in the *sit* mutant but had only minor effects on the WT (Fig. 7B).

Discussion

The role of ABA in shoot development has been the subject of debate for some time. While some recent authors still contend that the physiological role of ABA is to inhibit shoot growth [2], [8], [39] there is a growing body of evidence suggesting that it can in fact stimulate shoot growth, or at least contribute to its maintenance [12], [13], [21], [40], [41]. In the present study, the significant inhibition of hypocotyl growth was observed in ABA deficient etiolated seedlings. We found that exogenous ABA stimulated the growth of ABA deficient mutants and had no effect on WTs in nM concentration range. Only a high concentration (5 μ M) inhibited WTs growth. As mentioned by Sharp (2002), the interpretation of data related to the application of exogenous ABA are complicated by the uncertain effects of the exogenous treatment [42]. However, our data obtained through treatment with ABA in a wide concentration range suggested that the key factor is plant sensitivity to ABA and homeostatic regulation. It is highly probable that in WT seedlings the number of active ABA receptors corresponds to the signal compound concentration. We can hypothesize that in WT seedlings, the receptors are already saturated by endogenous ABA and the application of exogenous ABA either cannot trigger further response or it can trigger an "over-dose" response that leads to growth inhibition. In ABA deficient seedlings, the endogenous ABA content is too low to activate or saturate the receptors. Thus the *sit* and *not* seedlings are able to respond efficiently to the exogenous ABA treatment. It is important to consider not only the presence or absence, but also the quantity of the signal within the living organism. Then the same compound could evoke opposite responses depending on the concentration used, as has been previously shown for auxin [43] or cytokinins [44]. This can also explain the different sensitivity of *sit* and *not* mutants to ABA. Whereas *sit* seedlings are impaired in the last step of ABA synthesis, the *not* mutation affects the earlier step of conversion of 9'-*cis*-neoxanthin to xanthoxin (LeNCED enzyme). While both mutants produce consistently less ABA than WTs [45], [46], [47], their endogenous ABA content differs (4% and 13% of the WTs for *sit* and *not*, respectively). Thus the difference in sensitivity observed between the two mutants can reflect the difference in their endogenous ABA content. The dose-dependent increase of hypocotyl growth of the mutants suggests that a homeostatic imbalance could be restored by exogenous ABA. Our results suggested that in plants with

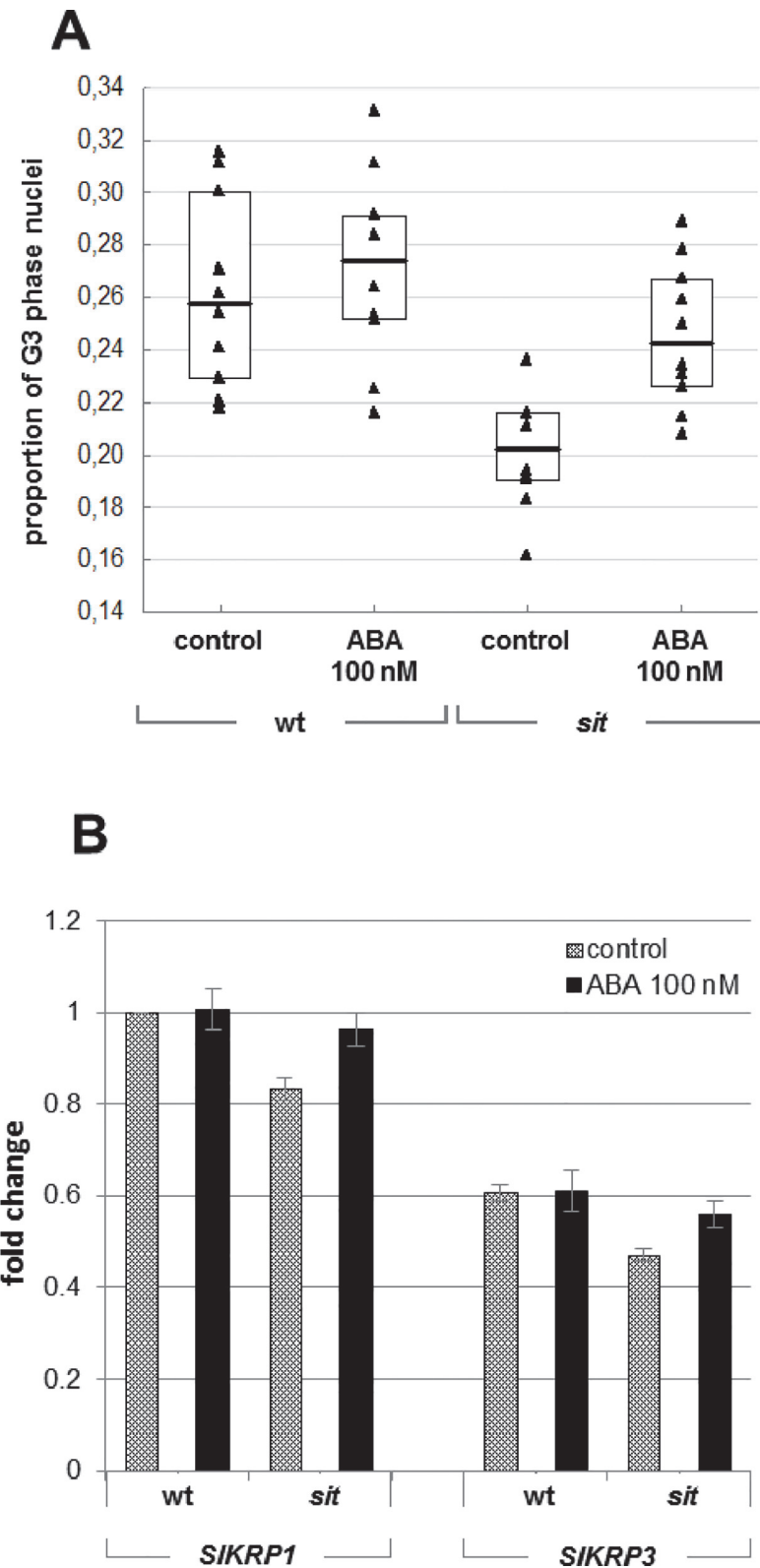


Fig 6. The effects of ABA on endoreduplication. The influence of ABA on nuclear ploidy was investigated using hypocotyl segments of *sit* and WT seedlings grown in darkness on untreated media and media containing 100 nM ABA (A). Triangles represent all measured values (n = 40) for each genotype and

treatment. The bars within the boxes indicate the median values in each case, while the boxes' upper and lower boundaries indicate the boundaries of the first and third quartiles. Three independent experiments were performed. The Kruskal-Wallis ANOVA test with multiple comparisons revealed that only the *sit* control sample differed significantly from the WT control ($p < 0.01$). No other significant differences were found. (B) Analysis of the expression of the *SIKRP1* and *SIKRP3* genes based on the mean of three independent experiments \pm SE. *Tip41like* and *PP2ACs* were used as housekeeping genes. All expression values are quoted relative to those for the "WT control" sample.

doi:10.1371/journal.pone.0117793.g006

normal (physiological) ABA levels, additive exogenous ABA will lead to an "over-dose" effect causing growth inhibition, but in the ABA deficient plants the ABA action could be revealed in a more physiological context.

To see the effects of ABA deficiency on the hypocotyl growth the application of ABA bio-synthetic inhibitor was performed also as an alternative to genetic approach. Although possible unspecific effects of the chemical treatment should be considered, the application of fluridone led to reduced hypocotyl elongation in dark-grown WT seedlings that further supported the data obtained in genetic experiments. The tomato *sit* mutant was an important genetic tool in this work because it is deficient in the very final step of ABA biosynthesis. Thus, results obtained on this mutant clearly identified the role of ABA in the studied physiological processes. Under conditions with no water stress, the ABA deficient seedlings grown in the dark had significantly shorter hypocotyls than WT plants grown under the same conditions. Previous analysis of the *Arabidopsis aba1* loss-of-function mutant also indicated that ABA may significantly contribute to the process of skotomorphogenesis [16]. However, because the ABA1 enzyme catalyzes an early step in ABA biosynthesis (Fig. 1) whose product is also a precursor of carotenoids, the authors concluded that one of the carotenoid precursors of ABA is required for etiolated growth rather than ABA itself. In the present study, very similar results were obtained with the tomato *sit* mutant, which was deficient in the final step of ABA synthesis, i.e. the conversion of ABA-aldehyde into ABA. Therefore our results strongly suggest that ABA rather than one of its carotenoid precursors promotes the hypocotyl elongation observed during skotomorphogenesis.

Plants defective in ABA signalling are also a good material to investigate the role of ABA during vegetative development. The family of *abscisic-acid insensitive (abi)* mutants was the first group of plants discovered with impaired ABA signal transduction [48]. To our knowledge only *abi5* was tested for etiolated hypocotyl elongation and no significant difference was observed between mutant and WT. Even the overexpression of *ABI5* construct in the WT did not change the hypocotyl growth [39]. However, it is hard to determine how the ABA signalling is involved in skotomorphogenesis because of the high level of redundancy between ABA signalling components [49], [50], [51]. In light-grown seedlings a strong inhibition of growth was reported for the *abi8* mutant [52]. Among the ABA receptors the most highly expressed in most developmental stages are PYR1, PYL1, PYL4, PYL8, PYL5, and PYL2. The sextuple mutant showed a strong inhibition of vegetative growth in adult *Arabidopsis* plants [53]. It corresponds to the results obtained with ABA deficient *Arabidopsis* [13] and tomato [12] plants, confirming the importance of proper ABA signalling for maintaining shoot growth.

The postulated correlation between ABA content and tomato hypocotyl growth was further supported by the measurement of endogenous ABA in dark-grown seedlings and in seedlings grown under continuous BL. The dark-grown seedlings undergoing skotomorphogenesis accumulated substantially higher amounts of ABA than those undergoing photomorphogenesis. The fact that seedlings growing under BL still accumulate ABA supports the idea that ABA contributes to the maintenance of steady-state seedling growth. Analyses of the expression of genes involved in ABA synthesis and catabolism suggested that both processes contribute to

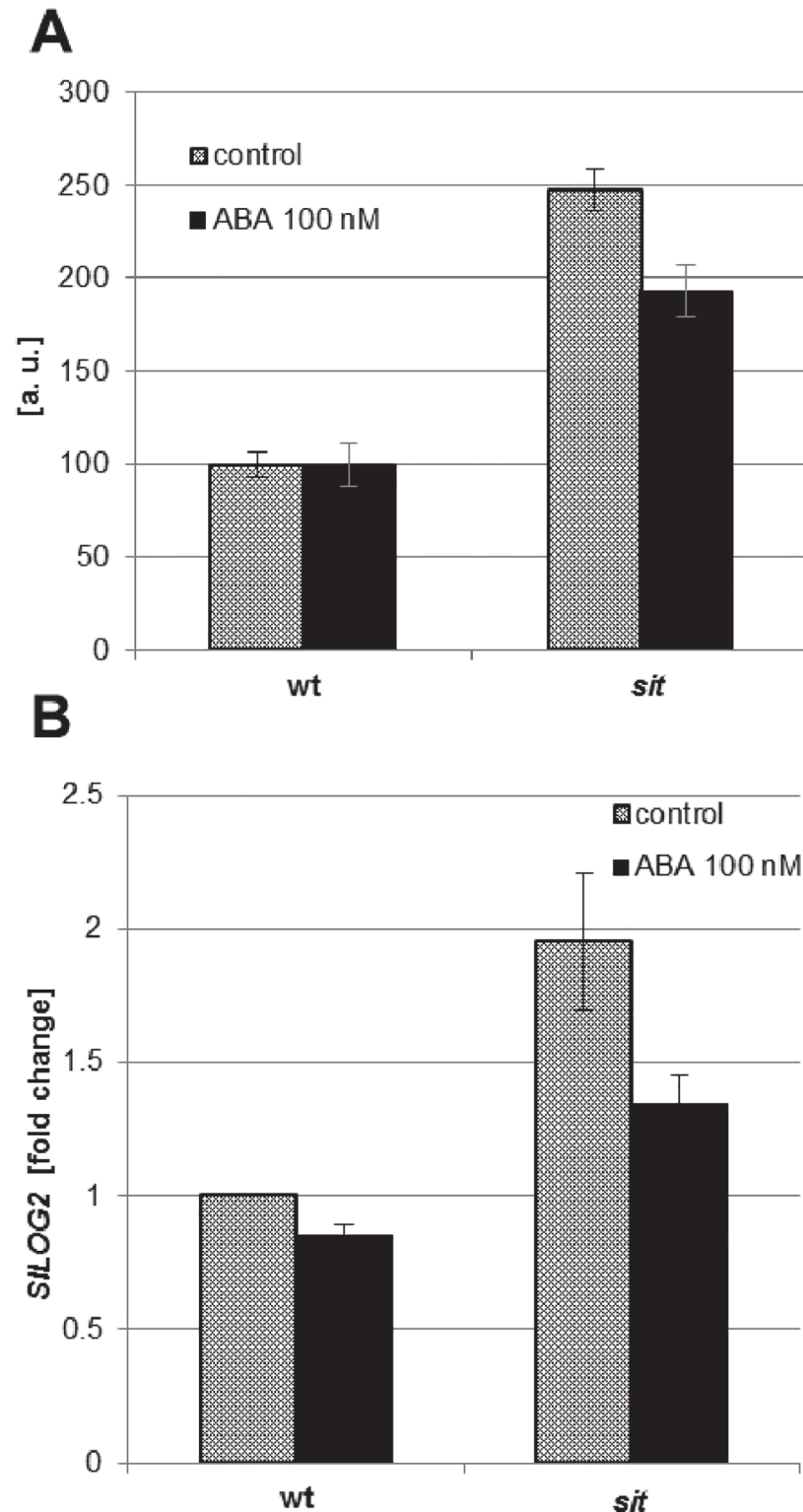


Fig 7. The effects of ABA deficiency on biosynthesis and overall CK levels in etiolated tomato seedlings. Overall CK levels are quoted as the mean of the relative values [a. u.] \pm SE for three independent experiments. All measurements are expressed in relation to those for the “WT control” sample, which was assigned a value of 100a.u. (A). The expression of the *SILOG2* gene is presented as the mean of three independent experiments \pm SE. *Tip41like* and *PP2ACs* were used as housekeeping genes. Expression was quantified in relation to that of the specified reference genes in the “WT control” sample (B).

doi:10.1371/journal.pone.0117793.g007

the regulation of ABA by light. Thus, the transcript of the *LeNCED1* gene, which is involved in ABA synthesis, was undetectable prior to seed germination (in accordance with the fact that ABA in the tomato seeds was synthesized during their maturation) but accumulated during the development of the young seedlings. The accumulation of *LeNCED1* transcripts in the BL-grown seedlings was considerably lower than in the etiolated seedlings. The differential accumulation of *LeNCED1* transcripts observed between dark- and BL-grown seedlings correlated with their differential accumulation of endogenous ABA. The analysis of catabolic genes revealed that *SICYP707A1* was not detected in our experimental conditions, consistent with its preferential localization in pollinated ovaries [33]. Under our conditions, *SICYP707A3* was the only ABA 8'-hydroxylase whose expression differed appreciably between dark- and BL-grown tomato hypocotyls, suggesting that this enzyme plays a role during the onset of photomorphogenesis. Continuous exposure to BL led to a decrease of ABA accumulation in the seedlings, driven by the reduction in synthesis and the strong but transient stimulation of catabolism. This suggests that the BL-induced reduction or limitation of endogenous ABA is important in de-etiolation and the onset of photomorphogenesis. Of course, an analysis of protein levels and enzymatic activities would be required to confirm our conclusions. However, we are not the first to report that light regulates endogenous ABA. Indeed, Kraepiel and co-authors demonstrated that the pea phytochrome-deficient *pew-1* mutant had a higher content of ABA in its seeds and leaves than the WT, suggesting that light plays an important role in regulating ABA accumulation [54]. Similarly, Weatherwax and co-authors reported that red light reduced the concentration of ABA in etiolated *Lemna gibba* and also that dark treatment of previously light-grown *Arabidopsis* and *Lemna gibba* plants caused significant ABA accumulation [55]. Moreover, Symons and Reid observed reductions in the ABA content of etiolated pea seedlings after 4 hours of exposure to white light [56].

Skotomorphogenesis is characterized by the rapid elongation of the hypocotyl across a basipetal gradient. This elongation is mainly due to cell expansion, with cell division being restricted to the development of stomata [34]. It has been described previously that leaf epidermal cells of the *sit* mutant are significantly reduced [57]. In the present study, we demonstrated that the shorter hypocotyls of the mutants are due to the reduction of cell expansion. Cell expansion is triggered by two processes: an increase in the cell ploidy by endoreduplication and the expansion of the cell itself, which is driven by water uptake [58]. Whereas there is no doubt about the importance of ABA for water regulation, in this study we focused on the possible influence of ABA on endoreduplication. DNA endoreduplication is a consequence of cell multiplication without division, leading to increased ploidy of the cell. Cell division is regulated via the activity of cyclin-dependent kinases (CDKs) which are regulated by cyclin D-type proteins (CYCD). The initiation of endoreduplication requires the suppression of proteins of the CDK B-family. The activity of the CDK-CYC complexes can be blocked by the inhibitor of CDK/KIP-related (ICK/KRP) proteins. The expression of ICK/KRPs stimulated endoreduplication restricts the G2/M transition [59]. Recently, Bergougnoux and co-authors reported that the switch from skoto- to photomorphogenesis is characterized by the inhibition of endoreduplication [35]. Similarly to studies of ABA effects on shoot growth, existing reports concerning the influence of ABA on endocycles are also contradictory. For example, del Castelano and co-authors reported that treatment with high concentrations (μM) of exogenous ABA inhibited endocycles in *Arabidopsis* leaf primordia, but not in root meristems [60]. Conversely, different studies suggested that ABA promoted endoreduplication by up-regulating the expression of ICK/KRPs in *Arabidopsis* [36] and in an alfalfa cell suspension culture [61]. In our study, the ABA deficiency of the *sit* mutant correlated to a lower expression of the *SIKRP1* and *SIKRP3* genes compared to the WT, and to reduced endoreduplication. The expression of *SIKRP*s as well as the level of endoreduplication was decreased by about 20% in *sit* compared to the WT,

corresponding to the growth reduction rate observed in this mutant. Such correlation suggests a direct link between endoreduplication and hypocotyl growth. Overall, these results prompted us to hypothesize that the stimulation of endoreduplication is at least one important aspect of the mechanism by which ABA triggers hypocotyl elongation during skotomorphogenesis.

The postulated growth-promoting effect of ABA is supported by the work of Sharp and co-authors [12]. The authors found that under well-watered, non-stressed conditions, the ABA deficient tomato *flacca* mutant exhibited impaired leaf growth and ethylene content two times higher than that of the WT. Exogenous ABA partially restored the mutant's growth and significantly reduced the accumulation of ethylene. This led to the hypothesis that endogenous ABA maintains shoot elongation in adult tomato plants in a non-hydraulic way by restricting ethylene production. Moreover, studies of the ABA-deficient and ethylene-insensitive *Arabidopsis aba2-1/etr1-1* mutant suggested ethylene-independent mechanisms for the maintenance of shoot growth [13], which implies that some other hormone may be responsible for the relevant processes.

Interaction between ABA and other phytohormones is expected to contribute to the control of stem growth during skotomorphogenesis. Aside from its ethylene-suppressing effects, ABA is also known to be antagonistic to gibberellins (GAs) during seed germination. However, GAs stimulate etiolated hypocotyl growth [62] and are rapidly degraded in response to light [56]. It is more likely that CKs counteract the effects of ABA in stimulating hypocotyl growth, in keeping with their established role during plastid development [63]. Recently it was shown in *Arabidopsis* that CK counteracts ABA by degrading the ABI5 protein [64]. The inhibitory effects of CKs on endoreduplication in tobacco and petunia leaves were reported [65]. Recently the negative regulation of endoreduplication by CKs in the *Arabidopsis* shoot apical meristem has been shown by Scofield and co-authors [66]. This response seems to be shoot-specific since the CK-dependent stimulation of endocycling activity in roots has been reported [67]. Here, we focused on ABA-CK interaction as it was found that CKs inhibit endoreduplication and cell expansion during de-etiolation in tomato seedlings [35]. Indeed the exposure of etiolated tomato seedlings to BL induced the accumulation of CK in the elongating zone of the hypocotyl and the accumulation of *SILOG2* transcripts; *SILOG2* encodes an enzyme that is responsible for the synthesis of CK free bases. This is accompanied by the inhibition of endoreduplication, prompting the conclusion that CKs inhibit stem growth by inhibiting endoreduplication and other processes. Our results showed that ABA stimulates endoreduplication and thereby contributes to stem elongation in dark-grown seedlings. This clarifies the previously discussed antagonism between ABA and CKs during seedling development. Indeed, ABA is known to stimulate the accumulation of cytokinin oxidase/dehydrogenase transcripts which encode the proteins responsible for CK degradation [68], while CKs repress the expression of ABA-associated genes [69], [64]. Our data showed that appropriate control of the endogenous ABA balance is necessary to regulate endogenous CK. The insufficient biosynthesis of ABA in the *sit* mutant led to the up-regulation of *SILOG2* and the concomitant accumulation of endogenous CKs. These effects were partially reversed by treatment with exogenous ABA. Nevertheless, the fact that ABA treatment fully restored the *sit* growth, while the overall amount of CKs was not suppressed to the WT level, raised several questions. These results provided an insight into the interactions between ABA and CKs during skotomorphogenesis, but a more focused study will be required to fully clarify the regulation of CK metabolism.

In conclusion, the results presented here demonstrate that ABA is important for promoting the rapid growth of tomato hypocotyls during skotomorphogenesis. Consistent with previous reports on adult plants we have shown that ABA is necessary to promote growth in young seedlings during the skotomorphogenic stage of development. It seems that this response is masked by homeostasis of endogenous ABA in the WT and can only be observed in ABA

deficient mutants. On the other hand, in the WT seedlings the significant increase in endogenous ABA levels could be observed during fast etiolated growth compared to the growth of de-etiolated seedlings. This shows the importance of ABA for cell elongation. Based on our results, we hypothesize that finely-tuned control of ABA metabolism during skotomorphogenesis promotes hypocotyl growth: ABA acts by stimulating the expression of the CDK inhibitors *SIKRP1* and *SIKRP3* and by inhibiting CK biosynthesis, both of which ultimately stimulate endoreduplication and cell expansion. While the full mechanisms of ABA action during skoto- and photomorphogenesis remain to be determined, our observations shed new light on the role of ABA during the development of young seedlings, and strongly suggest that at least in some stages of tomato seedling development, ABA stimulates growth.

Supporting Information

S1 Table. The hypocotyl length values used for data normalization.

(PDF)

S2 Table. Absolute quantification of free ABA.

(PDF)

S3 Table. Absolute quantification of free ABA in hypocotyls of ABA-deficient mutants.

(PDF)

S4 Table. Absolute quantification of CK levels.

(PDF)

S1 File. Supporting Information Tables. Table A in [S1 File](#) Fold change of *LeNCED1* transcript expression. Table B in [S1 File](#) Fold change of *SICYP707A3* transcript expression. Table C in [S1 File](#) Fold change of *SIKRP1* and *SIKRP3* transcript expression. Table D in [S1 File](#) Fold change of *SLOG2* transcript expression.

(PDF)

S1 Fig. The hypocotyl elongation of the *not* mutant treated with various concentrations of ABA.

(PDF)

S2 Fig. The effect of the *sit* mutation on hypocotyl length in BL-grown seedlings.

(PDF)

S3 Fig. The endogenous ABA content in fluridone treated WT hypocotyls (cv. Rutgers).

(PDF)

S4 Fig. The effect of fluridone on hypocotyl growth in dark-grown seedlings.

(PDF)

S5 Fig. The relative expression of the *SICYP707A2* and *SICYP707A4* genes.

(PDF)

Acknowledgments

The authors thank Renáta Plotzová, Jarmila Greplová and Věra Chytilová for their excellent technical support and seed propagation. We thank David Zalabák (Palacký University in Olomouc) for important help with the fixation of hypocotyl segments. We further thank Jan Nauš (Palacký University in Olomouc) for his measurements of the photon fluence rates and Nuria de Diego (Palacký University in Olomouc) for valuable discussion and critical reading of the

manuscript. We thank Tomáš Fürst (Palacký University in Olomouc) for revision of statistical analysis and Dave Richardson (Palacký University in Olomouc) for proof-reading of the manuscript.

Author Contributions

Conceived and designed the experiments: JFH VB. Performed the experiments: JFH MJ JŠ AP OT JR. Analyzed the data: JFH MJ AP JR ON. Contributed reagents/materials/analysis tools: MF. Wrote the paper: JFH VB MF.

References

1. Hansen H, Grossmann K (2000) Auxin-induced ethylene triggers abscisic acid biosynthesis and growth inhibition. *Plant Physiol* 124: 1437–1448. PMID: [11080318](#)
2. Davies PJ (2010) The plant hormones: their nature, occurrence, and functions. In: Davies PJ, editor. *Plant hormones: biosynthesis, signal transduction, action!* Dordrecht, The Netherlands: Springer. 9–11 p.
3. Rai MK, Shekhawat NS, Gupta AK, Phulwaria M, Ram K, et al. (2011) The role of abscisic acid in plant tissue culture: a review of recent progress. *Plant Cell Tiss Org* 106: 179–190.
4. Zhang J, Davies WJ (1990) Does ABA in the xylem control the rate of leaf growth in soil-dried maize and sunflower plants? *J Exp Bot* 41: 1125–1132.
5. Creelman RA, Mason HS, Bensen RJ, Boyer JS, Mullet JE (1990) Water deficit and abscisic acid cause differential inhibition of shoot versus root growth in soybean seedlings: Analysis of growth, sugar accumulation, and gene expression. *Plant Physiol* 92: 205–214. PMID: [16667248](#)
6. Munns R, Cramer GR (1996) Is coordination of leaf and root growth mediated by abscisic acid? *Opinion. Plant Soil* 185: 33–49.
7. Wakabayashi K, Sakurai N, Kuraishi S (1989) Role of the outer tissue in abscisic acid-mediated growth suppression of etiolated squash hypocotyl segments. *Physiol Plantarum* 75: 151–156.
8. Hayashi Y, Takahashi K, Inoue S-I, Kinoshita T (2014) Abscisic acid suppresses hypocotyl elongation by dephosphorylating plasma membrane H(+)-ATPase in *Arabidopsis thaliana*. *Plant Cell Physiol* 55: 845–853. doi: [10.1093/pcp/pcu028](#) PMID: [24492258](#)
9. Quarrie SA (1987) Use of genotypes differing in endogenous abscisic acid levels in studies of physiology and development. In: Hoad GV, Lenton J R, Jackson MB, Atkin RK, editors. *Hormone action in plant development—a critical appraisal*. London: Butterworths. pp. 89–105. doi: [10.1111/tpj.12742](#) PMID: [25624480](#)
10. Takahashi K (1972) Abscisic acid as a stimulator for rice mesocotyl growth. *Nat New Biol* 238: 92–93.
11. Saab IN, Sharp RE, Pritchard J, Voetberg GS (1990) Increased endogenous abscisic acid maintains primary root growth and inhibits shoot growth of maize seedlings at low water potentials. *Plant Physiol* 93: 1329–1336. PMID: [16667621](#)
12. Sharp RE, LeNoble ME, Else MA, Thorne ET, Gherardi F (2000) Endogenous ABA maintains shoot growth in tomato independently of effects on plant water balance: evidence for an interaction with ethylene. *J Exp Bot* 51: 1575–1584. PMID: [11006308](#)
13. LeNoble ME, Spollen WG, Sharp RE (2004) Maintenance of shoot growth by endogenous ABA: genetic assessment of the involvement of ethylene suppression. *J Exp Bot* 55: 237–245. PMID: [14673028](#)
14. Barrero JM, Piqueras P, González-Guzmán M, Serrano R, Rodríguez PL, et al. (2005) A mutational analysis of the *ABA1* gene of *Arabidopsis thaliana* highlights the involvement of ABA in vegetative development. *J Exp Bot* 56: 2071–2083. PMID: [15983017](#)
15. Arsovski AA, Galstyan A, Guseman JM, Nemhauser JL (2012) Photomorphogenesis. In *The Arabidopsis Book*. e0147. doi: [10.1199/tab.0147](#)
16. Barrero JM, Rodríguez PL, Quesada V, Alabadí D, Blázquez MA, et al. (2008) The *ABA1* gene and carotenoid biosynthesis are required for late skotomorphogenic growth in *Arabidopsis thaliana*. *Plant Cell Environ* 31: 227–234. PMID: [17996011](#)
17. Taylor IB, Linforth RST, Al-Naieb RJ, Bowman WR, Marples BA (1988) The wilty tomato mutants *flacca* and *sitiens* are impaired in the oxidation of ABA-aldehyde to ABA. *Plant Cell Environ* 11: 739–745.
18. Tal M, Nevo Y (1973) Abnormal stomatal behavior and root resistance, and hormonal imbalance in three wilty mutants of tomato. *Biochem Genet* 3: 291–300. PMID: [4701995](#)

19. Neill SJ, Horgan R (1985) Abscisic acid production and water relations in wilted tomato mutants subjected to water deficiency. *J Exp Bot* 36: 1222–1231.
20. Burbidge A, Grieve TM, Jackson A, Thompson A, McCarty DR, et al. (1999) Characterization of the ABA-deficient tomato mutant *notabilis* and its relationship with maize Vp14. *Plant J* 17: 427–431. PMID: [10205899](#)
21. Thompson AJ, Thorne ET, Burbidge A, Jackson AC, Sharp RE, et al. (2004) Complementation of *notabilis*, an abscisic acid-deficient mutant of tomato: Importance of sequence context and utility of partial complementation. *Plant Cell Environ* 27: 459–471.
22. Murashige T, Skoog A (1962) A revised medium for rapid growth and bio assays with tobacco tissue cultures. *Physiol Plantarum* 15: 473–497.
23. Schneider CA, Rasband WS, Eliceiri KW (2012) NIH Image to ImageJ: 25 years of image analysis. *Nat Methods* 9: 671–675. PMID: [22930834](#)
24. Pěňčík A, Rolčík J, Novák O, Magnus V, Barták P, et al. (2009) Isolation of novel indole-3-acetic acid conjugates by immunoaffinity extraction. *Talanta* 80: 651–655. doi: [10.1016/j.talanta.2009.07.043](#) PMID: [19836533](#)
25. Hoyerová K, Gaudinová A, Malbeck J, Dobrev PI, Kocábek T, et al. (2006) Efficiency of different methods of extraction and purification of cytokinins. *Phytochem* 67: 1151–1159. PMID: [16678229](#)
26. Dobrev PI, Kamínek M (2002) Fast and efficient separation of cytokinins from auxin and abscisic acid and their purification using mixed-mode solidphase extraction. *J Chromatogr A* 950: 21–29. PMID: [11990994](#)
27. Svačinová J, Novák O, Plačková L, Lenobel R, Holík J, et al. (2012) A new approach for cytokinin isolation from *Arabidopsis* tissues using miniaturized purification: pipette tip solid-phase extraction. *Plant Methods* 8: 17. doi: [10.1186/1746-4811-8-17](#) PMID: [22594941](#)
28. Dekkers BJ, Willems L, Bassel GW, van Bolderen-Veldkamp RP, Ligterink W, et al. (2012) Identification of reference genes for RT-qPCR expression analysis in *Arabidopsis* and tomato seeds. *Plant Cell Physiol* 53: 28–37. doi: [10.1093/pcp/pcr113](#) PMID: [21852359](#)
29. Doležel J, Greilhuber J, Suda J (2007) Estimation of nuclear DNA content in plants using flow cytometry. *Nat Protoc* 2: 2233–2244. PMID: [17853881](#)
30. Parks BM, Cho MH, Spalding EP (1998) Two genetically separable phases of growth inhibition induced by blue light in *Arabidopsis* seedlings. *Plant Physiol* 118: 609–615. PMID: [9765547](#)
31. Parks BM, Spalding EP (1999) Sequential and coordinated action of phytochromes A and B during *Arabidopsis* stem growth revealed by kinetic analysis. *P Natl Acad Sci USA* 96: 14142–14146. PMID: [10570212](#)
32. Kitahata N, Asami T (2011) Chemical biology of abscisic acid. *J Plant Res* 124: 549–557. doi: [10.1007/s10265-011-0415-0](#) PMID: [21461661](#)
33. Nitsch LM, Oplaat C, Feron R, Ma Q, Wolter-Arts M, et al. (2009) Abscisic acid levels in tomato ovaries are regulated by *LeNCED1* and *SICYP707A1*. *Planta* 299: 1335–1346.
34. Traas J, Hülskamp M, Gendreau E, Höfte H (1998) Endoreduplication and development: rule without dividing? *Curr Opin Plant Biol* 1: 498–503. PMID: [10066638](#)
35. Bergougnoux V, Zalabák D, Jandová M, Novák O, Wiese-Klinkenberg A, et al. (2012) Effect of blue light on endogenous isopentenyladenine and endoreduplication during photomorphogenesis and de-etiolation of tomato (*Solanum lycopersicum* L.) seedlings. *PLoS One*. 7, e45255. doi: [10.1371/journal.pone.0045255](#) PMID: [23049779](#)
36. Wang H, Qi Q, Schorr P, Cutler AJ, Crosby WL, et al. (1998) *ICK1*, a cyclin-dependent protein kinase inhibitor from *Arabidopsis thaliana* interacts with both *Cdc2a* and *CycD3*, and its expression is induced by abscisic acid. *Plant J* 15: 501–510. PMID: [9753775](#)
37. Bisbis B, Delmas F, Joubés J, Sicard A, Hernould M, et al. (2006) Cyclin-dependent kinase (CDK) inhibitors regulate the CDK-cyclin complex activities in endoreduplicating cells of developing tomato fruit. *J Biol Chem* 281: 7374–7383. PMID: [16407228](#)
38. Nafati M, Fagne N, Hernould M, Chevalier C, Gévaudant F (2010) Functional characterization of the tomato cyclin-dependent kinase inhibitor SIKRP1 domains involved in protein-protein interactions. *New Phytol* 188: 136–149. doi: [10.1111/j.1469-8137.2010.03364.x](#) PMID: [20618916](#)
39. Chen H, Zhang J, Neff MM, Hong S-W, Zhang H, et al. (2008) Integration of light and abscisic acid signaling during seed germination and early seedling development. *P Natl Acad Sci USA* 105: 4495–4500 doi: [10.1073/pnas.0710778105](#) PMID: [18332440](#)
40. Mäkelä P, Munns R, Colmer TD, Peltonen-Sainio P (2003) Growth of tomato and an ABA-deficient mutant (*sitiens*) under saline conditions. *Physiol Plantarum* 117: 58–63.

41. Aroca R, Del Mar Alguacil M, Vernieri P, Ruiz-Lozano JM (2008) Plant responses to drought stress and exogenous ABA application are modulated differently by mycorrhization in tomato and an ABA-deficient mutant (*sitiens*). *Microb Ecol* 56: 704–719. doi: [10.1007/s00248-008-9390-y](https://doi.org/10.1007/s00248-008-9390-y) PMID: [18443845](https://pubmed.ncbi.nlm.nih.gov/18443845/)
42. Sharp RE (2002) Interaction with ethylene: changing views on the role of abscisic acid in root and shoot growth responses to water stress. *Plant Cell Environ* 25: 211–222. PMID: [11841664](https://pubmed.ncbi.nlm.nih.gov/11841664/)
43. Taiz L, Zeiger E (2006) *Plant Physiology*, fourth edition. Sunderland, Massachusetts: Sinauer Associates, Inc., Publishers. Pp. 485–486. doi: [10.1016/j.ijssu.2006.06.025](https://doi.org/10.1016/j.ijssu.2006.06.025) PMID: [19059154](https://pubmed.ncbi.nlm.nih.gov/19059154/)
44. Dolezal K, Popa I, Krystof V, Spíchal L, Fojtíková M, et al. (2006) Preparation and biological activity of 6-benzylaminopurine derivatives in plants and human cancer cells. *Bioorg Med Chem* 14: 875–884. PMID: [16214355](https://pubmed.ncbi.nlm.nih.gov/16214355/)
45. Jones HG, Sharp CS, Higgs KH (1987). Growth and water relations of wilted mutants of tomato (*Lycopersicon esculentum* Mill.). *J Exp Bot* 38: 1848–1856.
46. Sindhu RK, Walton DC (1988) Xanthoxin metabolism in cell-free preparations from wild type and wilted mutants of tomato. *Plant Physiol* 88: 178–182. PMID: [16666262](https://pubmed.ncbi.nlm.nih.gov/16666262/)
47. Groot SP, Yperen II, Karssen CM (1991) Strongly reduced levels of endogenous abscisic acid in developing seeds of tomato mutant *sitiens* do not influence in vivo accumulation of dry matter and storage proteins. *Physiol Plantarum* 81: 73–78.
48. Leung J, Giraudat J (1998) Abscisic acid signal transduction. *Annu Rev Plant Physiol Plant Mol Biol* 49: 199–222. PMID: [15012233](https://pubmed.ncbi.nlm.nih.gov/15012233/)
49. Cutler SR, Rodriguez PL, Finkelstein RR, Abrams SR (2010) Abscisic acid: emergence of a core signaling network. *Annu Rev Plant Biol* 61: 651–679. doi: [10.1146/annurev-arplant-042809-112122](https://doi.org/10.1146/annurev-arplant-042809-112122) PMID: [20192755](https://pubmed.ncbi.nlm.nih.gov/20192755/)
50. Rushton DL, Tripathi P, Rabara RC, Lin J, Ringler P, et al. (2012) WRKY transcription factors: key components in abscisic acid signalling. *Plant Biotechnol J* 10: 2–11. doi: [10.1111/j.1467-7652.2011.00634.x](https://doi.org/10.1111/j.1467-7652.2011.00634.x) PMID: [21696534](https://pubmed.ncbi.nlm.nih.gov/21696534/)
51. Finkelstein R (2013) Abscisic acid synthesis and response. *Arabidopsis Book* 11: e0166. doi: [10.1199/tab.0166](https://doi.org/10.1199/tab.0166) PMID: [24273463](https://pubmed.ncbi.nlm.nih.gov/24273463/)
52. Brocard-Gifford I, Lynch TJ, Garcia ME, Malhotra B, Finkelstein RR (2004) The Arabidopsis thaliana ABCISIC ACID-INSENSITIVE8 locus encodes a novel protein mediating abscisic acid and sugar responses essential for growth. *Plant Cell* 16: 406–421. PMID: [14742875](https://pubmed.ncbi.nlm.nih.gov/14742875/)
53. Gonzalez-Guzman M, Pizzio GA, Antoni R, Vera-Sirera F, Merilo E, et al. (2012) Arabidopsis PYR/PYL/RCAR receptors play a major role in quantitative regulation of stomatal aperture and transcriptional response to abscisic acid. *Plant Cell* 24: 2483–2496. doi: [10.1105/tpc.112.098574](https://doi.org/10.1105/tpc.112.098574) PMID: [22739828](https://pubmed.ncbi.nlm.nih.gov/22739828/)
54. Kraepiel Y, Rousselin P, Sotta B, Kerhoas L, Einhorn J, et al. (1994) Analysis of phytochrome- and ABA-deficient mutants suggests that ABA degradation is controlled by light in *Nicotiana plumbaginifolia*. *Plant J* 6: 665–672.
55. Weatherwax SC, Ong MS, Degenhardt J, Bray EA, Tobin EM (1996) The interaction of light in the regulation of plant gene expression. *Plant Physiol* 111: 363–370. PMID: [8787022](https://pubmed.ncbi.nlm.nih.gov/8787022/)
56. Symons GM, Reid JB (2003) Hormone levels and response during de-etiolation in pea. *Planta* 216: 422–431. PMID: [12520333](https://pubmed.ncbi.nlm.nih.gov/12520333/)
57. Nagel OW, Konings H, Lambers H (1994) Growth rate, plant development and water relations of the ABA deficient tomato mutant *sitiens*. *Physiol Plantarum* 92: 102–108.
58. Perrot-Rechenmann C (2010) Cellular responses to auxin: division versus expansion. *Cold Spring Harb Perspect Biol*. 2: a001446. doi: [10.1101/cshperspect.a001446](https://doi.org/10.1101/cshperspect.a001446) PMID: [20452959](https://pubmed.ncbi.nlm.nih.gov/20452959/)
59. Wen B, Nieuwland J, Murray JAH (2013) The Arabidopsis CDK inhibitor ICK3/KRP5 is rate limiting for primary root growth and promotes growth through cell elongation and endoreduplication. *J Exp Bot* 64: 1–13. doi: [10.1093/jxb/ers358](https://doi.org/10.1093/jxb/ers358) PMID: [23264638](https://pubmed.ncbi.nlm.nih.gov/23264638/)
60. del Castellano M, Boniotti MB, Caro E, Schnittiger A, Gutierrez C (2004) DNA replication licensing affects cell proliferation or endoreplication in a cell type-specific manner. *Plant Cell* 16: 2380–2393. PMID: [15316110](https://pubmed.ncbi.nlm.nih.gov/15316110/)
61. Pettko-Szandtner A, Meszaros T, Horvath GV, Bako L, Csordas-Toth E, et al. (2006) Activation of an alpha cyclin-dependent kinase inhibitor by calmodulin-like domain protein kinase. *Plant J* 46: 111–123. PMID: [16553899](https://pubmed.ncbi.nlm.nih.gov/16553899/)
62. Alabadí D, Gallego-Bartolomé J, García-Cárcel L, Orlando L, Rubio V, et al. (2008) Gibberellins modulate light signalling pathways to prevent Arabidopsis seedling de-etiolation in darkness. *Plant J* 53: 324–335. PMID: [18053005](https://pubmed.ncbi.nlm.nih.gov/18053005/)

63. Yamburenko MV, Zubo YO, Vankova R, Kusnetsov VV, Kulaeva ON, et al. (2013) Abscisic acid represses the transcription of chloroplast genes. *J Exp Bot* 64: 4491–4502. doi: [10.1093/jxb/ert258](https://doi.org/10.1093/jxb/ert258) PMID: [24078671](https://pubmed.ncbi.nlm.nih.gov/24078671/)
64. Guan C, Wang X, Feng J, Hong S, Liang Y, et al. (2014) Cytokinin antagonizes abscisic acid-mediated inhibition of cotyledon greening of promoting the degradation of ABSCISIC ACID INSENSITIVE5 protein in Arabidopsis. *Plant Physiol* 164: 1515–1526. doi: [10.1104/pp.113.234740](https://doi.org/10.1104/pp.113.234740) PMID: [24443524](https://pubmed.ncbi.nlm.nih.gov/24443524/)
65. Valente P, Tao W, Verbelen JP (1998). Auxins and cytokinins control DNA endoreduplication and deduplication in single cells of tobacco. *Plant Sci* 134: 207–215.
66. Scofield S, Dewitte W, Nieuwland J, Murray JA (2013) The Arabidopsis homeobox gene SHOOT MER-STEMLESS has cellular and meristem-organisational roles with differential requirements for cytokinin and CYCD3 activity. *Plant J* 75: 53–66. doi: [10.1111/tpj.12198](https://doi.org/10.1111/tpj.12198) PMID: [23573875](https://pubmed.ncbi.nlm.nih.gov/23573875/)
67. Takahashi N, Kajihara T, Okamura C, Kim Y, Katagiri Y, et al. (2013) Cytokinins Control Endocycle Onset by Promoting the Expression of an APC/C Activator in Arabidopsis Roots. *Curr Biol* 23: 1812–1817. doi: [10.1016/j.cub.2013.07.051](https://doi.org/10.1016/j.cub.2013.07.051) PMID: [24035544](https://pubmed.ncbi.nlm.nih.gov/24035544/)
68. Brugiere N, Jiao S, Hantke S, Zinselmeier C, Roessler JA, et al. (2003) Cytokinin oxidase gene expression in maize is localized to the vasculature, and is induced by cytokinins, abscisic acid, and abiotic stress. *Plant Physiol* 132: 1228–1240. PMID: [12857805](https://pubmed.ncbi.nlm.nih.gov/12857805/)
69. Rivero RM, Gimeno J, Van Deynze A, Harkamal W, Blumwald E (2010) Enhanced cytokinin synthesis in tobacco plants expressing PSARK::IPT prevents the degradation of photosynthetic protein complexes during drought. *Plant Cell Physiol* 51: 1929–1941. doi: [10.1093/pcp/pcq143](https://doi.org/10.1093/pcp/pcq143) PMID: [20871100](https://pubmed.ncbi.nlm.nih.gov/20871100/)
70. Nambara E, Marion-Poll A (2005) Abscisic acid biosynthesis and catabolism. *Annu Rev Plant Biol* 56: 165–185. PMID: [15862093](https://pubmed.ncbi.nlm.nih.gov/15862093/)

Supporting table S1 The values of hypocotyl length used for data normalization. Medians, first and third quartiles are given. The control sample used for data normalization is marked as “norm.”

Figure	Genotype and/or treatment	Median hypocotyl length [mm]	1st quartile [mm]	3rd quartile [mm]	
2A	WT control	98	91	104	norm.
	WT 100 nM ABA	101	98	103	
	sit control	80	72	84	
	sit 100 nM ABA	99	94	106	
2B	control	53	46	62	norm.
	50 nM	76	67	81	
	100 nM	83	78	87	
	500 nM	74	69	80	
	1 μ M	74	64	80	
	5 μ M	46	38	52	
2C	control	73	66	83	norm.
	50 nM	77	67	81	
	100 nM	80	71	92	
	500 nM	74	63	85	
	1 μ M	69	56	78	
	5 μ M	41	22	58	
2D	WT control	101	95	104	norm.
	WT 50 nM ABA	100	91	106	
	not control	91	86	96	
	not 50 nM ABA	103	99	112	
S1	control	52	46	64	norm.
	50 nM	81	75	81	
	100 nM	84	77	86	
	500 nM	71	67	76	
	1 μ M	75	67	80	
	5 μ M	40	36	45	
S2	WT	28	22	33	norm.
	sit	26	23	27	
S4	control	68	62	73	norm.
	fluridone 10 μ M	53	51	57	

Supporting table S2 Absolute quantification of free ABA in tomato seedlings based on three independent experiments \pm SE from three technical replicates.

Sample	Set I.	Set II.	Set III.
	ABA [pmol/g FW]	ABA [pmol/g FW]	ABA [pmol/g FW]
6 h – D	29 \pm 2.5	9 \pm 0.7	45 \pm 3.6
12 h – D	18 \pm 5.4	6 \pm 0.4	25 \pm 4.2
24 h – D	5 \pm 0.1	4 \pm 0.3	n. a.
48 h – D	2 \pm 0.2	2 \pm 0.3	3 \pm 0.3
72 h – D	1 \pm 0.2	1 \pm 0.1	7 \pm 1.4
96 h – D	8 \pm 1.7	7 \pm 0.9	26 \pm 1.0
96 h – BL	5 \pm 0.7	3 \pm 0.5	8 \pm 1.2
120 h – D	11 \pm 0.5	15 \pm 0.6	32 \pm 0.8
120 h – BL	7 \pm 0.2	8 \pm 0.6	12 \pm 1.6

n. a.: not analyzed - sample lost during the analysis

Supporting table S3 Absolute quantification of free ABA in hypocotyls of ABA-deficient mutants and corresponding WTs based on two biological repeats \pm SE from two technical replicates.

Sample	Set I.	Set II.
	ABA [pmol/g FW]	ABA [pmol/g FW]
<i>sit</i>	0.8 \pm 0.2	0.8\pm0.1
WT (cv. Rheinlands-Ruhm)	17.9 \pm 0.4	18 \pm 1.9
<i>not</i>	2.6 \pm 0.5	2.9 \pm 0.0
WT (cv. Lukullus)	21.8 \pm 0.6	19.5 \pm 1.4

Supporting table S4 Absolute quantification of CK levels in tomato seedlings \pm SE based on three independent experiments. <LOD indicates that the levels of the corresponding compound were below the limit of detection; cZ *cis*-zeatin compounds, tZ *trans*-zeatin compounds, DHZ dihydrozeatin compounds, iP isopentenyladenine compounds, xR ribosides, xOG O-glucosides, x9G 9-glucosides, xMP monophosphates, x7G 7-glucosides.

CKs	wt control			wt 100 nM ABA			sit control			sit ABA 100 nM		
	[pmol/g FW] \pm SE			[pmol/g FW] \pm SE			[pmol/g FW] \pm SE			[pmol/g FW] \pm SE		
cZ	0.09	\pm	0.03	0.13	\pm	0.01	0.14	\pm	0.02	0.10	\pm	0.01
cZR	0.37	\pm	0.04	0.42	\pm	0.05	1.13	\pm	0.40	0.33	\pm	0.05
cZOG	0.09	\pm	0.03	0.13	\pm	0.02	0.14	\pm	0.01	0.08	\pm	0.01
cZ9G	0.15	\pm	0.00	0.14	\pm	0.01	0.11	\pm	0.02	0.10	\pm	0.01
cZROG	0.15	\pm	0.01	0.15	\pm	0.02	0.41	\pm	0.15	0.18	\pm	0.04
cZRMP	0.36	\pm	0.01	0.55	\pm	0.20	0.43	\pm	0.14	0.64	\pm	0.23
cZ7G	8.55	\pm	0.59	8.79	\pm	0.26	10.76	\pm	0.35	8.29	\pm	0.65
tZ	0.17	\pm	0.02	0.09	\pm	0.02	0.21	\pm	0.04	0.16	\pm	0.01
tZR	1.35	\pm	0.09	0.55	\pm	0.02	1.12	\pm	0.17	0.60	\pm	0.08
tZOG	0.10	\pm	0.02	0.07	\pm	0.02	0.13	\pm	0.03	0.08	\pm	0.01
tZ9G	0.28	\pm	0.03	0.18	\pm	0.00	0.46	\pm	0.06	0.28	\pm	0.05
tZROG	0.57	\pm	0.06	0.51	\pm	0.09	1.34	\pm	0.07	1.01	\pm	0.10
tZRMP	0.66	\pm	0.08	0.28	\pm	0.02	0.53	\pm	0.06	0.57	\pm	0.05
tZ7G	8.26	\pm	0.47	5.33	\pm	0.43	15.44	\pm	0.50	9.34	\pm	1.88
DHZ	0.01	\pm	0.00	0.01	\pm	0.00	0.02	\pm	0.00	0.01	\pm	0.00
DHZR	0.10	\pm	0.01	0.05	\pm	0.01	0.14	\pm	0.02	0.09	\pm	0.05
DHZOG	0.06	\pm	0.00	0.08	\pm	0.01	0.11	\pm	0.03	0.07	\pm	0.02
DHZ9G	<LOD			<LOD			<LOD			<LOD		
DHZROG	0.73	\pm	0.08	1.10	\pm	0.38	2.19	\pm	0.17	1.82	\pm	0.50
DHZRMP	<LOD			<LOD			<LOD			<LOD		
DHZ7G	23.29	\pm	1.40	26.91	\pm	4.26	73.61	\pm	0.61	44.07	\pm	3.54
iP	0.24	\pm	0.02	0.42	\pm	0.09	0.33	\pm	0.06	0.32	\pm	0.12
iPR	0.12	\pm	0.03	0.14	\pm	0.04	0.31	\pm	0.07	0.26	\pm	0.06
iP9G	0.12	\pm	0.02	0.15	\pm	0.04	0.13	\pm	0.01	0.15	\pm	0.02
iPRMP	0.40	\pm	0.07	0.31	\pm	0.09	0.49	\pm	0.06	0.41	\pm	0.06
iP7G	14.43	\pm	0.94	14.09	\pm	1.02	40.38	\pm	3.59	48.05	\pm	1.12
SUMA	60.64	\pm	4.02	60.58	\pm	7.12	150.07	\pm	6.63	117.00	\pm	8.66

Supporting table A Fold change in *LeNCED1* transcript expression based on three independent experiments.

Sample	Set I. Relative expression	Set II. Relative expression	Set III. Relative expression
6 h – D	0.07	0.00	0.00
12 h – D	0.00	0.00	0.00
24 h – D	0.04	0.00	0.00
48 h – D	0.00	0.00	0.00
72 h – D	0.24	0.04	0.17
96 h – D	0.75	0.30	0.54
96 h – BL	0.32	0.12	0.23
120 h – D	1.00	1.00	1.00
120 h – BL	0.46	0.34	0.51

Supporting Table B Fold change in *SICYP707A3* transcript expression based on three independent experiments.

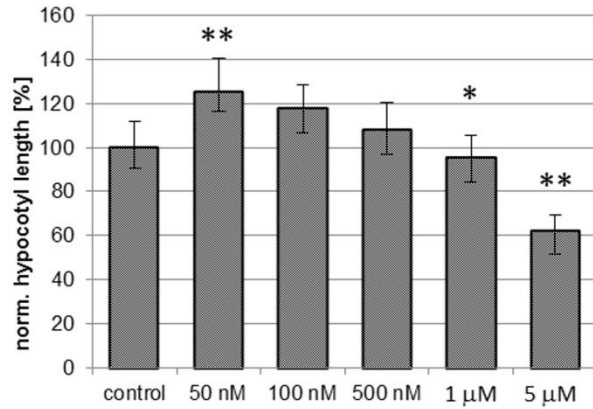
Sample	Set I. Relative expression	Set II. Relative expression	Set III. Relative expression
6 h – D	0.60	1.13	0.72
12 h – D	1.33	1.36	1.72
24 h – D	1.42	2.29	1.22
48 h – D	3.64	1.90	2.14
72 h – D	1.33	2.21	0.73
96 h – D	0.91	1.17	0.82
96 h – BL	1.63	5.37	2.34
120 h – D	1.00	1.00	1.00
120 h – BL	1.73	1.02	1.88

Supporting table C Fold change in *SIKRP1* and *SIKRP3* transcript expression based on three independent experiments.

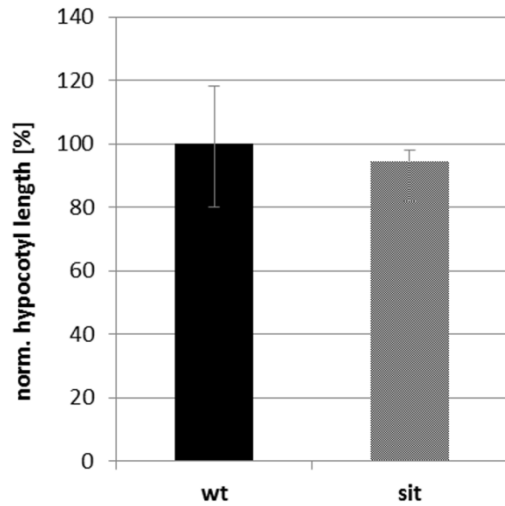
Gene	Sample	Set I. Relative expression	Set II. Relative expression	Set III. Relative expression
<i>SIKRP1</i>	wt control	1.00	1.00	1.00
	wt ABA 100 nM	0.91	1.00	1.11
	<i>sit</i> control	0.83	0.78	0.89
	<i>sit</i> ABA 100 nM	0.95	0.89	1.04
<i>SIKRP3</i>	wt control	0.57	0.60	0.64
	wt ABA 100 nM	0.50	0.66	0.67
	<i>sit</i> control	0.46	0.45	0.50
	<i>sit</i> ABA 100 nM	0.55	0.50	0.62

Supporting table D Fold change in *SILOG2* transcript expression based on three independent experiments.

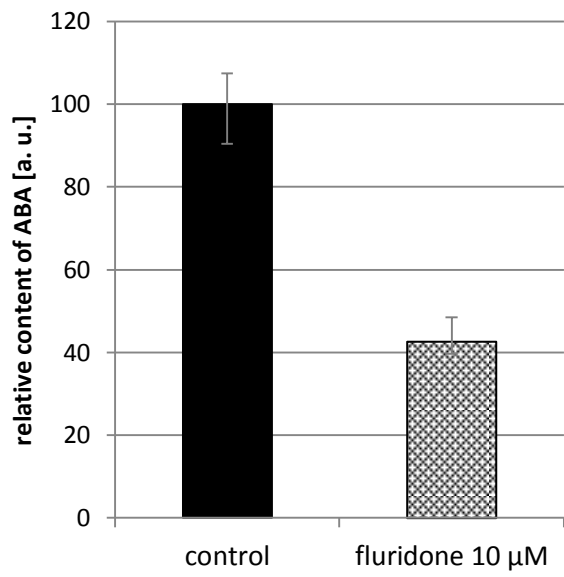
Sample	Set I. Relative expression	Set II. Relative expression	Set III. Relative expression
wt control	1.00	1.00	1.00
wt ABA 100 nM	0.76	0.93	0.88
<i>sit</i> control	1.39	2.49	1.98
<i>sit</i> ABA 100 nM	1.12	1.57	1.35



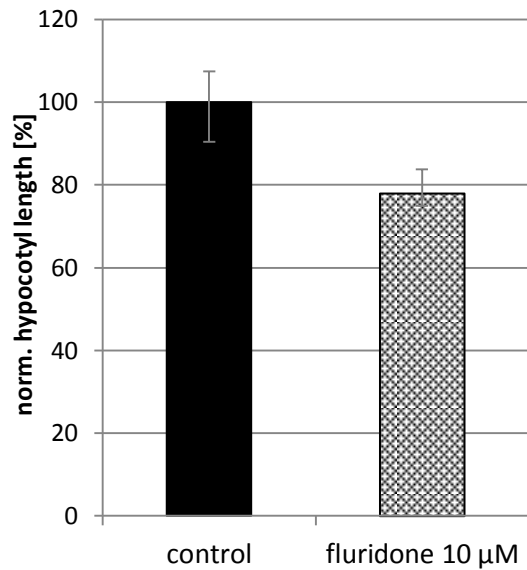
Supporting figure S1 The hypocotyl elongation of *not* mutant treated with various concentrations of ABA. Germinated seeds were transferred on basal media (control) or media supplemented with ABA and grown in the dark for 4 days. The results shown in the figure represent the medians of normalized length of hypocotyls from 1 independent experiment; the error bars represent the boundaries of the first and third quartiles. The sample “control” was set as 100% hypocotyl length and all other values (medians, quartiles) are expressed as percentage of this value. To prove significance the Kruskal-Wallis ANOVA with multiple post-hoc comparison was performed. Asterisks denote values that differ significantly from “control” sample (** $p < 0.01$, * $p < 0.05$; $n=135$).



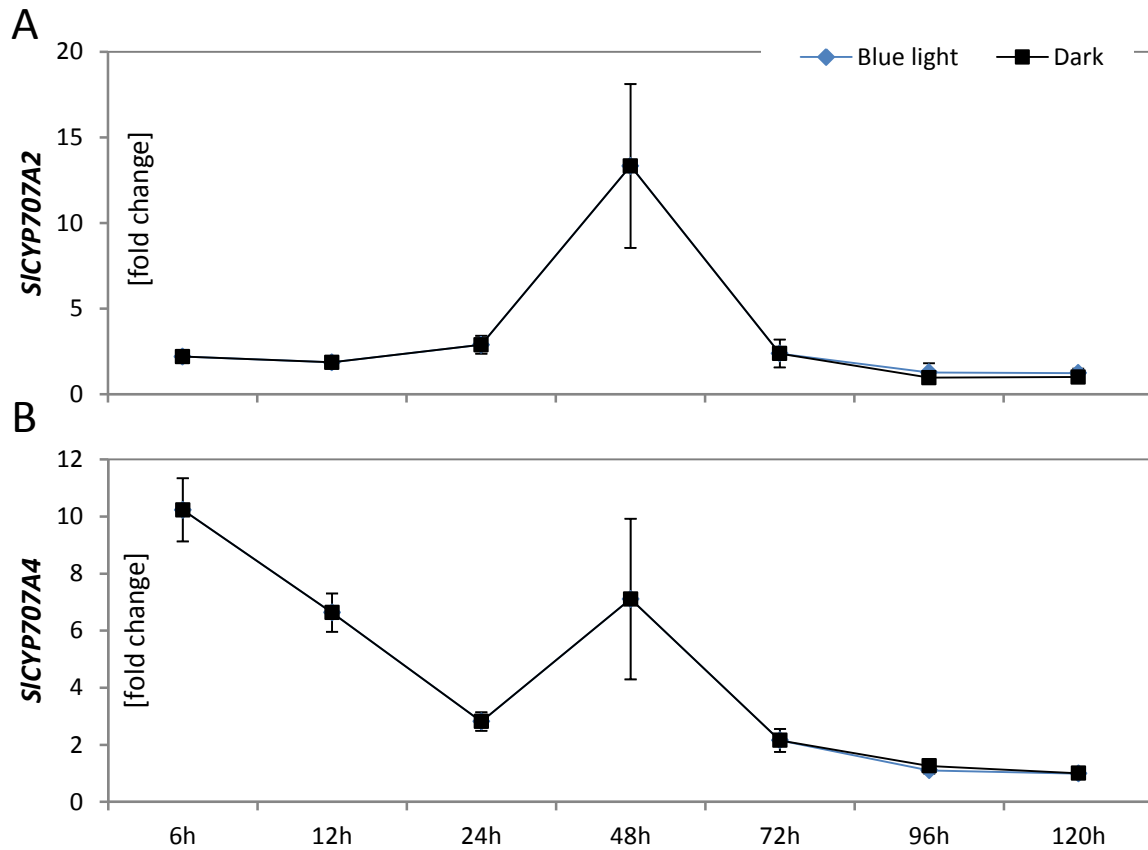
Supporting figure S2 The effect of the *sit* mutation on hypocotyl length in BL-grown seedlings. Seeds of the WT (cv. Rheinlands Ruhm) and *sit* mutant were germinated in darkness and then grown under continuous BL for 4 days. The results shown in the figure represent the medians of normalized length of hypocotyls from 1 independent experiment; the error bars represent the boundaries of the first and third quartiles. The sample "wt" was set as 100% hypocotyl length and all other values (medians, quartiles) are expressed as percentage of this value (Mann-Whitney test, $p > 0.05$, $n=40$).



Supporting figure S3 The endogenous ABA content in fluridone treated WT hypocotyls (cv. Rutgers). Free ABA levels are reported as relative means [a.u.] \pm SE based on two independent experiments. The control sample was assigned a value of 100 a.u.



Supporting figure S4 The effect of fluridone on hypocotyl growth in dark-grown seedlings. Germinated seeds of WT (cv. Rutgers) were transferred to media supplemented with 10 μM fluridone and grown for 4 days in darkness. The results shown in the figure represent the medians of normalized length of hypocotyls from 2 independent experiments; the error bars represent the boundaries of the first and third quartiles. The control sample was set as 100% hypocotyl length. Other values (medians, quartiles) are expressed as percentage of these values. The statistical significance was evaluated by Mann-Whitney U test; $p < 0.02$.



Supporting figure S5 The relative expression of the A) *SICYP707A2* and B) *SICYP707A4* ABA catabolic genes. Values shown are the geometric means of three biological replicates \pm SE. *Tip41like* and *PP2ACs* were used as housekeeping genes. All values are expressed in arbitrary units relative to the expression of the corresponding gene in the 120h-Dark¹ sample.

Supplement VI

Von Schwartzberg, K., Lindner, A. C., Gruhn, N., **Šimura, J.**, Novák, O., Strnad, M., Gonneau, M., Nogué, F., & Heyl, A. (2015). CHASE domain-containing receptors play an essential role in the cytokinin response of the moss *Physcomitrella patens*. *Journal of Experimental Botany*, 67(3), 667-679.



RESEARCH PAPER

CHASE domain-containing receptors play an essential role in the cytokinin response of the moss *Physcomitrella patens*

Klaus von Schwartzberg^{1,†,*}, Ann-Cathrin Lindner^{1,†}, Njuscha Gruhn², Jan Šimura³, Ondřej Novák³, Miroslav Strnad³, Martine Gonneau⁴, Fabien Nogué⁴ and Alexander Heyl^{2,5,*}

¹ Biozentrum Klein Flottbek, Universität Hamburg, Ohnhorststr. 18, D-22609 Hamburg, Germany

² Institute for Biology/ Applied Genetics, Dahlem Centre of Plant Sciences, Freie Universität Berlin, Albrecht-Thaer-Weg 6, D-14195 Berlin, Germany

³ Laboratory of Growth Regulators & Department of Chemical Biology and Genetics, Centre of the Region Haná for Biotechnological and Agricultural Research, Palacký University & Institute of Experimental Botany ASCR, Šlechtitelů 27, CZ-783 71 Olomouc, Czech Republic

⁴ Institut Jean-Pierre Bourgin, UMR1318 INRA-AgroParisTech, INRA Centre de Versailles-Grignon, Route de St-Cyr, 78026 Versailles Cedex, France

⁵ Biology Department, Adelphi University, Science 116, 1 South Avenue, PO Box 701, Garden City, NY 11530-070, USA

* To whom correspondence should be addressed. E-mail: klaus.von.schwartzberg@uni-hamburg.de or ahey@adelphi.edu

† These authors contributed equally to this work.

Received 15 June 2015; Revised 7 October 2015; Accepted 12 October 2015

Editor: James Murray, Cardiff University

Abstract

While the molecular basis for cytokinin action is quite well understood in flowering plants, little is known about the cytokinin signal transduction in early diverging land plants. The genome of the bryophyte *Physcomitrella patens* (Hedw.) B.S. encodes three classical cytokinin receptors, the CHASE domain-containing histidine kinases, CHK1, CHK2, and CHK3. In a complementation assay with protoplasts of receptor-deficient *Arabidopsis thaliana* as well as in cytokinin binding assays, we found evidence that CHK1 and CHK2 receptors can function in cytokinin perception. Using gene targeting, we generated a collection of CHK knockout mutants comprising single ($\Delta chk1$, $\Delta chk2$, $\Delta chk3$), double ($\Delta chk1,2$, $\Delta chk1,3$, $\Delta chk2,3$), and triple ($\Delta chk1,2,3$) mutants. Mutants were characterized for their cytokinin response and differentiation capacities. While the wild type did not grow on high doses of cytokinin (1 μ M benzyladenine), the $\Delta chk1,2,3$ mutant exhibited normal protonema growth. Bud induction assays showed that all three cytokinin receptors contribute to the triggering of budding, albeit to different extents. Furthermore, while the triple mutant showed no response in this bioassay, the remaining mutants displayed budding responses in a diverse manner to different types and concentrations of cytokinins. Determination of cytokinin levels in mutants showed no drastic changes for any of the cytokinins; thus, in contrast to *Arabidopsis*, revealing only small impacts of cytokinin signaling on homeostasis. In summary, our study provides a first insight into the molecular action of cytokinin in an early diverging land plant and demonstrates that CHK receptors play an essential role in bud induction and gametophore development.

Key words: Bryophyte, cytokinin, cytokinin receptor, evolution, moss, *Physcomitrella patens*, phytohormone, plant growth regulator, signaling, two-component system.

Introduction

Phytohormones regulate many processes in plants such as the development of tissues and organs and the response to changes in the environment. One class of phytohormones, the cytokinins, is comprised of adenine derivatives carrying an isoprenoid or an aromatic side chain at the N^6 -position (Mok and Mok, 2001). Cytokinin signaling is mediated via a multistep His-to-Asp phosphorelay system, a variant of the bacterial two-component system (TCS). While this type of signaling system is widespread in prokaryotes, it is unique to plants among multicellular eukaryotes (Heyl and Schmölling, 2003). For *Arabidopsis thaliana*, the current model of this signaling pathway predicts that the cytokinin ligand is bound by hybrid histidine kinase receptors via the cyclases/histidine kinases associated sensory extracellular (CHASE) domain (Anantharaman and Aravind, 2001; Mougél and Zhulin, 2001; Heyl *et al.*, 2007). These CHASE domain-containing histidine kinases (CHKs) were shown to localize mainly to the endoplasmic reticulum (ER) (Caesar *et al.*, 2011; Lomin *et al.*, 2011; Wulfetange *et al.*, 2011). The binding of the cytokinin ligand causes an autophosphorylation of the CHK receptor. After an intramolecular phosphotransfer, the signal is transmitted by phosphorylation to histidine phosphotransmitter proteins (HPTs), which shuttle between the cytoplasm and the nucleus (Punwani *et al.*, 2010). In the nucleus, the HPTs activate type-B response regulators (RRBs), transcriptional regulators belonging to the class of Myb transcription factors via phosphorylation. Subsequently these transcription factors initiate the transcription of their target genes, one group of which are the type-A RRs (RRAs). RRA proteins have been shown to be involved in a negative feedback mechanism of the cytokinin signaling pathway (Hwang and Sheen, 2001; To *et al.*, 2004). Most of the research on this signaling pathway has been done using the model plant *Arabidopsis*, but work in other plants species also contributed to the elucidation of the functioning of the pathway (Heyl *et al.*, 2006a; Hellmann *et al.*, 2010).

One of the open questions in cytokinin biology is the origin and evolution of this regulatory system and its contribution to the conquest of land by plants. Nevertheless, our knowledge of the cytokinin biology of algae and early diverging land plants is very limited (Tarakhovskaya *et al.*, 2007; Pils and Heyl, 2009; von Schwartzberg, 2009; Frébort *et al.*, 2011; Spíchal, 2012; Gruhn and Heyl, 2013). The streptophyta alga *Klebsormidium flaccidum* was recently shown to code for all parts of the TCS system in the evolution of the green lineage prior to the conquest of land (Hori *et al.*, 2014). The moss *Physcomitrella patens* as an early diverging land plant also encodes all protein families involved in cytokinin biosynthesis, metabolism, and signaling (Pils and Heyl, 2009; Frébort *et al.*, 2011; Spíchal, 2012; Gruhn and Heyl, 2013; Gruhn *et al.*, 2014). Due to its simple developmental differentiation and its responsiveness to several plant hormones, *P. patens* is a long-standing model regarding hormonal action and homeostasis (Wang *et al.*, 1981; Cove, 2005; Decker *et al.*, 2006; von Schwartzberg, 2006, 2009). Twenty different endogenous cytokinins were detected and quantified

in *P. patens*, and the generation of cytokinin-deficient plants revealed the importance of extracellular cytokinins for bud formation (von Schwartzberg *et al.*, 2007). Furthermore, the apparent absence of adenylate isopentenyltransferases (IPTs), the key enzymes for cytokinin production in flowering plants, makes *P. patens* an interesting organism for studying cytokinin biology in general (Yevdakova and von Schwartzberg, 2007; Yevdakova *et al.*, 2008; Frébort *et al.*, 2011; Patil and Nicander, 2013; Lindner *et al.*, 2014). While cytokinin metabolism has a long tradition as a topic in *P. patens* research (reviewed by von Schwartzberg, 2009), the signaling of this phytohormone has only recently attracted the attention of researchers (Pils and Heyl, 2009; Ishida *et al.*, 2010). Last year a new subfamily of cytokinin receptors was described containing eight members from *P. patens* (Gruhn *et al.*, 2014). This discovery makes this moss the only plant which encodes both classical and newly identified cytokinin receptors in its genome, and it raises the question of the biological role of both receptor subfamilies in *P. patens*.

Here we present the characterization of the three classical CHASE domain-containing histidine kinase cytokinin receptors from *P. patens*. Following the suggested nomenclature (Heyl *et al.*, 2013), we refer to them as CHK1, CHK2, and CHK3 and describe their role in differentiation processes of the moss. Our results show that the proteins can function as cytokinin receptors in different assays, and analysis of single, double, and the triple mutants demonstrated that CHK1, CHK2, and CHK3 are necessary for cytokinin perception by the moss. The results highlight the importance of these receptors for the cytokinin response in this early diverging land plant species.

Materials and methods

CHK full-length cDNAs

For the functional assays it was essential to isolate the respective cDNA clone for each of the three receptor genes (genomic loci: *CHK1*, Pp1s50_141; *CHK2*, Pp1s194_72; *CHK3*, Pp1s252_49; see <http://www.cosmoss.org>; Lang *et al.*, 2005). By using degenerated *AHK4* primers (degAHK4 for, genathgaycargaracnttygc; and degAHK4 rev, tngngtytgngcrtartc) on wild-type protonemal cDNA, two 942 bp fragments (*CHK1*-942 and *CHK2*-942) were amplified, subcloned, and sequenced. To retrieve the *CHK1* sequence (accession no. KJ697768, 3123 bp), the *CHK1*-942 fragment was used as a probe to isolate *CHK1* from a *P. patens* λ ZAPII cDNA library (Strepp *et al.*, 1998), according to standard procedures. Full-length *CHK2* (accession no. KJ697769, 3249 bp) was achieved by RACE (rapid amplification of cDNA ends) (SMART 5' and 3' RACE cDNA amplification kit; Clontech) with gene-specific primers (*cre2* 5' RACE, gcagtagacggcgaagtgtaaca; and *cre2* 3' RACE, tgccgtcatagcgaagtctcagt) on Δ *chk1* cDNA. To retrieve *CHK3* (accession no. KJ697770, 3306 bp), specific primers (*chk3* for, atgagacaagaacagttgatcaatcc; and *chk3* rev, attcgctggaa-gaaatgctttgcaacc) were used to amplify and subclone *CHK3* from cDNA derived from 4-week-old gametophores. Partial sequencing served to prepare a complete cDNA by commercial gene synthesis (GenScript, Piscataway, NJ, USA).

Cytokinin binding assay

The cytokinin binding assay was performed as has been described previously (Romanov and Lomin, 2009). In brief, the respective

cytokinin receptor (*AHK4*, *CHK1*, *CHK2*, and *CHK3*) was cloned into the pDEST15 vector (Invitrogen, Karlsruhe, Germany) and expressed using the *Escherichia coli* strain BL21 (DE) pLys. The empty pDEST15 vector was used as a negative control. Tritium-labeled *trans*-[³H]zeatin (*tZ*; 592 GBq mmol⁻¹) was obtained from the Isotope Laboratory of the Institute of Experimental Botany (Prague, Czech Republic).

In planta complementation assay

A protoplast transactivation assay (PTA) using protoplasts from the *Arabidopsis ahk2, ahk3* double mutant was conducted as previously described (Choi *et al.*, 2012). In brief, mesophyll protoplasts were isolated from 5- to 6-week-old *Arabidopsis* plants of the *ahk2, ahk3* double cytokinin receptor knockout. The 350 bp promoter fragment of the type-A response regulator *ARR6* was used as a reporter construct and the type-B response regulator *ARR2* as an effector. As an activator, the cDNAs of *CHK1*, *CHK2*, and *CHK3* as well as that of *AHK4* as a positive control were co-expressed with *ARR2*, respectively. The empty expression vector served as a negative control. The enzyme neuraminidase (NAN) was used as an internal control to standardize expression levels and to calculate relative expression levels (Kirby and Kavanagh, 2002). The details of the PTA protocol and the analysis of the results have been published previously (Ramireddy *et al.*, 2013).

P. patens culture

The sequenced wild-type *P. patens* Hedw. Bruch & Schimp strain used in this study was collected from Gransden Wood, Huntingdonshire, UK in 1968 (Rensing *et al.*, 2008). Standard growth conditions were 25 °C, in white light (100 μE m⁻² s⁻¹) for a light:dark cycle of 16:8 h. For transformation and cytokinin profiling, liquid cultures were regularly disintegrated and grown in A'BCD(N)TV medium [0.356 mM Ca(NO₃)₂, 1.01 mM MgSO₄, 1.84 mM KH₂PO₄, 10 mM KNO₃, 0.044 mM FeSO₄ supplemented with Hoagland trace element solution (1 ml l⁻¹) and the vitamins nicotinic acid (8 μM), *p*-aminobenzoic acid (1.8 μM), and thiamine HCl (1.5 μM)] according to Wang *et al.* (1981). For phenotyping, budding assays, and quantitative real-time PCR, cultivation was performed on KNOP agar medium according to Hahn and Bopp (1968).

Generation of chk knockout mutants

A Δ *chk* mutant collection comprising three single mutants, three double mutants, and one triple mutant was generated by sequential protoplast transformation with gene-disrupting vectors. The targeted loci, details on mutant generation [vector cloning, transformation protocol, and antibiotic selection Supplementary Table S1], as well as characterization [proof of insertion via PCR (see Supplementary Fig. S3) and absence of transcript (via RT-PCR (see Supplementary Fig. S4)], are given as the Supplementary data available at *JXB* online. For the Δ *chk1* mutants, a 300 bp fragment has been deleted (scaffold_50:1326711..1326313), for Δ *chk2* 77 bp (scaffold_194:351,070..351,147), and for Δ *chk3* 5016 bp (scaffold_252:345,051..350,06 (5016 bp).

Budding assay

Budding assays were performed as previously described by von Schwartzenberg *et al.* (2007) after cultivation of protonema for 10 d.

Cytokinin analysis by UHPLC-MS/MS

Liquid cultures of the wild type and the three double mutants (Δ *chk1,2*; Δ *chk1,3*; Δ *chk2,3*) as well as the triple mutant were grown for 21 d and harvested as previously described (von Schwartzenberg *et al.*, 2007). Three biological replicates were grown separately for the wild type and each mutant line. The extraction and purification

was carried out in two technical replicates for each biological replicate. Samples (5 mg DW) were homogenized under liquid nitrogen, extracted in modified Bielecki buffer (methanol/ water/formic acid, 15/4/1, v/v/v) (Novák *et al.*, 2008), and then purified using two solid phase extraction columns, a C18 octadecylsilica-based column (500 mg of sorbent, Applied Separations) and after that an MCX column (30 mg of C18/SCX combined sorbent with cation-exchange properties, Waters) (Dobrev and Kamínek, 2002). Analytes were eluted by two-step elution using a 0.35 M NH₄OH aqueous solution and 0.35 M NH₄OH in 60% (v/v) MeOH solution. Cytokinin levels were determined using ultra high performance liquid chromatography-electrospray tandem mass spectrometry (UHPLC-MS/MS) with stable isotope-labeled internal standards as a reference (Svacinova *et al.*, 2012).

RNA isolation and real-time PCR

RNA was extracted from the wild type as well as from the three double mutants and the triple mutant using the Trifast Reagent (Peqlab, Germany) according to the manufacturer. After DNaseI (Fermentas, Germany) treatment, cDNA was synthesized using peqGOLD M-MULV H plus (Peqlab). Real-time PCR was performed on a SteponePlus cycler (Applied Biosystems) using gene-specific primers and KAPA SYBR FAST Universal (Peqlab). Ribosomal protein L21 (Wang and Irving, 2011) was used as an endogenous control, and a primer efficiencies >95% were established for all targets (primers are given in Supplementary Table S2 at *JXB* online). Calculations were performed using the Stepone Software V. 2.3 with the $\Delta\Delta$ Ct method.

Results

CHK1 and CHK2 bind *trans*-zeatin in an *in vivo* binding assay

The sequences for the three *CHK*-coding sequences were retrieved by PCR cloning and submitted to the NCBI (*CHK1*, KJ697768; *CHK2*, KJ697769; and *CHK3*, KJ697770). In order to test the functionality of the three cytokinin receptors, we employed a cytokinin binding assay (Suzuki *et al.*, 2001; Yamada *et al.*, 2001; Romanov and Lomin, 2009). The cloned receptors and the respective controls were expressed in *E. coli* and the binding of radiolabeled *tZ* was tested. The assay was performed with *AHK4* and the empty vector as positive and negative controls, respectively (Romanov *et al.*, 2005; Heyl *et al.*, 2007). *CHK1* and *CHK2* showed binding of *tZ* that was clearly above background (Fig. 1). Surprisingly, in this assay we did not detect any *tZ* binding for *CHK3* although the protein was expressed in sufficient quantities (see Supplementary Fig. S1 at *JXB* online).

CHK1 and CHK2 function as cytokinin receptors in an *in planta* complementation assay

In order to test the *in vivo* functionality of the three cytokinin receptors, we employed an *in planta* complementation assay in which a candidate receptor is expressed in protoplasts from *Arabidopsis* plants in which two of the three cytokinin receptors are mutated (*ahk2, ahk3*) (Choi *et al.*, 2012). The complementation was quantified using a β -glucuronidase (GUS) reporter gene. All genes were individually expressed under the control of the 35S promoter

and the cells were treated with *tZ*. Using the cytokinin receptor AHK4 from *Arabidopsis* as a positive control, *ahk2,ahk3* was complemented as described previously, while the empty vector as negative control showed only a weak activation of the reporter gene (Fig. 2). Of the three cytokinin receptors, only CHK1 and CHK2 showed a complementation in the double mutant. In fact, they complemented the *ahk2,ahk3* double mutant even better than AHK4. However, no receptor activity was detected in this assay for CHK3 as compared with the controls (Fig. 2).

Taking the results of the binding and complementation assay together, it was shown that at least two of the three classical CHK proteins fulfill the requirements to function as a cytokinin receptor.

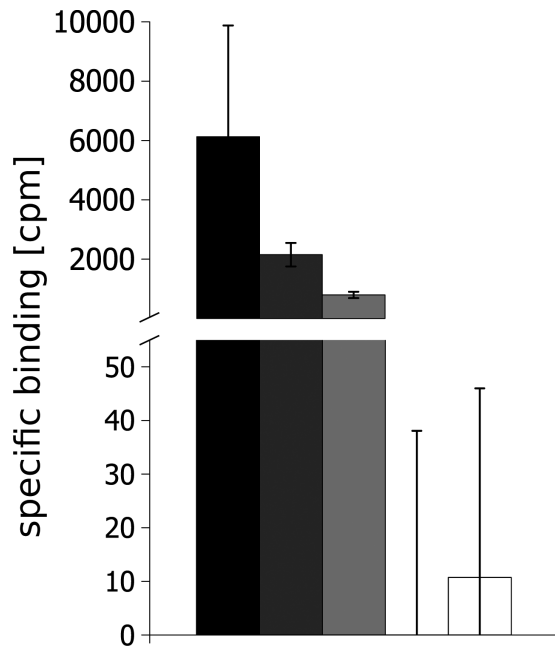


Fig. 1. CHK1 and CHK2 bind *tZ* in an *in vivo* cytokinin binding assay. All receptors were expressed as GST fusion proteins in *E. coli* strain BL21 (DE) pLys. The specific binding to *trans*-[2-³H]zeatin was analyzed according to Romanov and Lomin (2009). Shown are biological replicates ($n=3$) and their SD (error bars). Expression of the different fusion proteins was confirmed by western blot (see Supplementary Fig. S1 at *JXB* online).

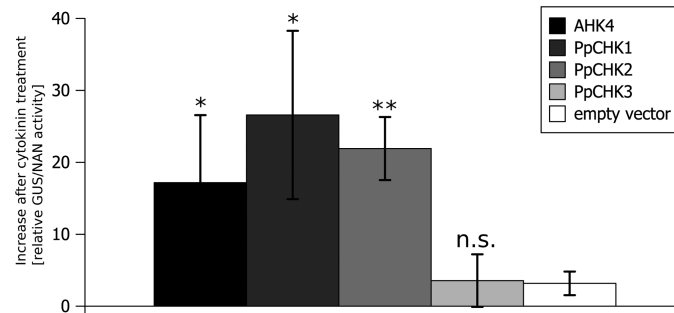


Fig. 2. *P. patens* cytokinin receptors PpCHK1 and PpCHK2 activate the cytokinin-dependent TCS in *ahk2-5,ahk3-7* double knockout mutant of *Arabidopsis*. Cytokinin perception-deficient protoplasts (*ahk2-5,ahk3-7*) (Riefeler *et al.*, 2006) were co-transformed with the cytokinin-responsive *ARR2* (effector), the *ARR6* promoter fused to β -glucuronidase (reporter), 35S::NAN (internal reference), and the indicated cytokinin receptor (activator) under the control of the 35S promoter. Protoplasts were incubated overnight with and without *trans*-zeatin; subsequently *ARR6* promoter *trans*-activation was measured. Results were normalized by the internal reference, and the specific activity upon cytokinin treatment was calculated (normalized reporter activity with cytokinin minus normalized reporter activity without cytokinin). Depicted results are mean values of three biological replicates, and whiskers represent the SD ($n=3$, mean \pm SD, *t*-test different from vector control, * $P<0.05$; ** $P<0.005$; n.s., not significant).

Generation of Δchk knockout mutants

In order to characterize the *in planta* function of the CHK1, CHK2, and CHK3 receptors in *P. patens*, a mutant collection comprising single ($\Delta chk1$, $\Delta chk2$, and $\Delta chk3$), double ($\Delta chk1,2$; $\Delta chk1,3$; and $\Delta chk2,3$), and triple ($\Delta chk1,2,3$) mutants was generated by protoplast transformation using gene targeting constructs for each locus. Detailed information of the generation and characterization of this collection are provided in Supplementary Fig. S2 at *JXB* online. Each of the constructs harbored a different resistance cassette (for selection on G418, hygromycin B, and zeocin, respectively), thus enabling selection of plants with up to three *CHK* loci targeted. Mutants were analyzed by detailed PCR-based characterization of genomic DNA (see Supplementary Fig. S3) and cDNA (see Supplementary Fig. S4) which proved that (i) the respective *CHK* loci were targeted and (ii) the corresponding transcripts were no longer detectable. Furthermore, it was confirmed that the mutants had maintained the haploid status using flow cytometry (not shown).

Phenotype of *CHK* knockout mutants: protonema and gametophore development

Knockout of a single receptor in $\Delta chk1$ or $\Delta chk2$ altered the growth morphology of moss grown on agar medium. Wild-type colonies showed a large area with undifferentiated protonema in the outer parts, and displayed bud and gametophore formation in the inner parts. The $\Delta chk1$ and $\Delta chk2$ single mutants had a smaller colony diameter and fewer protruding protonema. In contrast, $\Delta chk3$ did not exhibit a reduction of the colony size (Fig. 3C, E, G). For the double mutants, the colony size was most strongly reduced for $\Delta chk1,3$ (Fig. 3D, F, H). Detailed data on colony diameter over 6 weeks are given in Supplementary Fig. S5A at *JXB* online).

While the gametophores formed by $\Delta chk1$ mutants had an average size comparable with the wild type, the size of gametophores of $\Delta chk2$ and $\Delta chk3$ was reduced. The size of the gametophores formed by $\Delta chk1,2$ was

drastically reduced compared with the wild type and the single mutants (Fig. 3D). Gametophores of the $\Delta chk1,3$ and the $\Delta chk2,3$ mutants were smaller compared with the wild type, although they were larger than gametophores of $\Delta chk1,2$. This indicates the relevance of CHK1 and CHK2 for gametophore development. The development of gametophores in the double mutants occurred as for the wild type within 2 weeks of culture (Supplementary Fig. S5B at *JXB* online). All three *CHK* double mutants eventually developed antheridia and archegonia, produced a sporophyte after water-mediated fertilization, and finally completed the entire life cycle with the germination of haploid spores.

The triple receptor mutant $\Delta chk1,2,3$ showed a minor reduction in colony diameter compared with the wild type. However, the number of gametophores per colony was reduced as the colony consisted mainly of protonema. Gametophore formation was delayed by ~1 week (Supplementary Fig. S5B at *JXB* online). Furthermore, even after 14 weeks, the size of the gametophores was <20% of the size of the wild type, indicating the importance of all three receptors not only for bud initiation but also for gametophore development (Fig. 3B). This result functionally links two essential processes in the development of the moss, namely the onset of budding and gametophore formation, to the cytokinin receptors. Moreover, no antheridia and archegonia were observed for the triple mutants which arrested their life cycle at the gametophore stage, further highlighting the importance of the classical cytokinin receptors for the life cycle of *P. patens*.

CHK mutants display an altered cytokinin tolerance and response

Next, we investigated the effect of cytokinin treatment on the different mutant lines in a cytokinin tolerance assay. Plants of the *CHK* mutant collection were inoculated on KNOP agar medium supplemented with 1 μ M benzyladenine (BA), representing a concentration far beyond the range measured for endogenously produced cytokinins in *P. patens* (von Schwartzberg *et al.*, 2007). We have further chosen BA for this experiment as it is less prone to degradation by cytokinin oxidase/dehydrogenase compared with isoprenoid cytokinins (Avalbaev *et al.*, 2012). At a concentration of 1 μ M BA, the protonemal growth of the wild type was strongly inhibited, and malformed buds developed. In contrast, the high dose of BA did not lead to growth reduction and bud formation in the $\Delta chk1,2,3$ triple mutant, indicating a strong cytokinin insensitivity of this mutant (Fig. 4).

The exposure of the other members of the *chk* mutant collection to high doses of BA showed that the presence of a single *CHK* receptor is sufficient to confer sensitivity to an excess of cytokinin (Fig. 4). While all single and double mutant genotypes showed a brown or pale color, the protonema of the triple $\Delta chk1,2,3$ mutant was not visibly affected in pigmentation by the BA overdose. The tolerance assay showed that all three classical *CHK* receptors are involved in growth

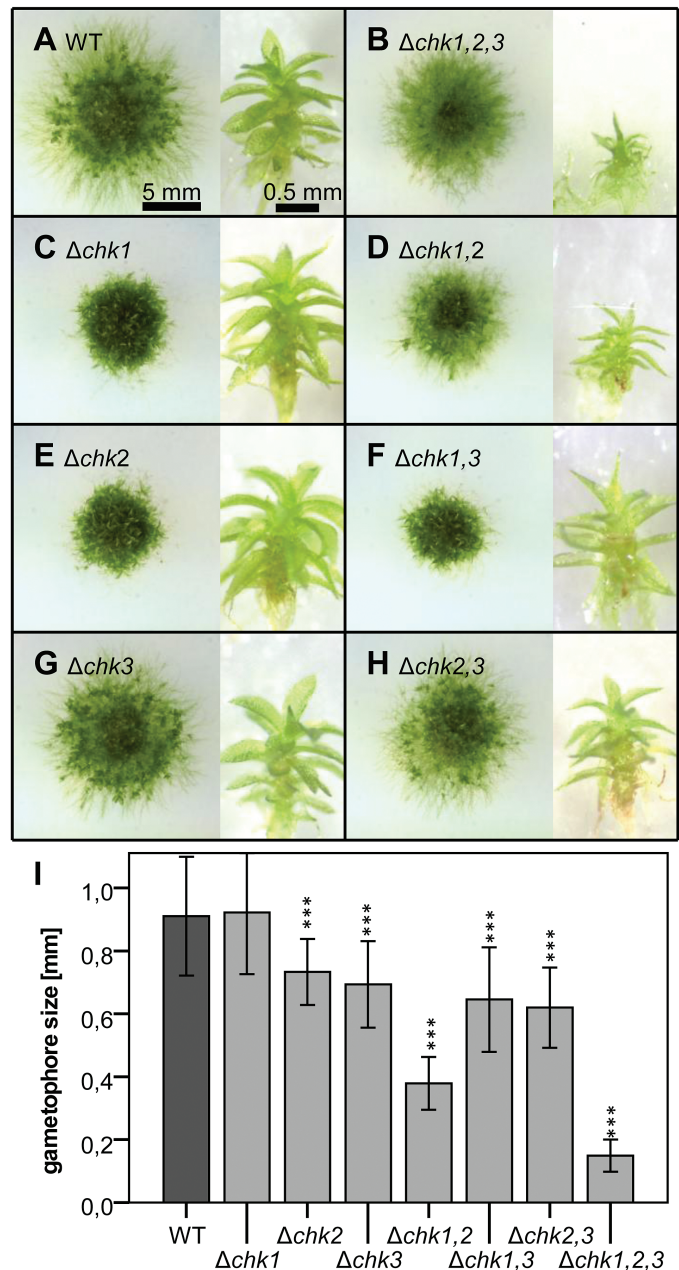


Fig. 3. (A–H) Phenotypes of single, double, and triple mutants of *CHK1*, *CHK2*, and *CHK3*. Each panel shows moss colonies (7 weeks old) on the left and isolated gametophores (14 weeks old) on the right. Cultures were grown on KNOP agar medium. Corresponding pictures were taken at the same magnification; scale bars are given in (A). (I) Mean size of gametophores after 14 weeks [mean \pm SD, *t*-test different from the wild type (WT), *** $P < 0.001$].

inhibition as well as in the formation of malformed buds, which are typical responses of *P. patens* to a high dose of cytokinin (von Schwartzberg, 2009).

Budding bioassay reveals differences in the biological roles of *CHK1*, *CHK2*, and *CHK3*

Cytokinins affect many aspects in the development of mosses (for a review, see von Schwartzberg, 2009), with the induction of buds being the most striking. In order to establish

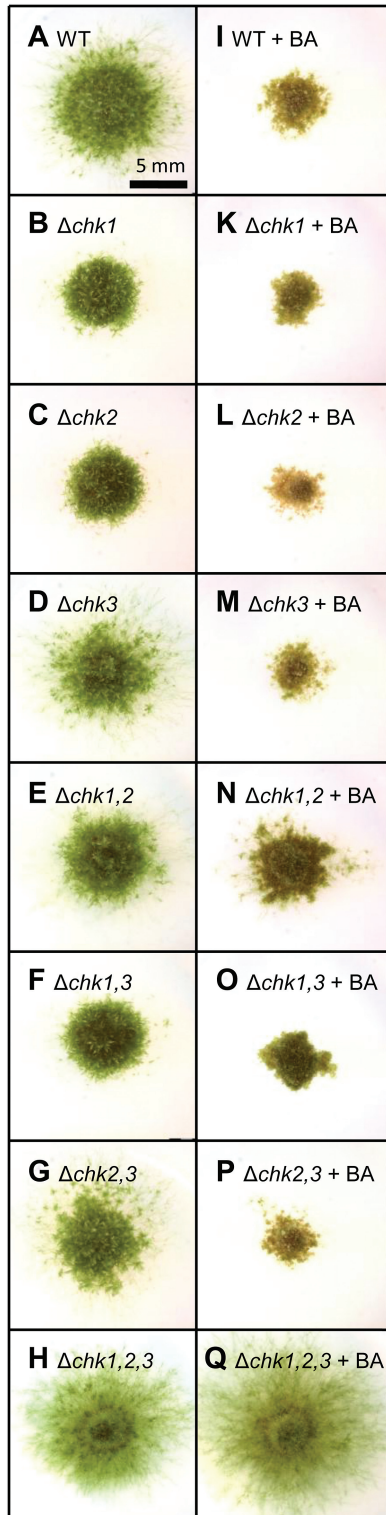


Fig. 4. Tolerance of single, double, and triple mutants of *CHK1*, *CHK2*, and *CHK3* to a high dose of cytokinin in comparison with the wild type. Seven-week-old cultures grown on KNOP agar plates. (A–H) No exogenous cytokinin, (I–Q) 1 μ M benzyladenine (BA). All pictures are at the same scale; the scale bar is given in (A).

whether one or more of the three *CHKs* under investigation are involved in this process, the *CHK* mutant collection was tested in a dose-dependent budding assay (Hahn and Bopp, 1968). The number of buds was counted after 10 d of growth

on different concentrations of isopentenyladenine (iP; 50, 100, and 400 nM). For the genotypes $\Delta chk1$, $\Delta chk3$, $\Delta chk1,3$, and $\Delta chk2,3$, a slightly reduced budding was observed (Fig. 5); however, the high variability of these bioassays results should be taken into account. For the genotypes $\Delta chk2$ and $\Delta chk1,2$ only minimal bud formation was recorded. These genotypes only responded to concentrations of iP >50 nM (Supplementary Table S3 at *JXB* online), whereas in the wild type and most of the other mutants bud induction was already clearly detectable at 50 nM iP. Strikingly, in this bioassay, the triple mutant $\Delta chk1,2,3$ did not exhibit any budding response.

From the results for the different double mutant combinations tested in the budding assay it can be deduced that *CHK1* and *CHK2* alone are capable of mediating budding as a response to increased iP concentrations. The response to iP in the presence of *CHK1* alone (in $\Delta chk2,3$) was slightly weaker than in the presence of *CHK2* alone (in $\Delta chk1,3$). Only a very low budding response was observable in the double mutant $\Delta chk1,2$ mediated by *CHK3* alone. Noticeably, the *CHK3* receptor in the absence of *CHK2* and *CHK1* was insufficient to transduce the iP signal in order to result in significant budding (Fig. 5). In summary all three receptors participate in the budding response in this short-term assay. The absence of all three receptors leads to a complete lack of cytokinin-dependent bud induction, thus indicating an essential role for the *CHKs* in this developmental transition.

Differential budding in response to distinct cytokinins

In order to investigate how the three *CHK* receptors differ in their response to different cytokinins, we performed the budding assay with the three double mutants as well as the triple mutant using the cytokinins iP, *tZ*, and BA (each at 400 nM, Fig. 6) known to be the most active in this assay (von Schwartzenberg *et al.*, 2007). As determined in the $\Delta chk2,3$ mutant background, the receptor *CHK1* alone is capable of mediating a budding response to all applied cytokinins. In $\Delta chk1,3$, where only the *CHK2* receptor is present, the budding response was high with iP but strongly impaired for *tZ* and BA—indicating a preference for iP. A strongly reduced response for all the three cytokinin bases was noted for the $\Delta chk1,2$ double mutant, indicating that *CHK3* alone is not very active—at least in the protonemal stage. No budding response at all was found for the $\Delta chk1,2,3$ triple mutant no matter which of the three cytokinins was applied (Fig. 6).

Relative expression of *CHK* genes in Δchk mutant backgrounds

In order to investigate compensatory interaction between the different receptors on the transcript level, quantitative real-time-based analysis of *CHK* gene expression in the mutants and wild type was carried out. This analysis revealed that *CHK1* expression is not or is only slightly affected by the knockout of *CHK2*, *CHK3*, or both receptors. However, expression of *CHK2* seems to be 3- to 5-fold up-regulated in the single, and the double mutants of *CHK1* and *CHK3*

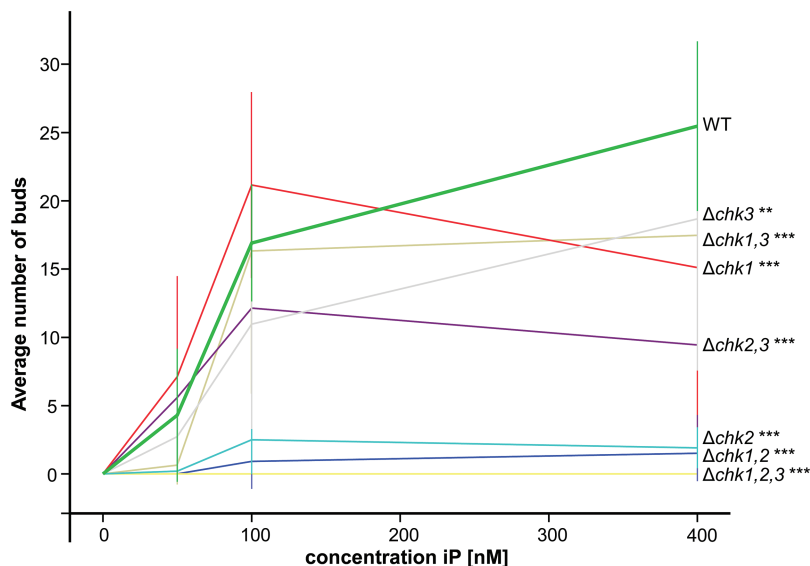


Fig. 5. Dose-dependent budding response to isopentenyladenine (iP) in the wild type (WT), and single, double, and triple Δchk mutants. Equal amounts of protonema were suspended on KNOP agar medium containing 0–400 nM iP, and bud formation was analyzed microscopically after 10 d under standard conditions. The average number of buds corresponds to one microscopic view field (3.8 mm²). At least two different biological replicates were counted in 5–10 view fields (mean \pm SD, *t*-test different from the WT at 400 nM, ***P*<0.01, ****P*<0.001; the complete data set is given in [Supplementary Table S3](#) at *JXB* online).

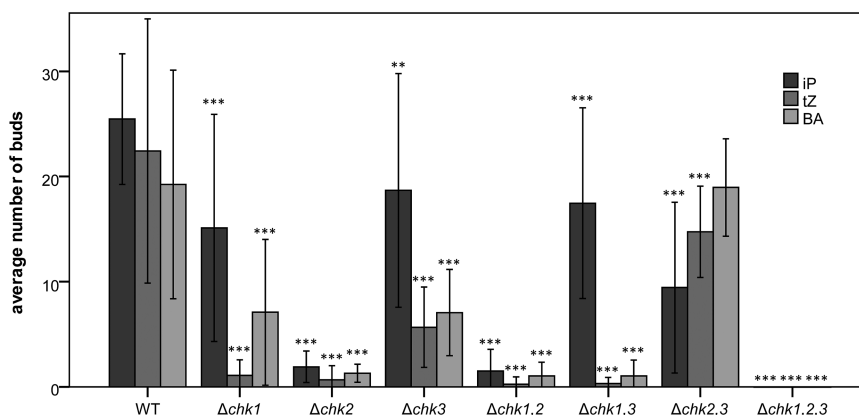


Fig. 6. Budding response of the wild type (WT), and double and triple Δchk mutants to iP, tZ, and BA. The budding response of the different genotypes was assessed after 10 d on KNOP agar medium supplemented with 400 nM iP, tZ, and BA, respectively. Equal amounts of protonema were suspended on KNOP agar medium and bud formation was analyzed microscopically after 10 d under standard conditions. The number of buds corresponds to one microscopic view field (3.8 mm²). At least two different biological replicates were counted in 5–10 view fields (mean \pm SD, *t*-test different from the WT for each individual cytokinin, ***P*< 0.01, ****P*<0.001); the complete data set is given in [Supplementary Table S3](#) at *JXB* online).

compared with the expression level measured for the wild type. The expression of *CHK3* was found to be up-regulated in $\Delta chk2$ and $\Delta chk1,2$, but not in $\Delta chk1$ (Fig. 7). Thus while the expression of *CHK1* is quite stable regardless of the genetic background, the transcript level of both *CHK2* and *CHK3* increased in most receptor mutant backgrounds.

Cytokinin profiles of Δchk mutants

The transcriptional response of *CHK2* and *CHK3* to a receptor deficiency led to the question of whether there is a connection between cytokinin signaling and metabolism in *P. patens*. Previously, it has been shown in *Arabidopsis* that deficiencies in cytokinin receptors can result in changes of cytokinin homeostasis (Riefler *et al.*, 2006). Thus we established the

cytokinin profiles of the three double mutants ($\Delta chk1,2$, $\Delta chk1,3$, and $\Delta chk2,3$) and the triple mutant $\Delta chk1,2,3$ using UHPLC-MS/MS measurements and compared them with the profile of the wild type (Fig. 8). Each of the genotypes was cultured three times independently as a protonemal culture in liquid medium, and two technical replicates were made for each extract. Although there were individual changes, a general increase of all types of cytokinins, as described for *Arabidopsis* (Riefler *et al.*, 2006), was not found for the moss mutants. *cis*-Zeatin riboside *O*-glucoside (*cZROG*), which is by far the most abundant cytokinin in *P. patens* (von [Schwartzberg et al.](#), 2007), was only found at slightly higher levels in the $\Delta chk1,3$ mutant. However no significant changes in cytokinin levels were measured in the cytokinin receptor mutants when compared with the wild type.

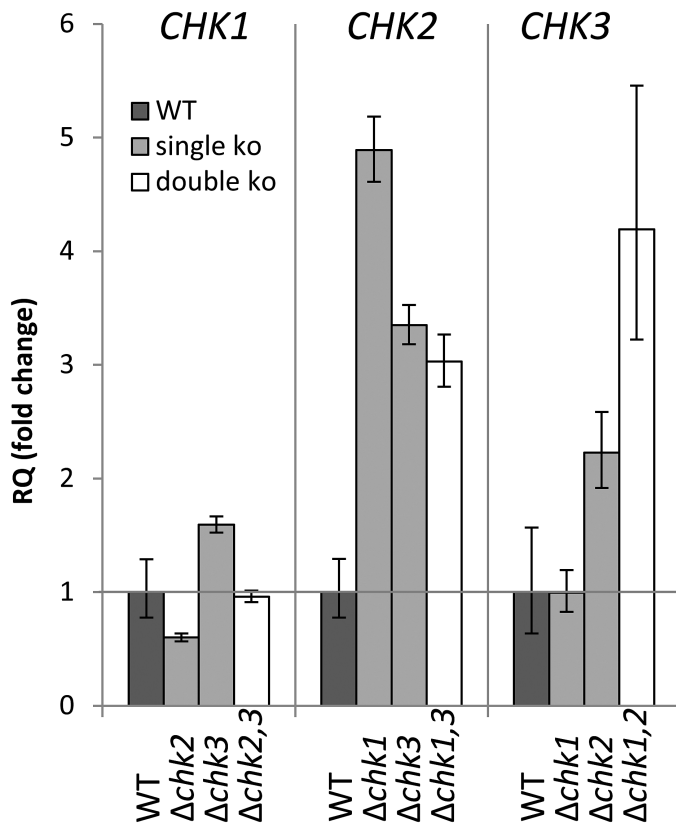


Fig. 7. Relative expression of *CHK1*, *CHK2*, and *chk3* in the respective single and double mutants. Three biological replicates were measured (7-day-old plants grown on KNOP agar, under standard conditions) with three technical replicates. 60S ribosomal protein L21 (Wang and Irving, 2011) served as the endogenous control, and gene expression was normalized to wild-type (WT) levels. Analysis of RQ (relative quantities) was performed with StepOne Plus software (Life Technologies®). Mean \pm SD from technical replicates. *t*-test for differences from the WT for each target among biological replicates yielded no significant differences.

Discussion

The aim of this study was to characterize the properties and biological roles of the three classical cytokinin receptors of *P. patens*. In order to test the functionality of the three cloned receptors *CHK1*, *CHK2*, and *CHK3*, we used two well-established cytokinin receptor assays, the cytokinin binding assay and the *in planta* complementation assay (Mizuno and Yamashino, 2010; Choi *et al.*, 2012). The assays confirmed the activity of *CHK1* and *CHK2* in hormone binding (Fig. 1), as well as their translation into downstream signaling, at least in *Arabidopsis* (Fig. 2). To our surprise, for *CHK3* no activity was confirmed in either of these assays (Fig. 1, 2). However, this does not mean that the third receptor is not functional in *P. patens*. In fact the analysis of the knockout lines clearly shows that *CHK3* has a role as a cytokinin receptor in the moss.

CHK receptors are functional *in planta*

To confirm the function of *CHKs* as cytokinin receptors in *P. patens*, different cytokinin-dependent assays using a collection of receptor knockout mutants were conducted.

In flowering plants it is known that high concentrations of cytokinins can induce senescence and programmed cell death (Carimi *et al.*, 2003; Vescovi *et al.*, 2012). Our experiments confirmed the growth-inhibiting effect of 1 μ M BA in *P. patens* (Thelander *et al.*, 2005). We clearly demonstrated that this cytokinin-dependent growth inhibition is mediated via the *CHK* receptors, as the $\Delta chk1,2,3$ triple mutant was not affected by a high dose of BA. The cytokinin tolerance assay (Fig. 4) confirmed a role for *CHK3* in cytokinin perception as the $\Delta chk1,2$ double mutant, with only *CHK3* left as a functional receptor, was more affected by BA than plants with a simultaneous knockout of all three classical receptors ($\Delta chk1,2,3$). We deduce from the *in planta* experiments that *CHK3* is capable of reacting to BA. The absence of a *tZ*-mediated response in the complementation and binding assays could be explained by either an incorrect protein processing in a heterologous system or a general low functionality of *CHK3*. While a *tZ* binding and a *tZ*-dependent response of *CHK3* remains unclear, it can be stated that *CHK3* mediates a clear *iP* response in the budding assay (Fig. 6) and a clear BA response in the tolerance assay (Fig. 4).

This experiment also indicates that apart from *CHK1*, *CHK2*, and *CHK3*, no other receptor is necessary to confer sensitivity to a cytokinin overdose, at least at this growth stage of the moss (Fig. 4).

A more detailed analysis using the well characterized cytokinin-dependent budding response (Hahn and Bopp, 1968) revealed that each *CHK* receptor, including *CHK3*, mediates a cytokinin response *in planta* as all three double mutants respond to cytokinins. *CHK2* has a prominent role in this developmental process as all mutants in which this cytokinin receptor was missing showed a much weaker cytokinin response and (almost) no response to low levels of *iP* (50 nM; Fig. 5; Supplementary Table S3 at *JXB* online) when compared with those missing *CHK1* or *CHK3*. In contrast, the mutants $\Delta chk1$, $\Delta chk3$, $\Delta chk1,3$, and $\Delta chk2,3$ were less affected in budding frequency, also at high cytokinin concentrations (Fig. 5). In order to check if these effects depend on the type of cytokinin used, the assay was extended using three different cytokinins at 400 nM (Fig. 6). These experiments showed weak budding when only *CHK3* was present regardless of the cytokinin used, which indicates that this receptor is functional, but does not play a critical role for the transition from protonema to gametophore during the moss life cycle. In contrast, *CHK1* responded to a broader cytokinin spectrum as all three tested cytokinins led to bud formation. Only *CHK2* showed a preference for one particular cytokinin, *iP*, as this cytokinin had a far stronger bud-inducing effect than *tZ* or BA in the $\Delta chk1,3$ mutant (Fig. 6). We conclude from the *in planta* cytokinin response assays that all three receptors mediate a cytokinin-dependent signal independently from each other. Despite its responsiveness towards high doses of cytokinin, *CHK3* seems to be of only minor importance for bud formation. *CHK1* and *CHK2* play a major role in triggering this developmental process, however with differences in the cytokinin preference.

The differences and redundancies among the investigated cytokinin receptors were further highlighted by the changes

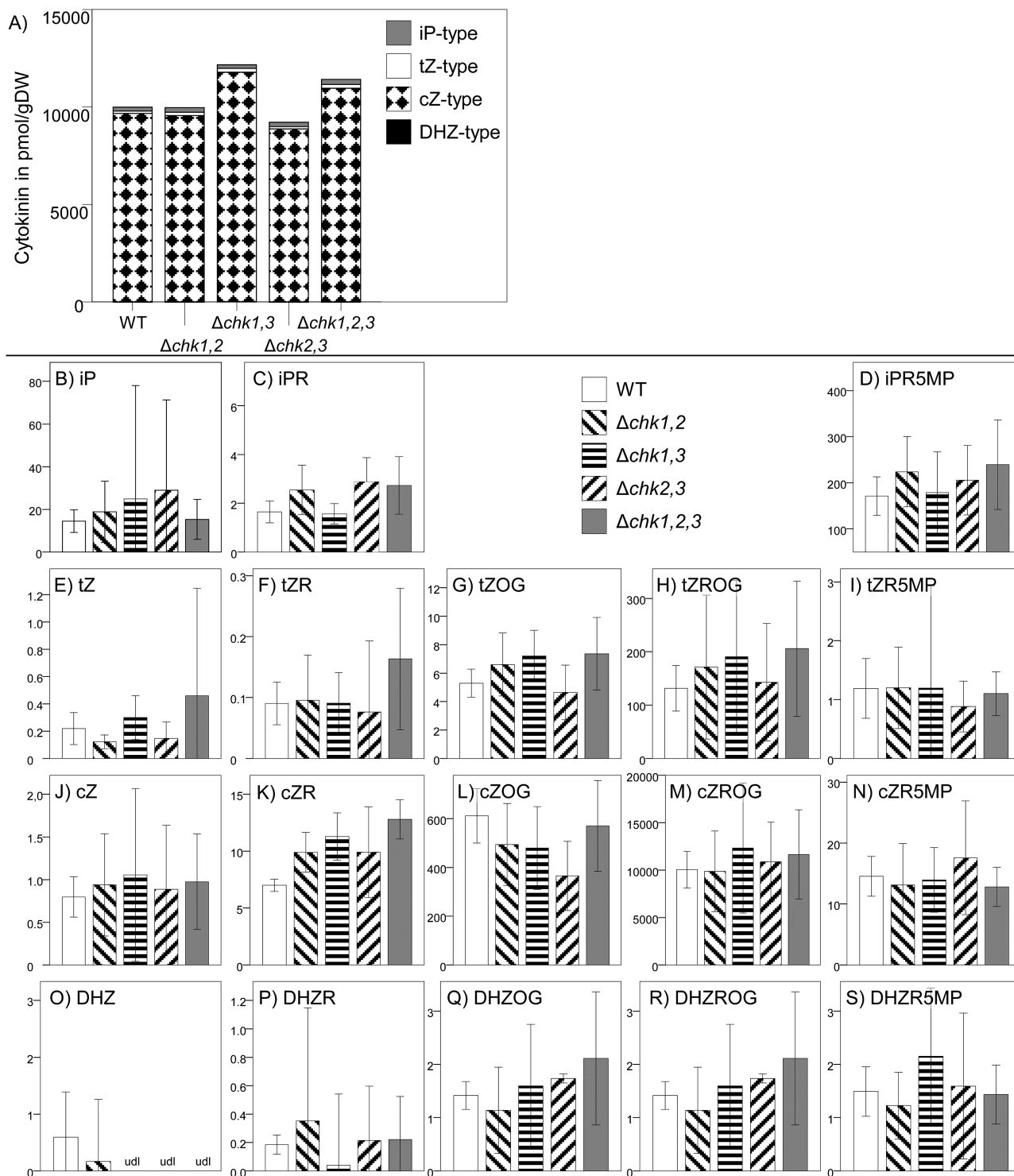


Fig. 8. Average level of isoprene-type cytokinins in tissue of *P. patens* wild type and the cytokinin receptor mutants $\Delta chk1,2,3$ (triple) and $\Delta chk1,2$; $\Delta chk1,3$ and $\Delta chk2,3$ (double). Each genotype was cultured three times independently for 21 d, sampled at three independent time points, and measured by UHPLC-MS/MS ($n=9-24$). Data present mean values with 95% confidence intervals. Cytokinin content in the mutants was compared with that in the wild type by independent samples Kruskal-Wallis test (confidence interval 95%, significance level 0.5); no significant changes compared in all samples with the wild type. Values are given in pmol g⁻¹ DW. (A) Sum of all measured cytokinins. (B-S) Levels of each individual cytokinin; columns are the same as indicated in (A). tZ, *trans*-zeatin; tZOG, *trans*-zeatin O-glucoside; tZR, *trans*-zeatin riboside; tZRMP, *trans*-zeatin riboside-5'-monophosphate; tZROG, *trans*-zeatin riboside O-glucoside cZ, *cis*-zeatin; cZOG, *cis*-zeatin O-glucoside; cZR, *cis*-zeatin riboside; cZRMP, *cis*-zeatin riboside-5'-monophosphate; cZROG, *cis*-zeatin riboside O-glucoside; DHZ, dihydrozeatin; DHZOG, dihydrozeatin O-glucoside; DHZR, dihydrozeatin riboside; DHZRMP, dihydrozeatin riboside-5'-monophosphate; DHZROG, dihydrozeatin riboside O-glucoside; iP, N⁶-isopentenyladenine; iPR, N⁶-isopentenyladenosine; iPRMP, N⁶-isopentenyladenosine-5'-monophosphate. udl, under the detection limit.

in their expression in the different mutant backgrounds. The peculiar finding of a higher sensitivity of the $\Delta chk2,3$ mutant compared with the $\Delta chk2$ mutant to iP can be explained by taking into account the expression level of *CHK1*. In $\Delta chk2$, but not in the $\Delta chk2,3$ mutant, the *CHK1* level is reduced, which could contribute to the reduced sensitivity of $\Delta chk2$. However, in what way and to what extent the regulation and redundancies among the receptors are realized remain to be investigated. The *CHK2* and *CHK3* transcript levels were elevated in mutants still expressing the respective receptor. Thus it seems possible that the relatively small loss of bud formation observed in $\Delta chk1,3$ (Fig. 5) was partly due to an up-regulated *CHK2* expression in this mutant. The expression levels of *CHK1* either remained constant or increased slightly in $\Delta chk2$ mutants (Fig. 7).

P. patens development depends on functional CHK receptors

The phenotypic characterization of colony shape and gametophore size revealed differences between the mutants and wild type. Single mutants expressed minor phenotypic changes (reduced colony diameter of $\Delta chk1$ and $\Delta chk2$) or were even indistinguishable from the wild type ($\Delta chk3$), thus indicating again that *CHK3* is not a major player for cytokinin perception in *P. patens*. The apparent minor role of *CHK3* was further corroborated by the similar phenotype of the $\Delta chk1,2$ double mutant and the triple mutant $\Delta chk1,2,3$, which both exhibited reduced differentiation and a reduction of gametophore size. However, the *CHK3* receptor possesses enough activity to provide basal functions in cytokinin activity as the $\Delta chk1,2$ double mutant like the $\Delta chk1,3$ and $\Delta chk2,3$ mutants, is able to undergo its entire life cycle including the formation of gametangia, sporophyte, and viable spores (not shown).

The importance of the cytokinin receptors for sexual reproduction was further emphasized by the inability of the triple mutant to form sporophytes. A similar phenotype was also observed when the cytokinin oxidase gene *AtCKX2* was over-expressed in *P. patens*. These plants with a lowered content of cytokinins also showed a reduced budding response and absence of sporophyte formation (von Schwartzenberg *et al.*, 2007). The life cycle of *P. patens* is apparently dependent on a functionality in the level of cytokinin homeostasis as well as of cytokinin perception.

A detailed developmental analysis of vegetative and generative stages in *CHK* mutants employing approaches such as presented by Coudert *et al.* (2015) and Landberg *et al.* (2013) is the subject of ongoing studies.

Classical *CHKs* play a key role in cytokinin perception and moss development

The experiments of this study clearly demonstrate the crucial role of *CHK1*, *CHK2*, and *CHK3* for cytokinin perception and especially for the cytokinin-triggered formation of buds in moss. Recently, an additional subfamily of cytokinin receptors has been discovered (Gruhn *et al.*, 2014). While sharing

the same overall domain structure with the classical *CHKs*, their CHASE domain shows a lower conservation compared with the classical cytokinin receptors (Gruhn *et al.*, 2014). One of the eight members of the new *P. patens* *CHK* subfamily, *CHK4*, has been characterized, and cytokinin binding and cytokinin-dependent activation of a two-component signaling chain was shown. The results of the analysis presented in this study of the classical Δchk mutants raise the question of the biological role of the receptors of the new subfamily. In particular, the facts that the triple mutant was completely resistant to the applied cytokinins in the tolerance assay and that bud formation was strongly delayed seem to indicate that these new receptors might not be critical in the cytokinin biology of the moss. However, one has to consider that budding is not the only developmental process regulated by cytokinin in *P. patens* and that small gametophores did form eventually in the $\Delta chk1,2,3$ triple mutant. Furthermore the transition from chloronema to caulonema, the formation of secondary chloronema, and the development of brachycytes and terna cells, amongst other processes, are influenced by cytokinin (von Schwartzenberg, 2009). It will be interesting to test if those processes are also affected in the $\Delta chk1,2,3$ mutant or if the newly identified receptors function in one or more of these developmental processes. While the biological function of these ‘novel’ *CHKs* is not yet clear, their evolutionary origin is clearly different from those of the other cytokinin receptors (Gruhn *et al.*, 2014). Interestingly, sequences from charophyceae algae [i.e. EST (expressed sequence tag) evidence from *Spirogyra pratensis* and the sequenced genome of *Klebsormidium flaccidum*] clustered between both clades of *CHKs* and those might be ancestral to both (Gruhn *et al.*, 2014; Hori *et al.*, 2014; E. Kaltenecker and A. Heyl, unpublished data). It is conceivable that they represent an ancestral type of cytokinin receptor that evolved into the classical *CHK* receptors found in land plants (e.g. *PpCHK1*, *AtAHK4*, and others).

Comparison of cytokinin signaling between *P. patens* and Arabidopsis

Given the importance of cytokinin as a regulator of plant growth and development (Hwang *et al.*, 2012; Kieber and Schaller, 2014), it is surprising that *A. thaliana* is the only species in which cytokinin receptors have been analyzed systematically.

On the protein level, the classical *CHK* receptors from Arabidopsis and *P. patens* show a high degree of similarity with respect to their domain architecture of the whole protein and on the sequence level, also within the CHASE domain (Gruhn *et al.*, 2014, 2015). These structural similarities also translate to functional similarities as we were able to complement *ahk2,ahk3* deficiency in Arabidopsis protoplasts by transient expression of *PpCHK1* and *PpCHK2* (Fig. 1).

This study investigated the classical cytokinin receptors of the moss *P. patens* in detail, thus allowing phenotypic comparisons of cytokinin receptor mutants of an early diverging and a flowering plant. In both cases, the single mutants showed weak or no phenotypes, indicating a high level of redundancy among

the receptors. While in *Arabidopsis* the simultaneous knockout of all cytokinin receptors (*ahk2, ahk3, ahk4*) leads to a severe dwarf plant (Higuchi *et al.*, 2004; Nishimura *et al.*, 2004; Riefler *et al.*, 2006), the respective *P. patens* $\Delta chk1,2,3$ mutant showed a protonemal growth area that is comparable with that of the wild type. However, gametophores which appeared delayed in the $\Delta chk1,2,3$ triple mutant when compared with the wild type also exhibited a strong dwarf phenotype (Fig. 3, Supplementary Fig. S5B at *JXB* online). Both the *Arabidopsis* triple mutant shoot and the *P. patens* triple mutant gametophore are strongly impaired in growth and development. Further, both plants are highly resistant to exogenous cytokinin treatment. In both plant species, different mutant combinations show a distinct response to certain cytokinins, indicating different biological roles for the respective receptors (Higuchi *et al.*, 2004; Nishimura *et al.*, 2004; Riefler *et al.*, 2006; Stolz *et al.*, 2011). Despite the similarities in the cytokinin signaling mechanisms of flowering plants and bryophytes, we uncovered differences in the impacts of cytokinin signaling on the homeostasis of these hormones. In *Arabidopsis*, it has been shown that deficiency in cytokinin perception results in drastic changes of cytokinin homeostasis; notably, with increasing number of deleted receptors, a significantly increased concentration of numerous cytokinin species was found. In the *Arabidopsis* triple receptor mutant, there was, for example, a 15-fold increase of *tZ* compared with the wild type (Riefler *et al.*, 2006). The levels of active cytokinins in *P. patens* [iP, iPR, *tZ*, *tZR*, and dihydrozeatin (DHZ) (von Schwanzenberg *et al.*, 2007)] were not significantly altered in the analyzed Δchk mutants (Fig. 8). Thus the relatively small reduction in budding response for $\Delta chk1$, $\Delta chk3$, or $\Delta chk1,3$, for example (Fig. 5), cannot be explained by an increased production of active cytokinins to compensate the loss of function in the receptor system. In summary, in the moss *P. patens*—in contrast to flowering plants—there is only a minor contribution of the CHK1, CHK2, and CHK3 receptors to cytokinin homeostasis.

Conclusions

The study presented reveals that at the evolutionary stage of bryophytes, cytokinin signaling is fully established and uses classical receptors of the CHK gene family. The different experiments highlight the common and different properties of the receptors and their roles in developmental processes such as bud formation and gametophore development. The results of this study demonstrate the functionality of the classical PpCHK receptors, which are crucial for key steps in the life cycle of *P. patens*. Currently studies are under way to investigate the impact of the CHK receptors on multiple physiological and developmental aspects, and we expect that this and the presented research will contribute to the understanding of how hormonal regulation was established at the level of bryophytes.

Supplementary data

Supplementary data are available at *JXB* online.

Supplementary Fig. S1. Expression control of the fusion proteins analyzed in Fig. 1.

Supplementary Fig. S2. Overview of the *chk* knockout plants generated by transformation with the listed vectors.

Supplementary Fig. S3. PCR screening of knockout mutants.

Supplementary Fig. S4. RT-PCR screen of the different mutant lines.

Supplementary Fig. S5. (A) Average colony radius; (B) time course of gametophore frequency.

Supplementary Table S1. Generation of the *chk* mutant collection.

Supplementary Table S2. Primer sequences.

Supplementary Table S3. Data for the budding assay (Figs 5, 6).

Acknowledgements

The authors thank Vera Schwekendiek (University of Hamburg) for excellent assistance related to moss culturing and bioassays, and Hana Martinková and Michaela Glosová (Palacký University, Olomouc) for sample purification and hormone analyses. The contributions of Florian Gelhaar and Niels Wegner (University of Hamburg) in an early phase of the project are acknowledged; furthermore, Frank Woihe (University of Hamburg) is acknowledged. Susanne Bringe (University Hamburg), who sadly passed away in 2014, deserves special recognition for her technical contributions to the project. NG and AH are grateful for the financial support of the Volkswagen Foundation to NG (Az I/83 477). AL appreciates support from the Estuary and Wetland Research Graduate School Hamburg (ESTRADE) as a member of the State Excellence Initiative (LEXI) funded by the Hamburg Science and Research Foundation. JŠ, ON, and MS acknowledge the Ministry of Education, Youth and Sports of the Czech Republic (the National Program for Sustainability I, grant no. LO1204) and the Internal Grant Agency of Palacký University (IGA_PrF_2015_024 and IGA_PrF_2015_021).

References

- Anantharaman V, Aravind L.** 2001. The CHASE domain: a predicted ligand-binding module in plant cytokinin receptors and other eukaryotic and bacterial receptors. *Trends in Biochemical Science* **26**, 579–582.
- Avalbaev AM, Somov KA, Yuldashev RA, Shakirova FM.** 2012. Cytokinin oxidase is key enzyme of cytokinin degradation. *Biochemistry (Moscow)* **77**, 1354–1361.
- Caesar K, Thamm AM, Witthoft J, Elgass K, Huppenberger P, Grefen C, Horak J, Harter K.** 2011. Evidence for the localization of the *Arabidopsis* cytokinin receptors AHK3 and AHK4 in the endoplasmic reticulum. *Journal of Experimental Botany* **62**, 5571–5580.
- Carimi F, Zottini M, Formentin E, Terzi M, Lo Schiavo F.** 2003. Cytokinins: new apoptotic inducers in plants. *Planta* **216**, 413–421.
- Choi J, Lee J, Kim K, Cho M, Ryu H, An G, Hwang I.** 2012. Functional identification of OsHk6 as a homotypic cytokinin receptor in rice with preferential affinity for iP. *Plant and Cell Physiology* **53**, 1334–1343.
- Coudert Y, Palubicki W, Ljung K, Novak O, Leyser O, Harrison CJ.** 2015. Three ancient hormonal cues co-ordinate shoot branching in a moss. *Elife* **4**.
- Cove D.** 2005. The moss *Physcomitrella patens*. *Annual Review of Genetics* **39**, 339–358.
- Decker EL, Frank W, Sarnighausen E, Reski R.** 2006. Moss systems biology en route: phytohormones in *Physcomitrella* development. *Plant Biology* **8**, 397–405.
- Dobrev PI, Kaminek M.** 2002. Fast and efficient separation of cytokinins from auxin and abscisic acid and their purification using mixed-mode solid-phase extraction. *Journal of Chromatography A* **950**, 21–29.
- Frébort I, Kowalska M, Hluska T, Frébortova J, Galuszka P.** 2011. Evolution of cytokinin biosynthesis and degradation. *Journal of Experimental Botany* **62**, 2431–2452.
- Gruhn N, Halawa M, Snel B, Seidl MF, Heyl A.** 2014. A subfamily of putative cytokinin receptors is revealed by an analysis of the evolution

of the two-component signaling system of plants. *Plant Physiology* **165**, 227–237.

Gruhn N, Heyl A. 2013. Updates on the model and the evolution of cytokinin signaling. *Current Opinion in Plant Biology* **16**, 569–574.

Gruhn N, Seidl MF, Halawa M, Heyl A. 2015. Members of a recently discovered subfamily of cytokinin receptors display differences and similarities to their classical counterparts. *Plant Signaling and Behavior* **10**, e984512.

Hahn H, Bopp M. 1968. A cytokinin test with high specificity. *Planta* **83**, 115–118.

Hellmann E, Gruhn N, Heyl A. 2010. The more, the merrier: cytokinin signaling beyond Arabidopsis. *Plant Signaling and Behavior* **5**, 1384–1390.

Heyl A, Braut M, Frugier F, Kuderova A, Lindner AC, Motyka V, Rashotte AM, Schwartzberg KV, Vankova R, Schaller GE. 2013. Nomenclature for members of the two-component signaling pathway of plants. *Plant Physiology* **161**, 1063–1065.

Heyl A, Schmülling T. 2003. Cytokinin signal perception and transduction. *Current Opinion in Plant Biology* **6**, 480–488.

Heyl A, Werner T, Schmülling T. 2006. Cytokinin metabolism and signal transduction. In: *Annual Plant Reviews Volume 24: Plant Hormone Signaling*. Oxford: Blackwell Publishing, 93–123.

Heyl A, Wulfetange K, Pils B, Nielsen N, Romanov GA, Schmülling T. 2007. Evolutionary proteomics identifies amino acids essential for ligand-binding of the cytokinin receptor CHASE domain. *BMC Evolutionary Biology* **7**, 62.

Higuchi M, Pischke MS, Mahonen AP, et al. 2004. *In planta* functions of the Arabidopsis cytokinin receptor family. *Proceedings of the National Academy of Sciences, USA* **101**, 8821–8826.

Hori K, Maruyama F, Fujisawa T, et al. 2014. *Klebsormidium flaccidum* genome reveals primary factors for plant terrestrial adaptation. *Nature Communications* **5**, 3978.

Hwang I, Sheen J. 2001. Two-component circuitry in Arabidopsis cytokinin signal transduction. *Nature* **413**, 383–389.

Hwang I, Sheen J, Müller B. 2012. Cytokinin signaling networks. *Annual Review of Plant Biology* **63**, 353–380.

Ishida K, Yamashino T, Nakanishi H, Mizuno T. 2010. Classification of the genes involved in the two-component system of the moss *Physcomitrella patens*. *Bioscience, Biotechnology, and Biochemistry* **74**, 2542–2545.

Kieber JJ, Schaller GE. 2014. Cytokinins. *Arabidopsis Book* **12**, e0168.

Kirby J, Kavanagh TA. 2002. NAN fusions: a synthetic sialidase reporter gene as a sensitive and versatile partner for GUS. *The Plant Journal* **32**, 391–400.

Landberg K, Pederson ER, Viaene T, Bozorg B, Friml J, Jonsson H, Thelander M, Sundberg E. 2013. The moss *Physcomitrella patens* reproductive organ development is highly organized, affected by the two SHI/STY genes and by the level of active auxin in the SHI/STY expression domain. *Plant Physiology* **162**, 1406–1419.

Lang D, Eisinger J, Reski R, Rensing SA. 2005. Representation and high-quality annotation of the *Physcomitrella patens* transcriptome demonstrates a high proportion of proteins involved in metabolism in mosses. *Plant Biology* **7**, 238–250.

Lindner AC, Lang D, Seifert M, Podlesakova K, Novak O, Strnad M, Reski R, von Schwartzberg K. 2014. Isopentenyltransferase-1 (IPT1) knockout in *Physcomitrella* together with phylogenetic analyses of IPTs provide insights into evolution of plant cytokinin biosynthesis. *Journal of Experimental Botany* **65**, 2533–2543.

Lomin SN, Yonekura-Sakakibara K, Romanov GA, Sakakibara H. 2011. Ligand-binding properties and subcellular localization of maize cytokinin receptors. *Journal of Experimental Botany* **62**, 5149–5159.

Mizuno T, Yamashino T. 2010. Biochemical characterization of plant hormone cytokinin-receptor histidine kinases using microorganisms. *Methods in Enzymology* **471**, 335–356.

Mok DWS, Mok MC. 2001. Cytokinin metabolism and action. *Annual Review of Plant Physiology and Plant Molecular Biology* **52**, 89–118.

Mougel C, Zhulin IB. 2001. CHASE: an extracellular sensing domain common to transmembrane receptors from prokaryotes, lower eukaryotes and plants. *Trends in Biochemical Science* **26**, 582–584.

Nishimura C, Ohashi Y, Sato S, Kato T, Tabata S, Ueguchi C. 2004. Histidine kinase homologs that act as cytokinin receptors possess

overlapping functions in the regulation of shoot and root growth in Arabidopsis. *The Plant Cell* **16**, 1365–1377.

Novák O, Hauserova E, Amakorová P, Doležal K, Strnad M. 2008. Cytokinin profiling in plant tissues using ultra-performance liquid chromatography-electrospray tandem mass spectrometry. *Phytochemistry* **69**, 2144–2224.

Patil G, Nicander B. 2013. Identification of two additional members of the tRNA isopentenyltransferase family in *Physcomitrella patens*. *Plant Molecular Biology* **82**, 417–426.

Pils B, Heyl A. 2009. Unraveling the evolution of cytokinin signaling. *Plant Physiology* **151**, 782–791.

Punwani JA, Hutchison CE, Schaller GE, Kieber JJ. 2010. The subcellular distribution of the Arabidopsis histidine phosphotransfer proteins is independent of cytokinin signaling. *The Plant Journal* **62**, 473–482.

Ramireddy E, Brenner WG, Pfeifer A, Heyl A, Schmülling T. 2013. In planta analysis of a cis-regulatory cytokinin response motif in Arabidopsis and Identification of a novel enhancer sequence. *Plant and Cell Physiology* **54**, 1079–1092.

Rensing SA, Lang D, Zimmer AD, et al. 2008. The *Physcomitrella* genome reveals evolutionary insights into the conquest of land by plants. *Science* **319**, 64–69.

Riefler M, Novak O, Strnad M, Schmülling T. 2006. Arabidopsis cytokinin receptor mutants reveal functions in shoot growth, leaf senescence, flowering size, germination, root development, and cytokinin metabolism. *The Plant Cell* **18**, 40–54.

Romanov GA, Lomin SN. 2009. Hormone-binding assay using living bacteria expressing eukaryotic receptors. *Methods in Molecular Biology* **495**, 111–120.

Romanov GA, Spichal L, Lomin SN, Strnad M, Schmülling T. 2005. A live cell hormone-binding assay on transgenic bacteria expressing a eukaryotic receptor protein. *Analytical Biochemistry* **347**, 129–134.

Spichal L. 2012. Cytokinins—recent news and views of evolutionally old molecules. *Functional Plant Biology* **39**, 267–284.

Stolz A, Riefler M, Lomin SN, Achazi K, Romanov GA, Schmülling T. 2011. The specificity of cytokinin signalling in *Arabidopsis thaliana* is mediated by differing ligand affinities and expression profiles of the receptors. *The Plant Journal* **67**, 157–168.

Strepp R, Scholz S, Kruse S, Speth V, Reski R. 1998. Plant nuclear gene knockout reveals a role in plastid division for the homolog of the bacterial cell division protein FtsZ, an ancestral tubulin. *Proceedings of the National Academy of Sciences, USA* **95**, 4368–4373.

Suzuki T, Miwa K, Ishikawa K, Yamada H, Aiba H, Mizuno T. 2001. The Arabidopsis sensor His-kinase, AHK4, can respond to cytokinins. *Plant and Cell Physiology* **42**, 107–113.

Svacinova J, Novak O, Plackova L, Lenobel R, Holik J, Strnad M, Doležal K. 2012. A new approach for cytokinin isolation from Arabidopsis tissues using miniaturized purification: pipette tip solid-phase extraction. *Plant Methods* **8**, 17.

Tarakhovskaya ER, Maslov Yu I, Shishova MF. 2007. Phytohormones in algae. *Russian Journal of Plant Physiology* **54**, 163–170.

Thelander M, Olsson T, Ronne H. 2005. Effect of the energy supply on filamentous growth and development in *Physcomitrella patens*. *Journal of Experimental Botany* **56**, 653–662.

To JP, Haberer G, Ferreira FJ, Deruere J, Mason MG, Schaller GE, Alonso JM, Ecker JR, Kieber JJ. 2004. Type-A Arabidopsis response regulators are partially redundant negative regulators of cytokinin signaling. *The Plant Cell* **16**, 658–671.

Vescovi M, Riefler M, Gessuti M, Novák O, Schmülling T, Lo Schiavo F. 2012. Programmed cell death induced by high levels of cytokinin in Arabidopsis cultured cells is mediated by the cytokinin receptor CRE1/AHK4. *Journal of Experimental Botany* **63**, 2825–2832.

von Schwartzberg K. 2006. Moss biology and phytohormones—cytokinins in *Physcomitrella*. *Plant Biol* **8**, 382–388.

von Schwartzberg K. 2009. Hormonal regulation of development by auxin and cytokinin in moss. In: Knight C, Perroud P-F, Cove D, eds. *Annual Plant Reviews: The Moss Physcomitrella patens*, Vol. **36**. Wiley-Blackwell, 246–281.

von Schwartzberg K, Fernandez Núñez MF, Blaschke H, Dobrev PI, Novák O, Motyka V, Strnad M. 2007. Cytokinins in the bryophyte

Physcomitrella patens: analyses of activity, distribution, and cytokinin oxidase/dehydrogenase overexpression reveal the role of extracellular cytokinins. *Plant Physiology* **145**, 786–800.

Wang TL, Beutelmann P, Cove DJ. 1981. Cytokinin biosynthesis in mutants of the moss *Physcomitrella patens*. *Plant Physiology* **68**, 739–744.

Wang YH, Irving HR. 2011. Developing a model of plant hormone interactions. *Plant Signaling and Behavior* **6**, 494–500.

Wulfetange K, Lomin SN, Romanov GA, Stolz A, Heyl A, Schmülling T. 2011. The cytokinin receptors of *Arabidopsis* are located mainly to the endoplasmic reticulum. *Plant Physiology* **156**, 1808–1818.

Yamada H, Suzuki T, Terada K, Takei K, Ishikawa K, Miwa K, Yamashino T, Mizuno T. 2001. The *Arabidopsis* AHK4 histidine kinase is a cytokinin-binding receptor that transduces cytokinin signals across the membrane. *Plant and Cell Physiology* **42**, 1017–1023.

Yevdakova NA, Motyka V, Malbeck J, Trávníčková A, Novák O, Strnad M, von Schwartzberg K. 2008. Evidence for importance of tRNA-dependent cytokinin biosynthetic pathway in the moss *Physcomitrella patens*. *Journal of Plant Growth Regulation* **27**, 271–281.

Yevdakova NA, von Schwartzberg K. 2007. Characterisation of a prokaryote-type tRNA-isopentenyltransferase gene from the moss *Physcomitrella patens*. *Planta* **226**, 683–695.

Supplementary data

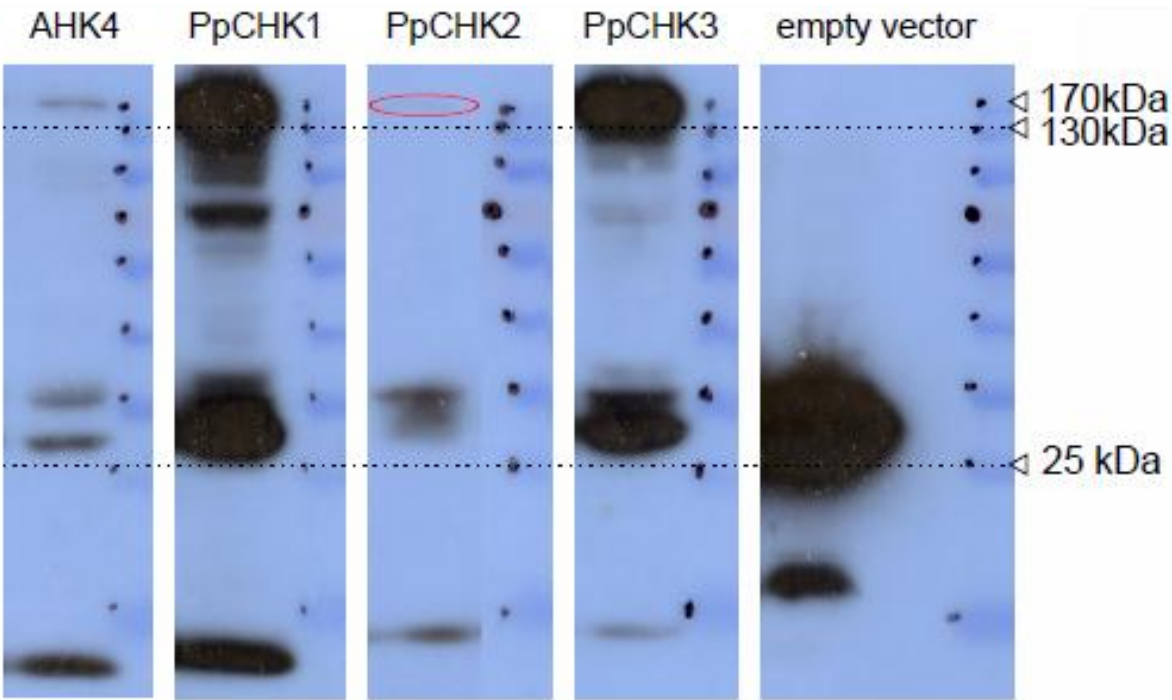


Fig. S 1. Expression control of the fusion proteins analysed in Fig. 1. Immunoblot detection was carried out using the pellet of 1 mL bacterial culture that was separated by SDS-PAGE, blotted to a PVDF membrane and GST-containing bands were stained using a GST specific antibody. White arrowheads mark the position of the protein marker. Encircled in red is the band for PpCHK2.

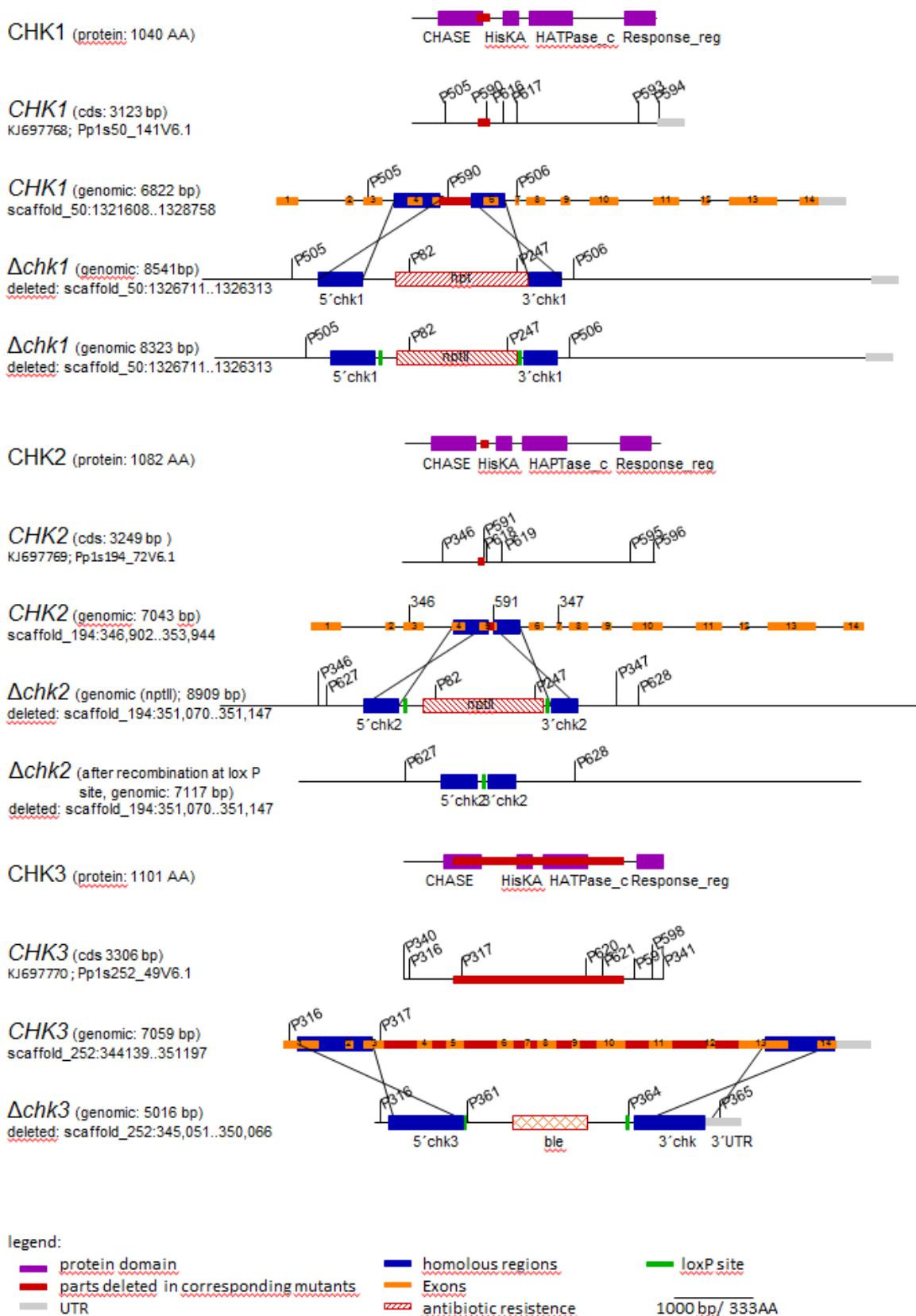


Fig. S 2. Overview of the *CHK* genes, proteins and knockout plants generated by transformation with the vectors listed in Tab. S 1. Double and triple mutants were generated by sequential transformation. The protein domains are shown in purple. The primers used for PCR (Fig. S 3) and RT-PCR (Fig. S 4) screening, as well as Real-time PCR Assays (Fig. 7) are indicated and sequences can be found in Tab. S 2. The accession numbers, as well as the Cosmoss gene (locus) IDs (cosmoss.org) are shown. Further the deleted regions in the corresponding mutants are shown in red and the deleted fragments are given by their scaffold location.

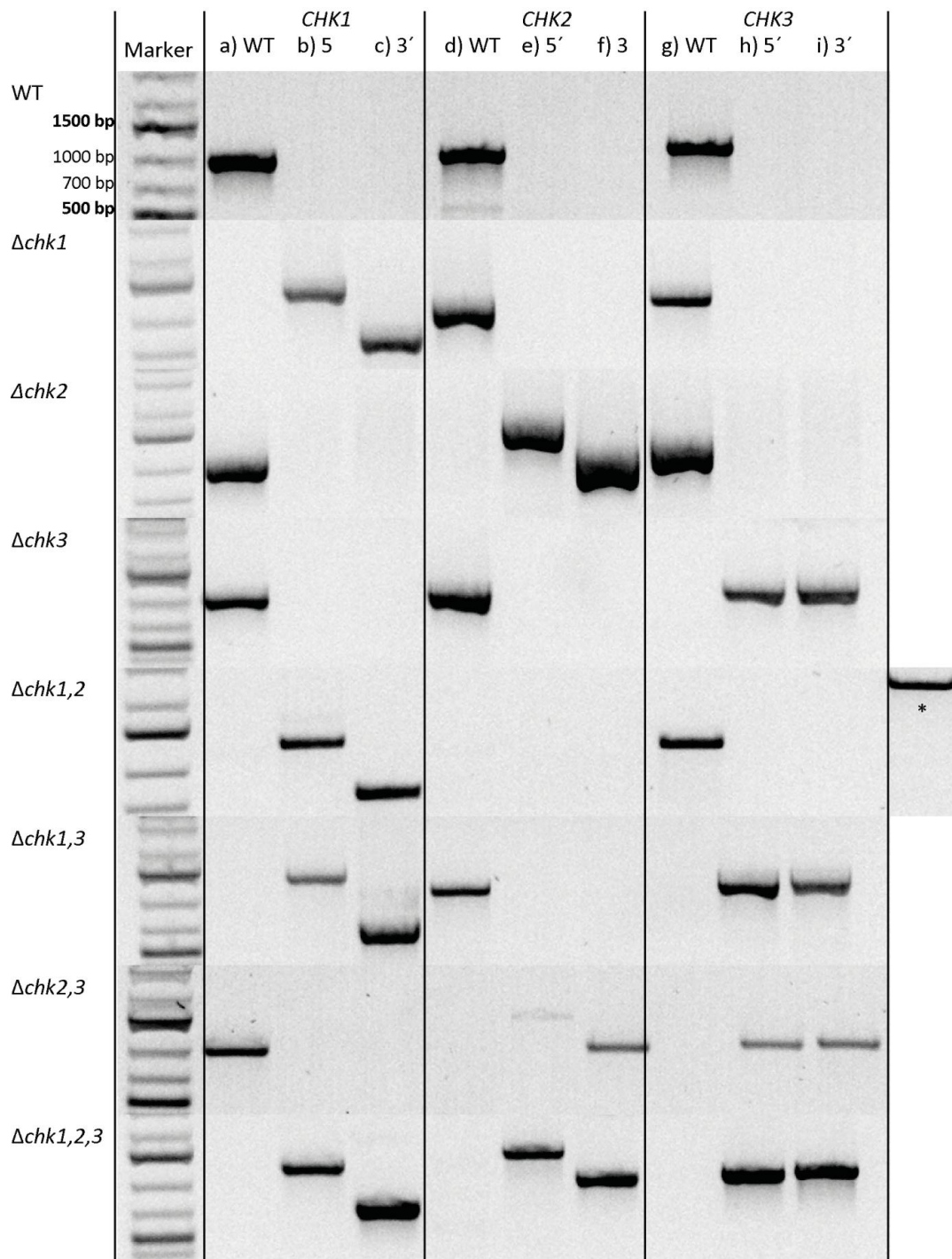


Fig. S 3. PCR screening of knockout mutants. DNA has been isolated (<http://moss.nibb.ac.jp>) from one colony of each stable mutant. For the WT and each mutant nine PCRs have been performed as described in Kamisugi and Cuming (2009, In Annual Plant Reviews: The Moss Physcomitrella patens, Vol 36. pp 76-112: For each locus forward and reverse primers were picked adjacent to the 5' homolog fragment of the respective locus (WT) to test the presence/absence of the WT locus. The same forward primer together with a reverse primer from the resistance cassette (5') as well as a forward primer from the resistance cassette together with a reverse adjacent to the 3' homolog fragment (3') were applied to show the correct integration at both sides after homologous recombination. *CHK1*: a) WT(P505/P590), b) 5'(P505/P82), c) 3'(P247/P506); d) *CHK2*: WT(P346/P591), e) 5'(P346/P82), f) 3'(P247/P347); g) *CHK3*: WT(P316/P317), h) 5'(P316/P361), i) 3'(P364/P365). * The nptII resistance cassette in the $\Delta chk1,2$ mutants was removed from the *chk2* locus by transient CRE recombinase expression. Thus the products e and f are missing. Instead an additional PCR (P627/P628) was performed and the product was sequenced to confirm the deletion of a 77bp fragment. All primers are indicated in Fig. S 2 and are given in Tab. S 2.

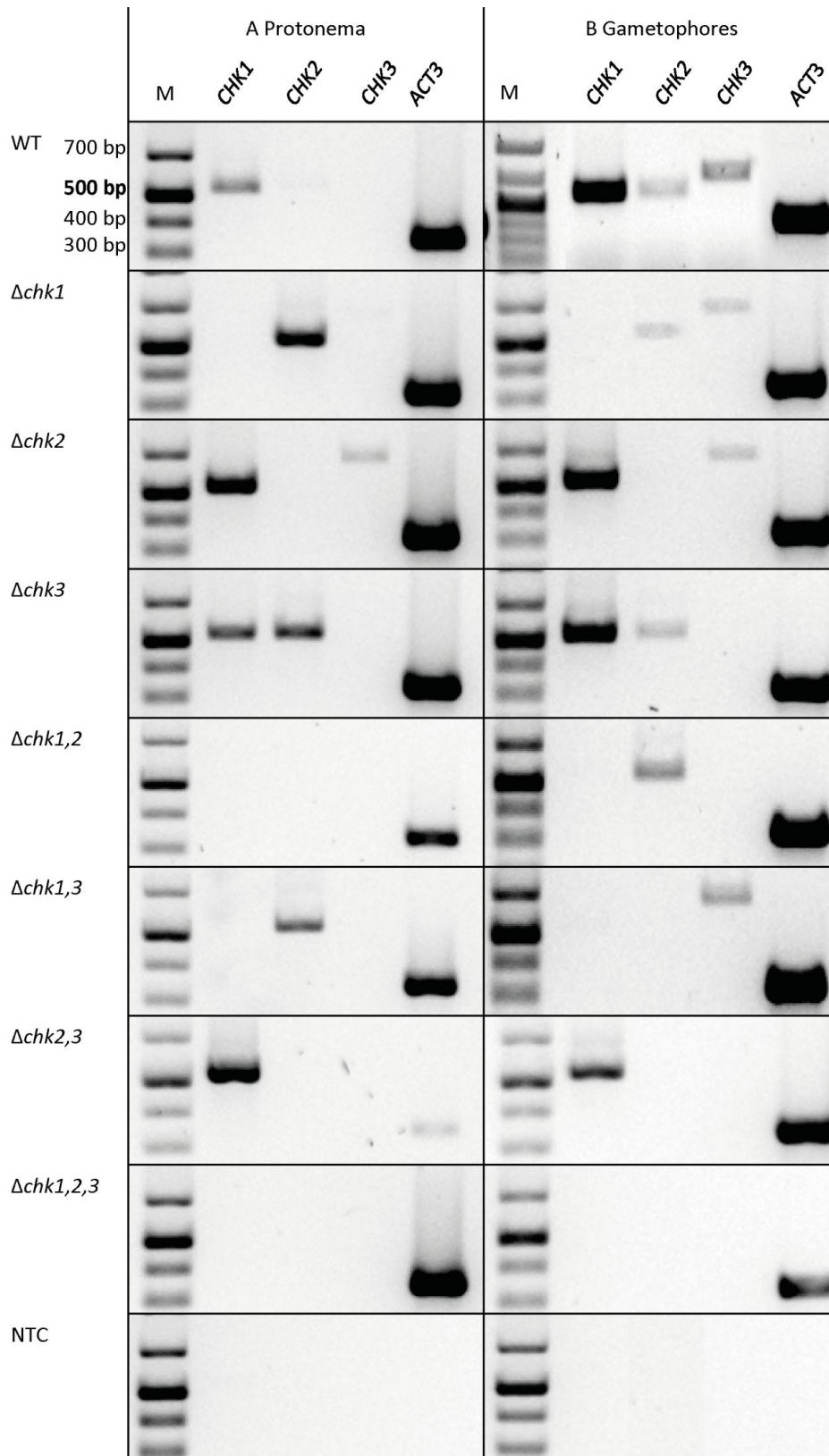


Fig. S 4. RT-PCR screen of the different mutant lines. RNA has been isolated from protonema (7-day-old) and gametophores (8-weeks-old) grown on solid medium in order to check the presence/absence of the chk transcripts in the mutants. Two different stages of development were chosen here due to the fact that especially *chk3* is on low abundance and thus not clearly detectable in protonema stages. RNA isolation and DNase digestion has been performed as described in Material and Methods section. cDNA synthesis has been performed with RevertAid H Minus Reverse Transcriptase (Thermo Scientific). *CHK1* (P505/P590); *CHK2* (P346/P591); *CHK3* (P316/P317). NTC = non template control. All primers are indicated in Fig. S 2 and are given in Tab. S 2.

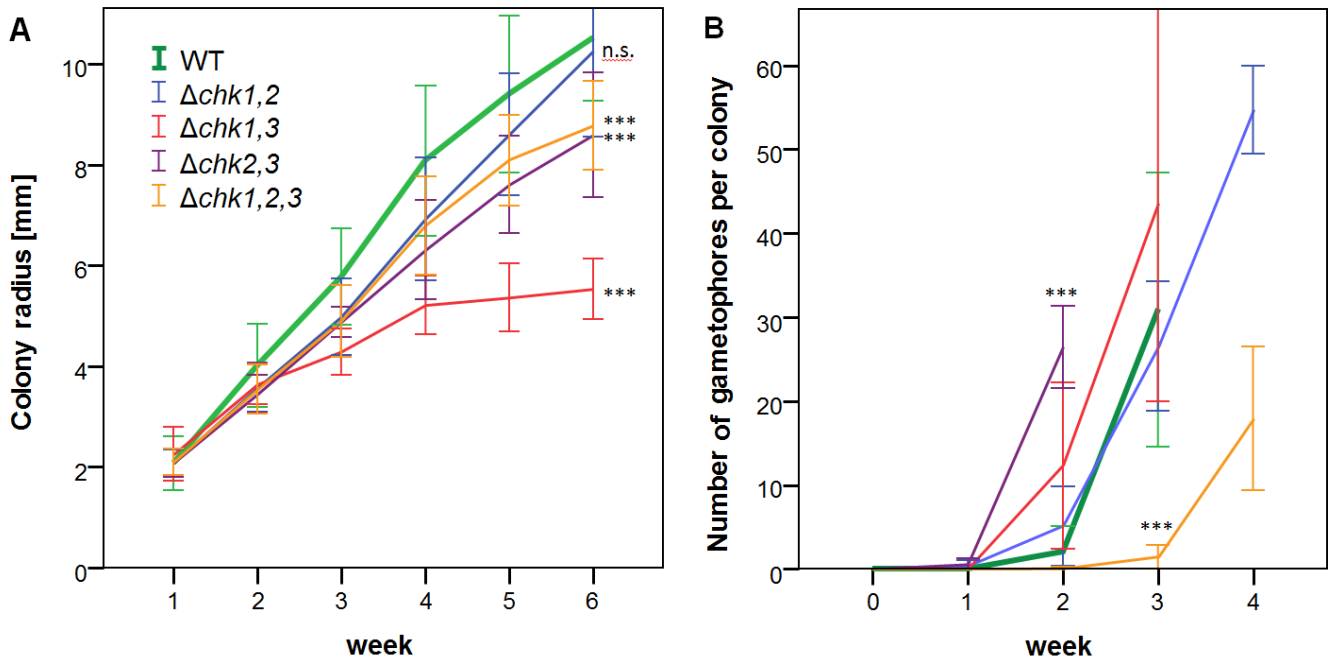


Fig. S 5. A) Average colony radius over the course of six weeks after inoculation of KNOP-Agar. B) Time course of gametophore frequency. Gametophores with at least three developed leaflets were counted up to 60 gametophores per colony (beyond that quantification was not further possible). Mean \pm SD, t-test difference from WT, *** $p < 0.001$, otherwise no significant differences.

Tab. S 1. Generation of *CHK* mutant collection.

Four different vectors were generated targeting the loci of *CHK1*, -2, and -3 individually. They were designed using three different resistance cassettes in order to allow the generation of double and triple mutants by subsequent re-transformation of already characterized single and double mutants respectively. At least 330 bp of homologous region were cloned from genomic DNA on two sides of the resistance cassette aiming at targeted integration and subsequent disruption of one specific locus. The following characterization (antibiotic selection, PCR screen, RT/PCR screen and flow cytometry) were performed prior to re-transformation with another construct in order to guarantee ideal mutants. The *nptII* resistance cassette in the Δ *chk1,2* mutant was eliminated by site specific recombination using the *cre/lox* system by transient expression of Cre recombinase (Albert et al. 1995, Plant J 7: 649-659, Troulliet et al. 2006, Nucleic Acids Res 34: 232-242).

Vectors for generation of mutants of up to three different constructs. **pNPTIIRev* and *pNPTIIFor* were obtained from Schaefer DG and Zryd JP (1997, Plant J 11: 1195-1206) and are a modified version of *pHP23b*. *pHP23b* was subcloned in the *pBSII-KS* plasmid (Stratagene) using *EcoRI* as restriction enzyme in reverse and forward orientation, leading respectively to the *pNPTIIRev* and *pNPTIIFor* plasmids. For *pHygro*, the *NptII* cassette of *pNPTIIFor* was removed by *EcoRI* digestion and the hygromycin resistance marker gene from the *pCambia* vector (*pC1304*) was cloned at the blunted *EcoRI* site. ***pBZR* was obtained from Schaefer et al. (2010, DNA Repair 9: 526-533) and is a modified version of *pBNR*. The *EcoRI/NotI* fragment of *pBNR*, corresponding to the *NPTII* gene was replaced by an *EcoRI/NotI* PCR amplified fragment of *pLGZ2* (Kubo et al. (2013) Plos One 8: e77356) corresponding to the zeocin resistance gene leading to *pBZR*. The final alternations of the three different loci are shown in Fig. S 2.

Protoplastation and PEG mediated transformation using linearized Plasmid DNA was performed according to Schaefer et al. (1991, Mol Gen Genet 226: 418-424). Stable mutants were selected after three rounds of growth on solid medium with the corresponding antibiotic (G418 (50 μ g/ml), Hygromycin B (30 μ g/ml) and zeocin 30 μ g/ml). The selected, stable mutants grow easily on antibiotic containing media whereas the WT and mutants other resistances die or grow poorly.

Protoplast fusion is known to occur during protoplastation and PEG transformation and results in various phenotypic alterations Schween et al. (2005, Bryologist 108: 27-35). All mutants have been checked using the PA Analyzer (Partec) for their relative genome size and are in haploid stage (data not shown).

Mutant	Vector 1	Vector 2	Vector 3	Antibiotic-Resistance of mutants
Δ<i>chk1</i>	* <i>pNPTIIRev_PpCHK1</i>	-	-	Geneticin
Δ<i>chk2</i>	* <i>pNPTIIFor_PpCHK2</i>	-	-	Geneticin
Δ<i>chk3</i>	** <i>pBZR_PpCHK3</i>	-	-	Zeocin
Δ<i>chk1,2</i>	<i>pNPTIIFor_PpCHK2</i>	* <i>pHygro_PpCHK1</i>	-	Hygromycin B (<i>Geneticin resistance was eliminated by recombination</i>)
Δ<i>chk2,3</i>	*** <i>pNPTIIFor_PpCHK2</i>	<i>pBZR_PpCHK3</i>	-	Geneticin Zeocin
Δ<i>chk1,3</i>	<i>pNPTIIRev_PpCHK1</i>	<i>pBZR_PpCHK3</i>	-	Geneticin Zeocin
Δ<i>chk1,2,3</i>	<i>pNPTIIFor_PpCHK2</i>	<i>pHygro_PpCHK1</i>	<i>pBZR_PpCHK3</i>	Geneticin Hygromycin B Zeocin

Tab. S 2. Primer sequences. All Primers used in this study were obtained from Metabion (Planegg, Germany).

target/purpose	Primer	Sequence
nptII/hyg PCR screening	P82	actgtcggcagagcatctt
	P247	gggttcgctcatgtgtga
zeo cassette screening	P361	ggccggccagatctataac
	P364	cgaagttatctcgagtcgcg
<i>CHK1</i> PCR screening	P505	catatgccgagagagtcctc
	P590	caaagtccaagtcgctgaca
	P506	atctcgtgagacacagttgcc
<i>CHK2</i> PCR screening	P346	atttgctgaacgagtgctgc
	P591	gatctccgaaatccaagctg
	P347	gaattcatgtgatactgtcgcc
	P627	gacgaatatgccccaccac
	P628	acggcctgattcaattttg
<i>CHK3</i> PCR screening	P316	ggagtcagaagtgaagctagg
	P317	aaacggtctcttgagacattgta
	P365	atccaccttcacattcatgcg
<i>ACT3</i>	P214	cggagaggaagtacagtgtgtgga
	P215	accagccgtagaattgagcccag
Real-time 60S L21 Protein	P494	acgcaccggcatcgt
	P495	tgcttggtcatcacgacaccaa

Tab. S 3. Data for the budding assay (Fig. 5 & Fig. 6). Equal amounts of protonema were suspended on KNOP agar medium containing 0 - 400 nM iP as well as 400 nM tZ and BA and bud formation was analyzed microscopically after 10 days under standard conditions. The number of buds corresponds to one microscopic view field (3.8 mm²). At least two different biological replicates were counted in 5 - 10 view fields and mean values were calculated, n = number of viewfields counted. t-test different from Wt at 400 nM, ** p< 0.01*** p<0.001, equal variances not assumed.

	CK	c [nM]	n	mean	SD	t-test
WT	iP	0	60	0	0	
		50	50	4.30	4.83	
		100	35	16.91	4.22	
		400	45	25.47	6.14	
	tZ	400	54	22.43	12.44	
BA	400	80	19.25	10.81		
Δ chk1	iP	0	25	0	0	
		50	25	7.12	7.22	
		100	25	21.16	6.67	**
		400	27	15.11	10.60	***
	tZ	400	30	1.10	1.45	***
BA	400	30	7.10	6.82	***	
Δ chk2	iP	0	35	0	0	
		50	40	0.20	0.60	***
		100	30	2.50	2.46	***
		400	35	1.91	1.48	***
	tZ	400	40	0.68	1.33	***
BA	400	20	1.30	0.84		
Δ chk3	iP	0	35	0	0	
		50	40	2.73	2.38	*
		100	35	10.97	7.57	***
		400	35	18.69	10.95	**
	tZ	400	30	5.67	3.75	***
BA	400	30	7.07	4.02	***	
Δ chk1,2	iP	0	30	0	0	
		50	35	0	0	***
		100	35	0.91	1.98	***
		400	35	1.51	2.02	***
	tZ	400	35	0.26	0.69	***
BA	400	40	1.05	1.28	***	
Δ chk1,3	iP	0	30	0	0	
		50	25	0.64	1.38	***
		100	15	16.33	10.10	n.s.
		400	30	17.47	8.91	***
	tZ	400	40	0.33	0.57	***
BA	400	25	1.04	1.48	***	
Δ chk2,3	iP	0	35	0.00	0.00	
		50	40	5.60	3.33	n.s.
		100	20	12.15	4.50	**
		400	25	9.44	7.96	***
	tZ	400	20	14.75	4.23	***
BA	400	30	18.97	4.56	n.s.	
Δ chk1,2,3	iP	0	20	0	0	
		50	20	0	0	***
		100	20	0	0	***
		400	20	0	0	***
	tZ	400	20	0	0	***
BA	400	20	0	0	***	